

GEOCHEMICAL STUDIES OF THE LEWISIAN COMPLEX  
OF THE WESTERN ASSYNT REGION, N.W. SCOTLAND

by

JANE D. SILLS

Thesis submitted to the University of Leicester  
for the degree of Doctor of Philosophy

January

1981

UMI Number: U316055

All rights reserved

INFORMATION TO ALL USERS

The quality of this reproduction is dependent upon the quality of the copy submitted.

In the unlikely event that the author did not send a complete manuscript and there are missing pages, these will be noted. Also, if material had to be removed, a note will indicate the deletion.



UMI U316055

Published by ProQuest LLC 2015. Copyright in the Dissertation held by the Author.  
Microform Edition © ProQuest LLC.

All rights reserved. This work is protected against  
unauthorized copying under Title 17, United States Code.



ProQuest LLC  
789 East Eisenhower Parkway  
P.O. Box 1346  
Ann Arbor, MI 48106-1346



THESIS  
623097  
26.5.81

ABSTRACT

This work examines the petrogenesis of layered ultramafic-gabbro bodies from the Scourian and the metamorphic evolution of the Assynt district of Sutherland.

The layered bodies comprise ultramafic rocks (amphibole-spinel-lherzolites) and garnetiferous gabbros derived from the same tholeiitic magma which had about 15-20% MgO. The ultramafic rocks are partial cumulates formed by olivine and orthopyroxene after settling; with the gabbros being derivative liquids. The flat to LREE enriched patterns and trace element levels suggest the magma formed by 30-40% partial melting of undepleted mantle. The bodies are fragments of Archaean oceanic crust invaded by tonalitic magma generated at a convergent plate boundary followed by ductile deformation and metamorphism to granulite facies. The gabbros show evidence of two periods of granulite facies mineral growth, the first producing a clinopyroxene-garnet+plagioclase assemblage at about 12-15 kb and 1000°C. Uplift caused partial breakdown of the garnet to orthopyroxene-plagioclase+spinel+amphibole symplectites at about 800-900°C and 9-14 kb. Garnet stability depends on both P-T conditions and whole rock Fe/Mg ratio.

The Lewisian complex in Assynt suffered widespread retrogression during the Inverian caused by the influx of large volumes of mantle-derived hydrous fluids associated with the development of NW-trending monoclinial folds. During retrogression the development of a uniform hornblende-plagioclase+quartz assemblage in mafic and intermediate gneisses caused a redistribution of elements. Hornblende and biotite compositions depend on whole-rock composition and paragenesis. The assemblages developed suggest retrogression occurred with falling temperatures in the range 700-500°C remaining above 500°C for the duration of the Inverian and Laxfordian events. The style of deformation became more brittle with time as the complex was uplifted. Amphibolite dykes from Clashnessie Bay are tholeiitic andesites formed from a tholeiitic magma by hornblende fractionation. They were deformed and metamorphosed before the intrusion of the main Scourie dyke swarm. The Canisp shear zone was the site of deformation over a protracted period and there may have been 5-10 km of right-lateral displacement.

To ANDY

## TABLE OF CONTENTS

	Page
INTRODUCTION	1
ACKNOWLEDGEMENTS	8
CHAPTER 1 : STRUCTURAL EVOLUTION OF THE ASSYNT AREA	11
1.1 Introduction	12
1.2 General character of the gneiss	14
1.3 Main structural features of the Assynt region	20
1.4 Orientation of structures in the Assynt region	27
1.5 Folds	36
1.6 Description of the four structural divisions	43
1.7 Discussion	53
CHAPTER 2 : EARLY METAMORPHIC HISTORY OF LAYERED ULTRAMAFIC- GABBRO BODIES	
2.1 Introduction	56
2.2 Mode of occurrence	56
2.3 Petrography	65
2.4 Garnet breakdown reactions	70
2.5 Mineral chemistry	73
2.6 Temperature and pressure of metamorphism	84
2.7 Conclusions	95
CHAPTER 3 : PETROGENESIS OF LAYERED ULTRAMAFIC-GABBRO BODIES	
3.1 Introduction	99
3.2 Field Relationships	100
3.3 Cryptic layering in the Achiltibuie body	102
3.4 Whole rock chemistry	105
3.5 Discussion	129
3.6 Tectonic setting	137

CHAPTER 4 : DESCRIPTION AND PETROGENESIS OF MAFIC, ULTRAMAFIC AND		
METASEDIMENTARY ROCKS FROM ASSYNT		
4.1	Introduction	143
4.2	Description, geochemistry and petrogenesis of the larger mafic masses	143
4.3	Description and petrogenesis of mafic layers and lenses	154
4.4	Agmatites	155
4.5	Hornblendite pods and layers	157
4.6	Metasedimentary gneisses from the Assynt region	162
CHAPTER 5 : RETROGRESSION OF THE ASSYNT GNEISSES		
5.1	Introduction	170
5.2	Petrography	172
5.3	Mineral chemistry	186
5.4	Partitioning of elements between coexisting mineral pairs	209
5.5	Retrogression of ultramafic rocks	219
5.6	P-T conditions during retrogression	229
5.7	Possible changes in whole-rock chemistry during retrogression	238
5.8	Discussion	243
CHAPTER 6 : DESCRIPTION AND PETROGENESIS OF AMPHIBOLITE DYKES		
FROM CLASHNESSIE BAY		
6.1	Introduction	250
6.2	Description and field relationships	250
6.3	Age of the amphibolite dykes	253
6.4	Chemistry	256
6.5	Petrogenesis	264

CHAPTER 7 : THE CANISP SHEAR ZONE	
7.1 Introduction	272
7.2 Main features of the Canisp shear zone	275
7.3 Comparison between the Canisp and Laxford front shear zones	283
7.4 Estimate of displacement	285
7.5 Relationship between deformation and metamorphism	287
7.6 Conclusions	289
SUMMARY OF CONCLUSIONS	293
REFERENCES	301
APPENDIX A : MINERAL CHEMISTRY	331
APPENDIX B : WHOLE ROCK CHEMISTRY	355
APPENDIX C : PARTITION COEFFICIENTS	388

## LIST OF FIGURES

	Page
Fig.1 Map of mainland Lewisian outcrop	6
Fig.2 Map showing Assynt district	7
CHAPTER 1	
1.1 Photographs of agmatites and intrusive trondjhemite sheets	16
1.2 Photographs of minor folds	19
1.3 Structural divisions of the Assynt area	21
1.4 Aeromagnetic anomalies over NW Scotland	21
1.5 Location of NW fold axes in Assynt	23
1.6 Sketch map of area south of Loch Roe	26
1.7 Stereoplots of foliations in Lochinver area	28
1.8 Stereoplots of foliations in the Stoer-Clashnessie area	30
1.9 Stereoplots of foliations in the Drumbeg area	31
1.10 Stereoplots of lineations in the Assynt region	34
1.11 Stereoplots of minor fold axes in the Assynt region	35
1.12 Photographs of minor folds	37
1.13 Sketches of minor folds	39
1.14 Sketches of folds from Clashnessie Bay	40
1.15 Photographs of folds from shear zones	41
1.16 Sketches of folds from shear zones	42
1.17 Sketch map of the area around L.Ardbhair	44
1.18 Sketch map of the area south of Lochinver	46
1.19 Sketch map of the area between Loch Poll and Gorm Loch Mor	48
1.20 Sketch map of the area around Clashnessie Bay	50
1.21 Diagrammatic map of the area around Clashnessie Bay	51
1.22 Sketch map of the area between Stoer and Clachtoll	52

## CHAPTER 2

2.1	Location of ultramafic-gabbro bodies	58
2.2	Photographs of ultramafic rocks	60
2.3	Sketch maps of ultramafic-gabbro bodies	62
2.4	Modal analyses of gabbros from Drumbeg and Achiltibuie	64
2.5	Photomicrographs of ultramafic and gabbroic rocks	66
2.6(a)	Pyroxene quadrilateral	76
	(b) Garnet (Alm-Py-Gr) diagram	
2.7	CaO, MnO and $\text{Cr}_2\text{O}_3$ against FeO for ortho- and clino-pyroxenes	78
2.8	$\text{Al}_2\text{O}_3$ against FeO for ortho- and clino-pyroxenes	79
2.9	$\text{Al}^{\text{iv}}$ against Na + K for amphiboles	83
2.10	P-T diagram for the granulite facies metamorphism	85

## CHAPTER 3

3.1	Cryptic variation in Achiltibuie body	103
3.2	Composition of coexisting garnet and clinopyroxene	103
3.3	AFM plot	109
3.4	$\text{SiO}_2$ against $\text{Al}_2\text{O}_3$ , $\text{TiO}_2$ and Y for all rock types	112
3.5	Major elements against MgO for ultramafic rocks and gabbros	114
3.6	Trace elements versus MgO for ultramafic rocks and gabbros	115
3.7	Dendrogram	117
3.8	Ti-Zr-Y and Ti-Zr-Sr plots	119
3.9	$\text{TiO}_2$ , Y and $\text{P}_2\text{O}_5$ against Zr	121
3.10	$\text{TiO}_2$ and Y against Zr	123
3.11(a)	REE analyses from Drumbeg	125
	(b) REE analyses from Scouriemore	
3.12	Comparisons of REE analyses with those from other mafic and ultramafic rocks	126

## CHAPTER 4

4.1	Photographs of amphibolite and agmatites	144
4.2	AFM plot for mafic rocks	146
4.3	TiO <sub>2</sub> vs Zr and Zr, CaO and TiO <sub>2</sub> against MgO for mafic rocks	147
4.4	Chondrite normalised REE plots for various mafic bodies	148
4.5	Sketch map of Cnoc an Sgriodaich	153
4.6	Photomicrographs of ultramafic pods	158
4.7(a)	TiO <sub>2</sub> against SiO <sub>2</sub> for metasediments and other gneisses	166
	(b) Ni against Sr for metasediments and other gneisses	166

## CHAPTER 5

5.1	Photomicrographs of mafic rocks	174
5.2	Photomicrographs of intermediate composition rocks	181
5.3	Photomicrographs of ultramafic rocks	184
5.4	Al <sup>iv</sup> against Na + K for all amphibole analyses	188
5.5(a)	mg (whole-rock) against mg(hornblende)	191
	(b) TiO <sub>2</sub> (hornblende) against TiO <sub>2</sub> (rock)	191
5.6(a)	correlation matrices for amphibole analyses	192
	(b) dendograms	192
5.7	Si, Ca, Na and MnO against mg for all analyses	193
5.8(a)	mg (whole-rock) against mg (biotite)	200
	(b) TiO <sub>2</sub> (whole-rock) against TiO <sub>2</sub> (biotite)	200
5.9	Plots for biotite	201
5.10	Garnet compositions	204
5.11(a)	Classification of chlorite	210
	(b) MnO (chlorite) against mg (chlorite)	210
	(c) Cr <sub>2</sub> O <sub>3</sub> (chlorite) against mg (chlorite)	210
5.12(a)	Mg.Fe (garnet) vs Mg/Fe (biotite)	212
	(b) Ca (garnet) vs K <sub>D</sub>	212
	(c) Mn (garnet) vs K <sub>D</sub>	212

5.13(a)	Mg/Fe (biotite) vs Mg/Fe (hornblende)	215
	(b) Mg/Fe (chlorite) vs Mg/Fe (biotite)	215
	(c) Mg/Fe (chlorite) vs Mg/Fe (hornblende)	215
5.14	Partitioning of elements between coexisting hornblende and biotite	218
5.15	T°C - X CO <sub>2</sub> plot for retrogression of ultramafic rocks	226
5.16	CaO - SiO <sub>2</sub> - MgO plot for ultramafic rocks	228
5.17	P-T plot for retrogression of Assynt region	231
5.18	CaO, Fe <sub>2</sub> O <sub>3</sub> , Na <sub>2</sub> O, K <sub>2</sub> O, Sr and Ba vs MgO for mafic rocks	240
5.19	CaO/Zr, Fe <sub>2</sub> O <sub>3</sub> /Zr, TiO <sub>2</sub> /Zr, Na <sub>2</sub> O/Zr and Sr/Zr against Zr for mafic rocks	242
CHAPTER 6		
6.1	Photographs of amphibolite dykes	251
6.2	Sketch plans of amphibolite dykes	252
6.3	Sketch map of the east end of Clashnessie Bay	254
6.4	Whole-rock lead-lead isochron for gneisses enclosing Clashnessie dykes	257
6.5(a)	TiO <sub>2</sub> - P <sub>2</sub> O <sub>5</sub> - K <sub>2</sub> O plot	261
	(b) SiO <sub>2</sub> vs Na <sub>2</sub> O + K <sub>2</sub> O	261
6.6	TiO <sub>2</sub> , Zr, Sr and Ba vs SiO <sub>2</sub> for Clashnessie and Scourie dykes	262
6.7	TiO <sub>2</sub> , Y, Ni, Sr, Ba and Rb vs Zr	263
6.8	K <sub>2</sub> O vs Rb	265
6.9	REE diagram for Clashnessie and Scourie dykes	268
CHAPTER 7		
7.1	Sketch map of Canisp shear zone	276
7.2	Cross section of Canisp shear zone	277
7.3	Sketch map of northern margin of shear zone	278

7.4	Photograph of small shear zones in a dyke	280
7.5(a)	folded Scourie dyke	281
	(b) general view of sheared gneisses	281
7.6	Photograph of small shear zone	286
7.7	Cross section through northern Lewisian	290

## LIST OF TABLES

	Page
CHAPTER 2	
2.1 Analyses of minerals from ultramafic rocks	74
2.2 Pyroxene analyses from Drumbeg and Achiltibuie gabbros	75
2.3 Garnet analyses	81
2.4 Amphibole analyses	82
2.5 Pressure and temperature estimates for the granulite facies metamorphism	88
2.6 Estimate for P-T of granulite facies metamorphism from other areas	91
2.7 Temperature estimates for Achiltibuie gabbros	93
CHAPTER 3	
3.1 Analyses of mafic and ultramafic rocks	106
3.2 Correlation matrix for all mafic and ultramafic analyses	107
3.3 Comparison of ultramafic rocks with those from other localities	110
3.4 Comparison of Lewisian gabbros with rocks from other localities	111
3.5(a) REE analyses from Drumbeg	127
(b) REE analyses from other mafic and ultramafic rocks	127
3.6 Estimates of initial magma composition	134
CHAPTER 4	
4.1 Analyses of anorthosites and granites from Gorm Loch	151
4.2 Whole rock and mineral analyses from hornblendite	160
4.3 Analyses of metasedimentary gneisses	164

## CHAPTER 5

5.1	Representative mineral assemblages	173
5.2	Composition of amphiboles rimming pyroxene	176
5.3	Changes in amphibole composition with retrogression	185
5.4	Biotite analyses	198
5.5	Garnet analyses	203
5.6	Epidote analyses	206
5.7	Chlorite analyses	208
5.8	Temperatures from garnet-biotite geothermometer	214
5.9	Distribution coefficients for various elements between coexisting hornblende and biotite	217
5.10	Possible mineral reactions for ultramafic rocks	221
5.11	Possible mineral reactions for ultramafic rocks	222
5.12	Feldspar temperatures	233

## CHAPTER 6

6.1	Whole-rock analyses of amphibolite dykes	258
6.2	Mineral analyses	259

## APPENDIX A

A1	Minimum detection limits, for microprobe analysis	332
	Pyroxene analyses	333
	Olivine analyses	339
	Garnet analyses	340
	Amphibole analyses	343
	Biotite analyses	352

## APPENDIX B

B1	Minimum detection limits for X.R.F. data	356
B2	Location of samples analysed by X-Ray fluorescence	358
B4	Whole rock analyses	366

## APPENDIX C

	Partition coefficients	388
--	------------------------	-----

INTRODUCTION

The Lewisian gneiss complex of NW Scotland is one of the best studied areas of Archaean gneiss in the world but many problems concerning the origin and subsequent evolution of the gneisses still remain. For this study an area extending from Kylesku westwards to Drumbeg and south to Lochinver has been examined (the area studied is shown in Figs.1 and 2).

There is a large literature on the Lewisian extending back to the beginning of the century when the classic Northwest Highlands Memoir (Peach et al., 1907) was published. The next major publication was that of Sutton and Watson (1951) who showed that the Lewisian formed in two major gneiss-forming events (the Scourian and the Laxfordian) separated by a period of dyke intrusion (the Scourie dykes). Subsequent isotopic work has shown that they were essentially correct. Moorbath et al. (1969) showed an Archaean age of ca 2.7 b.y. for the Scourian granulite facies event and a Proterozoic age for the Laxfordian reworking. Recent Sm-Nd isotopic work (Hamilton et al., 1979) showed that the gneiss-precursors equilibrated with a mantle source ca 2.92 b.y. This is in good agreement with the Pb-isotope work of Moorbath et al. (1975) and Chapman and Moorbath (1977) who demonstrated that the gneiss precursors separated from the mantle not more than 300 million years before the metamorphic event at ca 2.7 b.y. The Scourian gneisses therefore represent a significant addition of new crustal material.

Work in the Assynt region has shown the chronology to be more complex with the gneisses being reworked in NW-trending monoclinial fold belts before the intrusion of the Scourie Dykes (Evans, 1965; Sheraton et al., 1973b; Evans and Lambert, 1974). The effects of the Inverian deformation and retrogression are more extensive than implied in the literature and fresh granulites are rare in the area studied by the author. The deformation and metamorphic effects of the Inverian are discussed in Chapters 1 and 5.

There now seems to be a consensus of opinion regarding the origin of the quartzo-feldspathic gneisses; several authors believing them to be derived from a diorite-tonalite-granodiorite plutonic complex, possibly in a Cordilleran margin type environment (Holland and Lambert, 1975; Rollinson, 1978; Rollinson and Windley, 1980b; Weaver and Tarney, in press). The equivalence of Archaean high-grade granulite-gneiss belts to modern Cordilleran margins was originally suggested by Tarney (1976) and Windley and Smith (1976) and has received support from the geochemical evidence of Rollinson and Windley (1980b) and Weaver and Tarney (in press). In addition to the quartzo-feldspathic gneisses, there is a great variety of mafic and ultramafic rocks which make up about 10% (or possibly more) of the terrain. One of the aims of this study was to examine the mafic rock types, especially layered ultramafic-gabbro bodies, to see whether or not their origin is compatible with the above model which can account for the quartzo-feldspathic rocks.

The Assynt region comprises gneisses affected by all three Lewisian structural/<sup>and</sup>metamorphic events. Scourian granulites occur in low strain zones in the NE and extreme south of the area studied (see Fig.1) but the main part of the region was affected by the Inverian and then locally cut by Laxfordian shear zones (e.g. the Canisp shear zone). Davies (1974, 1976, 1978) used mafic-ultramafic layers as marker horizons to map out early Scourian structures and to determine how they were affected by the Laxford front (the "boundary zone" between Scourian granulites and Laxfordian migmatites; Sutton and Watson, 1951; Beach et al., 1974; Davies, op.cit.). It was hoped, in this study, to continue the work of Davies (op.cit.) southwards into the Canisp shear zone, but the large amount of Inverian deformation in Assynt has largely obliterated Scourian structures and the Canisp shear zone does not have

the concentration of ultramafic-gabbro bodies found in the Laxford front (see Chapter 7). However mapping of mafic units has helped in understanding Inverian structures.

This thesis then falls into two parts, firstly looking at the origin of the mafic rocks and secondly looking at the effects of the Inverian and Laxfordian events in Assynt. In the first part (Chapters 2 - 4), mafic and ultramafic rocks are examined in detail to help understand the evolution of the complex. In recent years, a number of P-T estimates for the granulite facies metamorphism have been published. O'Hara (1977), O'Hara and Yarwood (1978) and Barnicoat and O'Hara (1979) present evidence for very high peak conditions of 1000 - 1200°C and ca 15 kb, while other estimates (Wood, 1975; Rollinson 1978, 1980, 1980b) are lower (800 - 900°C, 10 - 14 kb). In Chapter 2 the granulite facies metamorphic history of layered ultramafic-gabbro bodies is examined and it is shown that there were two stages of granulite facies mineral growth, P-T estimates for both being made. In Chapter 3, the geochemistry and possible origins of these layered bodies is studied. This has caused considerable controversy notably between O'Hara (1961a, 1965) and Bowes et al. (1964, 1966). In view of the significance of these mafic rocks in understanding the early history of the complex (Davies, 1975) it was felt that a further study was necessary. Similar garnetiferous gabbros occur in other areas believed to be lower continental crust (Rivalenti et al., 1975; Okrusch et al., 1980) so an understanding of their genesis may help in understanding the evolution of the continental crust. Chapter 4 looks at other mafic, ultramafic and possibly metasedimentary rocks occurring in the Assynt region.

The second part of this thesis (Chapters 5 - 7) examines the Inverian and Laxfordian reworking of the Scourian granulites. Chapter 5

discusses the structural evolution of the area based on field mapping by the author and the work of Sheraton et al. (1973b). The area covered is indicated in Fig.1 and a map showing place names which may not be given grid references in the text is shown in Fig.2. All grid references quoted in this text are from the national grid area NC. In Chapter 5, the mineralogical changes occurring during the Inverian retrogression are documented, with an estimate of the P-T conditions. It is shown that retrogression was caused by the influx of mantle derived water. In Chapter 6 some small folded amphibolite dykes which are clearly not "normal" Scourie dykes are discussed. Chapter 7 examines the evolution of the Canisp shear zone from its initiation as the steep limb of the Lochinver antiform to the Laxfordian when a zone of sheared gneisses up to 0.5 km wide developed.

Note: Chapters 2 and 3 have been prepared for publication jointly with Dr. David Savage (Savage and Sills, 1980; Sills et al., in prep.) combining my work in Assynt with that of Savage (1979) on Scouriemore. In Chapters 2 and 3 I have tried to present my own data and acknowledge Dave Savage's work where necessary. All the data plotted in the figures for Chapter 3 marked "Scourie" are from Savage (1979).

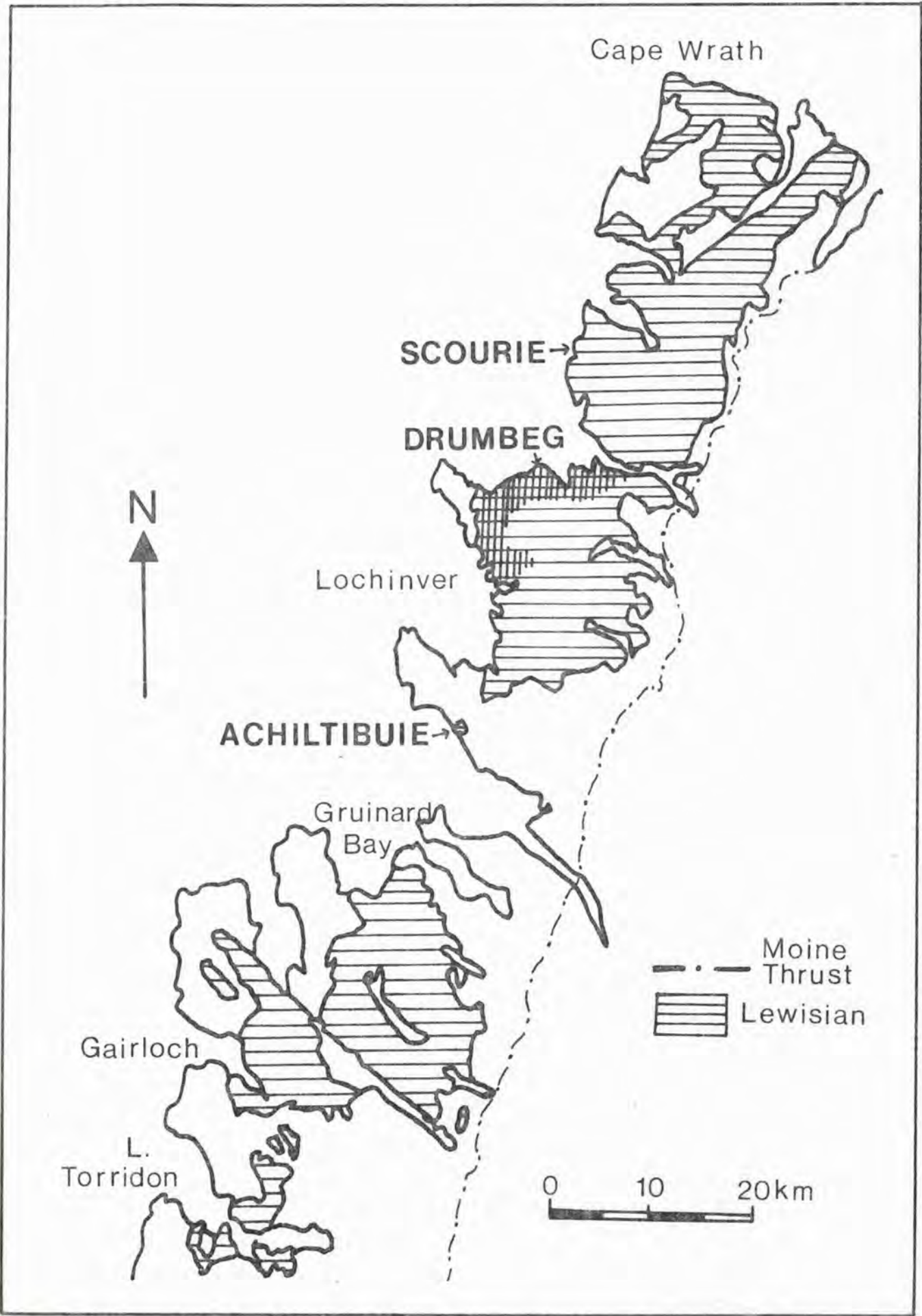


FIG. 1 Map showing the extent of the mainland Lewisian outcrop of NW Scotland. Area with vertical hatching indicates the area

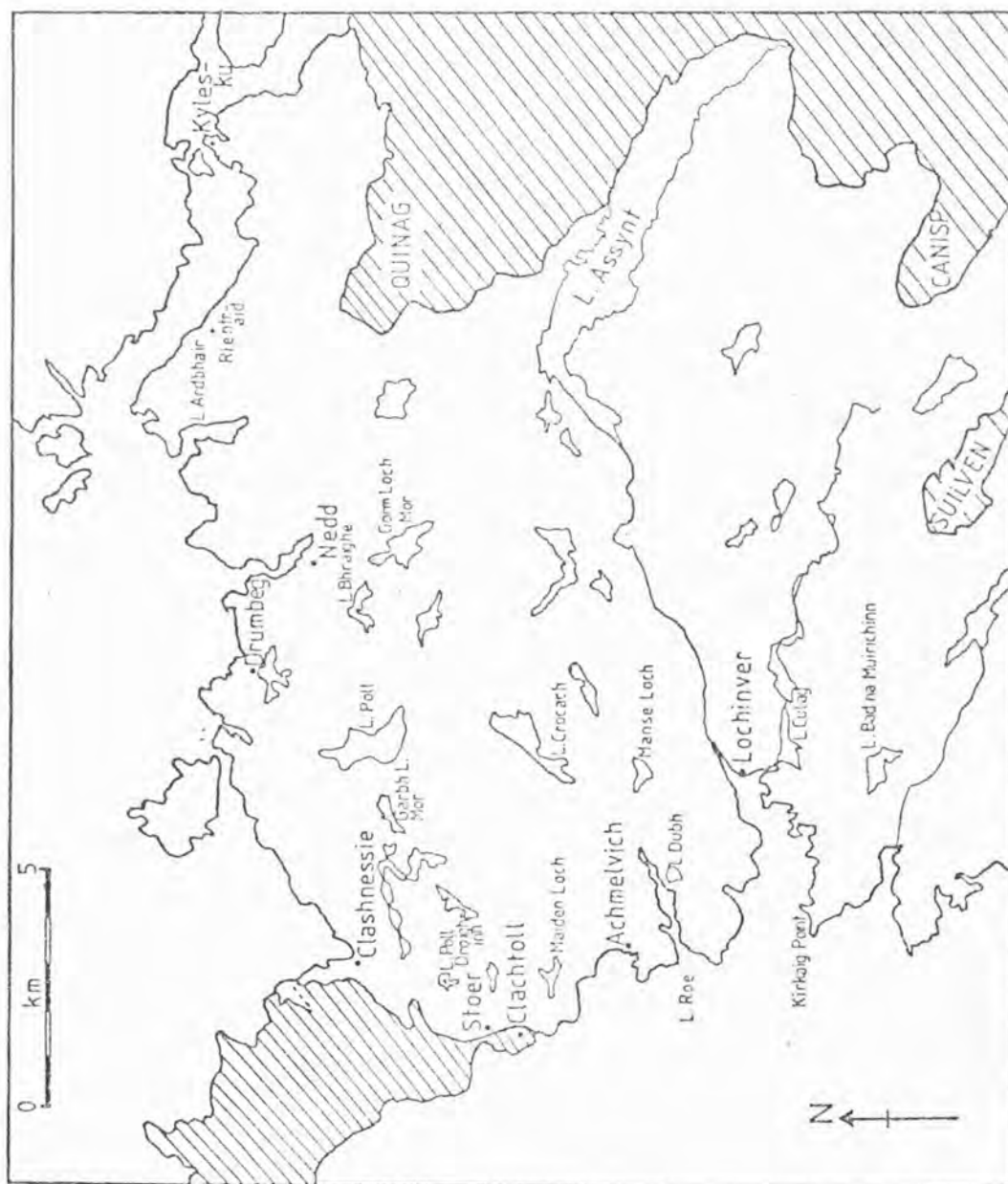


FIG. 2. Locality map, showing the location of villages and lochs mentioned in the text.

### Acknowledgements

I wish to thank Dr. Brian Windley for his supervision and encouragement during the course of this work. Rob Wilson instructed and guided me in the use of the electron 'probe' and computer and without his help much of this work would not have been possible. I would also like to thank Dr. Graham Hendry at the University of Birmingham for running most of the X.R.F. analyses and Dr. Giz Marrinner at Bedford College for the few remaining analyses. Thanks go to the technical staff of the Geology Department, Leicester, for producing thin sections and help with photography and diagrams. I would also like to thank the following for helpful discussions: Drs. Hugh Rollinson, David Savage, Barry Weaver and Mike Norry. The receipt of an NERC research studentship is gratefully acknowledged. Last but not least my thanks go to Andy who made the coffee.

TABLE 1 List of abbreviations used in this thesis

## A. Mineral names

opx	-	orthopyroxene
cpx	-	clinopyroxene
gt	-	garnet
ol	-	olivine
amph	-	amphibole
hb	-	hornblende
parg	-	pargasite
trem	-	tremolite
anth	-	anthophyllite
bi	-	biotite
phlog	-	phlogopite
musc	-	muscovite
chl	-	chlorite
serp	-	serpentine
tc	-	talc
ep	-	epidote
sp	-	spinel
magt	-	magnetite
ilmt	-	ilmenite
opq	-	opaque oxides
sulp	-	sulphides
qz	-	quartz
plag	-	plagioclase
micr	-	microcline
kfsp	-	potassium feldspar
cc	-	calcite
dol	-	dolomite
an	-	anorthite
ab	-	albite
ap	-	apatite
zr	-	zircon

## B. Thermochemical properties

P	-	pressure (kilobars)
T	-	temperature ( $^{\circ}\text{C}$ or K)
$P_{\text{H}_2\text{O}}$	-	partial pressure of water
$P_{\text{CO}_2}$	-	partial pressure of carbon dioxide
$f_{\text{O}_2}$	-	fugacity of oxygen
$\Delta S$	-	entropy
$\Delta H$	-	enthalpy
$\Delta V$	-	volume
$a_i^j$	-	activity of component $i$ in phase $j$
mg	-	$\text{Mg}/(\text{Mg} + \text{Fe}^{2+})$
MDL	-	minimum detection limit

C. Rayleigh Fractionation equation:

$$\frac{C_L}{C_O} = F^{K_D - 1}$$

where  $C_L$  is concentration in remaining liquid  
 $C_O$  is concentration in original liquid  
 $F$  is the fraction of liquid remaining  
 and  $K_D$  is the crystal-liquid partition coefficient  
 for the element concerned.

Shaw (1970) Batch melting equation:

$$\frac{C_L}{C_O} = \frac{1}{D + F(1 - P)}$$

where  $C_L$  is concentration in the liquid  
 $C_O$  is concentration in the source  
 $D$  is the bulk distribution coefficient for  
 the mineralogy of the source material  
 $F$  is the fraction of melting  
 and  $P$  is a constant  $(X^\alpha K_D^\alpha + X^\beta K_D^\beta + \dots)$   
 where  $X^\alpha$  is the proportion of phase  $\alpha$   
 entering the melt and  $K_D^\alpha$  is the  
 crystal-melt distribution coefficient  
 for phase  $\alpha$ .

All rocks in the Lewisian complex have been metamorphosed, hence rock names should be prefixed "meta-". However to avoid cumbersome terminology this prefix has generally been omitted.

CHAPTER 1

STRUCTURAL EVOLUTION OF THE  
ASSYNT REGION

## 1.1 INTRODUCTION

In this chapter the structural evolution of the Assynt area will be examined to provide a framework in which to discuss the geochemistry.

The Lewisian has been divided into a pre-Scourie dyke complex, the Scourian, metamorphosed at granulite facies, and a post-dyke complex, the Laxfordian, metamorphosed at amphibolite facies (Sutton and Watson, 1951). Due to the generally undeformed nature of the Scourie dykes in Assynt this region has usually been considered as part of the central Scourian block. Subsequent work by many authors has shown the situation to be more complex. The Scourian areas are characterised by a flat lying foliation and NE trending structures (e.g. Davies, 1976). Peach et al. (1907) originally, and then Evans (1965) recognised a series of NW trending structures, producing a steeper foliation, which predate the intrusion of the Scourie dykes. This deformation, which is associated with amphibolite facies retrogression, was termed the Inverian. These NW structures mark a sharp break in tectonic style from the flat structures of the Scourian. This NW trend is continued through the intrusion of the Scourie dykes to the fold structures and shear zones of the Laxfordian (Beach et al., 1974; Sheraton et al., 1973b). The status of the Inverian has caused some dispute, some authors e.g. Bowes (1969) ascribing it the status of a major orogeny, others believing Inverian structures to be the late stages of the Scourian. Park (1970) emphasised the unity of the Inverian, the intrusion of the Scourie dykes and some Laxfordian events. Studies in the Assynt area, the type area for the Inverian, have illuminated some of these problems. The NW structures, associated with retrogression, are clearly cut by undeformed Scourie dykes therefore a considerable amount of Inverian deformation is pre-Scourie dyke. Tarney (1963, 1973) and O'Hara (1961b) concluded that the Scourie dykes were intruded into fairly hot crust, perhaps at amphibolite facies. Tarney (1973) has outlined a complex

history of dyke metamorphism and alteration which demonstrates that the dykes were metamorphosed at amphibolite facies with no accompanying deformation and that some dykes were subsequently sheared in ESE shear zones. This suggests that the Inverian event lasted for a considerable time, starting with NW trending folds, then the Scourie dykes were intruded and metamorphosed towards the end of the event. The dykes and gneisses were then cut by shear zones. These late shear zones, as they affect the dykes, are assigned to the Laxfordian after the definition of Sutton and Watson (1951) but they could represent the last stages of the Inverian event in Assynt. The close association of dykes with major shear zones is common, e.g. the Nagssugtoqidian of W.Greenland (Escher et al., 1976).

Recent isotopic studies of the Lewisian allows the following time scale for the Assynt region to be constructed:

- (1) Derivation of the gneiss precursors from the mantle at 2.9 by ago (Hamilton et al., 1979).
- (2) Metamorphism of the complex, mainly at granulite facies, at 2.7 by ago (Chapman and Moor bath, 1977).
- (3) Intrusion of potash rich pegmatites at 2.54 by ago (Evans and Lambert, 1974).
- (4) Beginning of the Inverian deformation establishing a NW structural trend.
- (5) Intrusion of the Scourie dykes at 2.39 by ago (Chapman, 1979).
- (6) Laxfordian shear zones.

The structural development of the Assynt region thus falls into two distinct parts:

- (1) Formation of the gneisses up to the peak of Scourian metamorphism and development of the main foliation and early lineation.
- (2) The modification of this granulite facies complex to amphibolite facies over a period of several hundred million years.

In this study the terms Scourian, Inverian and Laxfordian are taken to mean the following:

Scourian: the period up to and including the peak of granulite facies metamorphism and formation of the main flat lying foliation (the Badcallian of Park, 1970).

Inverian: the period from the onset of folding on NW axes to the intrusion and metamorphism of the Scourie dykes.

Laxfordian: discrete ESE shear zones which affect Scourian and Inverian structures as well as the Scourie dykes.

## 1.2. THE GENERAL CHARACTER OF THE GNEISS

The general character of the gneiss in the Assynt area has been well described by Sheraton et al. (1973b) and much of what follows reiterates what they have already said. The complex is extremely heterogeneous; the gneiss type often changing in both structural style and composition over distances as small as a few millimetres. The composition of the gneiss ranges from ultramafic to true granite but intermediate gneiss types are most abundant. The following rock types are found, some of which are discussed further in subsequent chapters.

- (a) Layered ultramafics with associated garnetiferous gabbros

(Bowes et al., 1964, 1966; O'Hara, 1961a, 1965; Savage, 1979; Savage and Sills, 1980); these complexes are discussed in detail in Chapters 2 and 3.

(b) Hornblendite pods, balls and layers (Chapter 4).

Ultramafic pods, commonly 10 cm to 1 m across, are usually composed of hornblendite with hornblende crystals up to 10 cm long. Some balls are zoned with a pale green hornblendite core and a darker hornblendite rim. Near Kylesku ultramafic pods with orthopyroxene and some phlogopite are found. The hornblendes are paragonitic and were probably stable during granulite facies metamorphism. The pods tend to occur in clusters in acid gneiss, away from any original source and they are believed to result from the extreme boudinage and fragmentation of mafic or ultramafic material early in the history of the Scourian, prior to granulite facies metamorphism. The pods are generally unfoliated and the gneiss foliation often swings round them, occasionally with quartzo-feldspathic material in the pressure shadow regions at the end of the pods. Trains of pods can only be followed along strike for a few metres.

(c) Agmatites (Fig.1.1a,b and Chapter 4). Larger areas of mainly ultramafic material, broken up by veins of quartzo-feldspathic composition are fairly common and range in size from about 1 m to perhaps 100 m across. The mafic or ultramafic part of the agmatite is usually unfoliated, but the felsic component often has a lineation indicating deformation in the early Scourian, the bodies tend to be flattened within the plane of the foliation and the margins may be strongly foliated, suggesting that agmatization occurred prior to the end of the granulite facies event. The ultramafic portion is composed dominantly of actinolite, sometimes with clinopyroxene cores. The composition is thus different to that of the hornblendite balls, although the agmatites presumably also formed by fragmentation of ultramafic or mafic bodies.

FIG. 1.1(a) Agmatite from near Cnoc an Sgriodaich (069295) where massive mafic rock (top of outcrop) is broken into blocks by the intrusion of felsic material.

FIG. 1.1(b) Agmatite from south of Drumbeg (125312) where ultramafic blocks composed of actinolite are broken up by felsic material.

FIG. 1.1(c) Intrusive trondjemite sheets (samples J104, J105, and J106) cutting mafic and ultramafic rocks at Achmelvich (056242).



**a**



**b**



**c**

Ultramafic and mafic bodies of all types often occur in low strain zones reflecting their greater competence. Some agmatites (Fig.1.1a) clearly show break up of mafic by felsic material, probably during the Inverian. The quartzo-feldspathic portions of the agmatites are generally microcline-free.

(d) Mafic rock (Chapter 4) of uncertain affinity. Mafic rock, usually at amphibolite facies, occurs as layers up to 20 m thick in the gneiss. It could be equivalent to the layered complexes or it may have a different origin, perhaps from supracrustal volcanics.

(e) Intermediate to acid gneisses. These are dioritic to trondjhemitic with tonalitic compositions predominating (Sheraton et al., 1973a). These gneisses are well banded, often on a millimetre scale (Fig.1.2c). Some intermediate gneisses may be derived by the interdigitation of acid gneisses and mafic rocks from layered complexes, as the contacts are sometimes diffuse, particularly where there has been Inverian deformation.

(f) Discordant acid sheets with variable amounts of microcline are common (Fig.1.1c). These are sometimes foliated, often have a good quartz rodding lineation and near Scourie they contain granulite facies assemblages suggesting they were intruded prior to the last stages of granulite facies metamorphism. These late sheets have been discussed by Rollinson (1978) and Rollinson and Windley (1980b).

(g) Minor amounts of metasediment are found in the mainland Lewisian. Brown weathering schists, common in the Laxford Front area, are considered to be metasediment (Davies, 1976) and a meta-ironstone has been reported from near the margin of a layered ultramafic-gabbro body at Scourie (Barnicoat and O'Hara, 1979). In the Assynt region gt-qz-bi rocks

occur locally and these have been interpreted as metasediment (Sheraton et al., 1973a).

(h) Potash-rich pegmatites, sometimes with biotite books, occur locally particularly south of Lochinver (Evans and Lambert, 1974).

#### 1.2.1. Foliation

The dominant structure in the region is a sub-planar banding due to alternating felsic and mafic layers. The banding is best developed in intermediate gneiss compositions (Fig.1.2c). The more extreme compositions, both ultramafic and granite, are fairly massive. The mafic bands may or may not have plagioclase and the banding is best defined where the compositional contrast is greatest. The thin bands (a few mm thick) can only be followed for a few metres, the thicker bands (10 - 20 cm thick) for a few hundred metres at most. Mafic rocks are not normally foliated but they often contain thin felsic veins which are parallel to the regional foliation. Similarly the most acid gneisses (trondjemite and granite) are fairly massive but contain thin streaks of mafic material, usually biotite.

There are ubiquitous tight to isoclinal folds with their axial planes sub-parallel to the foliation (Fig.1.2a). These folds usually occur singly or in pairs but plastic complex folds are found (Fig.1.2b). Isolated fold noses occur. The banding forming these early folds is often quite diffuse and irregular, suggesting recrystallisation after folding. The flat-lying foliation containing isolated sub-parallel folds suggests that the foliation was formed in more than one event. In some cases the banding is folded by later folds with much steeper axial planes (Fig.1.2c) which are Inverian in age.

FIG. 1.2 (a) Isoclinal fold, possibly refolded, in banded gneiss. Note the flat axial plane and the slightly "fuzzy" margins of the bands. South of Drumbeg (125314).

(b) Complex folds with flat axial planes in intermediate composition gneiss, near Drumbeg (128326).

(c) "Inverian" fold in well banded intermediate composition gneiss from Clashnessie Bay. The axial plane of this fold is steeper than those of the earlier intrafolial folds.



a



b



c

### 1.2.2. Lineation

A coarse early lineation formed by quartz rods or elongate mafic or felsic segregations is only patchily developed and the plunge is somewhat variable. In the Laxfordian shear zones a new penetrative lineation is developed.

### 1.3. MAIN STRUCTURAL FEATURES OF THE ASSYNT REGION

The part of the Assynt region studied by the author can be divided into four structural divisions (Fig.1.3):

(a) The extreme NE of the area and south of Strathan where granulite facies mineral assemblages are often preserved even in acid and intermediate gneisses. Quartz grains are often bluish and the early Scourian flat lying foliation is found.

(b) The area around Nedd and Drumbeg and south to Gorm Loch Mor and Loch na Loinne; where granulite facies assemblages are preserved in mafic rocks but not in acid and intermediate gneisses. This area is slightly affected by Inverian deformation, and "steep belts" are common.

(c) Clashnessie Bay to the Canisp shear zone where all gneiss types are at amphibolite facies and are highly folded, steeply dipping and cut by numerous WNW-ESE shear zones.

(d) The Canisp shear zone and other shear zones, notably near Stoer and Clachtoll. There is extreme attenuation of the gneiss banding and a new flaggy foliation is developed with a penetrative lineation. These shear zones in places affect the Scourie dykes and are usually termed Laxfordian (Tarney, 1973), but they may well be the last stages of the Inverian event.

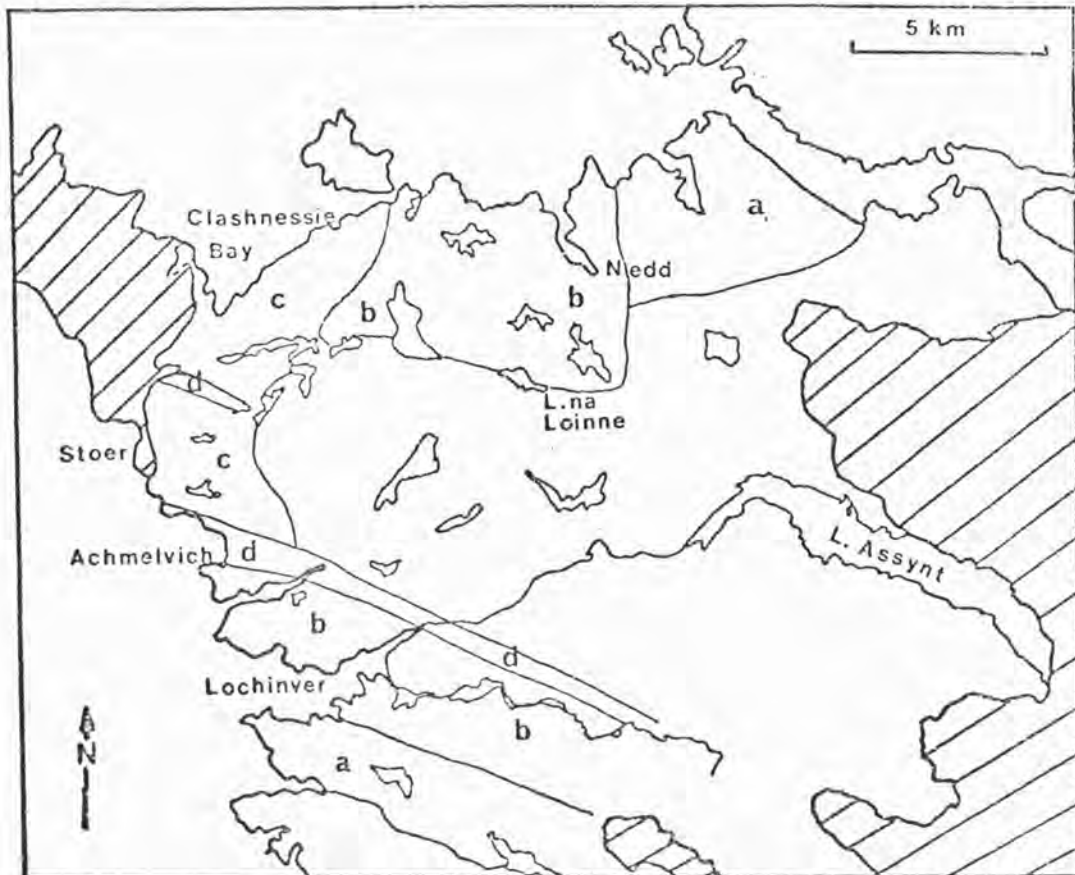


FIG. 1.3 Map of Assynt showing the structural divisions discussed in the text.



FIG. 1.4 Aeromagnetic anomalies over NW Scotland from Powell (1970). Contours are at 50 gamma intervals and magnetic lows are stippled. The Canisp shear zone and area of Inverian retrogression are marked by a significant low of more than -400 gamma. The coast line, where marked, is a thick line with cross hatching. CW- Cape Wrath, ST - Point of Stoer, To - Upper Loch Torridon, CF - Cromarty Firth, DF - Dornoch Firth.

The area of amphibolite facies retrogression (c and d above) shows up well as a magnetic low on the magnetic map of Powell (1970, Fig.1.4). The mineralogical and chemical changes brought about by the Inverian retrogression and Laxfordian shearing will be discussed in Chapter 5. The structure of the Assynt region can be simply described as a 10 - 12 km wide belt of amphibolite facies gneisses cutting granulites which is in turn cut by a 0.5 - 1.0 km wide shear zone.

### 1.3.1. Structures post-dating the main foliation

Due to the uniformity of structural trend from the onset of Inverian deformation to the Laxfordian it is often difficult to put structures in chronological order. Further deformation seems to tighten and steepen earlier folds. As mentioned above folds formed during or before the granulite facies metamorphism have flat axial planes while Inverian folds tend to have much steeper axial planes. A striking feature of Inverian deformation is its extreme heterogeneity; low strain zones where Scourian structures are preserved are very common. The following post-deformation structures can be recognised (Sheraton et al., 1973b):

(a) Open folds with NW trending axes plunging gently to the NW or SE. These folds are responsible for the variations in strike between Drumbeg and Kylesku. The wavelength of these folds ranges from 100 m to several kilometres. The main NW fold axes are shown in Fig.1.5. The axes of these folds tend to become more easterly and the folds become tighter as the Canisp shear zone is approached.

(b) Monoclinical folds with axial planes trending NE to N dipping either to the W or E. These folds are characterised by a steep short limb. This trend of fold is best developed in the area between Clashnessie and Drumbeg where N - NE strikes predominate (Sheraton et al., 1973b).

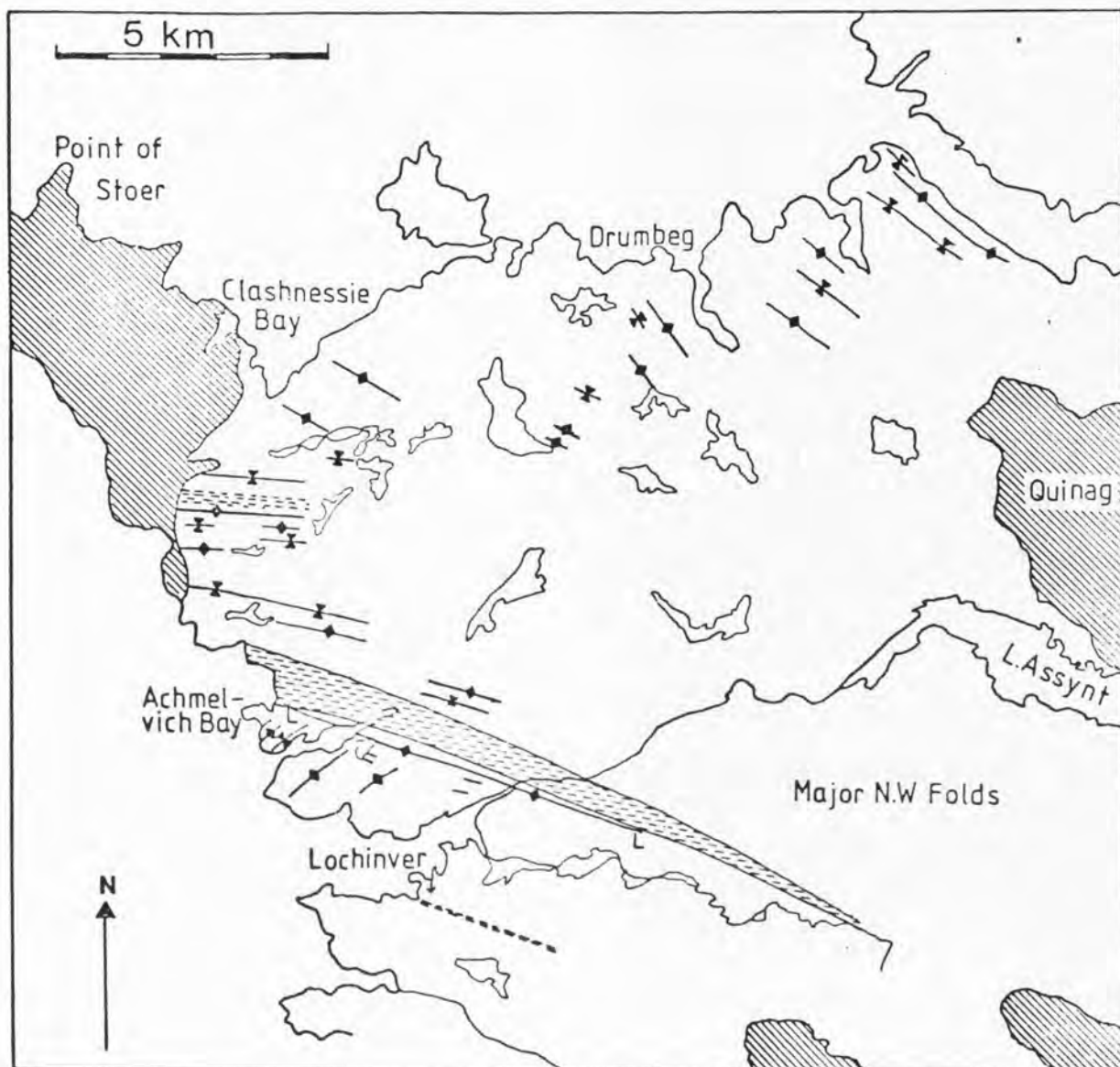


FIG. 1.5 Map of the Assynt area showing the approximate location of NW trending folds. Note that the folds become more easterly as the Glen Canisp shear zone is approached. Post Lewisian rocks are marked by cross hatching, the Glen Canisp shear zone by short dashes, the Stoer shear zone and the Strathan line are also marked. L - L is the Lochinver Antiform.

(c) Monoclinial folds with W to NW trending axes dipping either to the SW or NE. These folds are common throughout the area and are expressed as a series of steep belts. The steep limb of these folds may be attenuated but not to the same degree as in shear zones.

One of the problems in Assynt is the large number of minor folds which are not clearly related to any of these major structures. Around Clashnessie Bay there are numerous minor folds of extremely variable orientation (King, 1955).

(d) Shear zones trending ESE dipping at about  $70^\circ$  to the SSW. There is extreme attenuation, individual shears are rarely more than 25 m wide but wide shear belts such as the Canisp shear zone are composed of numerous small shear zones. Pre-existing Inverian steep belts clearly influenced the location of these Laxfordian shear zones.

(e) Brittle structures, i.e. faults and crush zones, are fairly common and affect all parts of the complex. The age of the structures is uncertain, some may be due to uplift before the deposition of the Torridonian but some faults are later than the intrusion of a suite of Caledonian alkaline dykes.

#### 1.3.2. The Lochinver Antiform

The Lochinver antiform is one of the major structures of the region (Sheraton et al., 1973b, Evans and Lambert, 1974). It can be traced eastwards from Achmelvich Bay for 8 km where it is cut by the Canisp shear zone. The southern limb dips gently SSW, extending as far south as Achiltibuie. The northern limb is more complex, it dips at about  $50^\circ$  to the NNE near the hinge but the dip then steepens. The northern limb is cut by the Canisp shear zone and near-vertical gneisses continue for 2 - 3 km northwards then more gentle NNE and NNW dips prevail. The axis of

the fold is nearly horizontal but it probably plunges very gently SE, the axial plane dipping about  $50^\circ$  to the SSW. It is difficult to decide whether the Lochinver antiform should be equated with the early NW open folds or with the WNW monoclinial folds. The present form resembles the WNW monoclinial folds but the northern limb of the Lochinver antiform is affected by a monoclinial fold (061247). It is possible that the Lochinver antiform is an open NW fold which has had the northern limb steepened by monoclinial folds and shear zones. However it is more likely that it is a monoclinial structure and there is more than one generation of monoclinial folds (Sheraton et al., 1973b). In Fig.1.6, the hinge zone in the region south of Loch Roe is seen to be a series of tight NW trending folds rather than a simple structure. The geology of this area is complicated by the presence of NE trending folds (Fig.1.6), these are affected by the Lochinver antiform and therefore predate it. These NE folds with a gentle SW plunge could be early Scourian in age.

### 1.3.3. The Canisp Shear Zone

The Canisp shear zone is a major structure of the region carefully mapped by Clough in Peach et al. (1907). This belt of highly deformed rocks extends eastwards from the coast, between Achmelvich and Clachtoll for 15 km where it reaches the Torridonian cover. The zone is up to 1 km wide in the west and thins eastwards. The zone is composed of numerous small shear zones which interlock in the manner described by Coward (1976) with low strain lenses in between. There is a new foliation and lineation, minor folds are ubiquitous and interference patterns are common. Most small shears indicate a downthrow to the SSW which is opposite to the sense of movement across the Lochinver antiform and Canisp shear zone as a whole. This indicates downthrow to the NNE bringing Inverian

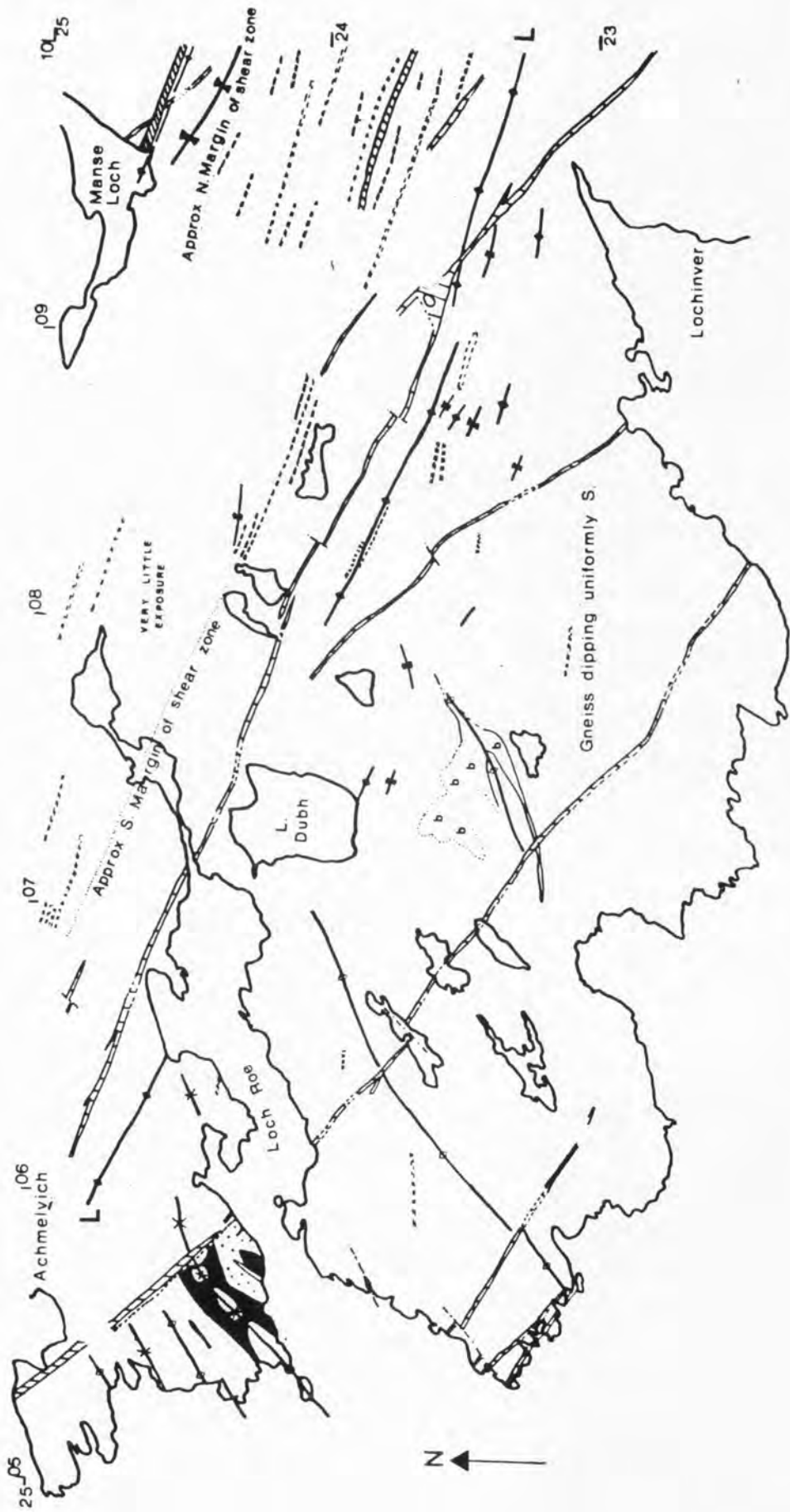


FIG. 1.6 Sketch map of the area between Achmelvich and Lochinver showing the Lochinver antiform L-L. Key as in Fig. 1.17, national grid numbers give the scale, a - mafic rock, early folds - open symbols, late folds - closed symbols.

amphibolites down to the same level as Scourian granulites, implying most of the vertical movement across this zone was Inverian and the shear zones are just a minor effect superimposed on the Inverian steep belt. Shear zones tend to follow pre-existing steep belts and the Canisp shear zone is also the locus for intrusion of ultramafic Scourie dykes (Tarney, 1973) which are rare elsewhere in the Lewisian complex. The shear zone will be discussed in detail in Chapter 7.

#### 1.4. ORIENTATION OF STRUCTURES IN THE ASSYNT REGION

##### 1.4.1. Foliation

In this section the range in strike of the foliation over the whole region will be examined. In the stereoplots all the foliations have been plotted, but no attempt to divide them into different ages has been made; however the diagrams show how the general structure changes from the south to the north of the area.

Fig.1.7 gives the contoured stereoplots for the Canisp shear zone, the area to the south and the northern margin of the shear zone. In the area to the south of the Lochinver antiform (area 1) the majority of points dip south at a low to moderate angle with a few vertical gneisses from ESE shear zones and the Strathan Bay fold. In area 2, which is south of the shear belt and includes the Lochinver antiform, the majority of gneisses still dip to the south but there is a significant clustering of northerly-dipping gneisses reflecting the influence of minor folds in the hinge zone of the Lochinver antiform (Fig.1.6). In the area around Achmelvich (area 3) the gneisses are folded around SW plunging folds (Fig. 1.6). In the Canisp shear zone (areas 4, 5 and 6) the gneisses are predominantly vertical or dipping very steeply to the south. There are a few more gentle dips from low strain zones. Along the northern margin of

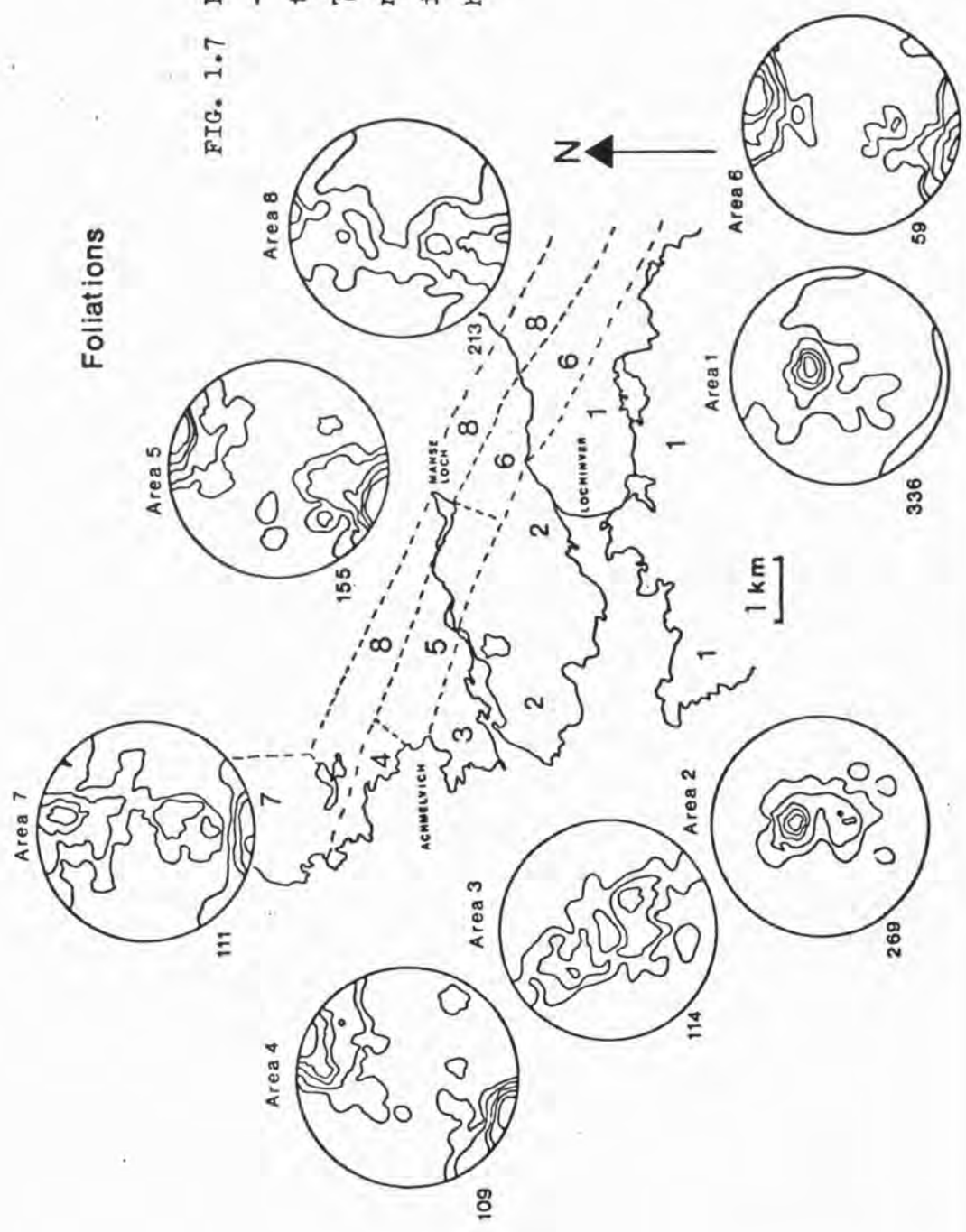


FIG. 1.7 Foliations in the Lochinver-Achmelvich area. Contours on the stereoplots are at 0, 2, 7, 11 and 20% intervals. The number of points in each plot is indicated in the bottom left hand corner of the circle.

Foliations

the shear zone (areas 7 and 8) there is still a large number of near-vertical gneisses, but there is a range in orientation of more gently dipping gneisses indicating folding around westerly-plunging axes. These plots indicate that the southern margin of the shear zone is sharp whereas the northern margin is diffuse.

In Fig.1.8, the stereoplots for the Clachtoll - Stoer - Clashnessie area are given. In the southern part of the map (areas 9, 10, 11 and 12) the vertical gneisses are still abundant with the more gently dipping gneisses folded by E - W folds. The vertical gneisses come from Inverian steep belts and Laxfordian shear zones. The structure around Clashnessie Bay is quite complex with two main elements; gneiss folded by WNW folds with WNW steep belts and N to NE striking steep belts (areas 14 and 17) where the dips are to the east ranging from  $20^{\circ}$  to vertical. In area 16 both the NNE steep belts and WNW folds are evident. Fig.1.9 shows the plots for the area east of Clashnessie. In areas 18 and 19 between Garbh Loch Mor and Loch Poll the foliations are so variable that there are almost no contours on the stereo plot. To the south and east of Drumbeg the gneisses are folded about gently plunging WNW folds with a few ESE shear zones and WNW monoclinial steep belts. In area 22 (which includes the Drumbeg body) the fold has a more north-westerly plunge. As one goes east, the number of steep belts decreases markedly and in the extreme east of the map the strike is predominantly 070, dipping either to the north or the south.

These diagrams show very clearly the Inverian belt with its WNW steep structures cutting across the more gently dipping Scourian gneisses.

#### 1.4.2. Lineations

As mentioned previously, lineations are only patchily developed. The early lineation is characteristically caused by quartz rodding; the

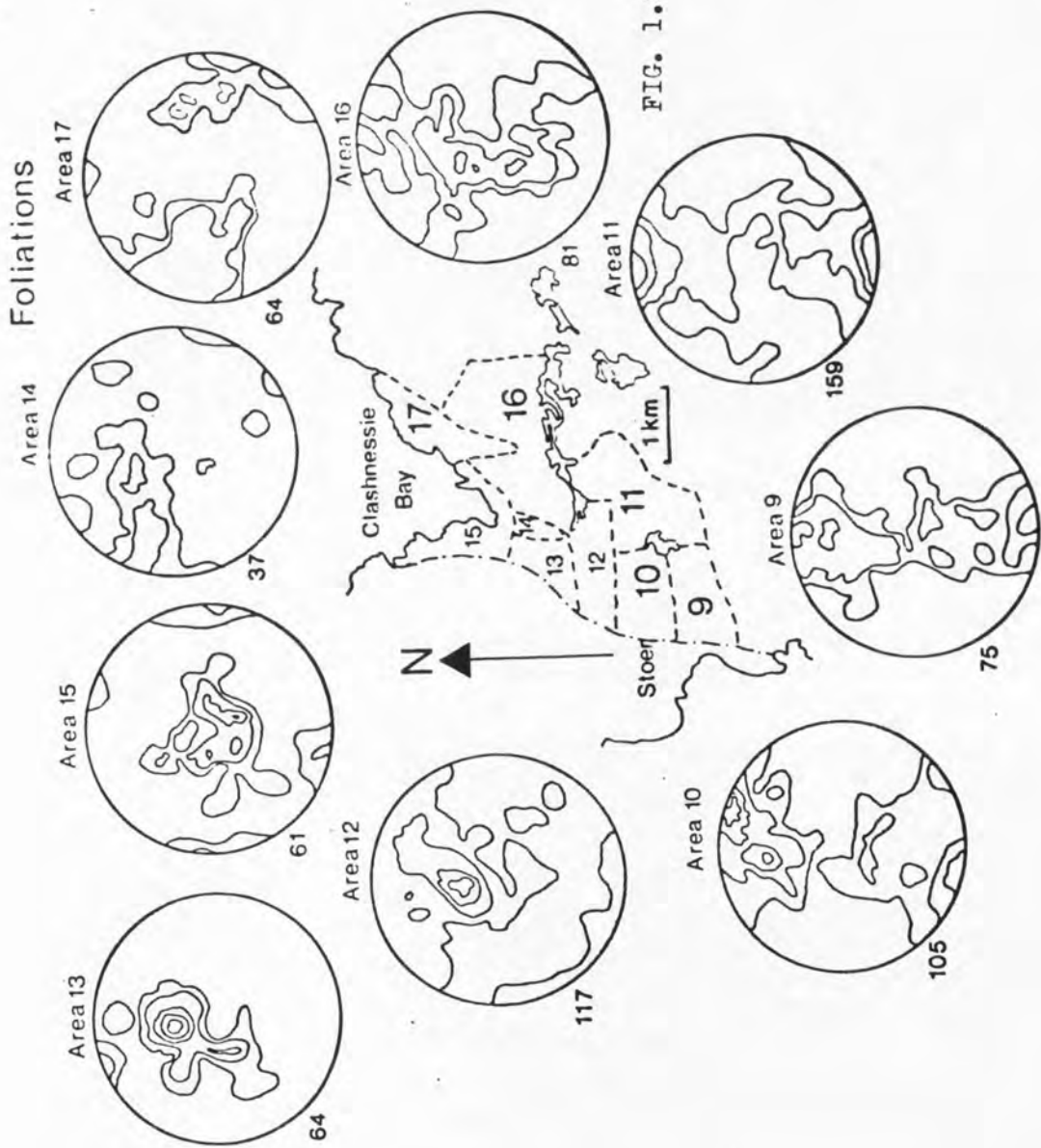


FIG. 1.8 Foliations in the Stoer-Clashnessie area; as FIG 1.7.

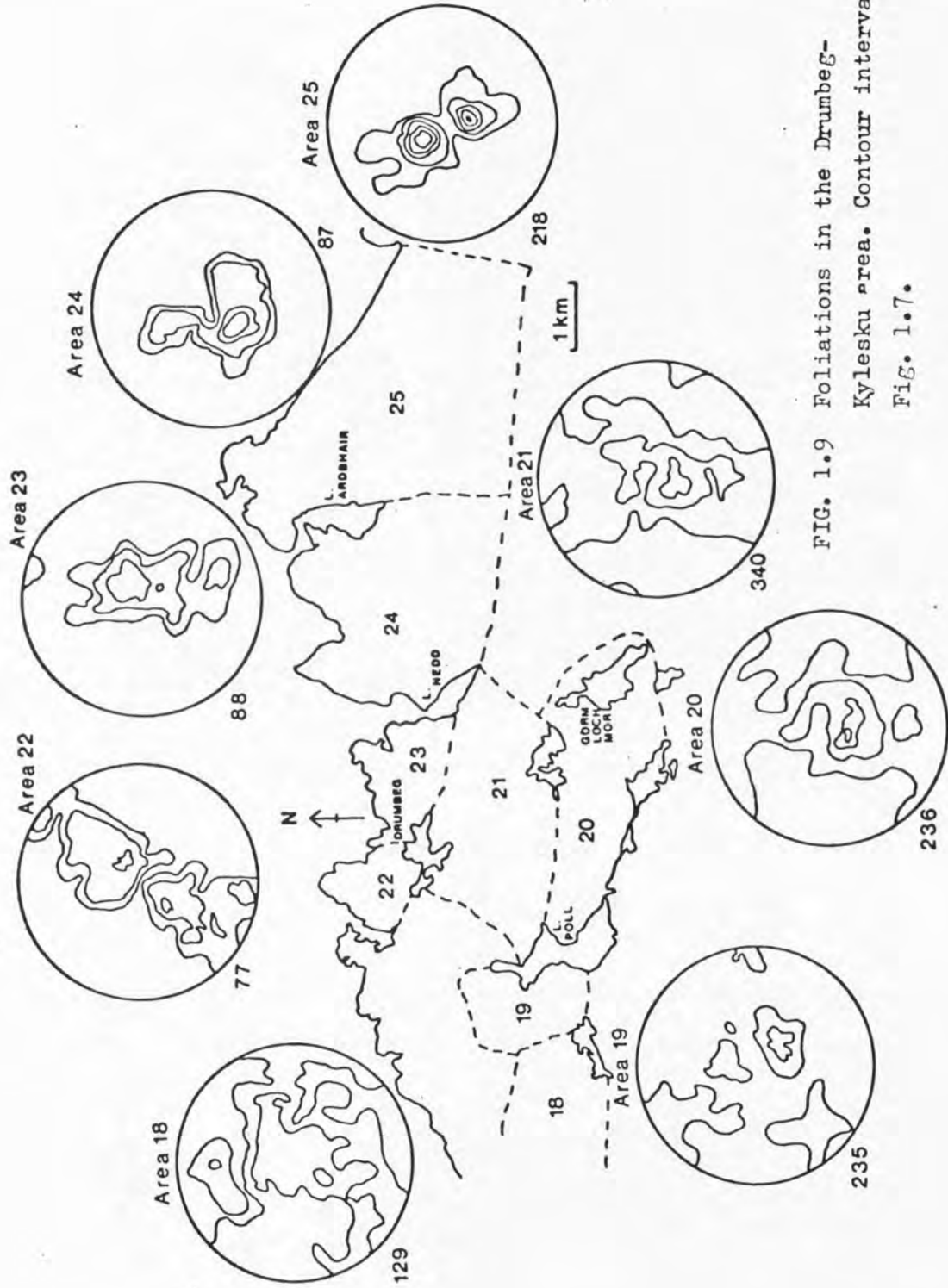


FIG. 1.9 Foliations in the Drumbeg-Kylesku area. Contour intervals as FIG. 1.7.

hornblendes in the layered ultramafics also tend to be aligned parallel to the same direction. In the Laxfordian shear zones there is a new penetrative lineation plunging at low angles (20 - 30°) to the ESE. This lineation results from the transposition of the coarse banding and mineral alignment of the old foliation onto the new foliation surface. In contrast Inverian monoclinial steep belts have no associated lineation. The early lineation is best preserved in regions where there is only a minor amount of Inverian deformation and is only found locally elsewhere. The age of the lineation is not at all certain. It is often parallel to the axes of intrafolial folds but this may not be significant. The plunge of the lineation varies over the region, due in part to folding around open NW folds and WNW monoclinial steep belts. The orientation of the lineation, where preserved, is more variable in the steep limbs of monoclinial folds.

In Fig.1.10 the lineations over the whole area studied by the author are plotted on contoured stereoplots. In the northeast the lineations plunge to the NW (centre of cluster 320/17°) with a few plunging to the SE. As one goes west to Drumbeg the distribution becomes bimodal, with plunges to the NW (centre of cluster 335/22°) and the SE (135/15°). Around Clashnessie SE lineations predominate (155/20°) but there are a few NW plunges (335/20°). On the west side of Clashnessie Bay the lineations change from a SE to a NW plunge as the gneisses are folded by a minor WNW fold, implying that this coarse lineation is Scourian. In the Clachtoll-Stoer area the lineations plunge in a variety of directions. Most lineations still plunge to the SE (155/25°) but there are a number of ESE plunges, some of which are from shear zones but some have been rotated. There are a few steep plunges especially in complex areas; again the early lineation has been affected by Inverian structures.

In the main shear zone (area 2, Fig.1.10) the lineations consistently plunge to the ESE (110/30°). South of the shear belt the majority of lineations plunge due south.

#### 1.4.3. Minor fold axes

Minor folds of several generations occur throughout the region. It is difficult to put the folds in chronological order as the different phases of folding tend to have approximately the same orientation. The similarity in style and orientation of folds of different ages places considerable doubt on the structural interpretation of Hopgood and Bowes (1972). It is also often difficult to measure the fold axes accurately due to the smooth glaciated outcrops.

In Fig.1.11, all minor fold axes have been plotted on contoured stereoplots. In the northeast (area 6) there are relatively few minor folds and these are mostly intrafolial isoclinal folds but a few WNW monoclines occur. The fold axes plunge mainly to the NW and SE, as do the lineations. Similarly, in the area around Drumbeg most minor fold axes plunge to the NW or SE with a few NE plunges. In area 7, between Clashnessie and Loch Poll, folds plunge in a variety of directions, with four clusters, NE, SE, S and SW. Around Clashnessie Bay (area 4) there are large numbers of minor folds (King, 1955) which plunge in all directions except WNW. There are three main clusters, plunging to the NNE ( $350 - 030^\circ$ ), NE ( $040 - 065^\circ$ ) and SSE ( $155 - 170^\circ$ ) but other directions also occur. In the Stoer - Clachtoll area the dominant plunge is to the SE with a few to the WNW, SSE and NE. Similarly in the shear zone the dominant plunge is to the ESE. In these two areas there are some steep plunges ( $60 - 70^\circ$ ) which are not found elsewhere; these may be folds which have been rotated and steepened by later deformation. South of the shear zone the plunge of fold axes is to the SSW with a few easterly and westerly plunges.

In general, except for the NE folds near Clashnessie, the plunge of minor folds parallels the lineations. The NE folds are presumably related to the NNE steep belts in the Clashnessie - Drumbeg area.

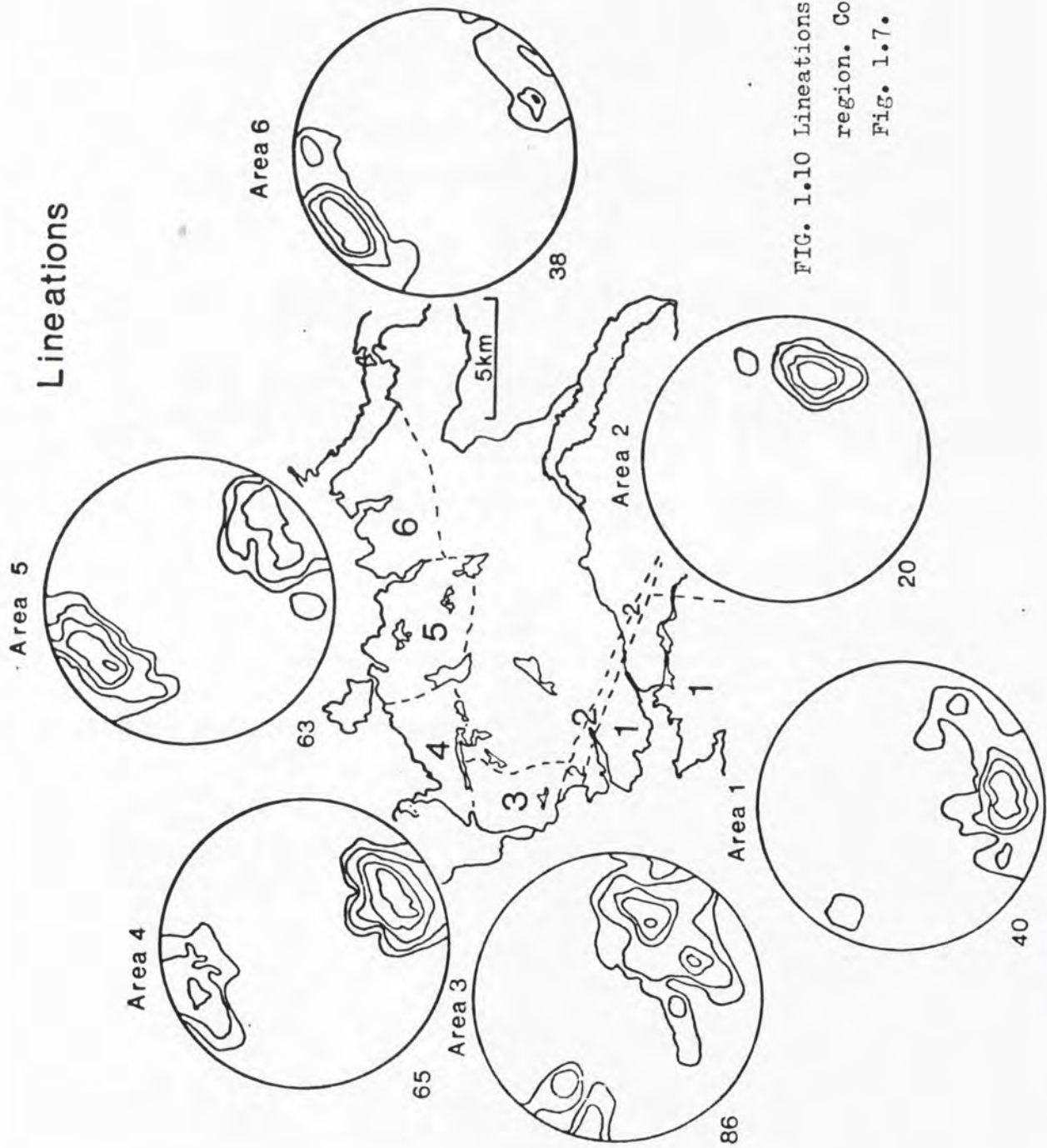


FIG. 1.10 Lineations for the whole Assynt region. Contour intervals as Fig. 1.7.

# Fold Axes

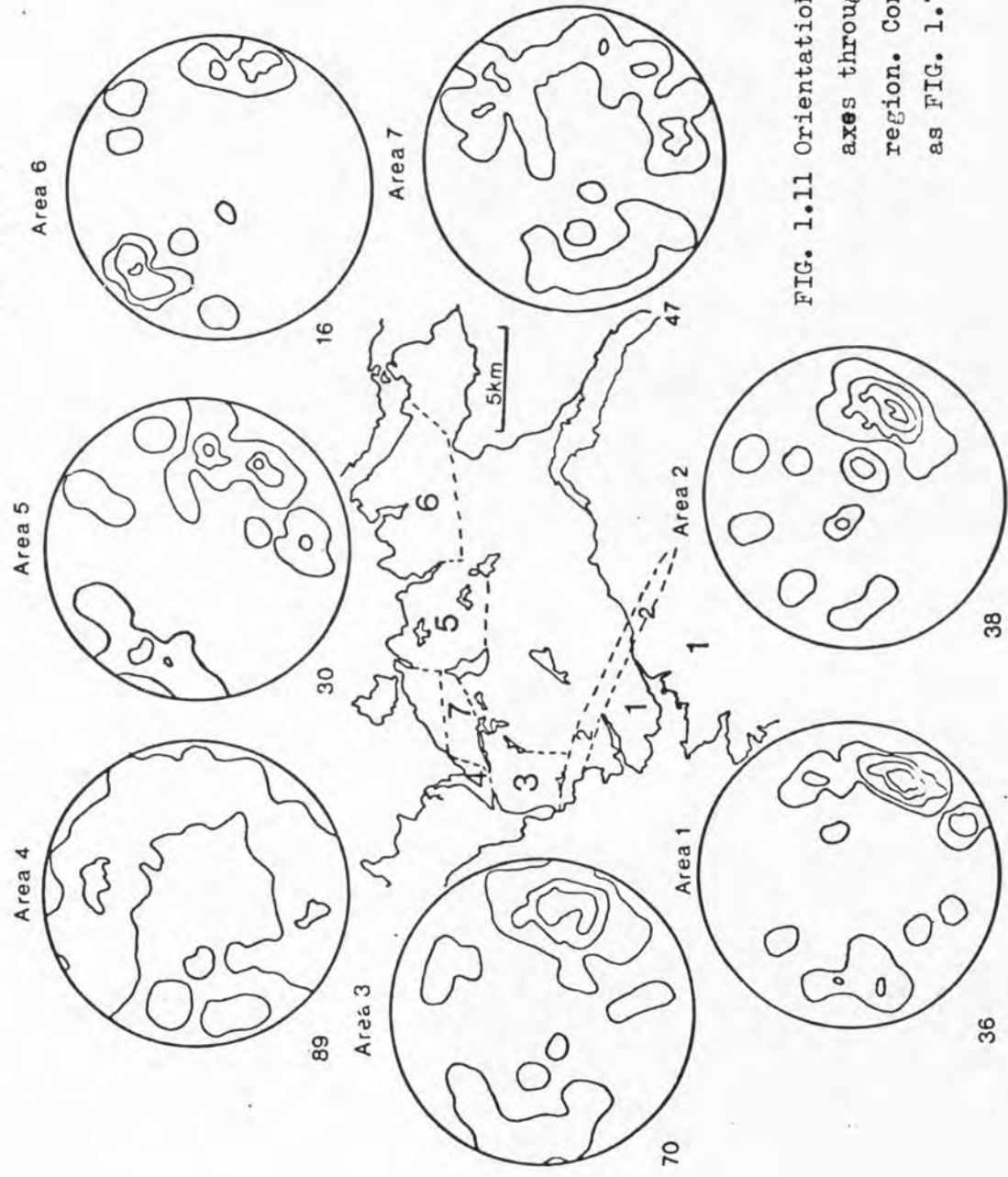


FIG. 1.11 Orientation of minor fold axes throughout the Assynt region. Contour intervals as FIG. 1.7.

## 1.5. FOLDS

Early Scourian folds: The large amount of Inverian deformation in the Assynt region has obscured most of the evidence for Scourian structures. The layered ultramafic-gabbro bodies such as Culag and Drumbeg sometimes have repeated ultramafic-gabbro successions which could be caused by isoclinal folding. On Scouriemore, near Scourie, where the effects of Inverian deformation are slight, the Camas nam Buth mafic body is clearly folded around an early Scourian isoclinal fold so that the base of the original body is now in the centre (Savage 1979).

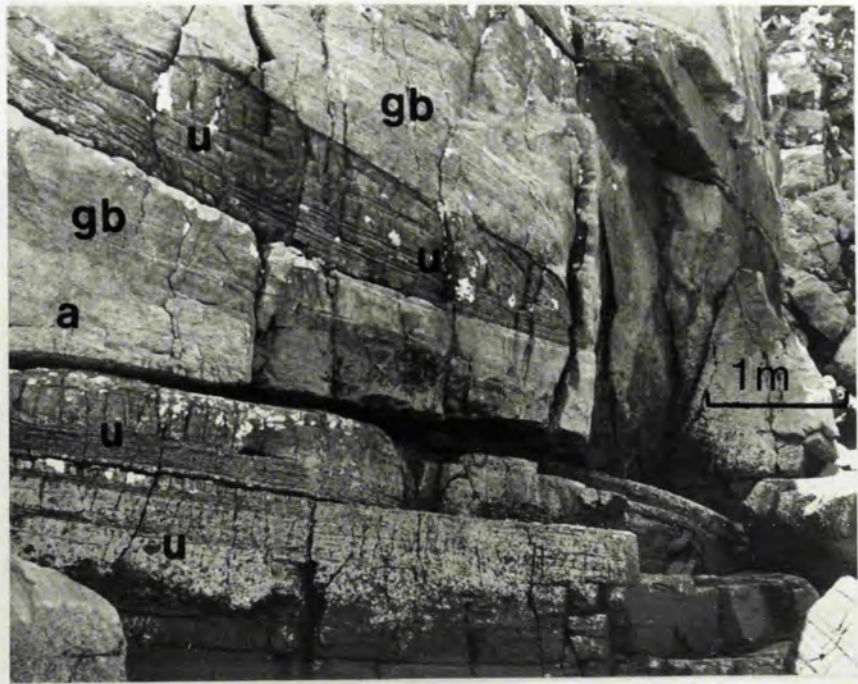
The most obvious Scourian structures in Assynt, apart from the foliation and lineation, are the intrafolial folds. These are folds with their limbs completely enclosed within thicker banded units; they are either tight or isoclinal (Fig.1.1a,b; Fig.1.13a,b) and their axial planes are sub-parallel to the regional foliation. The interlimb angles are usually less than  $30^\circ$  and rootless closures are common. In Fig.1.12a there is a larger intrafolial fold where layered ultramafic is infolded into gabbro. Thin felsic veins in the gabbro are highly folded.

Inverian folds: A brief description of the main types of Inverian fold has already been made; a more detailed discussion follows. The earliest Inverian structures are the open NW trending folds; occasional "arch" like folds could be small scale equivalents of these. The most characteristic Inverian structures are the WNW trending monoclines which occur on a variety of scales, the steep limbs ranging in size from a few centimetres to structures the size of the Lochinver antiform. In Fig.1.12c gently southerly-dipping gneiss is deflected into a WNW trending steep belt. The axial plane of this fold dips N with a downthrow to the SSW, but folds with a downthrow to the NNE are more common (e.g. the Lochinver antiform). The gneisses in the steep belts are always retrogressed to amphibolite

FIG. 1.12 (a) Fold in ultramafic-gabbro body at Poll Loisgann (067165) described by Bowes et al.(1964).  
u - ultramafic, gb - gabbro, a- trondjemite sheet.  
The ultramafic is folded into the gabbro which contains highly folded felsic veins.

(b) Fold from Clashnessie Bay. This fold has a gently dipping axial plane but is Inverian in age, clearly folding the main foliation.

(c) Monoclinial fold from Drumbeg harbour (121331). The foliation which dips at moderate angle to the south is folded into this steep belt which trends WNW. There is some attenuation of the steep limb.



facies even when they cut granulite facies gneisses (e.g. near Scourie) and these monoclines are thought to act as a route for water causing the retrogression. The steep limb may be attenuated but more commonly the banding becomes more marked and there is slight boudinage (pinch and swell) of mafic and ultramafic layers.

There is no lineation associated with these folds but occasionally the early lineation is folded around the hinge with a more variable orientation in the steep limb. The simplest of these structures (e.g. Fig.1.14a) are almost concentric and were probably initiated by buckling. Subsequent flattening caused the folds to tighten producing folds such as Fig.1.13g and h.

Many minor folds which clearly post-date the main foliation are not monoclines and their affinity is not certain. This type of fold, which can vary from S or Z folds (Fig.1.12b) to isoclinal folds, is very common especially in the Clashnessie area. They have a variety of orientations but commonly trend N to NE, and refolded folds are also abundant. They could be related to the NNE steep belts and have been affected by subsequent WNW folding. The NNE steep belts are also monoclinical in form and have axial planes dipping either to the west or east. Where NNE and WNW steep belts interfere, the structure becomes very complex and it is not at all clear which structure is the earlier. It is possible that they are simultaneous, but in general the NNE steep belts seem to be earlier. Fig.1.13 illustrates a range of Inverian fold styles, the tighter folds (h,i and j) monoclines that have been further deformed. A weak axial planar fabric may develop defined by the alignment of biotite crystals. Fig.1.14 shows a range of folds from Clashnessie Bay.

Shear zone folds: Similar style shear folds in the finely banded shear zones are ubiquitous. Laxfordian folds have their axes parallel to the

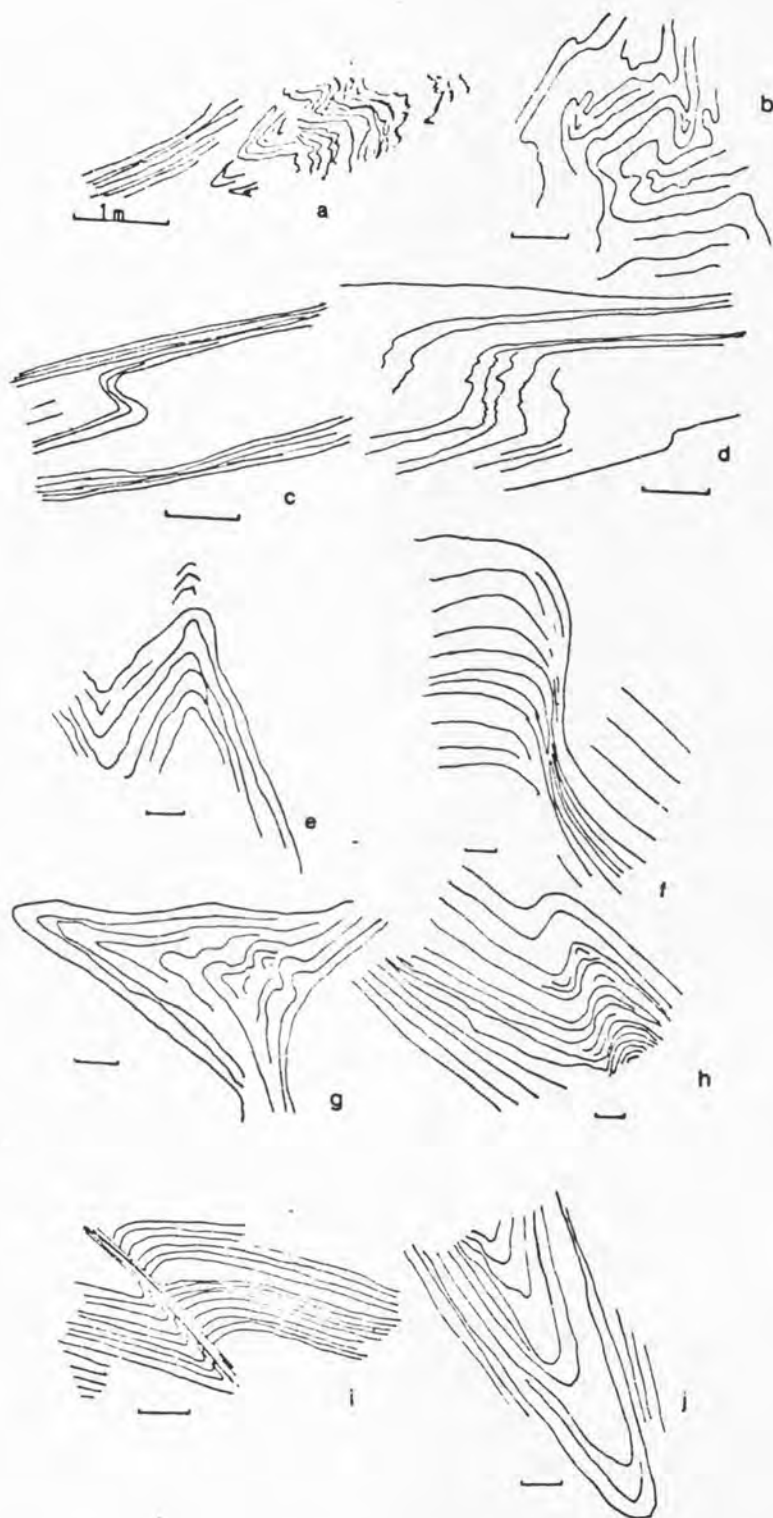


FIG. 1.13 Minor folds with a variety of styles. The scale bar is 10 cm unless otherwise indicated. a- plastic folds from near Drumbeg (129326), b- complex folds from shear zone margin (076255), c- monoclinial fold (126325), d- monoclinial fold (131322), e- steeply plunging isocline near Clachtoll (045272), f- monocline with attenuated vertical limb (123304), g- interference fold (128434), h- tightened monocline (126325), i- fold with shear zone along axial plane (126325), j- isoclinal fold with steeply dipping axial plane near Stoer (042287).

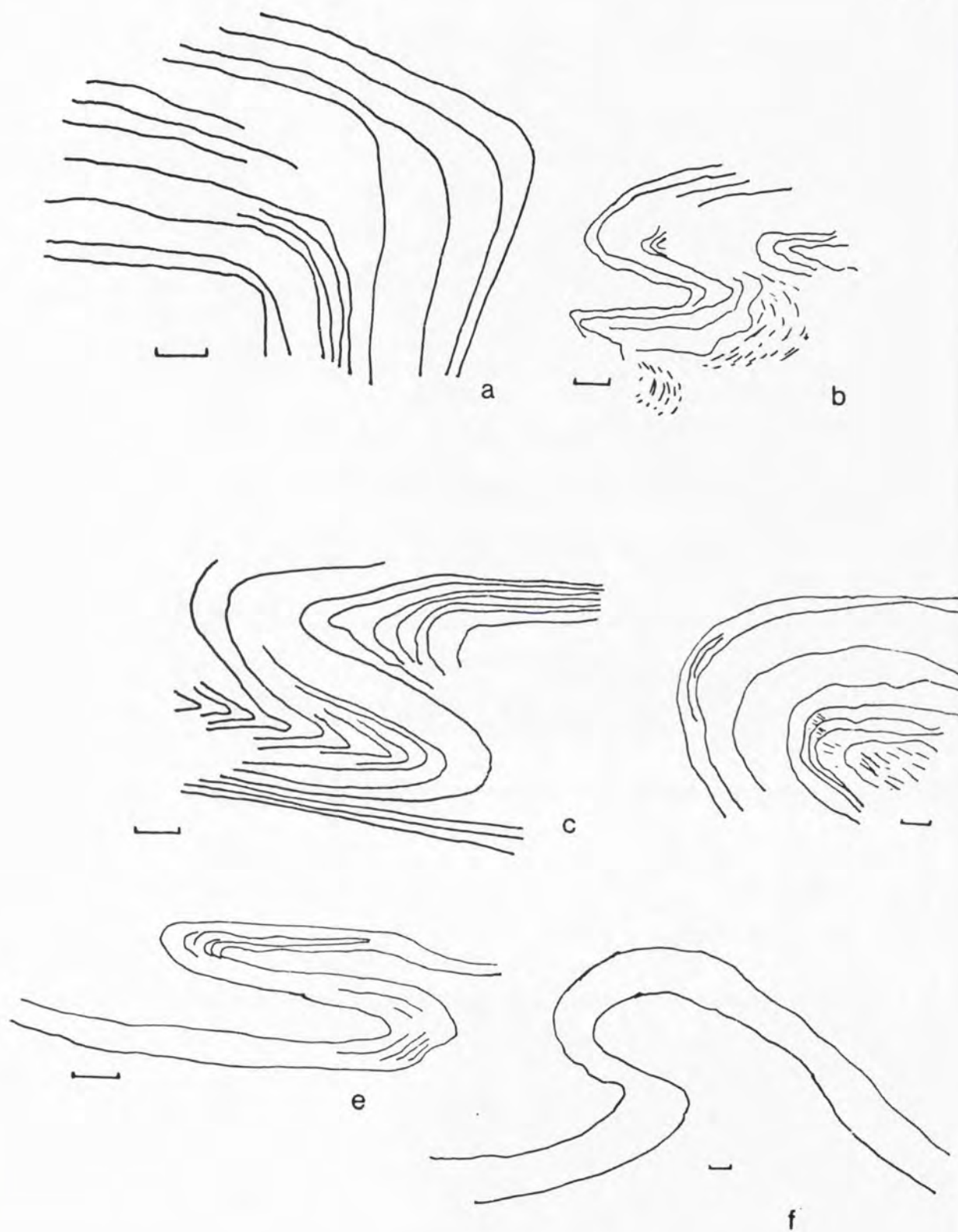


FIG. 1.14 Variety of styles of Fold from Clashnessie Bay. Scale bar is 10 cm.





**a**



**b**

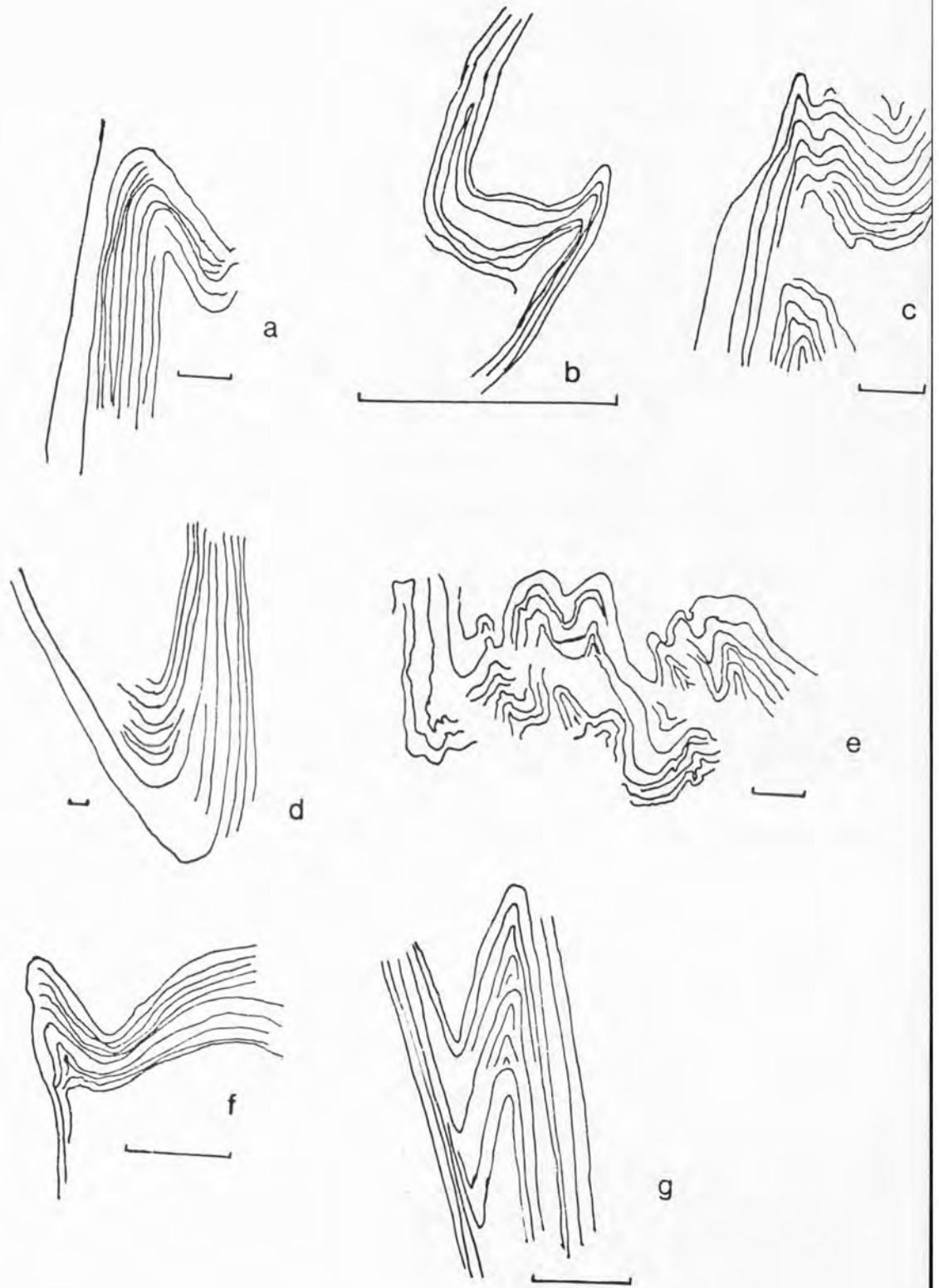


FIG. 1.16 Sketches of folds from the Canisp shear zone.  
Scale bar is 10cm.

lineation and their axial planes approach the plane of the foliation. Interference patterns indicate more than one phase of Laxfordian folding. Rotated Scourian and Inverian folds show more scatter, but they tend towards the same orientation as the Laxfordian folds. Figs. 1.15 and 1.16 show typical shear zone folds.

#### 1.6. DESCRIPTION OF THE FOUR STRUCTURAL DIVISIONS

In Section 1.3 the Assynt region was divided into four structural divisions; sketch maps of these areas and a more detailed discussion follow.

##### 1.6.1. Granulite facies areas

In the NE and S of the area (a in Fig.1.3) the effects of Inverian deformation are slight. The area between L.Nedd and Rientraid (Fig.1.17) is mainly composed of gneisses dipping to the NE. Mafic rocks proved useful markers; they can be followed along strike for considerable distances and are clearly folded around open NW trending folds axes. The variation in strike of the gneisses can be accounted for by folding around axes which plunge either to the NW or the SE.

To the SE of L.Ardhair there are a few WNW monoclinial folds and in this region the open folds have been tightened with rapid changes in the direction of dip. A Scourie dyke clearly cuts a NW trending fold axis (Fig.1.17). Shear zones are rare in this region but the ultramafic dyke extending along Glenn Ardbhair has a shear zone parallel to its margin.

There is a lot of mafic rock in this area, some of which is at granulite facies (opx-cpx-gt-plag), the rest being at amphibolite facies (plag-amph ± ep). A small amount of layered ultramafic occurs at (206301), suggesting that all the mafic rocks belong to layered complexes of the type discussed in Chapters 2 and 3.

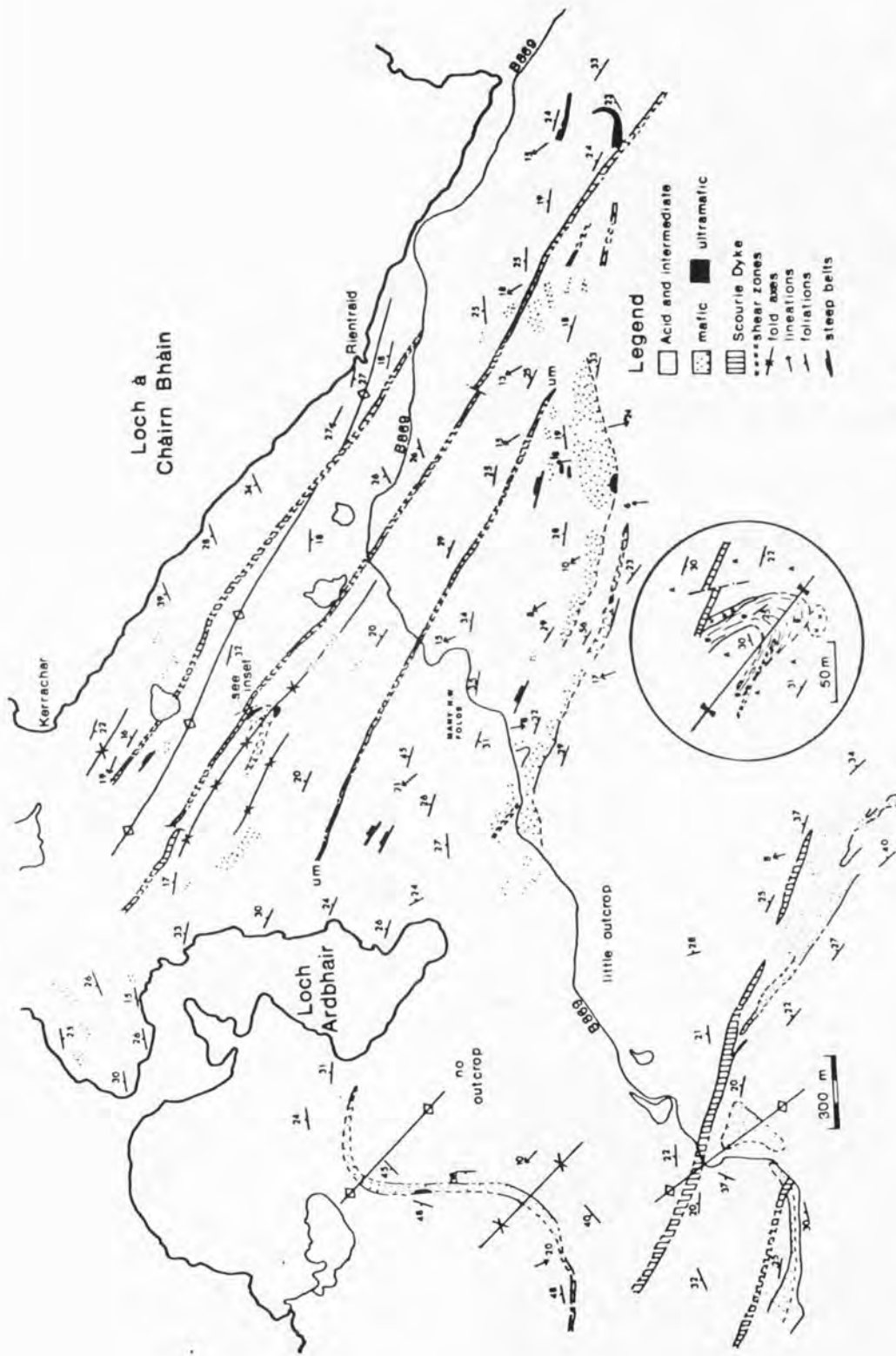


FIG.1.17 Sketch map of the area near L. Ardbhair. Inset shows a small area where mafic rocks are folded; G- gabbro, u- ultramafic, a- acid gneiss, um- ultramafic Scourie dyke.

### 1.6.2. Areas with some Inverian deformation

The areas around Drumbeg and Lochinver are intermediate with some Inverian deformation (areas b, Fig.1.3). A sketch map of the area south of Lochinver is given in Fig.1.18. This is part of the gently-dipping southern limb of the Lochinver antiform. To the south of the Strathan line (Fig.1.18) granulite facies assemblages are found locally, even in acid gneisses. In the area shown in Fig.1.18 both granulite and amphibolite facies mafic rocks occur, but the acid and intermediate rocks are at amphibolite facies. The main structure, marked by mafic rocks, has been termed the Strathan Bay structure (Evans and Lambert, 1974). South of Lochinver the gneiss generally strikes approximately E-W, but near Strathan it swings into a N-S vertical belt and then back to E-W again. This structure is cut off to the south by the Strathan line, a Laxfordian shear zone. In the west of the map area (Fig.1.18) there are some E-W trending folds which appear to be cut by the Strathan Bay structure. Evans and Lambert (1974) state that this type of structure is Badcallian (early Scourian) in age, but if the E-W folds cut by the structure are equivalent to similar folds further north, it must be Inverian in age. The Strathan Bay fold can probably be correlated with the NNE steep belts common near Clashnessie. A stereoplot of foliations (Fig.1.18) suggests folding around a southerly plunging axis ( $180/30^\circ$ ). This is a common lineation direction in the area (Fig. 1.10), but rare elsewhere in Assynt, so the lineation may be related to these structures.

The Culag body (see Chapter 2) crops out in the east of the map area (Fig.1.18). The repeated ultramafic-gabbro succession suggests folding around an early isocline, the axis of which now trends NW. The Culag body is at granulite facies whilst the mafic rocks in the Strathan

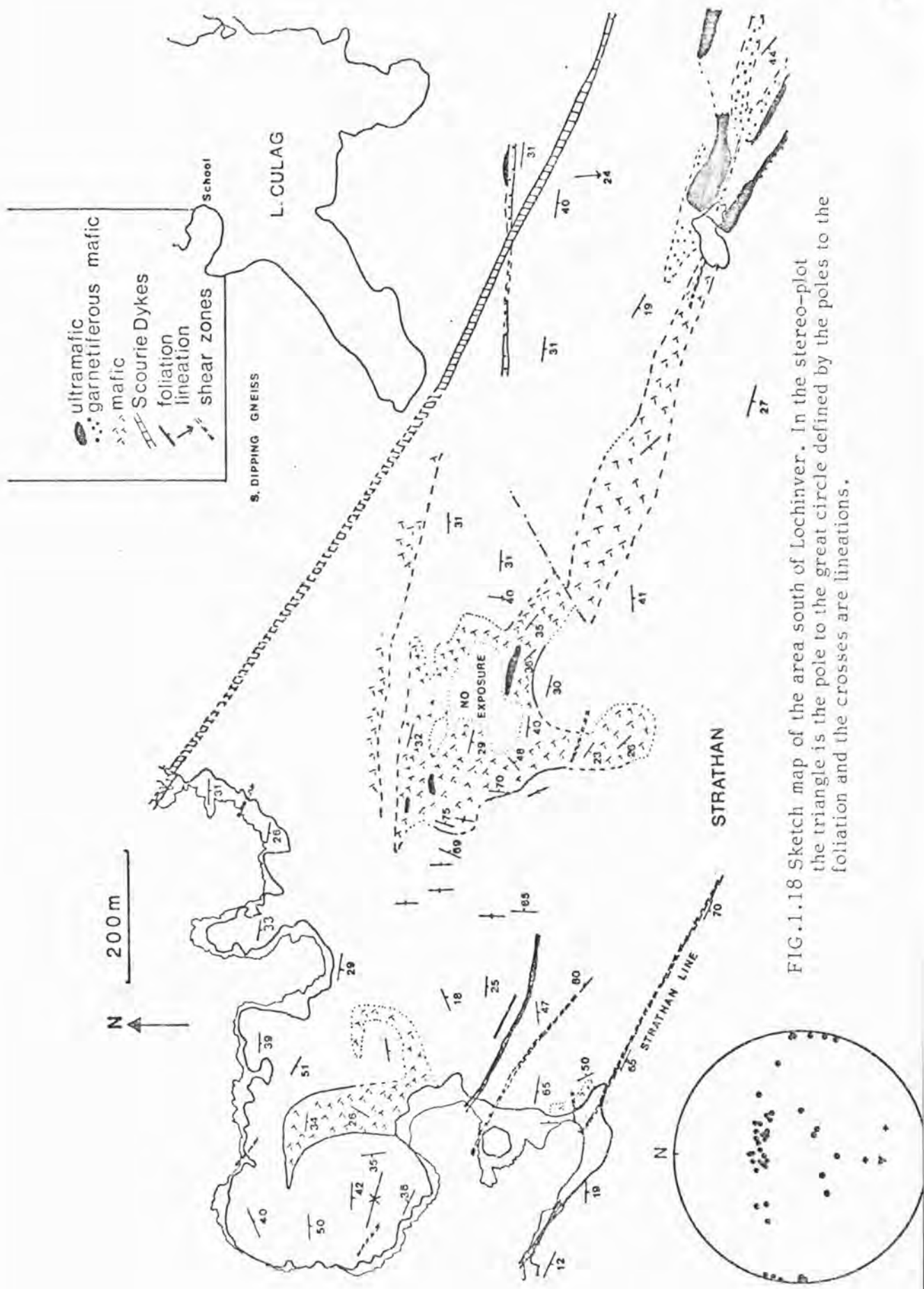


FIG. 1.18 Sketch map of the area south of Lochinver. In the stereo-plot the triangle is the pole to the great circle defined by the poles to the foliation and the crosses are lineations.

fold are at amphibolite facies, but rare remnants of granulite facies assemblages occur. It is thought that this mafic material is equivalent to the gabbros of the layered complexes and the retrogression to amphibolite facies is associated with the Strathan fold; further indication that the structure is Inverian.

There is a typical Laxfordian shear zone, the Strathan line (Evans and Lambert, 1974) which cuts the Strathan Bay fold. The Strathan line is monoclinial in form and there was probably originally a WNW monocline which was then the site for Laxfordian shearing.

Another area where Inverian deformation is only moderate is near Drumbeg; a sketch map of the area between Loch Poll and Gorm Loch Mor is given in Fig.1.19. A map of the Drumbeg area can be found in Sheraton (1969). The simple structure of this area is again emphasised by mafic and ultramafic bands. The Loch Poll body (see Chapter 2) crops out in the west of the area dipping gently to the NNE. Small outcrops of mafic rock can be followed along strike from the Loch Poll body to Loch na Loinne. Further east a band of ultramafic and gabbroic rocks can be followed from Loch Torr nam Uidhean to east of Gorm Loch Mor. This suggests folding about a NW-trending synform (not marked on the map). The detail, as can be seen from the sketch map, is much more complex with many NW trending folds, especially in the core of the major synform. The strike is further complicated by WNW steep belts.

### 1.6.3. Areas with a large amount of Inverian deformation

Clashnessie Bay. The structure of the area around Clashnessie Bay is fairly complex with NW trending folds, WNW and NNE trending steep belts and numerous minor folds which have a range of orientations.

On the west side of Clashnessie Bay amphibolite facies mafic rocks at Reidh Phort are interfolded with intermediate gneiss in tight E - W

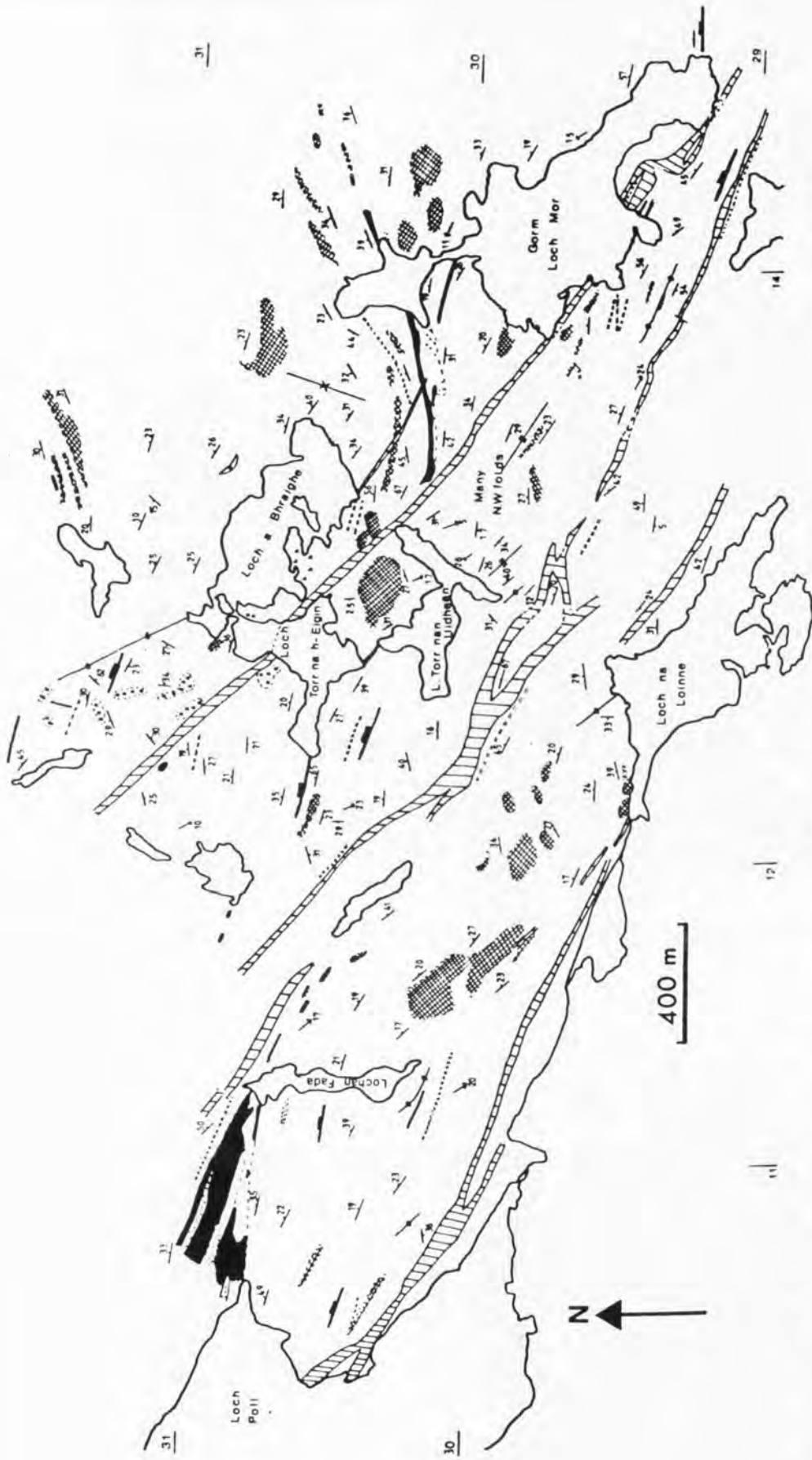


FIG. 1.19 Sketch map of the area between Loch Poll and Gorm Loch Mor. Key as in Fig. 1.17 with a= agmatite, h= hornblende and cross hatching-amphibolite facies mafic rock.

trending early folds, perhaps Scourian in age (Sheraton et al., 1973b, Fig.2). Fig.1.20, a sketch map of the Clashnessie Bay area, shows the extreme variability of the strike of the foliation and the simplified structure is shown in a diagrammatic sketch map, Fig.1.21. Open NW folds are clearly cut by the NNE steep belts. Where these two types of structure interfere, e.g. NW of Garbh Loch Mor, the foliation is extremely variable. There is very little mafic rock in this area to help map out major structures. In the NNE steep belts the early lineation plunges either to the N or S (it plunges NW or SE elsewhere).

Stoer-Clachtoll area: As one goes south towards the shear zone the gneisses become more deformed (Fig.1.22). A detailed map of the southern part of the area in Fig.1.22 is given in Tarney (1978) and a more detailed map of the NE corner is presented in Chapter 4. There are numerous monoclinial steep belts, commonly about 100 m wide, producing vertical dipping gneisses which are not attenuated. Between these steep belts the gneisses dip at moderate angles ( $40 - 60^\circ$ ) either to the N or S, reflecting E - W folds, which have been cut by the monoclines. Small areas, e.g. to the west of Loch Poll an Droighinn and (051289) and Cnoc an Sgriodaich (062296) are further complicated by the presence of N to NNE vertical structures resembling the Strathan Bay fold. Unfortunately the large number of Laxfordian shear zones and gaps in exposure make it very difficult to sort out the structures properly. In these N to NNE trending areas, the lineation, if present, may plunge quite steeply. There are many small shear zones, particularly near Stoer village (the Stoer shear zone of Beach, 1974). The shear zone foliation dips at about  $70^\circ$  to the south, while the Inverian steep belts are often vertical.

The shear zone (area d, Fig.1.3) will be discussed in Chapter 7.

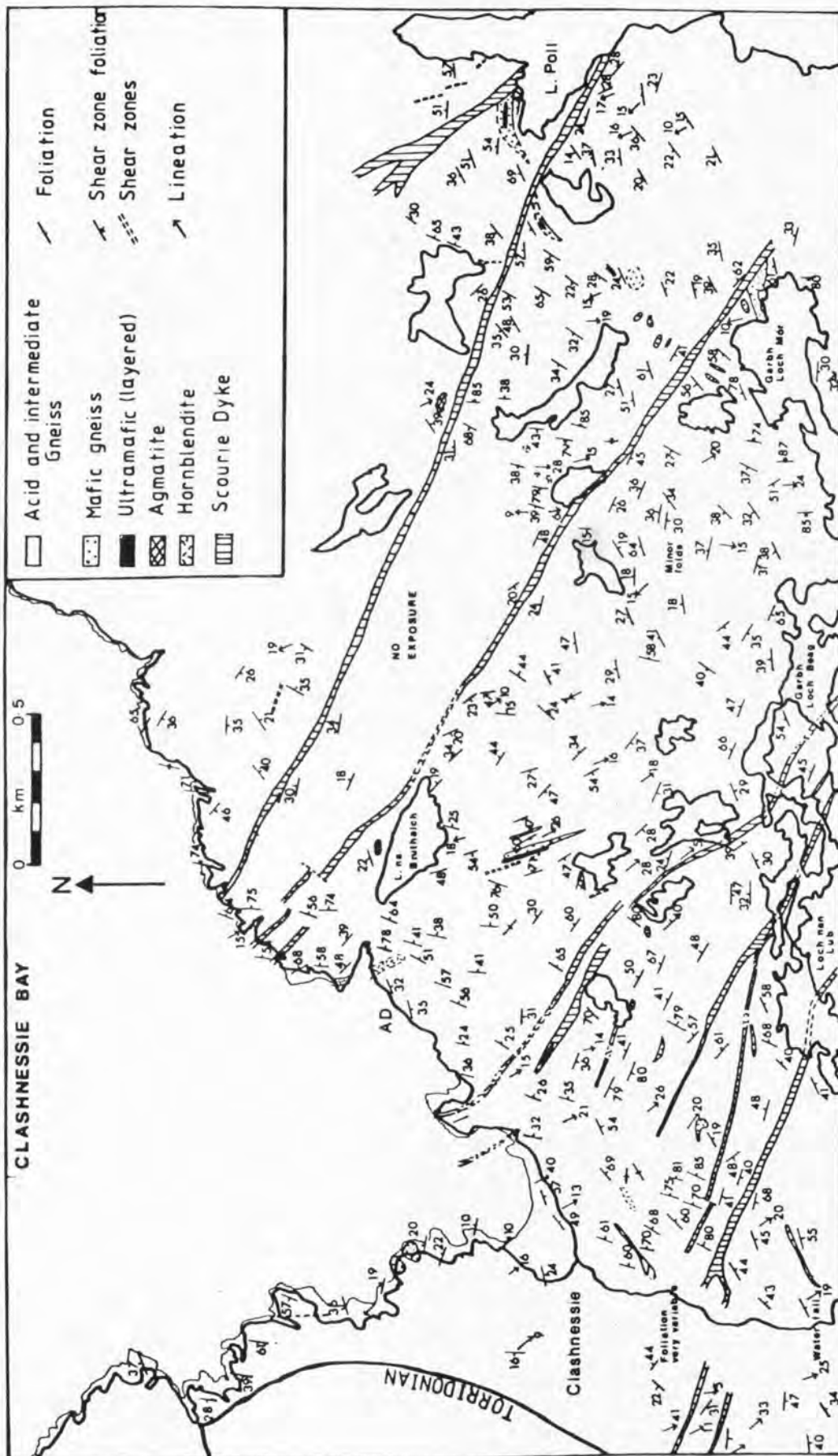


FIG. 1.20 Sketch map of the area around Clashnessie Bay showing the variable strike of the foliation.

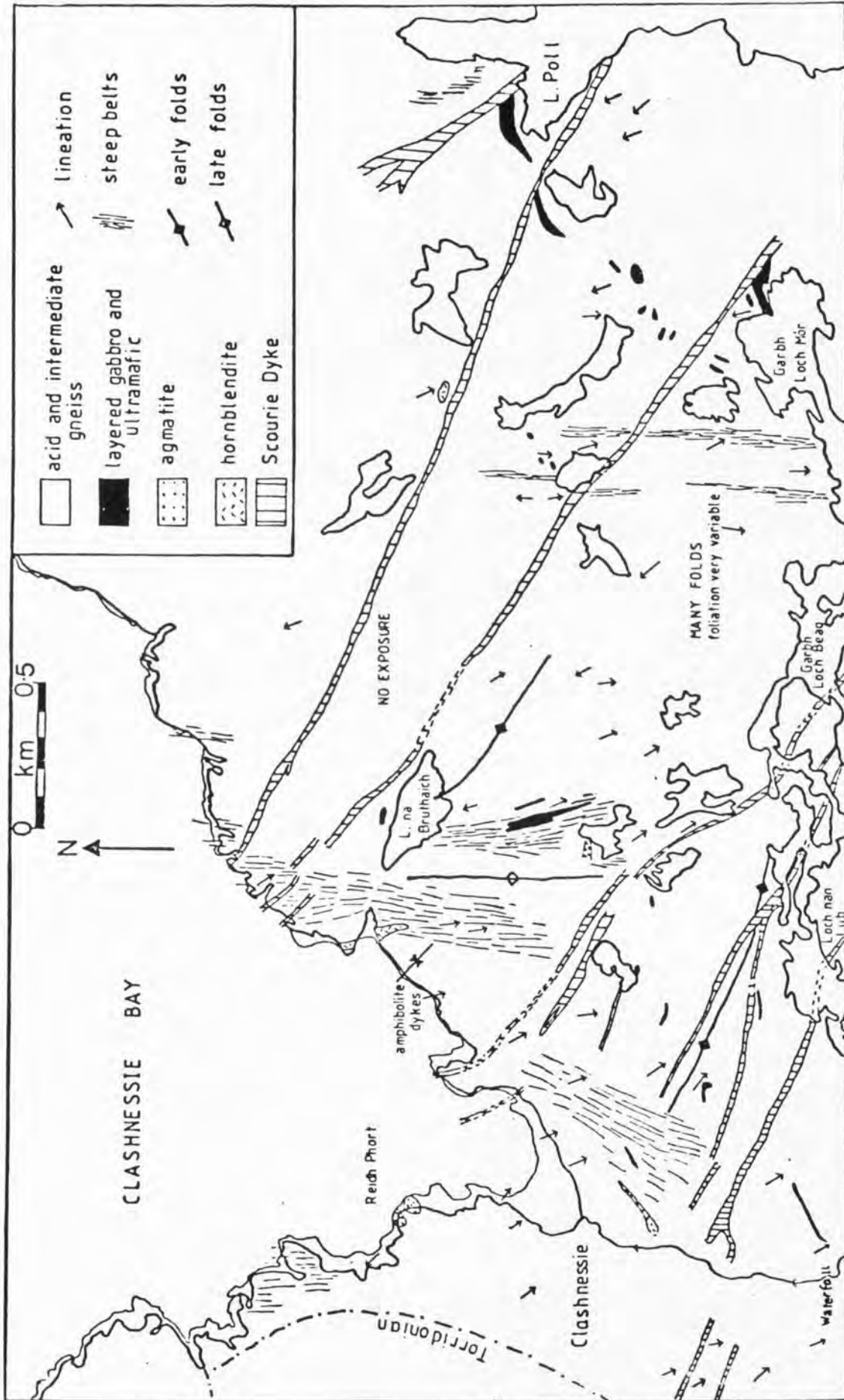


FIG. 1.21 Diagrammatic sketch map of the area around Clashnessie Bay.

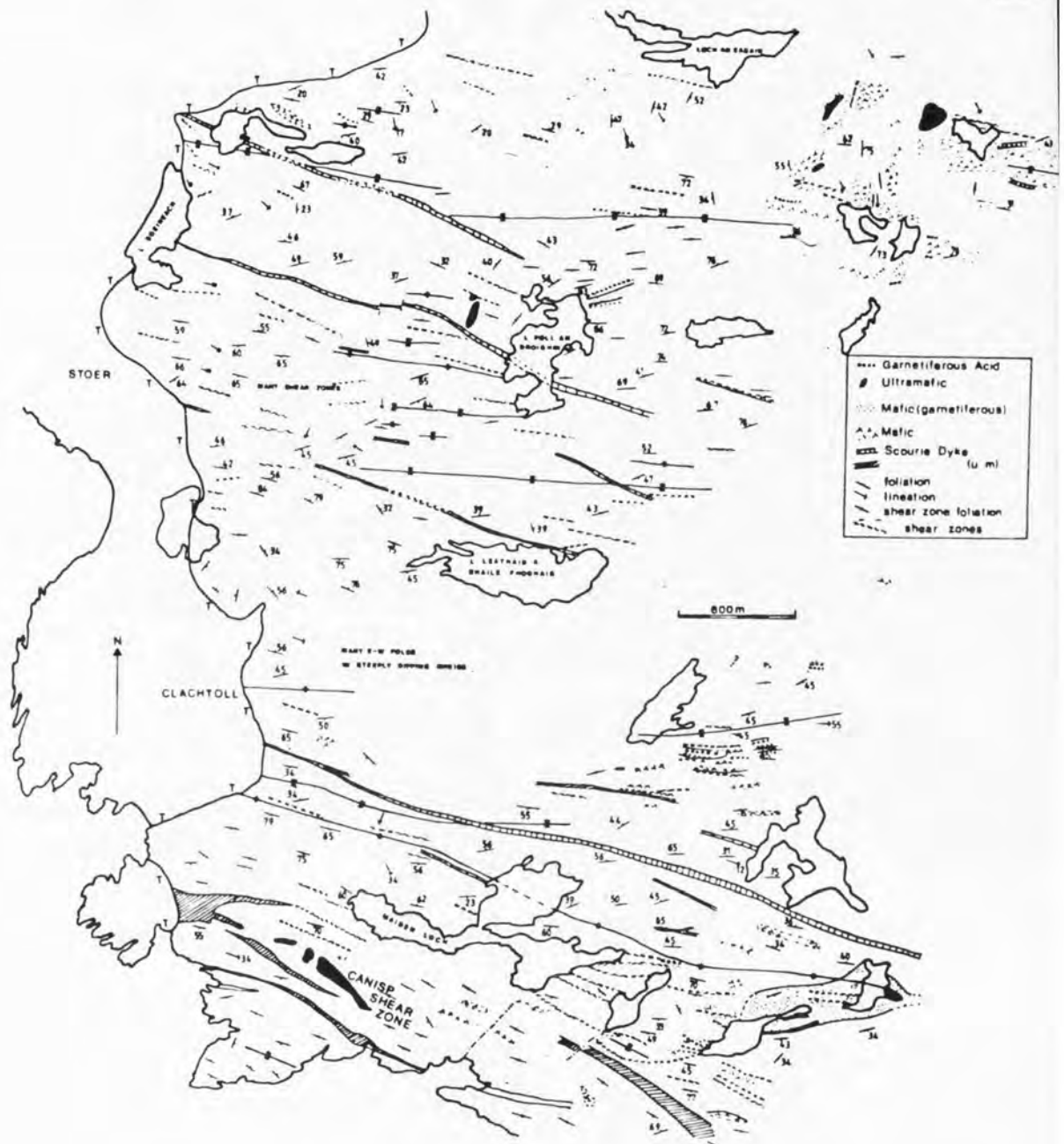


FIG. 1.22 Sketch map of the area between Stoer and Clachtoll.

T- Torridonian

## 1.7 DISCUSSION

The gneisses in the Assynt region evolved over a considerable period of time, at least 1000 million years, suffering three periods of deformation and metamorphism. The effects of Inverian and Laxfordian deformation are localised and not pervasive so that areas with a flat lying Scourian foliation remain.

The early evolution of the complex is speculative because later events have obscured most of the evidence for Scourian structures. It is clear that the original mafic and ultramafic rocks, that are now agmatites and hornblendite balls, were broken up prior to the peak of granulite facies metamorphism. The layered complexes were folded isoclinally, causing repetition of the successions, and were boudinaged and tectonically thinned before the end of the granulite facies event. Mafic rocks appeared to act more competently than intermediate and acid compositions. Scourian folds trend NE - SW in the Achmelvich area with gently SW plunging axes. The main flat lying foliation with associated intrafolial folds and coarse lineation developed in the Scourian. By the end of the granulite facies event, the Assynt region was a fairly rigid block of refractory gneisses depleted in LIL elements and more basic than the average crust (Sheraton et al., 1973a).

Inverian deformation, which began some time between 2.7 and 2.4 b.y. ago formed a series of monoclinial structures with vertical limbs:

$F_1$  - NW open folds, common the area between Nedd and Kylesku. Further south folds with a similar trend, causing the dip to change from north to south, could be the same generation of folds which have been tightened or monoclinial folds, e.g. the synform which follows the peat road from Stoer.

$F_2$  - N to NE trending monoclinial folds, varying from open to tight. The Strathan Bay fold and similar structures on the southern limb of the Lochinver antiform have this form and there may be an associated lineation but the coincidence of the fold axis plunge and the prevalent lineation in this southern limb may be fortuitous. N to NE steep belts east of Clashnessie are probably equivalent. Minor folds, with a variety of styles, but often with a N to NE plunge are so common in the Clashnessie area and are probably associated folds which have been refolded by WNW structures.

$F_3$  - WNW monoclinial folds such as the Lochinver antiform, producing steep belts without much attenuation.

$F_4$  - Further WNW monoclinial folds which affect the Lochinver antiform and cause tightening of earlier folds. These WNW folds have no associated lineation.

The steep belts are always retrogressed and where vertical structures are abundant the whole area, even the flat limbs, is amphibolitised. It is not known whether the vertical limbs developed and then acted as a route for the amphibolitising fluids or whether the deformation and metamorphism were synchronous. However, once the vertical limbs were established they continued as zones of weakness and were exploited by Laxfordian shear zones, which are commonly located along monoclinial steep belts, e.g. the Canisp shear zone which runs along the northern limb of the Lochinver antiform.

The tectonic expression of the Laxfordian in Assynt is thus marked by the reactivation of vertical belts and dyke margins. Ultramafic dykes, intruded into the northern limb of the Lochinver antiform and subsequently

metamorphosed to talcose assemblages have taken up substantial amounts of Laxfordian strain (Tarney, 1973). In general, though, mafic and ultramafic rocks are more competent than the surrounding acid gneisses. There is no migmatisation associated with the Laxfordian in Assynt, perhaps due to the low LIL content of the granulite facies Scourian rocks (Sheraton et al., 1973a). The Laxfordian areas which are migmatised could have been at a higher structural level during the Scourian than the Assynt area.

The metamorphic history of the Assynt region (discussed fully in Chapter 5) indicates gradually falling temperatures accompanied by the influx of water. The Laxfordian shear zone assemblages are much better crystallised than those in the Inverian vertical belts; this could either be due to a release of strain energy or to a rise in temperature. There has been a post-tectonic growth of prismatic hornblendes on foliation surfaces. The structural history concerns the development of narrow steep belts which acted as zones of weakness for later structures to exploit. The Assynt region thus consists of a series of low strain zones in which Scourian features may be preserved, surrounded by vertical-dipping high strain zones.

CHAPTER 2

EARLY METAMORPHIC HISTORY OF  
LAYERED ULTRAMAFIC - GABBRO BODIES

## 2.1. INTRODUCTION

The production of eclogitic assemblages during high grade metamorphism of rocks of basaltic composition is a process of petrological significance. Models of basalt and andesite genesis, geophysical models of the upper mantle and of plate tectonic processes depend on the mineralogical reconstitution of basic rocks in the lower crust and mantle (Ringwood, 1974). Consequently, great attention has been paid to the nature and physical conditions of the gabbro - eclogite transition both experimentally (Green and Ringwood; 1967; Ito and Kennedy, 1970) and on natural samples (Griffin and Heier, 1973; Whitney and McLelland, 1973; Loomis, 1977). This study concerns a suite of rocks of ultramafic and gabbroic composition which have been metamorphosed at garnet - granulite grade, a transitional stage in the gabbro - eclogite transition (Green and Ringwood, 1967). Archaean high grade gneiss terrains are commonly thought to represent the lower continental crust (Tarney and Windley, 1977) and these garnet - granulites provide a sensitive indicator of the metamorphic conditions that may prevail there.

## 2.2. MODE OF OCCURRENCE

Fig.2.1 shows the main occurrences of layered ultramafic gabbro bodies in the Assynt area. Two bodies were studied in detail; at Drumbeg (115328) and Achiltibuie (033079) but some information comes from other bodies, notably Achmelvich (055243) and from south of Loch Culag (097209).

The bodies occur as conformable lenses up to 100 m thick and 1 km long. No discordant contacts have been observed. The bodies thin rapidly along strike but the resulting trains of pods and lenses have been used to map out early Scourian NE trending structures (Davies, 1976).

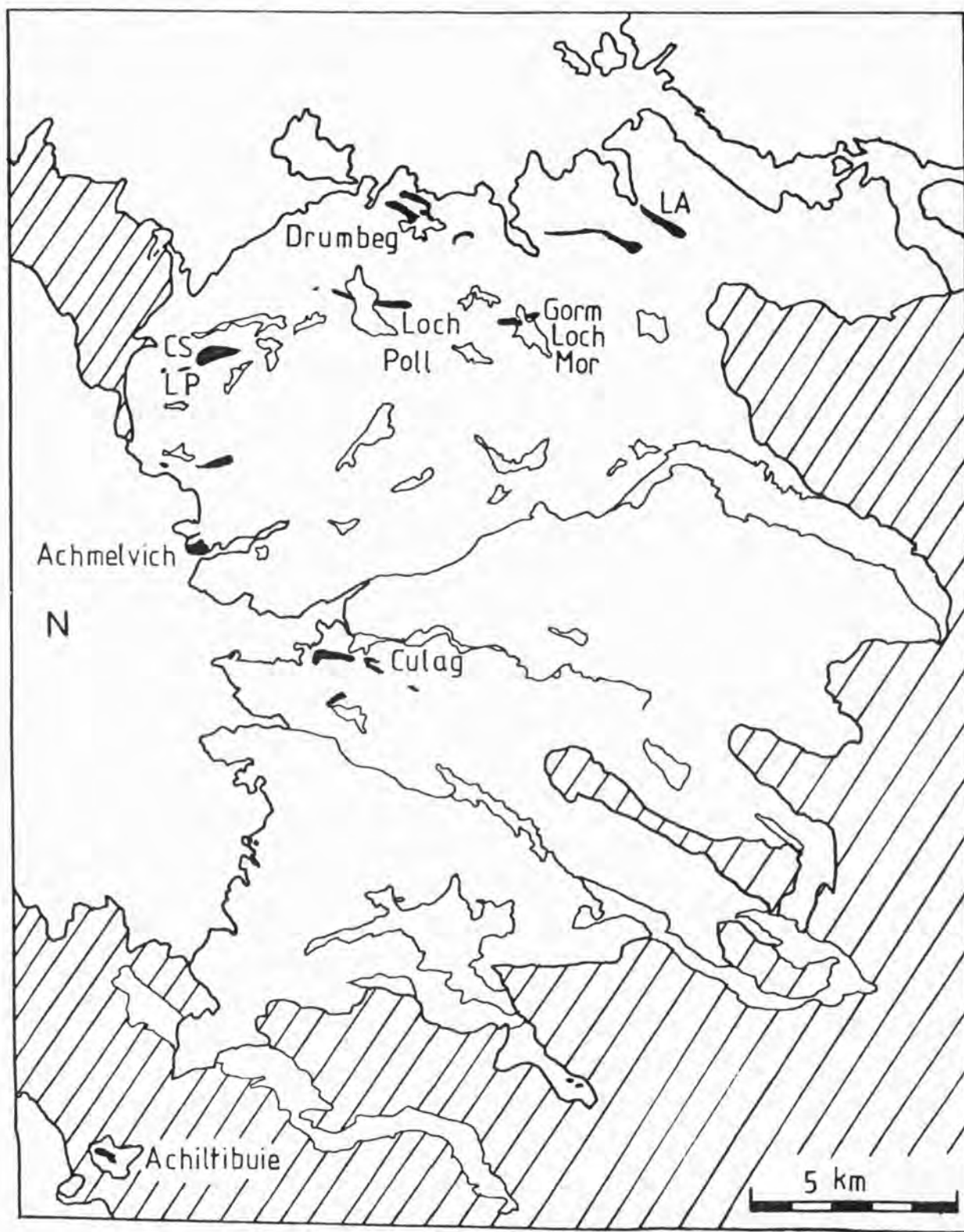


FIG 2.1 Map to show location of ultramafic-gabbro bodies in the Assynt area. LA- Loch Ardbhair, CS- Cnoc a Sgiorodaich, LP- Loch Poll an Droighinn. Hatched areas represent post Lewisian rocks.

This early Scourian deformation was responsible for boudinage and some thinning of the bodies. The ultramafic pyroxenites are more competent than the surrounding tonalitic gneisses and are found as low deformation lenses; but the gabbros are less competent than the pyroxenites, so in regions of intense late deformation the gabbros may become interbanded with the tonalitic gneisses to produce rocks of intermediate composition and the gabbros are indistinguishable.

In the Assynt region there was considerable retrogression associated with Inverian NW trending folds, but the ultramafic-gabbro bodies have often retained their granulite facies mineralogy even when the tonalitic gneisses are at amphibolite facies.

The layered bodies have two main components: an ultramafic portion consisting of amphibole-spinel lherzolites with minor dunite and harzburgite and a gabbroic portion consisting of plagioclase - two pyroxene-garnet rocks. These components are repeated in cyclic units providing a means for determining the way up of the body. On Scourimore, the Camas nam Buth sheet is anticlinally folded with an ultramafic core (Savage, 1979).

The ultramafics have a pronounced compositional layering (Fig.2.2a) made up of different proportions of the main component minerals: olivine, orthopyroxene and pargasite. The layers are commonly a few millimetres thick but some massive units reach 10 m. Occasional serpentinitised bands up to 3 m thick (e.g. at 154304, near Gorm Loch) are thought to represent dunite or harzburgite. The layering in the gabbros is less well marked, usually expressed by felsic or mafic schlieren and there are some sulphide-rich bands, which on Scourimore occur at the top of a gabbro under an ultramafic unit (Savage, 1979). The layering in the gabbros and ultramafics is conformable with that of the host gneisses. Minor intra-folial folds, probably of early Scourian age, have axial planes sub-

FIG. 2.2(a) Layering in an ultramafic outcrop from the Loch Poll body (NC 107308).

FIG. 2.2(b) Retrogressed ultramafic from Achmelvich (NC 058244). Note the presence of layering even though the mineral assemblages producing the original layering have disappeared. The rock is now a chlorite-tremolite assemblage.



a



b

parallel to the layering, and locally produce features resembling the cross-bedding of Bowes et al. (1964).

Drumbeg: This is the largest well preserved body in Assynt and consists of two main parts (Fig.2.3a). The northern part consists of a repeated ultramafic-gabbro succession dipping south westwards (Fig.2.4). The lower ultramafic unit, bounded by a shear zone, is retrogressed to a chlorite-tremolite assemblage. The main garnetiferous gabbro unit ranges up to 50 m thick and is fairly massive with modal plagioclase increasing up the section. The central ultramafic unit forms a prominent ridge of brown-weathering pyroxenites, serpentinised olivine-rich layers emphasising the layering. Above this, is a patchily developed, well foliated gabbro, more retrogressed than the middle unit. The southern part of the complex comprises numerous small outcrops cut by shear zones. Using increasing modal feldspar, as a way-up criterion, the northern part of the complex youngs southwards; accordingly the Drumbeg complex is part of an overturned synform with a NW-trending axis.

Achiltibuie: The Achiltibuie complex (Fig.2.3b) is less well exposed and crops out in an inlier in the Torridonian. The complex dips about  $40^{\circ}$ E and swings into an ESE steep belt in the north of the inlier. There is again a repeated ultramafic-gabbro succession, but only the upper part is well exposed with about 35 m of gabbro overlying 20 m of ultramafic. Modal (and normative) plagioclase increases up the section (Fig.2.4) indicating the body is the right way up.

Achmelvich: The Achmelvich body (Fig.2.3c) is very retrogressed. It is folded around a north east trending fold (plunging gently to the SW) which swings into the Canisp shear zone. The ultramafics have a fairly

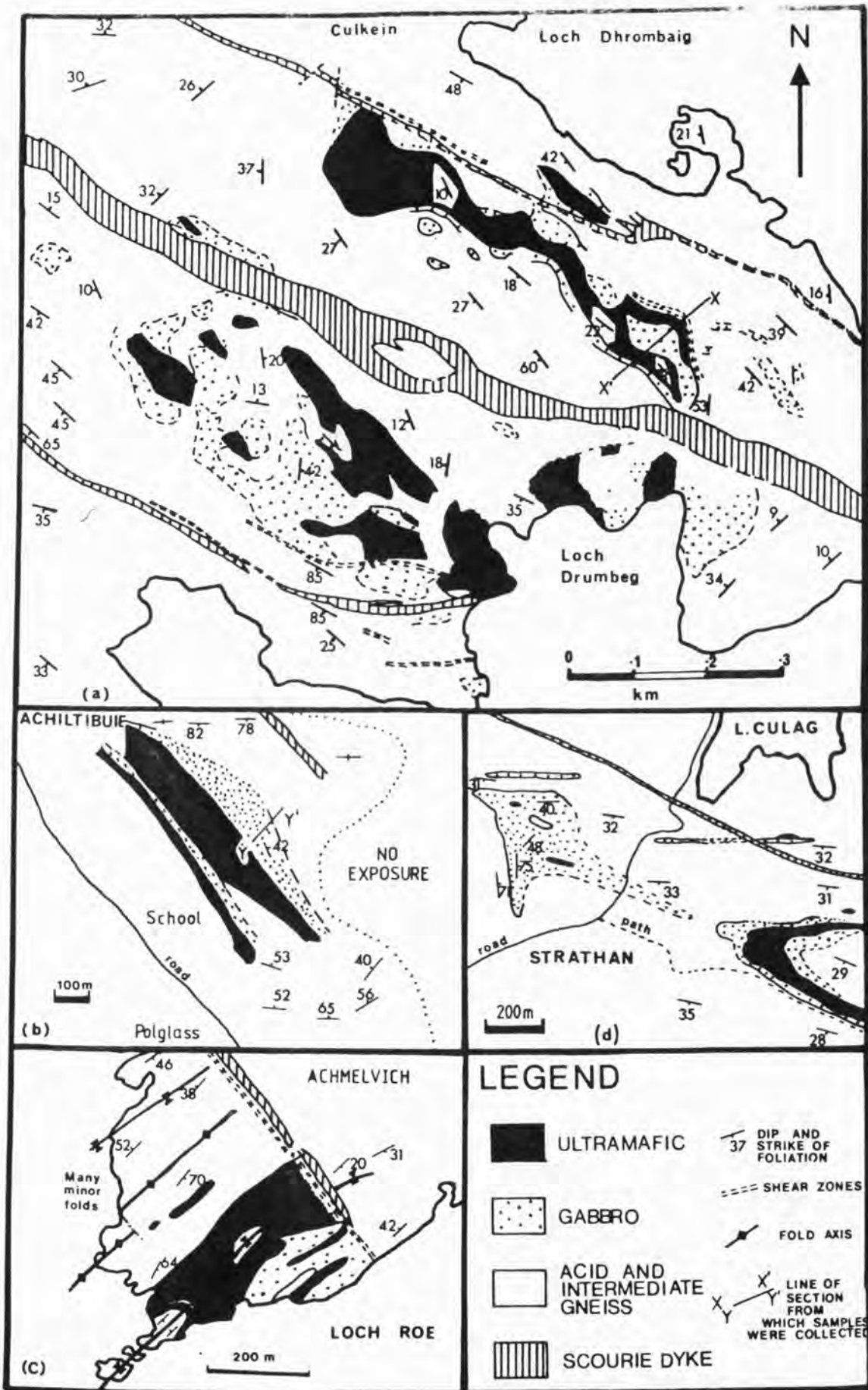


FIG. 2.3 Sketch maps of layered ultramafic-gabbro bodies.  
 (a) Drumbeg, after Sheraton (1969).  
 (b) Achiltibuie.  
 (c) Achmelvich.  
 (d) Culag, S. of Lochinver.

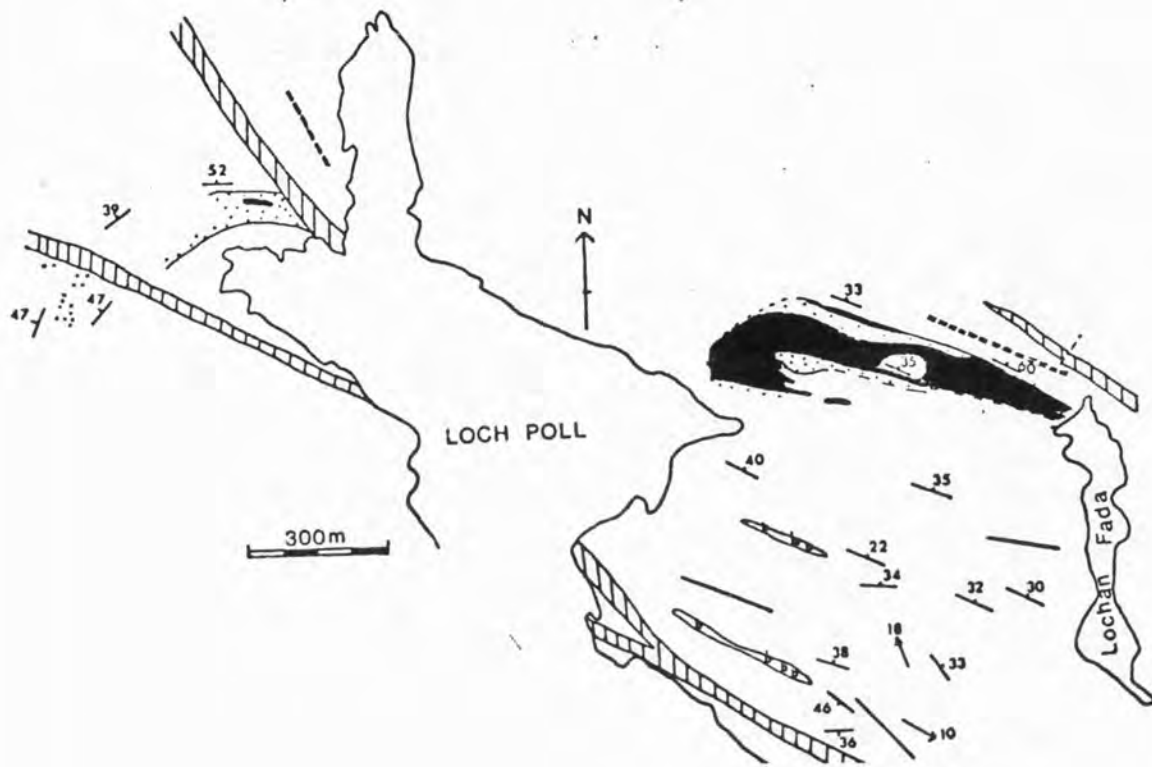


FIG. 2.3(e) Sketch map of the Loch Poll body.  
 Key as in Fig. 2.3a, small b symbols  
 represent basic lenses not obviously  
 part of the layered complex, and thick  
 black lines are steep belts.

## (a) Drumbeg

	%	plag	cpx	opx	gt	opq	amph	Section
10m gabbro	W13	41	28			1	30	Foliated with plag layers
	W12							
20m ultramafic	W11							opx-cpx-amph-ol-sp-magt. coarse opx-rich layer tremolite+chlorite+magt.
	W10							
	W9							
35m garnet gabbro	W8	30	26		19	2	23	1m W8 plag layers developing
	W7	23	25		13	2	37	7m W7
	W6	13	29		54	3	2	10m W6 1m garnetite layer
	W5	18	41	6	17	6	12	10m W5 0.6m sulphide-rich layer
	W4	33	25	3	22	2	15	6m W4
5m ultramafic								1m W3 3m tremolite+chlorite+opq 2m

-----  
sheared base

## (b) Achiltibuie

	%	Ht(m)	Plag	cpx	opx	gt	amph	Section
35m gabbro	W37B	31	26	44	7	17	6	minor anorthosite patches
	W37A	31	18	38	9	21	14	
	W36	19	29	35	10	12	14	gt gabbro
	W35	12	13	39	16	11	21	% plag increasing
	W34B	5	4	40	17	11	17	u/m layer 30cm thick
	W34A	5	13	35	31	—	31	hb-rich, gt free layer
	W32	2.5	13	42	14	10	20	gt-hornblende gabbro

Fig. 2.4 Modes from sections through (a) Drumbeg and (b) Achiltibuie bodies.

Modes are based on at least 2000 points over two thin sections

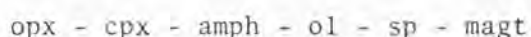
uniform tremolite-chlorite-magnetite assemblage but traces of the original layering can be seen on weathered surfaces (Fig.2.2b). The body is truncated in the north by a shear zone.

Culag: The Culag body (097209, Fig.2.3d) consists predominantly of massive and layered ultramafics with minor amounts of garnetiferous gabbro. It is folded around a NW-trending synformal axis.

Loch Poll: The Loch Poll body (107307) is up to 200 m thick and crops out between Loch Poll and Loch an Fada (Fig.2.3e). It is predominantly a well layered ultramafic (Fig.2.2a) with a subsidiary amount of garnetiferous gabbro. The body continues on the west side of Loch Poll for 500 m and small lenses can be traced south eastwards for up to 1 km.

### 2.3. PETROGRAPHY

Ultramafics: The ultramafic rocks are medium to coarse grained amphibole spinelherzolites with variable amounts of olivine. They have an equigranular, granoblastic texture, typical of the granulite facies (Fig.2.5a). The mineral assemblage at all localities is:

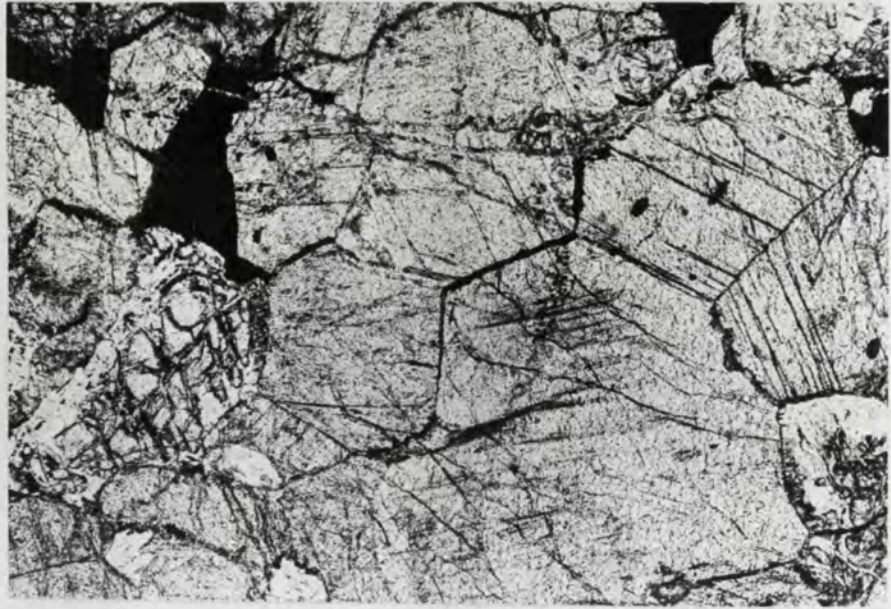


Orthopyroxene is most abundant (up to 60%), olivine reaches a maximum of 20%, but clinopyroxene and amphibole are of variable abundance and tend to be complementary. Orthopyroxenes are aluminous bronzites ( $\text{En}_{80-84}$ ,  $\text{Al}_{2-3} \text{O}_3$  up to 4.0 wt.%) and clinopyroxenes are aluminous diopsides ( $\text{En}_{42-44}$ ,  $\text{Wo}_{48-49}$ ,  $\text{Al}_{2-3} \text{O}_3$  up to 4.5 wt.%). Amphiboles are pargasites (nomenclature after Leake, 1978). Both pyroxenes contain profuse platelets of iron oxide in grain cores and along grain boundaries (Fig.2.5a) which is

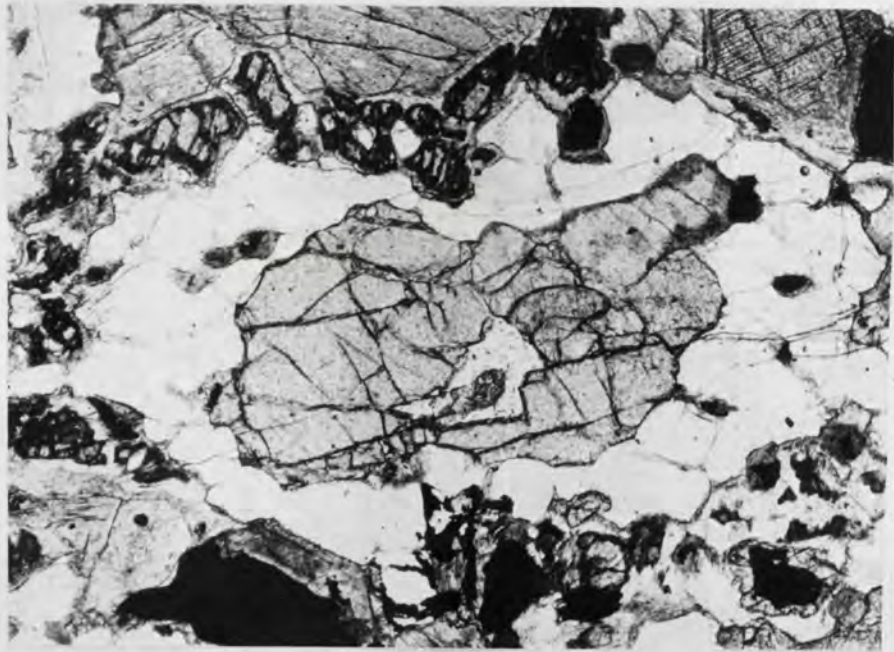
FIG. 2.5(a) Photomicrograph of an ultramafic (W4, Drumberg). Note the granoblastic texture, the exsolution of opaque oxides along grain boundaries and cleavage planes. Rounded cracked olivine grains (left of picture) and composite spinel-magnetite grains occur. Field of view 3.2mm.

FIG. 2.5(b) Garnet symplectite from an Fe-rich gabbro (W4, Drumberg). A large garnet porphyroblast is rimmed by plagioclase which is in turn rimmed by orthopyroxene and opaque oxides against clinopyroxene. Field of view 3.2mm.

FIG. 2.5(c) Small orthopyroxene grains against clinopyroxene in a Fe-rich gabbro (W4, Drumberg). The pyroxenes are partially replaced by a thin rim of actinolite or cummingtonite. Field of view 1.6mm.



a



b



c

probably a retrogressive feature. Spinels are olive green to opaque pleonastes forming rounded grains in association with magnetite, or more rarely, small rounded grains included in orthopyroxene.

Ultramafics may be retrogressed to a tremolite-chlorite-magnetite-anthophyllite assemblage adjacent to shear zones and Inverian folds and to a chlorite-talc-dolomite assemblage in shear zones.

Gabbros: The gabbros are less uniform than the ultramafics and are broadly divisible into two types: a more iron-rich type, such as at Drumbeg, with a whole-rock mg number less than about 0.5, and a magnesium-rich type such as at the base of the Achiltibuie body.

The Drumbeg gabbros are coarse to fine grained with an equigranular granoblastic texture consisting of: plag - cpx - gt  $\pm$  opx - magt - ilmt  $\pm$  sulph  $\pm$  green amphibole. They are characterised by two textural domains:

(a) a coarse granoblastic matrix of clinopyroxene with minor plagioclase and large garnet porphyroblasts (on average 2.3 mm, but may be up to 0.5 m!). The garnets may have inclusions of clinopyroxene and more rarely plagioclase.

(b) garnet-breakdown areas, which consist of a fine grained aggregate of orthopyroxene, plagioclase and opaque oxides. The garnets have embayed edges with a "collar" of plagioclase, an outer rim of pink orthopyroxene and ilmeno-magnetite against clinopyroxene (Fig.2.5b). Orthopyroxene only occurs in garnet-breakdown areas.

The textural evidence suggests two periods of granulite facies mineral growth, the earlier,  $M_1$ , producing a dominantly garnet-clinopyroxene assemblage with only minor plagioclase. The second,  $M_2$ , caused partial breakdown of garnet. There was a subsequent growth of

60  $\mu$  garnet fringes around opaque oxides; this garnet being richer in the almandine molecule than the porphyroblasts. In one iron-rich sample from a thin gabbro band near Kykesku (220338) this feature is particularly well developed (Fig.2.5f).

The Achiltibuie gabbros are similar to the above but have several significant differences (Fig.2.4):

(a) they have abundant (up to 30% modal) brown-straw-yellow pargasitic hornblende and no iron-titanium oxides, whilst at Drumbeg they have up to 6% opaque oxides and no pargasite. This is interpreted as being due to differing  $f_{O_2}$  conditions during metamorphism rather than during igneous fractionation because the whole-rock trends of the two bodies are similar.

(b) Garnet is embayed against a radial rim of anorthite, pargasite and orthopyroxene with an outer rim of orthopyroxene against clinopyroxene (Fig.2.5d). In the most magnesian samples (e.g. W 34 B Fig.2.5e) the garnet has been completely replaced by a symplectite of orthopyroxene, pargasite and anorthite (An 95).

(c) There is similarly a medium to coarse grained matrix of clinopyroxene which has 20  $\mu$  exsolution lamellae of orthopyroxene and minor plagioclase. However in the most magnesian samples, there is also polygonal pargasite and orthopyroxene in this matrix, but most of the orthopyroxene is in the garnet-breakdown areas.

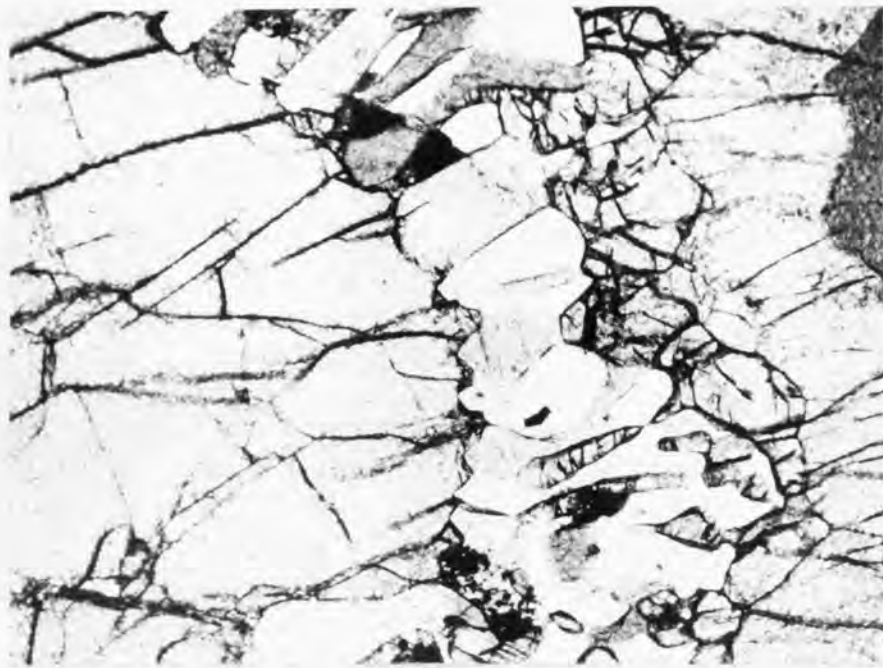
The earliest ( $M_1$ ) assemblage in the most magnesian gabbros was: cpx - gt - amph  $\pm$  opx; and in the others: cpx - gt  $\pm$  amph  $\pm$  plag.

The  $M_2$  assemblage in all but the most magnesian gabbros was: cpx - gt - amph - opx - plag. In the most mg-rich samples (as on Scouriemore, Savage, 1979) garnet was no longer stable during  $M_2$  conditions.

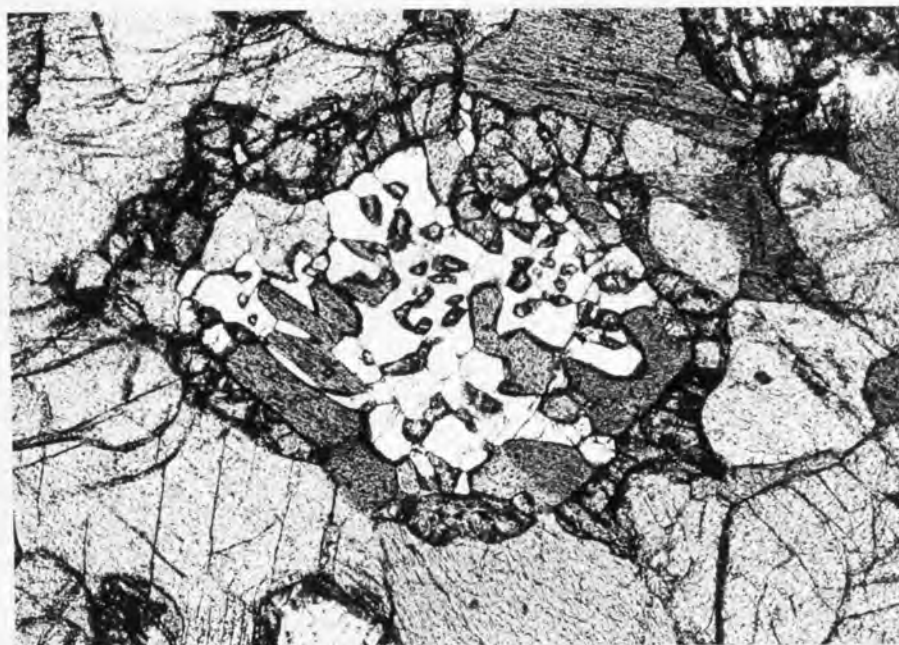
FIG. 2.5(d) garnet symplectite from an Mg-rich gabbro (W32, Achiltibuie). The large garnet porphyroblast is rimmed by a corona of plagioclase, orthopyroxene and pargasite against a rim of orthopyroxene which is in turn rimmed by clinopyroxene. field of view-3.2mm.

FIG.2.5(e) Symplectite of anorthite, pargasite and orthopyroxene from a Mg-rich gabbro which is thought to reflect the former presence of garnet. The symplectite area has an outer rim of orthopyroxene grains against clinopyroxene. Field of view-3.2mm.

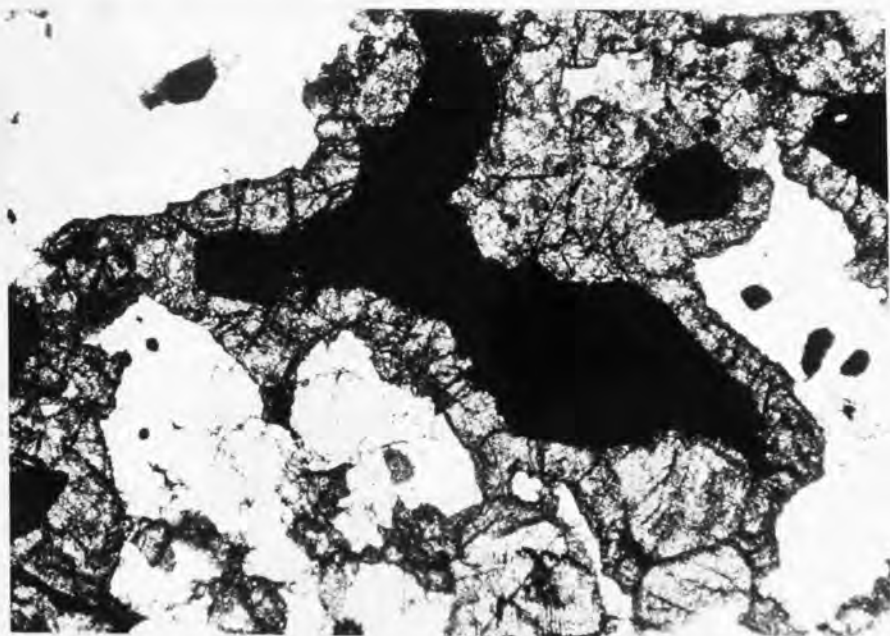
FIG. 2.5(f) Opaque oxide rimmed by garnet from an Fe-rich gabbroic band near Kylesku (230338). Field of view 3.2mm.



d



e



f

There is no conclusive evidence from either locality that the conditions during the peak of metamorphism ( $M_1$ ) were eclogitic, minor amounts of plagioclase or amphibole were present in  $M_1$  assemblages but the majority of the plagioclase was consumed in garnet and clinopyroxene.

Fringes of blue/green actinolite and cummingtonite rim pyroxenes in many samples and orthopyroxene is always the most altered (Fig.2.5c). Biotite commonly fringes opaque oxides and in the most retrogressed samples pyroxenes are rimmed by a green tschermakitic hornblende with tiny quartz inclusions.

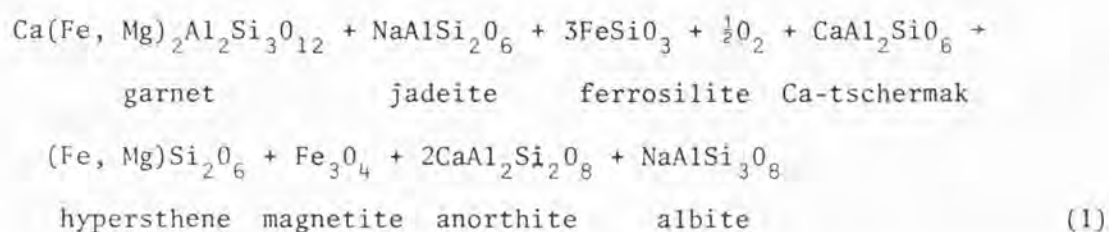
#### 2.4. GARNET-BREAKDOWN REACTIONS

In this section, garnet decomposition reactions are described with reference to the textural observations made previously. It is demonstrated that these reactions are retrogressive and that they document part of the slow uplift of the Lewisian complex from its inferred lower crustal position at 2.9 by ago to eventual exposure at the earth's surface about 1.0 by ago.

As mentioned above, it is believed that the earliest mineral assemblage in the gabbros was dominated by clinopyroxene and garnet with subsidiary amounts of plagioclase and amphibole. There are two types of garnet decomposition reaction in these rocks, but a third type in which spinel is a breakdown product is reported from Scourie (O'Hara and Yarwood, 1978; Savage, 1979; Savage and Sills, 1980).

(a) Iron-rich gabbros e.g. Drumbeg. The type of corona seen at Drumbeg (Fig.2.5b) has been interpreted (O'Hara, 1961a; O'Hara and Yarwood, 1978) as resulting from the exsolution of excess jadeite, Ca-tschermak's molecule, hypersthene and Fe-Ti oxide from an original high temperature pyroxene during slow cooling. However this hypothesis does not account for the bulk of the plagioclase and all the orthopyroxene occurring

adjacent to garnet, nor for the fact that large areas of mono-mineralic clinopyroxene occur without plagioclase or orthopyroxene. The textural evidence suggests a reaction between garnet and clinopyroxene; a coupled reaction would be:

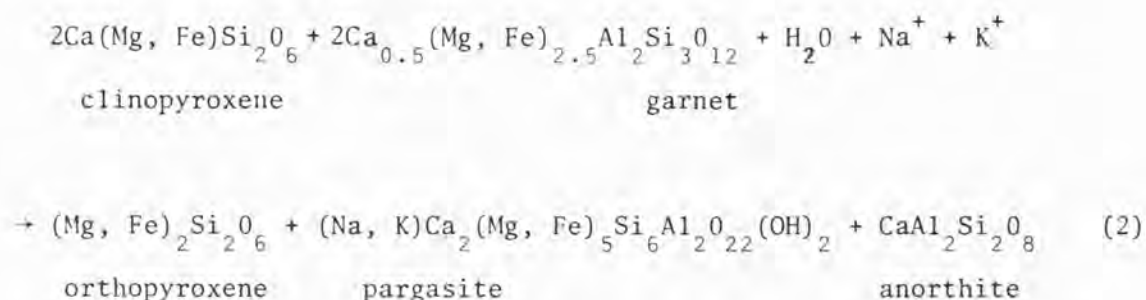


The plagioclase in the "collars" is about  $\text{An}_{50}$  but is more variable ( $\text{An}_{35-50}$ ) in the matrix. There is no detectable zoning in any of the mafic minerals.

(b) At Achiltibuie the earliest assemblage was again dominated by garnet and clinopyroxene, but some amphibole was also present. Amphibole, plagioclase and orthopyroxene all occur in two textural areas, the garnet-breakdown areas and the dominantly clinopyroxene matrix. The composition of the two types of orthopyroxene is very similar, but the symplectite orthopyroxene tends to have less  $\text{Al}_2\text{O}_3$ , although  $\text{Al}_2\text{O}_3$  contents are rather variable. Symplectite plagioclase is always richer in the anorthite molecule than the matrix plagioclase; the former ranges from  $\text{An}_{95}$  at the base of the body to  $\text{An}_{70}$  at the top, whilst the latter ranges from  $\text{An}_{75}$  to  $\text{An}_{50}$  and may be strongly reversed zoned. The pargasites are typical of the granulite facies (Binns, 1965) with up to 4.0 wt%  $\text{TiO}_2$  and up to 2.0 wt%  $\text{K}_2\text{O}$ . Symplectite amphiboles have a slightly lower FeO content, which is balanced by an increase in  $\text{Al}^{\text{vi}}$  rather than by MgO; this is thought (Binns, 1965) to reflect decreasing metamorphic grade.

A coupled garnet-clinopyroxene reaction to produce these coronas

would be:



The Na for the albite component of the plagioclase and a little Al for the pargasite has come from the jadeite molecule in the clinopyroxene in an analogous way to equation (1). Most grains show negligible zoning except for the symplectite plagioclase which may be richer in the anorthite molecule (2-3 % An) adjacent to the garnet.

It is apparent from the geometry of the coronas that nucleation and growth of the various phases were not random. For example, plagioclase rims garnet, whilst hypersthene and magnetite nucleate against clinopyroxene. This arrangement may be controlled by slow outward diffusion of aluminium from garnet to nucleating plagioclase. Some authors have suggested that diffusion of aluminium is much slower than that of other major silicate components and have noted the effect that this has on textures (Carmichael, 1969 ; Anderson and Buckley, 1973; Loomis, 1975, 1977). The exsolution of ferrosilite from clinopyroxene may also help nucleate hypersthene against clinopyroxene. Indeed O'Hara (1961a) has described mafic granulites from the Scourie district where hypersthene lamellae within the clinopyroxenes merge into the hypersthene grains associated with the coronas. It may be assumed therefore that corona geometry was controlled by a combination of slow intergranular diffusion of Al between garnet and plagioclase and preferential nucleation of orthopyroxene against clinopyroxene.

Intergranular diffusion in garnet may also have been important

as the rate-determining step in the kinetics of the coupled garnet-clinopyroxene reaction. Loomis (1977) suggested that this process is rate limiting in the eclogite-garnet granulite-gabbro retrogression. This may be expressed in chemical disequilibrium, such as zoning, in the garnet; zoning has not been observed in the Scourie samples, and may have been obliterated by high temperature metamorphism ( $T > 700^{\circ}\text{C}$ ) and slow cooling (cf. Yardley, 1977) despite diffusion in garnet being the rate limiting step. It is unlikely that diffusion in clinopyroxene would have been rate limiting as this process is believed to be relatively fast (Loomis, 1977; Fraser and Lawless, 1978). It is possible that armouring of garnet and clinopyroxene by plagioclase and hypersthene was important, hindering intergranular diffusion of components, and one would expect growth of the corona to reach a particular size and no more, beyond which reaction would be prohibitively slow.

## 2.5. MINERAL CHEMISTRY

All analyses were obtained from a Cambridge Instruments Microsan V electron probe at the University of Leicester. For full analytical details see Appendix A. Brief descriptions of the main features of the mineral chemistry follow.

Orthopyroxene. Representative analyses are given in Tables 2.1 and 2.2 and average compositions for each sample are plotted in the pyroxene quadrilateral (Fig.2.6a). All points plot near the enstatite-ferrosilite join; in the ultramafics they are aluminous bronzites (mg about 0.8) and in the gabbros they are aluminous hypersthene (mg 0.62 - 0.69). Calcium contents are low, typically less than 0.5 wt %, and lie in the range for metamorphic pyroxenes (Windley and Smith, 1974), as do the Mn and Cr

	cpx	opx	amph	ol	sp
SiO <sub>2</sub>	50.78	55.41	42.46	40.52	0.00
TiO <sub>2</sub>	0.49	0.08	1.53	0.00	0.00
Al <sub>2</sub> O <sub>3</sub>	4.51	3.57	13.47	0.00	58.58
FeO	4.21	10.08	6.60	14.64	18.56
MnO	0.17	0.23	0.08	nd	0.03
NiO	0.04	nd	nd	0.51	0.41
MgO	15.11	30.27	16.68	44.53	16.44
CaO	23.67	0.34	12.29	0.00	0.00
Na <sub>2</sub> O	0.28	0.00	2.56	nd	nd
K <sub>2</sub> O	0.00	0.00	0.64	nd	nd
Cr <sub>2</sub> O <sub>3</sub>	0.18	0.08	0.32	nd	5.36
TOTAL	99.44	99.96	96.70	100.20	99.38
No of oxygens	6	6	23	4	4
Si	1.877	1.936	6.184	1.015	-
Al	0.123	0.064	1.816	-	1.837
Al	0.073	0.077	0.495	-	-
Ti	0.013	0.002	0.168	-	-
Cr	0.005	0.003	0.036	-	0.113
Fe	0.130	0.298	0.804	0.304	0.413
Mn	0.005	0.008	0.010	-	0.001
Mg	0.832	1.573	3.621	1.655	0.652
Ca	0.937	0.019	1.918	-	-
Na	0.020	-	0.724	-	-
K	-	-	0.124	-	-

Table 2.1 Representative mineral analyses from layered ultramafics. Abbreviations are as follows:  
 cpx- clinopyroxene, opx - orthopyroxene, amph- amphibole, ol - olivine, sp - spinel.

	W5 cpx	W7 cpx	W34b cpx	W36 cpx	W5 opx	W34b opx	W36 opx
SiO <sub>2</sub>	49.23	49.07	51.19	51.00	51.45	52.11	51.09
TiO <sub>2</sub>	0.83	0.77	0.35	0.35	0.17	0.09	0.11
Al <sub>2</sub> O <sub>3</sub>	5.24	6.53	4.13	3.24	3.24	3.31	2.21
Cr <sub>2</sub> O <sub>3</sub>	0.04	0.02	0.11	0.14	0.03	0.10	0.08
FeO	9.44	10.11	7.31	8.84	21.61	19.41	24.02
MnO	0.09	0.16	0.13	0.19	0.18	0.27	0.37
MgO	12.27	11.46	13.78	13.22	22.72	24.43	21.75
CaO	21.66	20.92	22.55	22.30	0.53	0.51	0.47
Na <sub>2</sub> O	0.68	0.75	0.46	0.61	0.00	0.02	0.01
K <sub>2</sub> O	0.00	0.00	0.00	0.00	0.00	0.00	0.00
TOTAL	99.48	99.78	100.01	99.89	99.91	100.25	100.11
Si	1.858	1.844	1.899	1.908	1.910	1.909	1.920
Al	0.142	0.156	0.101	0.092	0.090	0.091	0.080
Al	0.091	0.133	0.060	0.051	0.052	0.052	0.018
Cr	0.001	0.000	0.004	0.004	0.001	0.003	0.002
Ti	0.024	0.022	0.010	0.010	0.005	0.002	0.003
Fe	0.298	0.318	0.228	0.277	0.673	0.595	0.755
Mn	0.003	0.005	0.004	0.006	0.006	0.008	0.012
Mg	0.690	0.642	0.762	0.743	1.257	1.335	1.219
Ca	0.877	0.844	0.896	0.894	0.021	0.020	0.019
Na	0.050	0.055	0.033	0.045	-	-	-

Table 2.2 Representative pyroxene analyses from Drumbeig and Achiltibuie gabbros. Sample numbers W4, W5, W7 are from Drumbeig and numbers W34b and W36 are from Achiltibuie.

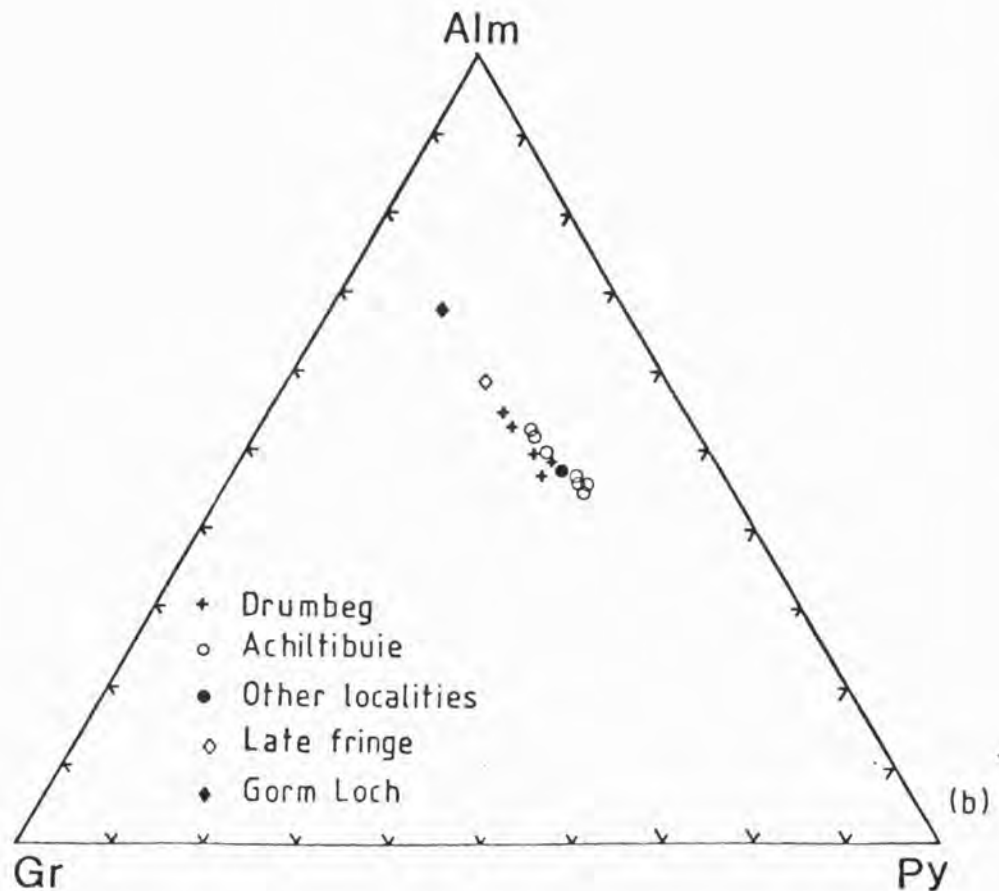
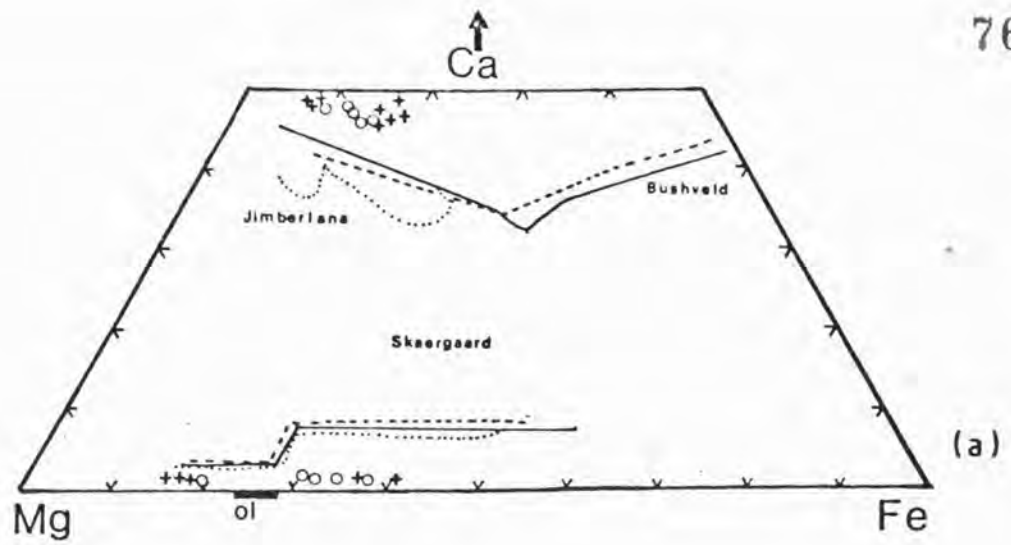


FIG. 2.6 (a) Pyroxene quadrilateral, key as in (b). The trends for Skaergaard and Bushveld are from Wager and Brown (1967) and the trend for the Jimberlana dyke is from Campbell (1977). (b) Garnet triangle for granulite facies garnets compared with the late fringes rimming opaque oxides and an amphibolite facies garnet (Gorm Loch). Alm-almandine, Py-pyrope, Gr- grossular

contents. Manganese contents are very low as Mn is preferentially partitioned into garnet, but in garnet-free samples the Mn content is significantly higher (see Fig.2.7).  $Al_2O_3$  contents are moderate (about 3.5 wt %) in the ultramafics and Drumbeg gabbros, but range from 1.75 to 3.5 wt % in the Achiltibuie gabbros where orthopyroxene is in equilibrium with an aluminous amphibole (Fig.2.8). These  $Al_2O_3$  contents are fairly typical for granulite facies pyroxenes. Chrome contents of the pyroxenes from the Drumbeg gabbros are below the minimum detection limit but are slightly higher (0.08 to 0.12 wt %  $Cr_2O_3$ ) in the Achiltibuie gabbros where there is no coexisting oxide phase.

Clinopyroxene. Representative analyses are given in Tables 2.1 and 2.2 and plotted in Fig.2.6a. Pyroxenes from the ultramafics are aluminous diopsides with less than 0.4 wt %  $TiO_2$ , low alkalis and moderate  $Al_2O_3$  (about 4.5 wt %). The gabbroic clinopyroxenes are aluminous salites with up to 6.5 wt %  $Al_2O_3$  in the Drumbeg gabbros and 3-4 wt %  $Al_2O_3$  in the Achiltibuie gabbros. Where tschermakitic rims are well developed (as in sample W13 from Drumbeg) the  $Al_2O_3$  contents of the clinopyroxene is reduced (Fig.2.8). Mn and Cr contents are similar to those described for orthopyroxene (Fig.2.7), mg numbers are in a similar range but are slightly higher which is consistent with crystal field theory.

A comparison with trends from un-metamorphosed layered basic intrusions is shown in Fig.2.6a. Although this diagram reveals the broad similarity of iron-enrichment trends for the pyroxenes in the intrusions, it highlights the calcium-rich nature of the clinopyroxenes and the calcium-poor nature of the orthopyroxenes from the Lewisian compared with the un-metamorphosed intrusions.

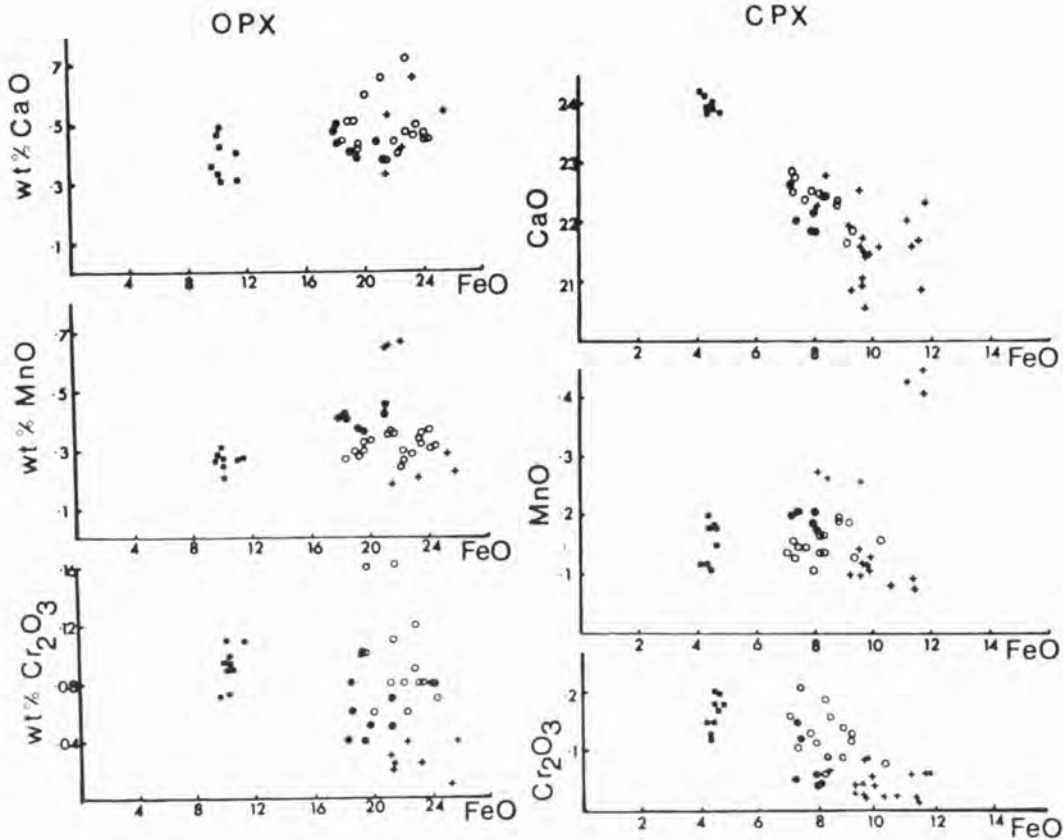


FIG. 2.7 Plots of CaO, MnO and  $\text{Cr}_2\text{O}_3$  against FeO for opx and cpx from ultramafics and mafic gabbros. Squares represent ultramafics, open circles gabbros from Achiltibuie, crosses gabbros from Drumbeg and filled circles gabbros from other localities.

In the MnO plots the three points from Drumbeg which have greater MnO contents than the others are from a garnet free sample.

The  $\text{Cr}_2\text{O}_3$  contents of the pyroxenes from the Achiltibuie gabbros are greater because there is no oxide phase.

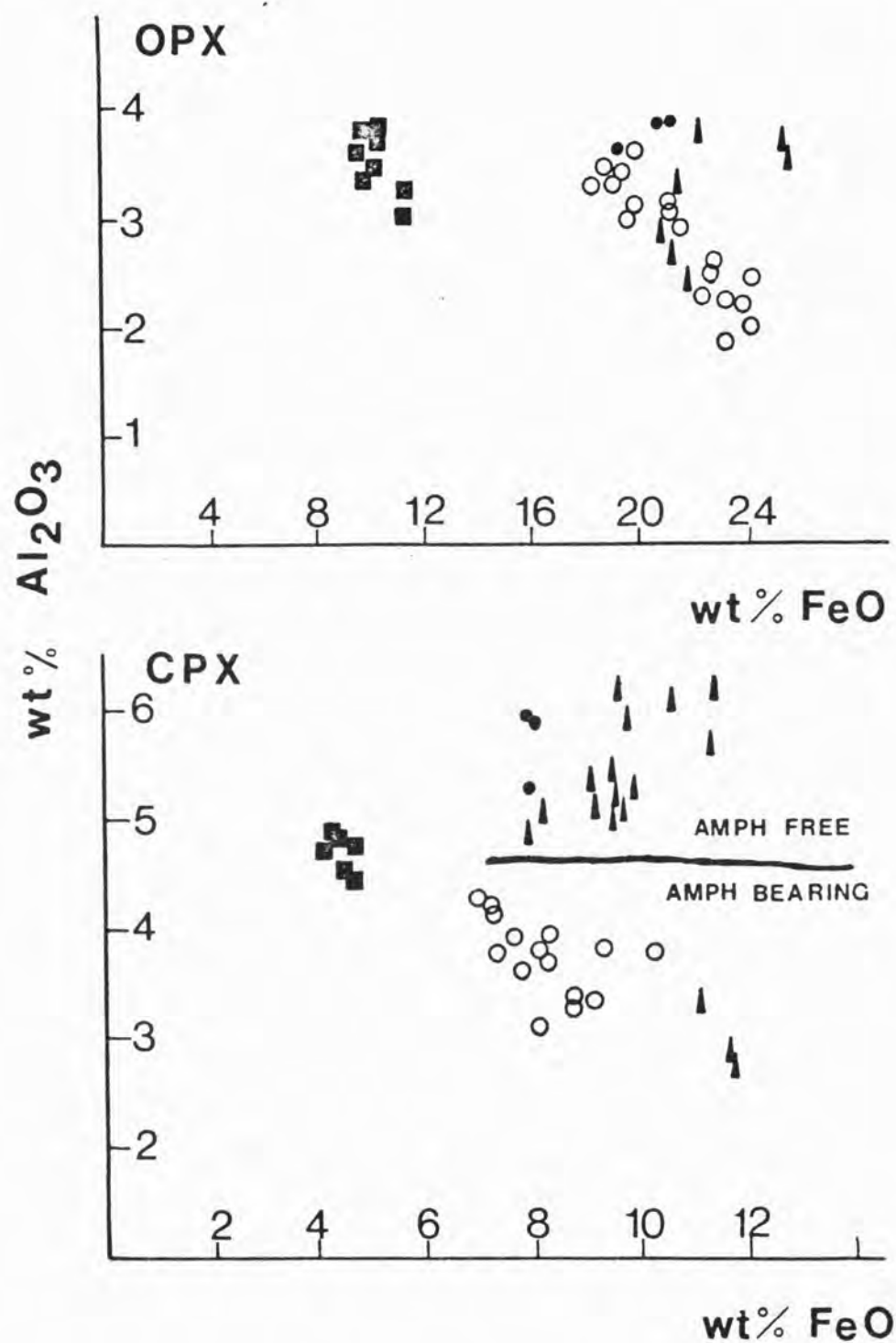


FIG. 2.8  $\text{Al}_2\text{O}_3$  vs FeO for pyroxenes from ultramafics and mafic gabbros. Squares are ultramafics, open circles Achiltibuie gabbros, filled circles are other localities and triangles gabbros from Drumbeg. Note the greater  $\text{Al}_2\text{O}_3$  contents of the pyroxenes in amphibole free samples.

Garnets: Average analyses for each sample are plotted in Fig.2.6b and presented in Table 2.3. All garnets are pyrope-almandine solid solutions with a constant grossular content (15 - 20 %) ; the percentage of all other end members is low. They plot towards the high pressure end of the granulite field of Chappell and White (1970). The garnets are often 1 cm or more across but no detectable zoning has been observed. 60  $\mu$  garnet fringes which occasionally rim opaque oxides are richer in almandine.

Amphibole: Representative analyses are shown in Table 2.1 and 2.4 and plotted in Fig.2.9. Amphiboles from ultramafics are pargasite and those from gabbros are ferroan pargasitic hornblende (nomenclature after Leake, 1978); mg is about 0.82 in the ultramafics and ranges from 0.60 to 0.70 in the Achiltibuie gabbros. There is a strong negative correlation between Mg and Fe and a weak negative correlation between Na and K. At Achiltibuie total Na + K increases up the stratigraphic section balanced by a decrease in  $Al^{vi} + Ti$ , and there is a slight negative correlation between  $Al^{vi}$  and Ti. The Achiltibuie gabbroic amphiboles have up to 0.5 wt%  $Cr_2O_3$  which is greater than the content for ultramafic amphiboles where Cr is partitioned into a coexisting spinel phase. Fluorine and chlorine were both below the MDL of the electronmicroprobe.

Olivine: All olivines plot in the range  $Fo_{82-86}$  (Fig.2.6a) and have about 0.5 wt% NiO. No other element was above MDL.

Oxides: As mentioned previously, the ultramafics contain composite spinel-magnetite grains. The spinels fall mid-way along the spinel-hercynite join and have up to 7 mol% chromite and 5 mol% magnetite in

	W32 (8)	W34b (4)	W35 (8)	W36 (13)	W37 (8)	W4 (8)	W5 (8)	W6 (7)	W4 (1)
SiO <sub>2</sub>	40.24	40.03	39.65	38.76	39.17	40.15	39.46	38.67	38.25
TiO <sub>2</sub>	0.04	0.07	0.04	0.07	0.07	0.12	0.10	0.11	0.03
Al <sub>2</sub> O <sub>3</sub>	22.13	22.09	22.38	21.89	21.90	21.71	22.08	21.68	21.85
Cr <sub>2</sub> O <sub>3</sub>	0.22	0.18	0.22	0.09	0.11	0.03	0.03	0.03	0.02
FeO	21.55	21.58	22.29	24.62	24.12	23.85	23.75	25.02	27.47
MnO	0.89	0.82	0.94	1.00	0.78	0.54	0.68	0.55	0.64
MgO	10.10	10.01	9.33	7.98	8.56	8.73	8.38	6.59	5.45
CaO	6.35	6.36	6.38	6.44	6.56	6.65	6.57	7.27	6.65
TOTAL	101.52	101.14	101.73	100.87	101.27	101.78	101.05	99.91	100.5

uv	0.66	0.54	0.66	0.28	0.34	0.09	0.09	0.09	0.06
py	38.23	38.00	36.96	30.69	32.84	33.87	31.97	25.60	21.22
sp	1.91	1.77	2.01	2.19	1.70	1.19	1.47	1.21	1.42
gr	16.61	16.81	16.58	17.53	17.76	18.45	17.93	20.21	18.55
alm	42.59	42.88	43.79	49.32	47.36	46.39	48.54	52.88	58.74

cations on the basis of 24 oxygens

Si	6.015	6.008	5.943	5.938	5.953	6.043	5.990	5.992	5.962
Al	3.899	3.908	3.954	3.953	3.923	3.852	3.950	3.960	4.111
Ti	0.004	0.008	0.005	0.008	0.008	0.014	0.011	0.013	0.003
Fe	2.694	2.709	2.794	3.154	3.066	3.003	3.015	3.243	3.580
Mn	0.113	0.104	0.119	0.130	0.100	0.069	0.087	0.072	0.082
Mg	2.250	2.239	2.196	1.822	1.939	1.959	1.896	1.522	1.266
Ca	1.017	1.023	1.025	1.057	1.069	1.073	1.069	1.207	1.112
Cr	0.026	0.021	0.026	0.011	0.013	0.004	0.004	0.004	0.002

TABLE 2.3 Average garnet analyses for each of the Drumbeig and Achiltibuie samples. Number of analyses included in average is shown in parentheses. Abbreviations are as follows: uv - uvarovite, py - pyrope, sp - spessartine, gr - grossular, alm - almandine.

	W32	W32	W34b	W34b	W35	W35	W36	W36	W37
	a	b	a	b	a	b	a	b	b
SiO <sub>2</sub>	42.51	43.00	41.39	41.99	40.71	40.64	40.77	41.88	40.95
TiO <sub>2</sub>	1.47	1.48	1.91	1.77	1.99	1.69	2.92	3.01	3.35
Al <sub>2</sub> O <sub>3</sub>	14.45	15.04	14.16	14.89	14.20	15.03	13.62	13.64	13.80
FeO	11.47	10.38	11.68	10.56	12.34	11.75	12.93	11.46	12.51
MnO	0.09	0.05	0.11	0.06	0.12	0.11	0.08	0.05	0.08
MgO	13.48	13.39	13.06	13.17	12.67	12.22	11.16	11.84	11.52
CaO	11.59	11.83	11.65	11.94	11.72	11.91	11.69	11.84	11.75
Na <sub>2</sub> O	2.67	2.56	2.38	2.29	2.48	2.17	1.85	1.65	2.04
K <sub>2</sub> O	0.31	0.32	0.60	0.52	0.98	1.22	1.89	2.04	1.43
Cr <sub>2</sub> O <sub>3</sub>	0.32	0.45	0.26	0.31	0.34	0.48	0.39	0.34	0.26
TOTAL	98.36	98.40	97.27	97.50	97.55	97.22	97.30	97.74	97.69
X <sub>Mg</sub>	0.67	0.70	0.66	0.69	0.64	0.65	0.60	0.65	0.62
Si	6.184	6.198	6.123	6.145	6.048	6.041	6.115	6.188	6.105
Al	1.816	1.802	1.877	1.855	1.952	1.959	1.885	1.812	1.895
Al	0.661	0.741	0.591	0.713	0.534	0.674	0.526	0.563	0.499
Ti	0.161	0.147	0.213	0.195	0.223	0.189	0.330	0.335	0.357
Fe	1.400	1.265	1.446	1.291	1.533	1.460	1.621	1.416	1.554
Mn	0.013	0.007	0.014	0.007	0.015	0.014	0.010	0.006	0.009
Mg	2.923	2.892	2.880	2.874	2.806	2.707	2.494	2.608	2.542
Cr	0.036	0.066	0.030	0.035	0.039	0.056	0.033	0.040	0.031
Ca	1.807	1.828	1.847	1.872	1.866	1.897	1.880	1.874	1.886
Na	0.754	0.716	0.683	0.652	0.715	0.630	0.538	0.471	0.586
K	0.057	0.062	0.113	0.096	0.187	0.232	0.361	0.382	0.271

TABLE 2.4. Amphibole analyses from each of the Achiltibuie gabbros. Cations are calculated on the basis of 23 oxygens in the water free formula. X<sub>Mg</sub> is the ratio Mg / (Mg + Fe + Mn). a refers to polygonal grains, b refers to symplectite grains.

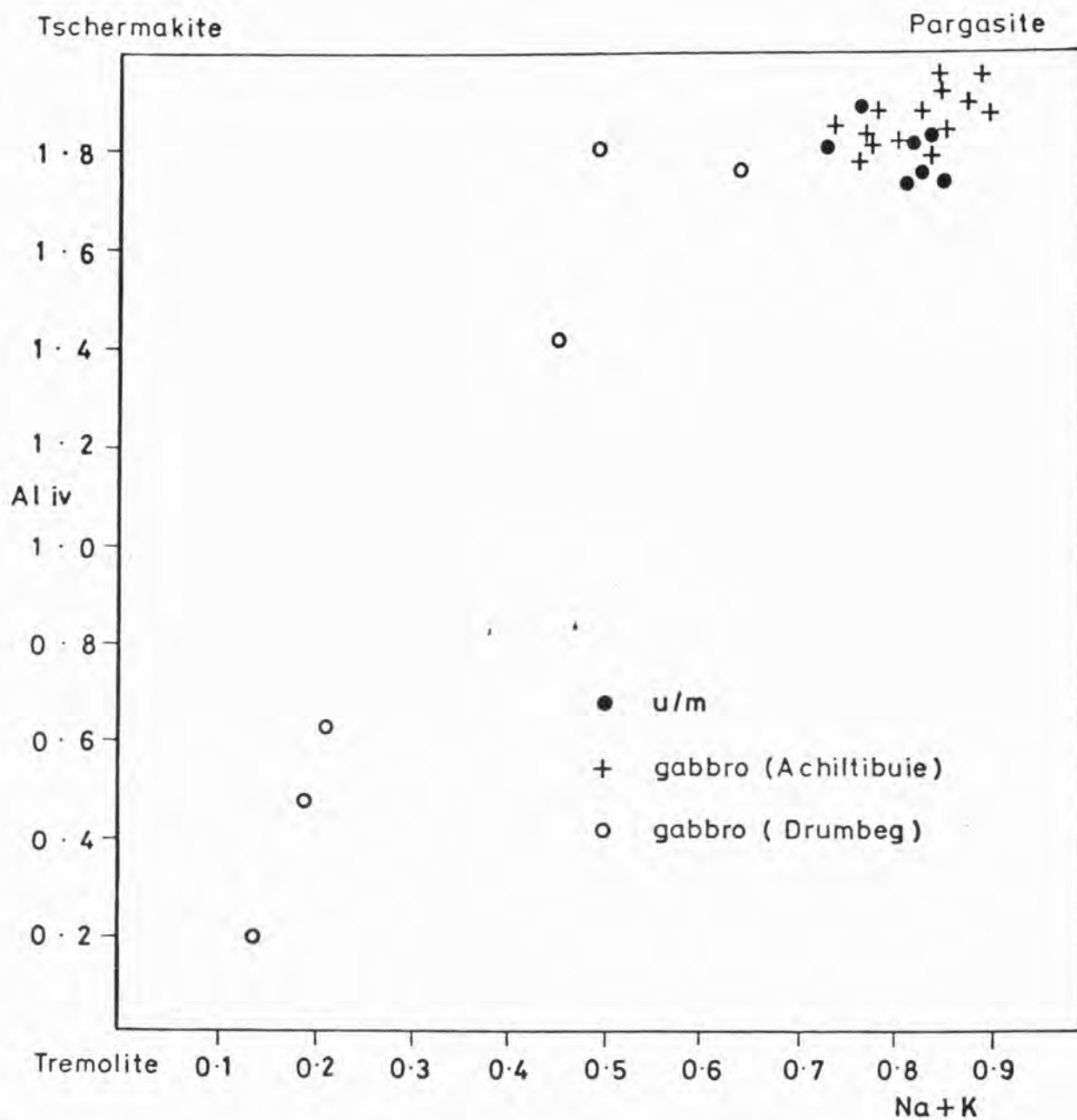


FIG. 2.9 Plot of amphiboles after fig.60 of Deer et al.(1966).

Cations are calculated on the basis of 23 oxygens in the water free formula. The open circles are retrogressive amphiboles rimming pyroxenes in the Drumbeg gabbros.

solid solution. The coexisting magnetites have up to 5 mol% chromite and very little spinel. These grains finally equilibrated at very low temperatures (400 - 450°C) but to rehomogenize them would require temperatures in the order of 860° (Turnock and Eugster, 1962). In the Drumbeg gabbros magnetite and ilmenite occasionally occur as composite grains. The  $R_2O_3$  component of ilmenite and the  $TiO_2$  content of coexisting magnetite are extremely low indicating final equilibration at temperatures of about 300 - 350°C (Buddington and Lindsley, 1964). MnO and MgO contents of ilmenite are antipathetic, neither being greater than 1 wt%. The chrome content of ilmenite is below MDL but there is up to 1 wt%  $Cr_2O_3$  in magnetite. Rare sulphide grains are pyrite with very low Ni and Co contents.

## 2.6. TEMPERATURE AND PRESSURE OF METAMORPHISM

It is intended in this section to provide some estimate of the physical conditions of granulite facies metamorphism of these rocks. Although two-pyroxene and pyroxene-garnet geothermometry and geobarometry are fraught with problems (O'Hara, 1977; O'Hara and Yarwood, 1978; Rollinson, 1978; Fraser and Lawless, 1978) it has been possible to reconstruct a reasonably self-consistent P - T grid using published mineral geothermometers and geobarameters (Fig.2.10). One of the main difficulties, apart from imprecise thermodynamic data and mixing models, is the problem of blocking temperatures, i.e. different mineral pairs close at different temperatures. This was outlined by Fraser and Lawless (1978) who state that Al-exchange between garnet and orthopyroxene stops at a higher temperature than Fe-Mg exchange between the two pyroxenes. The evidence for construction of the model presented in Fig.2.10 is discussed below.

It will be demonstrated in Chapter 3 (and in Sills et al. in prep) that a study of the whole-rock chemistry of the layered ultramafic-

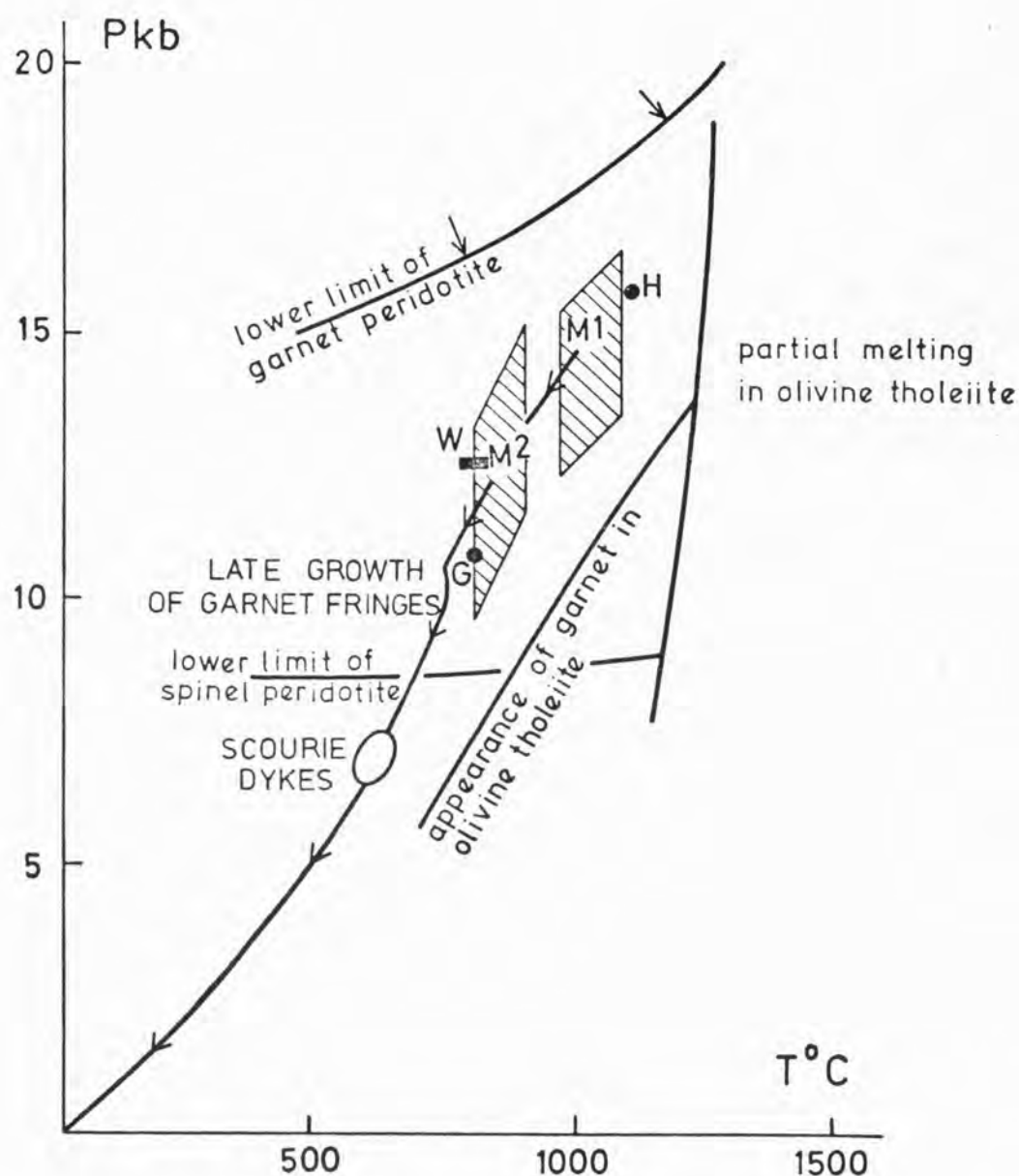


FIG. 2.10 Part of the P-T evolution of the Scourian based on the ultramafic-gabbro bodies. Parallelograms represent the P-T range for the  $M_1$  and  $M_2$  assemblages. H is the estimate of O'Hara and Yarwood (1978), W the estimate for S. Harris (Wood, 1975) and G the estimate for S.W. Greenland (Wells, 1979) for the granulite facies metamorphism. Other data is from: Green and Ringwood (1967), Green and Hibberson (1970), O'Hara et al. (1971) and Herzberg (1975). The P-T estimate for the Scourie dykes is taken from the data of O'Hara (1961b).

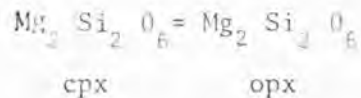
gabbro bodies suggests that the precursor igneous assemblage included two pyroxenes and olivine but no garnet. The large amounts of metamorphic garnet must either have formed from a reaction between olivine and plagioclase (as suggested by Wood, 1975) or from a reverse of the garnet-breakdown reactions. There could not have been enough igneous olivine in the gabbros for the first possibility, so presumably garnet formed from pyroxene and plagioclase reactions. For this to occur the igneous crystallisation pressure was increased to a metamorphic pressure, perhaps due to burial in a magmatically thickened crust as suggested by Wells (1980).

The earliest mineral assemblage ( $M_1$ ) has been inferred from textural evidence, but the present mineralogy is of little use in quantitatively estimating the P-T conditions of  $M_1$ ; nevertheless certain constraints may be placed upon these conditions. These conditions suggest 12 - 15 kb total pressure and a temperature of about  $1000^\circ\text{C} \pm 100^\circ\text{C}$ . The  $M_2$ , P-T estimate is based on mineral geothermometers and barometers (Fig.2.10). Slightly higher pressures and temperatures than those obtained for  $M_2$  are needed to account for the exsolution of orthopyroxene and minor plagioclase from clinopyroxene and for the garnet-breakdown reactions, which involve exsolution of ca-tschermak's molecule and jadeite from clinopyroxene. This places  $M_1$  to the right of  $M_2$  in Fig.2.10. The plagioclase-free ultramafics show no evidence of having been garnetiferous, thus restricting pressures to a maximum of 18 kb (O'Hara et al., 1971). The low mg gabbros show no evidence that plagioclase was totally consumed in clinopyroxene and garnet (i.e. eclogite), although plagioclase content was probably quite low. This limits pressure to approximately 16 kb (Green and Ringwood, 1967). However the high mg gabbros at Achiltibuie, which have no  $M_1$  plagioclase, contain  $M_1$  pargasite which formed partially at the expense of plagioclase; this means that the

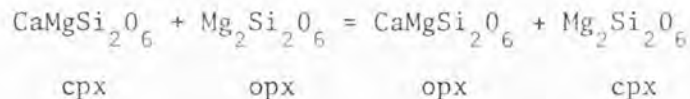
pressure could have been lower than this 16 kb limit. The tonalitic gneisses were never garnetiferous limiting pressure to a maximum of  $13 \pm 2$  kb (Wood, 1975). No evidence for large scale partial melting has been observed; this limits temperature to a maximum of 1150 to 1200°C (Green and Ringwood, 1967).

Temperatures for the formation of  $M_2$  assemblages were derived by the methods of Wood and Banno (1973), Wells (1977), Nehru and Wyllie (1974), Lindsley and Dixon (1976), Powell (1978), Råheim and Green (1974), Ganguly (1979), Ellis and Green (1979), and Danckwerth and Newton (1978). These two-pyroxene garnet methods concern only the exsolved clinopyroxene host, because it is intended to estimate the temperature after exsolution of orthopyroxene lamellae, due to changes in  $P-T$  from  $M_1$  to  $M_2$ .

The empirical geothermometer based on the reaction



of Wood and Banno (1973) and Wells (1977) gives values ranging from 750° to 940°C (Table 2.5). The experimental calibrations of Nehru and Wyllie (1974) and Lindsley and Dixon (1976) give much lower values (see Table 2.5). The equation



calibrated by Powell (1978) gives temperatures in the range 700 - 800°C. The iron-exchange reaction between garnet and clinopyroxene was calibrated experimentally by Råheim and Green (1974) and their 30 kb data have been extended to lower pressures as suggested by Wood (1977). The  $k_D$  is almost independent of pressure in this temperature range and values range from 750° - 850°C. Wood (1977) and Ganguly (1979) have shown that non-



ideal mixing in Ca-Mg garnets leads to a considerable error. The method of Ganguly (1979) yields temperatures about 150°C higher than those quoted above. Ellis and Green (1979) have experimentally recalibrated the original Råheim and Green (1974) equation to account for this non-ideality. Their equation yields temperatures in the range 780° to 870°C which is consistent with the two-pyroxene temperatures. Correction for  $\text{Fe}^{3+}$  (calculated stoichiometrically) lowers the temperatures by up to about 60°C.

Aluminous enstatite co-existing with spinel is a potentially useful geothermometer (Obata, 1976; Danckwerth and Newton, 1978). Using the experimental data of Danckwerth and Newton (1978) and assuming ideal mixing in spinel and olivine, temperatures again fall in the range 790°C to 940°C for pressures of 8 - 15 kb. The spinel-olivine geothermometer of Roedder et al. (1979) gives temperatures about 800°C.

Pressure has been derived from the geobarometer of Wood (1974) which depends on the alumina content of orthopyroxene co-existing with garnet. Values range from 4.6 to 18.5 kb (Table 2.5). This large range is due to:

- (a)  $X_{\text{Al}}$  depends critically on the correct estimation of the  $\text{Fe}^{3+}$  content of the orthopyroxene.
- (b) The reaction is strongly temperature dependent at these low pressures.
- (c) re-equilibration of the alumina distribution between mineral pairs (e.g. orthopyroxene and amphibole) during uplift and cooling.

Low pressures are derived from coarse, well crystallized orthopyroxenes. However the orthopyroxenes most likely to be in Al-exchange equilibrium with the garnet are those from the garnet-breakdown symplectites and these yield higher pressures, 9 - 15 kb on average for

the temperature range 800 - 900°C.

The best estimate of the P-T conditions for the  $M_2$  metamorphism is taken as the area outlined by the overlap of the garnet-pyroxene and two pyroxene temperatures and the pressures derived from the Wood (1974) geobarometer. These conditions are approximately 800 - 900°C and 10 - 14 kb. This is comparable with other estimates for the Scourian granulite facies metamorphism (Wood, 1975; Rollinson, 1978; Rollinson, 1980, see Table 2.6) but considerably lower than the estimate of O'Hara and Yarwood (1978) and Barnicoat and O'Hara (1979). The former is partially based on an alternative interpretation of the garnet-breakdown textures as previously discussed. The temperature of 1000°C obtained by Barnicoat and O'Hara (1979) from pyroxenes in a meta-ironstone could be correlated with the  $M_1$  temperature derived in this study. The  $M_1$  pressure and temperature are thought to represent the peak of metamorphism. Uplift of the Lewisian complex caused the garnet-clinopyroxene pairs to become unstable and the reaction coronas developed producing the  $M_2$  assemblages. Fe-Mg exchange between co-existing orthopyroxene, clinopyroxene and garnet ceased at about 800 - 900°C, which is the temperature quoted by some authors (Wood, 1975; Rollinson, 1980) for the peak of metamorphism.

This  $M_2$  temperature is slightly greater than the 800°C obtained by Wells (1979) for the Buksefjorden area of S.W. Greenland (with 10.5 kb pressure). It is believed that the Scourian represents a slightly lower structural level than that part of S.W. Greenland which is transitional between the granulite and amphibolite facies.

Minor regrowth of a more almandine-rich garnet has occurred around opaque oxide grains. This does not require any major thermal event and the temperature required to stabilise this iron-rich garnet could lie on a slope between the P-T for  $M_2$  assemblages and the intrusion of the

AUTHORS	AREA	PRESSURE (kb)	TEMPERATURE(°C)
This work	Lewisian (M <sub>1</sub> )	12-15	1000 <sup>±</sup> 100
This work	Lewisian (M <sub>2</sub> )	9-14	800-900
O'Hara & Yarwood (1978)	Scourie	15 <sup>±</sup> 3	1150 <sup>±</sup> 100
Wood (1975)	S.Harris	10-13	800-860
Rollinson (1980)	Scourie		830-890
Weaver et al. (1978)	S.India	9-10	720-840
Wells (1979)	Bukjesfjorden S.W.Greenland	10.5	810
Hensen & Green (1973)	Various (gt-cord pairs)	8-9	800-930

Table 2.6 Various estimates of P - T conditions for granulite facies metamorphism.

Scourie dykes (Fig.2.10). However some extra energy source may be required to nucleate this garnet. The composition of the garnet and clinopyroxene in the rocks yield temperatures in the range 650 - 700°C (Råheim and Green, 1974), but the garnet is not in textural equilibrium with the clinopyroxene. However iron-rich garnets are stabilised at lower temperatures than Mg-rich garnets (Green and Ringwood, 1967). This garnet regrowth could be correlated with the Inverian retrogression or may be due solely to uplift.

#### 2.6.1. Sensitivity of the Temperatures on Fe/Mg ratios

All mafic phases in the gabbros at Achiltibuie show decreasing mg up the stratigraphic section (Table 2.7, Chapter 3), so the temperatures generated by the various models were compared to see if there was any systematic changes correlated with Fe/Mg ratios and if any method was more sensitive than another. The data are presented in Table 2.7. There is no systematic variation and the range for each method is mostly within the estimated errors of  $\pm 30 - 50^\circ\text{C}$ .

#### 2.6.2. Estimation of water vapour pressure

Calculation of water vapour pressure during granulite facies metamorphism can be made by extending the simple amphibole component equilibria into more complex systems involving natural hornblendes (Wells, 1976, 1979), but there is considerable uncertainty due to the large differences in composition between tremolite and pargasitic hornblendes. Two further constraints can be placed on  $P_{\text{H}_2\text{O}}$  during granulite facies metamorphism:

(a) the experimentally determined breakdown of Mg-hornblende (Choudari and Winckler, 1967, Wells, 1979).

	mg OPX	mg CPX	mg GT	Wood + Banno	Wells	Nehru+ Wyllie +Dixon	Lindsley	Powell	Raheim +Green	Ganguly	Ellis+ Green
W32	0.693	0.804	0.445	819	798	1974 1976	1978	1974 1979	1979	836	836
W34A	0.689	0.770	0.443	851	840	687	712	792	930	836	836
W35	0.660	0.748	0.430	798	782	624	634	797	935	842	842
W36a	0.620	0.726	0.365	808	810	655	678	755	909	814	814
b	0.614	0.724	0.349	801	802	646	667	743	885	784	784
c	0.628	0.722	0.347	833	842	689	723	754	886	786	786
W37	0.630	0.713	0.380	808	807	651	673	751	920	828	828
Range of temps				53	60	65	89	42	52	50	52
Highest value				W34A	W36c	W36c	W36a	W35	W32, W35	W35	W35
Lowest value				W36b	W35	W35	W35	W36b	W36b, c	W36b, c	W36b, c

TABLE 2.7 Various temperatures for the Achiltibuie gabbros, W32 forms the base of the section, W37 the top.

(b) for the estimated P - T of 10 - 14 kb and 800 - 900°C for the Lewisian, under conditions of  $P_{\text{H}_2\text{O}} = P_{\text{TOT}}$  the quartzofeldspathic gneisses would have been largely molten at temperatures which are substantially above the experimentally determined  $\text{H}_2\text{O}$ -saturated solidus (Winckler, 1976).  $P_{\text{H}_2\text{O}}$  must have been less than  $P_{\text{TOT}}$  as there is no evidence for widespread partial melting coeval with granulite facies metamorphism. Limits can be placed on  $P_{\text{H}_2\text{O}}$  by assuming that the gneisses were on the point of melting which constrains  $P_{\text{H}_2\text{O}}$  values to between  $0.35 \pm 0.15 P_{\text{TOT}}$  at 9 - 12 kb total pressure (Wells, 1979).

It is possible to estimate  $P_{\text{H}_2\text{O}}$  from equilibria involving a fluid phase, if the relevant thermodynamic data are available, using the standard relationship:

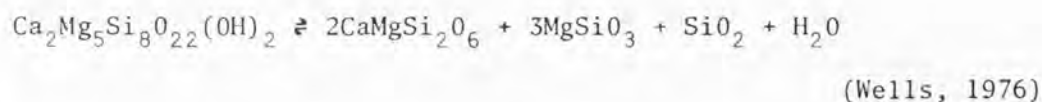
$$\Delta H_{1,T}^{\circ} - T \Delta S_{1,T}^{\circ} + (P-1)\Delta V_{1,298,\text{solids}}^{\circ} = -RT \ln K. \quad (\text{Wood and Fraser, 1976})$$

If the reaction involves a fluid phase, this can be rearranged to give the following relationship:

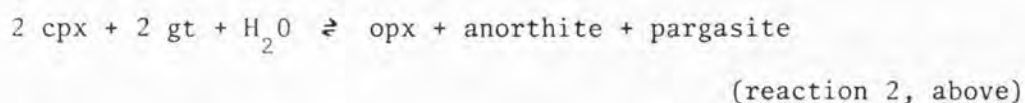
$$\ln a_f = \frac{1}{R} \left( \Delta S_{1,T}^{\circ} - \frac{\Delta H_{1,T}^{\circ}}{T} - \frac{(P-1)\Delta V_{1,298,\text{solids}}^{\circ}}{T} \right) - \ln K_{\text{solids}}$$

where  $a_f$  is the activity of the fluid phase (Wells, 1976).

Assuming the fluid phase is an ideal mixture,  $a_f$  is given by the product of its partial pressure and its fugacity coefficient (data from Burnham et al., 1969). The following equilibria can be considered:



and



The first of these equilibria is not really relevant to the Lewisian mafic

rocks because they do not contain quartz, but the mineral compositions yield a  $P_{\text{H}_2\text{O}}$  of about 2.5 kb which is in the same range as that obtained by Wells (1976) for S.W. Greenland. The second reaction, the garnet-breakdown reaction for the Achiltibuie gabbros, yields very low values of  $P_{\text{H}_2\text{O}} < 0.1 P_{\text{TOT}}$ . The activities of the Mg-component in the amphiboles and pyroxenes were estimated using an ideal mixing on sites model, the activity of the mg-garnet component was calculated using the data of Wood (1977) and the activity of the anorthite component was estimated using the data of Orville (1972). The thermodynamic data were taken from Robie et al. (1978) and Helgeson et al. (1978).

These data combined with the discussion of Wells (1979) limits the  $P_{\text{H}_2\text{O}}$  to approximately 0.1 - 0.4  $P_{\text{TOT}}$  during granulite facies metamorphism. The other fluid components were probably dominated by  $\text{CO}_2$ .

#### CONCLUSIONS

The original mafic-ultramafic bodies were subject to high pressure granulite facies metamorphism at pressures of 10 - 14 kb and temperatures of about 1000°C. This represents the peak of metamorphism. Trace element and rare-earth geochemistry suggests that garnet was not involved in the precursor igneous assemblages (Sills et al. in prep), thus implying burial of the bodies to  $M_1$  conditions. This burial could be due to an overaccreting magmatically thickened crust (Wells, 1979, 1980) which would also provide a source for the high temperatures. The coronas around garnet are retrogressive in origin, and their development is thought to be due to almost isothermal uplift of the Scourian complex after the peak of metamorphism. This is compatible with rapid uplift erosion shortly after this peak (England and Richardson, 1977). The Fe-Mg exchange reactions in pyroxenes and garnets "closed" at about 800 - 900°C but the oxide minerals continued to re-equilibrate to much lower temperatures

(Rollinson, 1980). The gneisses were held at these elevated temperatures ( $> 700^{\circ}\text{C}$ ) for a considerable period of time to obliterate any zonation in the mineral compositions.

Garnet stability during metamorphism was strongly dependent on the whole rock  $\text{FeO}/(\text{FeO} + \text{MgO})$  ratio of the sample concerned. A value of 0.3 seems to be the lowest value for which garnet was stable, as the low  $\text{FeO}/(\text{FeO} + \text{MgO})$  ultramafic granulites show no evidence of ever having been garnetiferous. All other samples, with ratios between 0.3 and 0.6, contained garnet at the peak of metamorphism. During uplift, in samples with a ratio of about 0.3 to 0.4, garnet broke down completely to spinel + opx + plag symplectites. (O'Hara and Yarwood, 1978; Savage, 1979; Savage and Sills, 1980) In the more iron-rich mafic granulites garnet was stable throughout although partial breakdown of the garnets occurred (reactions 1 and 2).

The rate of garnet corrosion was probably controlled by intra-granular diffusion in garnet, although some armouring of reactant garnet and clinopyroxene by product orthopyroxene, plagioclase and iron-oxides may have been important. The geometry of the coronas is probably a function of the slow diffusion of aluminium.

The garnet granulites studied show evidence of the mineral assemblages and reactions typical of the gabbro-eclogite transition (Green and Ringwood, 1967). Although similar examples are well documented from Phanerozoic suites, high pressure metamorphism of this type is the exception rather than the rule in Archaean metamorphic terrains. Indeed the absence of high pressure rocks such as eclogites and blueschists from the Archaean has been cited as direct evidence of a fundamental difference in tectonic processes and mechanisms of crustal growth during this period from later geological times (Green, 1975; Lambert, 1976). One suggested cause for this absence is the possible higher geothermal gradient in the

Archaean and the predicted instability of eclogite (Green, 1975; Fyfe, 1978). Estimates of pressure suggest depths of burial of 35 - 45 km at the peak of metamorphism. Geophysical data suggests a modern crustal thickness of 25 - 30 km under north-west Scotland, Lewisian type granulites extending to the crust mantle boundary (Bamford and Prodehl, 1977). If there has been no subsequent underplating this implies crustal thicknesses in the late Archaean of 60 - 75 km. As metamorphic isograds in the Lewisian are almost horizontal, this implies that mafic rocks in the region at 6 km depth at present would presumably have crystallized as eclogites if there had been no underplating (Fig.5).

For the Lewisian, at least, these conclusions question the assumption of a universally "thin" Archaean crust and concomitant conceptions of Archaean geological processes (Glikson, 1971, Fyfe, 1973, 1978; Kroner, 1977; Taylor and McLennan, 1979). Quite clearly, this particular segment of the Archaean crust shows many features attributable to growth by protoplate tectonic processes and is consistent with the suggestion (Windley and Smith, 1976) that Archaean high-grade terrains represent equivalents of deep levels in destructive plate boundaries.

It is becoming apparent that garnet metabasic rocks are a common component of the lower continental crust. These rocks are a common, but minor component of Archaean high-grade gneiss terrains which are thought to represent deep levels of the Archaean continental crust. Nodules of garnetiferous metabasic rocks (thought to be derived from the lower continental crust) in volcanic ejecta in the Eifel region of Germany show remarkable similarities to the Lewisian rocks described here (Okrusch et al., 1979). Garnetiferous metagabbro also forms a significant proportion of the Ivrea-Verbano zone, N. Italy, which is also a section of the Palaeozoic lower crust (e.g. Rivalenti et al., 1975).

## CHAPTER 3

PETROGENESIS OF LAYERED ULTRAMAFIC -  
GABBRO BODIES

### 3.1. INTRODUCTION

Remnants of layered igneous complexes occur in many high grade granulite gneiss terrains (Windley, 1977 pp.9-12). They typically form layers, lenses or pods up to 1 km thick, conformably bounded by gneisses, metavolcanic amphibolites or metasediments and were subject to the same intense deformation and high amphibolite to granulite grade metamorphism as their host rocks. There are broadly two types:

(1) Those composed dominantly of anorthosite and leucogabbro such as the Fiskenaasset complex, W.Greenland (Windley et al., 1973; Myers, 1976; Weaver et al. in press), the Sittampundi complex, S.India (Janardhan and Leake, 1975), the Messina complex in the Limpopo belt of Southern Africa (Hor et al., 1975; Barton et al., 1979), and the Rodil complex, S.Harris, Outer Hebrides, Scotland (Dearnley, 1963; Wittey, 1975).

(2) A lesser known group dominated by ultramafic and mafic rocks which is prominent in the Lewisian of the mainland of N.W.Scotland (Bowes et al., 1964).

The aim of this chapter is to examine the igneous history of this latter type of intrusion prior to granulite facies metamorphism in order to better understand the nature of Archaean magmatic processes and the evolution of the Archaean crust.

The origin of the Lewisian bodies has caused considerable controversy, five modes of formation have been proposed:

(1) Deformed, fragmented and metamorphosed layered igneous intrusions (Bowes et al., 1964, 1966; Bowes et al., 1970; Davies, 1974, 1976; Savage, 1979)

(2) 'Zoned' intrusions, the gabbroic rocks forming an aureole developed by diffusional mass transfer between igneous peridotite and acid gneisses under granulite facies conditions (O'Hara, 1961a, 1965).

(3) Basic and ultrabasic igneous rocks modified by metasomatic interchange with the surrounding acid gneisses (Bowdidge, 1969). He also proposed an alternative origin for both rock types as crystal cumulates with hornblende as the dominant cumulus phase.

(4) Fragments of undepleted mantle (Weaver and Tarney, in press), similar to the situation in the Ivrea-Verbano zone of N. Italy where iron-rich gabbros overly mantle peridotite (Rivalenti et al., 1975).

(5) Liquid compositions with komatiitic affinities, possibly representing thrust slices of Archaean oceanic crust (Weaver and Tarney, in press).

In order to clarify the issues new whole-rock data are presented.

### 3.2. FIELD RELATIONSHIPS

The field relationships and sketch maps of some ultramafic-gabbro bodies have been presented in Chapter 2, so only a few points relevant to the origin of these bodies will be given here.

The bodies occur as conformable lenses up to 1 km long and up to 100 m thick. No discordances have been seen by the author but a discordance between gabbro and tonalitic gneiss has been reported (Rollinson, 1978) which implies that the gneisses cut the ultramafic-gabbro body. Davies (1975) indicates that a small proportion of the quartzo-feldspathic gneisses and metasediment may predate the intrusion of the layered bodies which were subsequently broken up by the intrusion of large volumes of tonalitic magma. Lead isotopic studies (Chapman and Moorbath,

1977) cannot distinguish between the "older" and "younger" gneisses, so the age relationships between the ultramafic-gabbro bodies and the tonalitic gneisses are still unclear. Minor amounts of meta-sediment are occasionally found bordering these bodies (e.g. Barnicoat and O'Hara, 1979) and no really convincing metasediment has been found elsewhere; however this may be due to less thorough observation away from the layered bodies. Layered bodies are occasionally cut by discordant, thin (1 - 5 m) trondjemite or granite sheets (Rollinson and Windley, 1980b; Savage, 1979).

The bodies consist of a repeated ultramafic-gabbro successions with modal feldspar often increasing up the section, providing a means for determining the way-up of the body. In the Camas nam Buth body, Scouriemore, thin sulphide-rich horizons occur adjacent to ultramafic layers (Savage, 1979). By analogy with unmetamorphosed layered intrusions (e.g. Campbell, 1977) it is inferred that the ultramafics formed the base and the sulphides the top of what were originally gravity stratified units. The Camas nam Buth body was shown to be folded isoclinally during the early Scourian so that the stratigraphy has been repeated and the base is now in the centre (Savage, 1979). In the Assynt region, Inverian folding has obscured any early Scourian structures. Layered anorthosites, genetically related to the ultramafic-gabbro bodies have been reported; e.g. Achiltibuie (Bowes et al., 1964) and from Gorm Loch in the Laxford Front (Davies, 1974). However all anorthosites seen by the author are discordant "patches" (as at Achiltibuie, near Drumbeig and in the Culag body) or discordant sheets (as at Gorm Loch). The rare-earth patterns for these anorthosites are very steep, strongly HREE depleted with large, positive Eu anomalies. These could not be derived by crystal fractionation from the ultramafic-gabbro bodies which have flat to LREE enriched patterns (see later and Table 3.5). These

anorthosites may represent small scale, local partial melts of the surrounding gneisses (Weaver and Tarney, in press).

The ultramafics have a pronounced compositional layering (Fig. 2.2) due to differing proportions of the main component minerals: olivine, orthopyroxene and amphibole. Occasional totally serpentinitised layers (e.g. near Gorm Loch Mor, 136303) may represent dunite, and harzburgite occurs locally. The layers are commonly a few millimetres thick but massive units locally reach 10m (e.g. N shores of Loch Drumbeg, 118328). The layering in the gabbros is less well marked, usually expressed by felsic or mafic schlieren. The layering is always conformable to the foliation in the bordering gneisses. It is difficult to envisage how the layering in the ultramafics could have developed other than by mimicking original igneous layering. The proportion of ultramafic to gabbro varies considerably from body to body but in general is about one third ultramafic to two thirds gabbro.

### 3.3. CRYPTIC LAYERING IN THE ACHILTIBUIE BODY

This section examines the mineral chemistry in terms of possible cryptic variation with stratigraphic height. The Achiltibuie body was selected for this particular study because of the good preservation of granulite facies mineral assemblages throughout its thickness.

As can be seen from Fig.3.1, all mafic phases in the gabbro show an increase in FeO content and a decrease in Mg/Mg + Fe + Mn up the section; from 0.69 to 0.61 in orthopyroxene, from 0.77 to 0.725 in clinopyroxene, from 0.45 to 0.35 in garnet and from 0.70 to 0.61 in amphibole. The  $TiO_2$  content of the amphibole increases from 1.4 to 4.0 wt.% and  $K_2O$  increases from 0.4 to 2.0 wt.% up the section. The  $Na_2O$  content of the amphibole shows a slight decrease

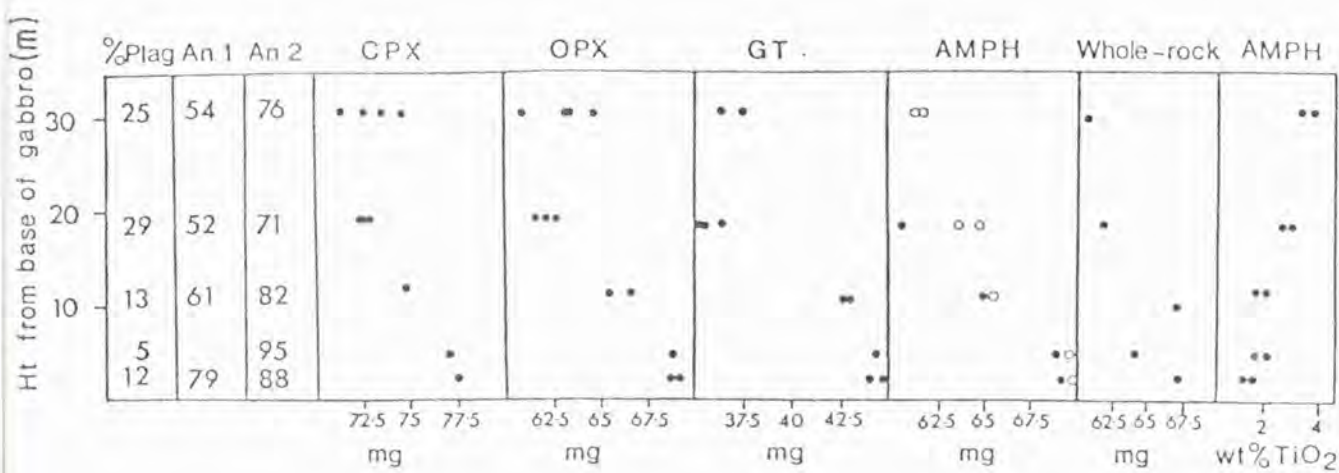


FIG 3.1 : Various parameters plotted against height from the base of the gabbro unit at Achiltibuie. Column 2 gives the An% of matrix plagioclase, Column 3 gives the An% of symplectite plagioclase, Columns 4-8 give mg for the phases indicated at the top of the column and column 9 gives the TiO<sub>2</sub> content of amphibole. Open circles in Column 7 refer to symplectite amphibole, filled circles to matrix amphibole.

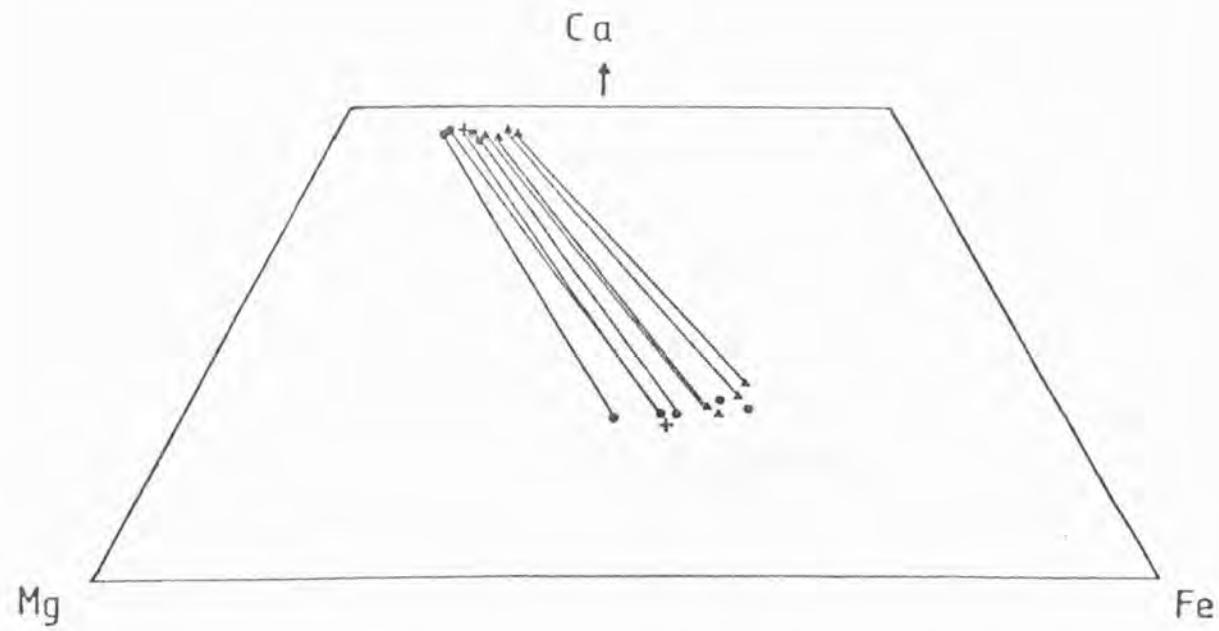


FIG 3.2 : Coexisting clinopyroxenes and garnets from Drunbeg (triangles), Achiltibuie (circles) and other localities (crosses) plotted in part of the Ca-Mg-Fe triangle. Tie lines join minerals from the same sample.

from 2.7 to 1.7 wt. %, corresponding to an increase in the albite content of the coexisting plagioclase. These trends are paralleled by the normative mineralogy. For example, there is an increase up the section in normative feldspar, which is coupled with a decrease in the anorthite content of this normative plagioclase from  $An_{77}$  to  $An_{61}$ . The whole-rock  $Mg / Fe + Mg$  ratio decreases from 0.67 to 0.60.

Although the present modal mineralogy is recognised as being entirely metamorphic, it is believed that this 'cryptic variation' mimics an upwards increase in  $Fe/Mg$  ratios in the original igneous assemblages. Metamorphic reactions are unlikely to have produced these trends because  $FeO$  contents of all mafic phases increase concomitantly (coexisting clinopyroxene and garnet are plotted in Fig.3.2, demonstrating that the most  $Fe$ -rich garnets coexist with the most  $Fe$ -rich clinopyroxenes). The cryptic variation apparently developed in response to increasing whole-rock  $Fe/Mg$  ratios with stratigraphic height. If these variations are founded on relict igneous fractionation trends then it follows that the metamorphism was isochemical (except for a few elements discussed below) over distances of 10 cm which is within the scale of the layering. One criticism of these trends representing the results of igneous processes is the small scale over which the variations occur (35 m). However there has been considerable tectonic thinning of these bodies, coupled with their break-up, associated with the intrusion of large amounts of invading tonalitic material, as envisaged for the Scourian gneisses by Davies (1975). Comparable cryptic variations over short stratigraphic distances are also reported from the Fiskenaeset complex, West Greenland (Windley and Smith, 1974) and the Messina complex, Southern Africa (Hor et al., 1975). Tectonic thinning of stratigraphic units of these bodies has also taken place during deformation associated with high grade metamorphism, but igneous cryptic variations can be locally preserved.

### 3.4. WHOLE-ROCK CHEMISTRY

Analytical Procedure: samples were analysed for major and trace elements by  $\chi$ -ray fluorescence using a Phillips P.W. 1450 spectrometer at the University of Birmingham. Full analytical details are given in Appendix B.

Representative analyses and a correlation matrix are presented in Tables 3.1 and 3.2 and full analyses in Appendix B.

Any assessment of the igneous fractionation processes which have taken place in the bodies prior to granulite facies metamorphism is dependent on the degree to which the metamorphism was isochemical. Depletion of granulite facies terrains, including the Lewisian, in some LIL elements, is well documented (Sighinolfi, 1971; Sheraton et al., 1973a; Heier, 1973; Rollinson and Windley, 1980a). Typically granulites are characterised by high K/Rb, Ba/Rb and low Rb/Sr, K/Sr and K/Ba ratios. In Tables 3.5 and 3.4 the average compositions of the ultramafic and mafic rock types are compared with unmetamorphosed igneous rocks of similar major and trace element chemistry. The gabbros have anomalous K/Rb and Rb/Sr ratios, but generally comparable Ba/Rb, K/Ba and K/Sr ratios when compared with unmetamorphosed rocks. This could be accounted for primarily by a depletion in Rb only. The ultramafics show no such depletion, probably due to the presence of pargasitic amphibole which is capable of holding the large Rb ion within its structure.

Although evidence exists for the mobility of K, and to a lesser extent Ba and Sr during retrogression to amphibolite facies (these elements increase in retrogressed samples), the general similarity of other elements and element ratios to unmetamorphosed igneous rocks (Tables 3.3, 3.4) suggests that the bodies remained isochemical during granulite facies metamorphism with the exception of Rb (and probably U, Th and Cs).

	W1	W9	W29	W4	W6	W32	W35	W36
SiO <sub>2</sub>	44.90	45.40	42.80	47.50	44.20	47.20	48.30	49.30
TiO <sub>2</sub>	0.37	0.36	0.18	1.02	1.97	0.63	0.61	0.53
Al <sub>2</sub> O <sub>3</sub>	4.1	5.5	3.0	13.1	11.0	10.1	11.2	12.1
Fe <sub>2</sub> O <sub>3</sub>	10.44	10.43	11.52	13.58	19.51	13.15	12.39	12.45
MnO	nd	nd	nd	nd	nd	0.20	0.17	0.24
MgO	30.43	29.19	32.90	7.89	8.15	13.39	12.29	9.96
CaO	7.19	7.11	6.06	12.27	12.59	13.37	12.75	13.49
Na <sub>2</sub> O	0.27	0.17	0.23	2.18	0.80	1.23	1.61	1.64
K <sub>2</sub> O	0.07	0.06	0.05	0.14	0.02	0.19	0.44	0.30
P <sub>2</sub> O <sub>5</sub>	0.02	0.01	0.01	0.05	0.16	0.01	0.02	0.06
TOTAL	97.79	98.13	96.75	97.92	98.40	99.47	99.88	100.07
Ni	1715	nd	nd	nd	nd	494	448	153
Cr	2869	2674	3096	491	511	1207	1199	502
Zn	73	92	143	115	124	78	87	77
Rb	1	2	1	< 1	2	2	< 1	< 1
Sr	33	29	20	268	29	59	84	71
Ba	16	16	30	52	23	12	21	82
Zr	18	21	20	43	39	17	17	26
Nb	2	2	2	2	9	1	1	1
Y	6	9	3	17	50	10	6	21
La	< 3	5	3	4	15	nd	nd	nd
Ce	< 3	< 3	< 3	14	20	nd	nd	33
Nd	< 3	< 3	< 3	nd	nd	nd	nd	17
Ca	9	7	4	18	14	14	12	11

TABLE 3.1 Representative analyses of ultramafics and gabbros. nd - element not determined. Full analyses and sample localities are given in Appendix B

	SiO <sub>2</sub>	TiO <sub>2</sub>	Al <sub>2</sub> O <sub>3</sub>	Fe <sub>2</sub> O <sub>3</sub>	limO	MgO	CaO	Na <sub>2</sub> O	K <sub>2</sub> O	P <sub>2</sub> O <sub>5</sub>	Cr	Ni	Zn	Rb	Sr	Y	Zr	Ba	Ga	
SiO <sub>2</sub>																				
TiO <sub>2</sub>	.38																			
Al <sub>2</sub> O <sub>3</sub>	.72	.39																		
Fe <sub>2</sub> O <sub>3</sub>	.64	.48	.30																	
limO		.24	.24	.08																
MgO		.32	.10	.10	.06															
CaO		.33	.28	.22	.06															
Na <sub>2</sub> O			.91	.86	.62															
K <sub>2</sub> O			.66	.44	.56															
P <sub>2</sub> O <sub>5</sub>			.69	.52	.52															
Cr			.43	.55	.44															
Ni			.70	.51	.70															
Zn			.72	.08	.72															
Rb			.19	.32	.19															
Sr			.39	.30	.30															
Y			.70	.34	.70															
Zr			.64	.64	.64															
Ba			.75	.75	.75															
Ga			.58	.58	.58															
			.60	.60	.60															
			.59	.59	.59															
			.76	.76	.76															
			.66	.66	.66															

TABLE 3.2 Correlation matrix for all the data from the ultramafics and gabbros. Correlations are significant for values of r greater than .45 at the 99.5% confidence limit.

The data for the ultramafics and mafic gabbros are plotted on an AFM (oxide) plot in Fig.3.3. This reveals an alkali-poor tholeiitic trend with a moderate degree of iron enrichment. Some ultramafics resemble peridotitic komatiites (Table 3.3, number 2) and picritic basalts (Table 3.3, number 4). This tholeiitic trend is in marked contrast to the Lewisian intermediate and acid gneisses which are calc-alkaline (Sheraton et al., 1973; Rollinson and Windley, 1980b). Indeed the tholeiitic trend contrasts sharply with the calc-alkaline trend of the ultramafics and gabbros analysed by Bowes et al. (1966) from layered bodies in the Drumbeg area. It is noticeable that the more retrogressed samples plot nearer the alkali apex of the AFM diagram. It is important to distinguish this late alkali metasomatism from the original geochemical characteristics of the rocks.

#### 3.4.1. Variation diagrams

A few plots (Fig.3.4) using  $\text{SiO}_2$  as an index of fractionation are presented to show the relationship between the ultramafic-gabbro bodies and the tonalitic gneisses. There is a sharp break in slope for some elements (Ti, P, Na, Ce, Y, and Al) at the boundary between the gabbros and the tonalites. Rollinson and Windley (1980b) present similar data which reveals the same features. The plots imply that the ultramafic-gabbro bodies cannot be a crystal residue extracted from the more silicic gneisses. Ti, Al, Y and Ce all increase with  $\text{SiO}_2$  in the gabbros and decrease in the tonalite to granodiorite gneisses. If these elements were removed from the tonalitic liquids by crystal fractionation the ultramafic-gabbro bodies cannot be the crystal fraction removed as they are depleted rather than enriched in these elements. The REE data are also inconsistent with the derivation of the ultramafic-gabbroic rocks from the tonalites; the former have flat to slightly LREE enriched

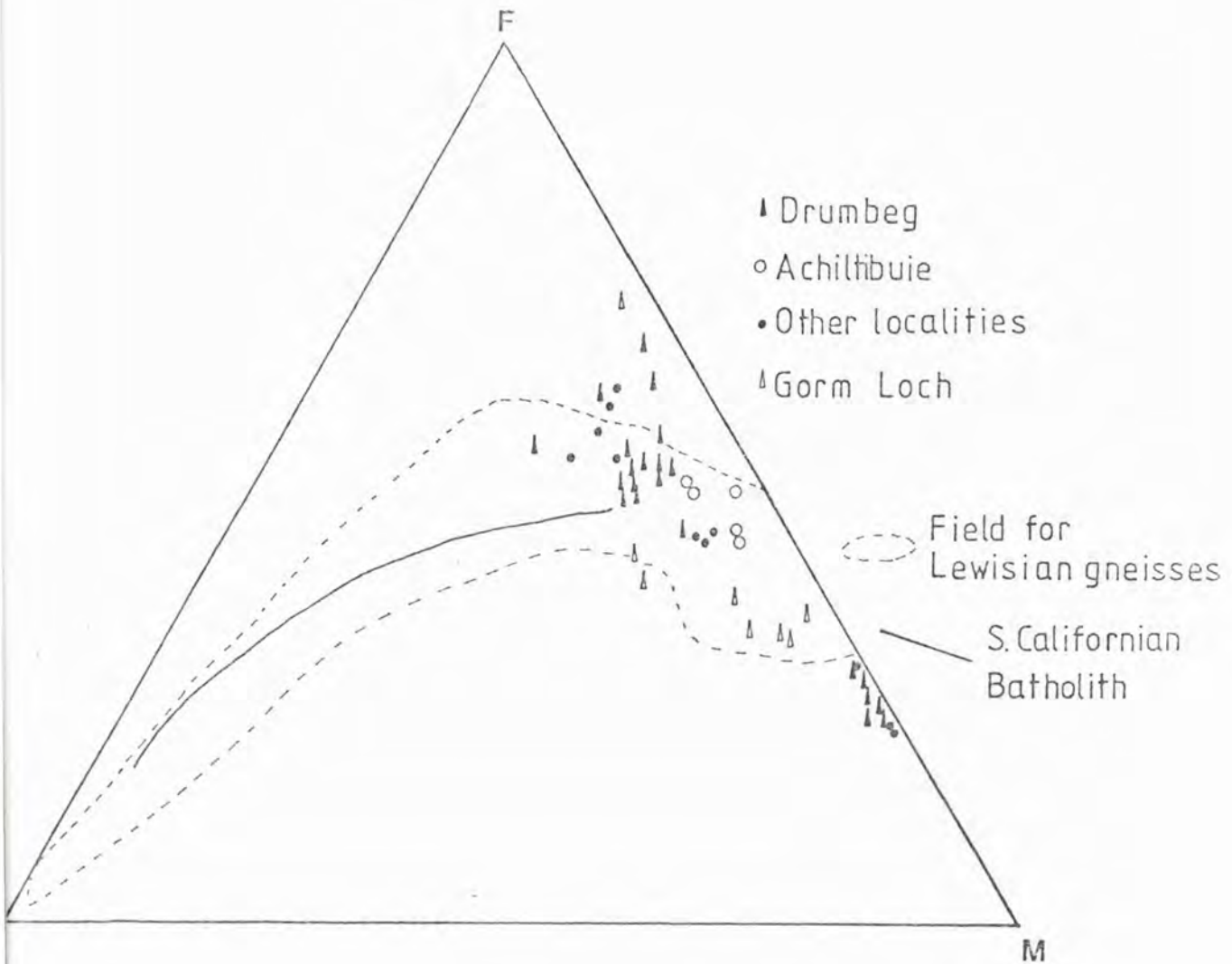


FIG. 3.3 A F M (oxide) plot for ultramafic-gabbro samples. A =  $\text{Na}_2\text{O} + \text{K}_2\text{O}$ , F = total iron as FeO and M = MgO. The field for Lewisian gneisses is from Rollinson (1978) and the trend for the S. Californian Batholith is from Carmichael et al. (1974).

	1	2	3	4	5	6
SiO <sub>2</sub>	46.09	54.02	47.41	44.00	44.43	49.50
TiO <sub>2</sub>	0.33	0.09	0.89	0.58	0.28	0.63
Al <sub>2</sub> O <sub>3</sub>	5.76	3.90	8.66	8.30	5.36	10.77
Fe <sub>2</sub> O <sub>3</sub>	12.45	0.82	2.81	2.20	12.53	1.39
FeO	-	4.22	11.15	8.80	-	11.26
MnO	0.21	0.03	0.20	0.19	0.22	0.20
MgO	25.77	31.76	19.29	26.00	31.72	17.80
CaO	7.18	1.92	6.76	7.30	4.87	7.54
Na <sub>2</sub> O	0.48	0.32	1.35	0.90	0.32	0.84
K <sub>2</sub> O	0.21	0.03	0.43	0.06	0.00	0.02
P <sub>2</sub> O <sub>5</sub>	0.02	0.01	0.10	0.07	0.02	0.05
H <sub>2</sub> O <sup>-</sup>		0.40	0.11			
LOI		2.01	1.45	0.97		
TOTAL	98.50	99.53	100.61	99.37	99.75	100.58
V	141	59	155		124	
Cr	2755	2300	290	2463	3100	706
Ni	1148	1300	500	1493	1655	222
Cu	19	<2	90	81		
Zn	102			60		
Rb	4			1	5	
Sr	39	<3	110	87	80	
Ba	17	2	150	44	4	
Zr	21	<20	90	45	17	
Y	7	<20	24	13	6	
K/Rb	436			498		
Ba/Rb	4.3			44	0.8	
Rb/Sr	0.10			.011	.063	
K/Ba	102	125	24	11		
K/Sr	45		32	6		

TABLE 3.3 Comparison of the layered ultramafics with other igneous rocks. 1 is the average Lewisian ultramafic (Sills et al. in prep; this average includes the data from this work and from Savage, 1979). 2 = orthopyroxenite, Central Indian Ridge (Engel and Fisher, 1975); 3 = Olivine dolerite, Palisades Sill (Walker, 1969); 4 = Picritic Basalt, Baffin Island (Clarke, 1970); 5 = Peridotitic Komatiite, Yilgarn Block, W. Australia (Nesbitt and Sun, 1976); 6 = Basaltic Komatiite, Belingwe Greenstone Belt (Nisbet et al., 1977).

	1	2	3	4	5	6	7
SiO <sub>2</sub>	47.47	50.60	50.67	51.57	46.37	48.56	47.09
TiO <sub>2</sub>	0.92	0.36	1.24	0.80	0.79	0.24	1.12
Al <sub>2</sub> O <sub>3</sub>	13.32	16.29	16.60	15.91	16.82	18.69	14.92
Fe <sub>2</sub> O <sub>3</sub>	13.57	1.87	1.33	2.73	1.52	2.27	3.82
FeO	-	4.12	7.37	7.04	10.44	4.30	7.30
MnO	0.24	0.09	0.16	0.17	0.09	0.11	0.20
MgO	9.11	9.59	8.02	6.73	9.61	9.26	9.05
CaO	12.17	14.33	11.58	11.74	11.29	12.67	12.67
Na <sub>2</sub> O	1.82	2.15	2.75	2.41	2.45	1.88	1.87
K <sub>2</sub> O	0.27	0.07	0.16	0.44	0.20	0.07	0.10
P <sub>2</sub> O <sub>5</sub>	0.08	0.04	0.11	0.11	0.06	0.02	0.10
H <sub>2</sub> O <sup>-</sup>	-	0.15		0.45	0.09	0.17	
LOT		0.52			0.29	1.72	
TOTAL	98.97	100.18	99.89	100.11	100.02	99.96	99.67
V	273	160	250	270	225	110	315
Cr	399	670	360	50	175	900	310
Ni	180	240	109	30	135	200	116
Cu	182	60	93		80	80	157
Zn	127					45	73
Rb	2			5			2
Sr	140	130	108	200	700	110	133
Ba	70	10	17	75	25	10	148
Zr	36	19	71	70	35	10	58
Y	21	10	35			25	28
K/Rb	1121			730			415
Ba/Rb	35			15			74
Rb/Sr	0.14			.025			.015
K/Ba	32	58	78	49	66	58	6
K/Sr	16	4	2	18	2	5	6

TABLE 3.4 Comparison of Lewisian gabbros with other igneous rocks.

1 is the average Lewisian gabbro (Sills et al. in prep; including data from this work and Savage, 1979). 2 = Average olivine gabbro, Central Indian Ridge (Engel and Fisher, 1975); 3 = Average low-K tholeiite, Central Indian Ridge (as 2); 4 = Average Island Arc Tholeiite, (Jakes and White, 1972); 5 = Average gabbro, Skaergaard LZB (Wager and Brown, 1967); 6 = Gabbro, Romanche Fracture (Nelson and Thompson, 1970) and 7 = Olivine tholeiite, Skye (Esson et al., 1975)

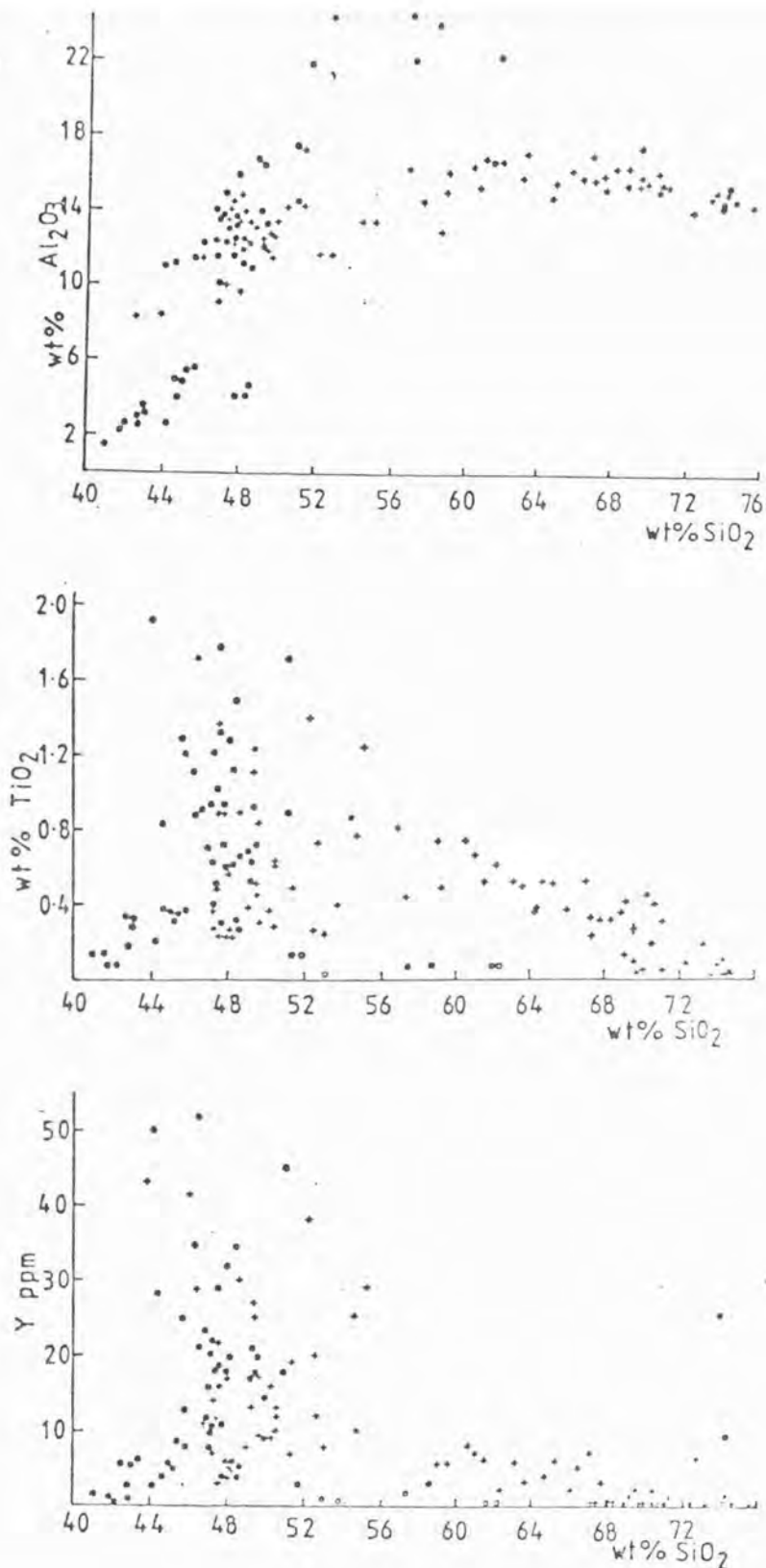


FIG. 3.4 SiO<sub>2</sub> versus Al<sub>2</sub>O<sub>3</sub>, TiO<sub>2</sub> and Y for all rock types.

Spots represent ultramafic-gabbro bodies, crosses all other gneiss types except for discordant quartzofeldspathic sheets (open circles).

patterns whilst the latter have strongly HREE depleted patterns (Weaver and Tarney, in press).

Any attempt to establish the phases controlling fractionation is handicapped by the fact that the granulite facies metamorphism has obliterated original textures and minerals. It is therefore necessary to establish using the whole rock data whether the bulk of the ultramafic gabbro bodies originated as cumulates (Bowes et al., 1964; Savage, 1979) or whether they represent primitive liquid compositions (Weaver and Tarney in press). Variation diagrams (Figs. 3.5 and 3.6) show the following features:

(a)  $\text{SiO}_2$  content is fairly constant, decreasing in only the most magnesian samples. This implies the fractionating phases had a combined  $\text{SiO}_2$  content of 45 to 48 wt.%, equivalent to the whole-rock concentrations.

(b) The  $\text{Al}_2\text{O}_3$ ,  $\text{CaO}$  and  $\text{Na}_2\text{O}$  contents all increase smoothly with fractionation; there are excellent correlations (Table 3.2) between  $\text{Al}_2\text{O}_3$  and  $\text{CaO}$ , and  $\text{Na}_2\text{O}$  and  $\text{MgO}$ .

(c) The  $\text{Fe}_2\text{O}_3$  (total iron) content is almost constant over the entire  $\text{MgO}$  range. The Zn variation is similar to iron.

(d) The Ni and Cr contents decrease markedly with decreasing  $\text{MgO}$ , implying that the liquid was rapidly depleted in these elements, presumably into early olivine and pyroxene. The ultramafics are characterised by high Ni (> 1000 ppm, up to 2500 ppm) and Cr (> 2500 ppm, up to 4000 ppm). These values may be greater than estimated compositions of the Archaean mantle (Sun and Nesbitt, 1977), implying these samples must have a cumulus component. The very high Cr contents may reflect a cumulus spinel component. Gabbros have Ni contents ranging from 500 to 50 ppm. The sulphide horizons found at the top of the rhythmic units at Camas nam Buth are depleted in Ni, further evidence that Ni was removed by an early fractionating phase (Savage, 1979).

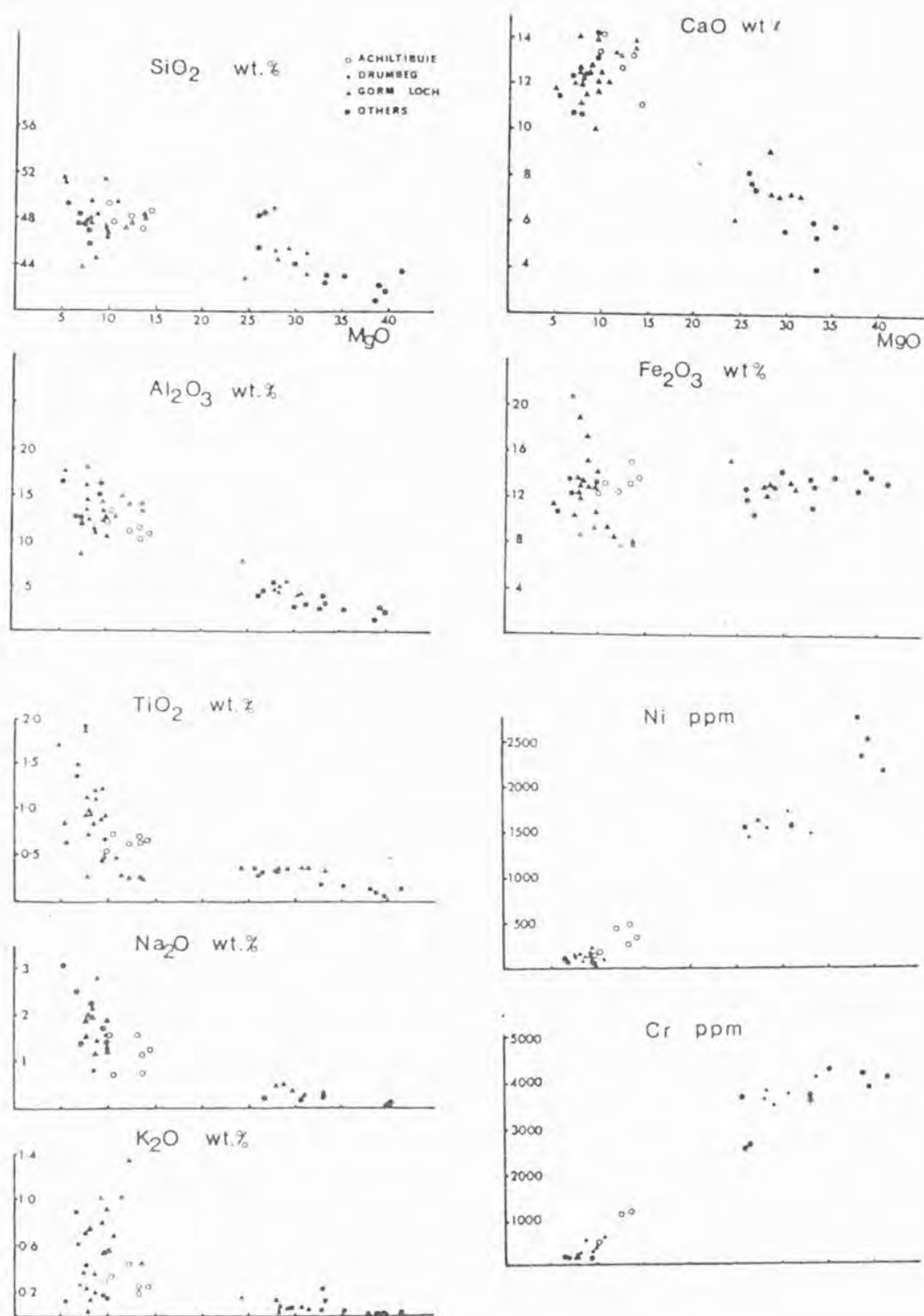


FIG. 3.5 MgO versus major elements and Ni and Cr for the ultra-mafic-gabbro bodies. Key at the top of diagram.

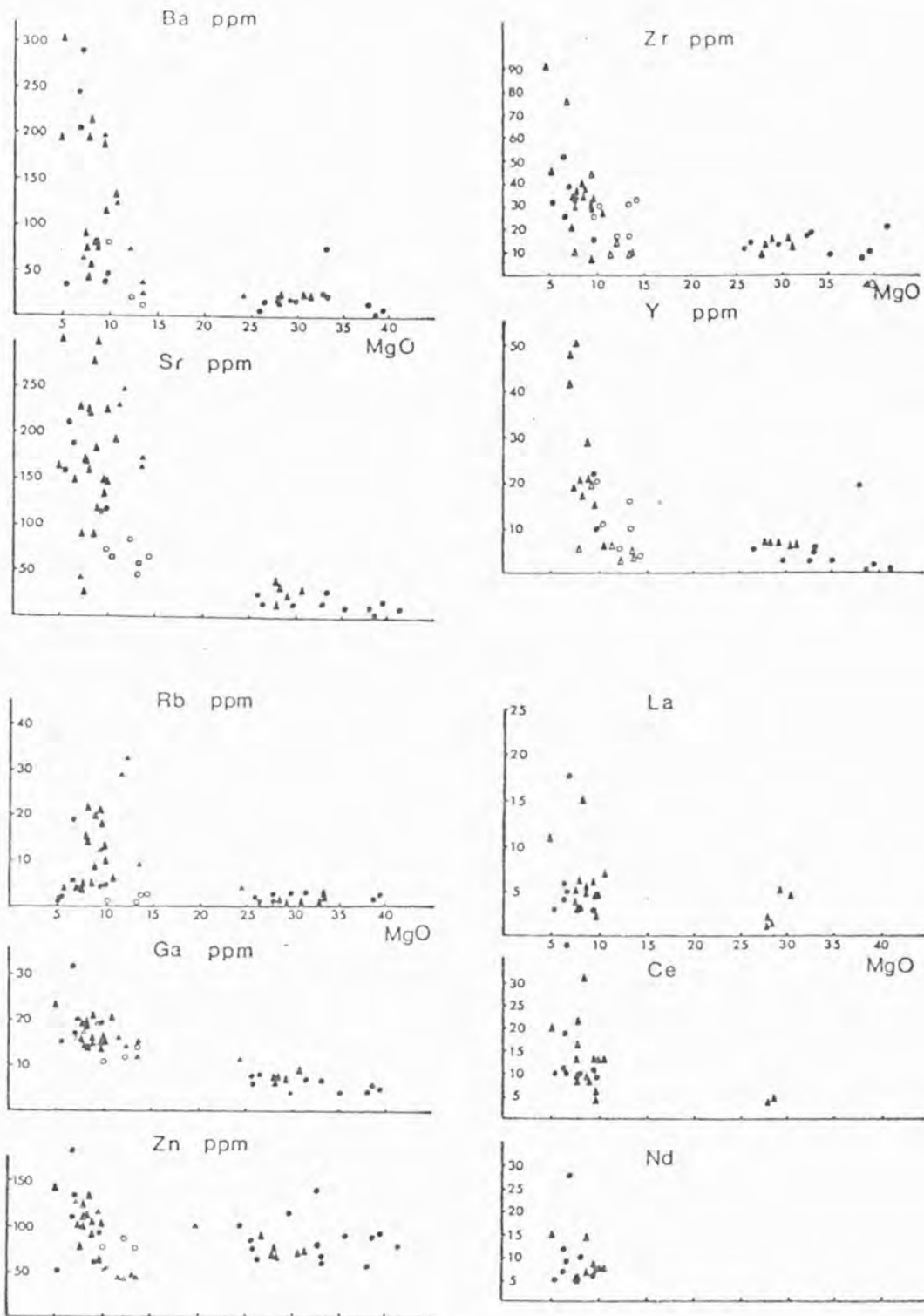


FIG. 3.6 Trace elements versus MgO for ultramafic-gabbro bodies.

Key as in Fig.3.5.

(e)  $TiO_2$  and V both increase with decreasing MgO (Savage, 1979). Fe, Ti and V are all generally concentrated in ilmenite and magnetite, and tholeiitic suites typically show an increase in these elements (Myashiro and Shido, 1975). This is taken to indicate a low ambient oxygen fugacity in the magma chamber (Osborn, 1962, 1969), suppressing ilmenomagnetite fractionation.

(f) The abundance of the relatively immobile incompatible elements (Ti, P, Y, Zr) increases with decreasing MgO. However the abundance of the more mobile incompatible elements (K, Rb, Sr and Ba), although showing the same general trend is much more scattered due to limited mobility during both granulite facies metamorphism and Inverian retrogression. Rocks which show signs of retrogression (e.g. amphibole fringes around pyroxene) have significantly higher K, Rb, Sr and Ba contents, e.g. Ba may be up to 300 ppm in retrogressed samples compared with 50 ppm in the granulite facies samples.

A correlation matrix (Table 3.2) has been computed by the method described by Beach and Tarney (1978) and an R-mode cluster dendrogram has been constructed from the correlation coefficient matrix using the weighted group mean pair method of Sokal and Sneath (1963). Four cluster groupings are apparent from the dendrogram (Fig.3.7): a Si-Ca-Al-Na-Sr-Ga-K-Ba grouping; and Fe/Mg-Ti-P-Zr-Y grouping; a Mg-Cr-Ni grouping and an Fe-Zn grouping. These groupings are less distinct than those for the Fiskenaesset complex (Weaver et al., in press). The Mg-Ni-Cr group clearly reflects a cumulus ferromagnesian component and the Ti-Fe/Mg-Zr-Y-P group are those elements which are incompatible in all likely fractionating phases. For Fiskenaesset, there is a distinct Si-Ca-Al-Na-Sr group which reflects cumulus plagioclase; this is not found for the Lewisian bodies. Instead this group contains Ba and K, elements not found in plagioclase. The general level of correlations for this

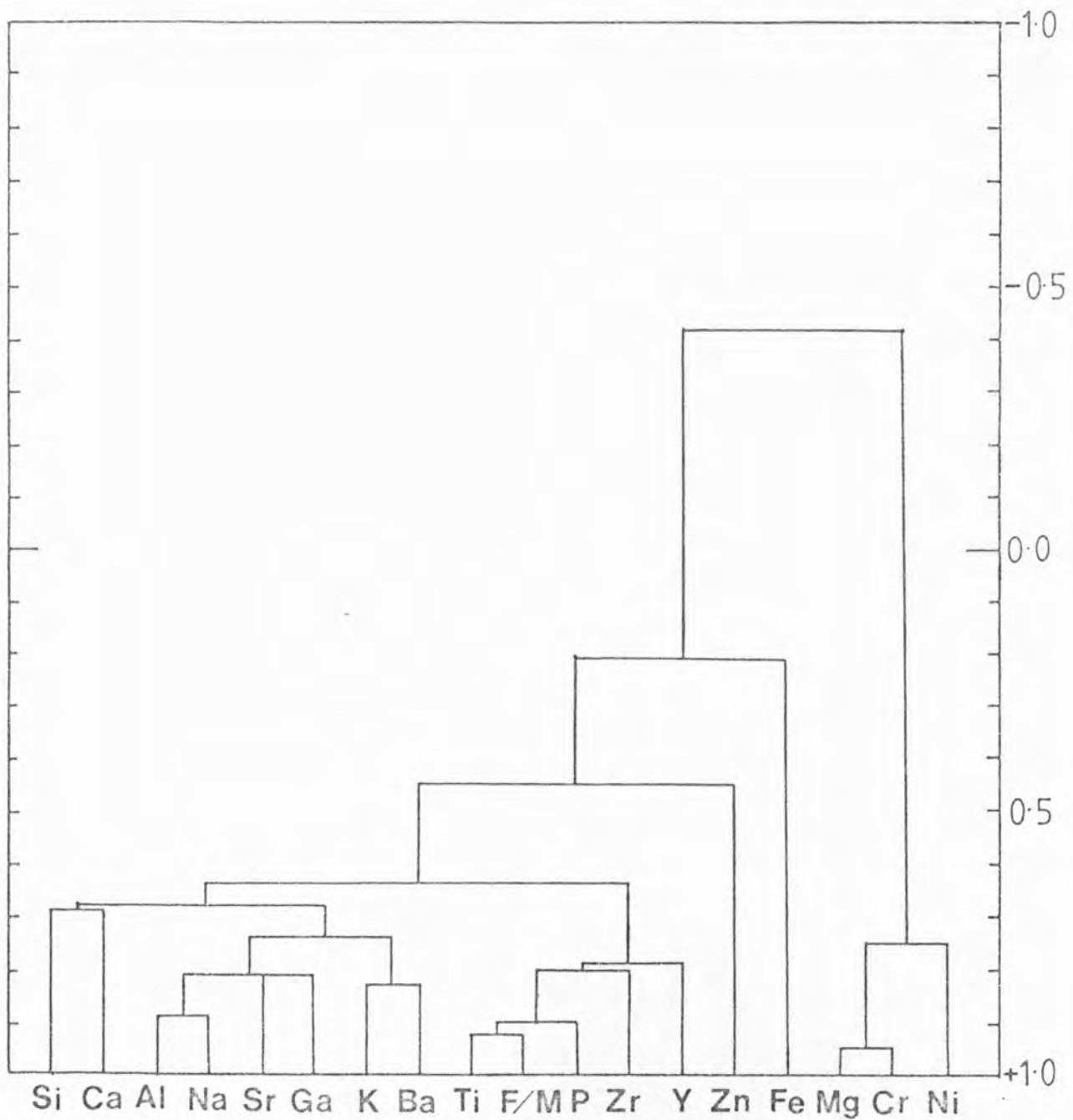


FIG. 3.7 Dendrogram showing clusterings of elements for ultramafic-gabbro bodies in the Assynt region. F/M is  $\text{Fe}_{\text{TOT}}/\text{Mg}$ .

group with the Ti-P-Y-Zr group implies both groups of elements behaved incompatibly and shows the lack of cumulus plagioclase.

#### 3.4.2. Ti-Zr-Y and Ti-Zr-Sr.

These triangular plots have been constructed by Pearce and Cann (1973) to discriminate the tectonic setting of basaltic rocks using incompatible trace element ratios. In Fig.3.8a it can be seen that most data plot in the low-K tholeiite or ocean floor basalt fields, but there is considerable scatter with two trends apparent. Serpentinised ultramafic rocks may have high Zr contents and plot towards the Zr apex and the gabbroic rocks from Scouriemore (Savage, 1979) tend to have higher Y contents. In the Ti-Zr-Sr plot (Fig.3.8a) the majority of data again plots in the low-K tholeiite and ocean floor basalt fields with a good deal of scatter. Two trends are again apparent, the Zr enrichment of the serpentinised ultramafics and Sr enrichment of the gabbros. There are a few gabbros which have a high Ti content outside any of the fields, implying enrichment of Ti relative to the other elements, presumably in a Ti-bearing cumulus phase. For most data the ultramafics and gabbros plot in the same fields. The retrogression of these rocks in Inverian steep belts will be discussed fully in Chapter 5, but these plots serve to show that care must be taken in interpreting the petrogenesis of these rocks using trace elements. However the plots do show that the unretrogressed granulites have probably retained their initial characteristics. The diagrams are of no use in determining the original tectonic setting because of the presence of cumulus phases.

#### 3.4.3. Ti-Zr-P-Y variations

These elements are all regarded as being incompatible in basaltic liquids, although they may have small but significant  $K_D$ 's in some

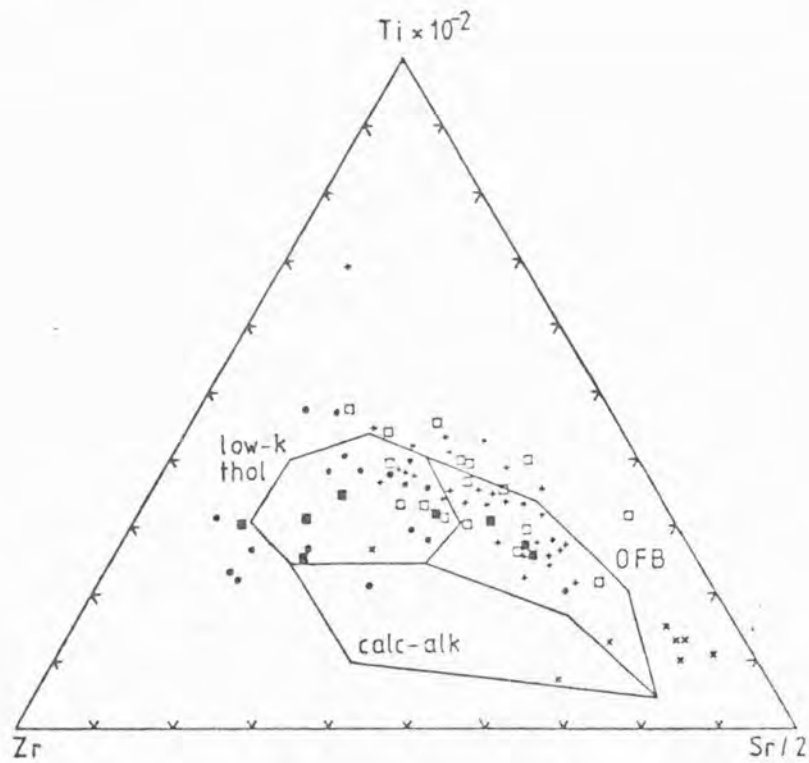
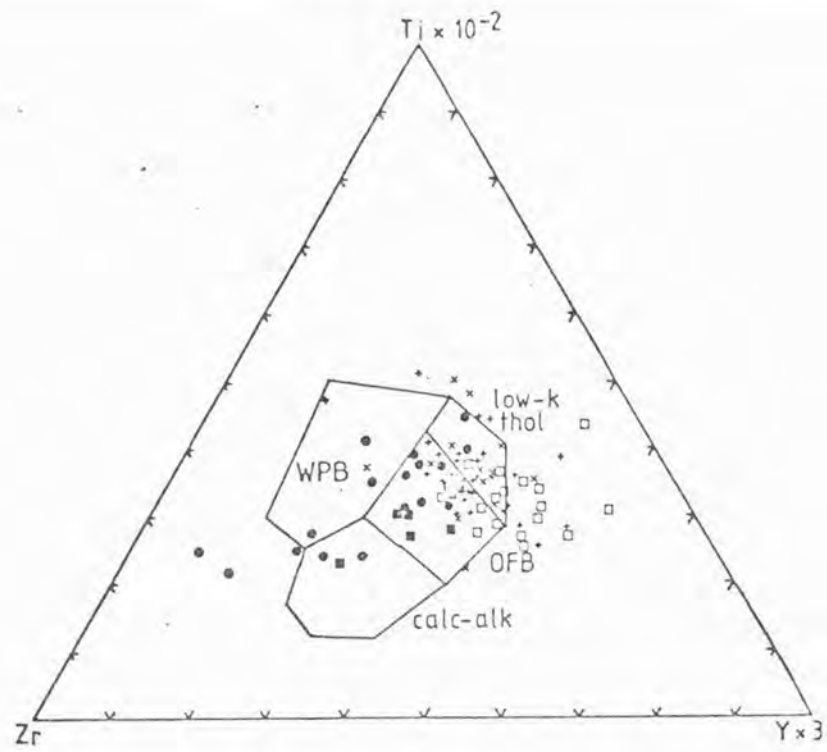


FIG. 3.8 Ti-Zr-Y and Ti-Zr-Sr plots after Pearce and Cann(1973) Key as in Fig 3.5 with filled squares being ultramafics and open squares gabbros from Camas nam Bath (Savage,1979). WPB- within plate basalts, OFB- ocean floor basalts.

phases e.g.  $K_Y^{\text{cpx/liq}} = 0.5$  , and  $K_{Ti}^{\text{magt/liq}} = 7.5$  (Pearce and Norry, 1979).

Nb is ignored in the following discussion because the X.R.F. values were very imprecise at these low concentrations (< 5 ppm). From the correlation matrix (Table 3.2) it can be seen that the correlations for all these element pairs are greater than 0.75. In Fig.3.9 all these elements are plotted against each other with a possible mantle ratio as a reference line (data from Nesbitt and Sun, 1976). All plots show a colinear relationship back through the origin, but with a fair degree of scatter, especially at the mafic end. If these rocks do represent primary liquid compositions, one would expect them to cluster around a mantle ratio, and the scatter is greater than for similar plots for komatiitic liquids (Nesbitt and Sun, 1976). This scatter could have several causes:

(a) mobilisation and redistribution of elements during granulite facies metamorphism. However these elements are all thought to be fairly immobile during metamorphism (Pearce and Cann, 1973; Floyd and Winchester, 1975),

(b) mantle heterogeneities, meaning that the source for the komatiites of Nesbitt and Sun (1976) was different to that which produced the Lewisian rocks,

(c) the presence of cumulus phases, which may contain minor amounts of these elements.

The correlation between pairs of incompatible elements is best held in the ultramafic rock types (Fig.3.9) and the  $TiO_2/Zr$  and  $Y/Zr$  ratios are more or less chondritic (Nesbitt and Sun, 1976). Ti and Zr will be fractionated very little, relative to each other, by olivine or pyroxene fractionation, but hornblende significantly takes Ti.

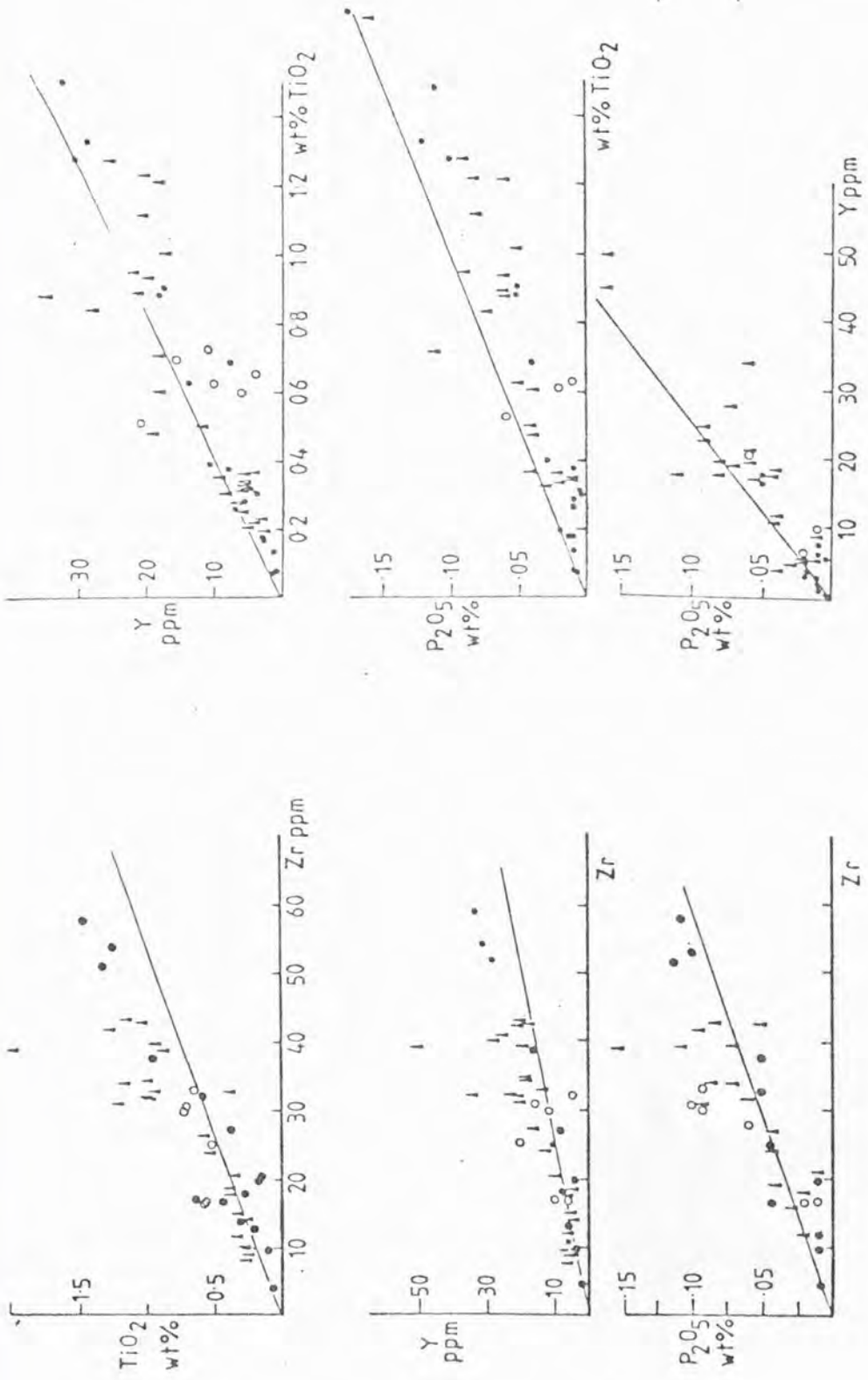


FIG. 3.9 TiO<sub>2</sub>, Y and P<sub>2</sub>O<sub>5</sub> against Zr for the ultramafic-gabbro bodies with a mantle ratio as a reference line (Mesbitt and Sun, 1976). Key as in Fig. 3.5.

Fractionation vectors for several phases for 50% fractional crystallisation were calculated according to the Rayleigh fractionation equation:

$$\frac{C_L}{C_0} = F^{K_D-1}$$

where  $C_L$  is the concentration in the remaining liquid,  $C_0$  the concentration in the original liquid,  $F$  is the fraction of liquid remaining and  $K_D$  is the distribution coefficient, using the distribution coefficient data of Pearce and Norry (1979). From Fig.3.10a it is apparent that neither hornblende or magnetite exerted any control over the trends. Similarly, for the Y against Zr plot (Fig.3.10b) it is clear that neither hornblende or garnet were involved. This means that the abundant pargasite in the ultramafics and the pargasite and garnet in the gabbros must be entirely metamorphic and had no control over the original igneous fractionation.

The very high Ni and Cr of some ultramafics suggests that some of the ultramafic rocks are at least partially cumulate with olivine and pyroxene controlling the trends. However the general level of incompatible elements (e.g. Zr of 10-20 ppm and REE levels of 5-8 times chondrite) are quite high for cumulates c.f. gabbro cumulates in the modern oceanic crust (Table 5.4, no.6 and Hodges and Papike, 1976) and ultramafic and gabbro cumulates from ophiolite complexes (Suen et al., 1979). This implies there must have been substantial amounts of intercumulus liquid in the Lewisian bodies. As none of the likely cumulus phases for the ultramafics take Ti, Zr or Y, the whole-rock ratios (Ti/Zr etc.) must equal that of the intercumulus liquid and hence the original liquid from which the ultramafics formed. Examination of the plots in Fig.3.9 yield the following ratios:  $Ti/Zr = 108$ ,  $Zr/Y = 2.2$  and  $Zr/P_2O_5 = 530$ .

In the gabbroic rocks there is a tendency for  $TiO_2$  and Y to become enriched relative to the mantle ratio, implying small amounts of a

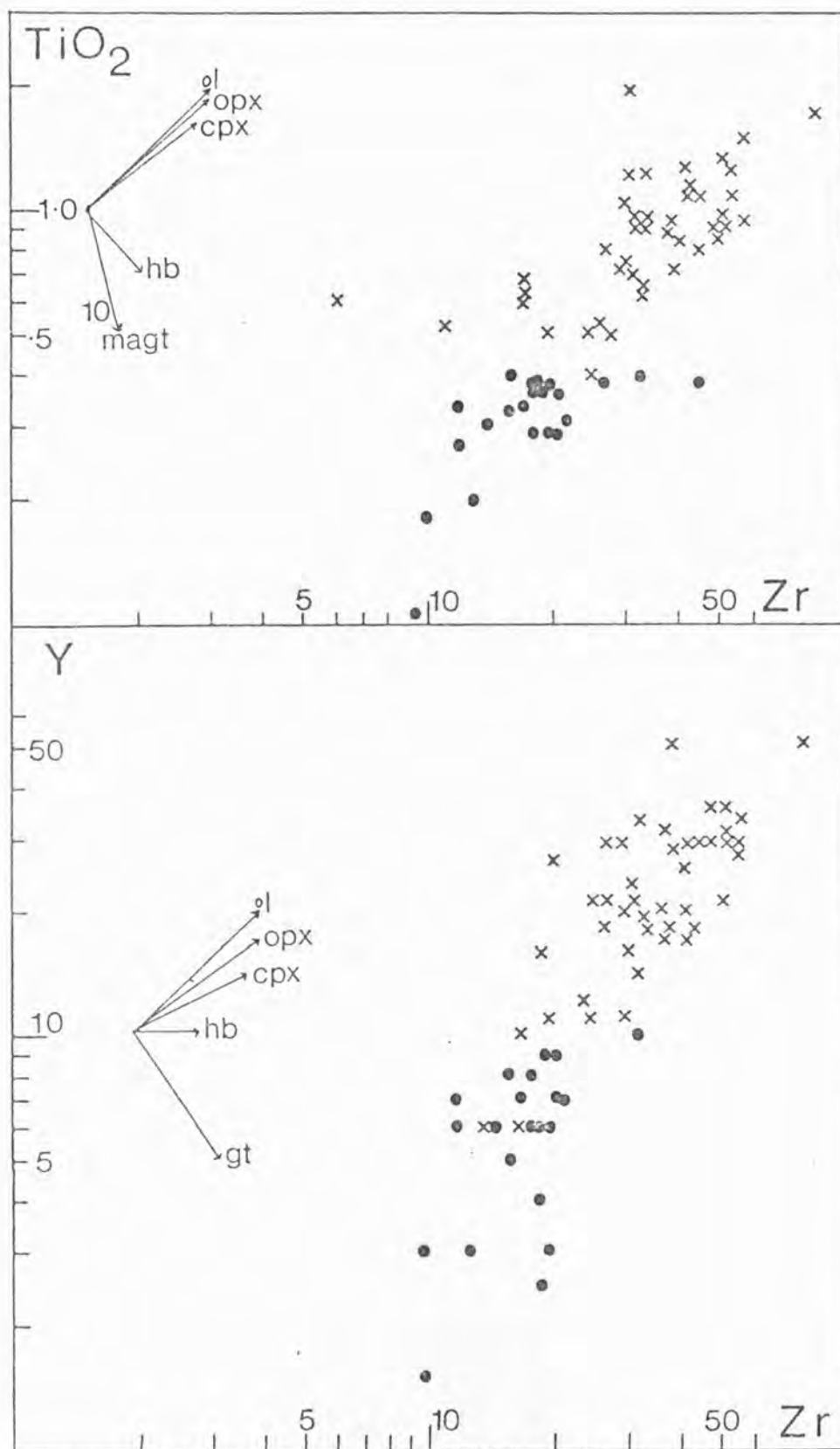


FIG. 3.10  $TiO_2$  and Y against Zr for ultramafic (circles) and gabbroic (crosses) rock types. The fractionation trends are <sup>those for the derivative liquids</sup> for 50% crystallisation of orthopyroxene, clinopyroxene, hornblende, garnet and 10% crystallisation of magnetite. ol is the olivine trend.

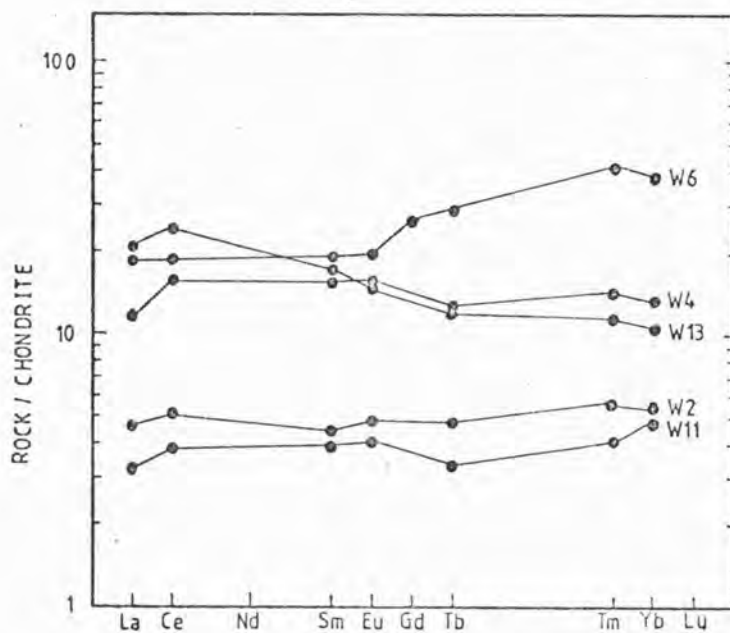
Ti and Y bearing cumulus phase, presumably clinopyroxene as the effect is not large enough for it to be caused by hornblende. It is unlikely to be due to ilmenite as the build up of FeO, Ti and V argue against ilmenite fractionation (Savage, 1979). The scatter on the  $P_2O_5$  plots is largely due to poor analytical precision.

In conclusion, the incompatible elements show the chemistry of the ultramafics to be controlled by olivine and pyroxene fractionation, not by hornblende as suggested by Bowdidge (1969). The gabbros may have some cumulus clinopyroxene. The abundant pargasite and garnet are entirely metamorphic.

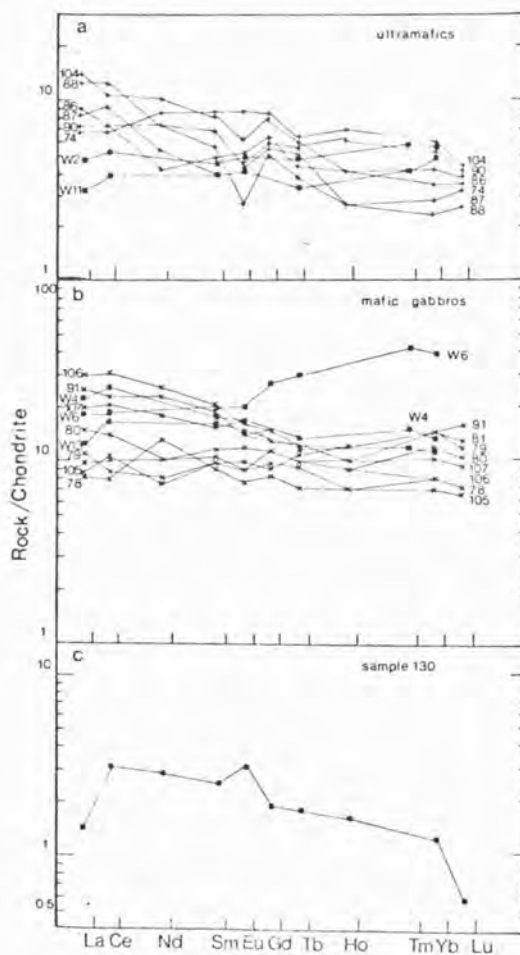
#### 3.4.5. Rare-earth element chemistry

5 samples from the Drumbeg body (Weaver and Tarney, in press) and 9 ultramafics and 11 gabbros from Camas nam Buth (Savage, 1979) have been analysed for rare-earth elements (REE). Although the analyses were not performed by the author, the results will be discussed here because of the importance of REE in understanding the petrogenesis of rock suites. Analyses are presented in Table 3.5, along with data from other ultramafic and mafic rock types. Chondrite normalised REE plots are given in Fig.3.11a and b and data from other areas are presented in Fig.3.12.

The REE are generally considered immobile during metamorphism (Green et al., 1972; Hamilton et al., 1979), although modification of REE patterns may take place, particularly LREE, if a large quantity of fluid has passed through the rocks (Menzies et al., 1977). Sample 130, a retrogressed ultramafic (Fig.3.11b) shows evidence of REE mobilisation, during recrystallisation at high  $P_{H_2O}$  during the Inverian retrogression. When compared with granulite facies samples from the same Camas nam Buth body, sample 130 shows lower total REE. Retrogression also causes



(a)



(b)

FIG.3.11 (a) REE patterns for ultramafic (W2, W11) and for gabbroic (W4, W6, W13) rocks. Data from Weaver and Tarney (in press).  
 (b) REE patterns for ultramafic(a), gabbroic (b) and retrogressed ultramafic(c) rocks from Scouriemore. Data from Savage(1979) and Sills et al.(in prep.).

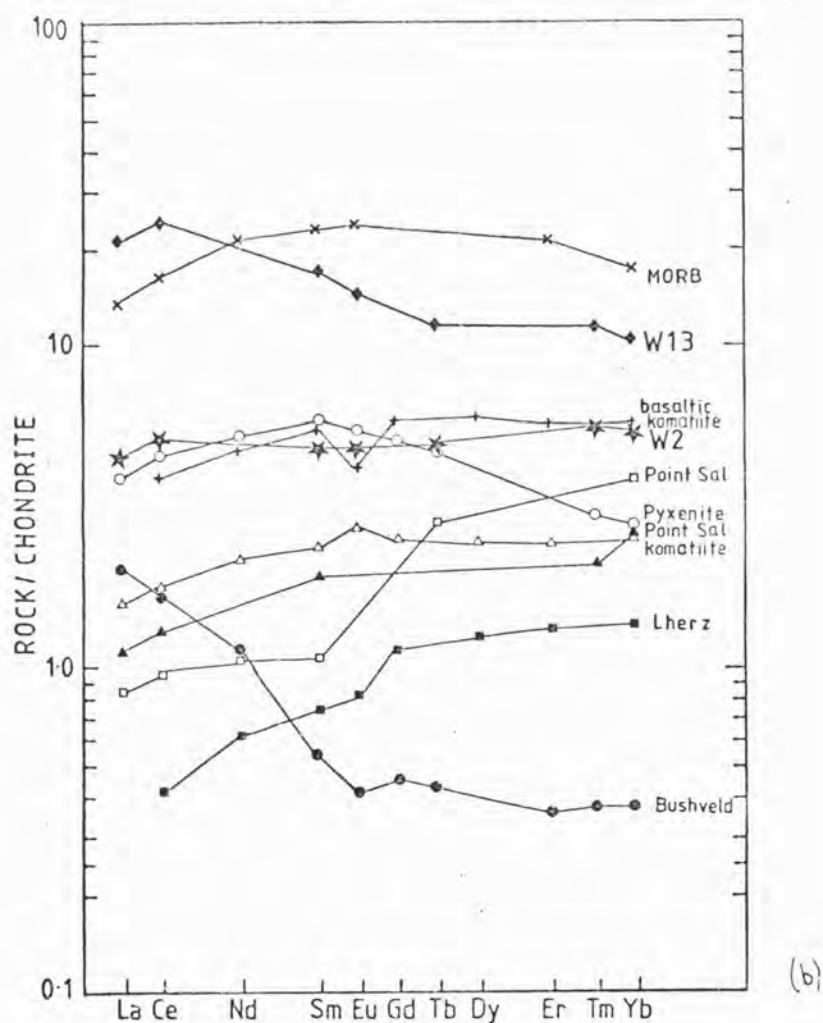
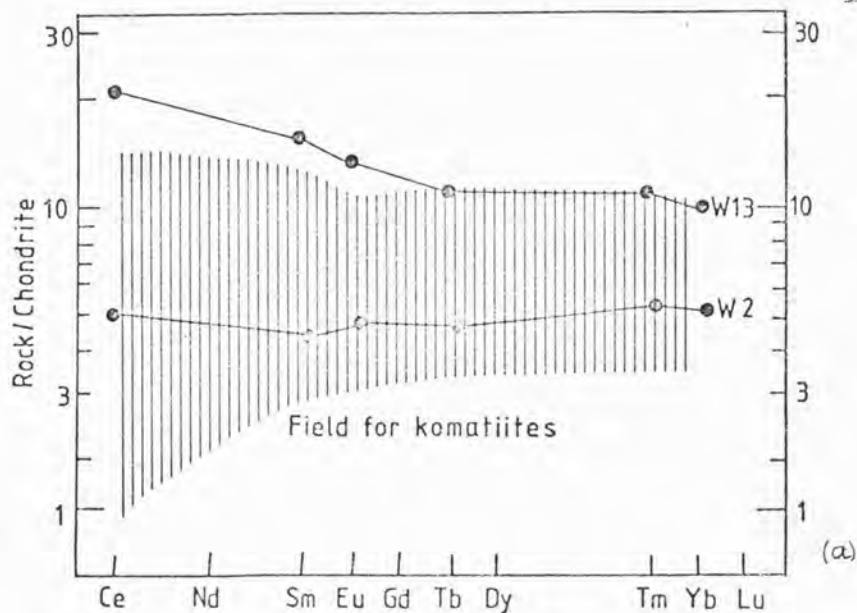


FIG. 3.12 (a) REE patterns of an ultramafic (W2) and a gabbro (W13) compared with the field for komatiites from Arth et al. (1977) from the Munro Township.

(b) REE patterns for an ultramafic (W2) and a gabbro (W13) compared with various other mafic and ultramafic rocks. Data are from Table 3.5.

(a)	W2	W11	W4	W6	W13	W15
La	1.50	1.04	3.80	6.10	6.90	33.20
Ce	4.40	3.30	13.70	16.20	21.30	54.10
Nd						14.00
Sm	0.89	0.79	3.10	3.90	3.50	1.27
Eu	0.37	0.31	1.19	1.53	1.14	1.58
Gd				7.10		
Tb	0.25	0.17	0.66	1.48	0.62	0.11
Tm	0.19	0.14	0.48	1.39	0.39	0.05
Yb	1.18	1.03	2.94	8.30	2.31	0.24
Eu <sub>N</sub> /Yb <sub>N</sub>	1.07	1.10	1.07	0.90	0.99	4.80
Ce <sub>N</sub> /Yb <sub>N</sub>	0.98	0.84	1.23	0.51	2.43	59.3
ΣREE	13.1	10.5	40.2	59.4	51.5	105.2

(b)	1	2	3	4	5	6	7	8
La	0.68	1.27		0.28	0.37	0.52		4.4
Ce	1.40	3.90	0.376	0.83	1.15	1.54	3.38	14.2
Nd	0.70	3.20	0.400			1.34	2.99	13.2
Sm	0.11	1.18	0.150	0.69	0.39	0.48	1.13	4.6
Eu	0.032	0.416	0.065	0.22	0.39	0.21	0.32	1.8
Gd	0.125	1.40	0.320			0.69	1.58	6.6
Dy		0.424				0.84	2.02	
Tb	0.025	0.241		0.15				
Er	0.081		0.300			0.55	1.27	4.6
Tm	0.013	0.099						
Yb	0.083	0.61	0.300	0.85	0.47	0.55	1.18	3.8
Lu		0.076		0.13	0.11			
Ce <sub>N</sub> /Yb <sub>N</sub>	4.4	1.68	0.33	0.26	0.64	0.74	0.75	0.95

TABLE 3.5

(a) REE analyses from the Drumbeg complex (Weaver and Tarney, in press); W2 and W11 are ultramafics, W4, W6 and W13 are gabbros, and W15 is from a discordant anorthositic "patch" cutting the Drumbeg complex. <sup>ΣREE includes interpolated values.</sup>

(b) REE analyses from the literature for various ultramafic and mafic rocks: 1=Bushveld pyroxenite (Frey et al., 1971); 2=Layered ultramafic (Potts and Condie, 1971); 3=Lherz alpine-peridotite massif (Loubet et al., 1975); 4=olivine gabbro, Point Sal Ophiolite (Menzies et al., 1977); 5=Cumulate pyroxenite, Point Sal Ophiolite (op cit) 6=Peridotitic komatiite (Sun and Nesbitt, 1978); 7=Basaltic komatiite, Belingwe (Hawkesworth and O'Nions, 1977); 8=MORB (Atlantic average, Kay et al. 1970)

loss of Ca and Sr from the ultramafics. One sample, W6 (Fig. 3.11a), which has about 60 percent modal garnet has enriched HREE abundances (Weaver and Tarney, in press) but this is probably due to metasomatic movement of HREE during metamorphic growth of garnet, because garnet has a strong affinity for the HREE (Arth, 1976). With these specific exceptions the regularity of the observed REE distributions reflects the original igneous patterns.

The ultramafics have slightly LREE enriched to flat REE patterns with  $Ce_N/Yb_N$  ratios ranging from 0.84 to 5.0 and HREE values of 3 to 6 times chondrite. Four samples have very slight negative Eu anomalies, four others slight positive anomalies, but these are probably insignificant. These patterns are in strong contrast to "Alpine-type" ultramafics (Loubet et al., 1975) which are strongly LREE depleted. The flat patterns resemble those from stratiform intrusions (Frey et al., 1971) but the Lewisian bodies have higher total REE abundances.

The gabbroic rocks have flat to slightly LREE enriched patterns,  $Ce_N/Yb_N$  ranging from 0.6 to 4.8, and  $La_N/Sm_N$  ranging from 0.93 to 1.95. There are no significant Eu anomalies. There is a tendency for total REE to increase with indices of fractionation such as  $FeO/FeO + MgO$ . These patterns are quite distinct from the LREE depleted REE patterns typical of MORB (Frey et al., 1974; Schilling, 1975) and ophiolitic pillow lavas and gabbros (Kay and Senechal, 1976; Menzies et al., 1977). Both ultramafic and gabbroic REE patterns show some resemblance to komatiitic patterns from the Munro Township area (Arth et al., 1977).

The low  $fO_2$ , indicated by suppression of ilmeno-magnetite fractionation and the iron enrichment trends, means that Eu would have been present as  $Eu^{2+}$  as well as  $Eu^{3+}$  (Drake and Weill, 1975).

The lack of europium anomaly in the gabbros suggests that plagioclase was an insignificant cumulus phase. This is consistent with the lack of plagioclase layers in the rocks.

The flattish REE patterns, taken together with the Ti-Zr-Y data presented earlier, imply neither hornblende nor garnet were residual in the source after partial melting, and were not involved in any subsequent fractionation. This implies a low pressure regime controlled the fractionation of these rocks in contrast to the tonalitic gneisses which have strongly depleted HREE patterns, thought to be due to residual garnet in the source (Weaver and Tarney, in press).

### 3.5. DISCUSSION

The original suggestion by O'Hara (1961a, 1965) that the mafic rocks formed by metasomatic interchange between homogeneous igneous peridotite and acid gneiss can be discounted on several grounds. The flat to slightly LREE enriched rare-earth patterns of the mafic rocks could not be due to simple mixing of the flat ultramafic patterns and the strongly HREE depleted patterns of the tonalitic gneisses (Weaver and Tarney, in press). It is also highly unlikely that this scale of metasomatic movement (i.e. over distances of at least 50 m) would have occurred under granulite facies conditions (or even under an earlier period of "wet" metamorphism), especially as small scale reaction textures are preserved (Savage, 1979; Savage and Sills, 1980). Finally ultramafic rocks sometimes occur with no associated mafic rocks and vice-versa. The first objection also applies to the model of Bowdidge (1969) according to which both ultramafic and mafic rocks represent igneous intrusions but their chemistry has been modified by metasomatic interchange with the acid gneisses. The resemblance of both ultramafic and mafic rock types to other igneous rocks and their common association suggests a related igneous

origin for both rock types. The suggestion (Weaver and Tarney, in press) that the ultramafics may represent fragments of undepleted mantle is unlikely as their MgO contents are too low (22-38 wt.% MgO).

The following points indicate a cumulate or partially cumulate origin:

(a) the rhythmic units at Camas nam Buth, Scouriemore, which have Ni depleted, sulphide-rich tops with each rhythmic unit showing decreasing Mg, Ni, Cr and normative An and increasing levels of incompatible elements with stratigraphic height (Savage, 1979),

(b) the iron-enrichment trends in all the mafic phases in the Achiltibuie body,

(c) the rapid depletion in Ni and Cr with decreasing MgO and the very high Ni and Cr contents of some ultramafic rocks,

(d) the mineral layering in the ultramafics.

However the moderately high level of incompatible elements suggests there must have been a substantial amount of intercumulus liquid.

Incompatible element versus MgO plots for ultramafic compositions can be projected back to intersect the MgO axis at 42 - 44 wt.% MgO. This is either the combined MgO content of any fractionating (accumulating) phases if the ultramafics are cumulate or the combined MgO content of the residual mantle phases with which a possible ultramafic liquid was in equilibrium. If this 42 - 44 wt.% represents olivine alone, it corresponds to a composition of  $Fe_{80-84}$  which is rather low for mantle olivine. Using similar graphical techniques Nesbitt and Sun (1976) and Nisbet et al. (1977) obtained values of 50.0 and 47.2 wt.% MgO respectively. If the MgO value is for olivine and orthopyroxene, it implies that orthopyroxene as well as olivine was a residual phase in the

source if the ultramafics represent liquids. This is unlikely for the large degree of partial melting required to produce ultramafic liquids. In CMAS (O'Hara, 1968) the ultramafics plot on an olivine-orthopyroxene control line.

To try and resolve the problem as to whether these rocks represent liquids or partial cumulates, attempts have been made to model the trace element variations in two ways:

(a) to see whether it is possible to produce the range of ultramafic rock compositions by partial melting alone,

(b) to assume the ultramafics are cumulate or partially cumulate and the gabbros are derivative liquids and to model whether simple olivine-pyroxene removal will produce the gabbros.

Partial Melting. The mantle was assumed to have the composition estimated for the Archaean mantle by Sun and Nesbitt (1977) which is similar to pyrolite. Partition coefficient data used are given in Appendix C; in general those for incompatible trace elements are from Pearce and Norry (1979) and for REE are from Arth (1976).

Ultramafics have a considerable range in trace elements concentrations from samples J21 and J22 with 2500 ppm Ni and 0.08 wt.%  $\text{TiO}_2$  to samples with 1000 ppm Ni and 0.40 wt.%  $\text{TiO}_2$ . The modelling of partial melting was done using the batch melting equation of Shaw (1970):

$$\frac{C_L}{C_0} = \frac{1}{D + F(1 - P)}$$

where  $C_L$  is the concentration in the liquid;  $C_0$  the concentration in the source mantle;  $D$  the bulk distribution coefficient for mantle mineralogies,  $F$  is the fraction of melting and  $P$  is  $p^\alpha k_D^\alpha + p^B k_D^B + \dots$  where  $p^\alpha$  is the proportion of phase  $\alpha$  in the melt and  $k_D^\alpha$  is the

distribution coefficient for that phase. As the incompatible trace element ratios are more or less chondritic, one can assume that no phase containing significant amounts of these elements (garnet, hornblende and possibly clinopyroxene) were residual. As the  $K_D$ 's for remaining phases (olivine and orthopyroxene) are so low one can assume that  $D$  approaches unity and the batch melting equation reduces to  $\frac{C_L}{C_0} = \frac{1}{F}$ .

The majority of the ultramafic samples have  $TiO_2$  contents of between 0.3 and 0.4wt.% and Zr contents of about 18 ppm; using the mantle composition estimated by Sun and Nesbitt (1977), 50 - 70% partial melting is required to generate these trace element levels. However the  $TiO_2$  content of 0.08 wt.%, Zr of 4 ppm and Y of 1 ppm in samples J21 and J22 are less than that of the estimated mantle composition (Sun and Nesbitt, 1977) and hence could not have been generated by partial melting alone. The Ni and Cr contents are higher than estimated mantle compositions. These harzburgite samples could not represent fragments of refractory mantle as their MgO content (36 - 38 wt.%) is too low. Arndt (1977) has suggested that it is improbable that melts could form by as much as 60% batch melting of pyrolite, as the rate of segregation of magma will be rapid compared with the rate of uprise of the mantle diapir which provides the heat of fusion by adiabatic decompression. Alternatively the source could be a more refractory mantle, where a lower degree of partial melting could produce the same trace element levels. However, the flat to slightly LREE enriched rare-earth patterns argue against a previously depleted source. In conclusion it seems unlikely that the ultramafic rocks represent liquid compositions.

Fractional crystallisation. To establish whether the range in ultramafic rock compositions could be established by crystal settling from a basaltic liquid it is necessary to make some estimate of its composition. The REE patterns suggest the liquid had a flat to slightly LREE enriched pattern, which is probably also a characteristic of the source. The Ti/Zr and Zr/Y ratios are approximately chondritic (a feature of many Archaean magma types, Nesbitt and Sun, 1976; Nesbitt et al., 1979).

Two methods of estimating the initial magma composition have been attempted. Firstly the rhythmic units at Camas nam Buth (Savage, 1979), Drumbeg and Achiltibuie were assumed as a first approximation to represent one "batch" of magma and the approximate bulk composition obtained by integration. Where the bodies are best preserved the ratio of gabbro to ultramafic is about 2:1. The average compositions (Tables 3.3 and 3.4) give an MgO content of 15 - 18 wt.% for the primary magma. Alternatively, consideration of the element versus MgO plots (Figs. 3.5 and 3.6) reveals a break in slope between 13 and 16 wt.% MgO for Ti, Al, Na, Zr, Y and Sr; the more magnesian samples representing partial cumulates, the less magnesian derived liquids. The composition estimated by both methods is given in Table 3.6 and the similarity is encouraging (although possibly fortuitous). The liquid composition used in subsequent modelling thus has 15 - 18 wt.% MgO, 0.5 wt.% Ti<sub>2</sub>O, 25 - 30 ppm Zr, and 12 - 15 ppm Y. This liquid could be generated by 30 - 40 % partial melting mantle of the composition of Sun and Nesbitt (1977). As outlined above the mantle had not undergone a previous partial melting episode. A liquid with this MgO content would probably have 500 - 600 ppm Ni (Sato, 1977; Cawthorn and McIver, 1977; Clarke and O'Hara, 1979) and about 1200 ppm Cr.

One must first establish whether it is possible to produce the range of Ni and MgO contents of the ultramafics by accumulation of

	1	2
SiO <sub>2</sub>	46-48	47
TiO <sub>2</sub>	0.5	0.72
Al <sub>2</sub> O <sub>3</sub>	10	10.83
Fe <sub>2</sub> O <sub>3</sub>	14	13.20
MgO	15	15
CaO	9-10	10.5
Na <sub>2</sub> O	1	1.38
K <sub>2</sub> O		0.25
Zr	20-30	31
Y	10-15	16
Sr	50-75	107

TABLE 3.6 Estimates of the initial magma composition.

1 - calculated from MgO versus element plots

2- aggregate of ultramafic and gabbro in the ratio  
one to two.

See text for details.

olivine and possibly pyroxene from this liquid. In the following discussion Cr is not considered, as the values seem too high, due in part to being Cr + V, and spinel has a marked and unquantifiable effect on Cr. The high Cr levels may reflect some cumulus spinel. Using the  $K_{Ni}^{ol/liq}$  data of Hart and Davis (1978) and a  $K_{Ni}^{opx/liq}$  of 1.25, it is possible to develop the range in Ni concentrations (2500 - 1000 ppm) and MgO variations (38 - 22 wt.%) by mixtures of varying proportions of olivine, orthopyroxene and liquid. The most extreme case, samples J21 and J22, can be made by a mixture of 60% olivine and 40% liquid. This gives the appropriate MgO, Ni and incompatible element levels (using the relationship of Roedder and Emslie, 1970 and  $K_D$  data of Pearce and Norry, 1979). As mentioned above, the MgO plots indicate control by olivine and a less magnesian phase, either clino- or ortho-pyroxene. At zero wt.%  $TiO_2$ , CaO and  $Al_2O_3$  contents are also very low (in fact CaO is negative) which may indicate the lack of clinopyroxene involvement. However some of the most magnesian samples are serpentinised and have lost Ca, implying any conclusions based on Ca may be invalid. It is assumed therefore that some orthopyroxene fractionated.

Production of one third of the body as ultramafic leads to reasonable Ni concentrations in the derived liquids; for example if 5% of the total magma formed as harzburgite like J21, this leaves 400 ppm Ni, if the next 10% crystallised as ultramafic with about 1500 ppm Ni, this leaves 275 ppm Ni and if the next 18% crystallised as ultramafic with about 1000 ppm Ni, this leaves 190 ppm. These are reasonable liquid trends as the Ni content of the gabbros ranges from 500 to 50 ppm, most samples having about 200 ppm.

The LREE, which are incompatible in all likely phases except plagioclase (which was not involved in fractionation, see earlier) are

enriched from the most primitive to the most enriched gabbro by a factor of 4.5, implying 75 - 80% fractionation. Using a value for  $F$  (the fraction of liquid remaining) of 0.22 bulk distribution coefficients ( $D$ 's) for the fractionating phases can be calculated using the Rayleigh fractionation equation. This gives  $D_{Ni} = 3.9$ ,  $D_{Ti} = 0.22$  and  $D_{Zr} = 0.23$ . The  $D_{Ni}$  is lower than one would expect if olivine were the sole liquidus phase ( $K_{Ni}^{ol/liq}$  ranges from 7.5 to 5.3 for 15 - 20 wt.% MgO, Davis and Hart, 1978), again implying the presence of liquidus orthopyroxene. Precise modelling is difficult as the trace elements are enriched by differing amounts; this may be due to different bodies having slightly different magmas or fractionation sequences.  $Ce_N/Yb_N$  does not increase significantly with fractionation implying clinopyroxene was not fractionating ( $K_{Yb}^{cpx/liq} = 0.62$ , Arth, 1976). The general level of REE increases with fractionation as one would expect with olivine and orthopyroxene removal as both these phases have insignificant  $K_{REE}^{xstal/liq}$  (Arth, 1976).

In conclusion, it is believed that the ultramafics formed by olivine (and minor orthopyroxene) settling from a tholeiitic magma with an MgO content between 15 and 20 wt.% and low trace element levels. The gabbros represent the derived liquids. A similar range in composition is found in Fred's Flow, a 120 m thick komatiitic lava flow from the Munro Township area, (Whitford and Arndt, 1979) where MgO ranges from 34 - 7.5 wt.% and  $TiO_2$  from 0.1 to 0.7 wt.% indicating it is possible to produce such a range in compositions in a small thickness.

It is envisaged that the following sequence of events took place:

(1) Partial melting of undepleted mantle to produce a tholeiitic liquid with 15 - 20 wt.% MgO and chondritic incompatible trace element ratios.

(2) Fractionation and settling of olivine and orthopyroxene to produce the ultramafic rock types.

(3) Continuing crystallisation of the derived liquids to produce the gabbroic rock types, possibly with some cumulus clinopyroxene.

(4) Delayed crystallisation of ilmeno-magnetite to increase FeO, TiO<sub>2</sub> and V contents.

(5) Precipitation at Camas nam Buth, of sulphide-rich horizons, enriched in Cu and Fe, but depleted in Ni (Savage, 1979).

### 3.6. TECTONIC SETTING

In assessing the regional setting in which the layered bodies formed, one must set the geochemical evidence presented above against that derived by other sources concerning the Lewisian complex as a whole.

Isotopic evidence suggests that the Lewisian contains no crustal material older than 3.0 b.y. and that the Scourian complex, including the layered bodies, was formed during a relatively short period of magmatism, deformation and metamorphism (Moorbath et al., 1969; Chapman and Moorbath, 1977; Hamilton et al., 1979). The field relationships suggested that some of the layered bodies, in particular those from the Laxford front region, south of Loch Laxford (Davies, 1974) were intruded into sediment and were subsequently disrupted by the intrusion of large volumes of tonalitic magma. An early phase of ductile deformation, before the peak of granulite facies metamorphism, caused isoclinal folding of the layered bodies and their enclosing gneisses, and extensive thinning and boudinage; with high strains being recorded. A flattened leucogabbro near Badcall (145418) appears to have suffered strains indicating that the original body was at least three times its present thickness

(J.V. Watson, pers. comm.; Sills et al., in prep.). Elsewhere strains were generally greater than those recorded at Badcall. The voluminous tonalitic gneisses which form the bulk of the Lewisian complex probably represent primary liquid compositions derived by partial melting of basaltic material with residual garnet in the source, (Weaver and Tarney, in press). They also suggest that the Lewisian crust grew by the underplating of tonalitic plutons in a continental margin environment so the tonalites originally crystallised at moderate pressures and temperatures. However there is no evidence for any older continental crust (see isotopic evidence, cited above) so one needs to consider the nature of pre-existing crust that the tonalites were underplating.

The geochemical evidence concerning the origin of the layered ultramafic-gabbro bodies presented earlier suggests that olivine and pyroxene were liquidus phases, implying that fractionation occurred at moderate pressures when the olivine-orthopyroxene reaction relationship is no longer operative. The pressure at which this occurs depends on both temperature and fluid pressure, but is in excess of 5 kb (Kushiro, 1972); equivalent to depths >15 km. This suggestion in conjunction with the field association with rocks of supracrustal origin, raises problems. Three possibilities are worth exploring:

(1) The magma was emplaced and fractionated at or near the base of an already thick continental crust. However this would allow for the implied pressures of fractionation but does not account for the presence of metasediment or for the suggestion that the layered bodies predate the tonalites (Davies, 1975).

(2) The layered ultramafic-gabbro bodies could represent fragments of Archaean oceanic crust and have been incorporated by lateral thrusting, along with a thin veneer of sediment, into the accreting

continental crust in a subduction zone environment. The high pressure (12 - 15 kb) recorded by the garnetiferous gabbros (Chapter 2) may indicate conditions in the downgoing slab. However some acid gneisses in the Lewisian also indicate similar high P-T conditions (O'Hara, 1977; O'Hara and Yarwood, 1978) indicating the whole complex probably experienced these extreme conditions.

(3) The mafic and ultramafic rocks along with the sediment represent parts of the early oceanic crust on which the Lewisian complex was founded. Assuming subduction had been initiated, the dehydration of the downgoing oceanic crust may have led to partial melting in the overlying mantle producing a thickened tholeiitic crust, the layered bodies possibly representing parts of this unit. This would be followed by melting of the subducting oceanic lithosphere itself to produce tonalitic liquids, which invaded and disrupted this primitive crust. This is essentially the model proposed for continental growth by Jakes (1973).

The injection of the basic material by tonalitic magma resulted in at least a four fold increase in volume causing an intimate mixing of rock types. The high pressures of metamorphism (as cited above) indicate parts of the crust were depressed to at least 45 km. Subsequent uplift may be due to further underplating. By 2.7 b.y. the Lewisian complex was of continental character as regards its composition and thickness.

To examine the feasibility of these proposals it is worth examining other areas which may have evolved in a similar manner. The essential features of the Scourian evolution are thus: formation of layered complexes with a thin veneer of sediment, intrusion of voluminous quantities of calc-alkaline tonalite-granodiorite making up the greater part of the terrain followed by deformation and metamorphism to high-amphibolite or granulite facies in a deep crustal environment.

In general terms the Archaean crust forming events recorded in the Lewisian resemble those in the Hebrides and other Archaean terrains where the layered complexes are of the leucogabbro-anorthosite type. In south-west Greenland for example, the Fiskenaesset complex is emplaced into tholeiitic metavolcanic and minor sediment (Windley et al., 1973; Myers, 1976). These volcanics have affinities with modern oceanic volcanics (Rivalenti, 1976) and the layered complex is believed to be derived from the same liquid (Weaver et al., in press). This is followed by phases of injection of vast volumes of tonalitic magma followed by isoclinal folding and metamorphism leading to a thickening of the crust. It differs from the Lewisian in that lower P-T conditions and generally lower strains are recorded, the Lewisian being a deeper crustal level.

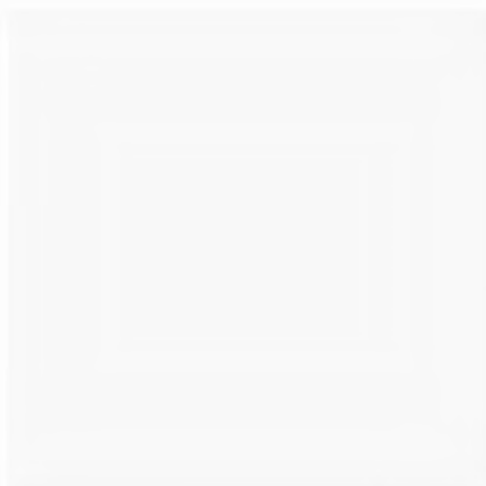
Under Phanerozoic regimes, the characteristic cycle of magmatism evolving from tholeiitic to calc-alkaline in combination with horizontal compressional stresses is most nearly matched at convergent plate boundaries of island arc or Andean type. In this connection the sequence of events is again similar to that recorded in the recently discovered Cretaceous Kohistan section in the Karakorum range of the Himalayas believed to be an upended section through the crust (Tahirkheli et al., 1979). There is a large cumulate norite body emplaced into oceanic metavolcanics succeeded in time by the intrusion of vast quantities of calc-alkaline diorites-granodiorites, the lower part of the succession being metamorphosed at granulite grade. The specific relevance of this Kohistan section to the Lewisian layered bodies lies in the Jijal complex which forms a tectonic wedge at the base of the section against the Indus suture (Jan and Howie, 1980; Jan, in press). This contains chromite layered peridotites and garnetiferous gabbros very like those of the Scourian. Mineral assemblages suggest pressures of about 15 kb.

Further comparison could be made with the layered cumulate mafic-ultramafic complexes of Palaeozoic age metamorphosed at granulite facies that occupy lower crustal segments in the Ivrea-Verbano zone (Rivalenti et al., 1975) and Calabria (Schenck, 1980). In both areas the mid to upper crust is occupied by calc-alkaline plutonics.

However these analogies can be taken too far as discrepancies exist between the evolution of the Scourian and these Phanerozoic examples. In the Kohistan and Ivrea sections calc-alkaline rocks are concentrated in the middle crust, overlying mafic rocks whilst in the Lewisian they are intimately mixed. However it is believed that the reason why the sequence of events in the Scourian bears strong resemblance to the younger crustal sections is because one is looking at comparable examples of the way in which the continental crust has grown.

In summary, it is tentatively suggested that the ultramafic-gabbro bodies of the Lewisian represent fragments of oceanic crust that was disrupted by the intrusion of vast volumes of tonalitic magma at a convergent plate margin.

CHAPTER 4  
DESCRIPTION AND PETROGENESIS OF  
MAFIC, ULTRAMAFIC AND METASEDIMENTARY  
ROCKS FROM ASSYNT



#### 4.1. INTRODUCTION

In this chapter the field relationships, geochemistry and petrogenesis of various mafic and ultramafic rocks and possible meta-sediments will be discussed. In Chapter 3 the origin of layered ultramafic - gabbro bodies was examined but in the Assynt region there are many occurrences of mafic rocks which are not clearly related to these layered bodies. As mafic rocks form a significant proportion of the Assynt gneisses (as much as 10%), their origin is of some importance.

There are several types of mafic and ultramafic rock which have been described briefly in Chapter 1. The following types will be discussed here:

- (1) Large (> 25 m thick) dominantly amphibolite masses such as those at Gorm Loch in the Laxford front, Reidh Phort in Clashnessie Bay, Cnoc an Sgriodaich, Loch Ardbhair and Strathan. The location of some of these masses is shown in Fig.2.1.
- (2) Thin layers and lenses of mafic rock which occur throughout the region.
- (3) Agmatites such as samples J48 and J70, shown in Figs.1.1a and b.
- (4) Ultramafic pods and lenses mostly composed of hornblendite.

#### 4.2. DESCRIPTION, GEOCHEMISTRY AND PETROGENESIS OF THE LARGER MAFIC MASSES

Whole-rock analyses of all samples are given in Appendix B, Table B4 and a brief description and sample locality in Table B2. Mineral analyses are given in Appendix A, Table 2 and the mineral chemistry is

FIG. 4.1(a) Reidh Phort amphibolite mass sitting on gently dipping micaceous trondjhemitic gneiss (O57316).

FIG. 4.1(b) The agmatized base of the Reidh Phort amphibolite mass (O57316)

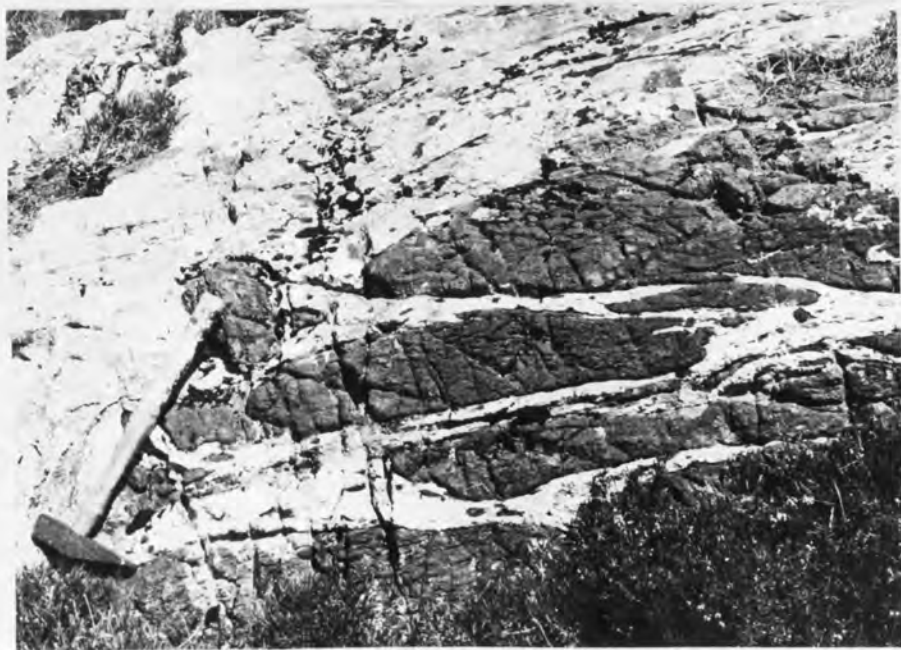
FIG. 4.1(c) Agmatite from (124310).



a



b

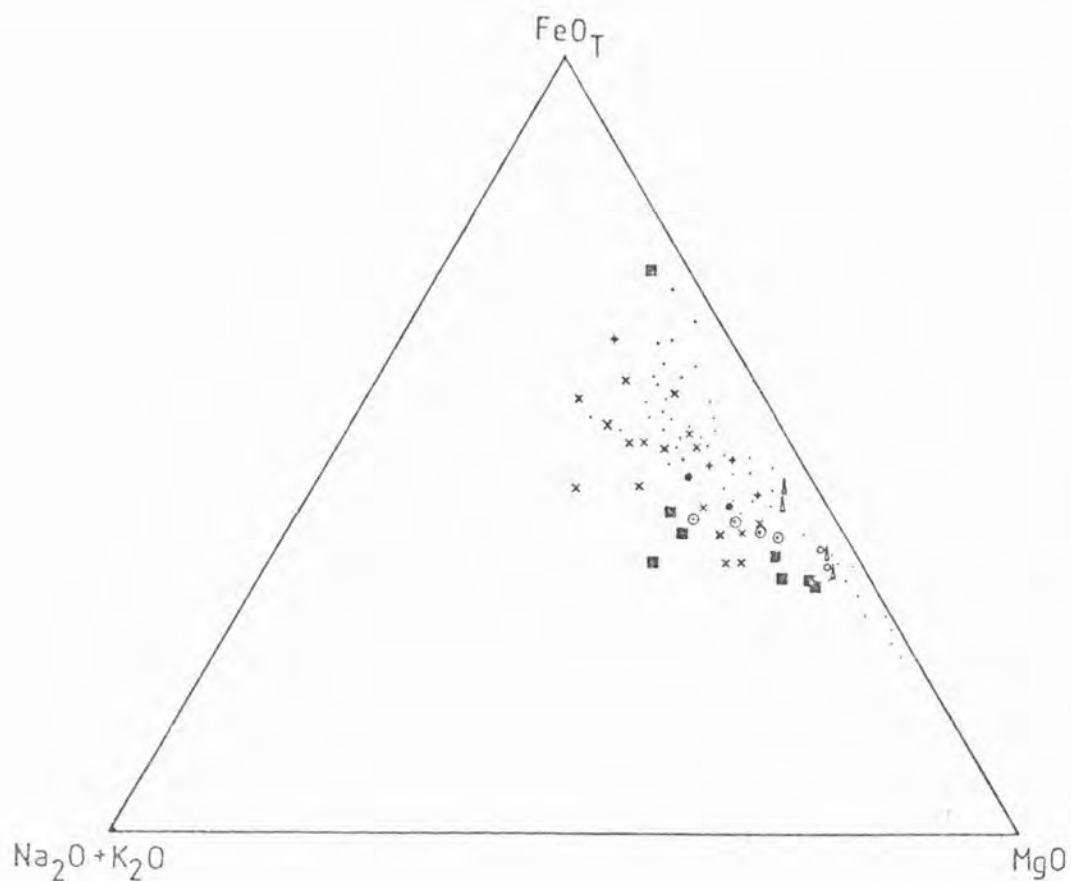


c

discussed in Chapter 5.

Strathan Body: A large mafic mass crops out just to the north of Strathan (088213; Figs.1.18 and 2.5). It continues along strike from the Culag body (see Chapter 2, Fig.2.5) and is folded by a southerly plunging Inverian fold. There is an assemblage of amph-plag-ep±qz. The texture is fairly coarse with irregular grain boundaries, suggesting the amphibolite facies mineralogy is pseudomorphing an earlier granulite facies assemblage. Locally gt-pyx-plag assemblages are preserved. The only sample analysed from this body (D35) is indistinguishable from the gabbros from layered bodies so it is suggested that the amphibolite facies mafic rocks at Strathan are retrogressed gabbros associated with the ultramafic rocks of the Culag body.

Reidh Phort: The Reidh Phort amphibolite mass crops out on the west side of Clashnessie Bay (057315). It is fairly massive sitting on gently dipping micaceous trondjhemitic gneisses (Fig.4.1a). Near the contact with the gneiss the amphibolite becomes agmatized with lenses of amphibolite veined by felsic material (Fig.4.1b). The central part of the mass is interfolded with the gneisses in a series of tight EW-trending folds (Sheraton et al., 1973b; their Fig.2). The rock is composed dominantly of hornblende with minor plagioclase and epidote. The lack of plagioclase may reflect the reaction  $\text{cpx} + \text{plag} \rightarrow \text{hb}$  by which granulite facies assemblages react to form amphibolite facies assemblages (Chapter 5). One more iron-rich sample contains trace amounts of garnet which is partially replaced by biotite. The analyses are compared with the layered complex gabbros on an AFM plot (Fig.4.2), various oxide-element plots (Fig.4.3) and simulated REE plots (Fig.4.4). As can be seen the Reidh Phort amphibolites are very similar to the gabbros on all diagrams.



- Layered complexes from Chapter 3.
- x Basic layers and masses, various localities.
- + Reidh Phort amphibolite mass.
- ⊙ Cnoc a Sgriodaich mafic mass,
- Gorm Loch mafic body, Laxford front.
- Agmatite.
- Hornblendite.
- ▲ Ultramafic lenses in gneiss.

FIG. 4.2 AFM (oxide) plot for the mafic rocks discussed in the text compared with the gabbros and ultramafic rocks from layered complexes.

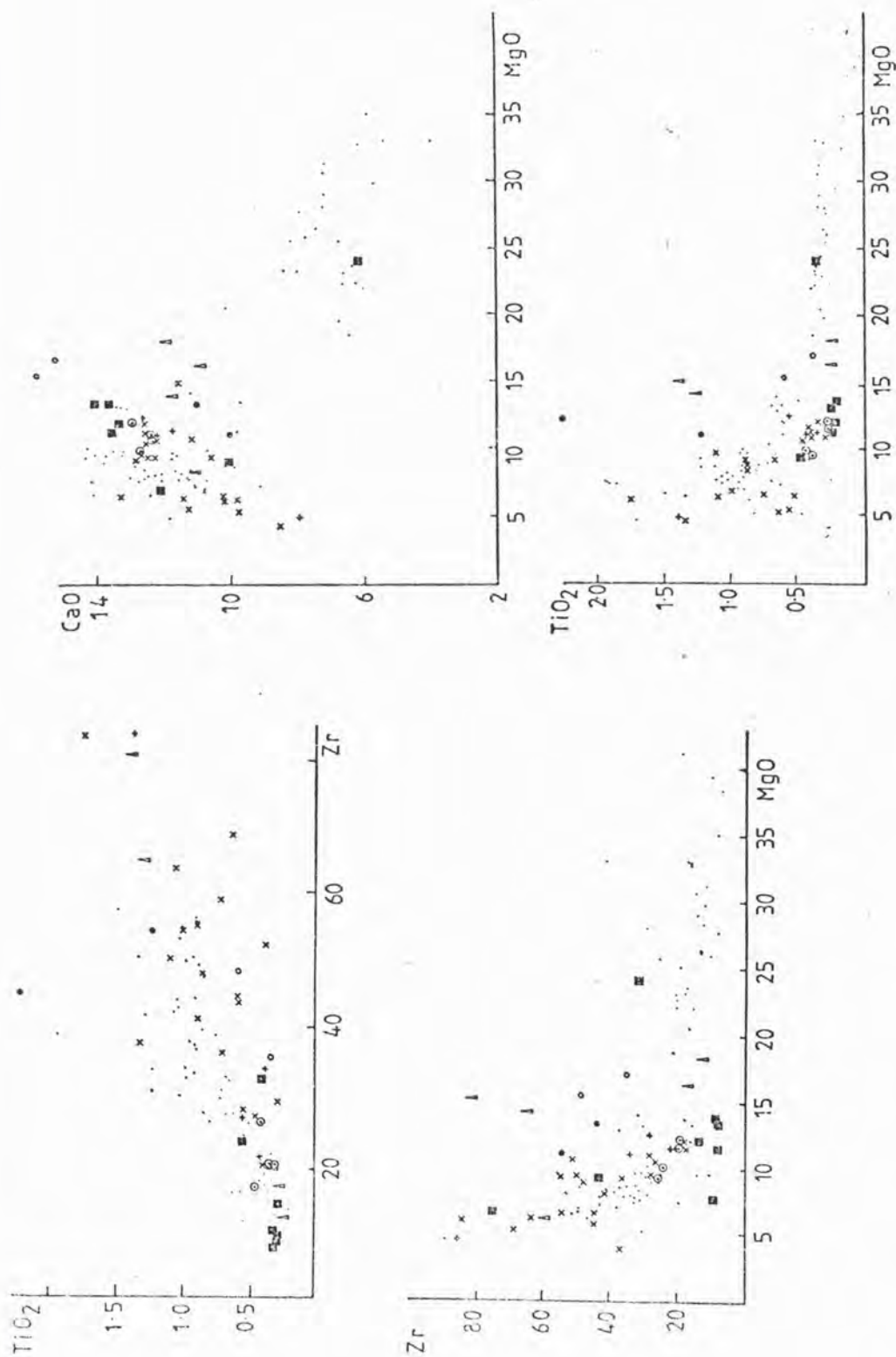


FIG. 4.3 TiO<sub>2</sub>(wt.%) against Zr (ppm) and Zr(ppm), CaO (wt.%) and TiO<sub>2</sub> (wt.%) against MgO (wt.%) for the mafic and ultramafic rocks discussed in the text compared with the rocks from layered complexes. Key as for Fig. 4.2.

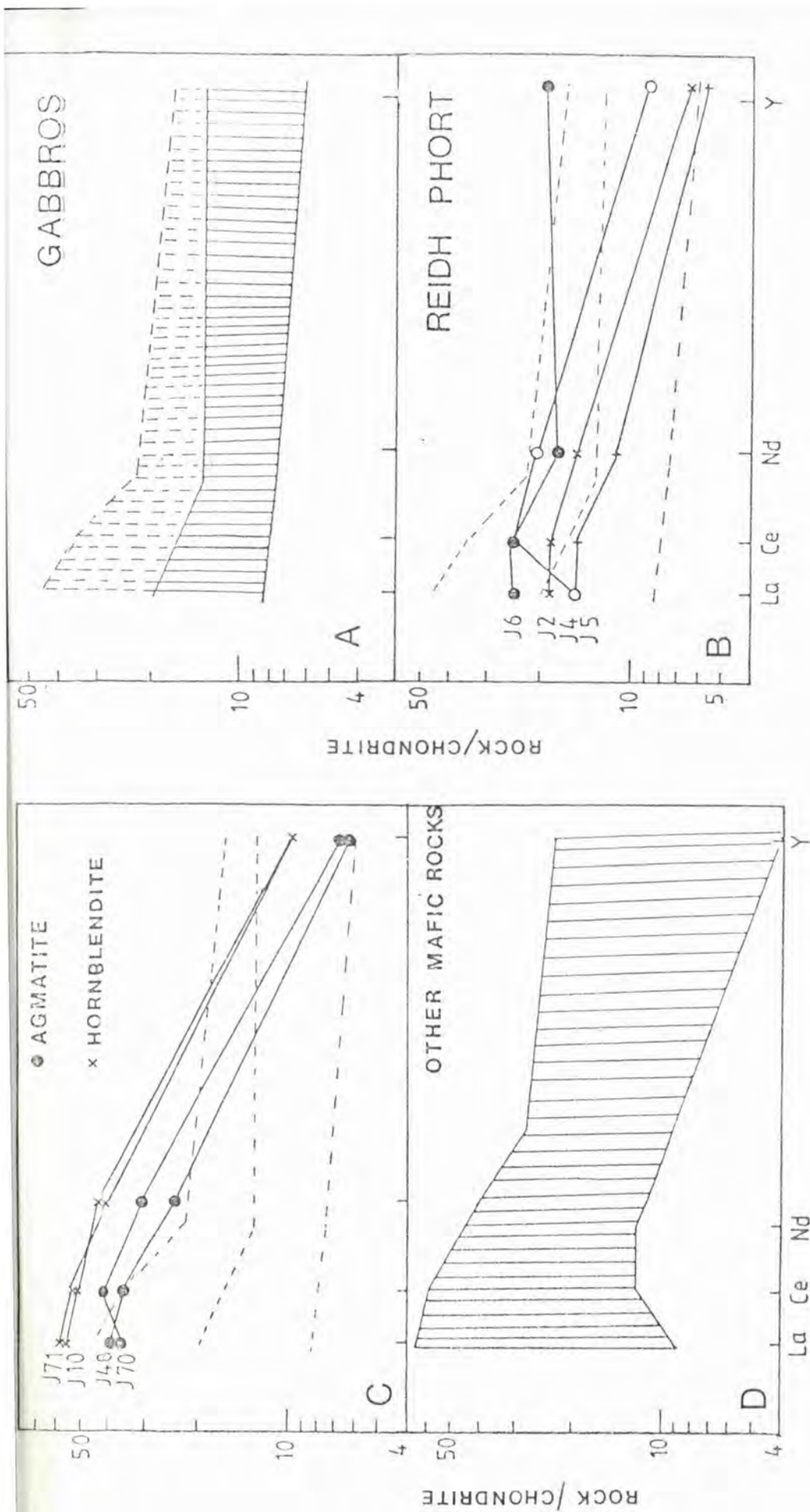


FIG. 4.4 Chondrite normalised simulated REE plots using La, Ce, Nd and Y to monitor the HREE, data are normalised using the values of Nakamura(1974). A- the field for gabbros from layered complexes, most samples falling in the field marked by the solid lines. B - Reidh Phort amphibolites compared with the field of gabbros from A. C - Agmatite and hornblende compared with the field of gabbros from A. D - Mafic layers and lenses.

It is therefore possible that this amphibolite mass is the retrogressed equivalent of the granulite facies gabbros discussed in Chapter 3.

Similarly samples from the large mafic body south of Loch Ardbhair have similar mineral chemistry (sample D27) and whole rock chemistry (samples D19 and D20) to the gabbros. This body also may be gabbro but with no associated layered ultramafic rock.

Gorm Loch, Laxford front: The samples W40-W54 were collected from the thickest part of the layered complex described by Davies (1974) from the Laxford front region NE of Scourie (215445), an area greatly affected by Inverian and Laxfordian deformation. Davies (1974, 1976) interprets this as being part of a more extensive layered complex or complexes which have been folded and thinned during the evolution of the Laxford front synform. The layered complexes are bordered by metasediment. There is a concentration of both metasediment and layered complexes in this region which does not appear to be found elsewhere in the mainland Lewisian.

Lenses of layered pyroxenite are found which closely resemble the ultramafic rocks from other localities (Fig.4.3) but the mafic rocks show several differences from the gabbros from layered bodies elsewhere, notably:

(1) The levels of incompatible trace elements such as Ti, Zr and Y are very low, being lower than in the ultramafic sample W49; e.g.  $\text{TiO}_2$  ranges from 0.22 - 0.48 wt.%, most samples being between 0.22 and 0.27, Zr ranges from 9 - 14 ppm with one sample having 43 ppm and Y ranges from 3 - 7 ppm with one sample having 19 ppm. However trace element ratios are still chondritic. This compares with typical values of 20 ppm Zr, 10 ppm Y and 0.65 wt.%  $\text{TiO}_2$  for gabbros with a similar MgO content. The La, Ce and Nd levels are

below the detection limit of the X.R.F. indicating that the REE content of the Gorm Loch rocks is also lower than that of gabbros.

- (2) The  $\text{Fe}_2\text{O}_3$  content tends to be slightly lower than that of the layered gabbros.
- (3) The  $\text{Al}_2\text{O}_3$  content tend to be slightly higher than that of layered gabbros.
- (4) The contents of Na , K , Sr and Ba are fairly high which can be seen in the AFM plot (Fig.4.2) but this may simply reflect the movement of these elements during metamorphism rather than an original chemical difference.

All these points, taken together with the slightly different field setting of the Gorm Loch mafic body suggests that it may have a different origin from the gabbros from the layered bodies. The low level of incompatible elements in some samples suggests that they may be cumulate. However samples W49 and W47 closely resemble the rocks from the layered bodies and hence may have formed in the same manner (Chapter 3). A final conclusion concerning the origin of the Gorm Loch body cannot be reached as Ni, Cr and REE data are not available.

The Gorm Loch body is cut by granitic sheets (samples W44, W51 and W54) as well as by anorthosites (samples W43, W48, W52 and W53; Table 4.1). Davies (1974) considered the anorthosites to be the final stages in the fractionation of a cumulate body analogous to the Fiskenaesset complex, West Greenland. Sample W43 is from a discordant vein and W48 from a 12 m thick discordant layer, however samples W52 and W53 come from a thick anorthositic sheet forming the uppermost unit of the body. This unit appears to be conformable with the mafic rocks but it grades into granite (sample W54), hence it may be

	W43	W48	W52	W53	W44	W51	W54
SiO <sub>2</sub>	53.0	54.8	51.8	53.9	74.7	74.4	74.1
TiO <sub>2</sub>	0.04	0.77	0.13	0.40	0.03	0.10	0.08
Al <sub>2</sub> O <sub>3</sub>	24.4	25.3	21.9	25.5	15.4	14.5	14.3
Fe <sub>2</sub> O <sub>3</sub>	3.25	2.87	5.59	2.64	0.89	0.87	1.28
MnO	0.08	0.07	0.11	0.04	0.05	0.04	0.08
MgO	2.58	1.14	4.01	1.44	0.32	0.15	0.24
CaO	8.04	6.03	9.11	9.46	3.56	0.87	0.78
Na <sub>2</sub> O	6.14	6.90	4.25	6.15	5.12	5.20	4.29
K <sub>2</sub> O	1.63	1.57	1.31	0.32	0.72	3.65	4.85
P <sub>2</sub> O <sub>5</sub>	0.00	0.15	0.01	0.08	0.02	0.01	0.01
TOTAL	99.17	99.60	98.22	99.93	100.81	99.79	100.01
Ni							
Cr							
Zn	10	5	58	6	9	5	8
Rb	39	36	26	4	8	113	194
Sr	578	775	483	492	447	205	83
Ba	172	580	162	165	286	606	411
Zr	109	46	16	42	28	71	79
Nb							
La	2	30		12		10	24
Ce	7	80	15	26		21	31
Nd		43	6	7		6	5
Y	1	10	3	<1	41	1	30
Ga	30	23	30	31	20	24	24

TABLE 4.1 Anorthositic and granitic rocks from the Gorm Loch body in the Laxford front (Davies, 1974).

related to the granitic rocks rather than the mafic body. Discordant anorthositic lenses from layered bodies elsewhere have very steep REE patterns indicating they could not be derived by crystal fractionation from the basaltic magma which gave rise to the mafic and ultramafic rocks. Weaver and Tarney (in press) proposed that they formed as local small scale partial melts. The anorthosites are composed of plagioclase (ca  $An_{50}$ ), this being much lower than the An content of plagioclase from large cumulate anorthosite bodies (e.g. Windley and Smith, 1974). The four anorthosites analysed are rather variable; W48 having high La and Ce contents typical of the discordant anorthosites and trondjemites found elsewhere (Weaver and Tarney, in press) while the other samples have much lower REE contents (Table 4.1). The other incompatible elements are also rather variable, for example sample W43 has very low  $TiO_2$  (0.04 wt.%) low REE (La - 2 ppm and Ce - 7 ppm) but the Zr content is very high (109 ppm). These analyses suggest that there may be two types of anorthosite, firstly the type with strongly LREE enriched patterns which are probably partial melts of the mafic rocks or gneisses (Weaver and Tarney, in press) and secondly cumulates with low levels of REE, Ti and Zr. Further information is needed before this problem can be resolved. The granite and trondjemite sheets are very similar to those described from the Scourie region (Rollinson and Windley, 1980b).

Cnoc an Sgriodaich: Mafic material crops out over a wide area near Cnoc an Sgriodaich (060295) as noted by Peach et al. (1907). The structure of this area is complex (Fig.4.5) with NW-trending open folds being folded by NNE-trending monoclinial folds in turn cut by ESE-trending shear zones. Most of the rocks are amphibolite or hornblendite with granulite facies assemblages preserved locally. Parts of the body are

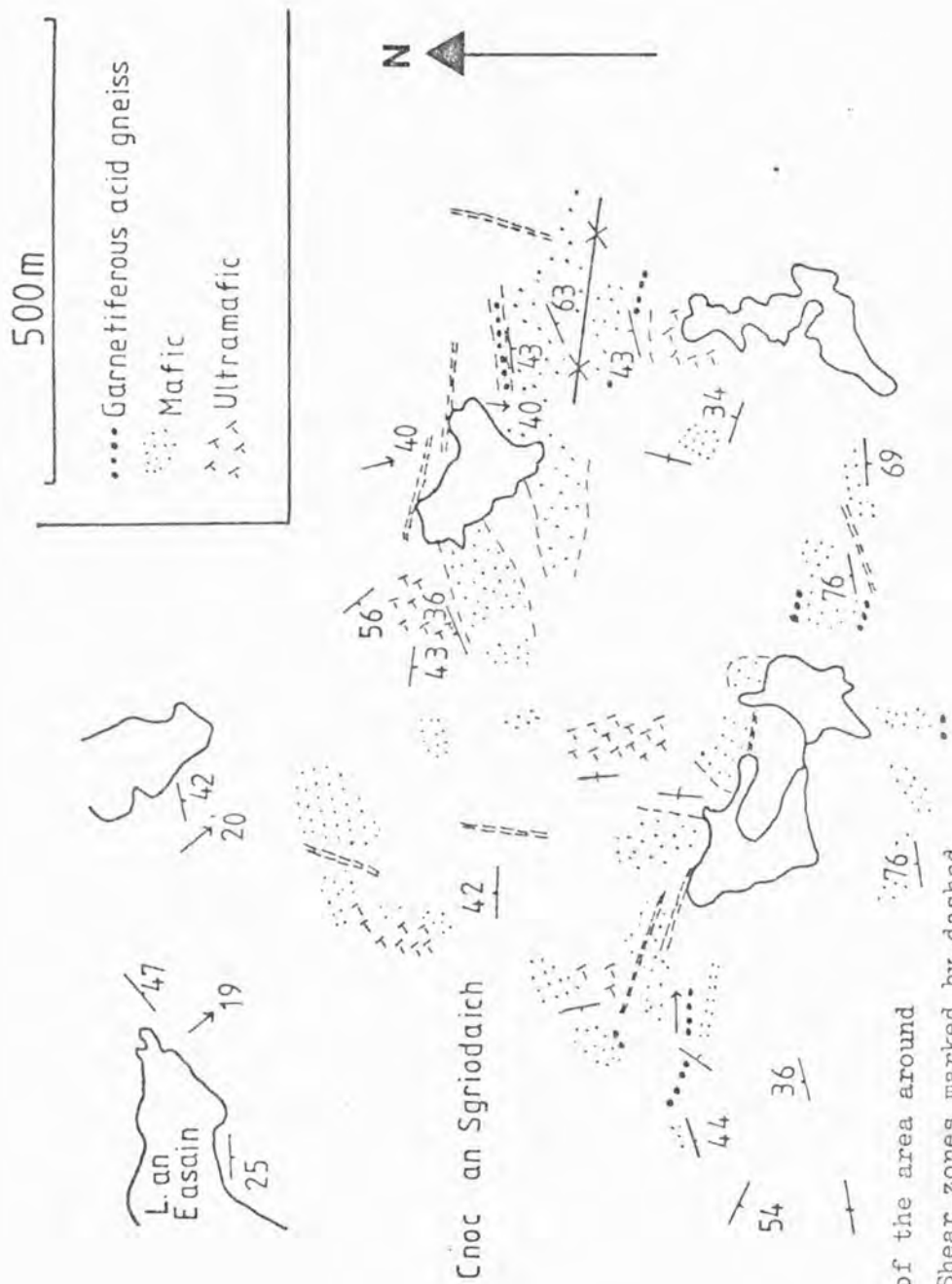


FIG. 4.5 Sketch map of the area around Cnoc an Sgrìodaich. Shear zones marked by dashed lines, fold axes by solid lines, lineations by arrows.

agmatized, where massive amphibolite grades into agmatite with amphibolite blocks in a felsic matrix (Fig.1.1a). Discordant anorthositic patches, with hornblende spots, are common as at Gorm Loch. The Cnoc an Sgriodaich amphibolites closely resemble those from Gorm Loch with low levels of incompatible elements ( $\text{TiO}_2$  ranges from 0.3 - 0.45, Zr from 17 - 27 ppm and Y from 2 - 11 ppm), and low  $\text{Fe}_2\text{O}_3$  (9 - 10 wt.%). The body is bordered in places by qz-gt-bi-plag-hb gneiss, believed to be metasediment (see later); another similarity with the Gorm Loch body which is also enclosed in sediment (Davies, 1974,1976).

In conclusion it appears that most of the mafic bodies have a very similar composition to the layered complexes discussed in Chapter 3 and presumably have a similar origin. However the Gorm Loch and Cnoc an Sgriodaich bodies are slightly different, having low levels of incompatible elements possibly indicating a cumulate origin. However the Gorm Loch body has very uniform MgO and the Ni content of the Cnoc an Sgriodaich rocks is quite low (70 - 160 ppm), lower than that of gabbros with similar MgO contents. More data is needed on the latter two bodies before any firm conclusion can be reached.

#### 4.3. DESCRIPTION AND PETROGENESIS OF MAFIC LAYERS AND LENSES

Layers and lenses of mafic material occur throughout Assynt and they could either be fragmented pieces of layered bodies or have a different origin such as being metavolcanics. These mafic layers plot on the same tholeiitic iron-enrichment trend (Fig.4.2) as the gabbros and have a similar range of trace element abundances and ratios (Fig.4.3) with similar LREE enriched rare-earth patterns (Fig.4.4). Occasionally gabbroic bands can be traced along strike from a layered complex

becoming thin amphibolite facies layers, demonstrating that it is possible to derive amphibolite from the granulite facies gabbros. The LREE enriched patterns and iron-enrichment trend are typical of many Archaean basalts (e.g. Arth and Hanson, 1975) and is contrasted with modern MORB (e.g. Schilling, 1975). The fairly low MgO contents of most samples (5 - 10 wt.%) argues against them being primary mantle liquids and suggests they have undergone some crystal fractionation. The low level of incompatible elements in some samples indicates they may be partially cumulate. The general similarity with the gabbros implies the mafic lenses may have been tectonically separated from the main gabbroic bodies during deformation possibly during an early phase of isoclinal folding which affected the layered complexes. However it is obviously not certain that all the mafic rocks originated in this way and some variety of modes of formation is possible.

#### 4.4. AGMATITES

Net-veined rocks (agmatites, Figs.1.1b and 4.1c) occur throughout the Assynt district and are clearly distinguishable from the ultramafic pods and balls, as the latter occur enclosed in gneiss whilst the agmatites comprise ultramafic blocks in a plag-qz matrix; the whole body being bordered by gneiss. The centres of the masses, which range up to 100m across, are generally unfoliated although the felsic veins may have a quartz-rodding lineation indicating they were in existence before the end of the early Scourian event which produced the main lineation. The margins of the bodies are foliated, often merging into banded gneiss as the ultramafic and felsic layers are flattened. Due to the intense deformation and metamorphism it is not possible to determine whether the felsic veins are a partial melt product of an original mafic or

ultramafic body or whether the mafic body was invaded and broken up by veins derived from the surrounding gneisses. However the veins are fairly evenly distributed throughout the body unlike the Reidh Phort and Cnoc an Sgrìodaich bodies which are partially agmatized near their contact with the gneisses which can be seen to invade the mafic body (Fig. 4.1b). This may indicate either a net-veined origin or agmatization very early in the history of the Lewisian.

Two samples have been analysed (J48 and J70; Appendix B4, mineral analyses from J48 are given in Appendix A2). The ultramafic blocks comprise pale green actinolitic hornblende wholly or partially replacing clinopyroxene, with trace amounts of plagioclase and epidote. They have a fairly high MgO content of 15 - 17 wt.% and Ni and Cr contents of 725 and 900 ppm respectively, this taken together with the high mg number of the minerals (0.78 for amphibole and 0.8 for clinopyroxene) suggests ultramafic affinities. The high CaO content of 15 - 16.5 wt.% reflects the high clinopyroxene content. However the incompatible trace element contents are fairly high with Zr ranging from 36 - 49 ppm,  $TiO_2$  from 0.36 - 0.61 wt.% and Y from 11 - 13 ppm. The La, Ce and Nd contents are very high for a rock with ultramafic affinities (Fig.4.4). A possible origin for these agmatites is as a clinopyroxene cumulate but the incompatible element contents, especially the LREE are too high. The  $K_D^{cpx-liq}$  for Ti, Zr and Y of 0.3, 0.1 and 0.5 respectively would lead to cumulates with high Ti/Zr and low Zr/Y ratios while the reverse is found. Alternatively these agmatites could be parts of layered ultramafic complexes which have been highly deformed and separated from the main bodies. However this does not account for the clinopyroxene rich nature of these rocks with a CaO content about twice that of any of the layered ultramafics. The origin of these agmatites is far from clear and more data is required before any

conclusion can be reached, but it is probable that metamorphic effects, possibly involving partial melting to produce the felsic veins, have altered the primary chemistry considerably.

#### 4.5. HORNBLENDITE PODS AND LAYERS

Hornblendite pods and balls occur throughout the Assynt district, tending to occur in clusters away from any obvious source. They presumably resulted from extreme boudinage and fragmentation of either mafic or ultramafic masses. In addition to the pods, which range up to 1 m in length, there are larger lenses or layers of hornblendite.

The smaller pods are generally composed of paragonitic hornblende although pyroxenite and gabbroic pods are found in the extreme east of the area near Kylesku. Most of the hornblendite pods and lenses are composed of a dark, coarse paragonitic hornblende but some comprise a paler, fine grained actinolitic hornblende. The colour of the hornblende is quite variable, possibly indicating a variety of sources. Both mafic and ultramafic rocks tend towards monomineralic hornblende with prolonged metamorphism. Many of the smaller pods have high Ni and Cr contents indicating an ultramafic source but variable Ni/Cr ratios may indicate a variety of sources (Tarney, 1978).

For this study no small pods have been analysed but a variety of hornblendite lenses enclosed in tonalitic gneisses from Clashnessie Bay have been analysed (see Table B4, Appendix B). These lenses are rather irregular, 1-5 m thick and up to 50 m long. The analyses are plotted on Figs. 4.2 - 4.4 as hornblendite and ultramafic layers in gneiss. The composition varies considerably from basaltic (e.g. sample J10 with 104 ppm Ni and 169 ppm Cr) to ultramafic (e.g. sample J61 with 800 ppm Ni and 3000 ppm Cr). The analyses cannot be compared directly with ultramafic rocks from layered complexes as the development

FIG. 4.6 (a) Photomicrograph of sample J10, showing large paragonitic hornblende, clouded with oxide dust and cut by flakes of biotite. Field of view 2.0mm.

FIG. 4.6(b) Photomicrograph of a phlogopite grain from sample D3, showing the exsolution of tiny brown chromite needles. Field of view about 1.0mm.



A



B

of a monomineralic hornblende assemblage has affected the composition, e.g. the CaO content is consistently about 11 wt.%, this being the CaO content of hornblende and is much higher than the CaO content typical of ultramafic rocks.

Sample J10, from a 5m thick layer, is composed of coarse (0.5 cm) crystals of pargasitic hornblende; the centres of grains being clouded with oxide dust and the edges being clear. Flakes of biotite occur along grain boundaries as well as cross-cutting the hornblende cleavage (Fig.4.6a). The biotite (5 modal %) can easily be derived from an earlier, more potassic hornblende. The whole rock analysis (Table 4.2) can be recalculated as a ferroan pargasitic hornblende with a  $\text{TiO}_2$  -  $\text{K}_2\text{O}$  - rich composition typical of granulite facies rocks (see Chapter 2), implying the pargasite was probably stable throughout the granulite facies event and that the disruption which produced the hornblende layers occurred early in the history of the complex. The  $\text{TiO}_2$  and Ba contents are higher than for other mafic rocks with similar MgO content. Both these elements are favoured by the hornblende structure, demonstrating that the development of a monomineralic hornblende assemblage influences the composition of the rock. The excess Ti and Ba were presumably derived from the enclosing gneisses.

The remaining hornblende lenses are composed of a finer grained actinolitic hornblende. It is not known whether this formed from the retrogression of granulite facies pargasite or from pyroxene-plagioclase assemblages. The  $\text{SiO}_2$  content of the actinolitic-lenses is correspondingly higher with  $\text{Al}_2\text{O}_3$  being lower. These layers are formed from both mafic (J69 and W59) and ultramafic (J15, J23 and J61) material. The latter two samples are similar to the ultramafics from layered bodies except for higher CaO and  $\text{SiO}_2$  and lower MgO. It is not certain whether these hornblende lenses are fragmented mafic and ultramafic

J 10 whole-rock	J10 amph- centre	J10 amph- edge	J10 biotite
SiO <sub>2</sub> 42.39	SiO <sub>2</sub> 42.04	43.28	37.59
TiO <sub>2</sub> 2.21	TiO <sub>2</sub> 2.15	0.76	1.21
Al <sub>2</sub> O <sub>3</sub> 11.16	Al <sub>2</sub> O <sub>3</sub> 13.58	13.02	16.22
Fe <sub>2</sub> O <sub>3</sub> 13.67	FeO 12.61	12.62	10.77
MnO 0.14	MnO 0.17	0.22	0.10
MgO 13.66	MgO 12.11	12.45	17.39
CaO 11.08	CaO 11.35	11.76	0.00
Na <sub>2</sub> O 1.68	Na <sub>2</sub> O 2.37	2.22	0.15
K <sub>2</sub> O 1.43	K <sub>2</sub> O 0.48	0.58	9.66
P <sub>2</sub> O <sub>5</sub> 0.03	Cr <sub>2</sub> O <sub>3</sub> 0.01	0.03	0.02
TOT 97.45	F 0.25	0.25	0.57
	TOT 97.14	97.21	94.10
Ni 104	Si 6.245	6.415	5.598
Cr 169	Al <sup>vi</sup> 1.755	1.585	2.402
Zn 92	Al <sup>iv</sup> 0.623	0.690	0.515
Rb 14	Ti 0.240	0.085	0.135
Sr 209	Cr 0.001	0.003	0.002
Ba 568	Fe 1.566	1.564	1.342
Zr 45	Mn 0.021	0.027	0.012
Nb <1	Mg 2.681	2.750	3.861
La 19	Ca 1.806	1.868	0.000
Ce 46	Na 0.683	0.639	0.045
Nd 26	K 0.091	0.109	1.835
Y 19			
Ga 17	mg 0.628	0.633	0.740
Th <3			
Pb <4			

TABLE 4.2 Whole-rock and mineral analyses from a hornblendite, sample J10, from the east side of Clashnessie Bay.

masses or whether they have resulted from metamorphic differentiation; however the concentration of hornblende found at the east end of Clashnessie Bay indicates that they may be derived from the fragmentation of a mafic body.

An unusual ultramafic pod enclosed in granulite facies gneisses from Kylesku (230337) is composed of partially serpentinised orthopyroxene and phlogopite with exsolved chromite needles (Fig.4.6b). The phlogopite has a fairly high  $\text{Cr}_2\text{O}_3$  content of 1 - 1.5 wt.% fairly low  $\text{TiO}_2$  of about 1.25 wt.% and a fluorine content of 0.6 - 0.75 wt.%. The exsolved brown spinel phase is variable with: 17 - 24 mol.% spinel, 50 - 61 mol.% chromite and 15 - 32 mol.% magnetite. This is in strong contrast to the green hercynite spinels from the layered ultramafics which have less than 7 mol.% chromite. Before the exsolution of this spinel the phlogopite would have had about 2 wt.%  $\text{Cr}_2\text{O}_3$ , this exsolution presumably occurring during slow cooling of the complex. This pod is unlike any other ultramafic rock found in the Lewisian and its provenance is unknown as no whole rock analysis is available. The Cr content of the pod must be very high as the orthopyroxene has a  $\text{Cr}_2\text{O}_3$  content of 0.55 wt.%, very much higher than in the pyroxenes from the layered ultramafics. The  $\text{Al}_2\text{O}_3$  content of 2.5 - 2.75 wt.% is fairly typical of granulites and its mg value is slightly less than that of the pyroxenes from other ultramafics (0.8 compared to about 0.83). The high Cr content taken together with the presence of phlogopite tends to suggest that this pod was not derived by fragmentation of layered pyroxenites. Phlogopite of a similar composition is found in the Finero mantle peridotite of the Ivrea zone (Brodie, 1980) but it is slightly more magnesian and the co-existing pyroxenes are far more Mg-rich (mg is about 0.9 for orthopyroxene). The relatively low mg-value of the Kylesku orthopyroxene suggests that the pod is unlikely to be a mantle fragment.

The ultramafic pods and lenses are thus rather variable, some being derived from mafic sources, others from ultramafic. The concentration of hornblende lenses in one area (the east end of Clashnessie Bay) tends to suggest they are fragmented mafic bodies rather than the result of metamorphic differentiation. Their petrogenesis is difficult to determine as the formation of a monomineralic hornblende assemblage has clearly affected the composition of the pods causing a uniform CaO content and increased Ti and Ba contents. For this change in chemistry to take place the disruption of the original mafic bodies must have occurred before the metamorphic event which produced the hornblendes as the chemistry of the larger mafic bodies has not been altered in the same manner.

From the above discussions it can be concluded that there is probably a variety of mafic and ultramafic rock types in the Lewisian gneisses but that the majority of them are layered gabbros and ultramafics or their retrogressed equivalents.

#### 4.6. METASEDIMENTARY GNEISSES FROM THE ASSYNT REGION

Metasedimentary gneisses have been reported from several parts of the Lewisian; notably from South Harris (Coward et al., 1969), from the Laxford front area (Davies, 1974, 1976), a meta-ironstone from Scourie Bay (Barnicoat and O'Hara, 1979) and gt-qz gneisses from Assynt (Sheraton et al., 1973a).

The vast majority of the acid and intermediate gneisses in Assynt are at amphibolite facies with the main ferromagnesian minerals being hornblende and biotite. However, rare intermediate composition gneisses containing garnet in addition to qz, plag, hb and biotite are found. These rocks tend to occur bordering mafic bodies and it is possible that

they have a sedimentary origin as suggested for similar qz-gt gneisses in the Assynt district (Sheraton et al., 1973a). Possible metasedimentary gneisses have been found at four localities:

(1) Bordering the Cnoc an Sgrìodaich body (Fig.4.5). These gneisses are very iron-rich with about 15 wt.% total iron as  $\text{Fe}_2\text{O}_3$  (Table 4.3; samples D17 and S4). They have an assemblage of gt-qz-plag-hb-bi-opq; with all the ferromagnesian minerals having low mg numbers (mg-garnet = 0.06, mg-amphibole = 0.15, mg-biotite = 0.21), much lower than for any other gneisses (see Chapter 5). Ni is below the minimum detection limit, but the  $\text{TiO}_2$  and Zr contents are fairly high (1.25 wt.% and 130 ppm respectively). The hornblende and biotite have higher  $\text{Al}^{\text{vi}}$  contents than minerals from other gneisses.

(2) Bordering the Loch Poll an Droighinn gabbros (055288; samples J94, J120, Table 4.3). These samples are composed of qz-plag-gt-bi, with the biotite wholly or partially replacing the garnet. J94 has a high  $\text{Al}_2\text{O}_3$  content (19.4 wt.%) and moderate  $\text{TiO}_2$ , Cr, Ni and Zr and of the samples analysed for this study most closely resembles the qz-gt gneisses of Sheraton et al. (1974a; Table 4.3). Sample J120 has qz-layers, high normative quartz, high  $\text{TiO}_2$  (2.7 wt.%) and high  $\text{P}_2\text{O}_5$  (1.45 wt.%).

(3) N.E. of Maiden Loch (058274). At this locality there is an Inverian steep belt containing a variety of rock types; normal tonalitic gneiss, qz-gt-plag-hb-bi-gneiss (samples J113, J114 (Table 4.3) and J98 (Appendix A2)), a trondjemite sheet and a peculiar brown weathering gneiss containing pale pink garnet with the following assemblage: qz-plag-gt-bi-hb-chl-anth-opq;sulp-ap. The hornblende from these samples has a high  $\text{Al}^{\text{vi}}$  content.

	D17	54	J94	J113	J114	J47	J96	S10	Assynt (Sheraton)	Lever- burgh	Flowerdale Schist	Av. Freywuicke Gondie(1957)	Feilite (Turney, 1977)	Semi-pelite vs-pelite	
SiO <sub>2</sub>	64.01	65.23	57.16	51.52	63.15	63.61	50.84	51.50	50.20	67.36	64.57	64.40	43.30	62.20	76.60
TiO <sub>2</sub>	1.00	1.26	0.94	1.04	0.51	1.14	0.78	1.43	0.76	0.64	0.81	0.62	2.41	1.20	0.92
Al <sub>2</sub> O <sub>3</sub>	12.97	12.79	19.59	17.49	16.85	14.04	12.99	19.66	16.50	14.61	14.03	15.50	20.40	15.10	7.20
Fe <sub>2</sub> O <sub>3</sub>	14.59	15.55	8.36	9.30	5.04	6.99	11.74	13.20	10.12	6.12	6.86	6.54	15.50	8.70	5.10
MnO	0.21	0.22	0.15	0.16	0.10	0.05	0.19	0.24	0.11	0.06	0.05		0.13	0.12	0.13
MgO	1.09	1.07	3.91	4.47	1.43	2.71	9.00	6.46	4.80	2.86	5.50	3.12	2.28	1.85	0.92
CaO	3.23	3.68	3.26	3.48	3.96	3.18	4.62	5.04	3.75	3.20	2.68	2.22	1.06	0.84	1.34
Na <sub>2</sub> O	2.02	1.79	5.90	4.18	4.91	4.08	2.24	3.05	3.10	2.52	2.29	3.74	0.38	1.12	1.46
K <sub>2</sub> O	1.54	1.43	1.75	0.95	1.79	2.34	0.85	1.09	2.56	2.75	2.95	2.44	6.91	4.55	2.04
P <sub>2</sub> O <sub>5</sub>	0.25	0.25	0.04	0.65	0.58	0.39	0.12	0.20	0.07	0.13	0.18		0.00	0.11	0.10
TOTAL	101.26	100.98	100.84	98.38	98.06	99.33	100.37	101.03	101.40						
Bi	<1	<1	107	13	29	<1	201	231	159	36	98	91	87	50	29
Cr	nd	nd	243	8	136	11	689	nd	355	120	482		323	105	77
Zn	nd	nd	75	107	66	62	210	nd					163	155	64
Pb	31	53	34	11	27	20	21	26	58	59	109	88	214	124	72
Sr	162	142	431	809	855	604	181	295	291	405	147	424	44	71	53
Ba	nd	nd	1127	698	1699	4450	167	nd	786	1100	562		698	574	583
Zr	127	159	317	434	174	958	86	96	103	288	221	199	323	180	361
Nb	6	15	11	6	<1	13	2	4	10	11	9		26	12	12
La	nd	nd	42	46	104	83	19	nd					28	29	21
Ce	nd	nd	76	107	189	175	38	nd					56	51	38
Md	nd	nd	26	57	75	92	19								
Y	62	58	30	26	15	39	23	23	24		24		30	28	24

TABLE 4.3 Analyses of possible metasedimentary gneisses. Assynt is the average of 6 gt-qz gneisses from Sheraton et al. (1973a); Leverburgh and Flowerdale schist analyses are from Winchester et al. (1980).

(4) A lens of biotite-rich gneiss with numerous tiny zircon crystals (J47) was found near Loch an Easain (057296). Although it does not border a mafic body and has no garnet, the composition is similar to samples D17 and S4 but less iron-rich. It has a very high Zr and Ba contents.

In high-grade gneiss terrains it is often difficult to distinguish between clastic metasediments and tonalitic gneisses, as the sediments are commonly derived from granitic crustal material and if the sediments are fairly immature they will have a similar composition. However differences in composition have been found which may enable ancient metasedimentary rocks to be recognised. If the original sediment contained a high proportion of clay minerals it is likely to be corundum-normative. In some metasedimentary sequences some inter-element correlations are opposite to those expected from an igneous suite; for example Tarney (1977) found K and Rb correlated with Mg, Cr and Ni. In most calc-alkaline series Zr increases with differentiation until very siliceous compositions when it falls suddenly; however in sedimentary rocks Zr may be present replacing Al in clay minerals as well as in detrital zircon, causing a more erratic variation of Zr contents (Van der Kamp et al., 1976). Similarly Ni and Cr fall off rapidly with differentiation in igneous suites whereas in sediments Ni and Cr are fairly constant over a wide silica range (Van der Kamp et al., 1976). Hence Zr, Ni, Cr and Ti contents of fairly siliceous sediments are often higher than for igneous rocks with the same silica content.

All the Assynt gneisses which could be of sedimentary origin, with the exception of sample J113, are corundum normative, but so are some of the trondjhemitic gneisses. However all the metasediments have

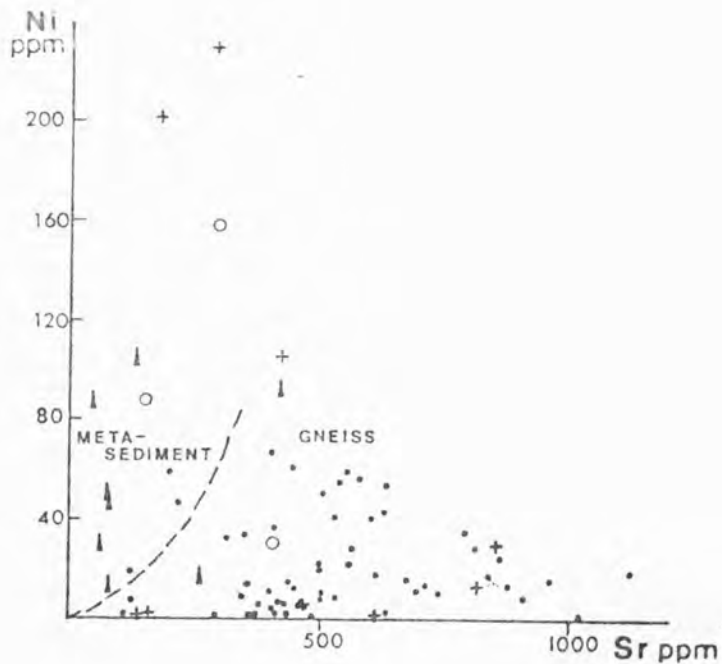
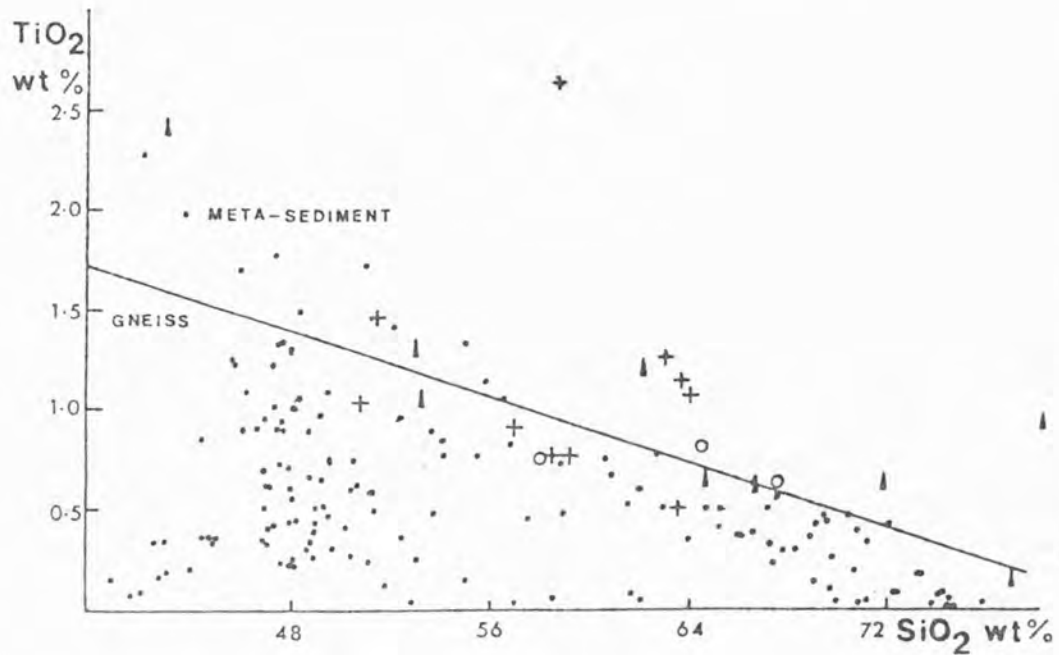


FIG.4.7(a)  $\text{TiO}_2$ - $\text{SiO}_2$  plot after Tarney(1977)

(b) Ni-Sr plot after Winchester et al(1980)

KEY: dots- gneisses, crosses- metasediment from this study, open circles-other Lewisian sediments and triangles-known sediment. All data from Table 4.3 except gneisses which are from Appendix B. In (b) only gneisses with more

less than 64 wt.%  $\text{SiO}_2$ , therefore this may be significant. Some samples have high Zr (especially J47) and  $\text{TiO}_2$  but not all of them; similarly the Ni contents are very variable, samples J96 and S10 having quite high Ni (200 ppm) while D17, S4 and J47 have a nickel content below the detection limit. These features are shown in Fig.4.7a and b and Table 4.3, where these metasedimentary gneisses are compared with known sediments from elsewhere (data from Tarney, 1977), other sedimentary gneisses from the Lewisian and a range of mafic-acid gneisses (data from this study). Tarney (1977) devised a plot to discriminate between sedimentary and igneous gneisses based on their  $\text{TiO}_2$  content. In Fig.4.7a it can be seen that some of the possible metasedimentary gneisses plot in the sedimentary field, while others do not. However the average Precambrian greywacke of Condie (1967) and the gt-qz gneisses of Sheraton et al. (1973a) also plot below the line. Similarly in Fig.4.7b, a Ni-Sr plot devised by Winchester et al. (1980) to discriminate between the two gneiss types, some samples plot in the sedimentary field, others in the igneous field. Interestingly the samples plotting in the sedimentary field in the  $\text{TiO}_2$  -  $\text{SiO}_2$  plot fall in the igneous field in the Ni-Sr plot. Samples J113 and J114 plot in the igneous field in both plots. A similar plot for Zr (not shown) reveals that, most but not all of the metasedimentary gneisses have a higher Zr content at a given  $\text{SiO}_2$  level than the igneous-gneisses. Samples J94, J113 and J114 are very similar to the gt-qz rocks of Sheraton et al. (1973a) and to the average Precambrian greywacke of Condie (1967).

Although rather inconclusive, the indication from these plots, taken together with the fact that these samples have a different mineralogy to the gneisses suggests that they may be metasediments. Comparisons with known sediments suggests they were probably fairly immature sediments such as greywackes. D17 and S4 are different in that their

iron content is so high. However an ironstone has been reported from Scourie (Barnicoat and O'Hara, 1979) so possibly they are related.

The presence of sediments in the Lewisian complex is of significance and adds a constraint to the models for generating this section of the crust. It is also significant that these sediments tend to occur bordering mafic bodies such as the Gorm Loch and Cnoc an Sgriodaich bodies, suggesting the sediment was incorporated into the dominantly plutonic complex along with the mafic bodies. In southern Chile, metasediment is found intercalated with the tonalitic gneisses and is believed to be part of a subducting accretionary prism that has been incorporated into the tonalitic gneisses (J. Tarney, pers. comm.). The metasediment could possibly have been incorporated into the Lewisian complex in a similar manner, but this involves considerable speculation. However it does provide another analogy between the Lewisian complex and the continental-margin of South America, as suggested by Windley and Smith (1976).

## CHAPTER 5

## RETROGRESSION OF THE ASSYNT GNEISSES

## 5.1. INTRODUCTION

In this chapter, the Inverian and Laxfordian retrogression of the Assynt gneisses will be examined. The reworking of Scourian granulites in WNW-trending Inverian steep belts and Laxfordian shear zones has been discussed in Chapter 1. The close association of metamorphism and deformation was emphasised. It is assumed that all the Assynt gneisses were originally metamorphosed at granulite facies, with a flat-lying foliation. The reasons for this assumption are that relict Scourian areas are found between Inverian steep belts and even in the Stoer-Clashnessie area, where steep belts are very close together and where retrogression has been extensive, granulite facies assemblages may be preserved in mafic and ultramafic rocks, e.g. harzburgite near Alltan na Bradhan (samples J21, J22; 054263) and garnet granulite near Loch Poll an Droighinn (055288). Outside Laxfordian shear zones the amphiboles are poorly crystallised and are clearly pseudomorphing an earlier granulite facies texture. Chemical comparisons would not be valid unless one was certain that the amphibolite facies rocks were derived from granulite facies assemblages. The retention of granulite facies assemblages in mafic rocks, when intermediate and acid gneisses are retrogressed, is a common phenomenon and is due to the fact that a larger amount of water is required to retrogress a mafic assemblage with 50-70 modal % mafic minerals than an acid gneiss with only 10% mafic minerals. There are few mafic rocks in Assynt without some replacement of pyroxene by amphibole.

The region can be divided into metamorphic divisions which are correlated with the structural divisions in Chapter 1. They are as follows:

- (a) areas with granulite facies assemblages (rare in Assynt),

- (b) areas with low amounts of Inverian deformation, retrogression being concentrated in steep belts. Acid and intermediate gneisses are retrogressed but mafic and ultramafic rocks retain their granulite facies assemblages,
- (c) areas with a large amount of Inverian deformation and extensive retrogression. In the latter two cases the metamorphism is "static" and the amphibolite facies minerals pseudomorph the granulite facies minerals with no recrystallisation,
- (d) fine grained completely recrystallised assemblages from Laxfordian shear zones. There is considerable reduction in grain size and extreme attenuation of the banding.

The detailed mineral chemistry of granulite facies gneisses from the Scourie area was studied by Muecke (1969) and Rollinson (1978). Apart from mafic rocks, no study of granulite mineralogy in the Assynt area can be made. Beach (1974a) discussed the amphibolitisation of Scourian granulites concluding that there was overall gain of Na and  $H_2O$  and loss of Ca and Mg. Beach and Fyfe (1972) and Beach (1973, 1976) examined shear zones in the Scourie area concluding that there was little overall change in composition during Inverian-type retrogression but shear zones were enriched in K and  $H_2O$ , depleted in Ca and Fe and oxidised relative to undeformed gneisses. The mineralogy of these shear zones indicates P-T conditions of about 600°C and 6kb (Beach, 1973) during Laxfordian shearing. Drury (1974) studied retrogression of gneisses from Coll and Tiree concluding that there was an increase in K, Rb, K/Ba and Rb/Sr in all rock types. Beach and Tarney (1978) discussed chemical changes that took place during retrogression by

comparing 39 granulite facies samples, 145 amphibolite facies samples and 52 samples from shear zones. The process of retrogression was shown to involve considerable large-scale chemical equilibration, with retrogressed samples having a more constant Fe/Mg ratio. Tarney (1973) studied the Inverian metamorphism of picritic Scourie dykes in the Lochinver area.

In this chapter the mineralogical changes occurring during retrogression will be discussed along with attempts to estimate the P-T conditions of retrogression and shearing. Any changes in the overall composition of the complex will be examined along with the composition of the fluid phase causing the retrogression.

## 5.2. PETROGRAPHY

### 5.2.1. Retrogression of mafic rocks

Mafic rocks without some amphibolitisation are rare in Assynt; representative mineral assemblages are given in Table 1. The first sign of retrogression is the alteration of orthopyroxene to a pale green to colourless, fibrous cummingtonite orientated parallel to the orthopyroxene cleavage. A detailed description of the alteration of Scourian orthopyroxene is given by Kerr (1979). Clinopyroxene begins to alter to a green actinolite. The cummingtonite is also fringed by actinolite. As the fringes develop, orthopyroxene and cummingtonite disappear completely and clinopyroxene is rimmed by blue-green to green hornblende. The rims range from a few microns thick to the whole grain being replaced by hornblende. The fringes are best developed between plagioclase and clinopyroxene, but they occur along all grain boundaries, even when in contact with other clinopyroxene grains. There is commonly a fringe of colourless epidote between plagioclase and hornblende. Occasionally (Fig.5.1a) these fringes are well developed. When the whole clinopyroxene

ULTRAMAFIC ROCKS	opx ± cpx - parg - magt ± sp - ol	(G)
	opx - ol - magt	(G)
	serp - chl - magt	(R)
	trem - chl ± dol ± anth ± tc - magt	(R)
	cpx - actinolite - opq	(R)
	opx - chl - phlog - opq	(R)
	hb - bi - opq	(R)
	chl ± trem - tc - dol - magt ± hem	(S)
	chl - tc - cummingtonite - opq	(S)
MAFIC ROCKS	plag - cpx ± opx ± gt ± parg ± ilmt ± magt	(G)
	plag - cpx - gt - hb - opq	(R)
	plag - hb - opq	(R)
	plag - hb - ep ± qz - opq ± sph	(R)
	plag - hb - bi ± qz - opq ± sph ± ep	(R)
	plag - hb - bi - gt - anth - chl - ap - opq	(R)
	plag - hb ± bi ± ep - opq	(S)
INTERMEDIATE AND ACID GNEISSES		
	qz - plag - hb (accessory - opq - ap - zr - sph - cc - ep)	
	qz - plag - hb - bi	(R)
	qz - plag - hb - bi - chl	(R)
	qz - plag - bi - hb - gt ± chl	(R)
	qz - plag - bi ± chl	(R)
	qz - plag - bi - musc ± chl	(R)
	qz - plag - bi - musc - micr ± chl	(R)
	qz - plag ± micr ± bi ± chl ± zr	(R)
	qz - plag - hb - bi - magt	(S)
	qz - plag - bi ± musc	(S)
	qz - plag - bi - chl	(S)
	qz - plag - hb - chl	(S)
	qz - plag - micr - gt ± chl	(R)

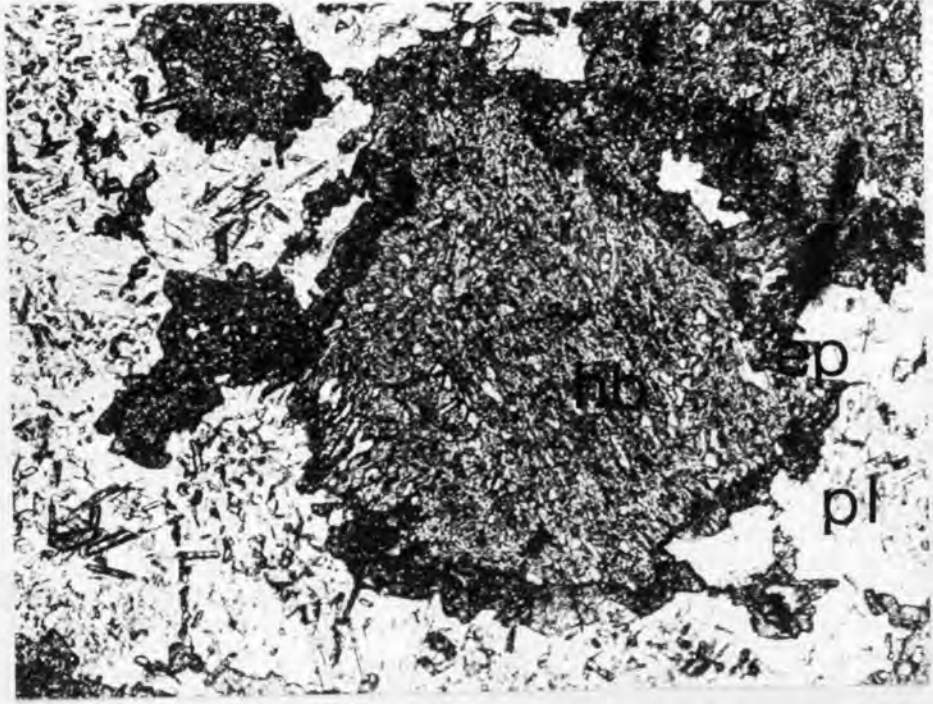
TABLE 5.1 Representative mineral assemblages from all rock types.  
G - granulite facies, R - retrogressed rocks, S - shear zone assemblages.

FIG. 5.1(a) Epidote rim around hornblende in sample D19, a mafic rock from near Loch Ardbhair (176326).

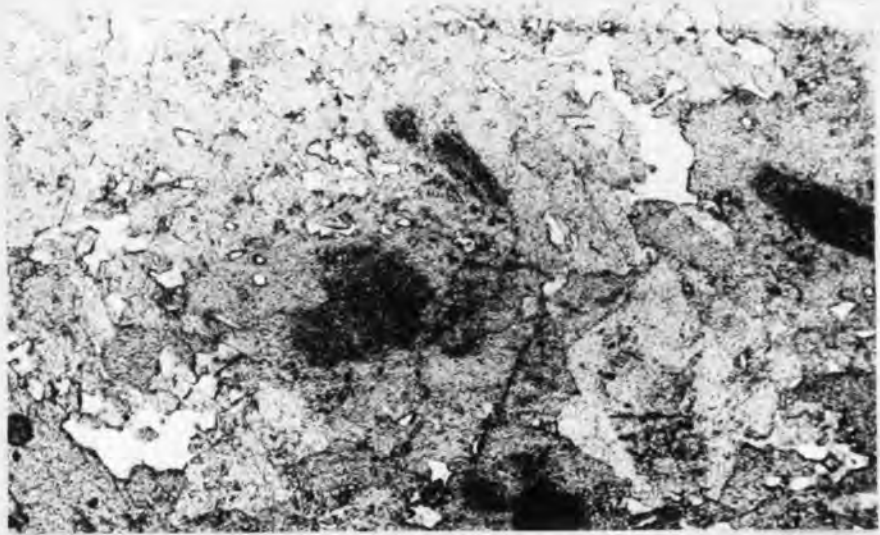
Note the quartz inclusions in the hornblende and the sutured grain boundaries. Field of view 3.2 mm.

FIG. 5.1(b) Poorly crystallised Inverian hornblendes, some with centres clouded with oxide dust. Sample J5, Reidh Phort amphibolite (056315). Field of view 3.2mm.

FIG. 5.1(c) Poorly crystallised Inverian hornblendes with euhedral recrystallised grains. Quartz aggregates to form larger grains. Sample J1 (057302). Field of view 3.2 mm.



a



b



c

grain is replaced, the hornblende has numerous tiny quartz inclusions (see also Beach, 1974a). The result is a green-yellow to green to blue-green hornblende sieved with quartz inclusions with an inclusion free rim sometimes fringed by epidote against plagioclase. The hornblende and plagioclase grains have irregular, sutured grain boundaries, but are clearly replacing a polygonal granulite facies texture. These Inverian hornblendes are usually poorly crystallised and generally consist of aggregates of tiny fibrous crystals. In Table 5.2 a range of hornblende fringe compositions is given. Plagioclase is commonly reversely zoned and may contain needles of epidote.

Several types of amphibole grain are found in completely retrogressed mafic assemblages:

- (a) grains clouded with inclusions of oxide dust (Fig.5.1b), but with clear rims, are derived from granulite facies paragonitic hornblendes by exsolution of opaque oxides,
- (b) grains with sutured edges and quartz inclusions developed from clinopyroxene (as above),

- (c) recrystallised grains without inclusions (Fig.5.1c).

The quartz and opaque oxides form discrete grains, but there is no noticeable difference in composition between these recrystallised grains and their Inverian counterparts. In Laxfordian shear zones there are fine-grained recrystallised amphiboles as well as relict Inverian grains.

Amphibolitisation of pyroxenes is accompanied by the development of sphene coronas around opaque oxides (presumably ilmenite). Biotite often overgrows opaque oxides. Biotite is found as discrete grains in

	W4 a	W4 b	W4 c	W13 d	W16 e
SiO <sub>2</sub>	53.66	53.43	42.03	41.87	42.99
TiO <sub>2</sub>	0.09	0.33	0.17	0.38	0.36
Al <sub>2</sub> O <sub>3</sub>	3.01	4.45	16.18	13.94	11.21
FeO	20.79	9.75	14.21	19.05	17.46
MnO	0.26	0.00	0.13	0.30	0.74
MgO	19.42	17.39	10.46	7.36	9.67
CaO	0.50	12.03	11.53	12.05	11.94
Na <sub>2</sub> O	0.45	0.64	2.16	1.07	1.14
K <sub>2</sub> O	0.00	0.08	0.16	0.78	1.02
Cr <sub>2</sub> O <sub>3</sub>	0.01	0.04	0.00	0.01	0.01
TOTAL	98.19	98.20	97.03	97.04	96.55

Cations recalculated on the basis of 23 oxygens

Si	7.699	7.541	6.234	6.381	6.568
Al <sup>iv</sup>	0.301	0.459	1.766	1.619	1.432
Al <sup>vi</sup>	0.208	0.282	1.063	0.884	0.587
Ti	0.010	0.035	0.019	0.043	0.042
Fe	2.494	1.150	1.762	2.427	2.231
Mn	0.032	0.007	0.016	0.039	0.096
Mg	4.152	3.659	2.313	1.726	2.203
Cr	0.001	0.004	0.000	0.001	0.001
Ca	0.176	1.819	1.832	1.968	1.954
Na	0.126	0.174	0.622	0.318	0.338
K	0.001	0.014	0.030	0.153	0.198
mg	0.622	0.760	0.570	0.490	0.486

TABLE 5.2 Range in composition of amphiboles rimming pyroxenes in partially retrogressed mafic gabbros from the Drumbeg complex.

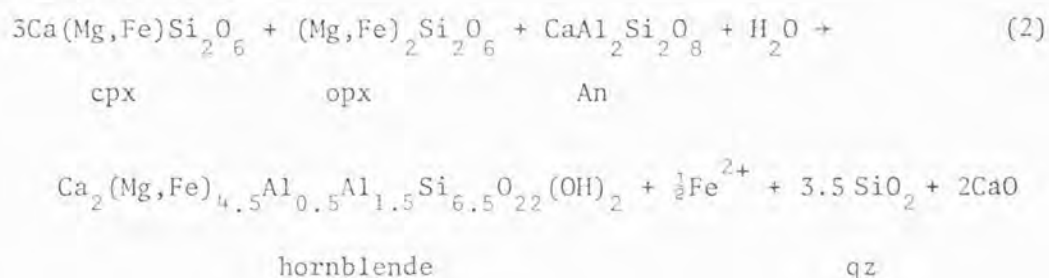
(a) cummingtonite rimming orthopyroxene

(b) actinolitic hornblende rimming clinopyroxene

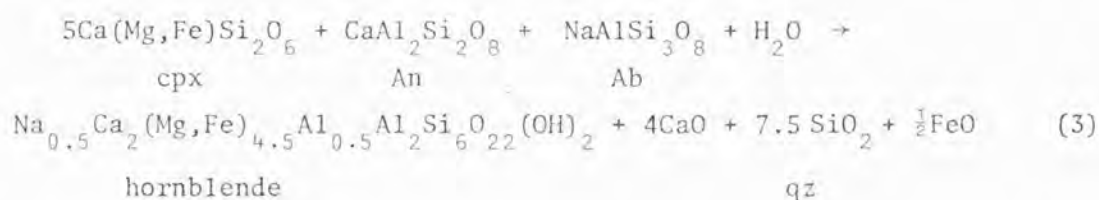
(c,d,e) hornblende rims around clinopyroxene



orthopyroxene (Chapter 2), and retrogressed assemblages are orthopyroxene free. The mg of the product hornblende is always less than that of the reactant clinopyroxene; e.g. in sample W4 clinopyroxene has an mg of 0.69, orthopyroxene 0.58, actinolite, which forms thin fringes, 0.76 and hornblende 0.57 and in sample W13 clinopyroxene has an mg of 0.62 and the replacing hornblende 0.45. A reaction involving both pyroxenes could be:



The hornblende also contains Na which is derived from the albite component of the plagioclase. The excess Al from this reactant albite could combine with the Ca + Fe from the above reaction to produce epidote. Any further excess Ca may form sphene coronas around oxides. Reaction 2 can only proceed until all the orthopyroxene is consumed. A more general reaction to form hornblende is:



This reaction produces a greater amount of excess Ca and Si. This Si forms the tiny quartz inclusions which form in the centre of hornblende grains. The edges of grains are inclusion free, implying that the excess silica found it increasingly difficult to diffuse out of the developing grain. The  $\text{TiO}_2$  content of the hornblende is presumably derived from opaque oxides. Granulite facies mafic assemblages

have a higher modal oxide content than their equivalent Inverian assemblages. The  $TiO_2$  and FeO thus released could enter hornblende (which has a lower mg than the reactant pyroxene). The potash content of these amphiboles is fairly low and could be derived from plagioclase. During retrogression the plagioclase becomes more sodic and the hornblende gains Na, possibly implying addition of Na to the complex during retrogression as suggested by Beach (1973, 1974a, 1976). However this is not necessary if the amount of modal plagioclase decreases. Unfortunately this is rather difficult to estimate, although many retrogressed mafic assemblages do have low plagioclase contents. Reaction 3 takes two parts anorthite to one part albite which would reduce the anorthite content of the plagioclase and does not involve addition of Na to the complex. The Ca released from the reactions may also account for the reverse zoning commonly observed in plagioclase from retrogressed samples.

#### 5.2.2. Retrogression of acid and intermediate gneisses

Unfortunately granulite facies acid and intermediate gneisses are rare in Assynt, so transitional stages of retrogression can rarely be observed; however retrogression of intermediate gneisses was described by Beach (1974a). Granulite facies gneisses have bluish quartz and greasy, dark plagioclase and are fairly coarse grained. They have a polygonal, granoblastic texture with straight to curved grain boundaries meeting in triple points. The plagioclase is coarse grained, twinned and often strained with bent twin lamellae. The composition is about  $An_{30-35}$ . Orthopyroxene is partially altered to a yellowish chlorite or serpentine and biotite overgrows opaque oxides.

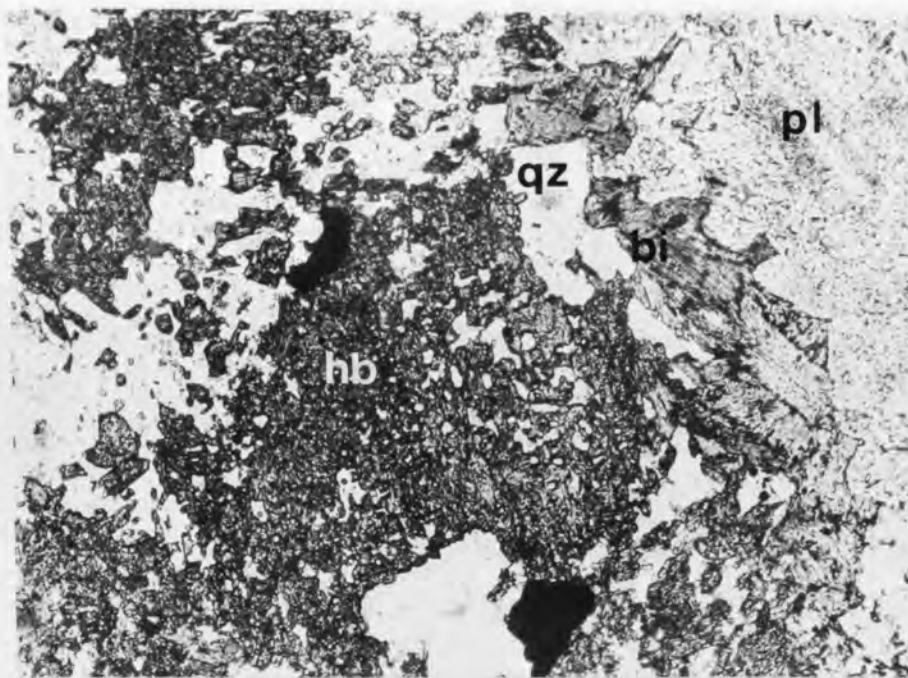
Amphibolite facies rocks are medium to coarse grained (average grain size is about less than 3 mm, quartz grains 2-3 mm, plagioclase 1 mm). Representative assemblages are given in Table 1, the most common being quartz-plagioclase-amphibole-biotite-magnetite. Accessory minerals are epidote, apatite, zircon (especially in discordant pegmatitic sheets cutting the Drumbeg body), opaque oxides, sphene and calcite. As the  $\text{SiO}_2$  content increases, the amount of biotite increases with a decrease in the hornblende content. Some assemblages contain muscovite (hornblende and muscovite are mutually exclusive), chlorite and microcline. Rare granite sheets contain garnet (partially replaced by chlorite). Hornblende generally has quartz inclusions (Fig.5.2a) and may be overgrown by biotite (especially in shear zones). Biotite is often altered to chlorite along cleavage planes. In or near Laxfordian shear zones biotite may be completely replaced by a pale green fibrous chlorite containing needles of haematite, but biotite and well developed chlorite aggregates do occur in the same sample. Epidote grains may be associated with biotite.

Plagioclase grains recrystallize during retrogression to a fine to medium grained aggregate of untwinned grains with curved to sutured grain boundaries (Fig.5.2b). Larger unrecrystallized grains with relict twinning have very irregular grain boundaries and are usually seriticised; the composition is generally between  $\text{An}_{20-30}$ . Recrystallized plagioclase grains from shear zones do not have epidote inclusions. Quartz tends to occur in lenses up to 2 cm long, which in acid gneisses define the foliation and lineation. They have recrystallized to a polygonal aggregate, although grains may have sutured edges (Fig.5.2b). Occasionally, in some trondjemite sheets the plagioclase is granulated to a very fine-grained aggregate.

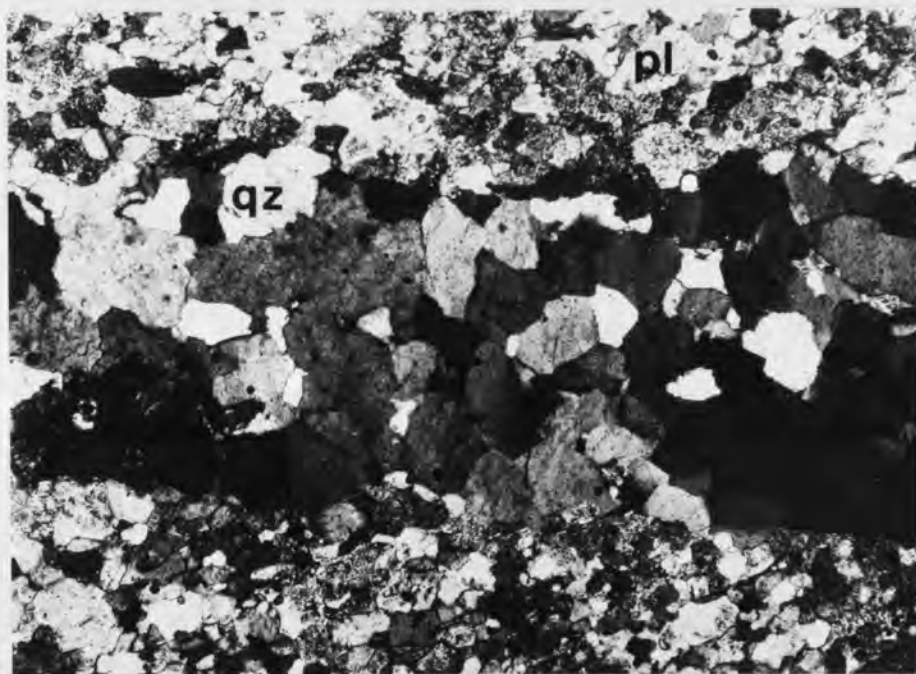
FIG. 5.2a Inverian hornblende with quartz inclusions partially rimmed by biotite in a gneiss of intermediate composition. Sample J91 (104223). Field of view 3.2mm.

FIG. 5.2b Recrystallized quartz lens with finer grained partially altered polygonal plagioclase. Sample 066 (158318). Field of view 3.2mm.

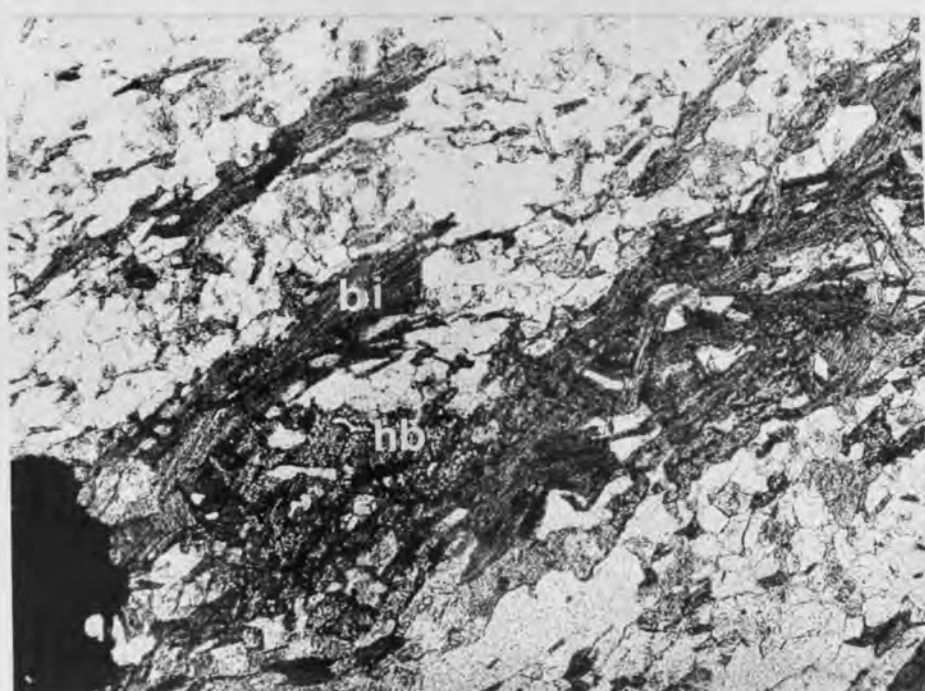
FIG. 5.2c Tonalitic gneiss from the Canisp shear zone; aligned biotite overgrows hornblende with a euhedral magnetite grain cutting the fabric. Sample D37 (054257). Field of view 3.2mm.



a



b



c

In shear zones, biotite overgrows hornblende and there is a post-deformational growth of euhedral magnetite (Fig.5.2c). Some samples particularly from the Strathan line, are rich in chlorite, which may replace hornblende.

### 5.2.3. Retrogression of ultramafic rocks from layered bodies

The rocks from layered bodies, especially the pyroxenites, are more competent than the surrounding gneisses. Consequently granulite facies and partially retrogressed ultramafic assemblages are found when all other rock types are completely retrogressed. However, once the ultramafic rocks are hydrated they become the least competent member of the complex. This is particularly noticeable in the picrite Scourie dykes near Clachtoll (Tarney, 1973). In fact, it becomes very difficult to distinguish between ultramafic dykes and rocks from layered bodies. Three types of retrogressive metamorphism of ultramafic rocks can be recognised:

- (a) retrogression without accompanying deformation in or near Inverian steep belts,
- (b) recrystallization accompanied by shearing in Laxfordian shear zones,
- (c) serpentinisation of olivine and orthopyroxene. This occurs to some extent in all olivine-bearing samples but it seems to increase eastwards across the Assynt region. Completely serpentinised rocks (J65, D28) occur away from any Inverian structures. Relict olivines in metamorphosed picrite dykes from the Canisp shear zone were serpentinised after the shearing (Tarney, 1973), implying the serpentinisation

was a very late stage event in the history of the Assynt gneisses, perhaps associated with the Caledonian or with the uplift prior to the deposition of the Torridonian.

Petrography. Granulite facies assemblages have a polygonal granoblastic texture (Chapter 2). The first sign of retrogression is the exsolution of opaque oxides along cleavage planes and grain boundaries (Figs. 2.5, 5.3a). This is due to the exsolution of excess  $TiO_2$  from granulite facies pargasite, associated with a change in colour from brown to green. Granulite facies amphiboles always have a higher  $TiO_2$  content than their amphibolite facies counterparts. In Table 5.5 the change in amphibole composition with retrogression is documented.

When ultramafic rocks recrystallize without the development of a fabric, they have the following assemblage:

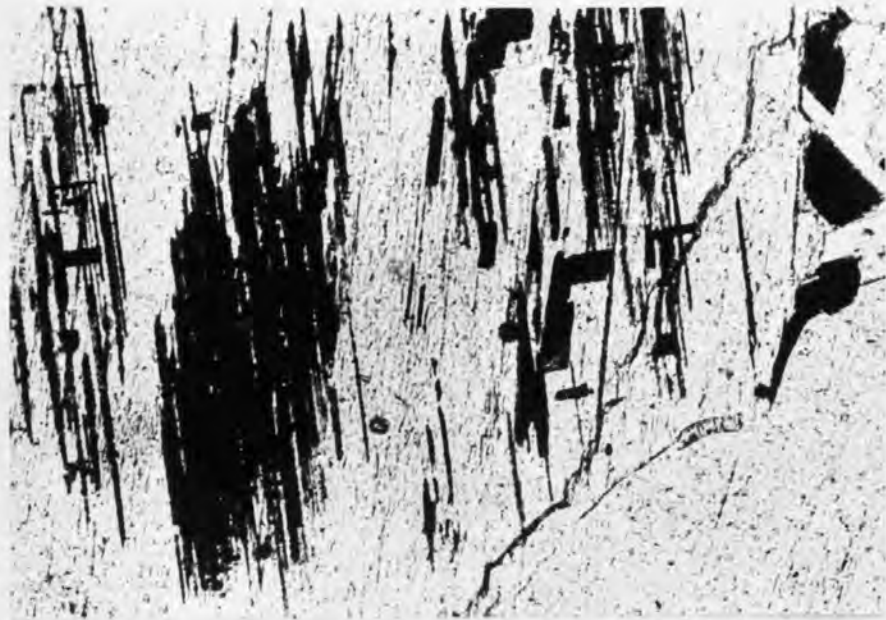
tremolite - chlorite  $\pm$  anthophyllite  $\pm$  talc  $\pm$  dolomite - magnetite

In partially retrogressed assemblages (W9,077a) anthophyllite needles replace orthopyroxene. Pargasite and clinopyroxene are replaced by tremolite.  $Al_2O_3$  thus released from pargasite and spinel forms chlorite. Chlorite is colourless and occurs either as fibrous masses or discrete needles. In completely retrogressed samples euhedral tremolite (sometimes twinned) develops (Fig.5.3b), cutting areas of fibrous tremolite, chlorite and anthophyllite which pseudomorph the granulite mineralogy. Chlorite forms fringes around magnetite, perhaps developing from the composite spinel-magnetite grains. Anthophyllite is only a transitional phase and is rarely present in completely retrogressed samples. Some dolomite and talc may be present but they are more abundant in shear zones. Inverian assemblages are thus dominated by tremolite and chlorite.

FIG. 5.3a Exsolution of opaque oxide in hornblende  
from sample W49, Gorm Loch, Laxford front.  
Field of view 1.6 mm.

FIG. 5.3b Retrogressed ultramafic rock from the margin  
of a shear zone cutting the Drumbeg complex.  
Euhedral tremolite grains cut the trem-chl  
intergrowths. Sample D25 (115327).  
Field of view 3.2mm.

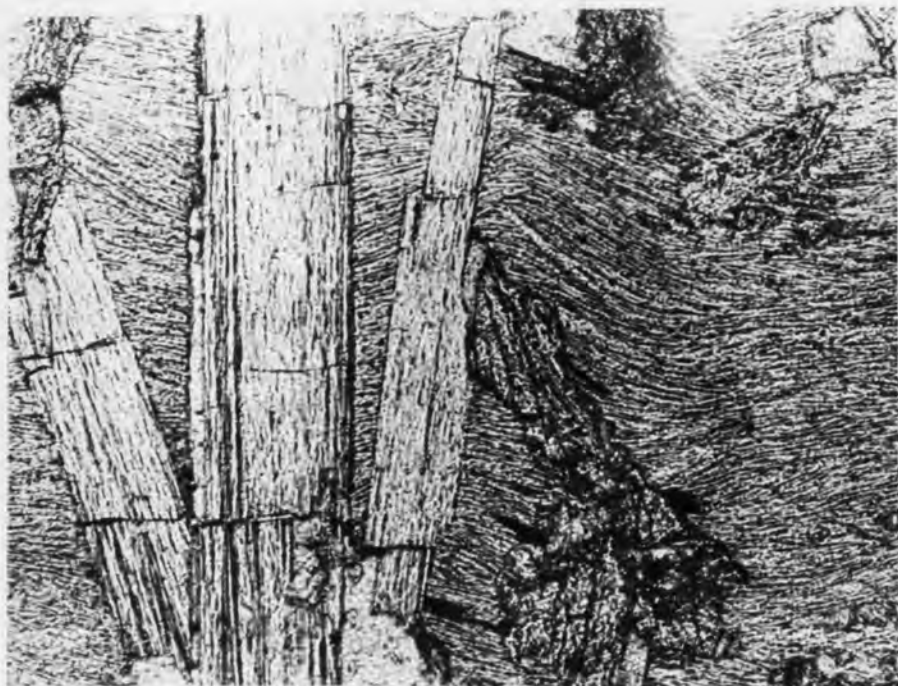
FIG. 5.3c Ultramafic rock from the Canisp shear zone.  
Cummingtonite needles cross-cut a fine grained  
talc-chlorite matrix. Sample S2 (054257)  
Field of view 3.2mm.



a



b



c

	W1	W11	W39	W49	D25
	(4)	(4)	(4)	(5)	(3)
SiO <sub>2</sub>	42.27	42.52	45.16	43.91	55.61
TiO <sub>2</sub>	1.55	1.06	0.73	0.40	0.06
Al <sub>2</sub> O <sub>3</sub>	13.46	13.87	12.78	14.72	1.44
FeO	6.20	6.26	6.48	8.59	5.15
MnO	0.07	0.08	0.10	0.14	0.17
MgO	16.81	17.12	17.13	15.26	21.47
CaO	12.38	12.26	12.68	12.31	12.45
Na <sub>2</sub> O	2.58	2.12	1.77	2.13	0.29
K <sub>2</sub> O	0.65	0.80	0.19	0.34	0.02
Cr <sub>2</sub> O <sub>3</sub>	0.32	0.23	0.41	0.02	0.05
TOT	96.34	96.32	97.43	97.83	96.71
Si	6.173	6.192	6.453	6.313	7.799
Al <sup>iv</sup>	1.827	1.808	1.547	1.687	0.201
Al <sup>vi</sup>	0.490	0.573	0.606	0.806	0.036
Ti	0.169	0.116	0.079	0.043	0.006
Cr	0.037	0.027	0.046	0.002	0.006
Fe	0.757	0.763	0.782	1.033	0.604
Mn	0.009	0.010	0.011	0.017	0.021
Mg	3.658	3.715	3.649	3.270	4.488
Ca	1.936	1.913	1.941	1.895	1.871
Na	0.730	0.598	0.490	0.595	0.078
K	0.121	0.148	0.035	0.063	0.004
mg	0.827	0.828	0.824	0.750	0.878

TABLE 5.3 Changes in amphibole composition with retrogression in ultramafic rocks. W1 and W11 are granulite facies assemblages in the Drumbeq body, W39 has some exsolution of opaque grains, W49 is a blue-green amphibole with extensive exsolution of opaque granules and D25 is a tremolite from a completely retrogressed assemblage. Cations are calculated on the basis of 23 oxygens in the water free formula. The number in parentheses is the number of point analyses included in the average.

In Laxfordian shear zones (e.g. sample D26) a strong fabric develops with parallel alignment of platy crystals and a segregation into silicate and carbonate layers. The following typical assemblage is found:

chlorite - talc - dolomite  $\pm$  tremolite  $\pm$  haemotite - magnetite

In the main Canisp shear zone dolomite often aggregates in fold closures (Tarney, 1973) and post-deformational prismatic amphibole grains cut the schistose fabric. These amphiboles resemble tremolite but microprobe determination reveals them to be cummingtonite (Fig.5.3c). This movement of dolomite produces an assemblage with no calcium mineral, leaving a chlorite - talc - cummingtonite assemblage.

Serpentinisation. All granulite facies samples show some serpentinisation but occasionally completely serpentinised rocks are found. The serpentine is a colourless, low birefringence antigorite, but where orthopyroxene has been altered, it may be a pale yellow. Pale green serpentine is also found. Serpentinites also contain a small amount of chlorite and abundant opaque oxide.

### 5.3. MINERAL CHEMISTRY

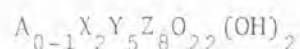
#### 5.3.1. Amphibole composition

Amphiboles occur in many rock types in the Assynt region - in mafic and ultramafic granulites, retrogressed rocks of all compositions except the most acid, and in recrystallized gneisses from Laxfordian shear zones. The composition ranges from Ca-free amphiboles to tremolite to pargasite. A wide range of substitutions occur in amphibole and the composition can depend on the following factors:

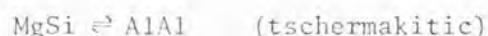
- (a) whole-rock composition
- (b) P-T conditions of formation
- (c) the paragenesis

In this section the influence of these factors will be examined.

The majority are Ca-amphiboles with Ca between 1.75 and 2.00 cations per formula unit (based on 23 oxygens). The general formula of Ca- amphibole can be written:



where A is Na or K ; X is Ca or Na ; Y is Mg, Fe<sup>2+</sup>, Mn, Fe<sup>3+</sup>, Al, Ti, Cr ; Z is Al or Si ; the hydroxyl ions may be wholly or partially replaced by Cl or F . The following are the main substitutions:



Pargasite is derived by a combination of edenite and tschermakite substitutions. As demonstrated in Fig.5.4, most of the Assynt amphiboles lie on a line between tremolite-actinolite and pargasite, with the richterite substitution being minor. Where actinolitic and tschermakitic amphiboles occur in the same sample, the former always has the higher mg number, emphasising the importance of the MgSi  $\rightleftharpoons$  AlAl substitutions.

The amphiboles from granulite facies assemblages (only mafic and ultramafic in Assynt) are very distinctive and have been discussed briefly in Chapter 2. The amphiboles from ultramafic rocks are olive-green to colourless pargasite (nomenclature after Leake, 1978), whilst those from mafic rocks are brown to straw yellow ferroan pargasitic

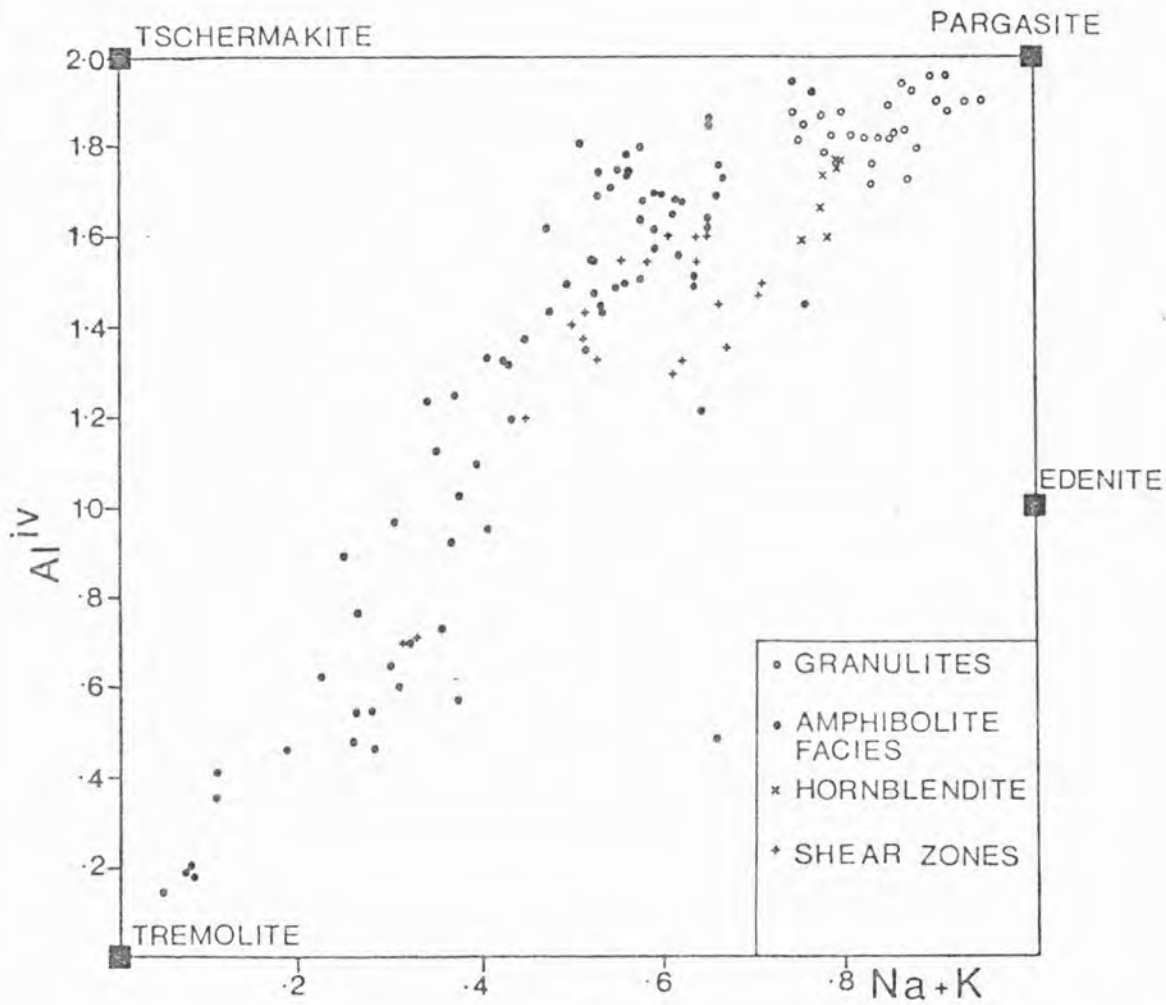


FIG. 5.4  $Al^{iv}$  versus  $Na+K$  for all amphiboles to show their classification after Fig.60 of Deer et al. (1966). Cations recalculated on the basis of 23 ions in the water free formula.

hornblende. The degree of brown colouration depends on the  $TiO_2$  content. When these amphiboles retrogress, they exsolve opaque oxide (presumably ilmenite) along cleavage planes and grain boundaries becoming green. Pargasites in the mafic granulites occur both as large matrix grains and in symplectites after garnet (Savage and Sills, 1980; Chapter 2). The latter have higher  $Al^{vi}$  contents.

In the amphibolite facies Inverian assemblages, nearly all amphiboles are between tremolite and pargasite (Fig.5.4) but occasional calcium-poor amphiboles are found as follows:

- (a) anthophyllite replaces orthopyroxene in partially retrogressed ultramafic rocks,
- (b) cummingtonite partially replaces orthopyroxene in retrogressed mafic rocks,
- (c) samples J96 and S10, which occur in a steep belt, have the following assemblage: quartz - plagioclase - garnet - anthophyllite - chlorite - biotite - hornblende - apatite - opaque oxides,
- (d) in the Canisp shear zone ultramafic rocks contain post-deformational laths of cummingtonite (Fig.5.3c).

The most common amphibole is a magnesio-tschermakitic hornblende or a ferroan-pargasitic hornblende; these will now be referred to simply as hornblende. Fringes of blue-green amphibole partially replacing clinopyroxene are actinolitic hornblende.

Various systematic grade-related changes in amphibole composition have been reported from other metamorphic terrains. These include  $TiO_2$ ,  $Mg/Mg + Fe$ ,  $Al^{iv}$  and total alkalis which may increase with temperature,  $Mn/Fe^{2+}$ , which may decrease with temperature and  $Al^{vi}$  which may

increase with pressure (Engel and Engel, 1962; Binns, 1965; Leake, 1965; Bard, 1970; Raase, 1974; Stephenson, 1977). However  $Al^{vi}$  and mg variations may correlate with whole-rock compositions. In Fig.5.5 the  $Mg/Mg + Fe$  ratio of all amphiboles is seen to mirror closely that of the host rock, whilst the  $TiO_2$  content is very much greater in granulite facies amphiboles and this does not correlate with whole rock  $TiO_2$  content. This difference in  $TiO_2$  is the most striking difference between amphibolite and granulite facies hornblendes.

Correlation matrices have been computed, firstly using all amphibole analyses and secondly excluding amphiboles from granulite facies assemblages (Fig.5.6a). R-mode cluster dendograms were then constructed (Fig.5.6b; method as in Chapter 3). The general degree of correlation is less when the granulite facies grains are included but the clusterings are similar, except for a clustering of Ti with K in the granulite facies grains. Surprisingly, considering the wide range of substitutions possible, the correlation between Mg and Fe is very high (-0.85).

All the analyses have been plotted using mg of the amphibole as abscissa and have been divided into three groups; granulite facies, retrogressive amphiboles in or near Inverian steep belts, and recrystallized grains from Laxfordian shear zones, to see if there is any systematic difference in composition between the groups which could be related to P-T conditions. A few analyses which are clearly partially retrogressed granulite facies grains have been plotted separately. Several of these plots are given in Fig.5.7.

In several plots the granulite facies hornblendes are clearly distinguishable from the retrogressive amphiboles. For high mg numbers the granulite facies grains are pargasite, whilst the amphibolite facies grains are tremolite. Granulite facies amphiboles have higher K ,

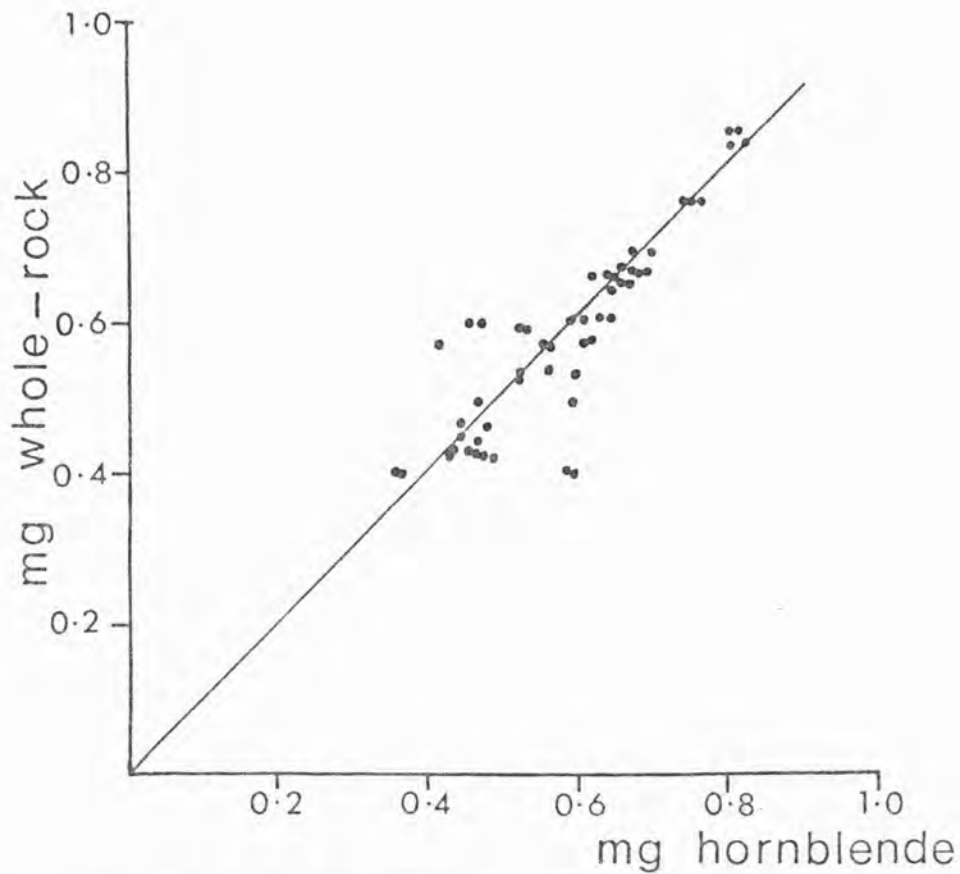


FIG. 5.5a mg( $\text{Mg}/\text{Mg}+\text{Fe}$ ) of hornblende versus mg of host rock.

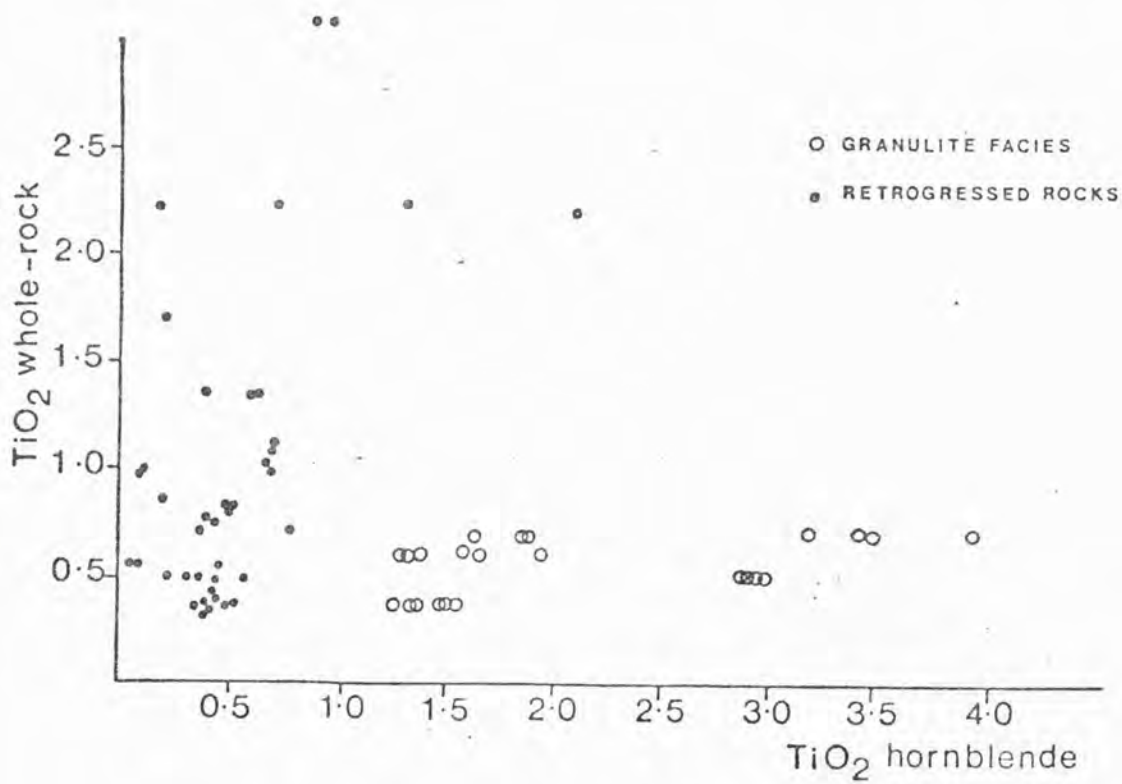


FIG. 5.5b  $\text{TiO}_2$  content of hornblende versus  $\text{TiO}_2$  content of the host rock.

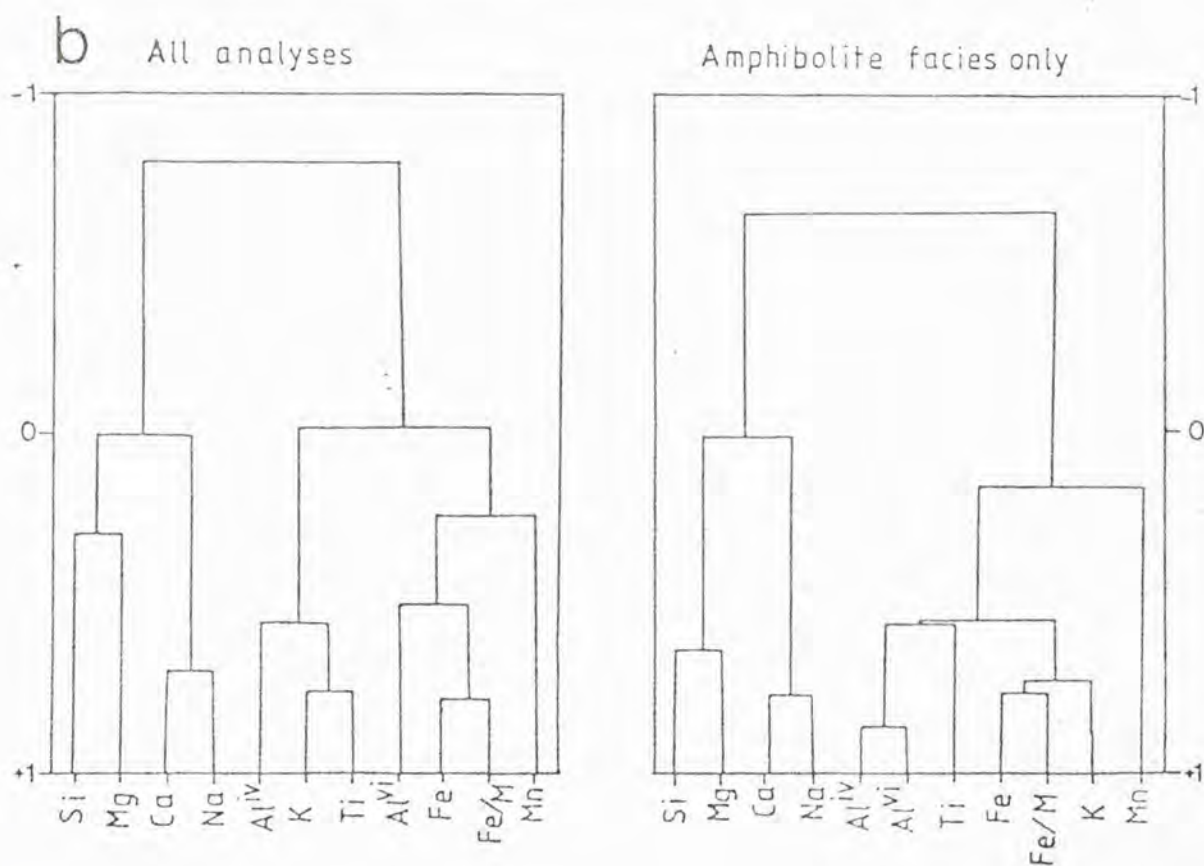
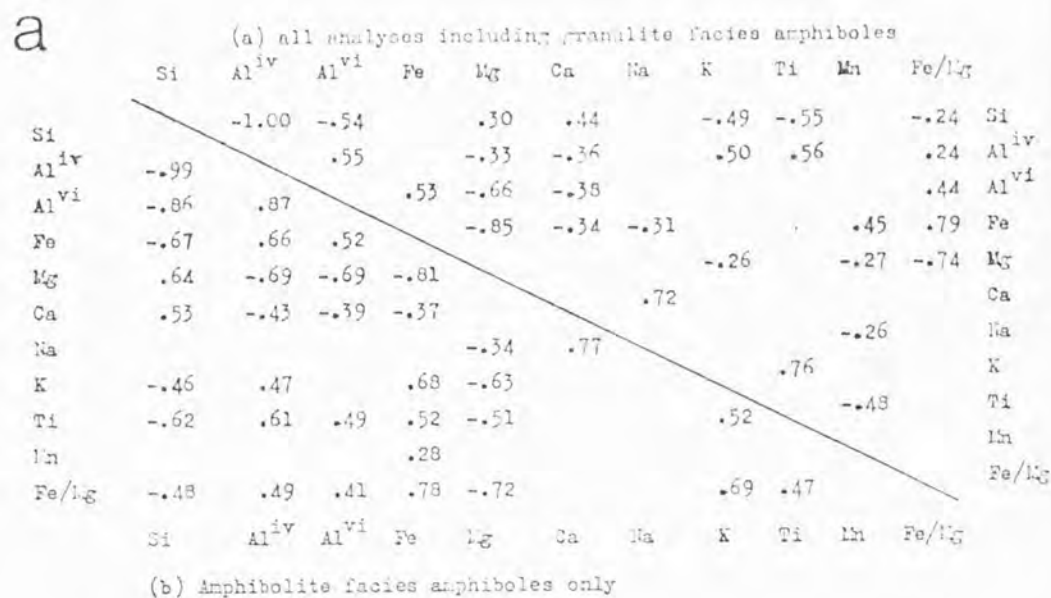


FIG. 5.6 (a) Correlation matrices for amphibole analyses as indicated; only correlations significant at the 99.5% confidence level shown.

(b) Cluster dendograms based on the correlation matrices.

$$\text{Fe/M} = \text{Fe}^{2+}_{\text{TOT}}/\text{Mg}.$$

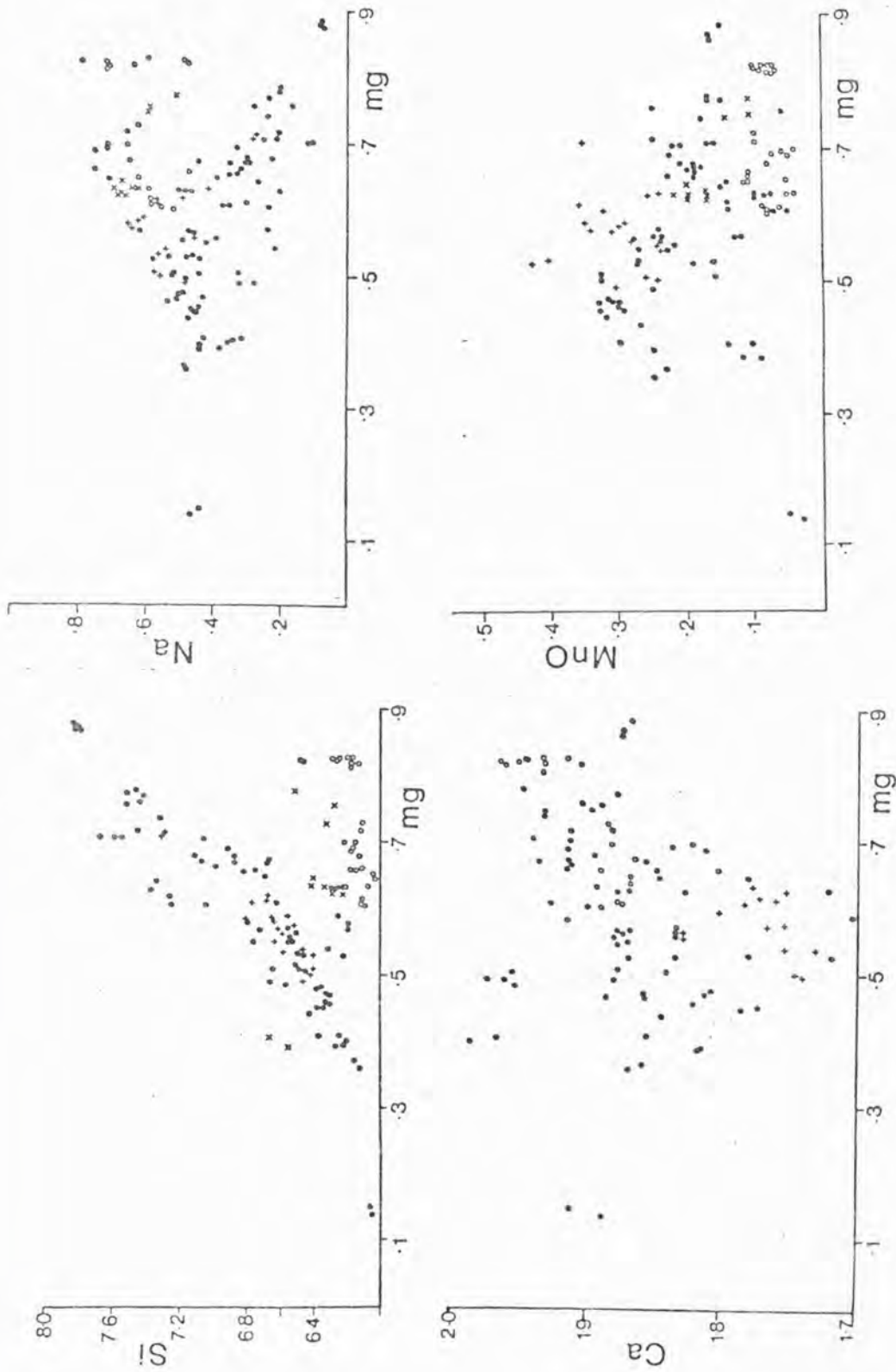


FIG. 5.7 Plots of Si, Na, Ca and MnO against mg for all Ca-amphiboles; key as in Fig. 5.4

Na + K, Ti, Cr and  $Al^{iv}$  than their amphibolite facies counterparts, while the  $Al^{vi}$  content is often lower. Binns (1965) suggests that  $Al^{vi}$  decreases with increasing grade; however the  $Al^{vi}$  is replaced by Ti in the granulite facies amphiboles and the  $Al^{vi} + Ti$  content is fairly constant.  $Cr_2O_3$  is below detection limit in most samples, but in the pargasites from ultramafic rocks and the hornblende from the Achiltibuie gabbros (where there is no oxide phase)  $Cr_2O_3$  contents are up to 0.5 wt.%. The  $Cr_2O_3$  content of amphibole is always greater than that of coexisting pyroxenes. In one retrogressed sample (D25, Fig. 5.3b) the euhedral tremolite has less than 0.05 wt.%  $Cr_2O_3$ , whilst the poorly crystallized tremolite has 0.20 wt.%. Granulite facies amphiboles have lower (OH) contents (from consideration of the totals of microprobe analyses) and may have up to 0.85 wt.% F with less than 0.05 wt.% Cl.

Considering now the Inverian amphiboles only, Si increases with decreasing mg, ranging from 6.05 to 7.80 atoms; Al obviously being the reverse. Ca shows a great deal of scatter but tends to decrease with mg. The MgO-rich grains are tremolite which have a high Ca content as there is little substitution of Al or Na. The narrow rims around clinopyroxene also have a high Ca content. Shear zone samples tend to have a slightly lower Ca-content, which is balanced by higher Na. Na, K and Na + K all tend to increase with decreasing mg and there is a slight tendency for Ti to decrease. MnO correlates with FeO, but is rather variable; the MnO content of amphibole coexisting with garnet is lower than that in garnet-free samples. MnO content of shear zone amphiboles is slightly higher; this does not correlate with the MnO content of the host rock and is thought to be due to the lower ilmenite content of shear zone assemblages. Stephenson (1977) concluded from a consideration of the  $Mn/Fe^{2+}$  ratio that granulite facies

hornblendes have a lower Mn content than amphibolite facies hornblendes. The  $\text{Mn}/\text{Fe}^{2+}$  ratio of the Assynt gneisses is very uniform, but the ratio of the hornblendes varies considerably. Shear zone amphiboles have the highest ratio, and those from garnetiferous samples the lowest. However granulite facies samples with no garnet also have low  $\text{Mn}/\text{Fe}^{2+}$  ratios. This suggests that the MnO content may be controlled by metamorphic grade as well as paragenesis, but the presence or absence of garnet has the most significant effect.  $\text{Al}^{\text{vi}}$  which is thought to increase with pressure, increases with decreasing  $m_{\text{g}}$ , but is generally between 0.5 and 0.8 atoms per formula unit. In a few samples  $\text{Al}^{\text{vi}}$  exceeds 1 atom but these samples all have above average  $\text{Al}_2\text{O}_3$  contents. The  $\text{Al}^{\text{iv}}$  content tends to be lower in samples with a significant amount of epidote.

The  $\text{Fe}_2\text{O}_3$  content has been estimated by charge balance (Papike et al., 1974). The estimate is only approximate but tends to indicate that shear zone amphiboles have a higher  $\text{Fe}_2\text{O}_3$  content than granulite or Inverian hornblendes. This suggests oxidation during recrystallization and shearing (Beach and Fyfe, 1972; Beach, 1973). Most grains contain no fluorine and only minor amounts of chlorine.

In summary, granulite facies samples have high Ti and K when compared with other samples; this does not depend on host rock composition or on the paragenesis. Shear zone samples are similar to retrogressed Inverian amphiboles except for slightly higher Ca and Mn contents and higher oxidation state. The shear zone samples all plot in the middle of the  $m_{\text{g}}$  range possibly indicating "mixing" of rock types during shearing, producing rocks of an average composition. Mn content seems to depend on the mineral assemblage. In amphibolite facies samples the presence of biotite does not seem to affect the Ti content of the hornblende. Biotite always has a higher Ti content ( $\text{Ti}_{\text{bi}}/\text{Ti}_{\text{hb}}$

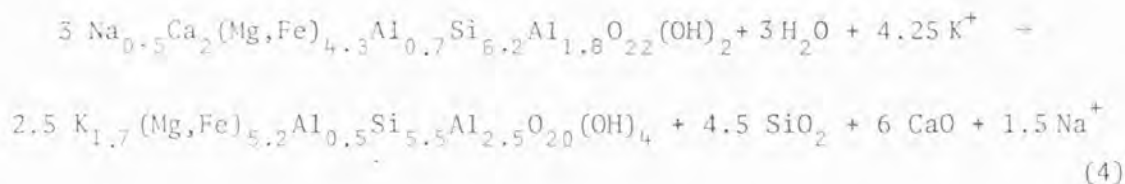
varies from 3.3 to 4.0). The mg of hornblende clearly depends on the whole-rock value apart from samples where hornblende and actinolite coexist where the former has a lower mg value. However this only occurs when clinopyroxene is partially replaced by hornblende and it is unlikely that equilibrium was reached.  $Al^{Vi}$ , thought by some authors to depend on pressure, seems to correlate with whole rock  $Al_2O_3$ . So apart from the Ti and K content, the chemistry of amphiboles, considered on their own, does not tell us much about the P-T conditions of formation.

Retrogression thus produces in rocks of mafic and intermediate composition a plagioclase - hornblende  $\pm$  quartz assemblage. The uniformity of the plagioclase and hornblende compositions imparts a homogeneity on the whole rock compositions which is reflected in increasing inter-element correlations with retrogression (Beach and Tarney, 1978). They showed that several element pairs notably Na-Al, Ti-Mg,  $Fe^{2+}$ -Mg and Ca-Ti all increase markedly from granulites to sheared gneisses. This was interpreted as being caused by the formation of a very uniform plagioclase and hornblende. Na and Al thus vary according to the modal proportion of plagioclase. Ti and Ca have uniform concentrations in hornblende, whilst in the granulite facies Ca is concentrated in clinopyroxene and plagioclase and Ti in opaques. The present study confirms the conclusions of Beach and Tarney (1978) in that plagioclase varies from  $An_{20}$  to  $An_{35}$  in retrogressed rocks of all compositions, whilst in granulites they range from  $An_{30}$  to  $An_{95}$ . The Ti content of retrogressed hornblende is fairly constant (0.4 to 0.8 wt.%) and with the exception of the ultramafic rocks the  $Mg/(Mg+Fe)$  ratio has a similar constant range (0.45 to 0.75).

5.3.2. Biotite

Biotite has been analysed from a variety of rock types - an unusual ultramafic pod near Kylesku, a hornblendite layer near Clashnessie, retrogressed mafic, intermediate and acid gneisses, a granulite facies acid gneiss near Kylesku and garnetiferous, possibly metasedimentary rocks. Representative analyses are presented in Table 5.4.

The development of biotite in shear zones is not as widespread as indicated by Beach (1973, 1976) for the shear zones near Scourie, but biotite is more abundant in shear zones than outside, often overgrowing hornblende. In the qz-plag-gt-bi-hb rocks biotite overgrows garnet. A possible reaction to form biotite from hornblende is:



This reaction implies addition of potash and water with the production of quartz and loss of Ca and Na.

As with hornblendes, various chemical changes in biotite are thought to relate to P-T conditions and include, increasing  $\text{Al}^{\text{iv}}$ , Ti and mg and decreasing  $\text{Fe}^{3+}/(\text{Fe}^{2+} + \text{Fe}^{3+})$  and increasing or decreasing Mn with rising temperature (Butler, 1967; Ramsay, 1973; Stephenson, 1977). Biotites from high-grade rocks have a deeper brown-red colour than lower grade biotites. All samples have less than the ideal 6 octahedral atoms but the precise number of vacancies is impossible to determine due to the lack of  $\text{Fe}^{3+}$  determinations. The mg of biotite correlates with whole-rock mg but is always higher than that of coexisting hornblende (Fig.5.8). As with hornblende the Ti content of biotite

	D3 (12)	J10 (3)	D41 (2)	J98 (12)	J51 (1)	D2 (6)	J8 (1)	D40 (4)	J47 (5)
SiO <sub>2</sub>	39.52	37.59	36.18	35.38	35.89	36.81	35.71	35.26	35.33
TiO <sub>2</sub>	1.29	1.21	2.38	1.80	1.61	3.51	3.37	2.92	3.70
Al <sub>2</sub> O <sub>3</sub>	14.66	16.62	16.38	18.07	17.10	15.08	16.60	17.31	16.84
FeO	4.69	10.77	17.19	19.05	18.63	13.04	19.00	20.26	21.14
MnO	0.02	0.10	0.14	0.07	0.11	0.05	0.25	0.17	0.24
MgO	22.98	17.39	12.81	10.29	11.03	15.71	9.86	9.16	8.29
CaO	0.02	0.00	0.00	0.02	0.01	0.20	0.02	0.03	0.00
Na <sub>2</sub> O	0.70	0.15	0.15	0.17	0.14	0.06	0.06	0.08	0.06
K <sub>2</sub> O	8.95	9.66	8.90	9.00	9.75	9.68	9.01	9.67	9.60
Cr <sub>2</sub> O <sub>3</sub>	1.24	0.02	0.04	0.07	0.01	0.01	0.04	0.01	0.01
Cl	0.02	0.02	0.04	0.08	0.11	0.04	0.04	nd	nd
F	0.66	0.57	0.00	0.00	0.00	0.24	0.00	0.00	nd
TOTAL	94.15	94.10	94.21	94.01	94.40	94.44	93.97	94.87	95.21
Cations on the basis of 22 oxygens									
Si	5.685	5.598	5.514	5.453	5.524	5.532	5.512	5.448	5.443
Al <sup>iv</sup>	2.315	2.402	2.486	2.547	2.476	2.478	2.498	2.552	2.557
Al <sup>vi</sup>	0.171	0.515	0.507	0.736	0.627	0.193	0.592	0.599	0.523
Ti	0.138	0.135	0.272	0.209	0.187	0.396	0.392	0.339	0.430
Fe	0.564	1.342	2.192	2.455	2.398	1.639	2.453	2.598	2.733
Mn	0.002	0.012	0.019	0.009	0.014	0.007	0.032	0.022	0.032
Mg	4.928	3.861	2.909	2.365	2.524	3.520	2.269	2.109	1.909
Cr	0.140	0.001	0.005	0.008	0.002	0.001	0.005	0.001	0.000
Ca	0.007	0.000	0.000	0.003	0.001	0.032	0.004	0.006	0.000
Na	0.194	0.045	0.044	0.050	0.043	0.017	0.018	0.023	0.016
K	1.642	1.835	1.730	1.769	1.914	1.857	1.775	1.906	1.892
mg	0.897	0.740	0.568	0.490	0.512	0.681	0.481	0.446	0.409

TABLE 5.4 Biotite compositions. Cation recalculation based on 22 oxygens in the water free formula. Number in parenthesis is the number of point analyses included in the average.

does not depend on whole-rock Ti content and increases with temperature (Figs.5.8b, 5.9). All samples have Si between 5.3 and 5.75 atoms per formula unit (based on 22 oxygens).  $Al^{vi}$  varies from 0.2 in the granulite facies sample to 0.8 in an  $Al_2O_3$ -rich rock. Unfortunately there are not enough samples to decide whether  $Al^{vi}$  is grade-dependent but it is clearly affected by whole-rock Al (Fig.5.9). Na and Ca contents are low. The K content is rather variable due to incipient alteration to chlorite along cleavage planes, with lowering of the K and raising of the (Mg,Fe) contents. Analyses with  $K_2O$  less than 8.75 wt.% and totals less than 93% have been rejected. This is particularly noticeable in samples from the Canisp shear zone; Beach (1980) states that these may be hydrobiotites with a lower potash and higher hydroxyl content than normal biotites, but these variations could be due to incipient chloritisation. The MnO content of biotite in garnet-free samples increases from 0.03 to 0.25 as mg decreases, but in garnetiferous samples biotite has a significantly lower MnO content. As with hornblende, examination of  $Mn/Fe^{2+}$  ratios reveals two trends; granulite facies and garnetiferous samples have lower MnO content than other samples. This does not depend on whole-rock Mn/Fe ratios. The phlogopite from an ultramafic pod and a hornblendite layer have between 0.5 and 0.75 wt.% F; most samples have trace amounts of Cl ranging up to 0.20 wt.%.

Muscovite occurs locally in a few trondjemite samples cross-cutting any fabric in the rock. There is thought to be some variation in muscovite composition with grade; for example a change from a phengitic composition to pure muscovite with increasing temperature (Butler, 1967). Muscovite has been analysed from three samples - two Inverian assemblages and one shear zone. All have some  $Fe_2O_3$ , MgO and  $TiO_2$  replacing  $Al^{vi}$  with a corresponding increase in the Si content.  $Fe_2O_3$  (total

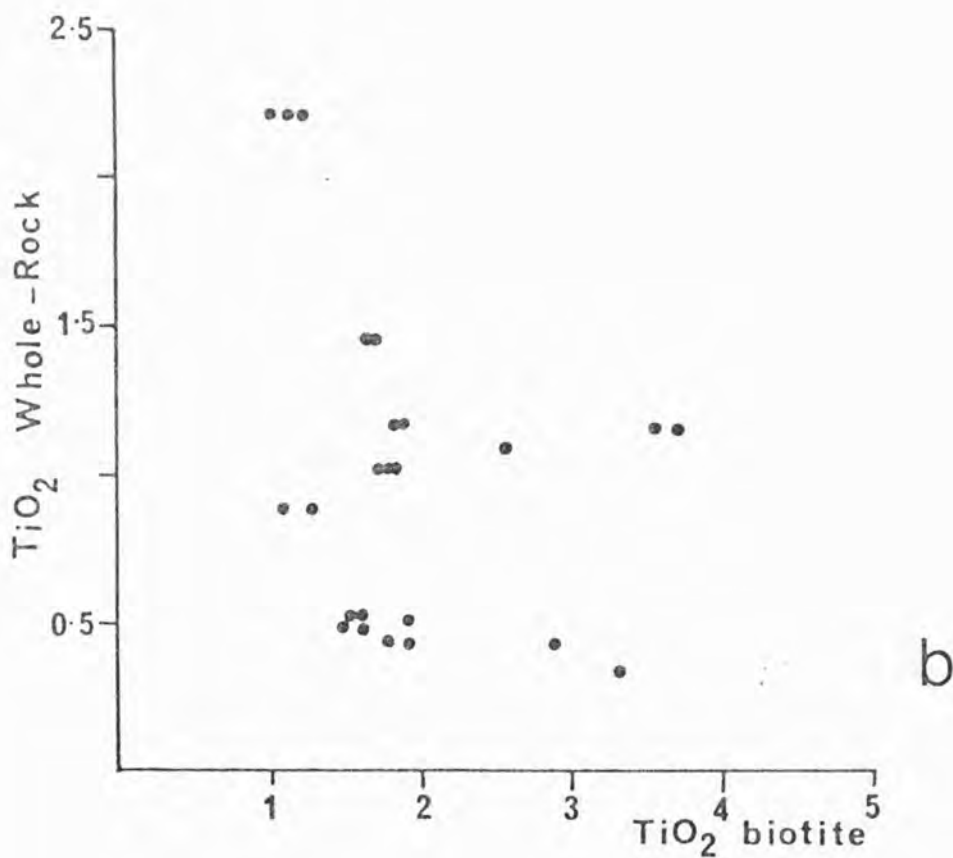
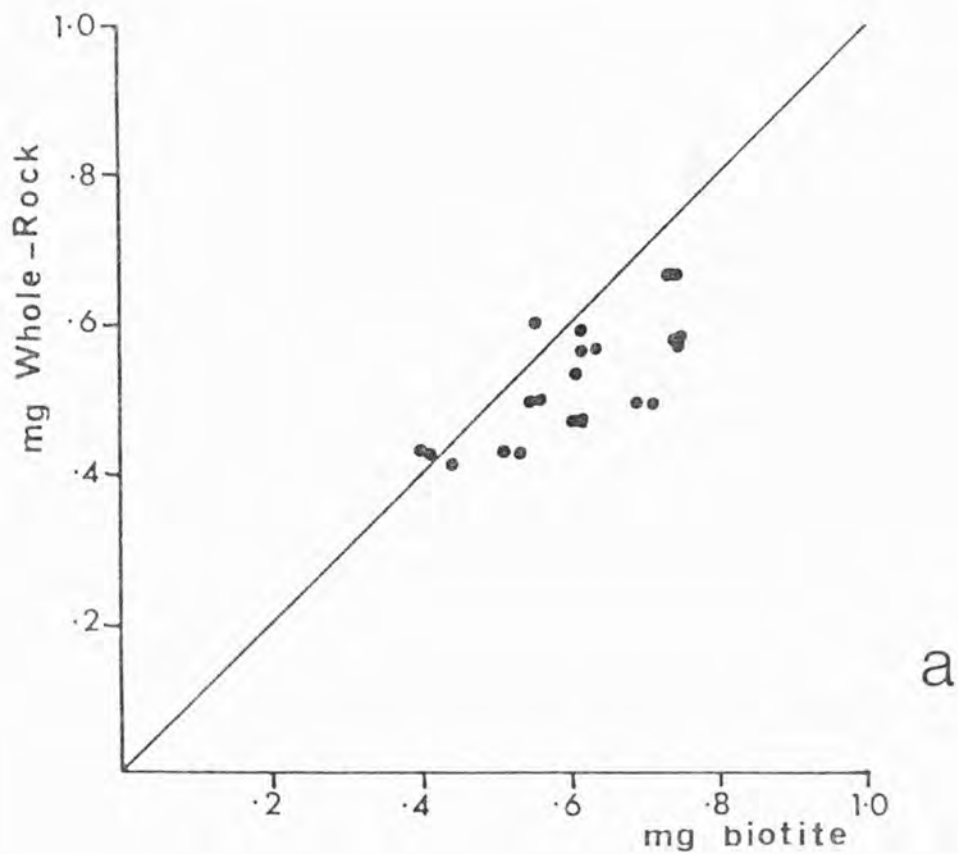


FIG. 5.8 mg (Mg/Mg+Fe) biotite against mg for the host rock, line represents a slope of 1.

b.  $\text{TiO}_2$  biotite against  $\text{TiO}_2$  host rock.

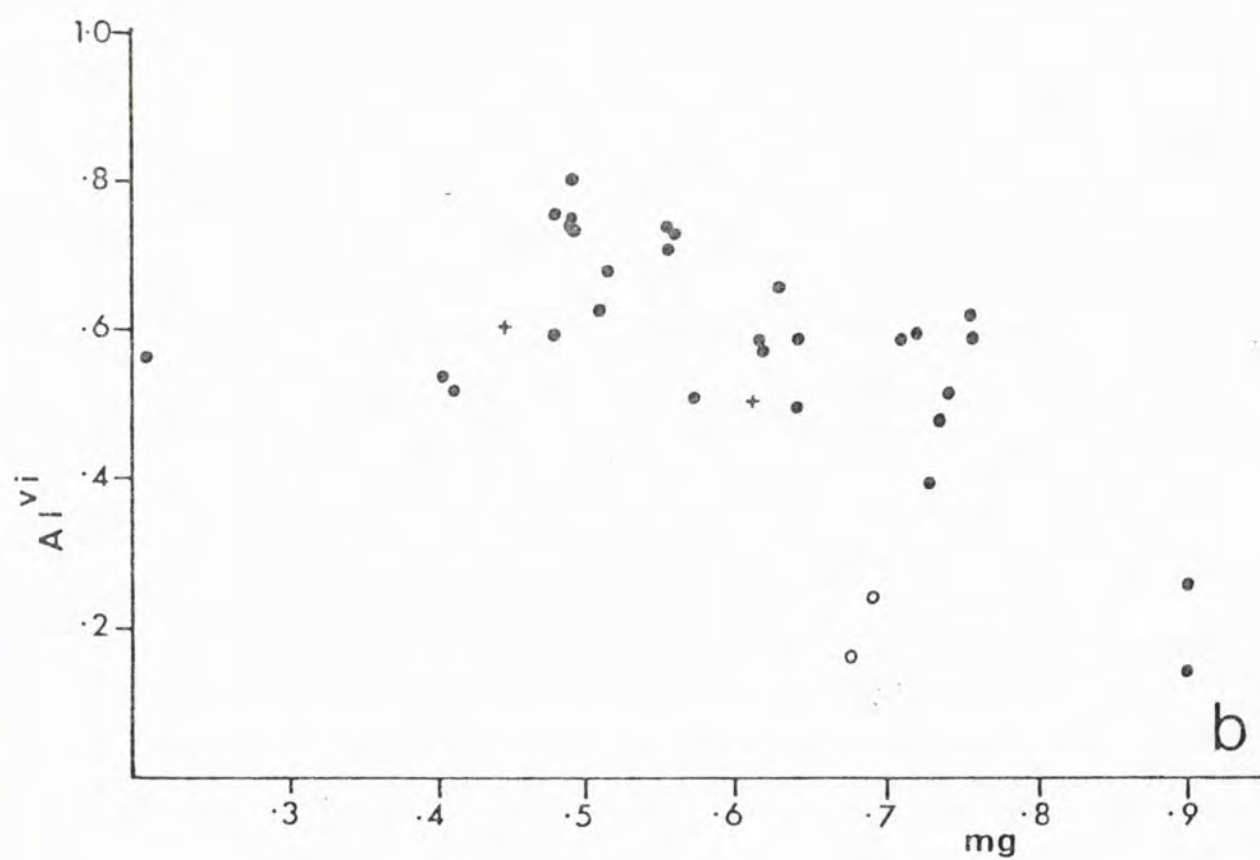
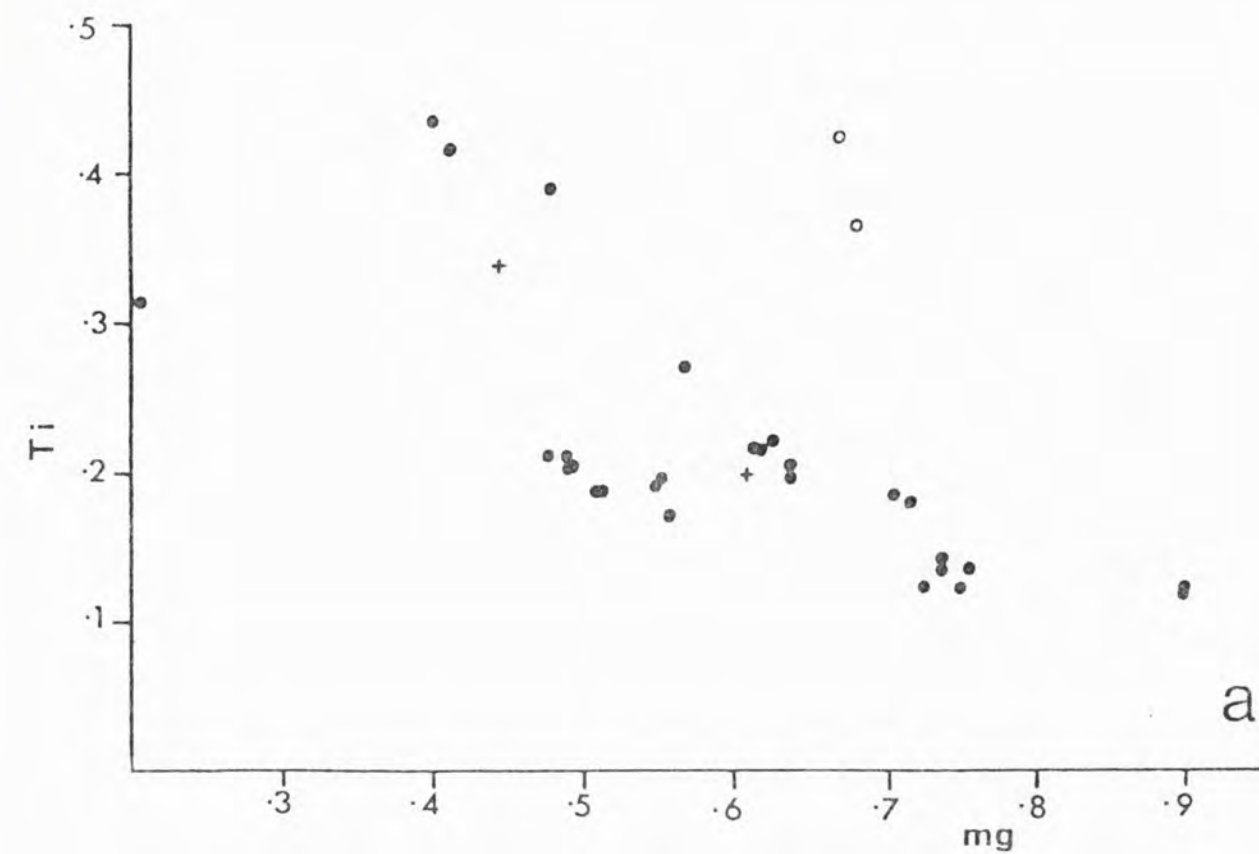


FIG. 5.9 Plots for biotite:

(a) Ti versus mg (Mg/(Mg+Fe))

(b) Al<sup>vi</sup> versus mg

Al, Ti, Mg and Fe based on 22 oxygens per formula unit.

iron) ranges from 4.8 to 5.9 wt.%; MgO from 1.14 to 2.0 wt.% and  $TiO_2$  from 0.75 to 1.05 wt.%. There is only a limited amount of paragonite solid solution - between 3 and 6%.

### 5.3.3. Garnet

Only a few Inverian assemblages contain garnet and those which do are either garnet amphibolite (J6 and W50) or possible metasediment (D17, S4, J36, J96, S10, J94, J98, J113). In the most iron-rich of the layered complex gabbros, there are garnet fringes around opaque oxides (Chapter 2). This garnet growth could be correlated with the Inverian retrogression, because its composition is similar to that from Inverian garnet amphibolites. All garnet analyses are presented in Table 5.5 and plotted in Fig.5.10a where they are compared with granulite facies garnets. They are all almandine-rich with up to 4 wt.% MnO. A few grains have a low Ca content. In Chapter 2 and Savage and Sills (1980) it was demonstrated that the stability of garnet depended on P-T conditions and the whole-rock Fe/Mg ratio. As the temperature was lowered, successively more iron-rich garnets were stabilised and garnet formed in rocks in which it was previously unstable. Inverian garnets occur in fairly Fe-rich rocks, e.g. in the Reidh Port amphibolite mass garnet occurs in sample J6 with a whole-rock  $mg$  of 0.4 but not in the remaining samples with  $mg$  between 0.62 and 0.67. There is a correlation between  $mg$  of garnet and that of the host rock (Fig.5.10b) with garnet always being more iron-rich. Garnet has a strong affinity for iron and the ratio  $(Fe/Mg)_{gt}/(Fe/Mg)_{rock}$  is always greater than 1 but is rather variable depending on the modal percentage of garnet in the rock. In sample J6, where there is only trace amounts of garnet, this  $K_D$  is 8, while in sample W6 which has 60 modal % garnet  $K_D$

SI O2	N50	J6	J96	J96	S10	J36
TI O2	39.48	37.93	39.49	38.53	37.81	38.23
AL2O3	.03	.16	.11	.03	.01	.04
FE O	21.62	20.61	22.02	21.63	22.15	21.53
MN O	29.74	28.62	24.13	29.04	30.28	30.68
MG O	.87	4.26	.88	1.11	1.23	3.33
CA O	3.13	2.02	8.14	6.44	5.83	4.87
CR2O3	7.39	7.31	5.82	3.13	2.81	3.45
TOTAL	102.35	101.41	100.70	100.45	100.16	111.55
UNIT FORMULA						
SI	6.091	6.010	6.018	6.005	5.934	5.467
TI	.009	.019	.013	.003	.003	.005
AL	3.933	3.850	3.956	3.963	4.093	3.980
FE	3.843	3.793	3.776	3.773	3.974	4.015
MN	.114	.573	.114	.145	.164	.411
MG	.727	.477	1.000	1.494	1.373	1.133
CA	1.222	1.326	1.930	1.532	1.471	1.197
CR	.001	.000	.025	.043	.000	.001
O	24.000	24.000	24.000	24.000	24.000	24.000
GARNET MOLECULES (RICKWOOD (1968))						
UVAROVIT	.03	.00	.64	1.15	0.00	.03
PYROPE	12.20	8.26	30.64	25.11	23.22	19.27
SPESSART	1.93	9.30	1.93	2.46	2.70	6.74
GROSSULA	22.63	22.96	15.55	7.73	7.93	3.68
ALMANDIN	65.15	58.88	51.55	63.51	66.03	64.48
SI O2	J98	J98	J98	D17	D17	
TI O2	38.32	38.13	37.71	37.33	37.51	
AL2O3	.12	.16	.11	.06	.25	
FE O	20.76	21.31	21.11	20.71	20.17	
MN O	29.78	29.24	29.63	29.71	32.68	
MG O	2.78	2.73	2.95	1.77	.89	
CA O	1.82	1.90	1.93	1.96	1.09	
CR2O3	7.89	7.84	6.79	7.97	7.94	
TOTAL	101.41	100.64	100.43	100.73	100.54	
UNIT FORMULA						
SI	6.054	6.063	6.011	6.000	6.030	
TI	.014	.016	.012	.005	.030	
AL	3.867	3.894	3.913	3.975	3.823	
FE	3.924	3.803	3.875	3.877	4.394	
MN	.372	.377	.394	.237	.121	
MG	.429	.447	.491	.333	.261	
CA	1.336	1.295	1.300	1.330	1.368	
CR	.012	.005	.003	.004	.001	
O	24.000	24.000	24.000	24.000	24.000	
GARNET MOLECULES (RICKWOOD (1968))						
UVAROVIT	.06	.13	.06	.03	.03	
PYROPE	7.38	7.65	8.40	5.32	4.50	
SPESSART	6.41	6.30	6.53	3.77	2.11	
GROSSULA	22.95	22.81	19.51	13.35	23.81	
ALMANDIN	63.19	64.89	63.63	69.44	69.49	

TABLE 5.5 Garnet analyses

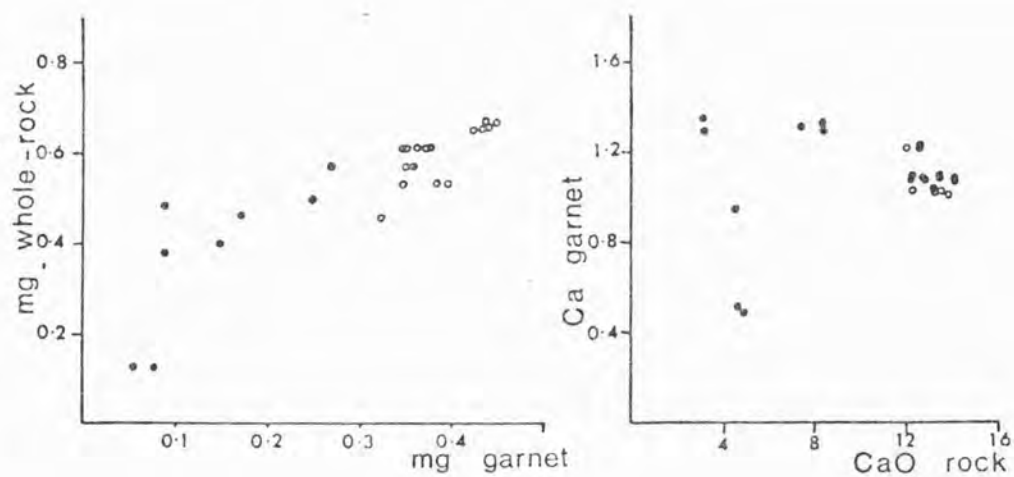
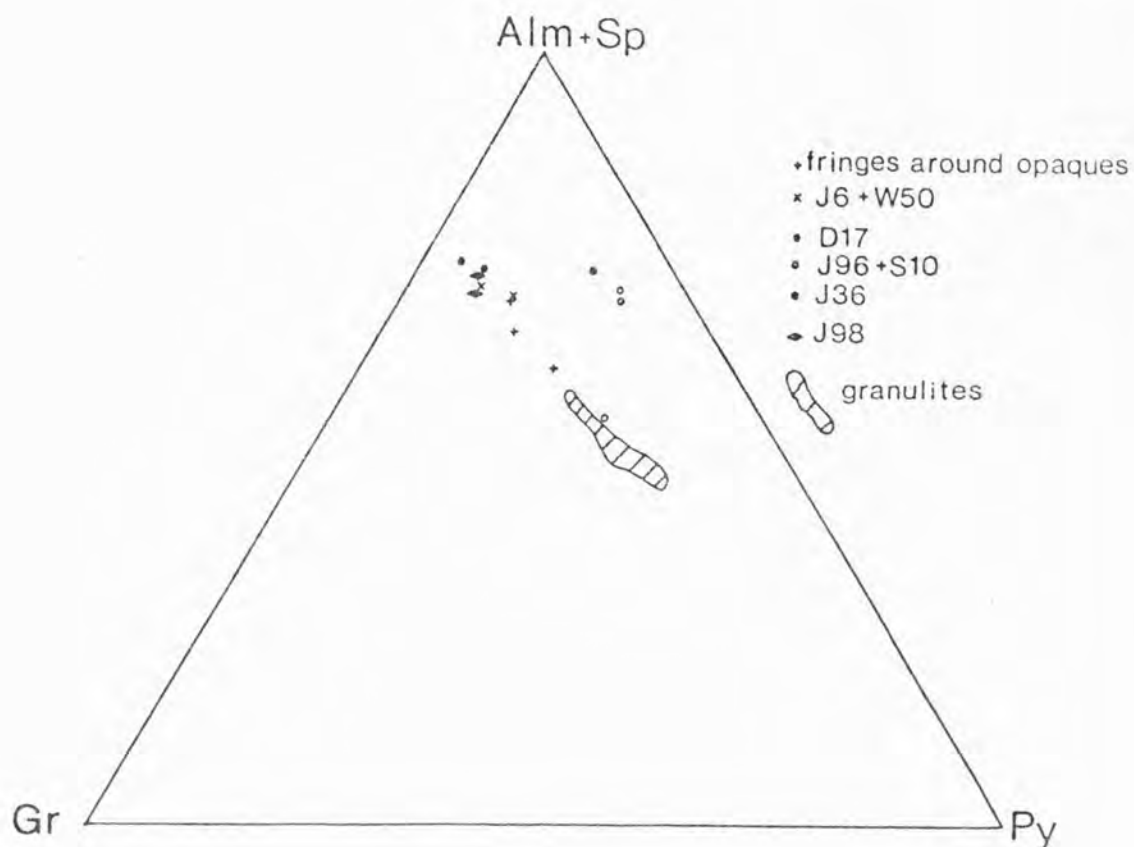


FIG. 5.10 (a) Garnet compositions plotted on a grossular (Gr)-Almandine+Spessartine(Alm+Sp) - Pyrope(Py) triangle.  
 (b) mg ( $Mg/(Mg+Fe)$ ) of garnet against mg of the host rock.  
 (c) Ca of garnet (based on 24 oxygens) against the CaO content of the host rock.

approaches unity. The influence of garnet on the whole rock chemistry of this sample is indicated by the high Y and HREE levels (Chapter 3). The MnO content shows no correlation with rock composition but is rather variable, again depending on the modal percentage of garnet in the sample; sample J6 has the highest MnO content (4.2 wt.%) and has only trace amounts of garnet. Garnet has a strong affinity for Mn, and thus all the Mn in the rock is likely to be concentrated in garnet; if garnet is only a minor phase its Mn content will consequently be higher. Ca content is fairly uniform apart from two grains and does not correlate with rock Ca content (Fig.5.10b) and in fact both Ca-poor and normal Ca grains occur in the same sample.

#### 5.3.4. Epidote

Epidote occurs in many Inverian mafic and intermediate gneisses in three textural varieties:

- (a) colourless needles in plagioclase. The age of saussurite - sation is uncertain. It occurs in plagioclases from Inverian rocks of all compositions but recrystallized grains from shear zones are often inclusion free,
- (b) fringes of colourless epidote between amphibole and plagioclase developed during retrogression of clinopyroxene. Amphiboles rimmed in this way (e.g. D19, Fig.5.1a) are often zoned. The epidote coronas may have tiny quartz inclusions and are zoned with respect to  $Fe^{3+}$ , being richer in Fe towards the amphibole,

	J100	J1	J55	D19	D19	D19	D19	D41	D41	J67
	(4)	(6)	(1)	(1)	(1)	(1)	(1)	(3)	(2)	(5)
SiO <sub>2</sub>	38.48	38.35	38.02	37.50	37.69	37.34	37.33	38.68	38.95	37.76
TiO <sub>2</sub>	0.03	0.05	0.11	0.00	0.04	0.06	0.03	0.12	0.25	0.07
Al <sub>2</sub> O <sub>3</sub>	24.45	25.81	25.02	27.95	26.00	26.13	26.37	23.46	23.90	24.10
Fe <sub>2</sub> O <sub>3</sub>	11.84	10.19	10.54	8.00	8.64	9.79	9.05	11.56	11.77	11.51
MnO	0.09	0.11	0.20	nd	nd	nd	nd	0.25	0.27	0.19
MgO	0.01	0.02	0.03	0.01	0.01	0.01	0.02	0.10	0.28	0.02
CaO	23.46	23.83	23.43	23.74	23.41	23.53	23.48	23.14	22.65	22.39
Cr <sub>2</sub> O <sub>3</sub>	0.00	0.01	0.01	nd	nd	nd	nd	0.84	0.04	0.00
TOTAL	98.38	98.37	97.36	97.20	95.80	96.89	96.28	98.15	98.12	95.04
Cations on the basis of 13(O)										
Si	3.149	3.125	3.135	3.068	3.136	3.082	3.096	3.178	3.190	3.159
Ti	0.001	0.002	0.007	0.004	0.002	0.004	0.002	0.006	0.015	0.004
Al	2.359	2.478	2.431	2.694	2.549	2.549	2.577	2.272	2.360	2.375
Fe <sup>3+</sup>	0.729	0.625	0.653	0.492	0.540	0.609	0.564	0.715	0.725	0.723
Mn	0.006	0.007	0.014	nd	nd	nd	nd	0.018	0.019	0.014
Mg	0.002	0.002	0.003	0.001	0.001	0.001	0.002	0.012	0.035	0.002
Ca	2.058	2.081	2.073	2.084	2.090	2.090	2.090	2.307	1.387	2.010
Cr	0.000	0.001	0.000	nd	nd	nd	nd	0.055	0.002	0.000

TABLE 5.6 Epidote analyses. nd means element not determined.

- (c) recrystallized grains of epidote again occurring between plagioclase and hornblende. These grains probably developed from the epidote coronas. They are yellow and have higher Fe contents (Table 5.6).

In Laxfordian shear zones the amphiboles have a more uniform composition and epidote has almost completely disappeared. It develops where there is excess Ca due to the breakdown of clinopyroxene and as the retrogressed rocks recrystallize and equilibrium is more likely to have been attained over a larger area, the epidote disappears. This ought to be correlated with a slight increase in the An content of plagioclase in shear zone assemblages, but this has not been detected. Epidote has low Mn and Cr contents with  $Fe^{3+}$  (total iron) ranging from 0.5 to 0.8 atoms per formula unit, based on 13 oxygens. Occasionally epidote grains are associated with biotite, perhaps forming from the excess Ca released when hornblende reacts to form biotite.

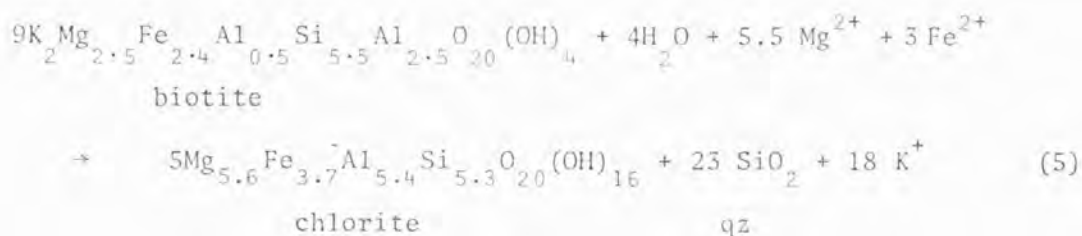
#### 5.3.5. Chlorite

Chlorite occurs in a wide range of rock types forming a major constituent of retrogressed ultramafic rocks. Chlorite commonly replaces biotite along cleavage planes. Well formed chlorite aggregates in mafic and intermediate composition gneisses only occur near shear zones or dyke margins. Complete replacement of biotite yields a pale green, pleochroic chlorite with needles of an opaque oxide (haematite?). This reflects the higher mg of the replacing chlorite, the excess iron forming haematite. In shear zones this type of chlorite pseudomorphing biotite has disappeared but a few samples contain abundant chlorite perhaps developed from hornblende. In samples J96 and S10 there are discrete needles of a colourless chlorite. Analyses are given in Table 5.7.

	J98	J36	J51	D34	D45	J96	D25	D26	J127	S2
	(4)	(2)	(4)	(3)	(3)	(3)	(3)	(15)	(5)	(1)
SiO <sub>2</sub>	24.74	26.32	25.59	26.72	26.93	26.75	28.86	29.59	29.28	30.79
TiO <sub>2</sub>	0.07	0.09	0.07	0.09	0.06	0.08	0.06	0.05	0.12	0.12
Al <sub>2</sub> O <sub>3</sub>	22.02	21.79	21.87	21.63	22.12	22.56	20.46	18.84	17.17	18.44
FeO	23.34	16.54	21.30	16.97	15.72	12.91	6.97	6.31	17.03	9.73
MnO	0.08	0.03	0.18	0.20	0.14	0.02	0.02	0.02	0.24	0.07
MgO	15.70	21.63	18.11	21.20	21.33	23.19	28.61	28.93	21.91	25.83
CaO	0.06	0.02	0.00	0.01	0.03	0.02	0.02	0.07	0.04	0.07
Cr <sub>2</sub> O <sub>3</sub>	0.06	0.00	0.01	0.09	0.01	0.26	0.45	0.81	0.20	0.55
NiO	nd	0.23	nd	0.23						
TOTAL	86.07	86.42	87.13	86.82	86.36	85.79	85.45	84.90	85.99	85.83
Cations on the basis of 28 oxygens										
Si	5.620	5.361	5.316	5.429	5.457	5.380	5.649	5.626	6.008	6.072
Ti	0.011	0.014	0.011	0.014	0.009	0.012	0.012	0.008	0.018	0.018
Al	5.517	5.230	5.374	5.180	5.283	5.348	4.270	4.370	4.151	4.285
Fe	4.149	2.817	3.672	2.833	2.664	2.171	1.142	1.040	2.922	1.605
Mn	0.014	0.000	0.032	0.035	0.023	0.004	0.003	0.003	0.042	0.012
Mg	4.974	6.566	5.576	6.389	6.443	6.951	8.347	8.484	6.699	7.581
Ca	0.013	0.004	0.002	0.003	0.006	0.004	0.003	0.016	0.009	0.015
Cr	0.010	0.000	0.000	0.014	0.003	0.042	0.071	0.126	0.032	0.085
Ni								0.037		0.040
mg	0.544	0.700	0.600	0.690	0.706	0.762	0.879	0.900	0.695	0.825

TABLE 5.7 Chlorite analyses

Using the classification of Deer et al. (1966, their Fig.81) all chlorites from Inverian mafic and intermediate assemblages are ripidolite (Fig.5.11), the mg ranging from 0.75 (colourless) to 0.5 (pale green). Chlorite from ultramafic assemblages is clinochlore. Although difficult to estimate, the amount of  $Fe^{3+}$  is probably quite small as the cation total is within 2% (usually <1%) of the ideal total of 20 when calculated on the basis of 28 oxygens.  $Cr_2O_3$  content is generally below minimum detection limit but in retrogressed ultramafics it is up to 0.9 wt.% (Fig.5.11b) and NiO is up to 0.25 wt.%. The Cr and Ni content of chlorite is greater than that of coexisting tremolite, implying that the Cr and Ni content of the granulite facies mafic minerals enters chlorite. MnO is low in garnetiferous samples. Chlorite could form from biotite by the following reaction:



This produces excess potassium and quartz.

#### 5.4. PARTITIONING OF ELEMENTS BETWEEN COEXISTING MINERAL PAIRS

As seen in the previous section the composition of individual hornblende and biotite grains does not give much information as to the pressure and temperature of formation. The composition was seen to depend on both the whole-rock composition and the paragenesis. However many studies have shown that the partitioning of elements between coexisting mineral pairs is sometimes P-T dependent and thus may be calibrated as a geothermometer or geobarometer; examples being the two-

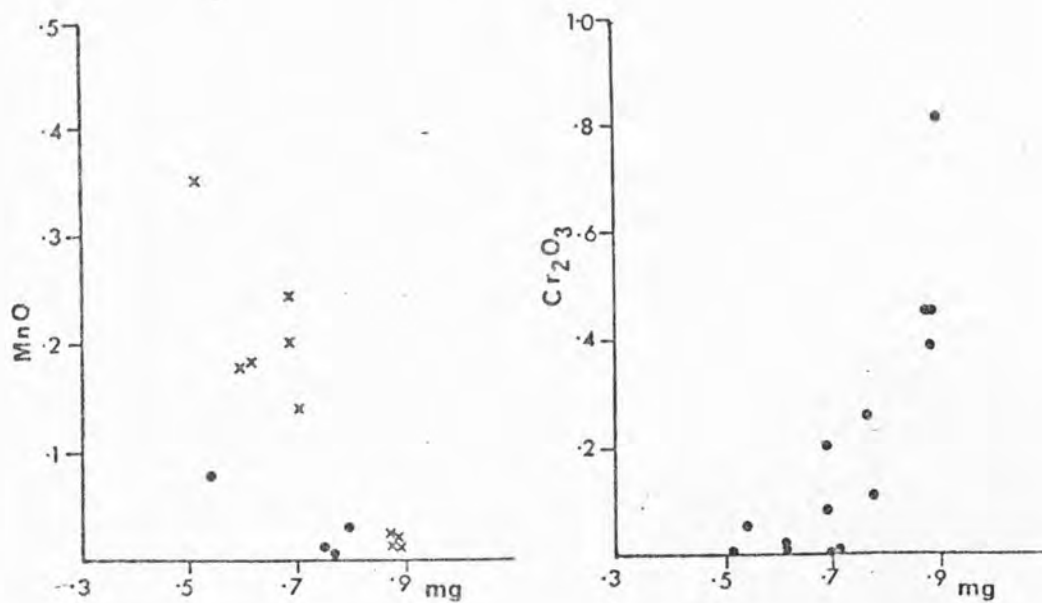
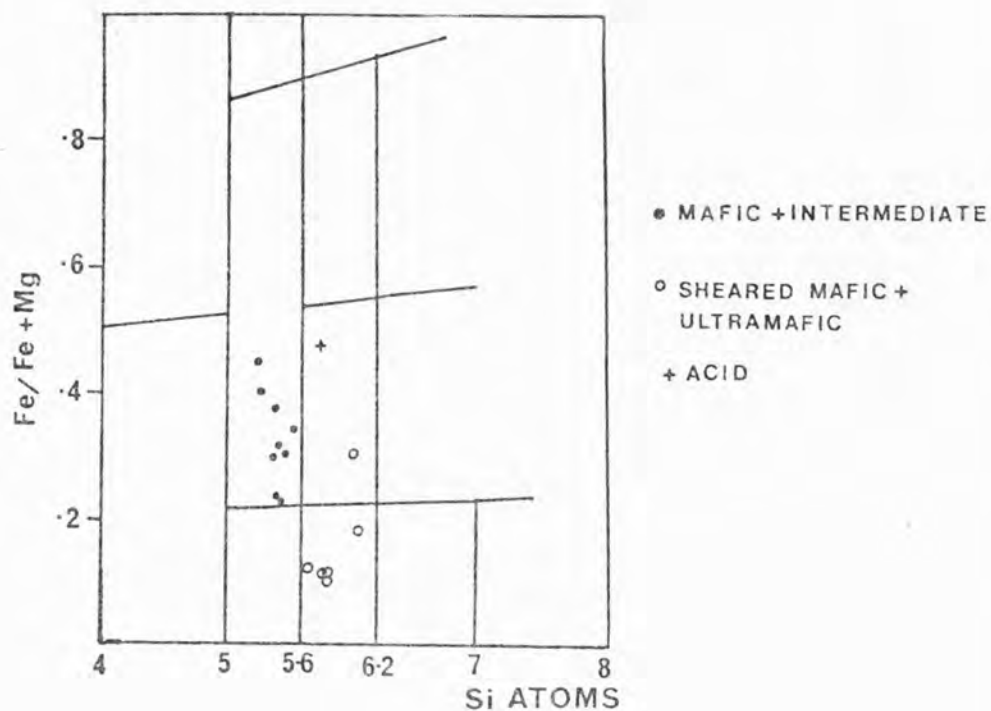


FIG. 5.11 (a) Classification of chlorites; those from Inverian mafic and intermediate gneisses are ripidolite, those from sheared mafic and ultramafic rocks are clinocllore. (b) MnO content of chlorite against mg of chlorite. (c) Cr<sub>2</sub>O<sub>3</sub> content of chlorite against mg of chlorite.

pyroxene and garnet-pyroxene geothermometry discussed in Chapter 2. However many distribution coefficients are strongly dependent on compositional variations between the minerals concerned. In this section partitioning of elements between various mineral pairs will be examined to see if any could be P-T dependent.

### Garnet-Biotite

The Fe-Mg exchange equilibrium between garnet and biotite is considered by many authors to depend on metamorphic grade (Saxena, 1969; Hietanen, 1969; Perchuk, 1970; Lyons and Morse, 1970; Goldman and Albee, 1977; Ferry and Spear, 1978; Baltatzis, 1979).

A literature study by Lyons and Morse (1970) suggested that  $K_{D}^{gt-bi}$  increases from an average of 0.13 in the garnet zone to 0.274 in the sillimanite zone. Hietanen (1969) found the  $K_D$  increases from 0.106 to 0.225 from the garnet to sillimanite-muscovite zones. In this study, garnet-biotite pairs have been analysed in 5 samples (D17, K98, J36, J96, S10). They have a fairly wide compositional range with  $m_{gt}$  of biotite ranging from 0.205 to 0.76 and that of garnet from 0.10 to 0.36. The  $K_{D}^{gt-bi}$  has been plotted in Fig.5.12a using the  $K_D$  values obtained by Lyons and Morse (1970) for comparison; the values obtained in this study do not fall on a straight line. Samples D17, J36 and J98 all occur in thin bands bordering retrogressed mafic assemblages and there is no reason to suggest that they formed at different temperatures. J96 and S10 come from an Inverian steep belt where there is some attenuation. In Fig.5.12b  $K_D$  is plotted against the Ca and Mn content of garnet but there is no clear relationship.

The  $K_D$  was calibrated as a geothermometer by Saxena (1969) who used multivariate statistics to define the dependence on compositional

pyroxene and garnet-pyroxene geothermometry discussed in Chapter 2. However many distribution coefficients are strongly dependent on compositional variations between the minerals concerned. In this section partitioning of elements between various mineral pairs will be examined to see if any could be P-T dependent.

#### Garnet-Biotite

The Fe-Mg exchange equilibrium between garnet and biotite is considered by many authors to depend on metamorphic grade (Saxena, 1969; Hietanen, 1969; Perchuk, 1970; Lyons and Morse, 1970; Goldman and Albee, 1977; Ferry and Spear, 1978; Baltatzis, 1979).

A literature study by Lyons and Morse (1970) suggested that  $K_{\text{gt-bi}}^{\text{(Mg-Fe}^{2+})}$  increases from an average of 0.13 in the garnet zone to 0.274 in the sillimanite zone. Hietanen (1969) found the  $K_D$  increases from 0.106 to 0.225 from the garnet to sillimanite-muscovite zones. In this study, garnet-biotite pairs have been analysed in 5 samples (D17, K98, J36, J96, S10). They have a fairly wide compositional range with mg of biotite ranging from 0.205 to 0.76 and that of garnet from 0.10 to 0.36. The  $K_{\text{gt-bi}}^{\text{(Mg-Fe}^{2+})}$  has been plotted in Fig.5.12a using the  $K_D$  values obtained by Lyons and Morse (1970) for comparison; the values obtained in this study do not fall on a straight line. Samples D17, J36 and J98 all occur in thin bands bordering retrogressed mafic assemblages and there is no reason to suggest that they formed at different temperatures. J96 and S10 come from an Inverian steep belt where there is some attenuation. In Fig.5.12b  $K_D$  is plotted against the Ca and Mn content of garnet but there is no clear relationship.

The  $K_D$  was calibrated as a geothermometer by Saxena (1969) who used multivariate statistics to define the dependence on compositional

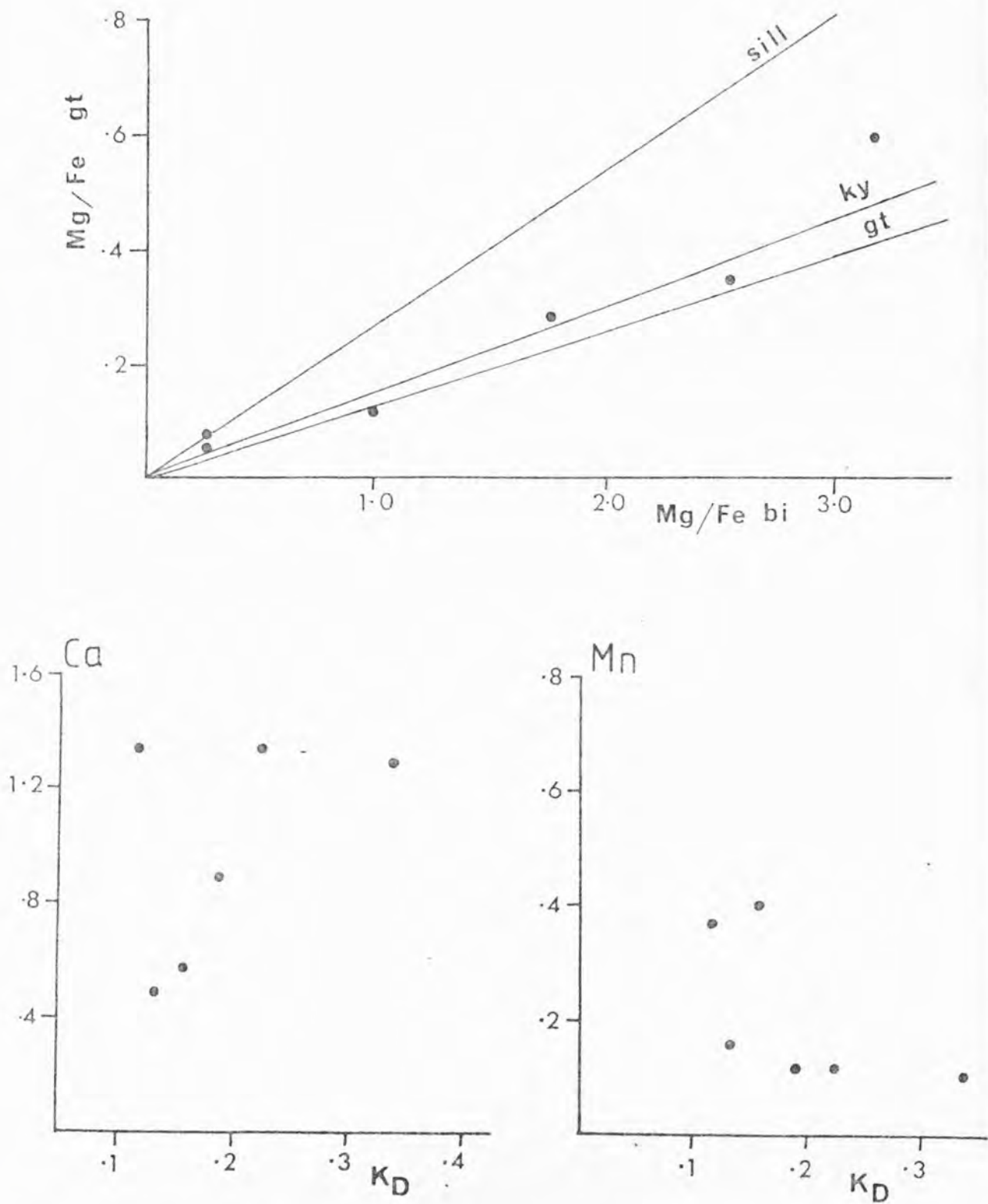


FIG. 5.12 Plots for coexisting garnet and biotite.

(a) Mg/Fe garnet against Mg/Fe biotite. The slopes for the sillimanite, kyanite and garnet zones are from Lyons and Morse (1970)

(b) Ca content of garnet (based on 24 O) against  $K_D^{Mg-Fe}_{gt-bi}$

(c) Mn content of garnet against  $K_D$

variables. Thompson (1976) devised a thermometer based on a direct correlation of Mg-Fe distribution coefficients between selected mineral pairs with metamorphic temperatures inferred from their host rock paragenesis and phase relations. Effects of non-ideal mixing and compositional factors were ignored. Goldman and Albee (1977) defined the  $K_D$  in terms of compositional factors and equilibrium temperatures estimated from  $^{18}O/^{16}O$  partitioning between quartz and magnetite. Ferry and Spear (1978) experimentally calibrated  $K_D$  between almandine-pyrope and annite-phlogopite; however this ignores Ti,  $Al^{Vi}$  and octahedral vacancies in biotite and the Ca and Mn content of garnet. The data of Stephenson (1979) indicate that the various thermometers give widely varying results, commonly much greater than the temperature range indicated by other thermometric methods and Bohlen and Essene (1980) advise caution in applying the various thermometers.

The results from this study are presented in Table 5.8. The  $K_D$  for the Ferry and Spear (1978) method has been modified to allow for some compositional variance. As can be seen, temperatures vary widely and it is concluded that garnet-biotite thermometry as it now stands is not reliable for non-pelitic rocks, although one can say that the temperature was probably between 450 and 700°C. This range in temperatures may be due to re-equilibration of one of the pair with another mineral e.g. biotite with opaque oxide.

#### Mg-Fe partitioning between hornblende, biotite and chlorite

Mg-Fe partitioning between hornblende, biotite and chlorite is shown in Fig.5.13. There is no difference between shear zone and retrogressed samples. The mg of chlorite > biotite > hornblende except for the retrogressed ultramafics where  $K_{(Mg-Fe)}^{chl-hb}$  approaches unity.

SAMPLE	$\ln K_D$	Ferry and Spear(1978) A	Ferry and Spear B	Ferry and Spear C	Thompson (1976) D	Saxena (1969) E
D17	-1.08	875	879	684	761	505
D17	-1.48	677	673	433	625	480
J98	-2.15	456	464	335	466	408
J36	-1.83	545	545	439	533	424
J96	-1.65	606	604	425	582	468
J96	-2.07	476	478	329	477	416
S10	-2.00	495	496	342	500	420
range		419	415	355	295	97

TABLE 5.8 Garnet-biotite temperatures ( $^{\circ}\text{C}$ ) derived as follows:-

- (A) Ferry and Spear(1978)
- (B) Ferry and Spear(1978) modified to account for compositional differences assuming an ideal mixing on sites model for both garnet and biotite
- (C) Ferry and Spear(1978) with  $K_D$  modified assuming an ideal mixing on sites model for biotite and using the mixing model of Ganguly and Kennedy(1974) for Ca-Mg garnets
- (D) Thompson(1976) Fig.1.b
- (E) Saxena(1969).

$$K_D \text{ is } \frac{\text{Mg/Fe}_{gt}}{\text{Mg/Fe}_{bi}}$$

range is the range in derived temperatures for each method.

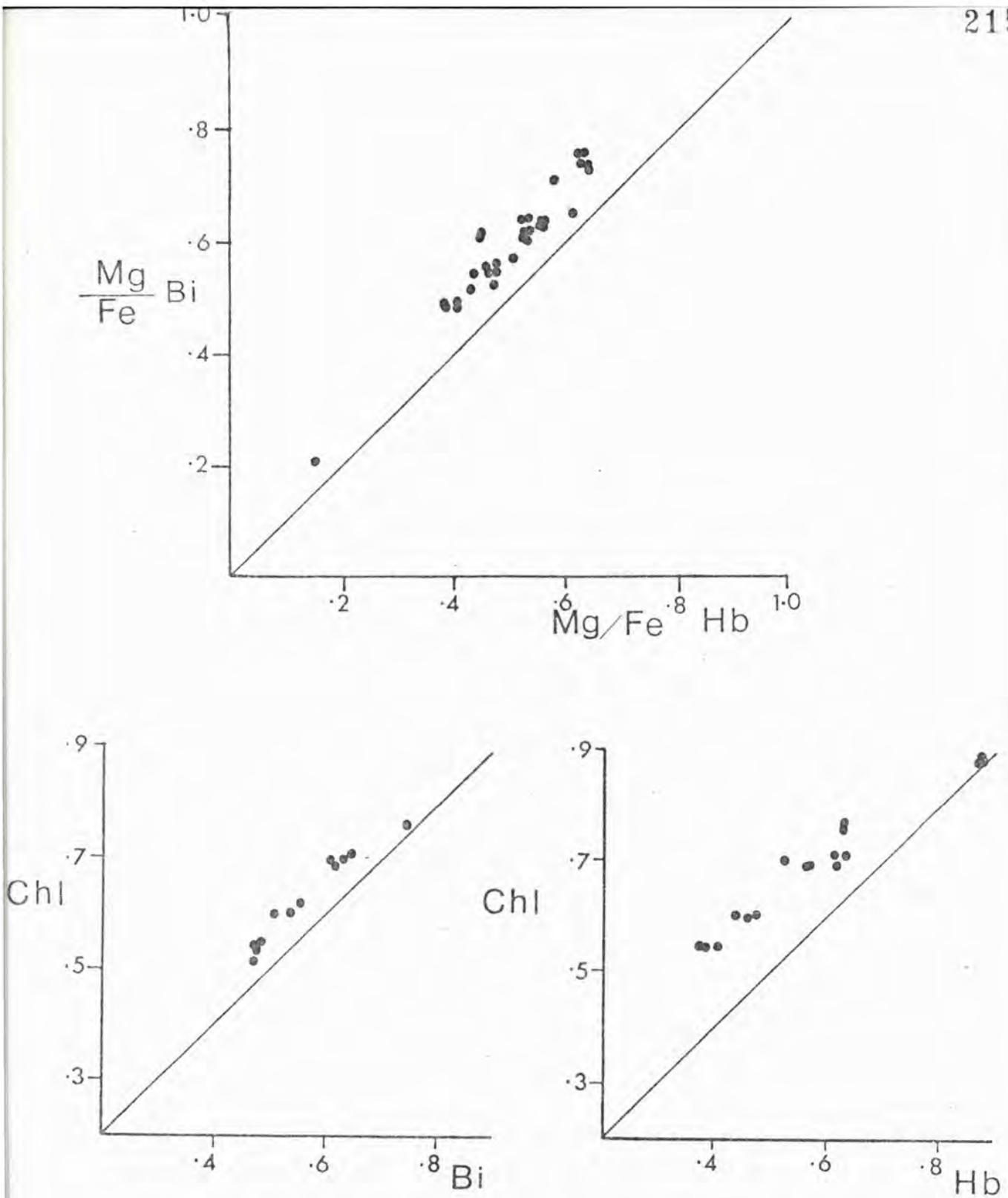


FIG. 5.13 Plots of Mg/Fe ratios for coexisting mineral pairs. The line represents a slope of unity.

- (a) Mg/Fe biotite versus Mg/Fe hornblende
- (b) Mg/Fe chlorite versus Mg/Fe biotite
- (c) Mg/Fe chlorite versus Mg/Fe hornblende

$K_{(Fe-Mg)}^{bi-hb}$  ranges from 0.51 to 0.88 but does not vary in any organised way so it is concluded that this particular Fe-Mg exchange is not temperature sensitive. It probably depends on compositional factors such as Al substitutions in hornblende and biotite. Stephenson (1977) came to a similar conclusion.

#### Partitioning of elements between hornblende and biotite

Hornblende and biotite coexist in many Inverian and Laxfordian shear zone assemblages, but unfortunately there are no granulite facies pairs. A study of the differences between granulite and amphibolite facies hornblende-biotite pairs has recently been made by Stephenson (1977).  $K_D$ 's for various elements have been calculated and the data and method of calculation given in Table 5.9. It can be seen that the biotite structure favours  $Al^{iv}$ , Mg and Ti and that the hornblende structure favours Fe/Mg,  $Fe^{2+}$ , Mn,  $Al^{vi}$  and  $Al^{vi} + Ti$ . Each  $K_D$  should be constant if the mineral pairs behave as ideal mixtures and reached equilibrium under constant P-T conditions. As can be seen in Table 5.9, the  $K_D$ 's are quite variable.

#### Tetrahedral ions

$Al^{iv}$  is favoured by biotite and  $K_{Al^{iv}}^{Bi-Hb}$  ranges from 1.35 to 1.9 in a shear zone pair. Gorbatshev (1969) showed that the distribution of  $Al^{iv}$  and Si between hornblende and biotite is non-ideal and that variations are systematically related to the  $Al^{iv}$  content of the hornblende; this is also the case in this study where  $K_{Al^{iv}}^{Bi-Hb}$  correlates with  $X_{Al^{iv}}$  in hornblende (Fig.5.14c). The substitution of Si by  $Al^{iv}$  in hornblende is coupled with increasing  $Al^{vi}$  and edenite alkalis, there being a weak correlation between  $K_{Al^{iv}}^{Bi-Hb}$  and  $Al^{vi} + Ti$  but no correlation with edenite alkalis (Fig.5.14d).

ROCK	$K_D^{\text{Bi-Hb}}_{\text{Al}^{\text{iv}}}$	$K_D^{\text{Bi-Hb}}_{\text{Fe-Mg}}$	$K_D^{\text{Bi-Hb}}_{\text{Fe}^{2+}}$	$K_D^{\text{Bi-Hb}}_{\text{Mg}}$	$K_D^{\text{Bi-Hb}}_{\text{Mn}}$	$K_D^{\text{Bi-Hb}}_{\text{Ti}}$	$K_D^{\text{Bi-Hb}}_{\text{Al}^{\text{vi}}}$	$K_D^{\text{Bi-Hb}}_{\text{Ti+Al}^{\text{vi}}}$
J98	1.643	0.694	0.868	1.587	0.503	4.099	0.507	0.645
J36	1.655	0.614	.764	1.647	0.202	4.270	0.480	0.622
D17	1.370	0.664	1.002	1.509	0.352	3.064	0.502	0.718
J96	1.354	0.548	0.768	1.400	0.081	2.887	0.424	0.500
S10	1.465	0.581	0.790	1.359	-	3.624	0.448	0.566
J51	1.782	0.758	0.843	1.352	0.355	2.595	0.681	0.828
W24	1.845	0.704	0.777	1.462	0.392	2.989	0.632	0.722
D34	1.723	0.775	0.884	1.141	0.332	3.666	0.689	0.843
D41	1.658	0.797	0.920	1.154	0.409	3.761	0.580	0.824
J55	1.932	0.807	0.970	1.459	0.447	3.033	0.516	0.684
J67	1.517	0.513	0.735	1.428	0.403	2.417	0.620	0.780
J10	1.737	0.606	0.671	1.658	0.386	1.215	0.619	0.702

TABLE 5.9 Various distribution coefficients ( $K_D$ ) for element pairs between coexisting biotite and hornblende, where:

$$K_D^{\text{Bi-Hb}}_{\text{A}} = \frac{X_A^{\text{Bi}}}{1 - X_A^{\text{Bi}}} \cdot \frac{1 - X_A^{\text{Hb}}}{X_A^{\text{Hb}}}$$

$K_D^{\text{Bi-Hb}}_{\text{Fe+Mg}}$  is the iron-magnesium exchange reaction distribution coefficient, calculated using the atomic ratio Fe/Fe+Mg;  $X_A$  for octahedral cations is  $A/\sum \text{octahedral}$ ;  $X_{\text{Al}^{\text{iv}}}$  is  $\text{Al}^{\text{iv}}/\text{Al}^{\text{iv}}+\text{Si}$ .

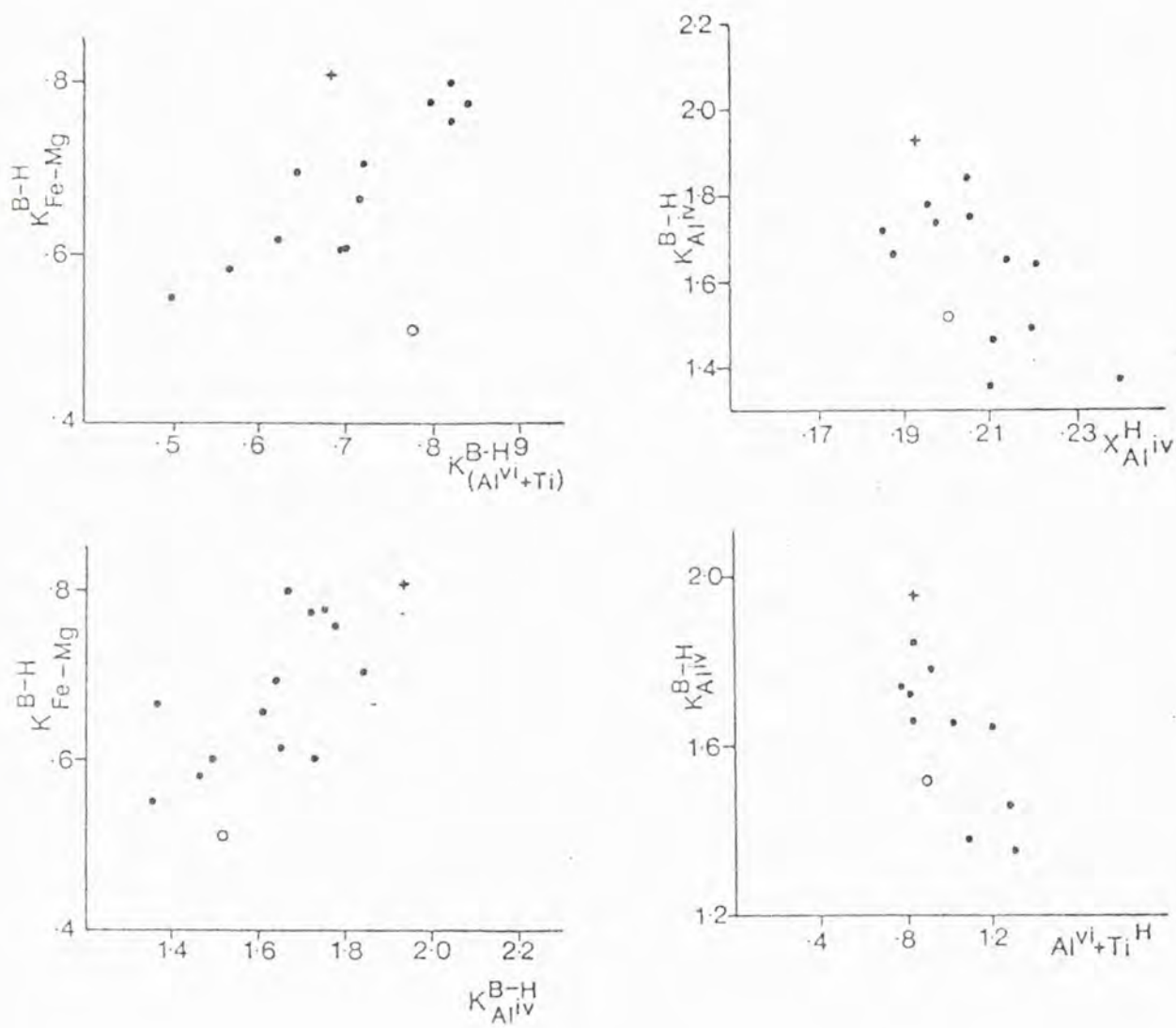


FIG. 5.14 Partitioning of elements between coexisting hornblende (H) and biotite (B).

$$K_{Fe-Mg}^{B-H} = (Fe/Mg)_B / (Fe/Mg)_H$$

other  $K_D$ 's are explained in Table 5.9.

$$X_{Al^{IV}}^H = Al^{IV} / (Al^{IV} + Si) \text{ in hornblende}$$

$(Al^{VI}+Ti)^H$  is the sum of tetrahedral Al and Ti based on 23 oxygens in the water free formula.

### Octahedral ions

The ratio  $(\text{Fe/Mg})_{\text{Bi}}/(\text{Fe/Mg})_{\text{Hb}}$  ranges from 0.51 to 0.88, being highest in shear zone samples. It is not dependent on the host rock composition or on  $X_{\text{Fe}}$  or  $X_{\text{Mg}}$  of the hornblende or biotite. Several studies (e.g. Stephenson, 1977) have concluded that this iron-magnesium exchange reaction is not P-T dependent, therefore the variation must be due to other factors such as the failure to reach equilibrium. This is likely as the biotite commonly partially replaces hornblende in reactions which failed to go to completion, presumably due to insufficient  $K^+$ . There is a positive correlation between  $K_{\text{Fe-Mg}}^{\text{Bi-Hb}}$  and  $K_{\text{Al}^{\text{iv}}}^{\text{Bi-Hb}}$  and  $K_{\text{Al}^{\text{vi}} + \text{Ti}}^{\text{Bi-Hb}}$  (Fig. 5.14a,b) indicating that replacement of Si by Al favours increasing substitution of Fe for Mg in the biotite structure.  $K_{\text{Mn}}^{\text{Bi-Hb}}$  does not vary greatly (except in samples where the Mn content is very low, approaching MDL) and is the most consistent of the  $K_D$ 's calculated. The partition of Mn between biotite and hornblende may be temperature dependent (Stephenson, 1977) and this may be reflected in the uniformity of  $K_{\text{Mn}}^{\text{Bi-Hb}}$  here as all the samples come either from Inverian or shear zone assemblages which probably formed at similar temperatures.

There are not enough data to conclude which, if any,  $K_D$ 's are temperature dependent but it is clear that some  $K_D$ 's depend on the composition of the minerals.

### 5.5. RETROGRESSION OF ULTRAMAFIC ROCKS

In this section the retrogression of the ultramafic rocks will be examined in detail. Ultramafic rocks have a fairly simple whole-rock chemistry when compared with mafic and acid rocks; the Lewisian ultramafics approximate to the system  $\text{MgO} - \text{CaO} - \text{Al}_2\text{O}_3 - \text{SiO}_2 - \text{CO}_2 - \text{H}_2\text{O}$  and

several experimental studies have been made on parts of this system, notably  $\text{MgO} - \text{SiO}_2 - \text{H}_2\text{O} - \text{CO}_2$  (Greenwood, 1963, 1967, 1971; Johannes, 1969). Studies have been made of the progressive metamorphism of serpentinites (Evans and Trommsdorff, 1970, 1974; Trommsdorff and Evans, 1972; Frost, 1975) but there are few studies of the retrogressive metamorphism of high-grade ultramafic rocks. Ultramafic rocks are more sensitive indicators of changing P-T conditions in the amphibolite facies than rocks of mafic and intermediate composition.

In Tables 5.10 and 5.11 a series of possible metamorphic reactions is presented to form the retrogressed and shear zone assemblages from the granulite facies assemblages. As retrogression in Inverian steep belts and then shearing proceeded, the following assemblages were produced;

opx - cpx - ol - parg - sp - magt (granulite facies);  
 trem - chl  $\pm$  anth - magt;  
 trem - chl  $\pm$  tc  $\pm$  anth - magt;  
 chl - tc - dol -  $\pm$  trem - magt  $\pm$  haem;  
 chl - tc  $\pm$  trem - cummingtonite - magt.

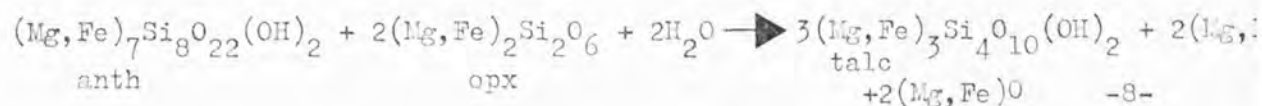
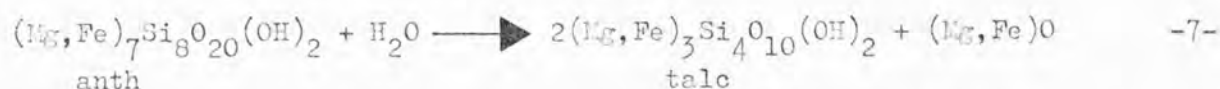
The most important reaction is number 4 (Table 5.10) where pargasite, orthopyroxene and spinel react to form chlorite and tremolite. In retrogressed samples fibrous intergrowths of chlorite and tremolite are found pseudomorphing the granulite facies texture (Fig.5.3b).

The granulite facies system can be approximated by  $\text{CaO} - \text{MgO} - \text{SiO}_2 - \text{Al}_2\text{O}_3 - \text{H}_2\text{O}$  and there are 5 main phases, hence 2 degrees of freedom (according to the phase rule). However as retrogression proceeds, the number of minerals decreases. In the Inverian assemblages (chl - trem -  $\pm$  anth  $\pm$  tc) there are 3 degrees of freedom and in shear zone assemblages  $\text{CO}_2$  becomes a significant component but there are no more phases;



A.

Reactions to produce talc from anthophyllite:-



B. Reactions to produce dolomite in shear zones:-

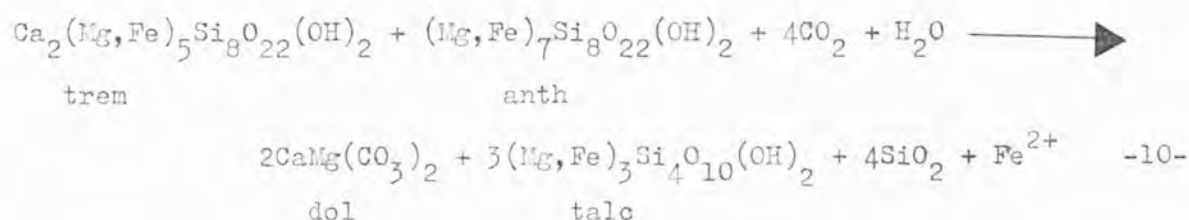
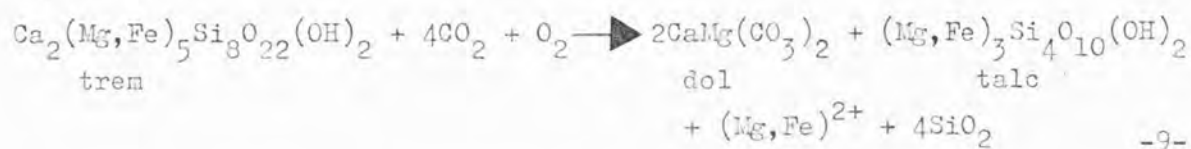


TABLE 5.11 Reactions to produce shear zone assemblages from Inverian assemblages in ultramafic rocks.

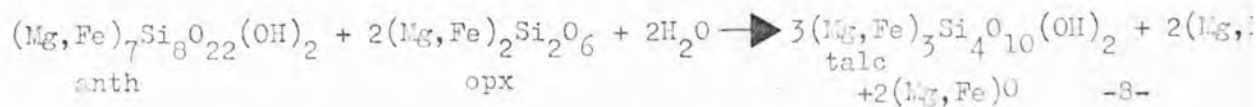
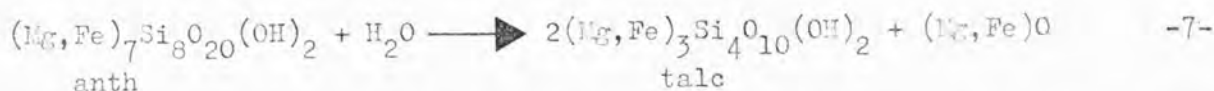
hence the variance may now be as much as four. This large variance means it is impossible to uniquely define the pressure and temperature without knowing the composition of the fluid phase, both  $X_{H_2O}$  and  $X_{CO_2}$  (although  $X_{CO_2} + X_{H_2O} = 1$ ) as well as the activity of ions in the fluid phase. As a result it will only be possible to define broad P-T fields in which the assemblages developed.

Anthophyllite is only a transitional phase forming from orthopyroxene, although it may be present in some shear zone assemblages. It either disappears by reactions with pargasite or diopside to produce tremolite or by reactions which produce talc (Table 5.11). There may be a local regrowth of anthophyllite in carbonated shear zones (Tarney, 1973). Many of the reactions in Tables 5.10 and 5.11 produce an excess of Fe or Mg which probably forms magnetite (which increases in abundance in retrogressed rocks) with a resulting increase in the Mg/Fe ratio in the silicate phases. The low temperature breakdown product of anthophyllite in the experimental systems is olivine + talc (Greenwood, 1963; Johannes, 1969) but no olivine is formed in the Lewisian rocks. In the retrogressed assemblages the only aluminous mineral is chlorite, whilst in the granulite facies assemblages there is spinel, pargasite and aluminous pyroxenes. This implies that  $Al_2O_3$  need no longer be considered as a component which affects the phase relationships, but this makes no difference to the amount of variance in the system discussed above.

In shear zones dolomite becomes abundant. Any possible reaction to produce dolomite (Table 5.11) produces excess silica; as no quartz is produced this silica must be removed. However in the Canisp shear zone, where retrogressed shear zone assemblages are best developed, there are abundant quartz veins especially in the vicinity of ultramafic rocks. These quartz veins are sometimes folded and could well be contemporaneous with some of the deformation. Finally cummingtonite (and possibly

A.

Reactions to produce talc from anthophyllite:-



B. Reactions to produce dolomite in shear zones:-

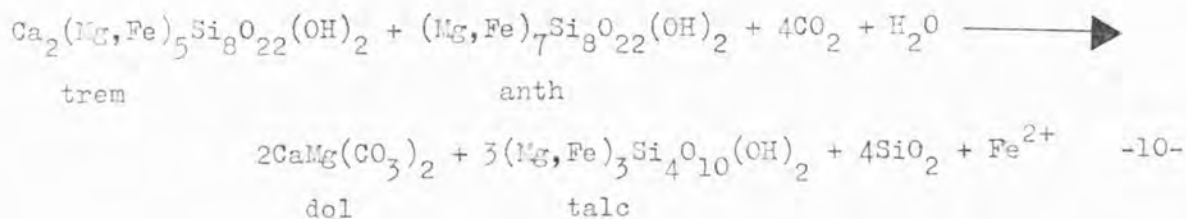
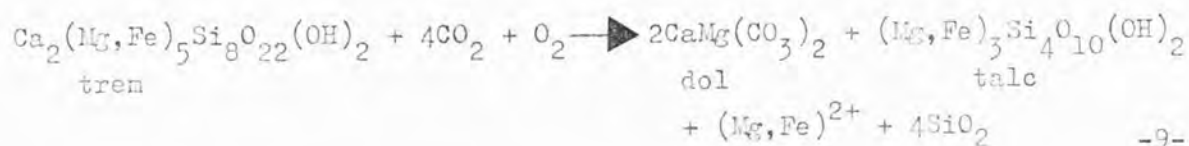


TABLE 5.11 Reactions to produce shear zone assemblages from Inverian assemblages in ultramafic rocks.

tremolite) laths develop from dolomite and the talc-chlorite matrix (Fig.5.3c); this reaction presumably releases  $\text{CO}_2$ .

It is possible to make an approximate estimate of the P-T-X conditions of the retrogression of the ultramafic rocks using the experimentally determined phase relationships in the pure Mg-system, although this may not be entirely valid as the reactions believed to have taken place in the Lewisian rocks are not necessarily the same as those investigated in the experimental systems.

The first mineral assemblage to form (tremolite-chlorite-anthophyllite) is entirely hydrous, whilst in and near shear zones and dyke margins dolomite becomes significant in ultramafic rocks and calcite is locally abundant in mafic and intermediate rocks. This indicates an evolution of the composition of the retrogressive fluid phase with time.

Anthophyllite, which is one of the first minerals to form, is only a transitory phase. The stability of anthophyllite has received a considerable amount of attention (Greenwood, 1963, 1971; Johannes, 1969; Popp et al., 1977) partly because of its limited stability range. In the pure  $\text{MgO} - \text{SiO}_2 - \text{H}_2\text{O}$  system it is stable between 667 and 745°C at 1 kb and between about 680 - 780°C at 7 kb (Greenwood, 1963) but it is stable down to 510°C if  $\text{CO}_2$  becomes the major proportion of the fluid phase (Johannes, 1969). The presence of up to 10% of the Fe-end member is not thought to affect the temperatures greatly (Trommsdorff and Evans, 1972) as all reactions involve the fluid phase and hence have a large entropy, so small amounts of Fe-Mg substitution are unlikely to have much effect. The data of Popp et al. (1977) for (Fe,Mg) amphiboles indicate that pyroxene and olivine would react to form anthophyllite at ca 730°C at an oxygen fugacity appropriate to the QFM buffer. As mentioned above the fluid phase is thought to have been dominated by  $\text{H}_2\text{O}$  initially, so the higher temperatures are more likely. Retrogression

thus began in the temperature range 650 - 750°C . The presence of Mg-chlorite is unfortunately not diagnostic, as it is stable to pressures and temperatures in excess of those estimated for the granulite facies metamorphism (Staudigel and Shreyer, 1977). Tremolite is also stable over any likely P-T range for the retrogression. In the pure MgO - SiO<sub>2</sub> - H<sub>2</sub>O - CO<sub>2</sub> system talc is stable between 400 and 700°C at 2 kb, and to higher temperatures as pressure is increased (Johannes, 1969). There is a limited field (ca 700°C at 2 kb) where talc and anthophyllite are both stable. The lack of any serpentinisation, except as a late stage phenomenon, suggests temperatures above 480°C (Scarfe and Wyllie, 1967; Johannes, 1969), although during Laxfordian shearing P<sub>CO<sub>2</sub></sub> was high enough for serpentine to be unstable at any temperature. The carbonate phase is always dolomite rather than magnesite; this again has a wide stability range and its presence reflects the CaO content of the system rather than temperatures in excess of the magnesite breakdown temperature (ca 500°C). The possible P-T evolution of the ultramafic rocks is as follows (Fig.5.15):

- (a) metamorphism at granulite facies at a P-T of 800-900°C and 10-14 kb (Chapter 2; Savage and Sills, 1980)
- (b) beginning of retrogression with a hydrous fluid phase at 700 ± 50°C
- (c) gradual cooling and further retrogression with the fluid phase containing a greater proportion of CO<sub>2</sub>
- (d) shearing and recrystallization in Laxfordian shear zones with dolomite becoming a major phase. Some shear zone assemblages (e.g. picrite dykes) contain anthophyllite (Tarney, 1973) indicating temperatures in excess of 500°C

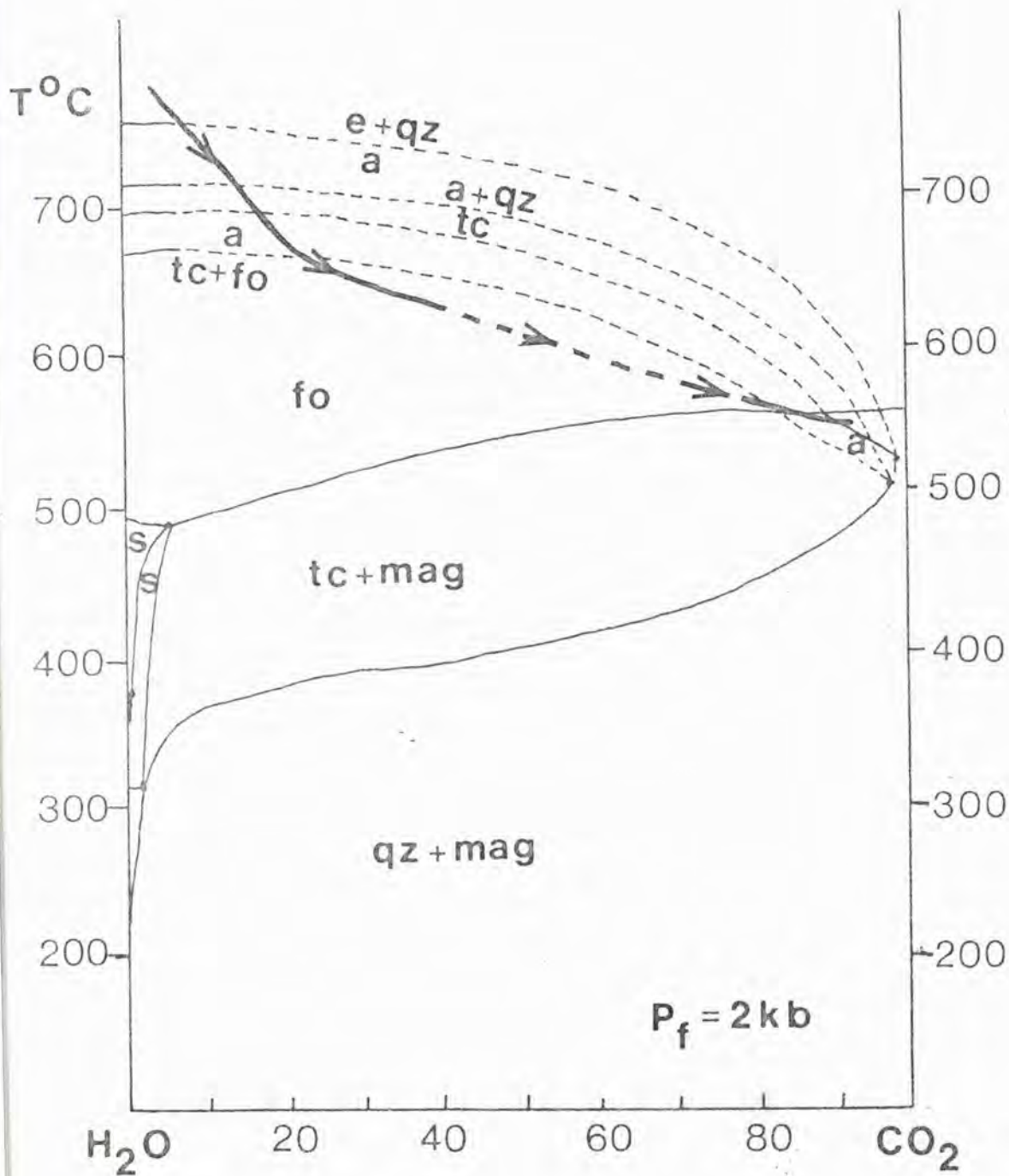


FIG. 5.15  $T^{\circ}\text{C} - X_{\text{CO}_2}$  plot after Johannes (1969) showing a possible  $T - X$  path for the retrogression of the ultramafic rocks; the dashed projection into  $\text{CO}_2$  rich fluids is based on the existence of tc-anthodol in metamorphosed picritic dykes (Tarney, 1973). e-enstatite, qz-quartz, a-anthophyllite, tc-talc, fo-forsterite, mag-magnesite, s-serpentine.

- (e) regrowth of tremolite and cummingtonite laths implying either a temperature increase or a reduction in  $P_{\text{CO}_2}$ . The pressure during retrogression is difficult to calculate but is probably in the range 5 - 8 kb.

#### Changes in whole-rock composition during retrogression

In order to make an assessment of whether the composition of the layered ultramafic rocks changed during retrogressive metamorphism, all analyses have been plotted in a CaO - MgO - SiO<sub>2</sub> (molecular) triangle with FeO added to MgO and Al<sub>2</sub>O<sub>3</sub> added to SiO<sub>2</sub> (Fig. 5.16). This diagram is not entirely suitable as Al<sub>2</sub>O<sub>3</sub> is not considered which results in meaningless crossing tie-lines. In Chapter 3, the whole-rock chemistry of the ultramafics was discussed in detail and it was shown that the ratios of immobile incompatible trace elements are more or less chondritic and that these elements retain the original characteristics of the rocks. Zr may have been increased (or Ti, Y and Sr lost) from serpentinised samples (Fig.3.10).

In Fig.5.16 the samples cluster around a line between tremolite and olivine or enstatite, the most magnesian samples plotting near serpentine, although two of these samples are serpentinites and two fairly fresh harzburgites. Three samples (W3, J101, 065, Inverian tremolite-chlorite assemblages), are slightly enriched in SiO<sub>2</sub>, but in general the granulite facies samples plot on a similar trend to the retrogressed samples.

The dominant minerals, tremolite and chlorite, must be accompanied by a more Mg-Fe rich mineral as all samples plot below the tremolite-chlorite join (Fig.5.16). Most samples have trace amounts of dolomite with magnetite up to 5 modal %. In shear zones dolomite is a major

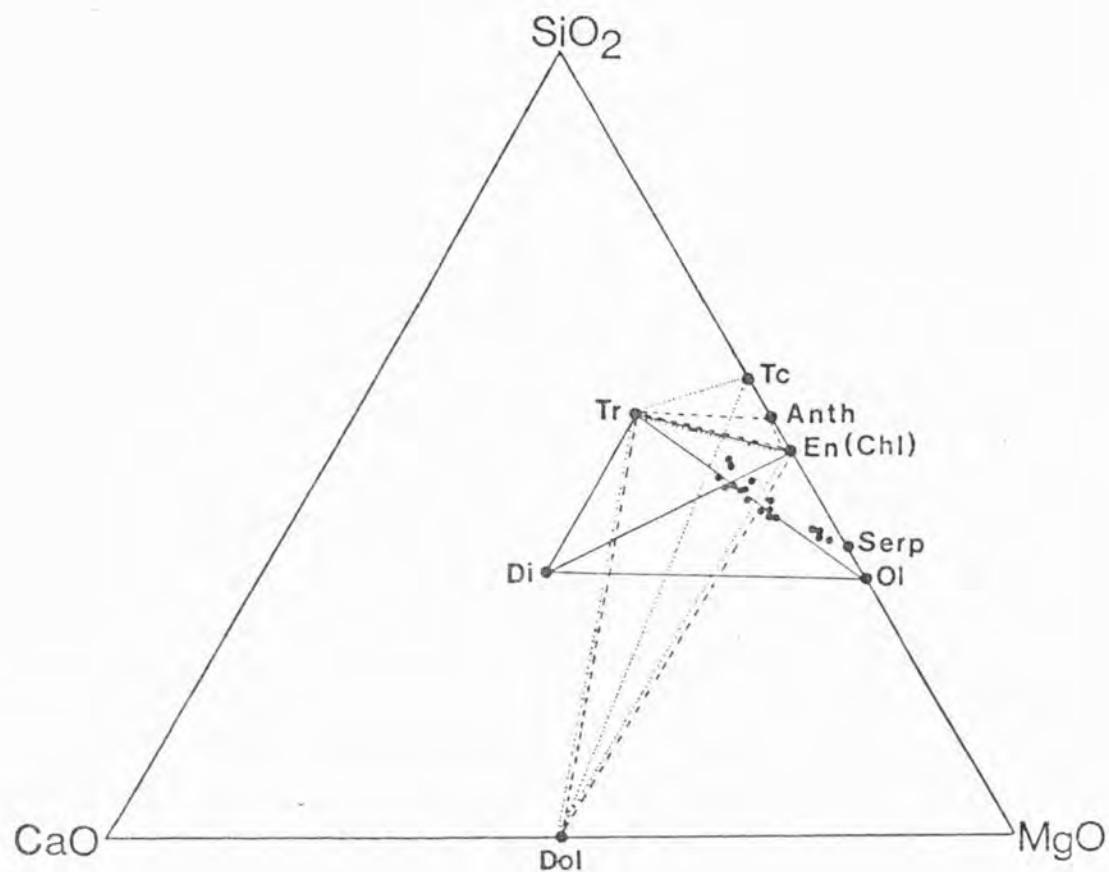


FIG. 5.16  $\text{CaO-SiO}_2\text{-MgO}$  triangle for ultramafic rocks.

Solid tie-lines are for granulite facies assemblages, dashed tie-lines are for Inverian assemblages and dotted tie-lines are for shear zone assemblages. Dol-dolomite, Di-clinopyroxene, Ol-olivine, serp-serpentine, En-orthopyroxene, chl-chlorite, anth-anthophyllite, tc-talc and tr-tremolite.

phase, being required to take  $\text{CO}_2$  but also Ca and Mg to retain the overall composition. Most granulite facies samples plot in the talc-dolomite-chlorite field, therefore no major changes in whole-rock chemistry are required to develop these assemblages. However all retrogressed assemblages have very low Na + K contents when compared with granulite facies rocks. In the granulite facies, Na + K is held in pargasite, whilst the Inverian amphibole, tremolite, has a very low alkali content. Na + K must therefore be lost from the ultramafic rocks during retrogression, but they need not have been totally removed as all other rock types seem to have gained Na during retrogression. The gabbros which are commonly associated with the ultramafics have often gained Na in hornblende and a more albitic plagioclase. Serpentinised samples may have lost Ca.

In conclusion, apart from the loss of alkalis and the gain of  $\text{H}_2\text{O}$  and  $\text{CO}_2$ , the whole-rock chemistry has not changed significantly from the granulite facies event to the development of Inverian retrogressed assemblages. Some silica may be lost during Laxfordian shearing.

#### 5.6. P - T CONDITIONS DURING RETROGRESSION

One of the aims of this study was to attempt to produce a P-T-time path for the evolution of the Lewisian complex in the Assynt region. The process of retrogression took place over a protracted period, starting prior to the intrusion of the Scourie dykes, through the metamorphism of the dykes to localised recrystallization in Laxfordian shear zones. One of the problems in constructing the P-T-time path is that similar metamorphic assemblages were formed at all stages and it is not always possible to determine the time that any

particular assemblage developed. It is also difficult to obtain precise temperature and pressure estimates because the variance of most assemblages is high ( $> 3$ ) and hence one needs to determine a large number of variables notably;  $P$ ,  $T$ ,  $P_{H_2O}$ ,  $P_{CO_2}$  and  $f_{O_2}$  as well as knowing the composition of the mineral phases (i.e. the Fe/Mg ratio of mafic phases and the An/Ab ratio of plagioclase). The main components of the Inverian mineral assemblages are micas, amphiboles and chlorite which have very poorly defined thermodynamic properties.

The Fe-Mg exchange equilibrium between garnet and biotite (Section 5.4) suggests temperatures between 475 and 675°C for the blocking of this exchange reaction. The formation of anthophyllite as an early phase in the retrogression of ultramafic rocks suggests temperatures of 675 - 750°C for the onset of retrogression. From a detailed study of composite ilmenite-magnetite grains, Rollinson (1980) has suggested that the introduction of a fluid phase, indicated by an increase in oxygen fugacity, occurred between 660 and 530°C. This range is compatible with the stability fields of the ultramafic assemblages (Section 5.5). Various phase equilibrium studies, both experimental and theoretical, can however place some limits on the P-T conditions. A diagram of the various relevant equilibria and a possible P-T path is presented in Fig.5.17.

#### Coexisting garnet and hornblende

It has been suggested (Saxena, 1968) that the Fe-Mg exchange equilibrium between garnet and hornblende is temperature dependent and Wells (1979a) has extracted the relevant thermodynamic data, from experimental studies, for the reaction:

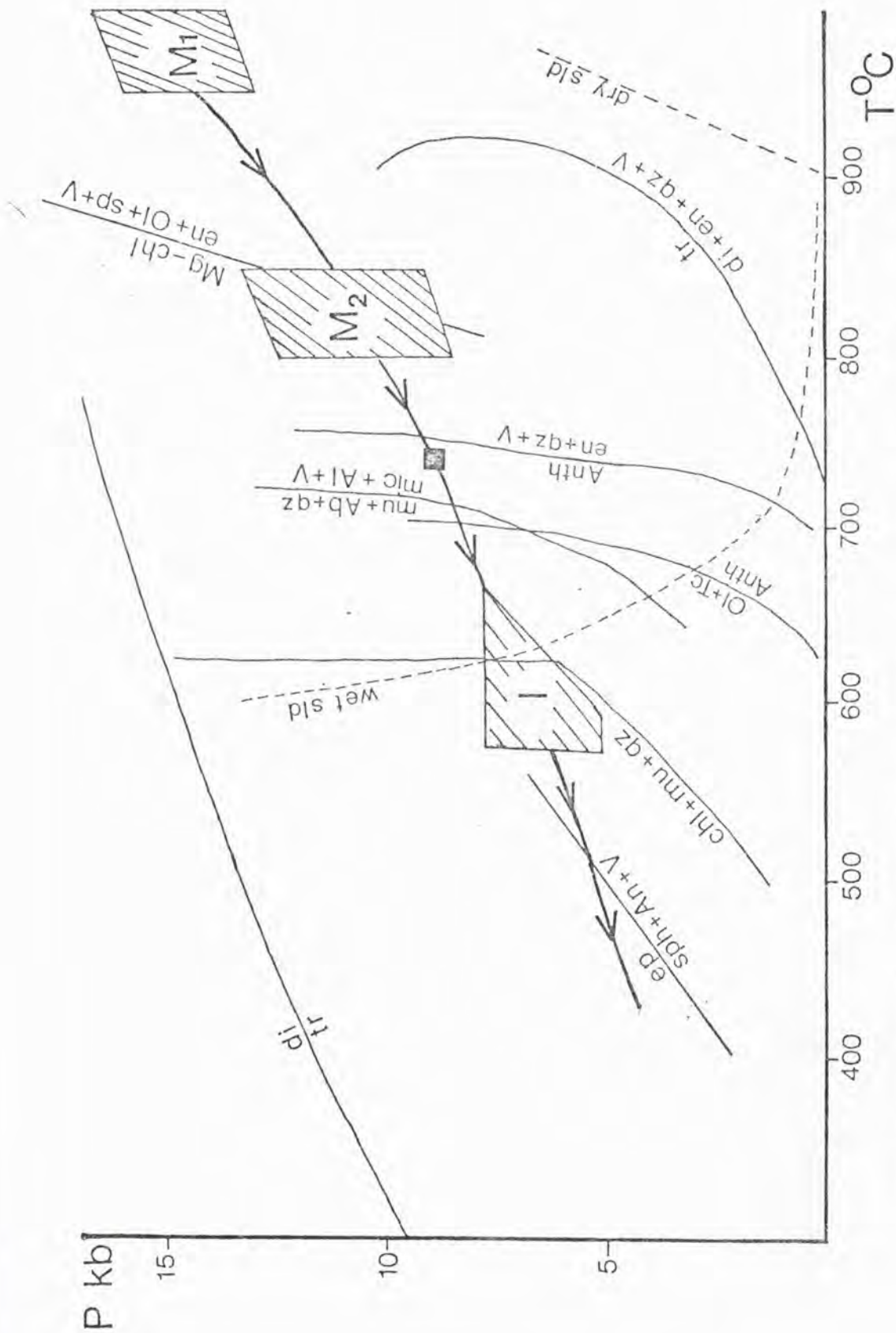
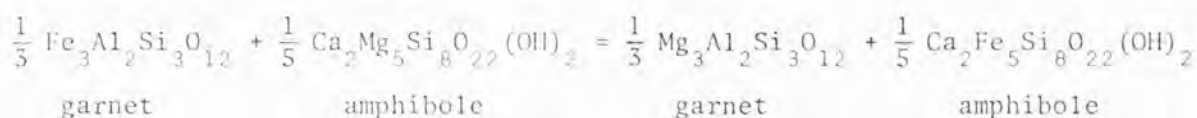


FIG. 5.17 Possible P-T path for the uplift of the Assynt gneisses.  $M_1$  and  $M_2$  are from Chapter 2. I - is the possible field for retrogression. The wet and dry granite minimum melting curves are from Winckler (1976). The remaining equilibria are discussed in the text.



Assuming an ideal mixing on-sites model for both garnet and hornblende (this is reasonable for garnets with less than 30% grossular; Wood, 1977), all samples with the exception of J96, give temperatures between 600°C and 650°C. These estimates are best  $\pm 50^\circ\text{C}$  because of the large extrapolation between tremolite-ferroactinolite and tschermakitic-hornblende. Some garnets have significant Mn (>Mg) which is not accounted for in the calculations. Sample J96 has garnets of two compositions, one Ca poor and one with a normal Ca content (20% grossular), which give temperatures between 650 and 750°C, consistent with the presence of anthophyllite in this rock.

#### Feldspar thermometry

A few trondjhemite and granite gneisses contain both sodic and potassic feldspar, but in the Assynt region there is no development of the complex perthites described by Rollinson (1978) for discordant granitic sheets in the Scourie area. Coexisting feldspar pairs have been analysed from two samples, J8 a trondjhemitic gneiss underlying the Rheidh Phort amphibolite mass and from J100, a peculiar quartz-free rock with the assemblage; plag - micr - amph - ep. In sample J100, analyses were performed by scanning across the grain to obtain an estimate of the pre-exsolution composition. It was not possible to analyse the exsolution lamellae as they were too small. In J8 there are no perthites, just homogeneous microcline and plagioclase grains. Temperatures and details are given in Table 5.12.

The equation of Stormer (1975) uses margules parameters calculated

Sample	Plag	Micr	T <sub>1</sub>		T <sub>2</sub>		T <sub>3</sub>		T <sub>4</sub>	
			5kb	10kb	5kb	10kb	5kb	10kb	5kb	10kb
J100	19	88	474	525	522	573	459	509	509	560
J100	19	92	404	450	450	497	389	434	438	484
J100	5	93	369	413	417	462	357	400	407	451
J100	5	78	541	597	610	668	525	579	594	651
J100	17	93	395	441	441	488	382	427	431	477
J100	22	78	581	640	645	706	541	596	606	663
(homog) J100	22	86	500	553	549	603	479	528	529	581
(homog) J8	16	95	370	414	418	462	368	412	418	462
J8	16	89	479	531	528	580	477	528	528	580
J8	2	95	351	393	399	443	349	391	399	443

TABLE 5.12. Feldspar temperatures °C calculated at 5 and 10 kb using the following methods:-

T<sub>1</sub> - equation of Stormer(1975)

T<sub>2</sub> - equation of Whitney and Stormer(1977)

T<sub>3</sub> - equation of Powell and Powell(1977)

T<sub>4</sub> - equation of Powell and Powell(1977) modified by Rollinson(1978).

Plag and micr are the An content of plagioclase and the  $KAlSi_3O_8$  content of microcline respectively. homog - scan analysis of grain to obtain composition prior to exsolution.

for the high-albite-sanidine solvus ( $T_1$ ), whereas Whitney and Stormer (1977) use margules parameters based on the low-albite-maximum microcline solvus ( $T_2$ ) and is therefore more applicable to slow cooling plutonic complexes, such as the Lewisian. Powell and Powell (1977) make allowance for the anorthite content of the alkali feldspar ( $T_3$ ) and their equation has been modified (Rollinson, 1978) incorporating thermodynamic data for the more ordered feldspars ( $T_4$ ); for full details of the theoretical background to feldspar thermometry see Rollinson (1978). Temperatures have been calculated for 5 and 10 kb (Table 5.12); the likely pressure for the retrogression being somewhere in between. The analysed grains are microcline (with cross-hatch twinning) so the data for the more ordered feldspars is applicable. Temperatures for the homogenised grains in sample J100 range from 529-645°C at 5 kb to 581-706°C at 10 kb. If the feldspars are disordered the equilibration temperatures are slightly lower. The uniform granular feldspars of sample J8 equilibrated down to 400°C.

Although these data are rather sparse, they again indicate temperatures of the order of 600°C for the retrogression.

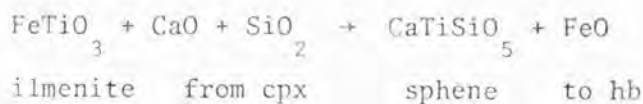
#### Stability of epidote

During progressive metamorphism, actinolite-albite-epidote assemblages are replaced by hornblende-labradorite; however in the Lewisian samples epidote grew at the same time as tschermakitic hornblende. In samples with a lot of epidote, there is a tendency for the amphiboles to have a lower Al content than in epidote poor samples (Si is ca 7 atoms per formula unit compared with 6.4), but the amphibole is always hornblende rather than actinolite. As demonstrated earlier, epidote develops when there is excess Ca produced from the breakdown of clinopyroxene to form hornblende. When there is complete

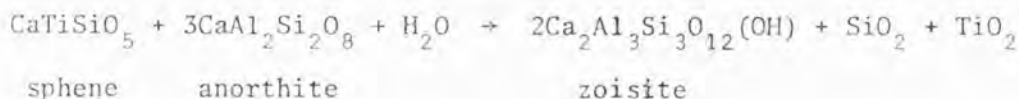
recrystallization and equilibrium is reached on a wider scale, epidote tends to disappear. This may reflect a slight increase in temperature in shear zones or may be solely due to the disappearance of a disequilibrium assemblage. Experimental studies in the  $\text{CaO} - \text{SiO}_2 - \text{Al}_2\text{O}_3 - \text{H}_2\text{O}$  system by Perkins et al. (1980) show that zoisite breaks down at  $800^\circ\text{C}$  at 6 kb, and is stable down to  $200^\circ\text{C}$ . Liou (1973) showed that the stability and composition of epidote depends on  $f\text{O}_2$  as well as temperature, the  $\text{Fe}^{3+}$  content increasing with  $f\text{O}_2$ . The composition of the Lewisian epidotes (Ps 15-24) suggests equilibration at or slightly below the NNO buffer (Liou, 1973) which is consistent with the ilmenite-magnetite data of Rollinson (1980). Liou (1973) suggests that at this  $f\text{O}_2$ , epidote of the composition  $\text{Ps}_{25}$  is stable up to  $650^\circ\text{C}$  at 5 kb.

#### Stability of sphene

The formation of amphibole and epidote from clinopyroxene is accompanied by the development of sphene coronas around ilmenite and more rarely rutile. Occasionally the sphene is itself rimmed by epidote. The stability of sphene has recently been studied by Hunt and Kerrick (1977) who show that the assemblage sphene + tremolite is stable over a wide T- $\text{XCO}_2$  space. Possible reactions to produce these coronas are:



and

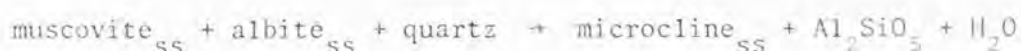


The latter reaction occurs at  $500^\circ\text{C}$  at 5 kb and  $430^\circ\text{C}$  at 3 kb with  $\text{XCO}_2 < 0.2$ . The assemblage tremolite + sphene breaks down to diopside + rutile + quartz +  $\text{H}_2\text{O}$  at temperatures above  $650^\circ\text{C}$  (Hunt and Kerrick, 1977).

### Stability of muscovite and quartz

Muscovite occurs locally in a few trondjhemitic and granitic gneisses, generally replacing feldspar but occasionally biotite. It occurs as large flakes cross-cutting the foliation defined by biotite and quartz lenses and the shear zone fabric, indicating that it grew at a late stage in the evolution of the complex. Several studies have been made on the upper stability of muscovite and quartz (Kerrick, 1972; Day, 1973; Thompson, 1974; Chatterjee and Froese, 1975) all giving similar results.

The reaction



is located at 705°C at 7 kb and 660°C at 5 kb (Chatterjee and Froese, 1975), which is in agreement with the thermodynamic data of Thompson (1974). The presence of significant amounts of  $\text{CO}_2$  in the fluid phase will lower this temperature; e.g. if  $X_{\text{CO}_2} = 0.5$  the reaction temperature is lowered by 100°C (Kerrick, 1972). The muscovite composition (paragonite 2 - 6%, 20 - 25% of the octahedral sites filled with  $\text{Mg} + \text{Fe}^{2+} + \text{Fe}^{3+}$ ) suggests it formed at temperatures lower than this maximum. Velde (1967) states that the  $\text{Si}^{4+}$  content of muscovite (an indication of the phengite content) is temperature dependent and his data imply temperatures in the range 550 - 650°C for pressures of 5 - 7 kb, indicating that they were still above 500°C at the end of deformation, when the muscovite developed.

### Stability of chlorite

Mg-chlorite is stable to pressures and temperatures in excess of any likely P-T conditions for the Inverian retrogression (Staudigel and

Shreyer, 1977), but the stability of Fe-Mg chlorite is more restricted. The assemblage Mg-chlorite + muscovite breaks down at ca 650°C at pressures of 5 - 7 kb (Bird and Fawcett, 1973); Fe-Mg chlorite may break down at a slightly lower temperature.

Although there is no reliable thermochemical method to estimate the P-T conditions during Inverian retrogression and Laxfordian shearing, all the evidence suggests that the retrogression took place at temperatures between 550 and 650°C and that the complex was held at above 500°C for the whole period. There may have been a slight increase in temperature after the end of the Inverian during Laxfordian shearing to account for the reduction in the amount of epidote and for the growth of anthophyllite in ultramafic Scourie dykes (Tarney, 1973). Pressures were probably between 5 and 8 kb. There is no evidence of partial melting associated with Inverian events, other than a few intrusive pegmatites (Evans and Lambert, 1974) which give a variety of ages but are post-Scourian and pre-dyke. If  $P_{\text{H}_2\text{O}} = P_{\text{TOT}}$  temperatures were less than the minimum granite melting curve, i.e. 660°C at pressures of ca 6 kb (Fig. 5.17). Prior to the intrusion of the Scourie dykes, the fluid phase was dominantly water, but during Laxfordian shearing high  $\text{CO}_2$  pressures built up locally with the development of dolomite in ultramafic rocks and calcite in rocks of mafic and intermediate compositions. Scapolite (Cl 0.4 - 0.6 wt.%, S below MDL) forms locally, adjacent to shear zones and dyke margins, replacing plagioclase showing that the fluid phase contained Cl as well as  $\text{H}_2\text{O}$  and  $\text{CO}_2$ . This scapolite contrasts with that found in a granulite facies mafic rock near Scourie which has 2.5% sulphur and no Cl (Rollinson, 1980b). The influx of retrogressing fluids caused an increase in the oxygen fugacity (Rollinson, 1980), and haematite may form in some assemblages in or near shear zones. The assemblage K - fsp - magt - biotite may be used to define  $P_{\text{H}_2\text{O}}$  (Wones and Eugster, 1965). This assemblage occurs in sample J8; however the uncertainty in

$fO_2$  and  $T$  are too large for meaningful results to be obtained. Using  $fO_2$  from Rollinson (1980) and a temperature of  $600^\circ\text{C}$ ,  $P_{\text{H}_2\text{O}}$  of 3.4 kb is derived, but altering  $fO_2$  by 1 log unit causes  $P_{\text{H}_2\text{O}}$  to alter by a factor of 2.

#### 5.7. POSSIBLE CHANGES IN WHOLE-ROCK CHEMISTRY DURING RETROGRESSION

In the Lochinver area retrogression took place in two main stages: first, amphibolitisation of granulites associated with NW trending Inverian monoclinial folds, and second recrystallization of Inverian gneisses with extreme attenuation of banding in Laxfordian shear zones. The development of new mineral assemblages took place during the first episode. The gneisses were often completely amphibolitised prior to the intrusion of the Scourie dykes. The time interval between retrogression and dyke intrusion is unknown but it is probably fairly short, as dyke intrusion and retrogression in NW trending steep belts are both part of the Inverian event (see Chapter 1).

Average analyses of 145 retrogressed gneisses and 52 shear zone gneisses are virtually identical (Sheraton et al., 1973a) but there is a considerable difference between these and their average granulite; notably higher Na and Si and lower Fe and Ca in the retrogressed samples. However this probably reflects a sampling problem rather than a real chemical change as mafic rocks retain their granulite assemblages longer than intermediate and acid gneisses, hence the granulite facies population of Sheraton et al. (1973a) is probably biased towards mafic rock types. Beach (1974a, 1976, 1980) has shown from a study of mineral reactions and whole rock chemistry that the gneisses from shear zones near Scourie are enriched in Na, K and  $\text{H}_2\text{O}$  and have lost Ca, Fe and possibly Si during shearing. The Assynt shear zones are

not greatly enriched in K because there is not the development of large amounts of biotite as at Scourie. To examine possible changes in whole-rock chemistry it is necessary to be able to trace a particular rock unit from the granulite facies into a shear zone. Unfortunately this is not possible in Assynt as shear zones cut previously retrogressed rocks that have not suffered notable deformation, and it is not possible to trace a specific horizon from the granulite facies to a retrogressed assemblage into a shear zone. However it is possible to analyse a range of compositions from all three metamorphic zones and compare the trends to see whether there are any systematic changes which could have been brought about by the retrogression. The considerable increase in correlation between major element pairs (Beach and Tarney, 1978) clearly reflects mobility of ions on a scale of a few metres, but it does not show whether there has been a net loss or a net gain of any elements by the complex as a whole.

For this study mafic rocks from the granulite facies, Inverian retrogressed assemblages and from Laxfordian shear zones have been analysed to examine whether there has been a change in composition. This cannot be achieved for intermediate and acid gneisses due to the rarity of granulites in the Assynt area. Various elements are plotted against MgO (Fig.5.18); showing the following:

(1) The CaO and  $\text{Fe}_{23}^{\text{(total iron)}}$  contents of granulite facies and amphibolite facies rocks are indistinguishable; so if Ca has been lost as suggested by Beach (1974a, 1976, 1980) the amount lost is not sufficient to show up in the major element analysis. Beach partially based his conclusion on the fact that all reactions produce excess Ca and there is no new Ca-bearing phase in the Scourie shear zones; however in Assynt there is the development of epidote in mafic and intermediate rocks.

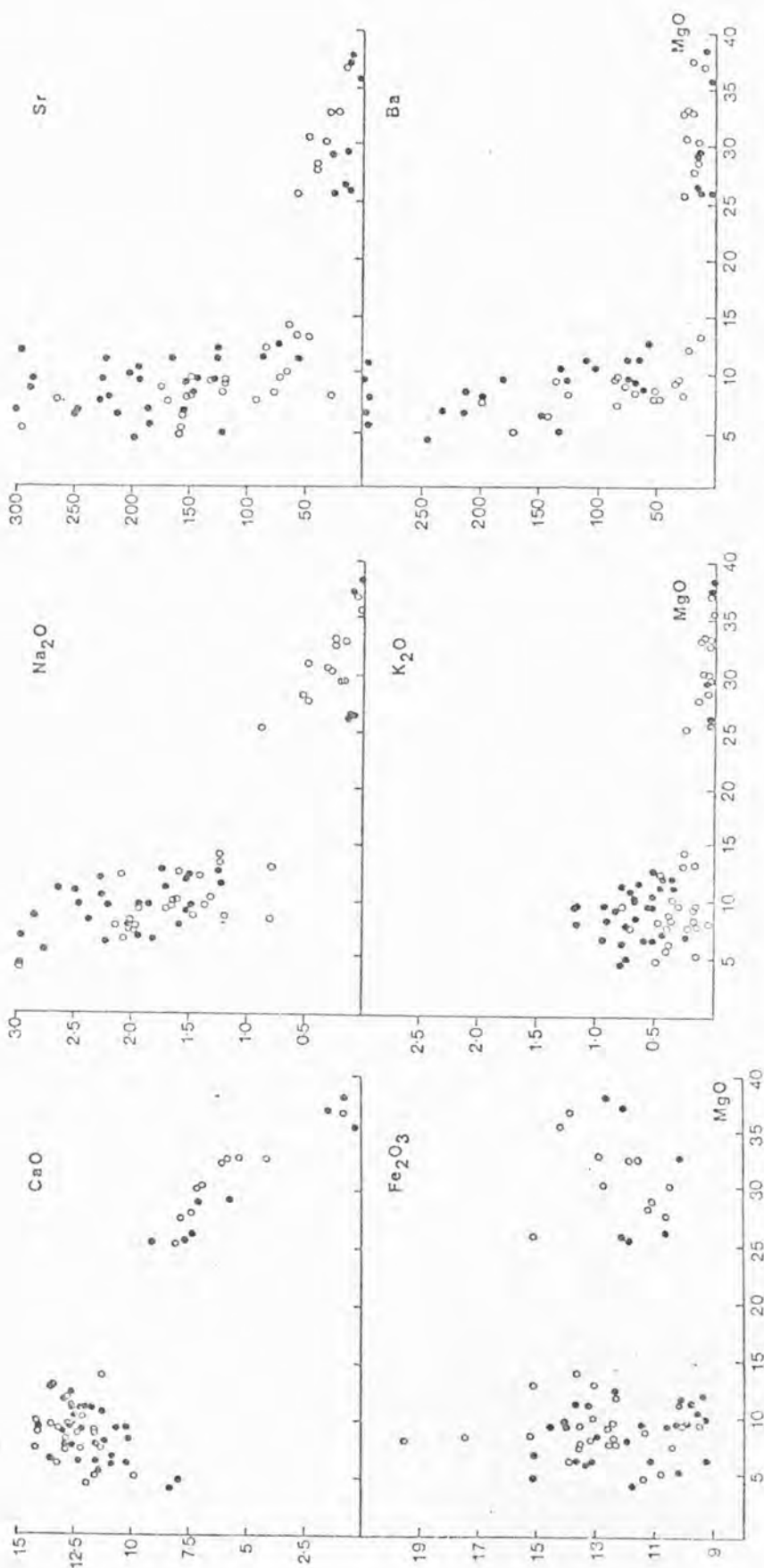


FIG. 5.18 CaO, Fe<sub>2</sub>O<sub>3</sub>, Na<sub>2</sub>O, K<sub>2</sub>O, Sr and Ba versus MgO for mafic and ultramafic rocks. Open circles are granulite facies samples, filled circles amphibolite facies.

(2) Retrogressed mafic rocks tend to have higher Na, K, Sr, Ba and Rb contents when compared with granulites, although there is some overlap. These elements all have higher concentrations in the bordering tonalitic gneisses so their increase may merely reflect a movement from high to low concentrations during retrogression.

(3) Similar plots for Zr and  $TiO_2$  show no difference between granulite and amphibolite facies rocks.

It is usually more instructive to compare element ratios rather than absolute abundances. Drury (1974) has shown that retrogressed mafic rocks on Coll and Tiree show an increase in K, Rb, Pb, K/Ba, and Rb/Sr with a decrease in K/Rb and Ba/Pb. Rb increases markedly in retrogressed Assynt samples with a concomitant decrease in K/Rb.

K/Rb ratios of ultramafic rocks are fairly constant. The K/Ba ratios are rather variable and show no systematic change, with most retrogressed samples having similar ratios to the granulites and a few having higher ratios. Similarly Rb/Sr ratios are very variable. As K, Rb, Sr and Ba have all probably moved during retrogression, the elements which may have been removed from or gained by the complex as a whole have been compared with Zr, an element which is relatively immobile during metamorphism. Various plots are shown in Fig.5.19. There is a good deal of scatter on all plots due in part to the fact that nearly all granulite facies mafic rocks show some replacement of pyroxene by hornblende. As a control it is seen that  $TiO_2/Zr$  is constant for granulite and amphibolite facies mafic rocks, whereas Sr/Zr and  $Na_2O/Zr$  tend to be higher in retrogressed rocks although there is considerable overlap. Some low Zr samples have high Sr/Zr and  $Na_2O/Zr$  ratios, possibly due to inaccuracies in the Zr value. The Sr/Zr and  $Na_2O/Zr$  ratios

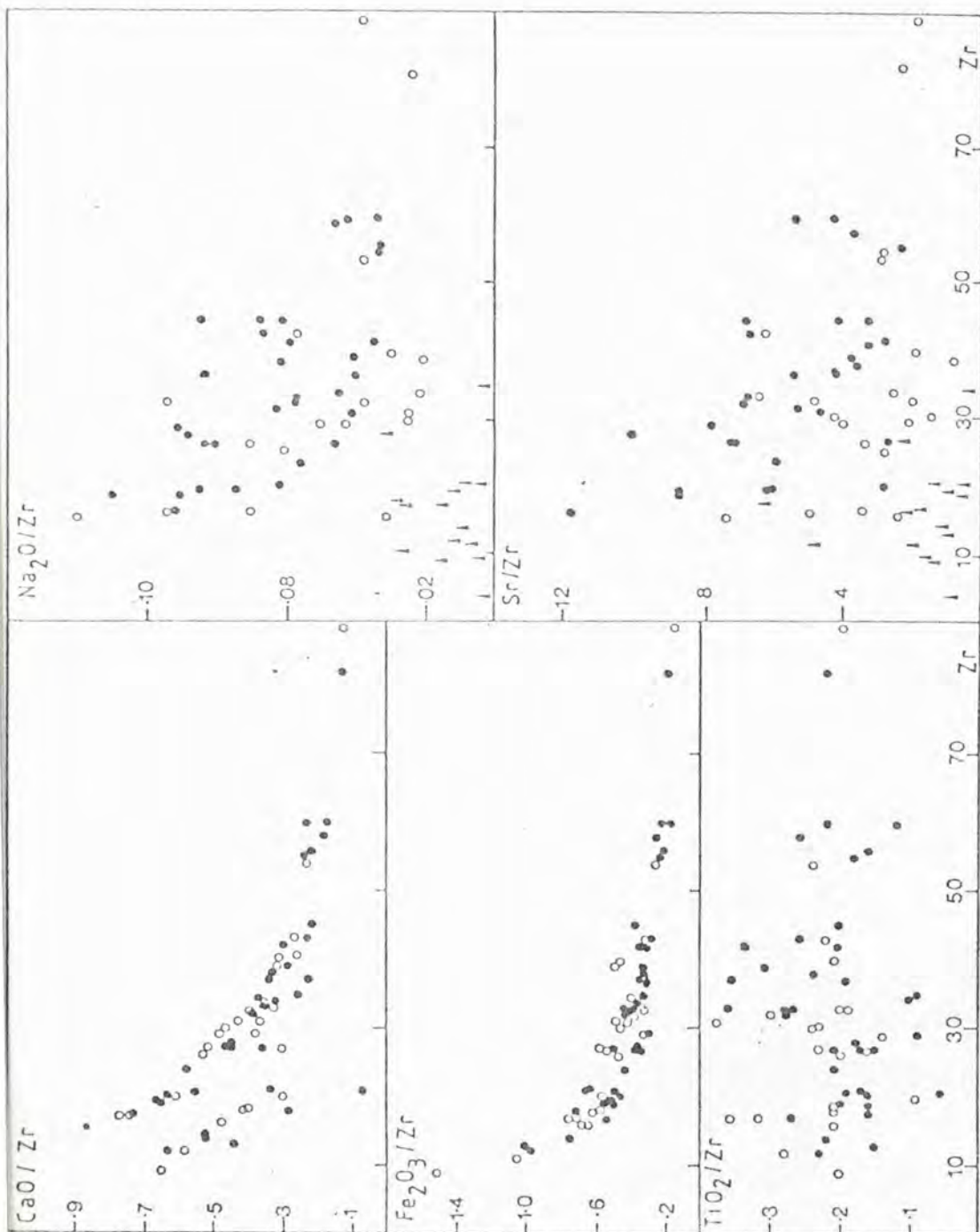


FIG. 5.19 CaO/Zr, Fe<sub>2</sub>O<sub>3</sub>/Zr, TiO<sub>2</sub>/Zr, Sr/Zr and Na<sub>2</sub>O/Zr for mafic and ultramafic rocks. Open symbols-granulite facies, filled symbols-amphibolite facies. In the Na and Sr plots, ultramafic rocks are shown by triangles, mafic rocks by circles.

decrease during retrogression of ultramafic samples indicating the loss of alkalis already mentioned. The  $\text{CaO/Zr}$  and  $\text{Fe}_2\text{O}_3/\text{Zr}$  ratios are similar for both groups.

This discussion shows that the composition of the mafic rocks has changed slightly during retrogression, mainly an increase in LIL elements; this may reflect a re-equilibration between different components of the complex rather than a net gain. However the decrease in anorthite content of plagioclase from intermediate composition gneisses, together with the formation of hornblende from pyroxene, implies a net gain of Na as suggested by Beach (1974a, 1976, 1980). The main chemical changes are then the gain of  $\text{H}_2\text{O}$ ,  $\text{CO}_2$ , Na and possibly the loss of some Ca; ultramafic rocks have lost Na, K, Sr, and Ba, but there is insufficient ultramafic rock in the Lewisian to provide enough Na to metasomatise the tonalites.

#### 5.8. DISCUSSION

Granulite facies gneisses were altered to amphibolite facies gneisses, mostly prior to the intrusion of the Scourie dykes; further retrogression occurred in which the dykes were involved with final, localised recrystallization in Laxfordian shear zones. A fairly uniform hornblende-plagioclase  $\pm$  quartz assemblage developed, with some biotite, especially in shear zones, but the introduction of potash was much less than in shear zones further north at Scourie (Beach, 1973). The uniform assemblage caused an increase in correlation of major element pairs (Beach and Tarney, 1978). The hornblende and biotite compositions (with the exception of  $\text{TiO}_2$ ) depend mainly on whole rock composition and to a lesser extent on paragenesis. The mineral assemblages indicate retrogression on a falling temperature path from about  $750^\circ\text{C}$  with temperatures still above  $500^\circ\text{C}$  at the end of deformation, indicated by the

presence of post-tectonic muscovite. Precise estimate of the P-T-X conditions is impossible because of the high variance of the assemblages.

There were no significant changes in whole rock composition, apart from the addition of  $H_2O$  and locally  $CO_2$ . However most reactions producing the Inverian mineral assemblages produce excess Ca, most of which is accommodated in epidote and sphene, but some may be lost to the fluid phase as suggested by Beach (1974a, 1976, 1980). There may also be a net gain of Na, and possibly K in shear zones, with a redistribution of LIL elements between the various components of the complex. The mineral data presented here suggest that most of the changes occurred during the Inverian and that Laxfordian events just emphasised these changes.

The formation of hornblende from pyroxene with the development of epidote and sphene coronas indicates that ions diffused on a scale of a few millimetres. The data of Beach and Tarney (1978) imply diffusion over much larger distances, perhaps as much as a few metres. Korzhinskii (1970) distinguished between two types of metasomatic process:

- (1) diffusion metasomatism, where ions and ionic complexes diffuse through a static pore fluid system, and
- (2) infiltration metasomatism, in which an aqueous fluid, carrying dissolved ions and ionic complexes, moves through a rock.

The latter process can obviously carry ions over much larger distances more quickly than diffusion. The redistribution of Ca in the formation of hornblende, sphene and epidote from clinopyroxene and plagioclase may have occurred by diffusion. However, if Na was gained by the complex as a whole, this presumably occurred by infiltration metasomatism.

It is interesting to speculate whether the water which was obviously present existed as a true fluid phase i.e. potentially mechanically separable from the solid phases, or whether it occurred as aqueous ions adsorbed onto grain boundaries. The second case allows  $P_f$  to be less than  $P_{TOT}$  and is likely to be the case during granulite facies conditions. However during the Inverian the following factors suggest that water probably existed as a true fluid phase:

(1) the complete alteration of a mafic granulite to an amphibolite facies assemblage requires the addition of a large amount of water; e.g. a rock with 70% hornblende indicates about 2.8 g of water per 100 g of rock and even in the intermediate gneisses which make up the bulk of the complex, 0.5 g of water per 100 g of rock is required (Beach, 1980)

(2) the large area over which the rocks have been retrogressed e.g. in the Drumbeg area intermediate composition rocks are retrogressed tens of metres from any vertical structure. Diffusion of  $(OH)^-$  and  $H^+$  ions over this distance would take a long time

(3) if excess water were available, the fluid phase may have the capacity to buffer the oxidation state of minerals. Beach and Tarney (1978) show that the retrogressed Assynt gneisses have a uniform  $Fe^{3+}/Fe^{2+}$  ratio suggesting that this buffering has occurred.

As a result of the above discussion, it is believed that water was present as a true fluid phase and that  $P_f = P_{TOT}$ . During the early stages of retrogression, when thin actinolite rims developed around pyroxene,  $P_f$  was probably less than  $P_{TOT}$ .

In Inverian assemblages hydrous phases predominate with only minor carbonate. In Laxfordian shear zones and near dyke margins carbonate may be locally abundant with minor replacement of plagioclase by a  $\text{Cl} - \text{CO}_2 - \text{H}_2\text{O}$  scapolite. This indicates that  $\text{CO}_2$  became a significant component of the fluid phase in the late shear zones. If mixed volatile reactions occur (i.e. reactions which involve both  $\text{H}_2\text{O}$  and  $\text{CO}_2$ , such as those to produce the *tc - trem - chl - dol* assemblages) the fluid composition may be buffered so that  $\text{CO}_2$  builds up with time (Kerrick, 1974). This may have happened in Assynt with early fluids being dominantly water, with a local build up of  $\text{CO}_2$ .

In conclusion the retrogression was caused by the influx of large volumes of water, locally buffered to produce  $\text{CO}_2$ -rich compositions, which enabled ions to be redistributed over large distances. The influx of this fluid caused an increase in  $f\text{O}_2$  (Rollinson, 1980). The retrogression was intimately associated with the formation of NW-trending structures which acted as channels for the fluids (Chapter 1). The source of fluids is uncertain, but the large volumes required are probably in excess of that which could be generated by the degassing of lower crustal granulites, so it is presumed that the fluids were mantle derived. The large scale chemical re-equilibration that took place during retrogression apparently did not occur during prograde metamorphism to produce the granulites (apart from the loss of K, Rb, Th and U; Sheraton et al., 1973a). As progressive and retrogressive metamorphism both involve a fluid phase it is thought that the precursors of the gneisses were originally metamorphosed directly into the granulite facies and never went through a progressive phase, as suggested by Beach and Tarney (1978). This is consistent with the idea of Spooner and Fairbairn (1970) that gneissic precursors were intruded into the lower crust and immediately adopted a granulite facies mineralogy.

The retrogression of Archaean granulite facies gneisses in the early Proterozoic has been reported from a number of areas (e.g. Watson, 1973; Bridgewater et al., 1973). It may be related in time to the intrusion of voluminous tholeiitic dyke swarms such as the Scourie dykes and the Kangâmiut swarm in West Greenland (Escher et al., 1976). These dykes have primary hydrous phases (Windley, 1969). In the Lewisian the influx of hydrous fluids slightly predates but overlaps the period of dyke activity.

A study of the geochemistry of the Scourie dykes (Weaver and Tarney, in prep.) suggests that the source mantle was enriched in LIL elements, this enrichment occurring either just prior to melting or during the genesis of the gneisses themselves. The dykes are mainly quartz-tholeiites and contain primary hydrous phases, both factors suggesting a role for water in their genesis (Weaver and Tarney, in prep.). It is interesting that the production of the Scourie dykes was shortly preceded by the influx of large volumes of hydrous fluids up vertical structures into the crust. It seems possible that the two processes were related.

The reason for the development of early Proterozoic dyke swarms is poorly understood, but these dykes are present in most cratons. In some cases it appears to be the last stage in the stabilisation of the Archaean crustal segment and is possibly related to a failed attempt at continental rifting. They could possibly be feeders to a continental flood basalt province. The cause of the influx of the fluid which may have triggered the generation of basaltic magma is uncertain; it could be:

(1) a hot spot process whereby an upwelling mantle diapir or convection cell brought up fluids which caused the retrogression and the lowering of the mantle solidus so that the tholeiitic liquids were generated.

(2) a subduction process. Fyfe and McBirney (1975) state that the first fluids formed by dehydration of the downgoing slab will be enriched in Na and Sr and depleted in Fe. These fluids would be appropriate to the retrogression of the Assynt gneisses as suggested by Beach and Tarney (1978). Further dehydration at greater depths may provide the fluids needed for the production of the dykes. The retrogression is closely associated with deformation of the crust. However there is no evidence for subduction in the Lewisian during the early Proterozoic.

In summary the retrogression was caused by the influx of large volumes of mantle-derived hydrous fluids but the reason for their genesis is unclear. However it is a widespread phenomenon in the early Proterozoic and may be related to lower crustal processes in general, or may be a feature of the stabilisation of continental crust which has not been repeated since.

CHAPTER 6  
DESCRIPTION AND PETROGENESIS OF AMPHIBOLITE DYKES  
FROM CLASHNESSIE BAY

## 6.1. INTRODUCTION

Several thin amphibolite dykes crop out in Clashnessie Bay. The age of these dykes is problematical as they have a different trend to the Scourie dyke swarm. In this chapter they will be described, an assessment of their age made and their chemistry discussed.

## 6.2. DESCRIPTION AND FIELD RELATIONSHIPS

Five thin (up to 2 m thick) amphibolite dykes crop out on the east side of Clashnessie Bay (065316) and one on the west side (058316). The dykes are clearly discordant (Fig.6.1a) cutting low deformation, amphibolite facies tonalitic to granodioritic gneiss, which contains numerous hornblendite lenses (analyses of the gneisses and ultramafic lenses are given in Appendix B). The dykes trend  $082/45S$  and can be followed along strike for 150 m when they disappear into the sea. The dyke on the west side of the bay could be a continuation of the eastern dykes. To the west the gneisses are overlain by the Torridonian sandstone. Photographs and sketch plans of the dykes are given in Figs.6.1 and 6.2. The trend of the dykes is cut by a well foliated ultramafic Scourie dyke, striking  $117^\circ$ , which crops out in Clashnessie Bay and a fairly unmetamorphosed Scourie dolerite dyke is found about 500 m to the east. As shown in Figs.6.1b and 6.2 there is some evidence that the dykes are folded. They are moderately well foliated with an assemblage of plag - hb - qz - bi - ep - opq. They are homogeneous with no signs of a chilled margin or a decrease in grain size towards the margins.

There are several differences which serve to distinguish these dykes from Scourie dykes. Scourie dykes vary considerably in width from less than a metre wide to up to 50 m (occasionally even wider). The

FIG. 6.1(a) Photograph showing discordant amphibolite dykes, E. side of Clashnessie Bay (65316).

FIG. 6.1(b) Photograph of amphibolite dyke, E. side of Clashnessie Bay. This dyke is possibly folded and contains gneiss inclusions and small folded quartz veins.



a



b

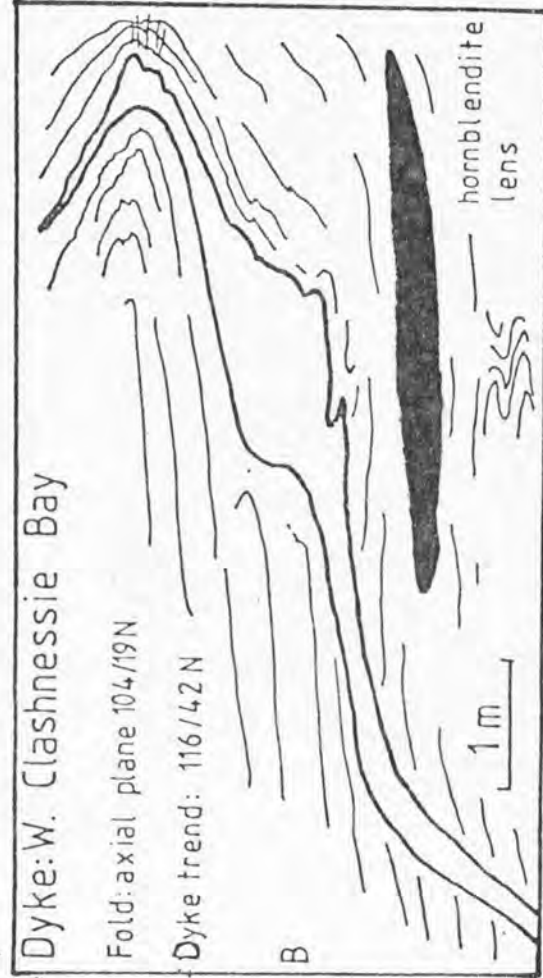
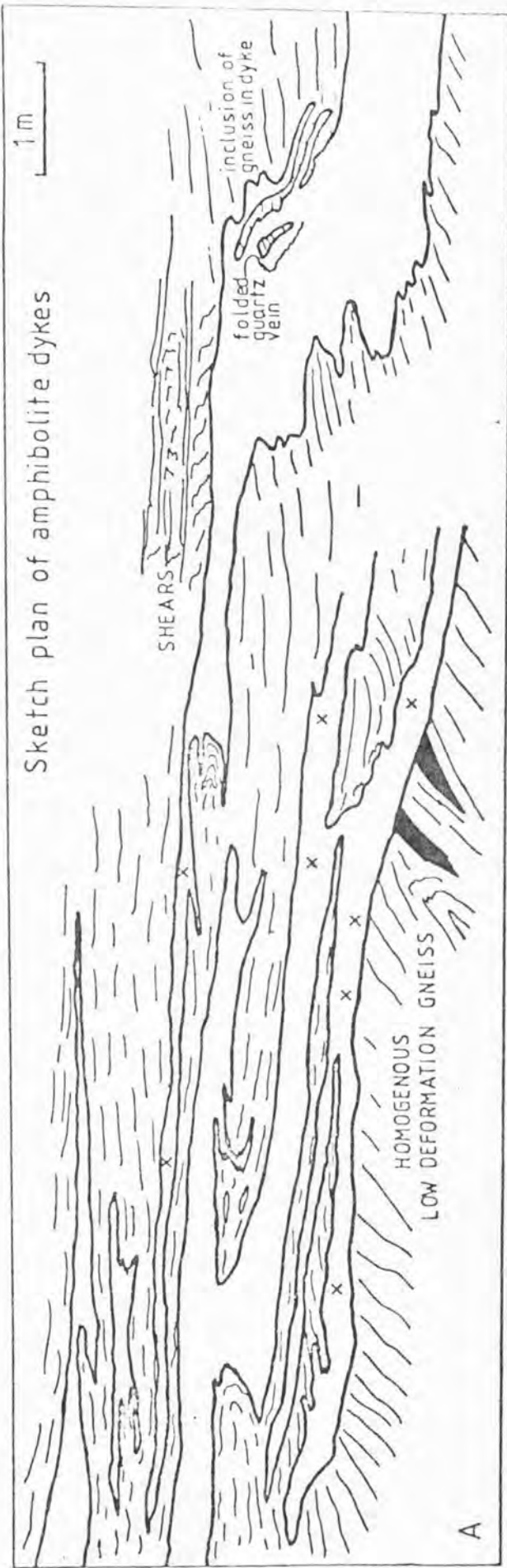


FIG. 6.2 (a) Sketch plan of the dykes on the E. side of Clashnessie Bay. x marks the location of samples, lines mark the trend of the banding and black marks hornblende. The photos in FIG. 6.1 are to the centre and right of the diagram. (b) Sketch of the dyke on the W. of Clashnessie Bay.

wide dykes usually have a coarse almost gabbroic centre with a fine grained margin. The margins are sometimes sheared so that the dykes develop a foliation. These shear zones are probably contemporaneous with dyke intrusion. King (1955) thought this deformation was Laxfordian, however it is Inverian using the terminology as defined in Chapter 1. The very thin Scourie dykes are sometimes metamorphosed to amphibolite with a foliation but they always have a NW-SE trend and a very steep dip ( $> 70^\circ$ ). The Clashnessie dykes however dip  $45^\circ$ , strike 082 and show evidence of folding.

The structure of the Clashnessie Bay area is rather complicated as outlined in Chapter 1. A sketch map of the east side of Clashnessie Bay is given in Fig.6.3. The area enclosing the dykes is composed of very gently-dipping gneisses possibly folded around an early NW-plunging fold ( $F_1$  of Fig.6.3). About 100 m to the east the gneisses are folded into a NNE trending steep belt ( $F_2$  of Fig.6.3). On the western limb of this fold there is abundant hornblendite, such as sample J10 (Chapter 4). Lineations consistently plunge to the SSE (Fig.6.3). The steep belt prevents the amphibolite dykes being followed eastwards as there was probably considerable vertical displacement across the zone. The dykes are therefore confined to a very small area and have not been found anywhere else. This indicates that the dykes may be related to the phase of deformation that produced the NNE-trending steep belts as these structures are well developed in this area and only poorly developed elsewhere.

### 6.3. THE AGE OF THE AMPHIBOLITE DYKES

These dykes are interestingly problematical because they cannot be normal Scourie dykes which are common in the area. No other similar dykes have been reported on the mainland Lewisian. Major problems

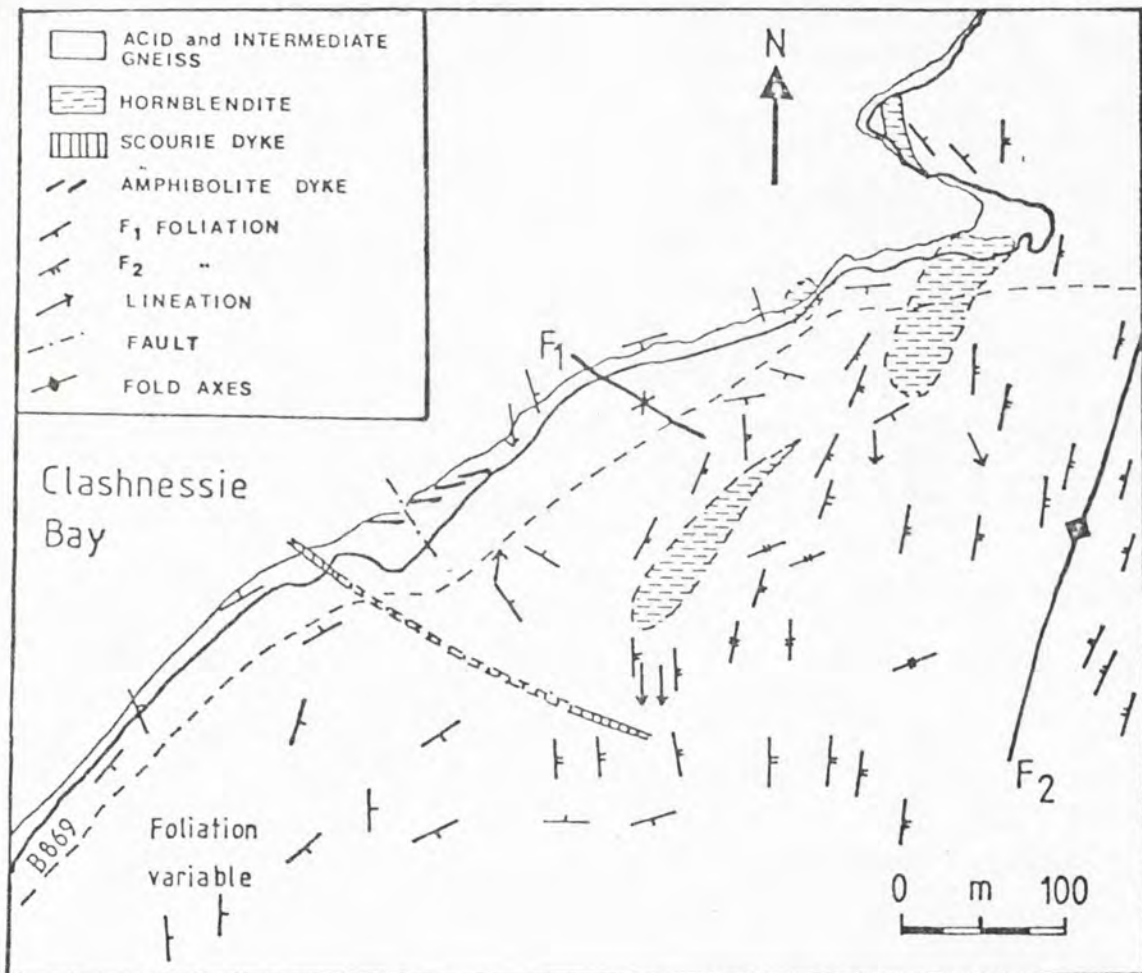


FIG. 6.3 Sketch map of the east end of Clashnessie Bay.

F<sub>1</sub> refers to early mainly flat lying foliation, F<sub>2</sub> to the foliation produced by the NNE trending steep belt.

concern their age relationships to the Scourie dykes, the gneisses and their structures. The possible relative ages are listed below and discussed afterwards:

(1) The host gneisses are "older gneisses" (pre-Scourian) which were intruded by the dykes; the gneisses with dykes were then invaded by large volumes of tonalitic magma which did not contain dykes, i.e. the dykes are equivalent to the Ameralik dykes of west Greenland (McGregor, 1973). Davies (1975) proposed a similar origin for some gneisses containing small dykelets at Scourie but the isotopic data of Chapman and Moorbath (1977) could not distinguish between the "older" and "newer" (Scourian) gneisses.

(2) The dykes were intruded during the Scourian event and metamorphosed and deformed before the end of the Scourian.

(3) The dykes are Inverian in age, contemporaneous with the NNE folding.

(4) They belong to a very early phase of Scourie dykes which were metamorphosed and deformed in the Inverian, before the main dolerite dykes swarm was intruded.

(5) They are a conjugate set to the main WNW-trending dykes.

(6) The dykes are Scourie dykes and there has been localised Laxfordian deformation which has caused rotation and deformation of the dykes.

To test the first hypothesis, samples of the host gneisses were analysed for their lead isotopes and the results are reported in Chapman (1978) and plotted in Fig.6.4. As can be seen, the Clashnessie gneisses and the "older" gneisses of Davies (1975) are indistinguishable from the main Scourian gneisses. The lead isotope data also suggest that there is no component of significantly older crust (greater than 3.0 b.y.) in the Lewisian complex (Chapman and Moorbath, 1977). It is therefore possible that the Clashnessie dykes were intruded in Scourian times, but they are not in significantly older crust.

The trend of the Clashnessie dykes is clearly cut by that of Scourie dykes which implies that the region is not a small area of Laxfordian reworking and that the dykes were intruded before the main Scourie dyke swarm. Point 5 is unlikely because if the Clashnessie dykes are a conjugate set there is no reason why they should be metamorphosed and folded when the Scourie dykes are not. The most likely answer is that the dykes were intruded early in the Inverian event and were deformed and metamorphosed to amphibolite facies before the intrusion of the main dyke swarm. If this is the case they were probably intruded into fairly hot crust, about  $650 \pm 50^\circ\text{C}$  (Chapter 5), so they could be metamorphosed fairly quickly.

#### 6.4. CHEMISTRY

Whole-rock analyses and mineral analyses are given in Tables 6.1 and 6.2. The mineral chemistry has been discussed in Chapter 5. The dykes are moderately well foliated, fine grained amphibolites. This is in contrast to the retrogressed granulite facies mafic rocks which are fairly coarse grained with very irregular grain boundaries. This probably indicates that the dykes were intruded after the granulite facies so they could be metamorphosed fairly shortly after intrusion. The

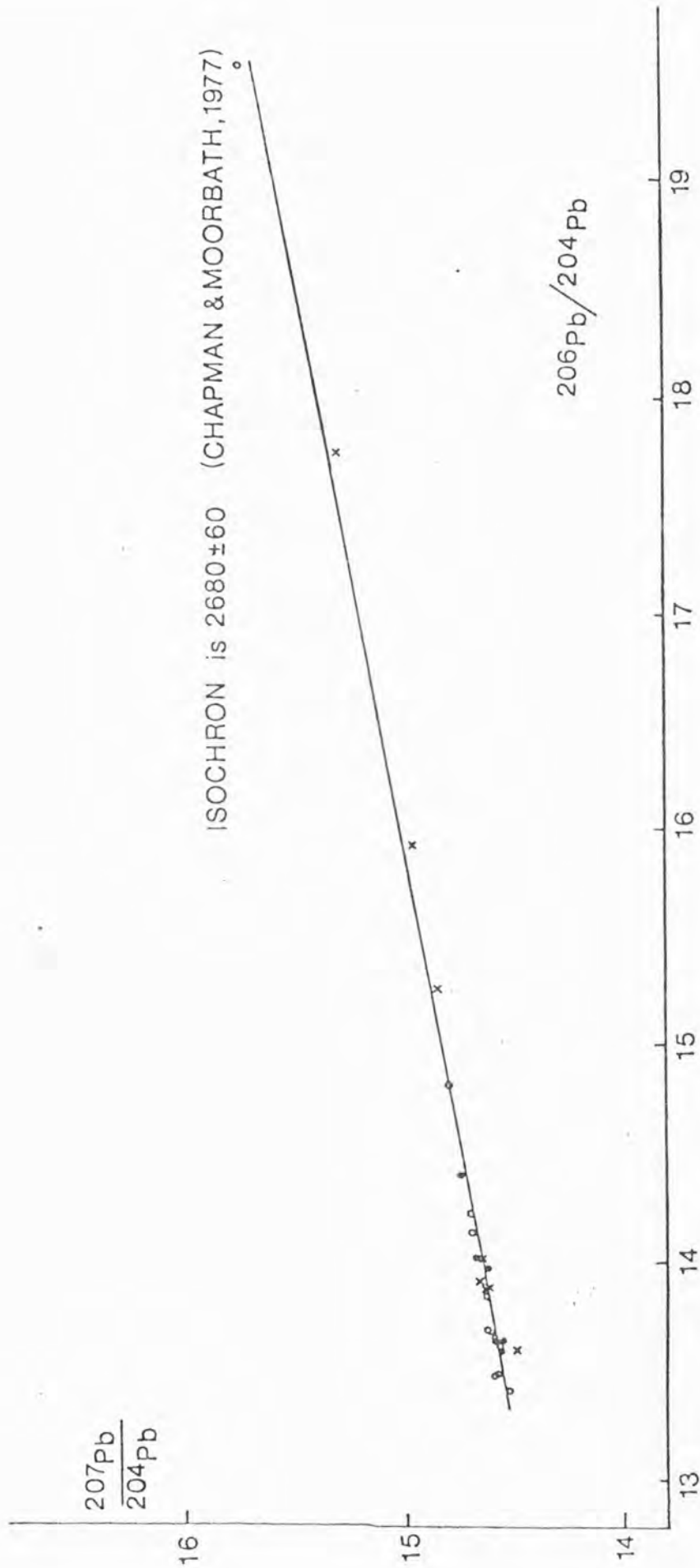


FIG. 6.4  $^{207}\text{Pb}/^{204}\text{Pb}$  versus  $^{206}\text{Pb}/^{204}\text{Pb}$  isochron for the Clashnessie Bay gneisses. Data is from Chapman and Moorbath (1977) and Chapman (1978). Plot is from P.N. Taylor (personal communication).  
 o F.B. DAVIES "older gneisses"  
 x Scourie gneisses  
 • Clashnessie gneisses

SAMPLE	W17	W19	W20	W21	W22	W23	J67	J68	average
SiO <sub>2</sub>	57.4	56.5	57.7	56.2	55.9	55.7	54.16	54.17	55.97
TiO <sub>2</sub>	1.13	1.05	1.14	1.61	1.59	1.16	1.18	1.18	1.26
Al <sub>2</sub> O <sub>3</sub>	12.10	11.80	12.1	12.1	12.1	12.6	12.04	12.04	12.11
Fe <sub>2</sub> O <sub>3</sub>	13.69	13.72	13.54	13.15	13.64	13.38	13.30	13.67	13.51
MnO	0.20	0.21	0.20	0.22	0.21	0.19	0.21	0.20	0.21
MgO	4.49	5.15	4.27	5.04	5.07	4.44	5.85	5.91	5.03
CaO	8.00	8.57	8.29	8.72	8.28	8.32	8.41	8.24	8.35
Na <sub>2</sub> O	2.38	2.42	2.40	2.63	2.74	2.87	2.50	2.51	2.56
K <sub>2</sub> O	0.70	0.57	0.70	0.60	0.70	0.53	0.73	0.77	0.66
P <sub>2</sub> O <sub>5</sub>	0.25	0.32	0.26	0.31	0.29	0.29	0.32	0.32	0.30
TOTAL	100.34	99.99	100.57	100.58	100.52	99.48	98.70	98.60	99.96
Cr	125	-	109	100	110	114	121	127	115
Ni	79	-	77	62	72	71	66	63	70
Zn	122	110	116	106	119	114	125	130	118
Rb	8	3	7	4	6	4	8	11	6
Sr	364	390	385	402	352	363	371	342	371
Ba	283	154	371	197	233	207	334	338	265
Zr	137	137	138	141	133	130	130	132	135
Nb	8	10	9	9	8	8	4	5	9
La	20	14	19	17	18	19	14	21	20
Ce	48	39	46	49	48	47	39	50	44
Nd	25	20	23	23	23	24	23	25	22
Y	28	27	28	28	32	30	29	30	29
Ga	24	20	19	24	20	22	17	16	20
Th	4	3	3	4	4	6	3	3	3
Pb	6	8	8	5	14	8	5	8	8

Table 6.1 Whole-rock analyses of the amphibolite dykes. Total iron is expressed as Fe<sub>2</sub>O<sub>3</sub>.

SAMPLE	W19	J67	J67	J67
MINERAL	Amph(8)	Amph(6)	Biot(6)	Epidote(5)
SiO <sub>2</sub>	42.29	41.52	36.26	37.76
TiO <sub>2</sub>	0.62	0.70	1.89	0.07
Al <sub>2</sub> O <sub>3</sub>	14.68	13.44	16.87	24.10
Fe <sub>2</sub> O <sub>3</sub>	-	-	-	11.59
FeO	17.77	18.21	15.11	-
MnO	0.29	0.33	0.16	0.24
MgO	8.71	8.56	13.83	0.02
CaO	11.71	10.81	0.00	22.39
Na <sub>2</sub> O	1.55	1.56	0.10	-
K <sub>2</sub> O	0.79	0.95	8.84	-
Cr <sub>2</sub> O <sub>3</sub>	0.05	0.02	0.03	0.00
TOTAL	98.46	96.10	93.09	96.17
Xmg	0.461	0.451	0.618	-
no.of oxygens	23	23	22	25
Si	6.308	6.374	5.533	6.074
Al <sup>iv</sup>	1.692	1.626	2.467	-
Al <sup>vi</sup>	0.888	0.805	0.560	4.602
Ti	0.070	0.080	0.217	0.008
Cr	0.006	0.002	0.004	0.000
Fe <sup>3+</sup>	-	-	-	1.290
Fe <sup>2+</sup>	2.218	2.339	1.925	-
Mn	0.037	0.042	0.019	0.033
Mg	1.930	1.959	3.139	-
Ca	1.873	1.778	0.000	3.861
Na	0.445	0.476	0.029	-
K	0.150	0.185	1.718	-

TABLE 6.2 : Mineral analyses from amphibolite dykes, amph - hornblende, biot - biotite, number in parentheses refers to the number of points included in the average. Total iron is calculated as FeO except for epidote where total iron is calculated as Fe<sub>2</sub>O<sub>3</sub>.

dykes have a very uniform megascopic appearance which is reflected in the uniformity of the whole-rock analyses (Table 6.1).

The Clashnessie dykes have an  $\text{SiO}_2$  content ranging from 54 - 57 wt.%, moderate total iron contents of 13 - 14 wt.%, low MgC of 4 - 6 wt.%, CaO of about 8 wt.%, fairly low alumina contents of 11.5 to 12.5 wt.% and fairly low alkalis with  $\text{K}_2\text{O}$  contents of 0.5 to 0.7 wt.%. They are best described as low-K tholeiitic andesites.  $\text{TiO}_2$  -  $\text{P}_2\text{O}_5$  -  $\text{K}_2\text{O}$  relations (after Pearce et al., 1975; Fig.6.5a) show the dykes plot as continental basalts. The Zr/Y ratios are consistent with an origin as within-plate basalts (Pearce and Norry, 1979). Fig.6.5b ( $\text{SiO}_2$  against  $\text{Na}_2\text{O} + \text{K}_2\text{O}$ ) emphasises the high  $\text{SiO}_2$  content of the Clashnessie dykes when compared with other dyke compositions.

The trace element data for the Clashnessie dykes has been compared with the early dolerite Scourie dykes (data from Weaver and Tarney, in prep. and O'Hara, 1961b) to determine whether the Clashnessie dykes could be related to the Scourie dykes. The  $\text{SiO}_2$  content of the Clashnessie dykes (54 - 57 wt.%) is always greater than that of the Scourie dykes, which ranges from 48 - 54 wt.%. In Fig.6.6, various elements have been plotted against  $\text{SiO}_2$  and it can be seen that  $\text{TiO}_2$ , Ba and Zr (as well as  $\text{K}_2\text{O}$ ,  $\text{P}_2\text{O}_5$ , Rb and Y) are all lower in the Clashnessie dykes than one would expect if the dykes belonged to the same trend as the Scourie dykes. The only element to plot on the same trend is Sr. In Fig.6.7, several elements are plotted against Zr to examine trace element ratios, which may give a better indication of whether the two dyke types could be derived from the same source. As shown in Fig.6.6 the Zr content of the Clashnessie dykes (130 - 140 ppm) is lower than that of the more evolved Scourie dolerite dykes (200 - 230 ppm). The  $\text{TiO}_2$  content of the Clashnessie dykes is fairly

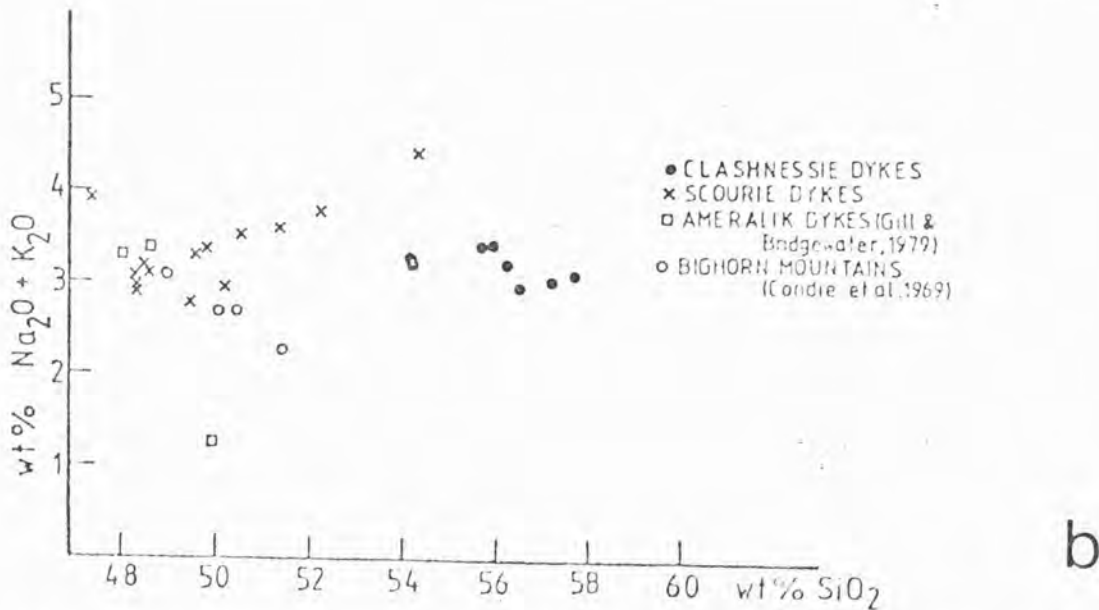
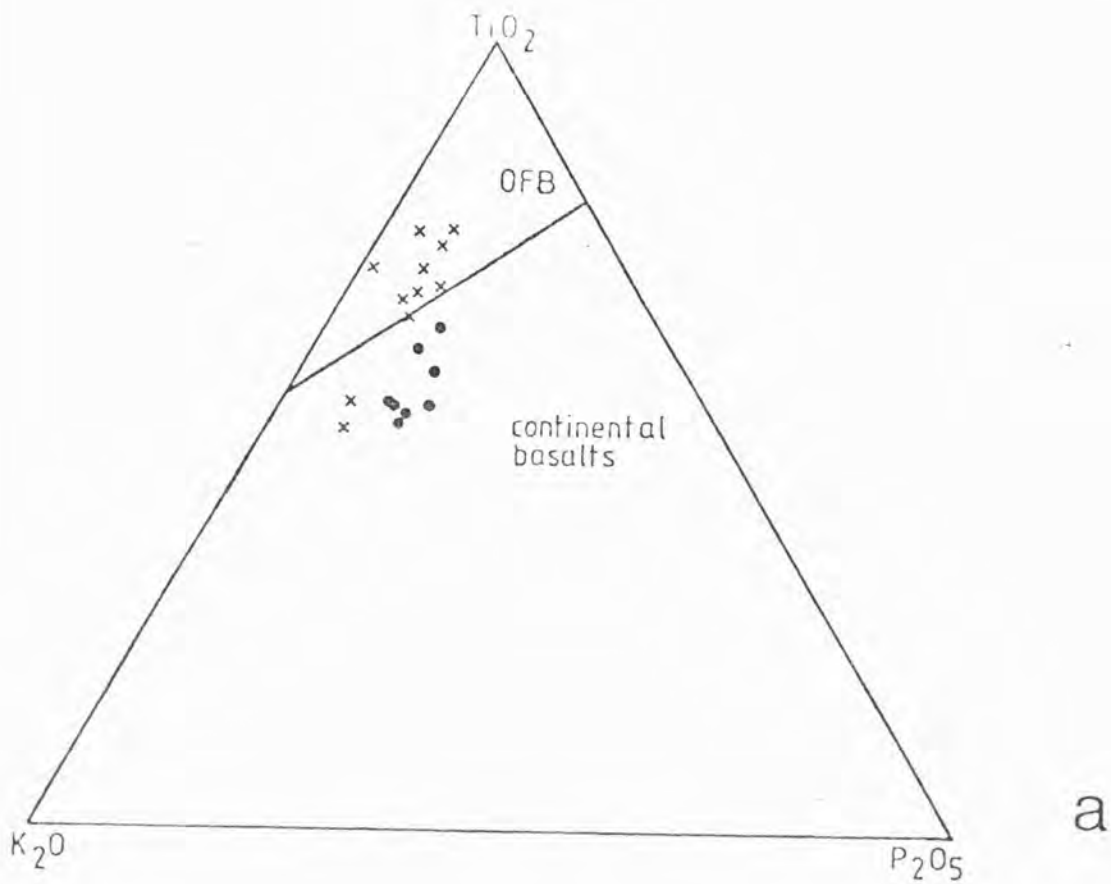


FIG. 6.5 (a)  $TiO_2 - K_2O - P_2O_5$  plot for the Clashnessie dykes, after Pearce et al., (1975). Key as in (b).

(b) Plot of  $SiO_2$  against  $Na_2O + K_2O$  for various dykes.

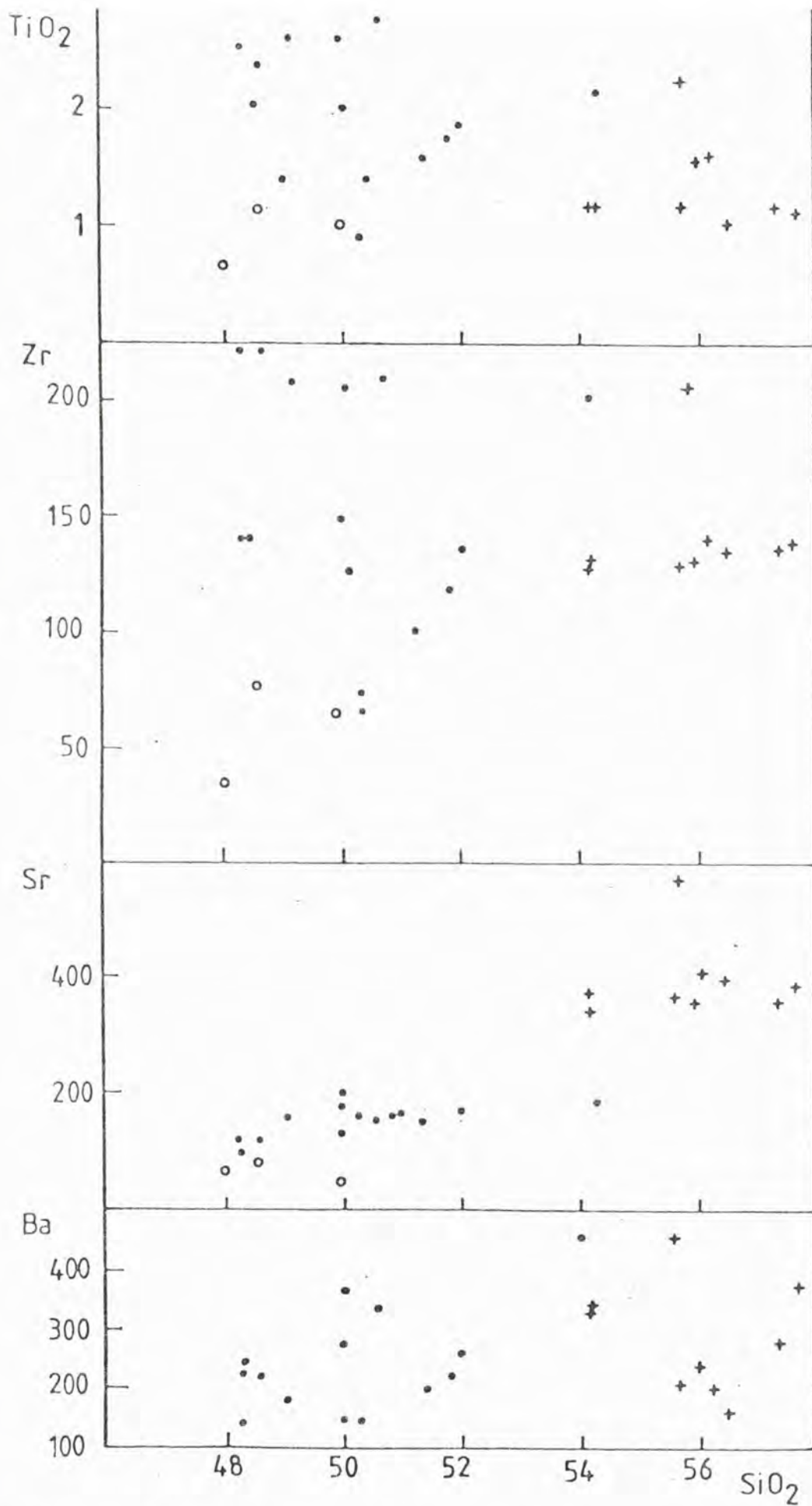


FIG. 6.6 TiO<sub>2</sub> (wt.%), Zr ppm, Sr ppm and Ba ppm against SiO<sub>2</sub> (wt.%) for Clashnessie dykes (crosses), Scourie dykes (filled circles, data from Weaver and Tarney, in prep. and O'Hara, 1961b) and

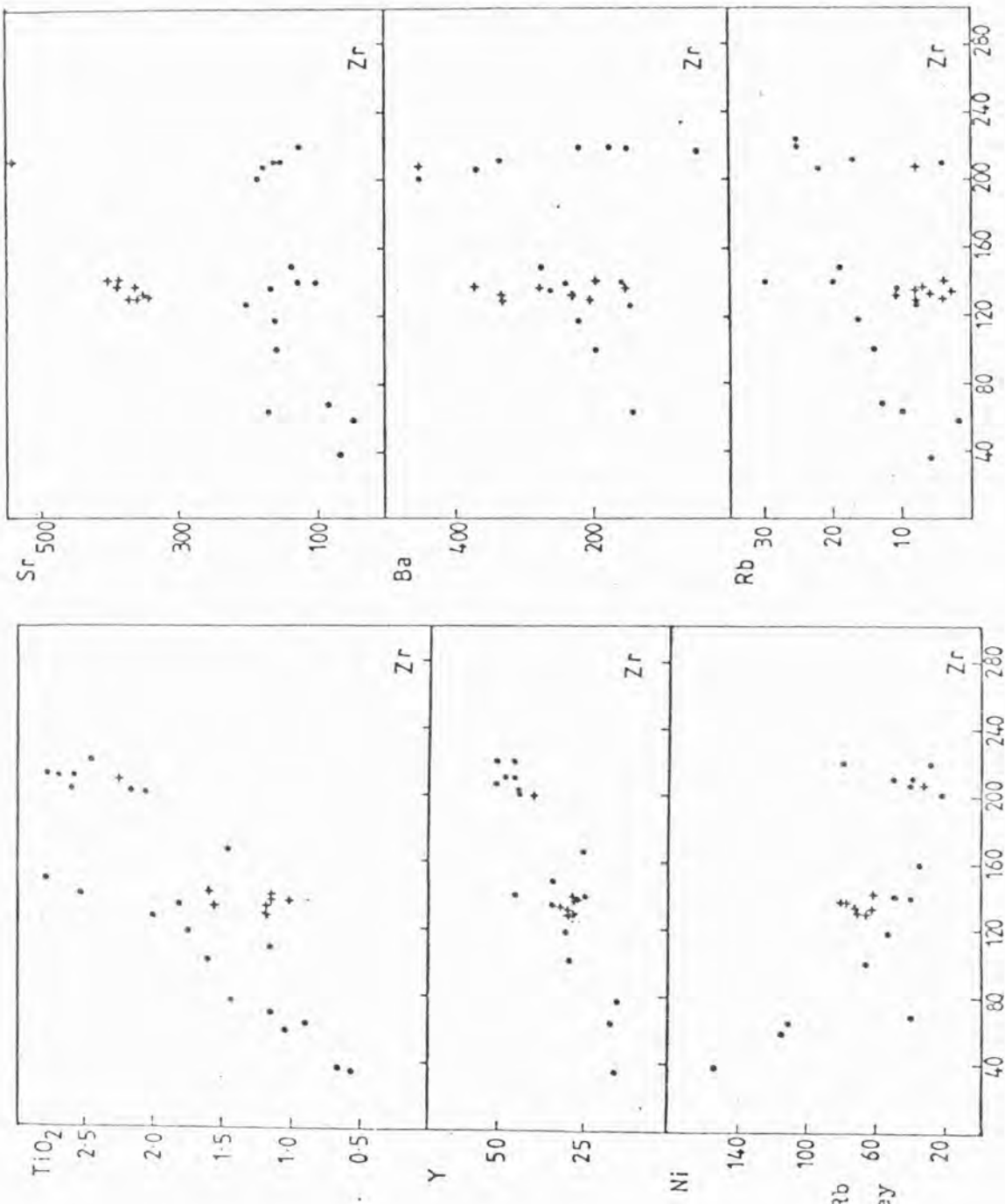


Fig. 6.7 TiO<sub>2</sub> (wt.%), Y, Ni, Sr, Ba and Rb against Zr (ppm) for various dykes. Key in Fig. 6.6.

low, leading to low Ti/Zr ratios of 45 - 75, lower than those of the Scourie dykes which also have low Ti/Zr ratios (65 - 90; Weaver and Tarney, in prep.). Both sets of dykes have similar Zr/Y ratios (about 5 for the Clashnessie dykes). Ni and Cr plot on a similar trend to the Scourie dykes. The Sr content of the Clashnessie dykes is much higher, Rb slightly lower and Ba similar to the Scourie dykes; these elements however are those most affected by metamorphism so the contents may not reflect the original composition. The low Rb contents (less than 11 ppm) lead to fairly high K/Rb ratios with an average of 1000 (Fig.6.8); compared with a K/Rb ratio of 300 - 500 for the Scourie dykes. The usual explanation of high K/Rb ratios in granulites involves the preferential removal of Rb over K either in a melt phase (e.g. Heier, 1973) or by CO<sub>2</sub>-rich fluids (Sheraton et al., 1973a; Rollinson and Windley, 1980a; Newton et al., 1980). However the very fine grained nature of these dykes implies they never went through a granulite facies event (see above), so the high K/Rb ratios may reflect those of the original liquid, and hence the source region.

These trace element variations, with most incompatible elements being lower than those of the most evolved Scourie dykes makes it impossible to relate the two dyke types by fractional crystallization.

#### 6.5. PETROGENESIS

As the dykes were completely recrystallized during amphibolite facies metamorphism, it is not known whether they had any phenocryst phases or to what extent the analyses represent liquid compositions; however the dykes are extremely homogeneous suggesting that they may be liquids. Their petrogenesis is rather difficult to determine as the

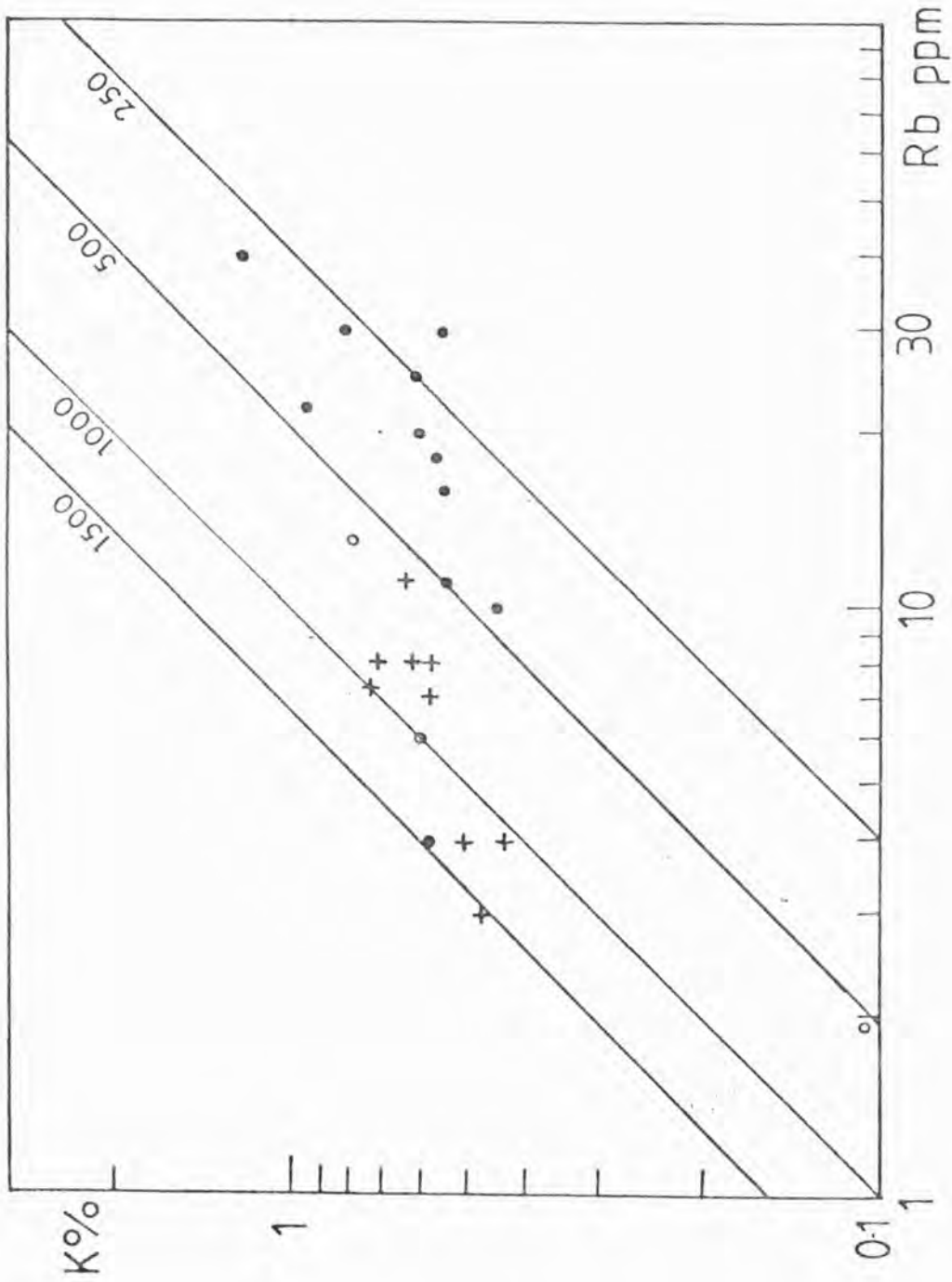


FIG. 6.8 K (wt.%) versus Rb (ppm) for Clashnessie and Scourie dykes.  
Key as in Fig.6.6. Lines refer to the K/Rb ratios indicated.

analyses are so similar that there are no trends apparent between different dykes. As outlined above, the Clashnessie amphibolite dykes cannot be related to the magma producing the Scourie dykes by fractional crystallization. They were probably intruded a fairly short time before the Scourie dykes so they may have been produced by the same segment of mantle. It is interesting to note that the first phase of Scourie dyke intrusion was represented by quartz normative tholeiitic dykes to be followed by olivine gabbro and picritic dykes (Tarney, 1973). The production of andesitic dykes shortly before the main Scourie dyke event is a continuation of the same trend of decreasing silica content of the dykes with time.

Due to the lack of any evidence to the contrary, it will be assumed that the dykes approximate to liquid compositions, i.e. any possible cumulus phases are ignored, to see whether it is possible to derive the dyke compositions as either primary mantle melts or as mantle-derived liquids modified by fractionation before intrusion. The Ti/Al and Ti/Cr ratios plot on the liquid trends of Pearce and Flower (1977). The element concentrations (with the exception of Sr) are more consistent with a silica content of 50 - 54 wt.% SiO<sub>2</sub> than 54 - 57 wt.% possibly implying contamination by silica. However the dykes are so uniform and the contents of fairly mobile lithophile elements such as Rb are low indicating that these silica contents may be primary.

The following points may help to understand the petrogenesis of these dykes:

(1) The  $Ce_N/Y_N$  ratio for the Clashnessie dyke ranges from 3.3 to 4.2. Complete REE data are not available but some elements (La, Ce, Nd and Y to monitor the HREE) have been analysed by X-ray fluorescence.

The data have been compared with selected patterns for Scourie dolerite dykes (Weaver and Tarney, in prep., Fig.6.9). The patterns are very similar, although the Clashnessie dykes may have slightly lower HREE contents. This implies the two dyke types may have had a similar source.

(2) The amphibolite dykes have low Ti/Zr ratios (average = 56) compared with a chondritic ratio of about 110 (Sun and Nesbitt, 1977). A low Ti/Zr ratio could be a feature of the source mantle (Weaver and Tarney (in prep.) put forward this theory to account for low Ti/Zr ratios in the Scourie dykes), or due to a Ti-bearing phase remaining in the source mantle after partial melting, or due to fractionation of a Ti-bearing phase before intrusion.

(3) The dykes have a Zr/Y ratio of about 4.7 compared with a chondritic mantle ratio of 2-3 (Sun and Nesbitt, 1977). The Ti/Y ratio of about 260 is close to the mantle value of Sun and Nesbitt (1977). This tends to imply that either Ti and Y contents are normal, while the Zr content is high or Ti and Y contents are low.

(4) There is a moderately high K/Rb ratio which could be:

(i) a feature of the source

(ii) due to a residual mantle phase containing Rb in preference to K

(iii) due to fractionation of a phase which removes Rb in preference to K. The only phase which has a higher  $K_D$  for Rb than K is phlogopite, but this also has a high  $K_D$  for Ba (Arth, 1976). The dykes have fairly high Ba contents, therefore the Rb

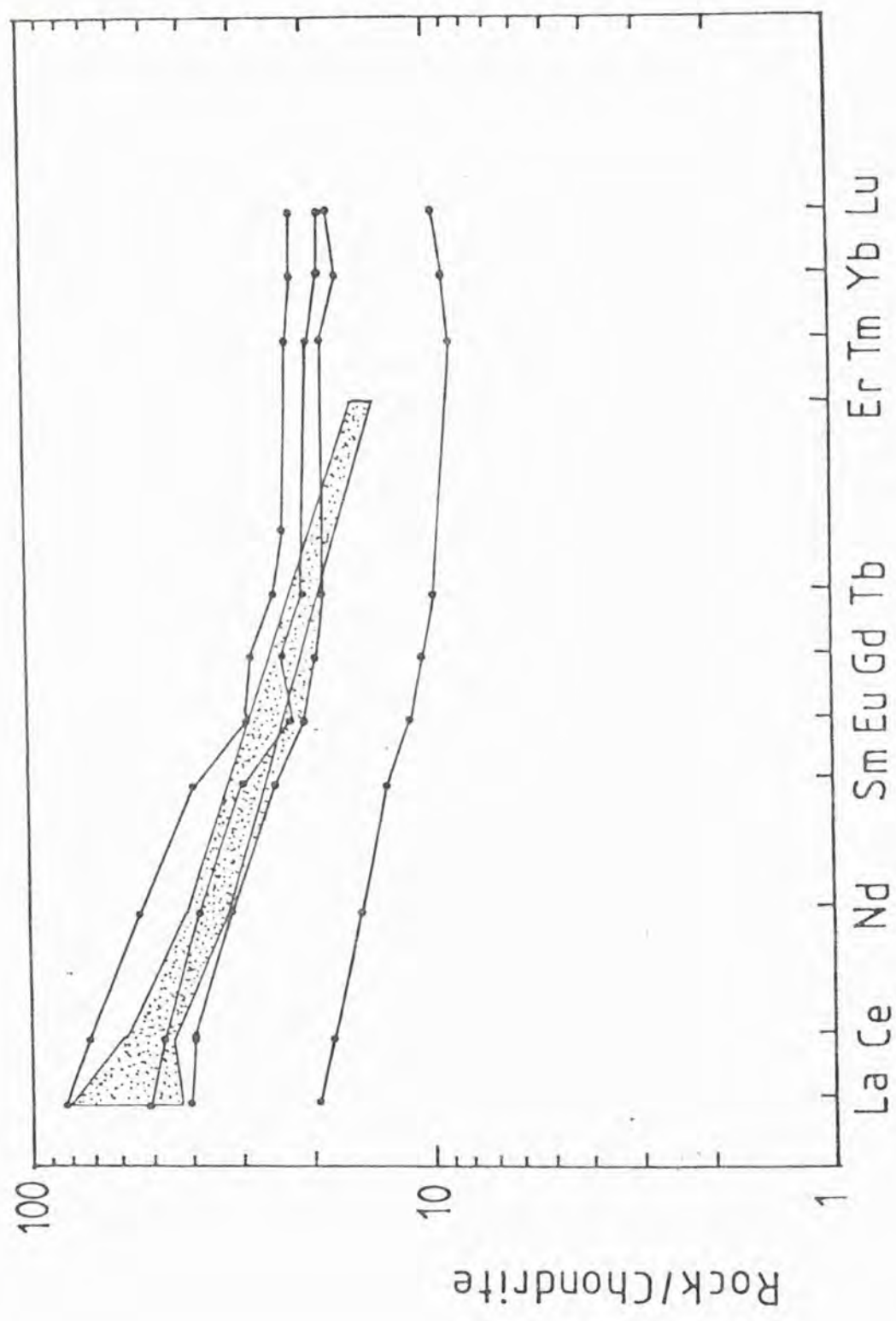


FIG. 6.9 Chondrite normalised REE plot for the Clashnessie dykes and selected Scourie dolerite dykes (data from Weaver and Tarney, in prep.). Dotted area is field for Clashnessie dykes.

could not be removed by phlogopite as this would also cause the removal of Ba which is not seen. In fact the Ba content (average of 265) is high compared to the levels of the other incompatible elements.

(iv) due to modification of K/Rb ratios by metamorphic processes.

The dykes are therefore moderately LREE-enriched and are either enriched in Zr or depleted in Ti and Y relative to chondritic ratios.

There are three main ways of generating liquids with a moderate degree of silica enrichment:

- (1) as primary mantle melts resulting from a very low degree or partial melting of anhydrous mantle
- (2) as primary mantle melts resulting from the partial melting of hydrous mantle
- (3) by fractional crystallization of a tholeiitic liquid leading towards more silica-rich compositions.

The first proposal is unlikely as the level of incompatible elements is fairly low, although it is possible that the source mantle was depleted in these elements. There has been considerable experimental work on the melting of hydrous mantle (e.g. Kushiro, 1972; Mysen and Boettcher, 1975) and of hydrous basaltic compositions (e.g. Holloway and Burnham, 1972) all of which suggests that it is possible to generate quartz-normative liquids in the presence of water. However, these liquids are

all calc-alkaline with high  $Al_2O_3$  contents, whilst the Clashnessie dykes have low alumina contents (ca. 13 wt.%). The MgO content of about 5 wt.% is rather low for primary mantle melts, so it is believed that the third possibility is most likely i.e. the dykes represent liquids that have undergone fractionation before emplacement. By fractionating a variety of phases it is possible to lower the MgO content and to alter the incompatible trace element ratios. However with the data available it is not possible to distinguish between phases residual in the mantle after melting, and phases which have fractionated between melting and emplacement.

A phase (or phases) is needed which will deplete the liquid in Ti and Y relative to Zr, keeping Ti/Y relatively constant, which will lower Rb, cause moderate LREE enrichment and allow moderate levels of Sr and Ba. The most suitable mineral is hornblende which has  $K_D$ 's for Ti and Y of 1.5 and 1.0 respectively for basaltic liquids and 3.0 and 2.5 for intermediate liquids (Pearce and Norry, 1979). Removal of hornblende would thus deplete the liquid in Ti, keep Y constant and cause Zr to increase. Calculations assuming Rayleigh fractionation require 50% fractional crystallization of hornblende to change the Ti/Zr ratio from a chondritic ratio of about 100 to a value of 50. It is possible that the source mantle already had a low Ti/Zr ratio (Weaver and Tarney, in prep.) in which case a smaller amount of fractionation is required to lower the ratio to about 50. Hornblende also concentrates the HREE (Arth, 1976) so hornblende fractionation could have caused the moderate LREE enrichment. Cawthorn (1976) suggests that ol - cpx - amph are likely fractionating phases from a quartz-normative liquid in the system  $CaO-MgO-Al_2O_3-SiO_2-Na_2O-H_2O$  at 5 kb water pressure. Clinopyroxene has a similar pattern of  $K_D$ 's to hornblende but fractionation of clinopyroxene has less effect.

It is tentatively suggested that the Clashnessie dykes evolved from a tholeiitic liquid by fractionation of hornblende. Some of the trace element ratios, such as  $K/Rb$ , may be inherited from the source. A heterogeneous source mantle is proposed by Weaver and Tarney (in prep.) to account for some of the features of the Scourie dykes and it is likely that some of the same heterogeneities were present in the source region of the Clashnessie dykes because the intrusion times of the two groups of dykes is fairly close. The generation of these amphibolite dykes may be related to the influx of water causing the retrogression of the Assynt gneisses and metamorphism of the dykes to amphibolite facies. This presence of water is consistent with the fractionation of hornblende from the tholeiitic liquid before emplacement. The dykes were probably intruded in the early stages of the Inverian event and were metamorphosed and deformed before the intrusion of the main Scourie dyke swarm.

CHAPTER 7  
THE CANISP SHEAR ZONE

## 7.1. INTRODUCTION

Archaean regions are commonly cut or bounded by major Proterozoic shear zones such as between the Limpopo mobile belt and the Kapvaal and Rhodesian cratons (Coward et al., 1973) and the southern margin of the Nagssugtoqidian belt of west Greenland (Bak et al., 1975). There is often a very large displacement across these zones e.g. up to 200 km across the Limpopo belt and up to 100 km across the Nagssugtoqidian. It is believed that these ductile shear zones are the deep crustal equivalents of high level brittle faults (Grocott, 1977; Davies, 1978). Watterson (1978) suggested the shear zones of Scotland and Greenland were deep seated equivalents of the transcurrent faults of China caused by the collision of the Indian and Eurasian plates; the Greenland shear zones being created by the northward collision of the Ketilidian block with the Archaean craton in early Proterozoic times.

The Scourian granulite facies gneisses are bounded in the north by the Laxford Front shear zone (Sutton and Watson, 1951; Beach et al., 1974; Davies, 1976, 1978; Coward et al., 1980). This structure has been in existence since the early Scourian with a total dextral displacement of at least 35 km (Davies, 1978). However Beach et al. (1974) interpreted the Laxford Front as a belt with sinistral, north-side-up sense of displacement. Davies (1978) based his interpretation on the rotation of Scourian fold axes into the shear zone, whilst Beach et al. (1974) based theirs on the sense determined from abundant small scale sinistral shear zones to the south. A dextral sense of shear would produce lineations rotated in a clockwise sense from the Scourian direction of about  $140^\circ$  which is not found, while lineations striking between  $140^\circ$  and the shear direction of about  $110^\circ$  are found (Coward et al., 1980). A sinistral sense of displacement however does not provide a fully satisfactory

explanation for the rotation of the Scourian fold axes. Davies (1978) considered that the small scale sinistral shears were mechanisms for accommodating some of the displacement in the narrow part of the shear zone.

In the Assynt region there are numerous late (Laxfordian) shear zones which commonly have a similar sinistral sense of movement, these structures usually being less than 1 m wide. The largest of these is the Canisp shear zone (Sheraton et al., 1973b; see also Chapter 1) which is over 0.5 km wide at the coast between Achmelvich and Clachtoll. Peach et al., (1907) discovered, and mapped, this zone of highly deformed gneiss for several kilometres eastwards until it disappears under the Torridonian cover. The zone thins eastwards until it is less than 100 m wide. The Laxfordian strain is very heterogeneous with numerous low strain zones occurring between the narrow shear zones; the Canisp shear zone is thus composed of many narrow shear zones which have merged. The zone has a long history of metamorphism and deformation spanning the period of dyke intrusion (Sheraton et al., 1973b; Chapter 1). It is clear that much of the amphibolite facies retrogression in NW-trending Inverian steep belts occurred before the intrusion of the dykes. Further metamorphism and deformation affecting the dykes was followed by localised recrystallization in Laxfordian shear zones. The history of the Canisp shear zone thus falls into two parts:

- (1) formation of the Lochinver antiform producing an Inverian steep belt with associated retrogression. This was followed by dyke intrusion and further deformation towards the end of the Inverian event,
- (2) recrystallization in Laxfordian shear zones located on the vertical limb of the Lochinver antiform.

The general features of the Canisp shear zone will now be described. Some of these features have already been mentioned in Chapters 1 and 5 but will be repeated here for the sake of clarity.

## 7.2. MAIN FEATURES OF THE CANISP SHEAR ZONE

The main structural features are shown in Figs.7.1 and 7.2 and sketches of minor folds in Figs.1.15 and 1.16. The southern margin of the shear zone is very sharp, but the northern margin is far more diffuse (Fig.7.2). To the south of the Canisp shear zone, the gneisses which dip gently south, extend as far as Achiltibuie. These gneisses have a lineation plunging S or SSW. Less than 500 m to the south of the shear zone at Achmelvich there is the Lochinver antiform (Figs.7.1 and 7.2; Chapter 1) which is a major Inverian structure that can be correlated with the NW-trending monoclinial folds in the Stoer-Drumbeg region (Sheraton et al., 1973b). The steeply-dipping northern limb was the focus for Laxfordian shearing. The Laxfordian shear zone cross-cuts the axial trace of the Lochinver antiform, which disappears into the shear zone to the east of Loch Bad na Goibhre (Fig.7.1). The dip of the gneisses steepens as the shear zone is approached from the south (Fig.7.2). The northern margin is less well defined with vertical or near-vertical Inverian gneisses extending 2-3 km northwards with NW or SE plunging lineations. The shear zone dies out in a series of narrow shears which decrease in frequency northwards. The shears tend to merge, enclosing low deformation lenses. Fig.7.3 is a sketch map of the northern margin of the shear zone near Alltan na Bradhan (057263).

In the Canisp shear zone Scourie dykes commonly have sheared and metasomatised margins (Tarney, 1973) and may be cut by small centimetre-scale shear zones which interlock in the manner described by Coward (1976;

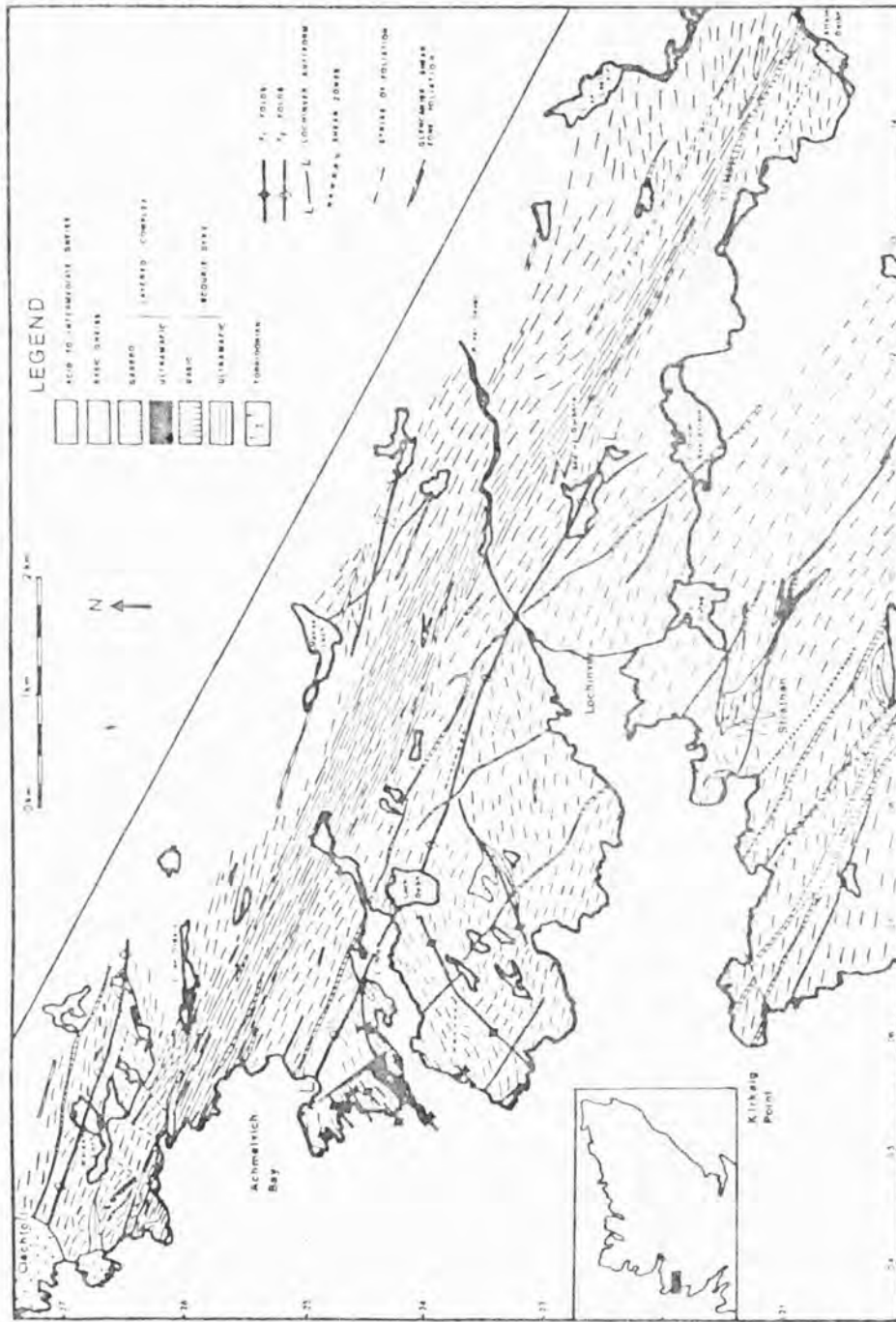


FIG. 7.1 Sketch map showing the Canisp shear zone and the Lochinver antiform. Dashes reflect the strike of the gneissic foliation and the rocks are more deformed when the dashes are close together.



FIG. 7.2 Cross section of the Canisp shear zone showing the Lochinver antiform and the belt of Laxfordian shearing. Discrete narrow shear zones shown by dashed lines.

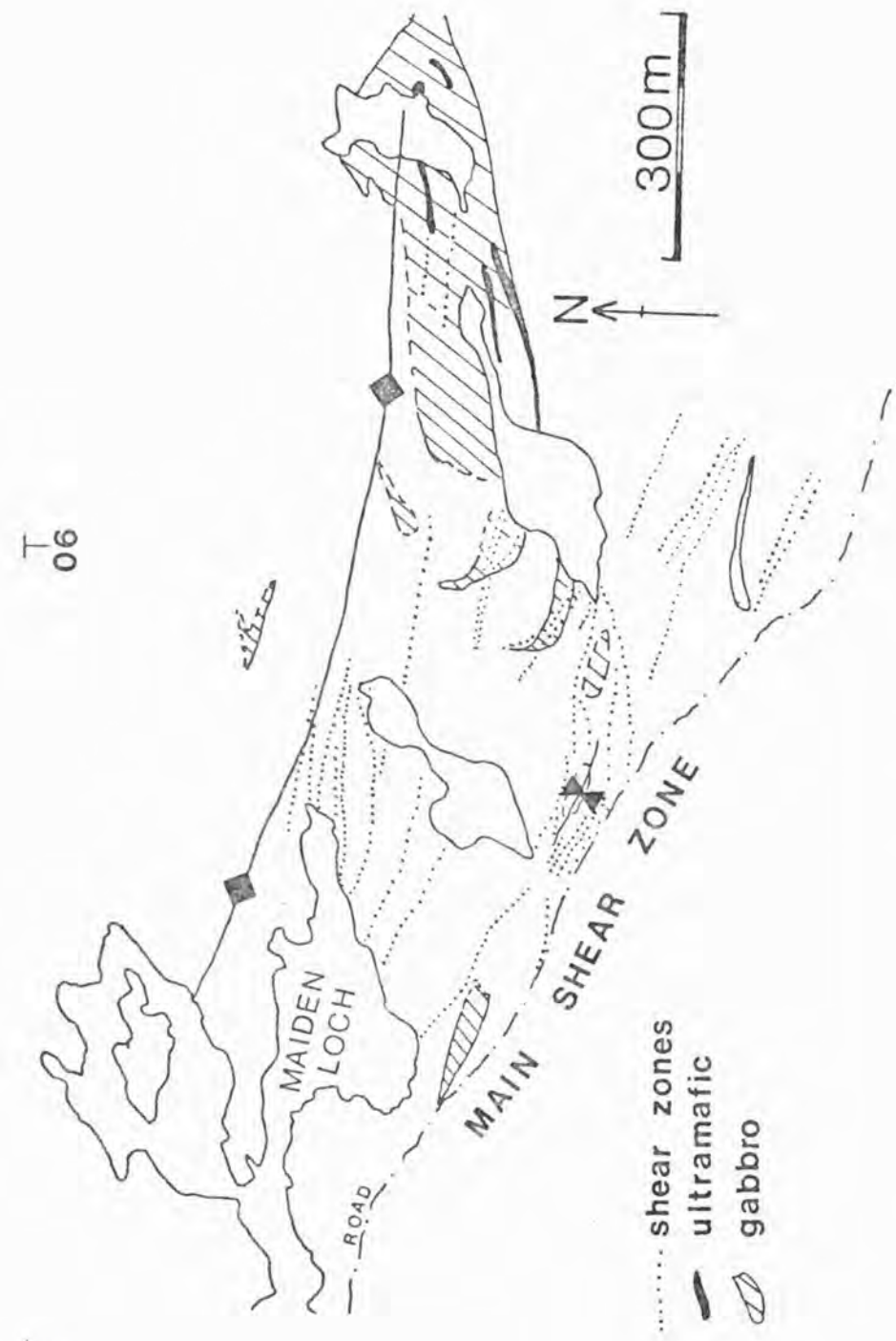


FIG. 7.3 Sketch map of the northern margin of the Canisp shear zone showing shear zones and fold axes.

Fig.7.4). Thin Scourie dykes may be transformed into amphibolite schists and locally folded e.g. at Port Alltan na Bradhan (050261; Fig.7.5a). Ultramafic dykes are highly metamorphosed and deformed (Tarney, 1973), often being more deformed than the bordering gneisses.

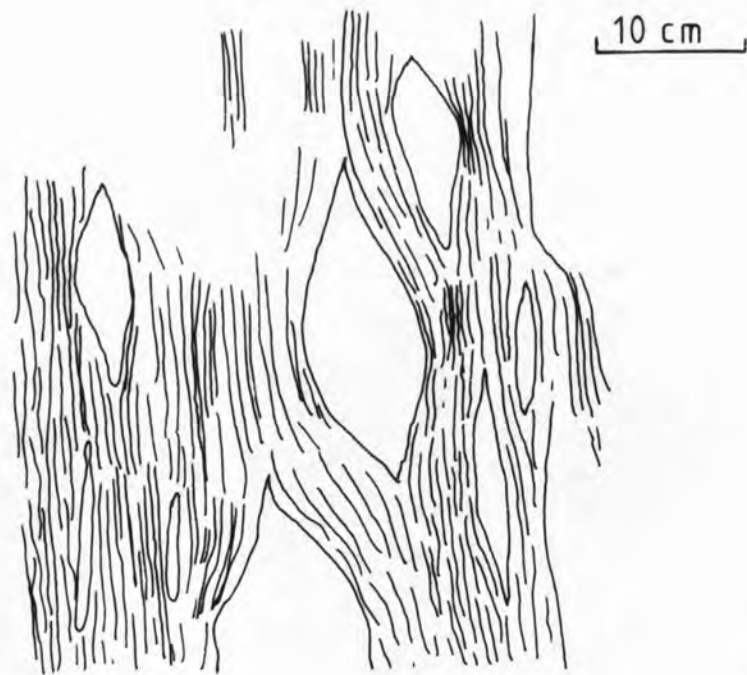
There is a strong foliation in the Laxfordian shear zones which consistently dips  $70 - 80^\circ$  to the SSW. This contrasts with the foliation in Inverian steep belts which is vertical. The Laxfordian shear zone reaches 0.5 km wide at the coast near Achmelvich, its gneisses dipping uniformly to the south (Fig.7.5b). There is a considerable reduction in grain size but the mineral assemblages are essentially the same as those developed during the Inverian retrogression (see Chapter 5). There has been static post-deformational growth of prismatic amphiboles (cummingtonite, tremolite and hornblende), muscovite and magnetite which cross-cut the schistose fabric (Fig.5.3c). These amphiboles are randomly orientated within the foliation surface often giving the rock a superficially massive appearance. There is a penetrative lineation plunging  $25 - 30^\circ$  to the ESE, parallel to the axes of minor Laxfordian folds. This lineation serves to distinguish these late shear zones from Inverian steep belts which have no associated lineation. Minor folds are ubiquitous, generally having steep axial planes parallel to the foliation. There are several fold generations which give rise to complex interference patterns (Fig.1.16). Many folds have a similar style developed during shearing, but some are Inverian or Scourian folds which have been rotated by the shear zone. The late Laxfordian shears tend to follow pre-existing vertical structures such as dykes or Inverian monoclinial steep belts.

FIG.7.4 (a) Photograph of small shear zone cutting a Scourie dyke on the southern margin of the Canisp shear zone, near Glencanisp Lodge, 133215.

(b) Sketch of the above photograph.



a



b

FIG. 7.5 (a) Photograph of a thin folded Scourie dyke  
from the Canisp shear zone, Port Alltan na  
Bradhan (051261).

(b) View of the Canisp shear zone in Achmelvich  
Bay, showing the well foliated gneisses  
dipping to the south (056255).



a



b

### 7.2.1. Sense of movement across the Canisp shear zone

Many of the late Laxfordian shear zones have a sinistral north-side-up sense of movement (Sheraton et al., 1973b) determined from the sense of minor folds. This is in contrast to the Inverian steep belts which generally have a downthrow to the north (Chapter 1). For example, just to the west of Imirfada in Clashnessie Bay (061312) there is a small shear zone with sigmoidal tension gashes exhibiting a sinistral displacement. However NE-trending fold axes in the Achmelvich-Loch Roe area appear to have been rotated with a dextral sense of shear into the Canisp shear zone (Fig.7.1). It is believed that a large amount of the deformation occurred during the Inverian, possibly with a dextral sense of movement and that the more brittle Laxfordian shear zones are a fairly minor effect superimposed on the steep limb of the Lochinver antiform. This view is consistent with that of Davies (1978) for the Laxford front area but is in conflict with that of Coward et al. (1980).

The NE-trending folds occurring in the Achmelvich region could be equivalent to the  $F_3$  folds of Coward et al. (1980) in the Scourie area. These  $F_3$  fold axes are rotated in the same manner as the Achmelvich folds by NW-trending  $F_4$  folds (late Scourian; Inverian of this study). It is possible that the outcrop pattern of the Achmelvich folds reflects refolding by the NW-trending Lochinver antiform rather than a component of simple shear in the Canisp shear zone. At present it is not really possible to decide whether the rotation of the NE-trending fold axes does reflect a dextral sense of movement or not. However it is clear that there has been a significant amount of vertical movement which has brought Inverian amphibolite facies gneisses of the northern limb of the Lochinver antiform down to the same structural level as fairly fresh granulites on the southern limb.

Faults occurring near the earth's surface are the result of brittle deformation while deep seated shear zones are the result of ductile deformation. However the Laxfordian shearing in the Canisp shear zone shows evidence of brittle-ductile behaviour (Ramsay, 1980). In a true ductile shear zone there are no discontinuities across the wall of the zone. In the Canisp shear zone the sheared gneisses stop abruptly against the Inverian gneisses at the southern margin. At the contact there are brecciated gneisses and quartz veining (058252) and a shear zone at 061312 has quartz-filled tension gashes, all features suggesting brittle-ductile behaviour (Ramsay, 1980). This implies that the Canisp shear zone may have formed at a higher crustal level than the Laxford Front.

### 7.3. COMPARISON BETWEEN THE CANISP AND LAXFORD FRONT SHEAR ZONES

There are several similarities and several differences between the Canisp and Laxford front shear zones which are summarised below:

(1) The Laxford front forms a boundary between Scourian granulites and Laxfordian migmatites, whereas the Canisp shear zone forms a boundary between slightly retrogressed granulites and amphibolite facies Inverian gneisses. In both cases the sense of vertical movement is the same, i.e. a downthrow to the south but the amount of movement was greater across the Laxford front.

(2) Late narrow shear zones in both areas have a sinistral, north-side-up sense of displacement, but there is still some dispute as to the direction of overall transcurrent displacement. If NE-trending folds were rotated by the shear zone, the displacement is dextral. Davies (1978) estimates that about 50% of the movement occurred by the end of the Scourian. In the Canisp shear zone most of the displacement occurred during the Inverian.

(3) The Laxford front appears to have been an anomalous zone throughout its history with a concentration of layered complexes bordered by metasediment (Davies, 1974, 1976, 1978). Davies (1978) states that the structure was in existence before the end of the granulite facies metamorphism. However there is no evidence to show the existence of the Canisp shear zone before the Inverian and there is approximately the same percentage of rock types within and outside the shear zone.

(4) Shear zones in the Scourie region cut granulite facies gneisses with the development of new mineral assemblages which formed at an estimated P-T of 6 kb and 600°C (Beach, 1973). The Canisp shear zone cuts already retrogressed gneisses and causes a reduction in grain size and a new schistosity rather than the development of new mineral assemblages. The mineral assemblages developed in Inverian steep belts and Laxfordian shear zones in the Assynt region have been discussed in Chapter 5 (see Table 5.1); typical assemblages being:

ultramafic rocks - trem-chl-mag ± anth ± tc (Inverian)  
 ± trem-chl-mag-tc-dol ± anth (Laxfordian)

mafic rocks - hb-plag ± qz ± bi ± ep ± sphere-opq  
 or actinolite

intermediate rocks - plag-qz-bi-hb ± chl-opq

acid rocks - qz-plag-bi ± chl ± musc-opq

The Laxford front assemblages have much more biotite (Beach, 1973).

(5) The Canisp shear zone was the locus for the intrusion of ultramafic Scourie dykes which are rare elsewhere in the Lewisian. This suggests the dykes preferentially intruded a zone of weakness and implies the shear zone extends right through the crust.

#### 7.4. ESTIMATE OF DISPLACEMENT

The rotation of marker horizons, such as fold axes, has been used by several authors (Coward et al., 1973; Bak et al., 1975, Davies, 1978) to obtain an estimate of displacement across shear zones. The formula, derived by Ramsay and Graham (1970) is:

$$\cot \alpha' = \cot \alpha - \gamma$$

where  $\gamma$  is the shear strain,  $\alpha$  is the initial angle between the marker horizon and the shear zone margin and  $\alpha'$  is the deformed angle. The NE-trending folds in the Achmelvich-Loch Roe area can be used in this way, assuming they have been rotated by simple shear. Beach (1974) used the displacement of Scourie dykes across Laxfordian shears to obtain an estimate of displacement but this method cannot be applied to the Canisp shear zone, because the dykes within the shear are conformable with the schistosity and there are no dykes which can be followed into the shear zone. The foliation south of the shear zone tends to swing into the shear but at the northern margin the Inverian gneisses already had a NW trending foliation prior to Laxfordian shearing along almost the same trend.

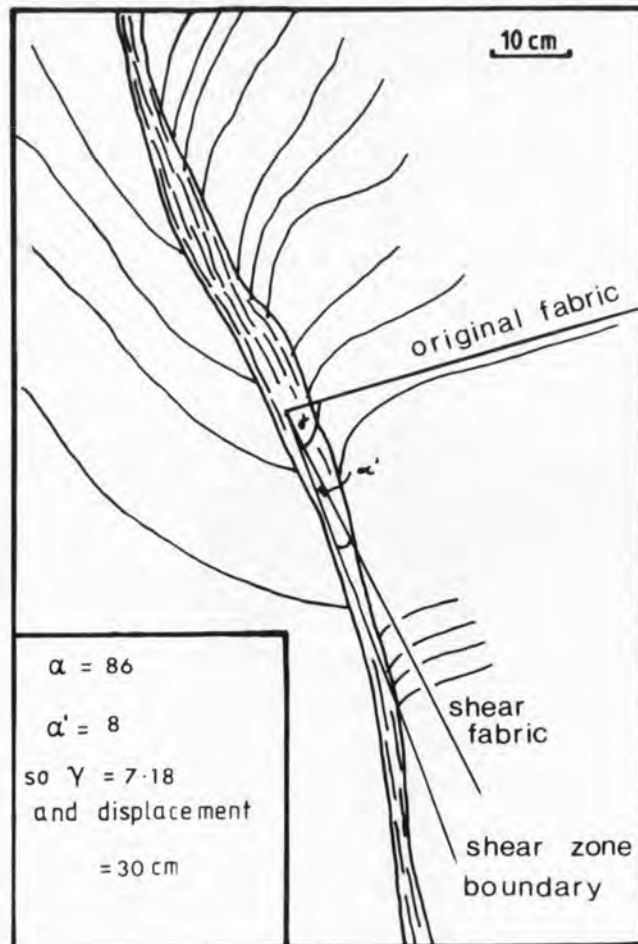
Using the above equation for the fold axes near Achmelvich (Fig. 7.1) an average value of  $\gamma$  of 6 - 10 is obtained. The main component of  $\gamma$  comes from  $\cot \alpha'$  which is a small and imprecisely determined value, partly due to lack of exposure and partly due to the non-perfectly planar margin of the shear belt. The shear belt varies in width from 0.5 to 1 kilometer which gives a displacement of 5 to 10 kilometers; this being a minimum value of displacement. The vertical face of a small 5 centimeter wide shear zone (Fig.7.6) gives a vertical displacement of 30 centimeters. This displacement across such a

FIG. 7.6(a) Small shear zone, just south of Lochinver (O88217).

FIG. 7.6(b) Diagram of the same shear zone showing an estimate of the displacement.



A



B

narrow zone indicates that it is possible to obtain large displacements across shear zones 0.5 km wide, such as the Canisp shear zone at Achmelvich. Unfortunately it is not possible to estimate how much movement occurred during the Inverian and how much during Laxfordian shearing.

#### 7.5. RELATIONSHIP BETWEEN DEFORMATION AND METAMORPHISM

It is obvious that deformation and metamorphism during both the Inverian and Laxfordian were intimately related, but it is very difficult to decide which came first. Fluids are essential for the Inverian retrogression and deformation is easier if fluids are present. Fyfe et al. (1978) suggest that it is metamorphism which triggers deformation, because the influx of water causes weakening of the rocks. However it is difficult to envisage how mantle-derived fluids could reach the middle crust unless deformation was in progress, and the vertical structures already in existence. This problem, in relation to the Lewisian, has recently been discussed by Beach (1976, 1980).

There are two main processes by which deformation occurs (Beach, 1980):

- (1) by diffusion along grain boundaries
- (2) by the movement of dislocations

Deformation causes an increase in the internal energy of a crystal resulting in the production of dislocations and recrystallization. This recrystallization to smaller aggregates of grains particularly the recrystallization of quartz lenses (Fig.5.2b) occurs during the Inverian. The resulting reduction in grain size produces a larger grain boundary area encouraging diffusion thus aiding further deformation. If

metamorphism is occurring with the nucleation of new phases the grain size is obviously going to be reduced; in turn facilitating deformation. Thus the development of new mineral assemblages with the associated grain size reduction, clearly enables deformation to proceed more easily. The catalyst for the metamorphic reactions is the influx of fluids, which is easier if deformation is proceeding. Thus the metamorphism seems to require deformation to occur first, while the deformation is more likely to occur if metamorphic reactions are taking place. What is clear however, is that once a zone of metamorphism and deformation with concomitant grain size reduction has developed, this will be a permanent zone of strain softening, explaining why structures are continually reactivated (Watterson, 1975). The 1 km wide Canisp shear zone has suffered deformation over a protracted period possibly as much as 300 million years. As the zone was uplifted with time the deformation style changed, becoming more brittle and confined to narrower zones (as discussed by Grocott, 1977). Presumably metamorphism and deformation ceased when fluid pressures fell.

The large amount of displacement that occurs across these zones suggests these structures are equivalent to faults, and presumably resulted from a stress system similar to that for faults. As discussed by Beach (1980) this stress system may enable fluid to migrate to a dilatant zone, as in the tectonic pumping model of Sibson et al. (1975). The influx of fluids then allows both deformation and metamorphism to proceed. This is consistent with the fact that the retrogression of Inverian assemblages occurred early in the history of Inverian/Laxfordian deformation.

## 7.6. CONCLUSIONS

The history of the Canisp shear zone falls into two main parts:

(1) formation of the steep limb of the Lochinver antiform with the associated retrogression of Scourian granulites to a plag-hb  $\pm$  qz  $\pm$  bi assemblage. This was followed by the intrusion of the Scourie dykes with the synchronous formation of shear zones

(2) deformation in Laxfordian shear zones with the development of a new schistosity and lineation and an associated reduction in grain size.

There was probably fairly continuous deformation from the onset of the Inverian, through the period of dyke intrusion to the late shearing. As mentioned in Chapter 1, these late shear zones are probably best described as the last phase of the Inverian event rather than Laxfordian. However, the Laxfordian terminology is still used to conform with the traditional usage.

The overall sense of vertical movement is south-side-up, bringing Inverian amphibolite facies rocks on the north side of the Canisp shear zone down to the same level as granulites to the south. This is the same sense of movement as determined by Davies (1976, 1978) for the Laxford front but differs from that of Beach et al. (1974). It is felt that the south-side-up interpretation is geologically more reasonable. The movement across these shear zones is given schematically in Fig.7.8, which shows how the northern mainland Lewisian can be divided into "faulted" blocks with zones of granulite facies gneisses between ductile shear zones. It is possible to consider the whole Lewisian as being part of a major shear zone with the granulite facies areas being low deformation lenses between areas of ductile deformation.

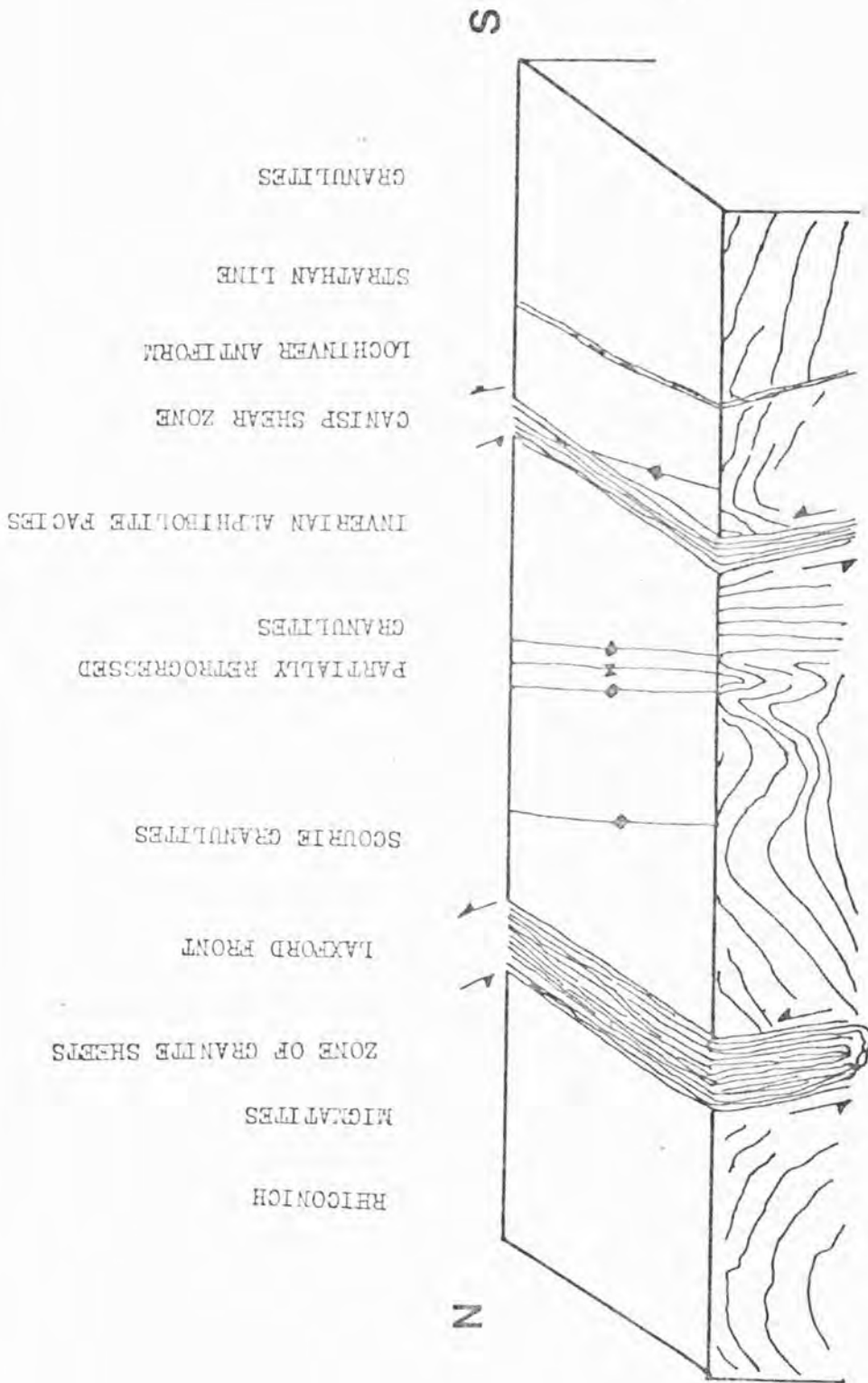


FIG. 7.8 Schematic cross section through the northern mainland Lewisian.

Fig.7.8 shows a schematic section from south to north, starting in gently southerly-dipping granulites. The first Inverian structure reached, as one goes north, is the Strathan line (Chapter 1; Evans and Lambert, 1974) which closely resembles the Canisp shear zone but is smaller. To the north of the Strathan line the gneisses have more Inverian structures and are more retrogressed than to the south. The Canisp shear zone has steeply dipping amphibolite facies gneisses to the north. Further northwards, one successively goes through amphibolite facies gneisses, partially retrogressed gneisses and then granulites (near Scourie) with the amount of Inverian deformation decreasing. This appears to be an oblique section through the crust. The Laxford front then brings down Laxfordian migmatites and amphibolite facies gneisses that appear never to have been through a granulite facies event (Sheraton et al., 1973a). There is probably also a large amount of horizontal movement across these zones; 35 km in the Laxford front (Davies, 1978) and possibly 5-10 km in the Canisp shear zone. This however depends on the interpretation of the rotation of NE-trending folds, which is equivocal.

The association of these ductile faults with retrogression by mantle-derived  $H_2O$  and the intrusion of dykes suggests they may extend down to the Moho.

The initial development of these zones appears to require the build up of a regional stress system, the cause of which is uncertain. Watterson (1978) relates these stresses and resulting transcurrent structures in the Archaean of Greenland and Scotland to the Proterozoic northwards collision and indentation of the Ketilidian block into the Archaean craton, in a way which is analogous to the recent transcurrent faults in S.China which are caused by the collision between the Indian

and Eurasian plates (Molnar and Tapponnier, 1977). Once the zone of weakness has been established due to grain size reduction, it will be continually reactivated (Watterson, 1975).

SUMMARY OF  
CONCLUSIONS

## CONCLUSIONS

This thesis falls into two main parts; the first looking at the petrogenesis and metamorphism of mafic rocks in the Assynt region providing information concerning the development of the continental crust in its early stages and its subsequent thermal evolution. This work is complementary to that of Weaver and Tarney (in press) who examined the petrogenesis of the quartzo-feldspathic rocks. The second part looks at the metamorphic and structural evolution of the Assynt region during later reworking. A list of the main suggestions made in this thesis will now be given.

(1) The sequence of events in the early evolution of the complex appears to be firstly the emplacement of ultramafic-mafic bodies into metasediment followed by the intrusion of vast volumes of tonalitic magma causing break up of the early mafic rocks. This was followed by a period of ductile deformation causing isoclinal folding and metamorphism to granulite grade. This sequence of events is essentially the same as that in the Fiskenaasset region of south-west Greenland and in the Kohistan region of the Karakorum range in Pakistan suggesting it is a feature of crustal growth in general.

(2) The layered bodies comprise ultramafic rocks (amphibole-spinel-herzolites) and mafic rocks (garnetiferous gabbros) believed to be derived from the same liquid. The rocks fall on a tholeiitic iron-enrichment trend and have moderate levels of incompatible trace elements with flat to LREE enriched rare-earth patterns. The ultramafic rocks are thought to be partial cumulates derived by olivine (and possibly orthopyroxene) settling from a tholeiitic magma with 15-20% MgO; the gabbros

being the derivative liquids. The magma was formed by 30-40% partial melting of an undepleted mantle. This liquid is more magnesian than most modern day oceanic lavas but in the Archaean the higher rate of heat production is likely to cause a greater degree of partial melting with the genesis of more magnesian liquids. The genesis of the ultramafic-gabbro bodies is not directly related to the formation of the tonalitic rocks.

(3) It is tentatively suggested that the mafic rocks in the Scourian are fragments of an early basaltic crust upon which the Scourian complex developed. There are many similarities between these Archaean high-grade gneiss terrains and the deeper levels of Cordilleran batholiths (Tarney 1976; Windley and Smith, 1976; Weaver and Tarney, in press) but in the Lewisian there is one significant difference; there is no older crust, i.e. there are no equivalents of the Amitsôq gneisses of West Greenland. So, in the initial stages, crustal growth must have taken place on oceanic crust. The generation of the tonalitic gneisses is best accounted for by the partial melting of the downgoing slab with a garnet residue and it is suggested that the mafic-ultramafic rocks formed the lower parts of a thickened oceanic crust at the base of an island arc. As plutonism continued and the amount of tonalitic rocks increased, the situation may have more nearly represented a Cordilleran margin, at any rate one can say that the complex developed at a destructive plate boundary. The mafic rocks are all tholeiitic but they differ from modern MORB in having higher LIL elements and LREE enriched patterns, they differ from island arc tholeiites in having higher Ni contents. However the depletion of modern MORB, and hence their source mantle, in LIL and the LREE is thought to be due to the fact that these elements reside in the crust. Before the period of widespread crustal growth that occurred

in the late Archaean (3.0 - 2.7 b.y.) the mantle would have had higher concentrations of these elements with the resulting mantle melts being slightly LREE enriched as is found in the Scourian and many other Archaean areas (e.g. Arth and Hanson, 1975; Condie, 1976).

(4) The ultramafic-gabbro bodies completely recrystallized at granulite facies, the peak conditions recorded by inferred gt-cpx±amph±plag assemblages being about 1000°C and 12-15 kb. Uplift and slow cooling caused complete or partial breakdown to opx+plag±sp±amph±magt symplectites. The Fe-Mg exchange reactions between coexisting gt-cpx and cpx-opx pairs "closed" at about 800-900°C at pressures of 9-14 kb. Oxide and spinel grains continued re-equilibrating to much lower temperatures. The uniform composition of the large garnets indicates that temperatures were in excess of 700°C for a considerable period of time (Yardley, 1977).

(5) The garnet stability was shown to depend on both P-T conditions and whole-rock composition, garnet becoming unstable in more magnesian rocks as the temperature fell, however temperatures were never high enough for garnet peridotite to be stable.

(6) It is possible that the mafic rocks were tectonically intercalated with the tonalitic gneisses by being pulled-off the downgoing slab in a subduction zone (Weaver and Tarney, in press) in which case the high P-T might reflect conditions in the slab. However calcic-mesoperthites found in discordant trondjhemitic sheets need very high temperatures to rehomogenize them; implying that the whole complex experienced these conditions. It would be interesting to date the formation of the garnet-clinopyroxene assemblages; this theoretically being

possible by the Nd-Sm method. It is believed however that the mafic rocks represent crust invaded by tonalite rather than the subducting slab itself. These pressures imply crustal thicknesses of 35-45 km ; the presence of a crust of 25-30 km thick in NW Scotland today (Bamford and Prodehl, 1977) either means the crust was at least 60 km thick in the Archaean or that it has since grown by further underplating.

(7) One of the problems in examining the thermal evolution of an area is the fact that the precise date of mineral growth is unknown. This problem is particularly critical in a complex that has cooled very slowly, such as the Scourian. For example it is not known at what time the garnet symplectites developed. The granulite facies conditions recorded here seem to indicate a fairly rapid decline in temperature at a fairly constant pressure, i.e. the geotherm is convex towards the temperature axis as was also suggested by O'Hara (1977) and Rollinson (1978). This is more consistent with a magmatically thickened crust than a tectonically thickened one (England and Richardson, 1977; Wells, 1980). This seems reasonable in light of the vast amounts of new tonalitic magma added to the crust.

(8) Large amphibolite facies mafic masses, and amphibolite facies layers and lenses which are not obviously related to the layered bodies have a similar chemistry and are believed to be retrogressed equivalents. However small hornblendite pods and lenses, which may be derived from mafic or ultramafic material, have had their composition modified by the prolonged metamorphism so that their origin is unclear. These pods result from the extreme fragmentation of mafic material before the peak of the granulite facies event. Minor amounts of gt-qz-bi±hb gneisses commonly bordering mafic bodies are believed to be semi-pelitic metasediment.

(9) After the granulite facies event the complex was reworked during the Inverian, the style of deformation becoming more brittle as the Lewisian complex was uplifted. One of the main features of Inverian and Laxfordian deformation in Assynt is its extreme heterogeneity. The Inverian event began with the development of NW-trending open folds followed by NW-trending monoclinical folds associated with the retrogression of the granulites to amphibolite facies. Most of the retrogression occurred before the intrusion of the Scourie dykes; both dykes and gneisses however suffering minor amounts of further Inverian deformation. The Laxfordian in Assynt is represented by the development of narrow shear zones, no major chemical changes occurring, only recrystallization of pre-existing amphibolite facies assemblages with concomitant grain size reduction.

(10) The production of a uniform hb-plag±qz assemblage caused a redistribution of elements within the complex resulting in greater inter-element correlations (Beach and Tarney, 1978). This study demonstrates the formation of a very uniform plagioclase composition ( $An_{25-30}$ ) in gneisses of all compositions and a uniform tschermakitic or pargasitic hornblende. The hornblende and biotite compositions are shown to depend on both whole-rock composition and paragenesis.

(11) Granulite facies ultramafic rocks retrogress to a chl-trem-magt±tct±anth assemblage with dolomite becoming abundant in Laxfordian shear zones. The succession of assemblages developed suggest that retrogression was caused by the addition of water and took place along a falling temperature path. It is impossible to define P-T conditions precisely but they were probably in the range 700°-500°C and moderate pressures throughout the Inverian and Laxfordian. Retrogressed ultramafic rocks have lost Na and Sr and serpentinitised samples have lost Ca.

(12) Granulite facies mafic rocks retrogress to a plag-hb-ep±qz assemblage by the reaction  $\text{cpx} + \text{plag} \rightarrow \text{hb}$ ; the excess Ca forming epidote. When the rocks recrystallized in Laxfordian shear zones much of this epidote disappeared.

(13) The assemblages developed in the Inverian together with gt-bi and feldspar thermometry suggest temperatures were about 600°C and remained above 500°C throughout the Inverian and Laxfordian events. Pressures are not very well constrained but are probably in the range 5-8 kb. The thermal evolution deduced here is essentially the same as that of O'Hara (1977) except the peak granulite facies temperatures from this study are lower and the Inverian temperatures higher.

(14) The retrogression was caused by the influx of large volumes of mantle derived water with  $\text{CO}_2$  pressures building up locally. Although elements were redistributed, probably on the scale of a few metres, it is very difficult to establish whether or not elements were gained or lost by the complex as a whole, but it is possible that there was a net gain of Sr.

(15) Small, slightly deformed, amphibolite dykes from the east end of Clashnessie Bay are tholeiitic andesites and could be derived from a primary mantle melt by hornblende fractionation. The dykes are probably a very early phase of the Scourie dykes which were deformed and metamorphosed before the intrusion of the main dyke swarm.

(16) The Canisp shear zone, north of Lochinver, has an extended history of metamorphism and deformation from the beginning of the Inverian with the development of the Lochinver antiform. The steep limb of this fold was the focus for the intrusion of ultramafic Scourie dykes and

Laxfordian shearing. If the rotation of NE-trending folds in the Achmelvich area was caused by a component of simple shear in this zone, there has been at least 5 - 10 km of right lateral displacement across the Canisp shear zone. The Scourian is thus divided into a series of "faulted" blocks separated by long lived zones of weakness such as the Canisp and Laxford front shear zones (Davies, 1978).

In summary, therefore, the mafic and ultramafic rocks are thought to represent parts of the Archaean oceanic crust, possibly thickened under an island arc, broken up and invaded by the intrusion of large volumes of tonalitic magma. The thickened crust and the thermal input from the magmas gave rise to the high P-T conditions recorded for the peak of metamorphism. The Assynt region was then reworked in NW-trending vertical belts, ca 2.4 b.y., with associated retrogression caused by the influx of mantle derived hydrous-fluids. The reason for the influx of these fluids is far from clear. The retrogression, dyke emplacement and shearing took place along a falling temperature scale in the range 700 - 500°C. The Assynt region thus provides an excellent area for the examination of the evolution of a gneiss complex as it is uplifted and cooled over a long period of at least 1.0 b.y. .

## REFERENCES

## REFERENCES

- D.E. ANDERSON and G.R. BUCKLEY (1973) Zoning in garnets-diffusion models. *Contrib. Mineral. Petrol.* 40, 87-104.
- N.T. ARNDT (1977) Ultrabasic magmas and high-degree melting of the mantle. *Contrib. Mineral. Petrol.* 64, 205-221.
- N.T. ARNDT, A.J. NALDRETT and D.R. PYKE (1977) Komatiitic and iron-rich tholeiitic lavas of Munro Township, Northern Ontario. *J. Petrol.* 18, 319-369.
- J.G. ARTH (1976) Behaviour of trace elements during magmatic processes - a summary of theoretical models and their applications. *J. Res. U.S. Geol. Surv.* 4, 41-47.
- J.G. ARTH, N.T. ARNDT and A.J. NALDRETT (1977) The genesis of Archaean komatiites from Munro Township, Ontario: trace element evidence. *Geology* 5, 590-594.
- J.G. ARTH and G.N. HANSON (1975) Geochemistry and origin of the early Precambrian crust of north eastern Minnesota. *Geochim. Cosmochim. Acta* 39, 325-362.
- J. BAK, J. KORSTGART and K. SØRENSEN (1975) A major shear zone within the Nagssugoqidian of W. Greenland. *Tectonophys.* 27, 191-209.
- E. BALTATZIS (1979) Distribution of Fe-Mg between coexisting garnet and biotite in Scottish Barrovian zones. *Mineral. Mag.* 43, 155-157.
- D. BAMFORD and C. PRODEHL (1977) Explosion seismology and the continental crust-mantle boundary. *J. Geol. Soc. Lond.* 134, 139-151.

- J.P. BARD (1970) Composition of hornblendes formed during the Hercynian progressive metamorphism of the Aracena metamorphic belt (S.W. Spain). *Contrib. Mineral. Petrol.* 28, 117-134.
- A.C. BARNICOAT and M.J. O'HARA (1979) High temperature pyroxenes from an ironstone at Scourie, Sutherland. *Mineral. Mag.* 43, 371-375.
- J.M. BARTON, R.E.P. FRIPP, P. HORROCKS and N. McLEAN (1979) The geology, age and tectonic setting of the Messina layered intrusion, Limpopo mobile belt, southern Africa. *Am. J. Sci.* 279, 1108-1135.
- A. BEACH (1973) The mineralogy of high temperature shear zones at Scourie, N.W. Scotland. *J. Petrol.* 14, 231-248.
- A. BEACH (1974a) Amphibolitization of Scourian granulites. *Scott. J. Geol.* 10, 35-43.
- A. BEACH (1974) The measurement and significance of displacements on Laxfordian shear zones. *Proc. Geol. Ass.* 85, 13-22.
- A. BEACH (1976) The interrelations of fluid transport, deformation, geochemistry and heat flow in early Proterozoic shear zones in the Lewisian complex. *Phil. Trans Roy. Soc. Lond. A* 280, 569-604.
- A. BEACH (1980) Retrogressive metamorphic processes in shear zones with special reference to the Lewisian complex. *J. Struct. Geol.* 2, 257-263.
- A. BEACH, M.P. COWARD and R.H. GRAHAM (1974) An interpretation of the structural evolution of the Laxford Front, N.W. Scotland. *Scott. J. Geol.* 9, 297-308.
- A. BEACH and W.S. FYFE (1972) Fluid transport and shear zones at Scourie, Sutherland; evidence of overthrusting. *Contrib. Mineral. Petrol.* 36, 175-180.

- A. BEACH and J. TARNEY (1978) Major and trace element patterns established during retrogressive metamorphism of granulite facies gneisses, N.W. Scotland. *Precamb. Res.* 7, 325-348.
- R.A. BINNS (1965) Mineralogy of metamorphosed basic rocks from the Willyama Complex, Broken Hill district, New South Wales: Pt 1 Hornblendes. *Mineral. Mag.* 35, 306-326.
- G.W. BIRD and J.J. FAWCETT (1975) Stability relations of Mg-chlorite, muscovite and quartz between 5 and 10 kb water pressure. *J. Petrol.* 14, 415-428.
- S.R. BOHLEN and E.J. ESSENE (1980) Evaluation of coexisting garnet-biotite, garnet-clinopyroxene and other Mg-Fe exchange thermometers in the Adirondack granulites: summary. *Bull. Geol. Soc. Am.* 91, 107-109.
- C.R. BOWDIDGE (1969) Petrological studies of Lewisian basic and ultrabasic rocks near Scourie, Sutherland. Unpubl. Ph.D. thesis, Univ. of Edinburgh.
- D.R. BOWES (1969) The Lewisian of the north-west highlands of Scotland. In: *North Atlantic - Geology and Continental Drift Symposium* (M. Kay, ed.) *Mem. Amer. Assoc. Petrol. Geol.* 12, 575-594.
- D.R. BOWES, W.R. SKINNER and A.E. WRIGHT (1970) Petrochemical comparisons of the Bushveld igneous complex and other layered intrusions. *Spec. Pub. Geol. Soc. S.Afr* 1, 425-440.
- D.R. BOWES, A.E. WRIGHT and R.G. PARK (1964) Layered intrusive rocks in the Lewisian of the north-west highlands of Scotland. *J. Geol. Soc. Lond.* 120, 153-192.

- D.R. BOWES, A.E. WRIGHT and R.G. PARK (1966) Origin of ultrabasic and basic masses in the Lewisian. *Geol. Mag.* 103, 280-285.
- D. BRIDGEWATER, A. ESCHER and J. WATTERSON (1973) Tectonic displacements and thermal activity in two contrasting Proterozoic mobile belts from Greenland. *Phil. Trans. Roy. Soc. Lond.* A273, 513-535.
- K.H. BRODIE (1980) Variations in mineral chemistry across a shear zone in phlogopite peridotite. *J. Struct. Geol.* 2, 265-272.
- A.F. BUDDINGTON and D.H. LINDSLEY (1964) Iron titanium oxide minerals and synthetic equivalents. *J. Petrol.* 5, 310-357.
- C.W. BURNHAM, J.R. HOLLOWAY and N.F. DAVIS (1969) Thermodynamic properties of water to 1000°C and 10,000 bars. *Spec. Paper Geol. Soc. Am.* 132, 96 pp.
- B.C.M. BUTLER (1967) Chemical study of minerals from the Moine schists of the Ardnamurchan area, Argyllshire, Scotland. *J. Petrol.* 8, 233-267.
- I.H. CAMPBELL (1977) A study of macrorhythmic layering and cumulate processes in the Jimberlana intrusion, West Australia. Part 1: Upper layered series. *J. Petrol.* 18, 183-215.
- D.M. CARMICHAEL (1969) On the mechanism of prograde metamorphic reactions in quartz-bearing pelitic rocks. *Contrib. Mineral. Petrol.* 20, 244-267.
- I.S.E. CARMICHAEL, F.J. TURNER and J. VERHOOGEN (1974) *Igneous Petrology*. McGraw Hill, New York, 729 pp.
- R.G. CAWTHORN (1976) Melting relations in part of the system CaO-MgO- $Al_2O_3$ - $SiO_2$ - $Na_2O$ - $H_2O$  under 5 kb pressure. *J. Petrol.* 17, 44-72.

- R.G. CAWTHORN and J.R. McIVER (1977) Nickel in komatiites. *Nature* 266, 716-718.
- H.J. CHAPMAN (1978) Geochronological and isotope geochemistry of Precambrian rocks, N.W. Scotland. Unpubl. D.Phil. thesis, Univ. of Oxford.
- H.J. CHAPMAN (1979) 2390 Myr. Rb-Sr whole rock isochron for the Scourie Dykes of N.W. Scotland. *Nature* 277, 642.
- H.J. CHAPMAN and S. MOORBATH (1977) Lead isotope measurements from the oldest recognised Lewisian gneisses of N.W. Scotland. *Nature* 268, 41-42.
- B.W. CHAPPELL and A.J.R. WHITE (1970) Mineralogy of an "eclogite" from Sittampundi. *Mineral. Mag.* 37, 555-561.
- N.D. CHATTERJEE and E. FROESE (1975) A thermodynamic study of the pseudobinary join muscovite-paragonite in the system  $KAlSi_3O_8-Al_2O_3-SiO_2-H_2O$ . *Am. Mineral.* 60, 985-993.
- D.B. CLARKE (1970) Tertiary basalts of Baffin Bay: possible primary magma from the mantle. *Contrib. Mineral. Petrol.* 25, 203-224.
- D.B. CLARKE and M.J. O'HARA (1979) Nickel and the existence of high-MgO liquids. *Earth Plan. Sci. Lett.* 44, 153-158.
- A. CHOUDARI and H.G.F. WINCKLER (1967) Anthophyllit und hornblend in einigen metamorphen reactionen. *Contrib. Mineral. Petrol.* 14, 293-315.
- J.W. COLBY (1971) Magic IV a computer programme for quantitative electron microprobe analysis. Unpub ms.
- K.C. CONDIE (1967) Geochemistry of early Precambrian greywackes from Wyoming. *Geochim. Cosmochim. Acta* 31, 2135-2149.

- K.C. CONDIE (1976) Trace element geochemistry of Archaean greenstone belts. *Earth Sci. Rev.* 12, 393-417.
- K.C. CONDIE, C.K. BARSKY and P.A. MUELLER (1969) Geochemistry of Precambrian diabase dykes from Wyoming. *Geochim. Cosmochim. Acta* 33, 1371-1388.
- M.P. COWARD (1976) Strain within ductile shear zones. *Tectonophys.* 34, 181-197.
- M.P. COWARD, P.W. FRANCIS, R.H. GRAHAM, J.S. MYERS and J.V. WATSON (1969) Remnants of an early metasedimentary assemblage in the Lewisian complex of the Outer Hebrides. *Proc. Geol. Ass.* 80, 387-408.
- M.P. COWARD, R.H. GRAHAM, P.R. JAMES and J. WAKEFIELD (1973) A structural interpretation of the northern margin of the Limpopo orogenic belt. *Phil. Trans. Roy. Soc. Lond.* A273, 487-491.
- M.P. COWARD, J.H. KIM and J. PARKE (1980) A correlation of Lewisian structures and their displacement across the lower thrusts of the Moine thrust zone, N.W. Scotland. *Proc. Geol. Ass.* 91, 327-337.
- P.A. DANCKWERTH and R.C. NEWTON (1978) Experimental determination of the spinel peridotite to garnet peridotite reaction in the system  $MgO-Al_2O_3-SiO_2$  in the range  $900^\circ - 1100^\circ$  and  $Al_2O_3$  isopleths of enstatite in the spinel field. *Contrib. Mineral. Petrol.* 66, 189-201.
- F.B. DAVIES (1974) A layered basic complex in the Lewisian, south of Loch Laxford, Sutherland. *J. Geol. Soc. Lond.* 130, 279-284.
- F.B. DAVIES (1975) Origin and ancient history of gneisses older than 2800 m.y. in the Lewisian complex. *Nature* 258, 589-591.

F.B. DAVIES (1976) Early Scourian structures in the Scourie-Laxford region and their bearing on the evolution of the Laxford front. *J. Geol. Soc. Lond.* 132, 543-554.

F.B. DAVIES (1978) Progressive simple shear deformation on the Laxford shear zone, Sutherland. *Proc. Geol. Ass.* 89, 177-196.

H.W. DAY (1975) The high temperature stability of muscovite and quartz. *Am. J. Sci.* 58, 225-262.

R. DEARNLEY (1963) The Lewisian complex of South Harris, with some observations on the metamorphosed basic intrusions of the Outer Hebrides, Scotland. *J. Geol. Soc. Lond.* 119, 243-312.

W.A. DEER, R.A. HOWIE and J. ZUSSMAN (1966) An introduction to the rock-forming minerals. Longman (Lond.) 528 pp.

M.J. DRAKE and D.F. WEILL (1975) Partitioning of Sr, Ba, Ca, Y,  $\text{Eu}^{2+}$ ,  $\text{Eu}^{3+}$  and other REE between plagioclase feldspar and magmatic liquid: an experimental study. *Geochim. Cosmochim. Acta* 38, 689-712.

S.A. DRURY (1974) Chemical changes during retrogressive metamorphism of Lewisian granulite facies rocks from Coll and Tiree. *Scott. J. Geol.* 10, 237-256.

D.J. ELLIS and D.H. GREEN (1979) An experimental study of the effect of Ca upon garnet-clinopyroxene Fe-Mg exchange equilibria. *Contrib. Mineral. Petrol.* 71, 13-22.

A.E.J. ENGEL and C.G. ENGEL (1962) Hornblendes formed during progressive metamorphism of amphibolites, north west Adirondack mountains, New York. *Bull. Geol. Soc. Am.* 73, 1499-1514.

- C.G. ENGEL and R.L. FISHER (1975) Granitic to ultramafic rock complexes of the West Indian Ocean ridge system, Western Indian Ocean. Bull. Geol. Soc. Am. 86, 1553-1578.
- P.C. ENGLAND and S.W. RICHARDSON (1977) The influence of erosion upon the mineral facies of rocks from different metamorphic environments. J. Geol. Soc. Lond. 134, 201-213.
- A. ESCHER, S. JACK and J. WATTERSON (1976) Tectonics of the North Atlantic Proterozoic dyke swarm. Phil. Trans. Roy. Soc. Lond. A280, 529-539.
- J. ESSON, A.C. DUNHAM and R.N. THOMPSON (1975) Low alkali, high calcium olivine tholeiite lavas from the Isle of Skye, Scotland. J. Petrol. 16, 488-497.
- B.W. EVANS and V. TROMMSDORFF (1970) Regional metamorphism of ultramafic rocks in the Central Alps: parageneses in the system  $\text{CaO-MgO-SiO}_2\text{-H}_2\text{O}$ . Schweiz. Mineral. Petrog. Mitt. 50, 481-492.
- B.W. EVANS and V. TROMMSDORFF (1974) Stability of enstatite + talc and  $\text{CO}_2$  metasomatism of metaperidotites, Val d'Efra, Lepontine Alps. Am. J. Sci. 274, 274-296.
- C.R. EVANS (1965) Geochronology of the Lewisian basement near Lochinver, Sutherland. Nature 207, 54-56.
- C.R. EVANS and R. St.J. LAMBERT (1974) The Lewisian of Lochinver, Sutherland: the type area for the Inverian metamorphism. J. Geol. Soc. Lond. 130, 125-150.
- J.M. FERRY and F.S. SPEAR (1978) Experimental calibration of partitioning of Fe and Mg between biotite and garnet. Contrib. Mineral. Petrol. 66, 113-118.

- P.A. FLOYD and J.A. WINCHESTER (1975) Magma type and tectonic setting discrimination using immobile elements. *Earth Plan. Sci. Lett.* 27, 211-218.
- D.G. FRASER and P.J. LAWLESS (1978) Palaeogeotherms: implications for disequilibrium in garnet lherzolite xenoliths. *Nature* 273, 220-222.
- F.A. FREY, L.A. HASKIN and M.A. HASKIN (1971) Rare-earth abundances in some ultramafic rocks. *J. Geophys. Res.* 76, 2057-2070.
- F.A. FREY, W.B. BRYAN and G. THOMPSON (1974) Atlantic ocean floor geochemistry and petrology of basalts from Legs 2 and 3 of the Deep Sea Drilling Project. *J. Geophys. Res.* 79, 5507-5527.
- R.B. FROST (1975) Contact metamorphism of serpentinite, chloritic black-wall and rodingite at Paddy-Go-Easy Pass, Central Cascades, Washington. *J. Petrol.* 16, 272-313.
- W.S. FYFE (1973) The granulite facies, partial melting and the Archaean crust. *Phil. Trans. Roy. Soc. Lond.* A273, 457-461.
- W.S. FYFE (1978) The evolution of the earth's crust: modern plate tectonics to ancient hot spot tectonics? *Chem. Geol.* 23, 89-114.
- W.S. FYFE and A.R. McBIRNEY (1975) Subduction and the structure of andesitic volcanic belts. *Am. J. Sci.* 275-A, 285-297.
- W.S. FYFE, N.J. PRICE and A.B. THOMPSON (1978) *Fluids in the Earth's Crust.* Elsevier, 383 pp.
- J. GANGULY (1979) Garnet and clinopyroxene solid solutions and geothermometry based on Fe-Mg distribution coefficient. *Geochim. Cosmochim. Acta*, 43, 1021-1029.

- J. GANGULY and G.C. KENNEDY (1974) The energetics of natural garnet solid solution. 1 Mixing of alumina-silicate end members. *Contrib. Mineral. Petrol.* 48, 137-148.
- R.C.O. GILL and D. BRIDGEWATER (1979) Early Archaean basic magmatism in West Greenland: the geochemistry of the Ameralik dykes. *J. Petrol.* 20, 695-726.
- A.Y. GLIKSON (1971) Primitive Archaean element distribution patterns: chemical evidence and geotectonic significance. *Earth Plan. Sci. Lett.* 12, 309-320.
- D.S. GOLDMAN and A.L. ALBEE (1977) Correlation of Mg/Fe partitioning between garnet and biotite with  $^{18}\text{O}/^{16}\text{O}$  partitioning between quartz and magnetite. *Am. J. Sci.* 277, 750-767.
- R. GORBATSHEV (1969) Element distribution between biotite and Ca-amphibole in some igneous and pseudo-igneous plutonic rocks. *Neues. Jarbh. Miner. Abh.* 111, 314-342.
- D.H. GREEN (1975) Genesis of Archaean peridotitic magmas and constraints on Archaean geothermal gradients. *Geology* 3, 15-18.
- D.H. GREEN and W. HIBBERSON (1970) The instability of plagioclase in peridotite at high pressures. *Lithos* 3, 209-221.
- D.H. GREEN and A.E. RINGWOOD (1967) An experimental investigation of the gabbro to eclogite transformation and its petrological applications. *Geochim. Cosmochim. Acta* 31, 767-833.
- T.H. GREEN, A.O. BRUNFELT and K.S. HEIER (1972) Rare earth element distribution and K/Rb ratios in granulites, mangerites and anorthosites, Lofoten-Verstaalen, Norway. *Geochim. Cosmochim. Acta* 36, 241-256.

- H.J. GREENWOOD (1963) The synthesis and stability of anthophyllite.  
J. Petrol. 4, 317-351.
- H.J. GREENWOOD (1967) Mineral equilibria in the system  $MgO-SiO_2-H_2O-CO_2$ .  
In: Researches in Geochemistry Vol.2 (P.H.Abelson ed.) Wiley, pp.542-567.
- H.J. GREENWOOD (1971) Anthophyllite, corrections and comments on its  
stability. Am. J. Sci. 270, 151-154.
- W.L. GRIFFIN and K.S. HEIER (1973) Petrological implications of some  
corona structures. Lithos 6, 315-335.
- J. GROCOTT (1977) The relationship between Precambrian shear belts and  
modern fault systems. J. Geol. Soc. Lond. 133, 257-262.
- P.J. HAMILTON, N.M. EVENSON, R.J. O'NIONS and J. TARNEY (1979) Sm-Nd  
systematics of Lewisian gneisses: implications for the origin of granulites.  
Nature 277, 25-28.
- S.R. HART and K.E. DAVIS (1978) Nickel partitioning between olivine and  
silicate melt. Earth Plan. Sci. Lett. 40, 203-219.
- C.J. HAWKESWORTH and R.K. O'NIONS (1977) The petrogenesis of some  
Archaean volcanic rocks from South Africa. J. Petrol. 18, 487-520.
- K.S. HEIER (1973) Geochemistry of granulites and problems of their origin.  
Phil. Trans. Roy. Soc. Lond. A273, 429-442.
- H.C. HELGESON, J.M. DELANEY, H.W. NESBITT and D.K. BIRD (1978) Summary  
and critique of the thermodynamic properties of rock-forming minerals.  
Am. J. Sci. 278-A, 1-29.
- B.J. HENSON and D.H. GREEN (1973) Experimental study of the stability of  
cordierite and garnet in pelitic compositions at high pressures and  
temperatures. III Syntheses of experimental data and geological applica-  
tions. Contrib. Mineral. Petrol. 38, 151-166.

C.T. HERZBERG (1975) Phase assemblages in the system  $\text{CaO-Na}_2\text{O-MgO-Al}_2\text{O}_3\text{-SiO}_2$  in the plagioclase lherzolite and spinel lherzolite mineral facies. Unpubl. Ph.D. thesis Univ. of Edinburgh.

A. HIETANEN (1969) Distribution of Fe and Mg between garnet, staurolite and biotite in aluminium-rich schists in various metamorphic zones north of the Idaho batholith. *Am. J. Sci.* 267, 422-456.

F.N. HODGES and J.J. PAPIKE (1976) DSDP Site 334: magmatic cumulates from oceanic layer 3. *J. Geophys. Res.* 81, 4135-4151.

J.G. HOLLAND and R. St. J. LAMBERT (1975) The chemistry and origin of the Lewisian gneisses of the Scottish mainland: the Scourie and Inver assemblages and subcrustal accretion. *Precamb. Res.* 2, 161-188.

J.R. HOLLOWAY and C.W. BURNHAM (1972) Melting relations of basalts with equilibrium water pressures less than total pressure. *J. Petrol.* 13, 1-29.

A.M. HOPGOOD and D.R. BOWES (1972) Application of structural sequence to the correlation of Precambrian gneisses, Outer Hebrides, Scotland. *Bull. Geol. Soc. Am.* 83, 107-128.

A.K. HOR, D.K. HUTT, J.V. SMITH, J. WAKEFIELD and B.F. WINDLEY (1975) Petrochemistry and mineralogy of early Precambrian anorthositic rocks of the Limpopo Belt, Southern Africa, *Lithos* 4, 297-310.

J.A. HUNT and D.M. KERRICK (1977) The stability of sphene: experimental redetermination and geological implications. *Geochim. Cosmochim. Acta* 41, 279-288.

K. ITO and G.C. KENNEDY (1970) The fine structure of the basalt to eclogite transition. *Mineral. Soc. Am. Spec. Paper* 3, 77-83.

- P. JAKES (1973) Geochemistry of continental growth. In: Implications of Continental Drift to the Earth Sciences (D.H. Tarling and S.K. Runcorn, eds.) Academic Press, New York, 2, 999-1009.
- P. JAKES and A.J.R. WHITE (1972) Major and trace element abundances in volcanic rocks of orogenic areas. *Geol. Soc. Am. Bull.* 83, 29-40.
- M.Q. JAN (in press) Petrology of the obducted mafic and ultramafic metamorphites from the southern part of the Kohistan island arc sequence. *Proc. Geodynamics Conf. Peshawar Univ. Pakistan.*
- M.Q. JAN and R.A. HOWIE (1980) Ortho- and clino-pyroxenes from the pyroxene granulites of Swat, Kohistan, Northern Pakistan. *Mineral. Mag.* 43, 715-726.
- A.S. JANARDHAN and B.E. LEAKE (1975) The origin of meta-anorthositic gabbros and garnetiferous granulites of the Sittampundi complex, Madras. *J. Geol. Soc. India* 16, 391-408.
- W. JOHANNES (1969) An experimental investigation into the system  $MgO-SiO_2-H_2O-CO_2$ . *Am. J. Sci.* 267, 1083-1104.
- R.W. KAY, N.S. HUBBARD and P.W. GAST (1970) Chemical characteristics and origin of oceanic ridge volcanic rocks. *J. Geophys. Res.* 75, 1585-1613.
- R.W. KAY and R.G. SENECHAL (1976) The rare-earth geochemistry of the Troodos ophiolite. *J. Geophys. Res.* 81, 964-970.
- A. KERR (1979) The retrogressive breakdown of orthopyroxene in granulite-facies rocks, Sutherland. *Mineral. Mag.* 43, 443-445.
- D.M. KERRICK (1972) Experimental determination of muscovite + quartz stability with  $P_{H_2O} < P_{TOT}$ . *Am. J. Sci.* 272, 446-448.

- D.M. KERRICK (1974) Review of metamorphic mixed volatile ( $H_2O-CO_2$ ) equilibria. *Am. Mineral.* 59, 729-762.
- B.C. KING (1955) The tectonic pattern of the Lewisian around Clashnessie Bay, near Stoer, Sutherland. *Geol. Mag.* 92, 69-80.
- D.S. KORZHINSKII (1970) Theory of metasomatic zoning. Clarendon Press (Oxford). 162 pp.
- A. KRONER (1977) The Precambrian geotectonic evolution of Africa: plate accretion versus plate destruction. *Precamb. Res.* 4, 163-213.
- I. KUSHIRO (1969) The system forsterite-diopside-silica with and without water at high pressures. *Am. J. Sci.* 267, 269-294.
- I. KUSHIRO (1972) Effect of water on the composition of magma formed at high pressures. *J. Petrol.* 13, 311-334.
- R. St. J. LAMBERT (1976) Archaean thermal regimes, crustal and upper mantle temperatures and a progressive evolutionary model for the earth. In: *The Early History of the Earth* (B.F. Windley ed.) Wiley, Lond. 363-387.
- B.E. LEAKE (1965) The relationship between tetrahedral Al and the maximum possible octahedral Al in natural calciferous and subcalciferous amphiboles. *Am. Mineral.* 50, 843-851.
- B.E. LEAKE (1978) The nomenclature of amphiboles. *Mineral Mag.* 42, 533-563.
- B.E. LEAKE, G.L. HENDRY, A. KEMP, A.G. PLANT, P.K. HARVEY, J.R. WILSON, J.S. COATS, J.W. AUCOTT, T. LUNEL and R.J. HOWARTH (1969) The chemical analysis of rock powders by automatic X-ray fluorescence. *Chem. Geol.* 5, 7-86.

- D.H. LINDSLEY and S.A. DIXON (1976) Diopside-enstatite equilibria at 850-1400°C, 5-35 k bar. *Am. J. Sci.* 276, 1285-1301.
- J.G. LIOU (1973) Synthesis and stability relations of epidote,  $\text{Ca}_2\text{Al}_2\text{FeSi}_3\text{O}_{12}(\text{OH})$ . *J. Petrol.* 14, 381-413.
- T.P. LOOMIS (1975) Reaction zoning of garnet. *Contrib. Mineral. Petrol.* 52, 285-305.
- T.P. LOOMIS (1977) The kinetics of a garnet-granulite reaction. *Contrib. Mineral. Petrol.* 62, 1-22.
- M. LOUBET, N. SHIMIZU and C.J. ALLEGRE (1975) Rare earth elements in Alpine peridotites. *Contrib. Mineral. Petrol.* 53, 1-12.
- J.B. LYONS and S.A. MORSE (1970) Mg/Fe partitioning in garnet and biotite from some granitic, pelitic and calcic rocks. *Am. Mineral.* 55, 231-245.
- V.R. MCGREGOR (1973) The early Precambrian gneisses of the Godthab district, West Greenland. *Phil. Trans. Roy. Soc. Lond.* A273, 343-357.
- W.G. MELSON and G. THOMPSON (1970) Layered basic intrusion in the oceanic crust, Romanche fracture, equatorial Atlantic. *Science* 168, 817-820.
- M. MENZIES, D. BLANCHARD, J. BRANNON and R. KOROTEV (1977) Rare-earth and trace element geochemistry of a fragment of Jurassic sea floor, Point Sal, California. *Geochim. Cosmochim. Acta* 41, 1419-1430.
- P. MOLNAR and P. TAPPONNIER (1977) Relations of the tectonics of Eastern China to the Indian-Eurasian collision: application of slip-line field theory to large scale continental tectonics. *Geology* 5, 212-216.

- S. MOORBATH, J.L. POWELL and P.N. TAYLOR (1975) Isotopic evidence for the age and origin of the "grey gneiss" complex of the Southern Outer Hebrides, Scotland. *J. Geol. Soc. Lond.* 131, 213-222.
- S. MOORBATH, H. WELKE and N.H. GALE (1969) The significance of lead isotope studies in ancient high grade metamorphic basement complexes as exemplified by the Lewisian rocks of North West Scotland. *Earth Plan. Sci. Lett.* 6, 616-625.
- G.K. MUECKE (1969) Petrogenesis of granulite facies rocks from the Lewisian of N.W. Scotland. Unpub. D.Phil. Thesis, Univ. of Oxford.
- A. MYASHIRO and F. SHIDO (1975) Tholeiitic and calc-alkaline series in relation to the behaviours of titanium, vanadium, chromium and nickel. *Am. J. Sci.* 275, 265-277.
- J.S. MYERS (1976) Stratigraphy of the Fiskenaesset complex, North West Greenland, and comparison with the Bushveld and Stillwater complexes. *Rapp. Grønlands Geol. Unders.* 80, 87-92.
- B.O. MYSEN and A.L. BOETTCHER (1975) Melting of a hydrous mantle II. Geochemistry of crystals and liquids formed by anatexis of mantle peridotite at high pressures and temperatures as a function of controlled activities of water, hydrogen and carbon dioxide. *J. Petrol.* 16, 549-593.
- N. NAKAMURA (1974) Determination of REE, Ba, Fe, Mg, Na and K in carbonaceous and ordinary chondrites. *Geochim. Cosmochim. Acta* 38, 757-775.
- C.E. NEHRU and P.J. WYLLIE (1974) Electron microprobe measurement of pyroxenes, coexisting with H<sub>2</sub>O undersaturated liquid on the join CaMgSi<sub>2</sub>O<sub>6</sub>-Mg<sub>2</sub>Si<sub>2</sub>O<sub>6</sub>-H<sub>2</sub>O at 30 kilobars with applications to geothermometry. *Contrib. Mineral. Petrol.* 48, 221-228.

- R.W. NESBITT and S.-S. SUN (1976) Geochemistry of Archaean spinifex-textured peridotites and magnesian and low magnesian tholeiites. *Earth Plan. Sci. Lett.* 31, 433-453.
- R.W. NESBITT, S.-S. SUN and A.C. PURVIS (1979) Komatiites: geochemistry and genesis. *Can. Mineral.* 17, 165-186.
- R.C. NEWTON, J.V. SMITH and B.F. WINDLEY (1980) Carbonic metamorphism, granulites and crustal growth. *Nature* 288, 45-50.
- E.G. NISBET, M.J. BICKLE and A. MARTIN (1977) The mafic and ultramafic lavas of the Belingwe greenstone belt, Rhodesia. *J. Petrol.* 18, 521-566.
- M. OBATA (1976) The solubility of  $Al_2O_3$  in orthopyroxene in plagioclase peridotite and spinel pyroxenite. *Am. Mineral.* 61, 804-816.
- M.J. O'HARA (1961a) Zoned ultrabasic and basic gneiss masses in the early Lewisian metamorphic complex at Scourie, Sutherland. *J. Petrol.* 2, 248-276.
- M.J. O'HARA (1961b) The petrology of the Scourie dyke, Sutherland. *Mineral. Mag.* 32, 848-865.
- M.J. O'HARA (1965) Origin of ultrabasic and basic masses in the Lewisian. *Geol. Mag.* 102, 296-414.
- M.J. O'HARA (1968) The bearing of phase equilibria studies in synthetic and natural systems on the evolution of basic and ultrabasic rocks. *Earth Sci. Rev.* 4, 69-133.
- M.J. O'HARA (1977) Thermal history of excavation of Archaean gneisses from the base of the continental crust. *J. Geol. Soc. Lond.* 134, 185-200.
- M.J. O'HARA, S.W. RICHARDSON and G. WILSON (1971) Garnet-peridotite stability and occurrence in crust and mantle. *Contrib. Mineral. Petrol.* 32, 48-68.

- M.J. O'HARA and G. YARWOOD (1978) High pressure-temperature point on an Archaean geotherm, implied magma genesis by crustal anatexis and consequences for garnet-pyroxene thermometry and barometry. *Phil. Trans. Roy. Soc. Lond.* A288, 441-456.
- M. OKRUSCH, B. SCHRODER and A. SCHNUTGEN (1979) Granulite facies metabasite ejecta in the Laacher See area, Eifel, West Germany. *Lithos* 12, 251-270.
- P.M. ORVILLE (1972) Plagioclase cation exchange equilibria with aqueous chloride solution: results at 700°C and 2000 bars in the presence of quartz. *Am. J. Sci.* 272, 234-272.
- E.F. OSBORN (1962) Reaction series for sub-alkaline igneous rocks based on different oxygen pressure conditions. *Am. Mineral.* 47, 211-266.
- E.F. OSBORN (1969) Genetic significance of V and Ni content of andesites: comments on a paper by Taylor, Kaye, White, Duncan and Ewart. *Geochim. Cosmochim. Acta* 33, 1553-1554.
- J.J. PAPIKE, K.L. CAMERON and K. BALDWIN (1974) Amphiboles and pyroxenes, characterisation of other than quadrilateral components and estimates of ferric iron from microprobe data. *Geol. Soc. Am. Abs.* 6, 1053-1054.
- R.G. PARK (1970) Observations on Lewisian chronology. *Scott. J. Geol.* 6, 379-399.
- B.N. PEACH, J. HORNE, W. GUNN, C.T. CLOUGH, L.W. HINXMAN and J.J.H. TEALL (1907) The geological structure of the N.W. Highlands of Scotland. *Mem. Geol. Surv. Gt. Britain* 668 pp.
- J.A. PEARCE and J.R. CANN (1973) Tectonic setting of basic volcanic rocks determined using trace element analyses. *Earth Plan. Sci. Lett.* 19, 290-300.

J.A. PEARCE and M.F. FLOWER (1977) The relative importance of petrogenetic variables in magma genesis at accreting plate margins; a preliminary investigation. *J. Geol. Soc. Lond.* 134, 103-127.

J.A. PEARCE and M.J. NORRY (1979) Petrogenetic implications of Ti, Zr, Y and Nb variations in volcanic rocks. *Contrib. Mineral. Petrol.* 69, 33-347.

T.H. PEARCE, B.E. GORMAN and T.C. BIRKETT (1975) The  $TiO_2$ - $K_2O$ - $P_2O_5$  diagram: a method of discriminating between oceanic and non-oceanic basalts. *Earth Plan. Sci. Lett.* 24, 419-426.

L.L. PERCHUK (1970) Equilibrium of biotite with garnet in metamorphic rocks. *Geochem. International* 7, 157-179.

D. PERKINS, E.F. WESTRUM Jr. and E.J. ESSENE (1980) Thermodynamic properties and phase relations of some minerals in the system  $CaO-Al_2O_3-SiO_2-H_2O$ . *Geochim. Cosmochim. Acta* 44, 61-84.

R.K. POPP, M.C. GILBERT and J.R. CRAIG (1977) Stability of Fe-Mg amphiboles with respect to oxygen fugacity. *Am. Mineral.* 62, 1-12.

M.J. POTTS and K.C. CONDIE (1971) Rare earth element distributions in a proto-stratiform ultramafic intrusion. *Contrib. Mineral. Petrol.* 33, 245-258.

D.W. POWELL (1970) Magnetised rocks from within the Lewisian of Western Scotland and under the Southern Uplands. *Scott. J. Geol.* 6, 353-369.

M. POWELL and R. POWELL (1977) Plagioclase-alkali feldspar geothermometry revisited. *Mineral. Mag.* 41, 253-256.

R. POWELL (1978) The thermodynamics of pyroxene geotherms. *Phil. Trans. Roy. Soc. Lond.* A288, 457-469.

- P. RAASE (1974) Al and Ti contents of hornblendes, indicators of pressure and temperature of regional metamorphism. *Contrib. Mineral. Petrol.* 45, 231-236.
- A. RAHEIM and D.H. GREEN (1974) Experimental determination of the temperature and pressure dependence of the Fe-Mg partition coefficient for existing garnet and clinopyroxene. *Contrib. Mineral. Petrol.* 48, 179-203.
- C.R. RAMSAY (1973) Controls of biotite zone mineral chemistry in Archaean metasediments near Yellowknife, N.W. Territories, Canada, *J. Petrol.* 14, 467-488.
- J.G. RAMSAY (1980) Shear zone geometry: a review. *J. Struct. Geol.* 2, 83-99
- J.G. RAMSAY and R.H. GRAHAM (1970) Strain variation in shear belts. *Can. J. Earth Sci.* 7, 786-813.
- A.E. RINGWOOD (1974) The petrological evolution of island arc systems. *J. Geol. Soc. Lond.* 130, 183-204.
- G. RIVALENTI (1976) Geochemistry of metavolcanic amphibolites from S.W. Greenland. In: *The Early History of the Earth* (B.F. Windley ed.) Wiley, Lond. 213-224.
- G. RIVALENTI, G. GARUTI and A. ROSSI (1975) The origin of the Ivrea-Verbano basic formation (Western Italian Alps) - whole rock geochemistry. *Bull. Soc. Geol. Italy* 94, 1149-1186.
- R.A. ROBIE, B.S. HEMMINGWAY and J.R. FISHER (1978) Thermodynamic properties of minerals and related substances at 298.15 K and 1 bar ( $10^5$  pascals) pressure and at higher temperatures. *U.S. Geol. Surv. Bull.* 1452, 456 pp.

- P.L. ROEDDER, I.H. CAMPBELL and H.E. JAMESON (1979) A re-evaluation of the olivine-spinel geothermometer. *Contrib. Mineral. Petrol.* 68, 325-334.
- P.L. ROEDDER and R.F. EMSLIE (1970) Olivine-liquid equilibrium. *Contrib. Mineral. Petrol.* 29, 275-289.
- H.R. ROLLINSON (1978) Geochemical studies on the Scourian complex of N.W. Scotland. Unpubl. Ph.D. thesis, Univ. of Leicester.
- H.R. ROLLINSON (1980) Iron-titanium oxides as an indicator of the role of the fluid phase during cooling of granites metamorphosed to granulite grade. *Mineral. Mag.* 43, 623-631.
- H.R. ROLLINSON (1980b) Mineral reactions in a granulite facies calc-silicate rock from Scourie. *Scott. J. Geol.* 16, 153-164.
- H.R. ROLLINSON and B.F. WINDLEY (1980a) Selective elemental depletion during metamorphism of Archaean granulites, Scourie, N.W. Scotland. *Contrib. Mineral. Petrol.* 72, 257-264.
- H.R. ROLLINSON and B.F. WINDLEY (1980b) An Archaean granulite-grade tonalite-trondjemite-granite suite from Scourie, N.W. Scotland: geochemistry and origin. *Contrib. Mineral. Petrol.* 72, 265-282.
- H. SATO (1977) Nickel content of basaltic magma: identification of primary magmas and a measure of the degree of olivine fractionation. *Lithos* 10, 113-120.
- D. SAVAGE (1979) Geochemistry and petrology of layered basic intrusions in the Lewisian complex around Scourie. Unpubl. Ph.D. thesis, Univ. of London.
- D. SAVAGE and J.D. SILLS (1980) High pressure metamorphism in the Scourian of N.W. Scotland: evidence from garnet granulites. *Contrib. Mineral. Petrol.* 74, 153-163.

- S.K. SAXENA (1968) Distribution of elements between coexisting minerals and the nature of solid solution in garnet. *Am. Mineral.* 53, 994-1013.
- S.K. SAXENA (1969) Silicate solid solutions and geothermometry 3. Distribution of Fe and Mg between coexisting garnet and biotite. *Contrib. Mineral. Petrol.* 22, 259-267.
- C.M. SCARFE and P.J. WYLLIE (1967) Serpentine dehydration curves and their bearing on serpentine deformation during orogenesis. *Nature* 215, 672-674.
- V. SCHENCK (1980) U-Pb and Rb-Sr radiometric date and the correlation with metamorphic events in the granulite-facies basement of the Serre, Southern Calabria (Italy). *Contrib. Mineral. Petrol.* 73, 22-38.
- J-G. SCHILLING (1975) Rare-earth variations across "normal segments" of the Reykjanes Ridge, 60° - 53° N, Mid-Atlantic Ridge, 29° S and the East Pacific Rise, 2° - 19° S and evidence for the composition of the underlying low velocity layer. *J. Geophys. Res.* 80, 1459-1473.
- D.M. SHAW (1970) Trace element fractionation during anatexis. *Geochim. Cosmochim. Acta* 34, 237-243.
- J.W. SHERATON (1969) The geology and geochemistry of the Lewisian rocks of the Drumbeg area, Sutherland. Unpubl. Ph.D. thesis, Univ. of Birmingham.
- J.W. SHERATON (1970) The origin of the Lewisian gneisses of N.W. Scotland with particular reference to Drumbeg, Sutherland. *Earth Plan. Sci. Lett.* 8, 301-310.
- J.W. SHERATON, A.C. SKINNER and J. TARNEY (1973a) The geochemistry of the Scourian gneisses of the Assynt district. In: *Early Precambrian Rocks of Scotland and Related Rocks of Greenland* (R.G. Park and J. Tarney eds.) Univ. of Keele, 13-30.

J.W. SHERATON, J. TARNEY, T.J. WHEATLEY and A.E. WRIGHT (1973b) The structural history of the Assynt district. In: The Early Precambrian Rocks of Scotland and Related Rocks of Greenland (R.G.Park and J. Tarney eds.) Univ. of Keele, 31-43.

R.H. SIBSON, J. McM. MOORE and A.H. RANKIN (1975) Seismic pumping - a hydrothermal fluid transport mechanism. J. Geol. Soc. Lond. 131, 653-659.

G.P. SIGHINOLFI (1971) Investigations into deep crustal levels: fractionating effects and geochemical trends related to high grade metamorphism. Geochim. Cosmochim. Acta 35, 1005-1021.

J.D. SILLS, D. SAVAGE, J.V. WATSON and B.F. WINDLEY (in prep.). Layered ultramafic-gabbro bodies in the Lewisian of N.W. Scotland: geochemistry and petrogenesis.

R.R. SOKAL and P.H.A. SNEATH (1963) Principles of Numerical Taxonomy. Freeman, 359 pp.

C.M. SPOONER and H.W. FAIRBAIRN (1970) Strontium 87/strontium 86 initial ratios in pyroxene granulite terrains. J. Geophys. Res. 75, 6706-6713.

H. STAUDIGEL and W. SHREYER (1977) The upper stability of clinocllore -  $Mg_5Al(AlSi_3O_{10})(OH)_2$  at 10-35 kb  $P_{H_2O}$ . Contrib. Mineral. Petrol. 61, 187-198.

N.C.N. STEPHENSON (1977) Coexisting hornblendes and biotites from the Precambrian gneisses of the South West coast of Western Australia. Lithos 10, 9-28.

N.C.N. STEPHENSON (1979) Coexisting garnets and biotites from Precambrian gneisses of the South West coast of Western Australia. Lithos 12, 73-87.

- J.C. STORMER (1975) A practical two-feldspar geothermometer. *Am. Mineral.* 60, 667-674.
- C.J. SUEN, F.A. FREY and J. MALPAS (1979) Bay of Islands ophiolite suite, Newfoundland: petrologic and geochemical characteristics with emphasis on rare earth element geochemistry. *Earth Plan. Sci. Lett.* 45, 337-348.
- S.-S. SUN and R.W. NESBITT (1977) Chemical heterogeneity of the Archaean mantle, composition of the earth and mantle evolution. *Earth Plan. Sci. Lett.* 35, 429-448.
- S.-S. SUN and R.W. NESBITT (1978) Petrogenesis of Archaean ultrabasic and basic volcanics: evidence from the rare earth elements. *Contrib. Mineral. Petrol.* 65, 301-325.
- J. SUTTON and J.V. WATSON (1951) The pre-Torridonian metamorphic history of the Loch Torridon and Scourie areas in the N.W. Highlands and its bearing on the chronology of the Lewisian. *J. Geol. Soc. Lond.* 106, 241-308.
- R.A.K. TAHIRKHELI, M. MATTHEWS, F. PROUST and P. TAPPONIER (1979) The India-Eruasia suture zone in Northern Pakistan - synthesis and interpretation of recent data at plate scale. In: *Geodynamics of Pakistan* (A. Farah and K.A. de Jong eds.) *Geol. Surv. Pakistan Quetta*, 125-130.
- J. TARNEY (1963) Assynt dykes and their metamorphism. *Nature* 199, 672-674.
- J. TARNEY (1973) The Scourie dyke suite and the nature of the Inverian event in Assynt. In: *The Early Precambrian of Scotland and Related Rocks of Greenland* (R.G. Park and J. Tarney eds.) *Univ. of Keele*, 105-118.
- J. TARNEY (1976) Geochemistry of Archaean high-grade gneisses, with implications as to the origin of the Precambrian crust. In: *The Early History of the Earth* (B.F. Windley ed.) *Wiley Lond.*, 405-417.

- J. TARNEY (1977) Petrology, mineralogy and geochemistry of the Falkland Plateau basement rocks, site 330, deep sea drilling project. In: Initial Reports of the Deep Sea Drilling Project, 36 (P.F. Barker and I.W.D. Dalziel eds.) Washington U.S.Govt. Printing Office, 893-921.
- J. TARNEY (1978) Achmelvich Bay, Assynt (Lewisian), Itinerary III. In: The Lewisian and Torridonian Rocks of North West Scotland. (A.J. Barber, A. Beach, R.G. Park, J. Tarney and A.D. Stewart). Geol. Ass. Guide No.21, 35-50.
- J. TARNEY and B.F. WINDLEY (1977) Chemistry, thermal gradients and evolution of the lower continental crust. J. Geol. Soc. Lond. 134, 153-172.
- J. TARNEY, A.D. SAUNDERS, S.D. WEAVER, N.C.B. DONELLAN and G.L. HENDRY (1979) Minor element geochemistry of basalts from Leg 49, North Atlantic Ocean. In: Initial Report Deep Sea Drilling Project (B.P. Luyendyk and J.R. Cann eds.) U.S.Govt. Printing Office, Washington, 49, 657-691.
- S.R. TAYLOR and S.M. McLENNAN (1979) Discussion on 'Chemistry, thermal gradients and evolution of the lower continental crust'. J. Geol. Soc. Lond. 136, 497-500.
- A.B. THOMPSON (1974) Calculations of muscovite-paragonite-alkali feldspar phase relations. Contrib. Mineral. Petrol. 44, 173-194.
- A.B. THOMPSON (1976) Mineral reactions in pelitic rocks: II Calculation of some P-T-X(Fe-Mg) phase relations. Am.J.Sci. 276, 425-454.
- V. TROMMSDORFF and B.W. EVANS (1972) Progressive metamorphism of anti-gorite schist in the Bergell Tonalite aureole (Italy). Am.J.Sci. 272, 423-437.
- A.C. TURNOCK and H.P. EUGSTER (1962) Fe-Al oxides, phase relations below 1000°C. J. Petrol. 3, 535-565.

- B. VELDE (1967)  $\text{Si}^{4+}$  content of natural phengites. *Contrib. Mineral. Petrol.* 14, 250-258.
- L.R. WAGER and G.M. BROWN (1967) *Layered Igneous Rocks*. Oliver and Boyd (Edin.) 588 pp.
- K.R. WALKER (1969) The Palisades sill: a reinvestigation. *Geol. Soc. Am. Spec. Pap.* 111, 178 pp.
- J.V. WATSON (1973) Effects of reworking on high-grade gneiss complexes. *Phil. Trans. Roy. Soc. Lond.* A273, 443-455.
- J. WATTERSON (1975) Mechanism for the persistence of tectonic lineaments. *Nature* 253, 520-522.
- J. WATTERSON (1978) Proterozoic intraplate deformation in the light of South-East Asian neotectonics. *Nature* 273, 636-640.
- B.L. WEAVER, J. TARNEY, B.F. WINDLEY, E.B. SUGAVANAM and V. VENKATA RAO (1978) Madras granulites: Geochemistry and P-T conditions of crystallization. In: *Archaean Geochemistry* (B.F. Windley and S.M. Naqvi eds.) Elsevier, Amsterdam, 177-204.
- B.L. WEAVER and J. TARNEY (in press) Rare-earth geochemistry of granulite-facies gneisses, N.W. Scotland: implications for the petrogenesis of the Archaean lower continental crust. *Earth Plan. Sci. Lett.* in press.  
[now published: *Earth. Plan. Sci. Lett.* (1980) 51, 279-296]
- B.L. WEAVER and J. TARNEY (in prep.) The Scourie Dyke suite: II. Petrogenesis and geochemical nature of the Proterozoic sub-continental mantle. In preparation.
- B.L. WEAVER, J. TARNEY and B.F. WINDLEY (in press) Geochemistry and petrogenesis of the Fiskenaesset anorthosite complex South-West Greenland: nature of the parent magma. *Geochim. Cosmochim. Acta* in press.

- P.R.A. WELLS (1976) Late Archaean metamorphism in the Buksefjorden region, S.W. Greenland. *Contrib. Mineral. Petrol.* 56, 229-242.
- P.R.A. WELLS (1977) Pyroxene thermometry in simple and complex systems. *Contrib. Mineral. Petrol.* 62, 129-139.
- P.R.A. WELLS (1979) Chemical and thermal evolution of Archaean sialic crust, South West Greenland. *J. Petrol.* 20, 187-226.
- P.R.A. WELLS (1979a) P-T conditions in the Moines of Central Scotland. *J. Geol. Soc. Lond.* 136, 663-672.
- P.R.A. WELLS (1980) Thermal models for magmatic accretion and subsequent metamorphism of the continental crust. *Earth Plan. Sci. Lett.* 46, 253-265.
- D.J. WHITFORD and N.T. ARNDT (1979) Rare-earth element abundances in a thick layered komatiitic lava flow from Ontario, Canada. *Earth Plan. Sci. Lett.* 41, 188-196.
- J.A. WHITNEY and J.C. STORMER (1977) Two feldspar geothermometry and geobarometry in mesozonal granitic intrusions: three examples from the piedmont of Georgia. *Contrib. Mineral. Petrol.* 63, 51-64.
- P.R. WHITNEY and J.M. McLELLAND (1973) Origin of coronas in metagabbros of the Adirondacks. *Contrib. Mineral. Petrol.* 39, 81-98.
- J.A. WINCHESTER, R.G. PARK and J.G. HOLLAND (1980) The geochemistry of Lewisian semipelitic schists from the Gairloch District, Wester Ross, Scott. *J. Geol.* 16, 165-179.
- H.G.F. WINCKLER (1976) *Petrogenesis of metamorphic rocks.* 4th Edition, Springer-Verlag, 334 pp.

B.F. WINDLEY (1969) Primary quartz ferro-dolerite/garnet amphibolite dykes in the Sukkertopen region, West Greenland. In: Mechanisms of Igneous Intrusion. (G. Newall and N. Rast, eds.) Geol. J. Spec. issue 2, 79-92.

B.F. WINDLEY (1977) The Evolving Continents. Wiley, London, 385 pp.

B.F. WINDLEY, R.K. HERD and A.A. BOWDEN (1973) The Fiskenaasset complex, West Greenland Part 1. A preliminary study of the stratigraphy, petrology and whole rock chemistry from Qeqertarssuatsiaq. Gron. Geol. Unders. Bull. 106.

B.F. WINDLEY and J.V. SMITH (1974) The Fiskenaasset complex, West Greenland Part 11. General mineral chemistry from Qeqertarssuatsiaq. Gron. Geol. Unders. Bull. 108.

B.F. WINDLEY and J.V. SMITH (1976) Archaean high-grade complexes and modern continental margins. Nature 206, 671-675.

G.J. WITTEY (1975) The geochemistry of the Roneval anorthosite, South Harris, Scotland. Unpubl. Ph.D. thesis, Univ. of London.

D.R. WONES and H.P. EUGSTER (1965) Stability of biotite: experimental theory and applications. Am. Mineral. 50, 1228-1272.

B.J. WOOD (1974) Solubility of alumina in orthopyroxene coexisting with garnet. Contrib. Mineral. Petrol. 46, 1-15.

B.J. WOOD (1975) The influence of pressure, temperature and bulk composition on the appearance of garnet in orthogneiss - an example from South Harris. Earth Plan. Sci. Lett. 26, 299-311.

B.J. WOOD (1977) The activity of components in clinopyroxene and garnet solid solutions and their application to rocks. Phil. Trans. Roy. Soc. Lond. A286, 33-342.

B.J. WOOD and S. BANNO (1973) Garnet-orthopyroxene and orthopyroxene-clinopyroxene relationships in simple and complex systems. *Contrib. Mineral. Petrol.* 42, 109-124.

B.J. WOOD and D.G. FRASER (1976) *Elementary Thermodynamics for Geologists.* Oxford, 303 pp.

B.W.D. YARDLEY (1977) An empirical study of diffusion in garnet. *Am. Mineral.* 62, 793-800.

APPENDICES

APPENDIX AMINERAL ANALYSES

All analyses were performed on carbon coated polished thin sections using a Cambridge Instruments Microscan V electron microprobe at the University of Leicester. An accelerating potential of 15 kV and a specimen current of about 200 n amps on Cu were used. The beam was focussed to a diameter of approximately 1 micron. Elements were analysed in pairs and a co-ordinate system was used to relocate points. A range of natural minerals, synthetic oxides and pure metals were used as standards.

The following standards were used:-

- K - synthetic microcline
- Na- natural jadeite
- Al- natural jadeite
- Ca- natural wollastinite
- Si- natural wollastinite
- Ti- either natural rutile or ilmenite
- Mg- synthetic MgO
- Fe- either pure metal or natural magnetite
- Mn- natural rhodonite
- Ni- pure metal
- Cr- pure metal
- Co- pure metal
- Cl- natural scapolite
- F - lithium fluoride
- S - zinc sulphide
- Zn- zinc sulphide
- Ba- natural barite

The minimum detection limits and precision depend on the mineral and on count rate and are therefore variable. Approximate values for pyroxene, amphibole and garnet are given in Table A.1.

All raw counts were corrected for dead time and full Z.A.F. corrections were applied using the computer programme MAGIC IV (Colby, 1971) modified by R.N. Wilson.

Lists of analyses are given in this appendix; biotite, chlorite and epidote analyses are given in Chapter 5.

	ABSOLUTE PRECISION $\pm$ wt.%oxide	% PRECISION	MINIMUM DETECTION LIMIT ppm oxide
SiO <sub>2</sub>	0.35	1.0	250
TiO <sub>2</sub>	0.03	5.0	120
Al <sub>2</sub> O <sub>3</sub>	0.15	1.5	150
FeO	0.15	1.5	220
MnO	0.03	15.0	200-300
MgO	0.12	1.5	125
CaO	0.10	1.0	125
Na <sub>2</sub> O	0.06	5.0	250-300
K <sub>2</sub> O	0.02	2.0	100
Cr <sub>2</sub> O <sub>3</sub>	0.03		320
Cl	0.01		50
F	0.25		250

TABLE A.1 Minimum detection limits (oxide ppm), absolute precision ( $\pm$  wt.% oxide) and percentage precision for silicate minerals. The actual values depend partially on count rate and hence vary. The precision is between 1 and 2 % for major oxides and between 10 and 20% for trace components.

## ORTHOPYROXENE FROM LAYERED ULTRAMAFICS

ROCK NO	W1	W1	W1	W1	W1	W1	W1	W1
SI02	55.53	55.31	55.72	55.98	55.47	55.52	54.89	54.80
TI02	.08	.08	.09	.07	.11	.09	.08	.08
AL203	3.66	3.57	3.43	3.28	3.64	3.78	3.64	3.74
FE0	10.38	10.08	10.29	10.12	10.15	10.34	10.12	10.40
MNO	.26	.23	.25	.22	.24	.25	.19	.22
MGO	30.17	30.27	30.52	30.50	30.12	29.96	30.26	30.02
CA0	.64	.34	.27	.34	.43	.54	.27	.19
NA20	0.00	0.00	0.00	.01	0.00	0.00	.01	0.00
K20	0.00	0.00	0.00	0.00	.01	0.00	0.00	0.00
CR203	.09	.08	.09	.04	.08	.07	.10	.11
TOTAL	100.80	99.96	100.64	100.57	100.24	100.55	99.54	99.56

## CATIONS RECALCULATED ON THE BASIS OF 6 OXYGENS

SI	1.934	1.938	1.940	1.948	1.939	1.936	1.932	1.931
AL4	.066	.062	.060	.052	.061	.064	.068	.069
AL6	.084	.085	.081	.083	.089	.092	.083	.086
TI	.002	.002	.002	.002	.003	.002	.002	.002
CR	.002	.002	.002	.001	.002	.002	.003	.003
FE	.302	.295	.300	.295	.297	.302	.298	.306
MN	.008	.007	.007	.006	.007	.007	.006	.007
MG	1.566	1.581	1.584	1.582	1.569	1.557	1.587	1.576
CA	.024	.013	.010	.013	.016	.020	.010	.007
NA	0.000	0.000	0.000	.001	0.000	0.000	.001	0.000
K	0.000	0.000	0.000	0.000	.000	0.000	0.000	0.000

## ORTHOPYROXENE FROM ULTRAMAFIC LAYERED COMPLEXES

ROCK NO	W1	W2	W2	W2	W11	W39	W39	W39
SI02	54.61	54.28	54.27	54.10	53.71	54.39	54.82	54.80
TI02	.05	.06	.07	.06	.05	.06	.06	.06
AL203	3.29	3.81	3.59	3.78	3.47	3.19	2.98	2.98
FE0	10.09	10.11	9.93	10.39	10.60	11.48	11.46	11.46
MNO	.31	.27	.26	.27	.26	.27	.27	.27
MGO	30.57	30.68	31.06	30.90	32.01	30.51	30.81	30.81
CA0	.33	.33	.36	.43	.40	.41	.30	.31
NA20	0.00	.02	.01	.01	0.00	0.00	0.00	0.00
K20	0.00	.01	.01	.02	0.00	.01	.01	.01
CR203	.11	.10	.09	.09	.07	.11	.11	.11
TOTAL	99.40	99.67	99.77	100.03	100.57	100.42	100.82	100.82

## CATIONS RECALCULATED ON THE BASIS OF 6 OXYGENS

SI	1.929	1.912	1.912	1.904	1.885	1.915	1.921	1.921
AL4	.071	.088	.088	.096	.115	.085	.079	.079
AL6	.066	.071	.061	.061	.029	.048	.045	.045
TI	.001	.002	.002	.002	.001	.002	.002	.002
CR	.003	.003	.003	.003	.002	.003	.003	.003
FE	.298	.298	.293	.305	.311	.338	.336	.336
MN	.009	.008	.008	.008	.008	.008	.008	.008
MG	1.609	1.611	1.631	1.621	1.675	1.601	1.609	1.609
CA	.012	.012	.014	.016	.015	.015	.011	.011
NA	0.000	.001	.001	.001	0.000	0.000	0.000	0.000
K	0.000	.000	.000	.001	0.000	.000	.000	.000

## ORTHOPYROXENE FROM ACHILTIBUIE GABBROS

ROCK NO	W32	W32	W32	W32	W32	W34B	W34B	W35
SI02	51.25	51.88	51.86	51.46	52.29	52.11	52.81	51.58
TI02	.07	.05	.05	.04	.06	.09	.10	.07
AL203	3.47	2.92	3.26	3.62	3.41	3.31	3.12	3.08
FE0	19.04	19.71	18.62	20.02	19.75	19.41	20.11	21.35
MNO	.29	.32	.26	.30	.29	.27	.33	.35
MGO	24.51	24.53	25.01	23.76	24.33	24.43	23.70	23.32
CA0	.52	.43	.44	.57	.42	.51	.60	.66
NA20	.02	.01	.02	.03	.01	.02	.02	0.00
K20	.02	.02	.01	.02	.01	.02	.02	.01
CR203	.10	.10	.20	.18	.15	.10	.06	.08
TOTAL	99.29	99.98	99.74	99.99	100.71	100.27	100.87	100.50

## CATIONS RECALCULATED ON THE BASIS OF 6 OXYGENS

SI	1.896	1.911	1.905	1.898	1.909	1.909	1.927	1.905
AL4	.104	.089	.095	.102	.091	.091	.073	.095
AL6	.048	.038	.046	.056	.056	.052	.061	.039
TI	.002	.001	.001	.001	.002	.002	.003	.002
CR	.003	.003	.006	.005	.004	.003	.002	.002
FE	.589	.607	.572	.618	.603	.595	.614	.660
MN	.009	.010	.008	.009	.009	.008	.010	.011
MG	1.352	1.346	1.369	1.306	1.324	1.334	1.289	1.284
CA	.021	.017	.017	.023	.016	.020	.023	.026
NA	.001	.001	.001	.002	.001	.001	.001	0.000
K	.001	.001	.000	.001	.000	.001	.001	.000

## ORTHOPYROXENE FROM ACHILTIBUIE GABBROS

ROCK NO	W35	W35	W35	W35	W36	W36	W36	W37
SI02	51.39	51.23	50.74	51.13	51.67	51.19	51.71	51.42
TI02	.03	.05	.04	.05	.11	.11	.11	.12
AL203	2.93	2.97	3.67	2.98	2.26	2.21	1.88	2.39
FE0	21.67	21.40	20.98	21.23	23.55	24.02	23.42	23.20
MNO	.35	.35	.31	.29	.35	.37	.34	.28
MGO	23.16	23.41	23.41	23.74	21.88	21.75	22.53	22.20
CA0	.38	.68	.46	.43	.50	.47	.46	.49
NA20	0.00	0.00	.01	0.00	.02	.01	.01	.01
K20	.02	.01	.01	.02	.02	.01	.04	0.00
CR203	.16	.14	.15	.16	.08	.08	.08	.08
TOTAL	100.09	100.24	99.79	100.02	100.44	100.12	100.58	100.19

## CATIONS RECALCULATED ON THE BASIS OF 6 OXYGENS

SI	1.909	1.900	1.886	1.898	1.928	1.920	1.927	1.921
AL4	.091	.100	.114	.102	.072	.080	.073	.079
AL6	.037	.030	.047	.028	.028	.018	.010	.026
TI	.001	.001	.001	.001	.003	.003	.003	.003
CR	.005	.004	.004	.005	.002	.002	.002	.002
FE	.673	.664	.652	.659	.735	.755	.730	.725
MN	.011	.011	.010	.009	.011	.012	.011	.009
MG	1.282	1.294	1.297	1.313	1.217	1.218	1.251	1.236
CA	.015	.027	.018	.017	.020	.019	.018	.020
NA	0.000	0.000	.001	0.000	.001	.001	.001	.001
K	.001	.000	.000	.001	.001	.000	.002	0.000

## ORTHOPYROXENE FROM DRUMBEG GABBROS

ROCK NO	W4	W4	W5	W5	W5	W14	W14	W14
SI02	51.36	50.76	50.84	51.45	50.21	51.15	51.56	51.31
TIO2	.14	.16	.20	.17	.17	.10	.11	.11
AL2O3	3.52	3.68	3.67	3.24	3.56	2.36	2.81	2.61
FE0	24.74	25.08	23.29	21.61	25.30	22.33	21.37	21.41
MNO	.14	.15	.20	.18	.28	.66	.64	.65
MGO	19.88	19.74	21.36	22.72	19.80	22.12	22.48	22.43
CAO	.58	.61	.66	.53	.54	.40	.42	.34
NA2O	.02	.03	.01	0.00	.01	.01	.03	.02
K2O	.01	.01	0.00	0.00	.02	.01	0.00	0.00
CR2O3	0.00	0.00	.03	.03	.01	.01	.03	.02
TOTAL	100.38	100.20	100.25	99.90	99.90	99.09	99.45	98.90

## CATIONS RECALCULATED ON THE BASIS OF 6 OXYGENS

SI	1.923	1.910	1.898	1.911	1.901	1.927	1.925	1.928
AL4	.077	.090	.102	.089	.099	.073	.075	.072
AL6	.079	.073	.060	.052	.060	.032	.049	.043
TI	.004	.005	.006	.005	.005	.003	.003	.003
CR	0.000	0.000	.001	.001	.000	.000	.001	.001
FE	.775	.789	.727	.671	.801	.703	.667	.673
MN	.004	.005	.006	.006	.009	.021	.021	.021
MG	1.109	1.107	1.189	1.257	1.117	1.242	1.251	1.256
CA	.023	.025	.026	.021	.022	.016	.017	.014
NA	.001	.002	.001	0.000	.001	.001	.002	.001
K	.000	.000	0.000	0.000	.001	.000	0.000	0.000

## ORTHOPYROXENE FROM GABBROS

ROCK NO	W37	W37	J125	J125	J125	J125	W45	W45
SI02	51.63	51.53	51.92	51.34	51.31	51.22	51.08	51.13
TIO2	.12	.12	.11	.14	.11	.12	.09	.08
AL2O3	2.28	2.60	3.66	4.34	3.89	3.86	4.39	4.34
FE0	22.39	22.97	19.51	19.85	21.41	21.25	19.58	20.28
MNO	.26	.28	.36	.35	.44	.41	.33	.35
MGO	22.88	22.13	24.06	23.45	22.70	22.65	23.89	23.06
CAO	.40	.47	.20	.38	.38	.44	.33	.36
NA2O	.01	.01	.01	.01	0.00	.01	0.00	0.00
K2O	.01	0.00	.01	.01	.02	.01	.01	.02
CR2O3	.10	.12	.04	.05	.05	.07	.04	.02
TOTAL	100.04	100.21	100.08	99.92	100.31	100.14	99.74	99.82

## CATIONS RECALCULATED ON THE BASIS OF 6 OXYGENS

SI	1.923	1.921	1.908	1.891	1.897	1.898	1.883	1.892
AL4	.077	.079	.092	.109	.103	.102	.117	.108
AL6	.023	.036	.067	.080	.067	.067	.074	.082
TI	.003	.003	.003	.004	.003	.003	.002	.002
CR	.003	.004	.001	.001	.001	.002	.001	.001
FE	.697	.716	.600	.611	.662	.659	.604	.628
MN	.008	.009	.011	.011	.014	.013	.010	.011
MG	1.270	1.230	1.318	1.287	1.251	1.251	1.313	1.272
CA	.016	.019	.008	.015	.015	.017	.013	.014
NA	.001	.001	.001	.001	0.000	.001	0.000	0.000
K	.000	0.000	.000	.000	.001	.000	.000	.001

## CLINOPYROXENE FROM DRJMBEG GABBROS

ROCK NO	D5	W4	W4	W4	W4	W5	W5	W6
SI02	50.81	50.19	50.27	50.43	50.14	49.68	48.77	49.15
TIO2	.38	.70	.62	.67	.86	.77	.77	.61
AL2O3	3.04	5.07	5.12	5.23	5.32	5.41	5.06	6.66
FEU	13.17	9.82	9.70	9.90	9.23	9.58	9.29	9.74
MNO	.27	.12	.12	.13	.10	.10	.10	.09
MGO	10.82	12.25	12.30	12.26	12.34	12.58	13.04	11.39
CAO	21.10	20.55	21.72	21.45	21.95	21.60	20.84	21.47
NA2O	.61	.92	.79	.81	.79	.77	.74	.78
K2O	0.00	0.00	0.00	0.00	0.00	0.00	0.00	0.00
CR2O3	0.00	.05	.06	.04	.03	.04	.02	.03
TOTAL	100.20	99.67	100.73	100.92	100.75	100.54	98.64	99.92

## CATIONS RECALCULATED ON THE BASIS OF 6 OXYGENS

SI	1.928	1.883	1.871	1.872	1.863	1.853	1.852	1.843
AL4	.072	.117	.129	.128	.137	.147	.148	.157
AL6	.064	.107	.096	.101	.096	.091	.079	.138
TI	.011	.020	.017	.019	.024	.022	.022	.017
CR	0.000	.001	.002	.001	.001	.001	.001	.001
FE	.418	.308	.302	.307	.287	.299	.295	.305
MN	.009	.004	.004	.004	.003	.003	.003	.003
MG	.612	.685	.682	.678	.683	.699	.738	.637
CA	.858	.826	.866	.853	.874	.863	.848	.863
NA	.045	.067	.057	.058	.057	.056	.054	.057
K	0.000	0.000	0.000	0.000	0.000	0.000	0.000	0.000

## CLINOPYROXENE FROM DRJMBEG GABBROS

ROCK NO	W6	W7	W13	W13	W14	W14	W14	W16
SI02	48.69	49.23	50.95	51.03	49.42	49.67	49.50	51.52
TIO2	.70	.81	.37	.33	.76	.67	.68	.26
AL2O3	5.69	6.27	3.34	2.79	5.02	4.97	4.84	2.66
FEU	11.38	9.63	11.17	11.78	9.56	8.37	8.10	10.25
MNO	.10	.15	.43	.41	.26	.26	.27	1.02
MGO	11.22	11.36	11.50	11.37	12.70	12.47	12.47	12.16
CAO	21.62	21.07	22.02	22.17	22.53	22.77	22.23	21.54
NA2O	.83	.73	.44	.37	.73	.69	.73	.61
K2O	.02	0.00	.02	.01	0.00	0.00	0.00	.02
CR2O3	.02	.02	.06	.06	.09	.06	.04	.01
TOTAL	100.25	99.23	100.30	100.32	101.07	99.86	99.10	99.45

## CATIONS RECALCULATED ON THE BASIS OF 6 OXYGENS

SI	1.839	1.856	1.919	1.928	1.842	1.862	1.871	1.939
AL4	.161	.144	.081	.072	.158	.138	.129	.061
AL6	.093	.134	.067	.052	.063	.081	.087	.057
TI	.020	.023	.010	.009	.021	.019	.019	.007
CR	.001	.001	.002	.002	.003	.002	.001	.000
FE	.360	.304	.352	.372	.298	.262	.256	.323
MN	.003	.005	.014	.013	.008	.008	.009	.033
MG	.632	.638	.645	.640	.706	.697	.702	.682
CA	.875	.851	.889	.897	.900	.914	.900	.869
NA	.061	.053	.032	.027	.053	.050	.053	.045
K	.001	0.000	.001	.000	0.000	0.000	0.000	.001

## CLINOPYROXENE FROM LAYERED ULTRAMAFIC

ROCK NO	W1	W1	W1	W1	W1	W1	W2	W39
SiO2	51.83	51.27	51.41	50.78	51.19	50.97	50.68	51.56
TiO2	.51	.45	.43	.49	.47	.49	.39	.32
Al2O3	4.89	4.54	4.45	4.51	4.59	4.74	4.41	3.51
FeO	4.42	4.51	4.20	4.21	4.40	4.62	4.56	4.09
MnO	.11	.19	.18	.17	.20	.18	.15	.12
MgO	14.51	15.30	15.75	15.11	14.98	14.68	15.28	15.92
CaO	23.92	24.03	24.04	23.67	23.74	23.76	23.92	24.40
Na2O	.30	.35	.30	.28	.32	.36	.37	.07
K2O	.01	0.00	0.00	0.00	0.00	0.00	.01	.01
CR2O3	.15	.17	.21	.18	.18	.18	.20	.15
TOTAL	100.65	100.86	100.63	99.44	99.70	100.03	100.07	100.15

## CATIONS RECALCULATED ON THE BASIS OF 6 OXYGENS

SI	1.889	1.873	1.872	1.877	1.880	1.876	1.870	1.893
AL4	.111	.127	.128	.123	.120	.124	.130	.107
AL6	.100	.068	.063	.074	.079	.082	.062	.045
TI	.014	.012	.012	.014	.013	.014	.010	.009
CR	.004	.005	.006	.005	.005	.005	.006	.004
FE	.135	.138	.128	.130	.135	.142	.141	.126
MN	.003	.006	.006	.005	.006	.006	.005	.004
MG	.788	.833	.855	.832	.820	.805	.840	.871
CA	.934	.940	.938	.938	.934	.937	.946	.960
NA	.021	.025	.021	.020	.023	.026	.026	.005
K	.000	0.000	0.000	0.000	0.000	0.000	.000	.000

## CLINOPYROXENE FROM ULTRAMAFIC/AGAMTITE/ACID GRANULITE

ROCK NO	W39	J48	J48	J48	D2	D27	D27	D5
SiO2	51.62	52.64	52.88	52.94	51.24	50.30	50.46	50.22
TiO2	.33	.16	.13	.18	.27	.20	.16	.41
Al2O3	3.56	2.35	1.95	2.10	2.62	5.54	5.53	3.25
FeO	4.26	6.06	6.11	6.17	10.41	7.18	7.37	13.48
MnO	.14	.20	.18	.19	.18	.20	.21	.43
MgO	15.75	14.26	14.55	14.36	13.16	13.09	12.59	10.70
CaO	24.35	22.94	22.97	23.11	21.15	22.68	22.01	20.66
Na2O	.09	.73	.76	.75	.83	.71	.68	.57
K2O	.02	0.00	.10	.10	.05	0.00	0.00	0.00
CR2O3	.12	.26	.27	.27	.03	.05	.12	0.00
TOTAL	100.24	99.67	99.90	100.16	99.94	99.94	99.14	99.72

## CATIONS RECALCULATED ON THE BASIS OF 6 OXYGENS

SI	1.894	1.952	1.957	1.955	1.927	1.870	1.887	1.918
AL4	.106	.048	.043	.045	.073	.130	.113	.082
AL6	.048	.055	.043	.047	.043	.112	.131	.065
TI	.009	.004	.004	.005	.008	.006	.005	.012
CR	.003	.008	.008	.008	.001	.001	.004	0.000
FE	.131	.188	.189	.191	.327	.223	.231	.431
MN	.004	.006	.006	.006	.006	.006	.007	.014
MG	.861	.788	.803	.790	.738	.725	.702	.609
CA	.957	.912	.911	.915	.852	.903	.882	.846
NA	.006	.052	.055	.054	.061	.051	.049	.042
K	.001	0.000	.005	.005	.002	0.000	0.000	0.000

## ORTHOPYROXENE FROM GABBROS AND ULTRAMAFIC PODS

ROCK NO	W45	D5	D27	D27	D27	D3	D3	D3
SI02	50.31	50.83	51.92	51.67	51.96	53.30	53.75	53.20
TIO2	.09	.12	.05	.03	.05	.05	.07	.05
AL2O3	4.26	1.74	4.54	4.47	4.67	2.44	2.96	2.70
FE0	19.87	29.32	18.62	18.66	18.21	12.36	12.52	12.51
MNO	.34	.86	.41	.39	.40	.26	.24	.25
MGO	23.39	16.48	23.97	23.96	24.29	29.48	29.51	29.38
CA0	.33	.55	.43	.49	.47	.90	.35	.50
NA2O	0.00	.05	.02	.03	.04	0.00	.02	0.00
K2O	.02	0.00	0.00	0.00	0.00	0.00	0.00	0.00
CR2O3	.01	0.00	.08	.06	.04	.55	.54	.54
TOTAL	98.62	99.95	100.04	99.76	100.12	99.29	99.96	99.13

## CATIONS RECALCULATED ON THE BASIS OF 6 OXYGENS

SI	1.882	1.963	1.898	1.895	1.894	1.914	1.914	1.913
AL4	.118	.037	.102	.105	.106	.086	.086	.087
AL6	.069	.042	.093	.089	.095	.017	.038	.027
TI	.003	.003	.001	.001	.001	.001	.002	.001
CR	.000	0.000	.002	.002	.001	.016	.015	.015
FE	.621	.947	.569	.572	.555	.371	.373	.376
MN	.011	.028	.013	.012	.012	.008	.007	.008
MG	1.304	.948	1.306	1.310	1.319	1.578	1.566	1.574
CA	.013	.023	.017	.019	.018	.035	.013	.019
NA	0.000	.004	.001	.002	.003	0.000	.001	0.000
K	.001	0.000	0.000	0.000	0.000	0.000	0.000	0.000

## CLINOPYROXENE FROM ACHILTIBUIE GABBROS

ROCK NO	W32	W34B	W35	W35	W36	W36	W36	W37
SI02	54.02	51.19	50.18	50.68	51.16	51.00	50.00	50.29
TIO2	.28	.35	.25	.22	.38	.35	.37	.43
AL2O3	4.27	4.13	3.78	3.76	3.36	3.24	3.34	3.69
FE0	7.01	7.31	8.18	7.39	8.80	8.84	9.14	8.92
MNO	.14	.13	.17	.15	.20	.19	.18	.13
MGO	13.67	13.78	13.57	13.65	13.45	13.32	13.59	13.49
CA0	19.71	22.55	22.44	22.75	22.36	22.30	21.66	22.33
NA2O	.46	.46	.61	.62	.61	.61	.61	.59
K2O	.02	.02	.02	.01	.02	.02	.01	.02
CR2O3	.16	.11	.19	.21	.08	.14	.13	.07
TOTAL	99.75	100.03	99.39	99.44	100.42	100.01	99.03	99.96

## CATIONS RECALCULATED ON THE BASIS OF 6 OXYGENS

SI	1.975	1.899	1.888	1.898	1.906	1.909	1.893	1.886
AL4	.025	.101	.112	.102	.094	.091	.107	.114
AL6	.159	.080	.055	.064	.053	.052	.042	.049
TI	.008	.010	.007	.006	.011	.010	.011	.012
CR	.005	.003	.006	.006	.002	.004	.004	.002
FE	.214	.227	.257	.231	.274	.277	.289	.280
MN	.004	.004	.005	.005	.006	.006	.006	.004
MG	.745	.762	.761	.762	.747	.743	.767	.754
CA	.772	.896	.904	.913	.893	.894	.879	.897
NA	.033	.033	.044	.045	.044	.044	.045	.043
K	.001	.001	.001	.000	.001	.001	.000	.001

OLIVINE FROM LAYERED ULTRAMAFIC ROCKS

ROCK NO	W1	W1	W1	W1	W2	W2	W2	W2	W11	W39	W39	W39	W39	W39
SI02	41.18	40.85	41.26	40.52	40.19	40.16	40.34	40.01	39.94	39.72	39.72	39.72	39.72	39.67
TI02	.01	.01	.01	0.00	0.00	0.00	.01	0.00	0.00	0.00	0.00	0.00	0.00	0.00
AL2O3	.01	.01	0.00	0.00	0.03	0.01	.20	0.00	0.00	0.00	0.00	0.00	0.00	0.00
FE0	14.05	14.37	14.65	14.64	13.19	13.78	13.29	14.71	17.17	17.43	17.43	17.16	17.16	17.13
MNO	0.00	0.00	0.00	0.00	0.00	0.00	0.00	0.03	0.27	0.29	0.29	0.31	0.27	0.27
MGO	45.05	44.80	44.86	44.53	46.18	45.75	46.21	47.02	43.91	44.10	44.10	44.01	44.01	43.86
CAO	0.00	0.00	.01	0.00	.03	.02	.02	.02	.01	.01	.01	.01	.01	.01
NIO	.52	.52	.54	.51	.49	.45	.43	.45	.39	.37	.37	.38	.38	.38
CR2O3	0.00	0.00	0.00	0.00	0.00	0.00	0.00	0.00	0.00	0.00	0.00	0.00	0.00	0.00
TOTAL	100.87	100.57	101.33	100.20	100.19	100.17	100.46	99.96	102.07	101.20	101.93	101.60	101.60	101.34

CATIONS RECALCULATED ON THE BASIS OF 4 OXYGENS

	SI	AL	TI	CR	FE	MN	MG	CA	NI
SI	1.019	1.015	1.018	1.013	1.000	1.000	1.000	1.000	1.000
AL	.000	.000	.000	0.000	0.000	0.000	0.000	0.000	0.000
TI	.000	.000	.000	0.000	0.000	0.000	0.000	0.000	0.000
CR	.291	.299	.302	.306	.275	.287	.303	.301	.358
FE	0.000	0.000	0.000	0.000	0.000	0.000	0.000	0.000	0.000
MN	0.000	0.000	0.000	0.000	0.000	0.000	0.000	0.000	0.000
MG	1.661	1.659	1.650	1.658	1.700	1.700	1.726	1.640	1.633
CA	0.000	0.000	.000	0.000	.001	.001	.001	.000	.000
NI	.011	.011	.011	.011	.009	.009	.009	.008	.008

## GARNET FROM DRUMBEG

	W4	W4	W5	W5	W6	W6	W7
O2	40.23	40.14	39.47	39.45	38.71	38.64	39.72
O2	.11	.13	.10	.10	.13	.10	.09
O3	21.72	21.69	22.11	22.04	21.70	21.67	21.69
O	24.07	23.47	23.57	24.06	24.51	25.40	23.85
O	.55	.52	.61	.75	.54	.54	.80
O	8.66	8.85	8.57	8.07	6.96	6.35	7.38
O3	6.65	6.67	6.59	6.55	7.37	7.20	6.62
AL	.04	.03	.03	.04	.03	.03	.06
AL	102.03	101.40	101.05	101.07	99.95	99.93	100.21

## T FORMULA

	6.045	6.041	5.985	5.997	5.984	5.996	6.083
	.012	.015	.011	.011	.015	.012	.010
	3.848	3.858	3.952	3.959	3.955	3.964	3.916
	3.025	2.961	2.989	3.059	3.169	3.296	3.055
	.071	.066	.078	.093	.071	.071	.104
	1.939	1.990	1.937	1.828	1.603	1.468	1.684
	1.071	1.078	1.071	1.067	1.221	1.197	1.086
	.005	.004	.004	.005	.004	.004	.007
	24.000	24.000	24.000	24.000	24.000	24.000	24.000

## NET MOLECULES (RICKWOOD (1968))

ROVIT	.12	.09	.09	.12	.09	.09	.19
JP	33.56	34.25	32.64	30.82	27.01	24.67	28.62
SSART	1.21	1.15	1.32	1.65	1.19	1.19	1.76
SSULA	18.41	18.52	17.95	17.85	20.47	20.02	18.27
ANDIN	46.70	45.88	48.00	49.54	51.24	54.02	51.16

## PERCENTAGE CATIONS ASSIGNED

	96.22	96.46	98.73	98.77	98.83	99.15	98.42
--	-------	-------	-------	-------	-------	-------	-------

	W4 LF	W4 LF	W16 LF	W16 LF	W31
SI O2	37.79	38.72	37.92	39.15	39.51
TI O2	.04	.03	.32	.15	.10
AL2O3	21.74	21.97	20.39	21.03	21.59
FE O	28.73	26.20	23.91	24.68	24.79
MN O	.66	.62	6.13	5.30	.81
MG O	4.83	6.08	1.94	2.15	7.82
CA O	6.27	7.03	8.80	8.40	6.76
CR2O3	.04	0.00	0.00	.02	.10
TOTAL	100.10	100.65	99.41	100.90	101.48

## UNIT FORMULA

SI	5.942	5.981	6.172	6.133	6.010
TI	.005	.003	.039	.018	.011
AL	4.030	4.001	3.849	3.880	3.872
FE	3.778	3.385	3.202	3.235	3.154
MN	.088	.081	.831	.704	.104
MG	1.132	1.410	.463	.505	1.773
CA	1.056	1.164	1.510	1.411	1.102
CR	.005	0.000	0.000	.002	.012
O	24.000	24.000	24.000	24.000	24.000

## GARNET MOLECULES (RICKWOOD (1968))

UVAROVIT	.13	0.00	0.00	.05	.31
PYROPE	19.05	23.40	8.02	8.65	30.43
SPESSART	1.43	1.36	14.40	12.05	1.79
GROSSJLA	17.65	19.45	26.15	24.12	18.60
ALMANDIN	61.69	55.79	51.43	55.11	48.86

## PERCENTAGE CATIONS ASSIGNED

	98.81	99.59	96.43	97.83	96.87
--	-------	-------	-------	-------	-------

## GARNET FROM ACHILTIBUIE

	W32	W32	W34B	W35	W35	W36
SI O2	40.23	40.26	41.03	39.68	39.63	38.67
TI O2	.05	.04	.07	.04	.05	.08
AL2O3	22.25	21.91	22.09	22.29	22.47	21.44
FE O	21.38	21.70	21.58	22.21	22.38	24.37
MN O	.90	.89	.82	.94	.94	.96
MG O	10.27	9.93	10.01	9.91	9.76	8.21
CA O	6.26	6.43	6.36	6.38	6.39	6.54
CR2O3	.19	.26	.18	.22	.23	.08
TOTAL	101.53	101.42	101.14	101.65	101.85	100.34

## UNIT FORMULA

SI	6.006	6.031	6.008	5.951	5.935	5.953
TI	.006	.005	.008	.005	.006	.009
AL	3.916	3.869	3.908	3.941	3.967	3.891
FE	2.669	2.718	2.709	2.785	2.803	3.138
MN	.114	.113	.104	.119	.119	.125
MG	2.285	2.217	2.239	2.212	2.178	1.881
CA	1.001	1.032	1.023	1.025	1.025	1.079
CR	.022	.031	.021	.026	.027	.010
O	24.000	24.000	24.000	24.000	24.000	24.000

## GARNET MOLECULES (RICKWOOD (1968))

UVAROVIT	.57	.79	.54	.66	.69	.25
PYROPE	38.68	37.89	37.98	37.18	36.70	32.15
SPESSART	1.93	1.93	1.77	2.01	2.01	2.14
GROSSULA	16.38	16.85	16.81	16.57	16.59	18.19
ALMANDIN	42.45	42.53	42.90	43.58	44.01	47.27

## PERCENTAGE CATIONS ASSIGNED

	98.34	97.41	98.12	98.77	98.54	97.00
--	-------	-------	-------	-------	-------	-------

	W36	W36	W37	W37	W37
SI O2	38.98	38.68	39.16	39.18	39.35
TI O2	.07	.07	.08	.07	.04
AL2O3	22.11	22.18	21.74	22.07	21.90
FE O	24.95	25.03	24.11	24.13	24.15
MN O	1.05	1.03	.78	.79	.78
MG O	7.81	7.78	8.49	8.63	8.53
CA O	6.44	6.43	6.56	6.55	6.56
CR2O3	.10	.07	.11	.11	.12
TOTAL	101.51	101.27	101.03	101.53	101.43

## UNIT FORMULA

SI	5.937	5.911	5.966	5.933	5.969
TI	.008	.008	.009	.008	.005
AL	3.970	3.996	3.905	3.943	3.916
FE	3.178	3.199	3.072	3.059	3.063
MN	.135	.133	.101	.101	.100
MG	1.773	1.772	1.928	1.949	1.928
CA	1.051	1.053	1.071	1.064	1.066
CR	.012	.008	.013	.013	.014
O	24.000	24.000	24.000	24.000	24.000

## GARNET MOLECULES (RICKWOOD (1968))

UVAROVIT	.30	.21	.34	.33	.37
PYROPE	29.86	29.98	32.80	32.84	32.71
SPESSART	2.28	2.26	1.71	1.71	1.70
GROSSULA	17.40	17.60	17.88	17.59	17.72
ALMANDIN	50.16	49.96	47.27	47.52	47.51

## PERCENTAGE CATIONS ASSIGNED

	98.55	98.02	97.56	98.45	97.89
--	-------	-------	-------	-------	-------

## GARNET

	W50	J6	J96	J96	S10	J36
SI O2	39.48	37.93	39.49	38.59	37.81	38.23
TI O2	.08	.16	.11	.98	0.00	.04
AL2O3	21.62	20.61	22.02	21.63	22.15	21.52
FE O	29.78	28.62	24.13	29.04	30.28	30.63
MN O	.87	4.26	.88	1.11	1.23	3.03
MG O	3.13	2.02	8.04	6.44	5.89	4.87
CA O	7.39	7.81	5.82	3.19	2.80	3.45
CR2O3	.01	0.00	.21	.37	0.00	.01
TOTAL	102.36	101.41	100.70	100.45	100.16	101.83

## UNIT FORMULA

SI	6.091	6.010	6.018	6.005	5.934	5.967
TI	.009	.019	.013	.009	0.000	.005
AL	3.933	3.850	3.956	3.968	4.098	3.961
FE	3.843	3.793	3.076	3.779	3.974	4.005
MN	.114	.572	.114	.146	.164	.401
MG	.720	.477	1.826	1.493	1.378	1.133
CA	1.222	1.326	.950	.532	.471	.577
CR	.001	0.000	.125	.046	0.000	.001
O	24.000	24.000	24.000	24.000	24.000	24.000

## GARNET MOLECULES (RICKWOOD(1968))

UVAROVIT	.03	0.00	.64	1.15	0.00	.03
PYROPE	12.20	8.26	30.61	25.17	23.22	19.57
SPESSART	1.93	9.90	1.90	2.46	2.76	6.74
GROSSULA	20.68	22.96	15.30	7.79	7.93	9.68
ALMANDIN	65.15	58.88	51.55	63.51	66.09	64.48

## PERCENTAGE CATIONS ASSIGNED

	98.72	95.97	99.56	99.31	98.78	98.73
--	-------	-------	-------	-------	-------	-------

	J98	J98	J98	D17	D17
SI O2	38.32	38.18	37.71	37.83	37.51
TI O2	.12	.13	.10	.25	.25
AL2O3	20.76	20.80	21.01	20.01	20.17
FE O	29.70	29.24	29.82	32.71	32.68
MN O	2.78	2.75	2.89	.78	.89
MG O	1.82	1.89	2.11	1.62	1.09
CA O	7.89	7.61	6.79	7.57	7.94
CR2O3	.02	.04	.02	.01	.01
TOTAL	101.41	100.64	100.45	100.79	100.54

## UNIT FORMULA

SI	6.054	6.063	6.011	6.053	6.030
TI	.014	.016	.012	.031	.030
AL	3.867	3.894	3.948	3.775	3.823
FE	3.924	3.883	3.976	4.377	4.394
MN	.372	.370	.390	.106	.121
MG	.429	.447	.501	.386	.261
CA	1.336	1.295	1.160	1.298	1.368
CR	.002	.005	.003	.001	.001
O	24.000	24.000	24.000	24.000	24.000

## GARNET MOLECULES (RICKWOOD(1968))

UVAROVIT	.06	.13	.06	.03	.03
PYROPE	7.38	7.65	8.46	6.82	4.55
SPESSART	6.41	6.32	6.58	1.87	2.11
GROSSULA	22.95	22.01	19.51	22.88	23.81
ALMANDIN	63.19	63.89	65.39	68.41	69.49

## PERCENTAGE CATIONS ASSIGNED

	96.74	97.64	98.77	94.24	95.43
--	-------	-------	-------	-------	-------

## AMPHIBOLES FROM LAYERED ULTRAMAFIC ROCKS

ROCK NO	W1	W1	W1	W2	W2	W2	W39	W39
SI02	42.25	42.27	42.46	42.72	43.00	42.96	45.16	45.31
TIO2	1.555	1.55	1.53	1.35	1.37	1.27	.73	.73
AL2O3	13.555	13.46	13.47	13.45	13.29	13.07	12.78	12.76
FeO	6.37	6.20	6.60	6.22	6.19	6.22	6.48	6.58
MNO	.09	.07	.08	.07	.07	.07	.10	.09
MGO	16.45	16.81	16.68	16.31	16.42	16.48	17.13	17.14
CAO	12.32	12.38	12.29	12.45	12.54	12.53	12.68	12.68
NA2O	2.50	2.58	2.56	2.71	2.62	2.78	1.77	1.76
K2O	.65	.65	.64	.42	.44	.43	.19	.19
CR2O3	.34	.32	.32	.28	.27	.25	.41	.41
CL	.04	.03	.05	0.00	0.00	0.00	0.00	0.00
F	.02	.02	.02	0.00	0.00	0.00	0.00	0.00
TOTAL	96.13	96.34	96.70	95.98	96.11	96.06	97.43	97.65

## CATIONS RECALCULATED ON THE BASIS OF 23 OXYGENS

SI	6.183	6.171	6.184	6.243	6.265	6.275	6.453	6.460
AL4	1.817	1.829	1.816	1.757	1.735	1.725	1.547	1.540
AL6	.521	.489	.497	.560	.549	.526	.606	.606
TI	.171	.170	.168	.148	.150	.140	.078	.078
CR	.039	.037	.037	.032	.031	.029	.046	.046
FE	.780	.757	.804	.760	.754	.760	.774	.785
MN	.011	.009	.010	.009	.009	.009	.012	.011
MG	3.588	3.658	3.620	3.552	3.566	3.588	3.648	3.642
CA	1.932	1.937	1.918	1.949	1.958	1.961	1.941	1.937
NA	.759	.730	.723	.768	.740	.787	.490	.487
K	.121	.121	.119	.078	.082	.080	.035	.035

## AMPHIBOLE FROM RETROGRESSED ULTRAMAFIC

ROCK NO	D25						
SI02	55.51	55.72	55.71	55.48	54.24	55.72	56.89
TIO2	.06	.06	.05	.09	.11	.06	.05
AL2O3	1.44	1.22	1.27	1.91	2.04	.43	.31
FeO	5.25	5.50	4.75	5.34	4.75	12.43	13.80
MNO	.17	.17	.15	.19	.17	.55	.56
MGO	21.47	21.48	21.55	21.59	21.65	23.79	25.06
CAO	12.45	12.50	12.42	11.70	12.18	1.59	.36
NA2O	.29	.27	.31	.46	.34	.15	.05
K2O	.02	.03	.02	.04	.03	.02	.02
CR2O3	.05	.02	.05	.16	.19	.05	.04
CL	0.00	0.00	0.00	0.00	0.00	0.00	0.00
F	0.00	0.00	0.00	0.00	0.00	0.00	0.00
TOTAL	96.71	96.97	96.28	96.98	95.71	94.82	97.15

## CATIONS RECALCULATED ON THE BASIS OF 23 OXYGENS

SI	7.799	7.808	7.833	7.758	7.688	7.983	7.966
AL4	.201	.192	.170	.242	.312	.017	.034
AL6	.037	.009	.041	.073	.029	.056	.017
TI	.006	.006	.005	.009	.012	.006	.005
CR	.006	.002	.006	.018	.021	.006	.004
FE	.604	.645	.558	.625	.563	1.489	1.616
MN	.020	.020	.018	.023	.020	.068	.066
MG	4.487	4.486	4.514	4.499	4.574	5.080	5.229
CA	1.871	1.877	1.871	1.753	1.850	.244	.054
NA	.079	.073	.084	.125	.093	.042	.014
K	.004	.005	.004	.007	.005	.004	.004

## AMPHIBOLES FROM ACHILTIRUIE GABBROS.

ROCK NO	W32	W32	W32	W32	W34B	W34B	W34B	W35
SiO <sub>2</sub>	42.74	42.51	43.17	42.51	42.17	41.81	41.39	40.71
TiO <sub>2</sub>	1.41	1.32	1.35	1.61	1.89	1.64	1.91	1.99
Al <sub>2</sub> O <sub>3</sub>	14.95	14.59	15.13	14.30	14.65	15.13	14.15	14.20
FeO	10.49	11.03	10.26	11.90	10.31	10.80	11.68	12.34
MnO	.05	.07	.06	.11	.04	.08	.11	.12
MgO	13.33	13.76	13.45	13.20	13.45	12.89	13.06	12.67
CaO	11.88	11.62	11.78	11.55	12.03	11.84	11.65	11.72
Na <sub>2</sub> O	2.57	2.67	2.56	2.67	2.31	2.28	2.38	2.48
K <sub>2</sub> O	.35	.28	.33	.34	.54	.49	.60	.98
Cr <sub>2</sub> O <sub>3</sub>	.57	.33	.44	.31	.33	.29	.26	.34
Cl	.02	.01	0.00	.01	0.00	.05	.05	.03
F	.05	.04	.01	.01	.02	.02	.02	.01
TOTAL	98.34	98.18	98.54	98.50	97.74	97.32	97.27	97.59

## CATIONS RECALCULATED ON THE BASIS OF 23 OXYGENS

Si	6.133	6.160	6.220	6.186	6.152	6.136	6.122	6.048
Al <sub>4</sub>	1.811	1.820	1.780	1.812	1.848	1.864	1.878	1.952
Al <sub>6</sub>	.741	.681	.790	.643	.672	.755	.591	.535
Ti	.154	.144	.145	.176	.207	.181	.212	.222
Cr	.055	.038	.050	.036	.038	.034	.030	.040
Fe	1.270	1.341	1.236	1.449	1.258	1.326	1.445	1.533
Mn	.006	.009	.007	.014	.005	.010	.014	.015
Mg	2.377	2.431	2.488	2.664	2.924	2.819	2.879	2.805
Ca	1.843	1.817	1.818	1.802	1.880	1.862	1.846	1.866
Na	.722	.753	.715	.754	.653	.649	.683	.714
K	.065	.052	.061	.063	.101	.092	.113	.186

## AMPHIBOLES FROM ACHILTIRUIE GABBROS.

ROCK NO	W35	W36	W36	W36	W37	W37	W36
SiO <sub>2</sub>	43.64	43.92	43.61	41.75	41.23	40.75	42.01
TiO <sub>2</sub>	1.59	2.92	2.92	3.03	3.43	3.11	2.99
Al <sub>2</sub> O <sub>3</sub>	15.03	13.57	13.57	13.79	13.67	14.01	13.48
FeO	11.75	12.89	12.97	11.08	12.62	12.58	11.84
MnO	.11	.18	.18	.25	.06	.09	.05
MgO	12.22	11.18	11.14	12.02	11.32	11.46	11.65
CaO	11.91	11.67	11.71	11.88	11.52	11.84	11.79
Na <sub>2</sub> O	2.17	1.92	1.78	1.66	2.03	2.03	1.63
K <sub>2</sub> O	1.22	1.84	1.93	2.06	1.38	1.45	2.03
Cr <sub>2</sub> O <sub>3</sub>	.48	.29	.27	.34	.32	.21	.35
Cl	.03	.09	.08	.06	.12	.07	.07
F	.01	.39	.40	.32	.06	.07	.36
TOTAL	97.25	97.76	97.55	98.04	97.76	97.67	98.25

## CATIONS RECALCULATED ON THE BASIS OF 23 OXYGENS

Si	6.040	5.126	6.099	6.166	6.124	6.068	6.210
Al <sub>4</sub>	1.960	1.874	1.901	1.834	1.876	1.932	1.790
Al <sub>6</sub>	.674	.522	.521	.568	.518	.528	.560
Ti	.189	.329	.330	.337	.383	.348	.332
Cr	.056	.034	.032	.040	.038	.025	.041
Fe	1.451	1.614	1.629	1.369	1.568	1.567	1.464
Mn	.014	.010	.010	.006	.008	.011	.006
Mg	2.707	2.494	2.494	2.646	2.506	2.543	2.567
Ca	1.897	1.872	1.885	1.880	1.833	1.889	1.867
Na	.625	.557	.518	.475	.585	.586	.467
K	.231	.351	.371	.388	.262	.275	.383

## RIMS AROUND PYROXENE IN PARTIALLY ALTERED GABBROS

ROCK NO	W4	W4	W4	W4	W4	W4	W13	W13
SiO <sub>2</sub>	42.03	41.73	50.73	49.50	52.57	53.66	41.87	44.22
TiO <sub>2</sub>	.17	.17	.20	.20	.12	.09	.38	.57
Al <sub>2</sub> O <sub>3</sub>	16.18	17.04	6.20	6.69	3.47	3.01	13.94	11.44
FeO	14.21	13.65	14.23	14.93	20.16	20.79	19.04	17.09
MnO	.13	.12	.08	.05	0.00	.26	.30	.25
MgO	10.46	10.38	13.65	13.39	17.66	19.42	7.60	9.47
CaO	11.53	11.57	11.53	11.89	3.17	.50	12.05	12.14
Na <sub>2</sub> O	2.16	1.66	.72	.86	.41	.45	1.07	.96
K <sub>2</sub> O	.16	.16	.10	.11	.10	0.00	.78	.66
Cr <sub>2</sub> O <sub>3</sub>	0.00	.02	.04	.06	0.00	.01	.01	.04
Cl	0.00	0.00	0.00	0.00	0.00	0.00	0.00	0.00
F	0.00	0.00	0.00	0.00	0.00	0.00	0.00	0.00
TOTAL	97.03	96.50	97.48	97.67	97.67	98.19	97.04	96.85

## CATIONS RECALCULATED ON THE BASIS OF 23 OXYGENS

Si	6.234	6.193	7.375	7.236	7.629	7.699	6.380	6.667
Al <sub>4</sub>	1.766	1.807	.625	.764	.371	.301	1.620	1.333
Al <sub>6</sub>	1.064	1.175	.438	.389	.222	.208	.885	.700
Ti	.019	.019	.022	.022	.013	.010	.044	.055
Cr	0.000	.002	.005	.007	0.000	.001	.001	.005
Fe	1.763	1.694	1.730	1.825	2.447	2.495	2.427	2.155
Mn	.016	.015	.010	.006	0.000	.032	.039	.032
Mg	2.312	2.296	2.958	2.917	3.819	4.152	1.726	2.126
Ca	1.832	1.840	1.796	1.862	.493	.077	1.968	1.961
Na	.621	.478	.203	.244	.115	.125	.316	.281
K	.030	.030	.019	.021	.019	0.000	.152	.127

## PARTIALLY ALTERED GABBROS

ROCK NO	W31	W31	W31	W31	W31	W13	W16	W16
SiO <sub>2</sub>	42.36	52.73	63.34	48.69	49.61	40.27	43.74	42.99
TiO <sub>2</sub>	.32	.10	.06	.20	.18	.99	.29	.36
Al <sub>2</sub> O <sub>3</sub>	11.70	3.19	2.79	5.16	4.80	14.46	16.65	11.21
FeO	17.04	11.61	11.73	14.60	13.88	18.74	16.75	17.46
MnO	.16	.17	.16	.14	.15	.25	.73	.74
MgO	9.91	16.42	16.57	13.35	14.12	7.10	10.27	9.67
CaO	12.10	12.88	12.71	12.50	12.40	12.04	11.99	11.94
Na <sub>2</sub> O	1.75	.37	.40	1.08	.93	1.20	1.11	1.14
K <sub>2</sub> O	.51	.06	.06	.24	.18	1.07	.97	1.02
Cr <sub>2</sub> O <sub>3</sub>	.93	.03	.06	.11	.12	.47	0.00	.01
Cl	.70	.05	.06	.34	.29	0.00	0.00	0.00
F	0.00	0.00	0.00	0.00	0.00	0.00	0.00	0.00
TOTAL	97.50	97.61	97.95	96.61	96.67	96.59	96.50	96.55

## CATIONS RECALCULATED ON THE BASIS OF 23 OXYGENS

Si	6.446	7.589	7.646	7.283	7.352	6.201	6.652	6.568
Al <sub>4</sub>	1.554	.411	.354	.717	.648	1.799	1.348	1.432
Al <sub>6</sub>	.546	.130	.117	.194	.191	.826	.562	.587
Ti	.037	.011	.006	.022	.020	.115	.033	.041
Cr	.12	.003	.007	.013	.014	.057	0.000	.001
Fe	2.169	1.397	1.406	1.827	1.720	2.413	2.131	2.231
Mn	.021	.021	.019	.018	.019	.033	.094	.096
Mg	2.248	3.522	3.540	2.976	3.118	1.629	2.328	2.202
Ca	1.973	1.986	1.952	2.004	1.969	1.986	1.954	1.955
Na	.516	.103	.111	.313	.267	.358	.327	.338
K	.099	.011	.011	.046	.034	.210	.138	.199

## AMPHIBOLES FROM BASIC ROCKS

ROCK NO	J1	J1	J6	J6	O19	O19	O27	O27
SiO <sub>2</sub>	47.66	48.79	40.27	40.39	44.21	48.98	41.71	41.66
TiO <sub>2</sub>	.36	.31	.62	.61	.46	.33	1.02	1.02
Al <sub>2</sub> O <sub>3</sub>	8.82	8.71	15.74	15.58	11.44	8.08	15.55	15.37
FeO	12.36	12.05	20.55	20.40	13.86	11.70	9.23	9.45
MnO	.19	.19	.25	.23	0.00	0.00	.12	.12
MgO	13.84	14.09	6.56	6.73	12.22	14.90	13.95	13.85
CaO	12.20	11.96	11.44	11.38	11.99	12.12	12.01	11.95
Na <sub>2</sub> O	1.13	1.10	1.64	1.66	1.27	.76	2.20	2.27
K <sub>2</sub> O	.30	.32	.85	.82	.41	.17	1.61	1.61
Cr <sub>2</sub> O <sub>3</sub>	0.00	0.00	.01	0.00	0.00	0.00	.12	.10
Cl	.03	.03	.13	.13	.03	0.00	.08	.08
F	0.00	0.00	0.00	0.00	0.00	0.00	.85	.85
TOTAL	96.89	97.55	98.06	97.93	95.95	97.04	98.42	98.36

## CATIONS RECALCULATED ON THE BASIS OF 23 OXYGENS

Si	6.984	7.068	6.138	6.158	6.625	7.104	6.101	6.107
Al <sub>4</sub>	1.016	.932	1.862	1.842	1.375	.836	1.899	1.893
Al <sub>6</sub>	.509	.555	.967	.958	.646	.466	.784	.762
Ti	.040	.034	.071	.070	.052	.036	.112	.114
Cr	0.000	0.000	.001	0.000	0.000	0.000	.014	.012
Fe	1.515	1.460	2.620	2.601	1.737	1.419	1.129	1.159
Mn	.024	.023	.032	.030	0.000	0.000	.012	.012
Mg	3.023	3.042	1.490	1.529	2.729	3.221	3.042	3.032
Ca	1.916	1.856	1.868	1.859	1.925	1.884	1.883	1.882
Na	.321	.309	.485	.491	.369	.214	.624	.649
K	.056	.059	.165	.159	.078	.031	.301	.299

ROCK NO	J100	J100	J100	J100	J50	J50	J50	J50
SiO <sub>2</sub>	52.01	52.08	43.76	45.71	45.52	45.82	46.31	46.51
TiO <sub>2</sub>	.08	.16	.59	.32	.42	.36	.33	.38
Al <sub>2</sub> O <sub>3</sub>	3.74	4.95	10.69	9.58	12.14	10.02	9.23	10.87
FeO	11.35	11.41	16.41	15.64	11.20	11.66	11.38	11.10
MnO	.22	.25	.27	.24	.20	.23	.21	.19
MgO	16.01	15.90	11.57	12.01	13.07	13.89	14.41	13.06
CaO	12.48	12.46	11.71	12.04	12.16	12.15	12.27	12.16
Na <sub>2</sub> O	.77	1.02	1.68	1.54	1.24	1.16	.90	1.01
K <sub>2</sub> O	.35	.53	1.40	1.04	.41	.33	.28	.31
Cr <sub>2</sub> O <sub>3</sub>	.02	.01	.03	.01	.03	.02	.05	.02
Cl	.05	.04	.19	.12	.05	.03	.03	.05
F	.12	.10	.21	.16	0.00	0.00	0.00	0.00
TOTAL	97.21	98.92	98.49	97.90	96.44	95.73	96.41	96.01

## CATIONS RECALCULATED ON THE BASIS OF 23 OXYGENS

Si	7.540	7.426	6.552	6.779	6.682	6.902	7.031	6.874
Al <sub>4</sub>	.460	.574	1.448	1.221	1.318	1.098	.969	1.126
Al <sub>6</sub>	.179	.259	.439	.454	.783	.642	.615	.757
Ti	.009	.017	.066	.036	.046	.040	.036	.042
Cr	.002	.001	.004	.001	.003	.002	.006	.003
Fe	1.376	1.361	2.055	1.940	1.375	1.313	1.263	1.367
Mn	.027	.030	.034	.030	.025	.029	.026	.024
Mg	3.459	3.379	2.582	2.654	2.859	3.048	3.126	2.859
Ca	1.939	1.904	1.879	1.913	1.913	1.917	1.913	1.914
Na	.216	.282	.488	.443	.353	.331	.254	.293
K	.065	.096	.267	.197	.077	.062	.052	.054

344

## AMPHIBOLES FROM AGMATITE

ROCK NO	J48	J48	J48	J48	J48
SI02	51.00	45.13	52.11	51.31	52.95
TIO2	.18	.56	.13	.16	.13
AL2O3	6.40	10.52	4.60	5.05	4.40
FE0	9.73	11.67	8.64	8.89	8.66
MNO	.18	.18	.17	.17	.15
MGO	16.19	13.68	17.45	17.14	17.25
CAO	12.59	12.24	12.70	12.59	12.81
NA2O	.89	1.57	.73	.87	.75
K2O	.41	1.11	.33	.37	.29
CR2O3	.43	.44	.23	.28	.28
CL	.02	.04	.01	.01	.01
F	0.00	0.00	0.00	0.00	0.00
TOTAL	97.71	97.14	97.10	97.14	97.68

## CATIONS RECALCULATED ON THE BASIS OF 23 OXYGENS

SI	7.280	6.659	7.457	7.384	7.521
AL4	.720	1.341	.543	.616	.479
AL6	.357	.489	.233	.241	.258
TI	.019	.062	.014	.017	.014
CR	.049	.051	.026	.032	.031
FE	1.162	1.440	1.034	1.070	1.029
MN	.022	.023	.021	.021	.018
MG	3.444	3.008	3.721	3.676	3.652
CA	1.326	1.935	1.947	1.941	1.950
NA	.246	.449	.203	.243	.207
K	.075	.209	.060	.068	.053

## AMPHIBOLES FROM HORNBLENDITE

ROCK NO	J10						
SI02	42.11	42.04	41.20	43.09	42.56	41.09	43.28
TIO2	1.31	2.15	1.55	.30	.75	1.80	.76
AL2O3	13.73	13.58	13.49	13.61	13.48	13.14	13.02
FE0	12.79	12.61	12.57	12.03	12.70	12.64	12.62
MNO	.17	.17	.20	.20	.18	.20	.22
MGO	12.05	12.11	12.07	12.57	12.36	12.22	12.45
CAO	11.62	11.35	11.30	11.58	11.76	11.30	11.76
NA2O	2.33	2.37	2.32	2.34	2.25	2.36	2.22
K2O	.67	.48	.53	.53	.63	.53	.58
CR2O3	.03	.01	.04	.03	.02	.01	.03
CL	.03	.03	.03	.03	.03	.03	.02
F	.22	.25	.35	.25	.30	.19	.25
TOTAL	97.06	97.14	95.63	96.56	97.02	95.31	97.21

## CATIONS RECALCULATED ON THE BASIS OF 23 OXYGENS

SI	6.271	6.244	6.234	6.406	6.336	6.237	6.414
AL4	1.729	1.756	1.766	1.594	1.664	1.763	1.586
AL6	.682	.623	.641	.791	.702	.589	.690
TI	.147	.240	.176	.034	.084	.183	.085
CR	.004	.001	.005	.004	.002	.001	.004
FE	1.593	1.566	1.591	1.496	1.581	1.605	1.564
MN	.021	.021	.026	.025	.023	.026	.028
MG	2.674	2.681	2.722	2.785	2.742	2.764	2.750
CA	1.854	1.806	1.832	1.845	1.876	1.833	1.868
NA	.673	.683	.681	.674	.649	.695	.638
K	.127	.091	.102	.101	.120	.103	.110



AMPHIBOLES FROM POSSIBLE METASEDIMENT

ROCK NO	J98	J93	J98	J36	J36	J96	J96	J96	J96	J96	017	017
SiO2	41.40	41.10	41.52	42.13	41.81	43.16	43.14	54.41	38.16	37.91		
TiO2	.46	.34	.46	.34	.40	.39	.32	.03	.82	.68		
Al2O3	16.67	13.91	16.00	15.01	15.32	17.13	17.25	2.24	15.20	15.89		
FeO	18.91	18.56	18.99	15.48	16.09	11.69	11.53	18.71	25.97	25.40		
MnO	.12	.14	.13	.16	.19	.10	.08	.22	.05	.03		
MgO	6.26	7.05	6.90	10.12	10.73	11.24	11.09	20.54	2.58	2.40		
CaO	11.27	11.37	11.22	11.08	10.73	11.60	11.18	.34	11.20	11.03		
Na2O	11.53	11.50	11.51	11.84	12.02	11.26	11.71	.14	1.57	1.52		
K2O	.61	.06	.08	.21	.26	.18	.24	.05	1.02	1.03		
Cl	.08	.08	.09	.08	.08	.11	.12	.00	.24	.24		
F	0.00	0.00	0.00	0.00	0.00	.29	.14	0.00	0.00	0.00		
TOTAL	97.95	95.81	97.48	95.49	97.13	97.27	96.98	96.69	97.24	96.45		

CATIONS RECALCULATED ON THE BASIS OF 23 OXYGENS

Si	6.219	6.254	6.272	6.321	6.253	6.285	6.304	7.829	6.176	6.056		
Al4	1.781	1.746	1.728	1.679	1.747	1.704	1.696	.171	1.924	1.944		
Al6	1.172	1.108	1.122	1.076	1.054	1.124	1.127	.209	1.929	1.950		
Ti	.052	.039	.052	.038	.045	.043	.035	.003	.098	.082		
Fe	.005	.007	.010	.001	.002	.021	.005	.006	.003	.004		
Mn	2.376	2.362	2.395	1.942	2.012	1.426	1.415	2.027	3.458	3.394		
Mg	.015	.018	.017	.020	.024	.012	.010	.027	.007	.004		
Ca	1.536	1.599	1.553	2.263	2.276	2.444	2.415	4.405	.612	.571		
Na	1.814	1.854	1.816	1.783	1.786	1.719	1.751	.052	1.911	1.888		
K	.449	.443	.442	.535	.586	.498	.485	.039	.441	.471		
	.117	.136	.118	.046	.050	.041	.045	.002	.319	.271		

## AMPHIBOLES FROM INVERIAN TONALITIC GNEISSES

ROCK NO	J51	J51	J51	W24	W24	J55	J55	D34
SiO2	42.08	41.72	41.86	42.49	41.94	42.98	43.16	43.89
TiO2	.56	.44	.23	.49	.51	.51	.48	.44
Al2O3	13.35	14.63	14.25	13.50	13.90	13.03	13.34	12.50
FeO	18.18	17.45	17.37	18.02	18.31	15.76	15.37	14.67
MnO	.27	.33	.31	.32	.30	.27	.27	.25
MgO	8.37	8.78	8.85	9.47	9.03	10.23	10.08	11.09
CaO	11.26	11.44	11.42	11.24	11.28	11.59	11.37	11.64
Na2O	1.62	1.76	1.73	1.70	1.83	1.68	1.60	1.63
K2O	.96	.54	.52	.50	.53	.50	.44	.35
CR2O3	.02	.01	.01	0.00	.01	.02	.05	.09
CL	.06	.06	.06	.03	.05	.05	.07	.02
F	0.00	0.00	.02	0.00	0.00	0.00	0.00	0.00
TOTAL	96.33	97.16	96.61	98.08	97.69	96.62	96.23	96.57

## CATIONS RECALCULATED ON THE BASIS OF 23 OXYGENS

SI	6.429	5.302	6.355	6.385	6.327	6.469	6.496	6.557
AL4	1.571	1.698	1.645	1.615	1.673	1.531	1.504	1.443
AL6	.834	.908	.906	.777	.799	.781	.863	.760
TI	.064	.050	.026	.055	.058	.058	.054	.049
CR	.002	.001	.001	0.000	.001	.002	.006	.011
FE	2.323	2.205	2.205	2.265	2.310	1.984	1.935	1.833
MN	.035	.042	.040	.041	.038	.034	.034	.032
MG	1.906	1.977	2.002	2.121	2.030	2.295	2.261	2.469
CA	1.843	1.852	1.858	1.810	1.823	1.869	1.834	1.863
NA	.487	.515	.529	.495	.535	.490	.467	.472
K	.109	.104	.101	.096	.102	.096	.084	.067

## AMPHIBOLES FROM INVERIAN TONALITIC GNEISSES

ROCK NO	D34	D41	D41	D29	D29	D29	D30	D30
SiO2	43.76	43.23	43.31	43.77	44.36	44.24	43.72	43.18
TiO2	.51	.55	.55	.37	.42	.39	.55	.54
Al2O3	12.97	12.94	12.58	12.20	11.79	12.11	12.13	12.28
FeO	14.80	15.52	16.53	15.11	15.61	15.07	15.41	15.32
MnO	.28	.33	.33	.29	.23	.28	.24	.22
MgO	11.06	9.74	9.88	11.17	11.06	11.29	11.03	10.76
CaO	11.73	11.44	11.64	11.24	11.40	11.47	11.70	11.55
Na2O	1.72	1.72	1.54	1.71	1.52	1.52	1.34	1.45
K2O	.35	.63	.70	.25	.38	.31	.54	.51
CR2O3	.12	.07	.04	.03	.02	.04	.11	.07
CL	.02	.04	.04	.01	.02	.02	.05	.06
F	0.00	0.00	0.00	.10	0.00	0.00	.01	0.00
TOTAL	97.22	97.26	97.14	96.26	96.79	96.75	96.83	95.84

## CATIONS RECALCULATED ON THE BASIS OF 23 OXYGENS

SI	6.504	6.490	6.511	6.575	6.630	6.600	6.548	6.529
AL4	1.496	1.510	1.489	1.425	1.370	1.400	1.452	1.471
AL6	.759	.781	.741	.737	.708	.731	.691	.718
TI	.057	.062	.062	.042	.047	.044	.062	.061
CR	.014	.008	.005	.004	.002	.005	.013	.008
FE	1.840	2.074	2.078	1.898	1.951	1.880	1.930	1.937
MN	.035	.042	.042	.037	.029	.035	.030	.028
MG	2.450	2.179	2.214	2.501	2.463	2.510	2.462	2.425
CA	1.868	1.840	1.875	1.809	1.826	1.834	1.878	1.871
NA	.496	.501	.449	.498	.440	.440	.389	.425
K	.066	.121	.134	.048	.072	.059	.103	.098

## AMPHIBOLES FROM LAXFORDIAN SHEAR ZONES

ROCK NO	D37	D37	J102	J102	D45	D45	D45	D45
SiO2	42.61	43.68	43.12	42.90	45.28	44.48	46.23	42.61
TiO2	.15	.13	.45	.44	.48	.35	.39	.31
Al2O3	13.79	13.44	13.92	14.13	12.20	12.83	10.97	12.91
FeO	16.07	16.18	17.11	16.92	13.02	14.27	13.01	17.34
MnO	.44	.41	.26	.24	.26	.30	.24	.31
MgO	19.41	10.82	10.03	9.71	12.21	11.53	12.85	9.55
CaO	10.85	10.89	10.96	10.89	11.21	11.04	11.28	11.55
Na2O	1.92	1.86	2.01	1.97	1.74	1.87	1.46	1.65
K2O	.25	.24	.36	.33	.17	.20	.20	.38
CR2O3	.11	.09	.02	.01	.06	.05	0.00	0.00
CL	0.00	0.00	.12	.13	.01	.01	0.01	0.00
F	0.00	0.00	0.00	.03	0.00	0.00	0.00	0.00
TOTAL	96.61	97.74	98.34	97.70	96.64	96.95	96.63	96.72

## CATIONS RECALCULATED ON THE BASIS OF 23 OXYGENS

Si	6.407	6.479	6.401	6.404	6.674	6.584	6.802	6.458
Al4	1.593	1.521	1.599	1.596	1.326	1.416	1.198	1.542
Al6	.853	.831	.838	.891	.794	.823	.706	.769
Ti	.017	.015	.048	.049	.053	.039	.043	.038
Cr	.013	.011	.002	.001	.007	.006	0.000	0.000
Fe	2.021	2.007	2.124	2.112	1.605	1.767	1.601	2.197
Mn	.056	.052	.033	.030	.032	.038	.031	.039
Mg	2.337	2.392	2.219	2.160	2.682	2.544	2.316	2.152
Ca	1.750	1.731	1.743	1.742	1.770	1.751	1.778	1.879
Na	.560	.535	.579	.570	.497	.537	.417	.479
K	.048	.045	.068	.063	.032	.038	.038	.073

## AMPHIBOLES FROM SHEARED MAFIC ROCK

ROCK NO	J127							
SiO2	45.13	44.01	43.61	45.14	50.46	50.75	44.35	44.83
TiO2	.27	.32	.29	.25	.20	.21	.33	.35
Al2O3	11.05	12.42	12.84	11.32	6.05	5.02	11.74	11.54
FeO	13.83	14.01	14.50	13.49	10.94	11.01	14.44	14.46
MnO	.32	.29	.31	.36	.35	.34	.34	.33
MgO	12.42	11.66	11.35	12.56	15.75	15.99	11.45	11.86
CaO	11.21	11.30	11.07	11.25	12.00	12.59	10.95	11.05
Na2O	1.97	2.13	2.28	2.02	.98	1.02	2.26	2.18
K2O	.22	.25	.24	.20	.22	.25	.25	.22
CR2O3	.17	.25	.33	.25	.04	.07	.31	.31
CL	0.00	0.00	0.00	0.00	0.00	0.00	0.00	0.00
F	0.00	0.00	0.00	0.00	0.00	0.00	0.00	0.00
TOTAL	96.59	96.65	96.82	96.85	96.99	97.76	96.43	97.11

## CATIONS RECALCULATED ON THE BASIS OF 23 OXYGENS

Si	6.705	6.554	6.501	6.680	7.307	7.296	6.631	6.648
Al4	1.295	1.446	1.499	1.320	.693	.704	1.369	1.352
Al6	.641	.735	.758	.655	.340	.317	.700	.665
Ti	.030	.036	.033	.028	.022	.023	.037	.039
Cr	.020	.029	.039	.029	.005	.008	.037	.036
Fe	1.718	1.745	1.808	1.670	1.325	1.324	1.805	1.793
Mn	.040	.037	.039	.045	.043	.041	.043	.041
Mg	2.750	2.588	2.522	2.770	3.399	3.426	2.551	2.621
Ca	1.783	1.803	1.768	1.784	1.862	1.862	1.754	1.756
Na	.567	.615	.659	.580	.275	.284	.655	.627
K	.042	.048	.046	.038	.041	.046	.048	.042

## BIOTITE FROM INVERIAN TONALITIC GNEISSES

ROCK NO	18	J51	J51	J51	J51	J51	W24	034
SiO2	35.71	36.20	35.89	35.89	36.25	35.76	35.68	36.39
TiO2	3.37	2.08	1.92	1.61	1.61	1.63	1.67	1.83
Al2O3	16.60	17.14	17.37	17.10	17.10	17.38	17.75	17.79
FeO	19.00	18.13	17.75	18.63	18.37	19.67	17.74	14.28
MnO	.25	.14	.14	.11	.11	.13	.14	.09
MgO	9.86	11.33	11.68	11.03	10.99	11.82	12.97	14.07
CaO	.02	.01	.03	.01	.03	.01	.05	.04
Na2O	.08	.10	.11	.14	.17	.14	.20	.06
K2O	9.01	8.22	8.65	9.75	9.27	8.91	8.03	9.37
CR2O3	.04	.03	.01	.01	.01	.01	0.00	0.00
CL	.04	.08	.07	.11	.09	.07	.04	.03
F	0.00	0.00	.03	0.00	0.00	0.00	.02	0.00
TOTAL	93.97	93.45	93.64	94.40	93.99	95.54	94.33	94.36

## CATIONS RECALCULATED ON THE BASIS OF 22 OXYGENS

SI	5.512	5.554	5.505	5.524	5.572	5.436	5.416	5.519
Al <sup>4</sup>	2.488	2.446	2.495	2.476	2.428	2.564	2.584	2.481
Al <sup>6</sup>	.533	.654	.647	.627	.671	.551	.594	.657
TI	.331	.240	.221	.186	.186	.186	.191	.206
CR	.005	.004	.001	.001	.001	.001	0.000	0.000
FE	2.453	2.326	2.277	2.398	2.362	2.501	2.252	1.787
MN	.033	.016	.013	.014	.014	.017	.018	.011
MG	2.258	2.591	2.670	2.530	2.518	2.678	2.934	3.137
CA	.003	.002	.005	.002	.005	.002	.008	.006
NA	.024	.030	.033	.042	.051	.041	.059	.017
K	1.774	1.629	1.693	1.915	1.818	1.728	1.555	1.788

## BIOTITE FROM INVERIAN TONALITIC GNEISS

ROCK NO	034	041	042	042	042	147	J47
SiO2	37.02	36.18	36.27	36.19	36.41	35.36	35.36
TiO2	1.98	2.38	1.48	1.57	1.61	3.62	3.77
Al2O3	17.43	16.38	17.69	17.68	17.77	16.78	16.89
FeO	14.39	17.19	16.67	17.09	16.78	21.15	21.14
MnO	.10	.14	.07	.06	.08	.23	.24
MgO	13.72	12.81	11.92	11.92	11.73	8.44	8.13
CaO	.02	0.00	.01	0.00	.01	0.00	0.00
Na2O	.21	.15	.19	.20	.13	.05	.06
K2O	9.16	8.90	9.37	9.11	9.47	9.64	9.56
CR2O3	0.00	.04	.08	.03	.05	0.00	.01
CL	.03	.04	0.00	0.00	0.00	0.00	0.00
F	0.00	0.00	0.00	0.00	0.00	0.00	0.00
TOTAL	93.94	94.21	93.75	93.86	94.03	95.27	95.09

## CATIONS RECALCULATED ON THE BASIS OF 22 OXYGENS

SI	5.559	5.513	5.538	5.523	5.544	5.459	5.457
Al <sup>4</sup>	2.441	2.487	2.462	2.477	2.456	2.541	2.543
Al <sup>6</sup>	.646	.457	.723	.704	.734	.514	.536
TI	.224	.273	.170	.180	.184	.420	.438
CR	0.000	.005	.010	.004	.006	0.000	.001
FE	1.808	2.191	2.129	2.181	2.137	2.731	2.733
MN	.013	.018	.009	.008	.010	.030	.031
MG	3.072	2.909	2.712	2.711	2.662	1.942	1.873
CA	.003	0.000	.002	0.000	.002	0.000	0.000
NA	.061	.044	.056	.059	.038	.015	.018
K	1.756	1.730	1.825	1.774	1.840	1.899	1.885

BIOTITE FROM POSSIBLE METASEDIMENT

ROCK NO	J98	J95	J98	J98	J36	J36	J36	J36	D17	D17	J96	J96
SI02	35.31	34.84	36.08	35.45	36.05	36.00	36.00	33.14	31.77	38.92	38.90	
TI02	1.82	1.76	1.85	1.76	1.70	1.56	1.56	2.59	2.20	1.12	1.25	
AL2O3	18.19	18.11	18.03	18.14	17.05	17.19	17.19	16.86	15.40	16.81	16.81	
FE0	18.95	19.24	19.23	19.06	14.58	16.70	16.70	28.74	29.97	10.01	10.06	
MNO	10.08	10.08	10.06	10.37	14.41	15.24	15.24	4.19	4.53	17.55	17.53	
MGO	10.35	10.59	10.16	10.37	14.45	15.24	15.24	4.02	4.07	17.01	17.01	
CAO	0.27	0.4	0.00	0.00	0.23	0.22	0.22	0.10	0.19	0.36	0.33	
NA2O	17.03	17.17	9.16	9.15	7.88	6.75	6.75	9.14	8.02	0.84	0.88	
K2O	9.08	8.62	9.05	9.06	7.03	6.03	6.03	0.00	0.00	0.25	0.25	
CR2O3	0.08	0.07	0.08	0.08	0.08	0.08	0.08	0.14	0.13	0.34	0.34	
CL	0.03	0.00	0.01	0.00	0.12	0.19	0.19	0.00	0.00	0.56	0.59	
F												
TOTAL	94.10	93.60	94.94	94.21	92.22	94.05	94.05	94.93	92.37	94.53	94.78	

CATIONS RECALCULATED ON THE BASIS OF 22 OXYGENS

SI	AL4	AL6	TI	CR	FE	MN	MG	CA	NA	K
5.436	2.737	2.11	0.10	0.10	0.10	0.10	0.10	0.10	0.10	0.10
5.564	2.737	2.11	0.10	0.10	0.10	0.10	0.10	0.10	0.10	0.10
5.705	2.737	2.11	0.10	0.10	0.10	0.10	0.10	0.10	0.10	0.10
5.892	2.737	2.11	0.10	0.10	0.10	0.10	0.10	0.10	0.10	0.10
5.922	2.737	2.11	0.10	0.10	0.10	0.10	0.10	0.10	0.10	0.10
5.939	2.737	2.11	0.10	0.10	0.10	0.10	0.10	0.10	0.10	0.10
5.992	2.737	2.11	0.10	0.10	0.10	0.10	0.10	0.10	0.10	0.10
6.000	2.737	2.11	0.10	0.10	0.10	0.10	0.10	0.10	0.10	0.10
6.023	2.737	2.11	0.10	0.10	0.10	0.10	0.10	0.10	0.10	0.10
6.094	2.737	2.11	0.10	0.10	0.10	0.10	0.10	0.10	0.10	0.10
6.658	2.737	2.11	0.10	0.10	0.10	0.10	0.10	0.10	0.10	0.10

## BIOTITE FROM SHEAR ZONE/GRANULITE/AMPHIBOLITE

ROCK NO	D40	D45	D37	D2	D2	J67	J67	J55
SiO2	35.26	33.18	35.58	36.85	36.76	36.48	36.03	36.11
TiO2	2.92	1.69	.56	3.80	3.22	1.90	1.88	1.73
Al2O3	17.31	17.27	17.03	15.09	15.07	16.86	16.87	16.90
FeO	20.26	14.44	16.30	13.29	12.79	15.02	15.20	15.83
MnO	.17	.10	.17	.06	.05	.15	.16	.14
MgO	9.16	15.44	15.08	15.60	15.81	13.64	14.02	14.11
CaO	.03	.08	.03	0.00	0.00	0.00	0.00	.06
Na2O	.08	.26	.17	.07	.04	.08	.11	.15
K2O	9.67	8.56	7.26	9.71	9.65	9.03	9.65	8.95
CR2O3	.01	.08	.05	.01	.01	.03	.04	.03
CL	0.00	.03	0.00	.04	.04	0.00	0.00	.06
F	0.00	.06	0.00	.20	.30	0.00	0.00	0.00
TOTAL	94.87	91.19	92.22	94.72	93.74	93.04	92.96	94.07

## CATIONS RECALCULATED ON THE BASIS OF 22 OXYGENS

SI	5.441	5.195	5.464	5.523	5.557	5.553	5.475	5.477
AL4	2.559	2.805	2.536	2.477	2.443	2.447	2.525	2.523
AL6	.591	.383	.548	.189	.244	.579	.498	.499
TI	.339	.199	.065	.428	.366	.218	.215	.197
CR	.001	.010	.016	.001	.001	.004	.005	.004
FE	2.615	1.891	2.093	1.666	1.617	1.912	1.932	2.008
MN	.022	.013	.022	.008	.006	.019	.021	.018
MG	2.107	3.603	3.451	3.484	3.562	3.094	3.175	3.189
CA	.005	.013	.005	0.000	0.000	0.000	0.000	.010
NA	.024	.079	.051	.020	.012	.024	.032	.044
K	1.904	1.710	1.422	1.857	1.861	1.754	1.871	1.732

## BIOTITE FROM ULTRAMAFIC ROCKS

ROCK NO	D3	D3	D3	J10	J10	J10
SiO2	39.52	39.79	39.52	35.79	36.87	37.86
TiO2	1.24	1.29	1.29	1.21	1.08	1.25
Al2O3	15.54	14.51	14.66	16.62	16.36	16.25
FeO	4.53	4.62	4.68	10.77	11.69	11.00
MnO	.04	.03	.02	.10	.11	.09
MgO	23.09	23.17	22.36	17.39	18.08	17.44
CaO	.02	.01	.02	0.00	.03	0.00
Na2O	.99	.72	.70	.15	.20	.24
K2O	8.22	8.99	8.95	9.66	9.11	9.72
CR2O3	.92	1.43	1.24	.02	.02	.03
CL	.62	.03	.02	.02	.02	.03
F	.75	.53	.66	.57	.43	.49
TOTAL	94.86	95.12	94.15	94.10	93.99	94.38

## CATIONS RECALCULATED ON THE BASIS OF 22 OXYGENS

SI	5.648	5.694	5.684	5.463	5.511	5.625
AL4	2.352	2.306	2.316	2.537	2.489	2.375
AL6	.267	.142	.170	.454	.395	.472
TI	.133	.139	.140	.139	.121	.140
CR	.104	.162	.141	.002	.002	.004
FE	.541	.553	.563	1.375	1.461	1.367
MN	.005	.004	.002	.013	.014	.011
MG	4.918	4.941	4.926	3.956	4.028	3.862
CA	.003	.002	.003	0.000	.005	0.000
NA	.274	.200	.195	.044	.058	.069
K	1.499	1.641	1.642	1.881	1.737	1.842

355

APPENDIX B.

WHOLE ROCK DATA

Samples were analysed by X-ray fluorescence for 25 elements using a Philips PW 1450 automatic spectrometer with a PW 1466 sixty-position sample changer at the University of Birmingham. Count data from the spectrometer were processed using a Digital PDP 11-03 computer. Four internal reference samples per batch were used to monitor long term precision.

Sample preparation: Approximately 500g (where possible) of each sample were crushed to millimetre size using a fly press. About 100g of each sample was then coarse crushed in a TEMA swing-mill, mostly using a tungsten carbide barrel although a few samples were crushed using agate. About half of the resulting powder was further crushed in the "TEMA" to a powder of -240 B.S. mesh. Pressed powder briquettes were made using 15g of powder and about 30 drops of MOIVAL resin as a binder, and then compressed at 15 tons against the polished steel faces of the die, producing briquettes of 46mm diameter.

Trace element analysis: Samples were excited using molybdenum, tungsten and rhodium tubes. The fluorescent radiation was dispersed using a  $\text{LiF}_{220}$  analysing crystal to achieve maximum peak separation.

Instrumental conditions were essentially as in Leake et al. (1969).

Wavelengths and choice of tube were as follows:-

Mo target: Y(K<sub>α</sub>), Sr(K<sub>α</sub>), Rb(K<sub>α</sub>), Th(L<sub>α</sub>), Pb(L<sub>1,4</sub>), Ga(K<sub>α</sub>), Zn(K<sub>α</sub>), Ba(L<sub>1,4</sub>), W(L<sub>α1</sub>).

Corrections were made for the overlap of RbK<sub>α</sub> on YK<sub>α</sub>, CeL<sub>α</sub> on BaL<sub>α</sub> and YK<sub>α</sub> on the MoK<sub>α</sub> Compton peak. Background profiles and contamination were determined using ultrapure samples of SiO<sub>2</sub>, MgO and Al<sub>2</sub>O<sub>3</sub>.

W or Rh target: Ni(K<sub>α</sub>), Cr(K<sub>α</sub>), Zr(K<sub>α</sub>), Nb(K<sub>α</sub>)

W target: La(L<sub>β</sub>), Ce(L<sub>β1,4</sub>), Nd( )

Corrections were made for the overlap of SrK<sub>β1,3</sub> on ZrK<sub>α</sub> and the target contamination on Ni and Cr. Because of the lack of precision inherent in the correction of CrK<sub>α</sub> for VK<sub>β</sub> from the overlapping TiK<sub>β</sub>, the results for Cr are presented uncorrected.

Calibration: Initial calibrations were prepared from a wide range of rock types spiked with the appropriate pure element compound (Leake et al., 1969). These values were then related using either the WL<sub>β</sub> or MoK<sub>α</sub> Compton peaks scattered by the sample to provide correction for total mass absorption for all emission lines shorter than the iron absorption edge. The slightly inferior method of correction using the W Rayleigh peak was adopted in automatic analysis to give immediate results.

Minimum detection limits: The following table gives estimated MDL for the trace elements concerned.

Ni	1 ppm	TABLE B.1.
Cr	2 "	Minimum detection limits
Zr	1 "	for trace elements
Ga	1 "	
Rb	1 "	
Sr	1 "	
Y	2 "	
Zn	1 "	
Nb	1 "	
Ba	4 "	
La	2 "	
Ce	3 "	
Nd	3 "	
Pb	4 "	
Th	3 "	

Major element analysis: Most samples were analysed on pressed powder briquettes but there are potential errors caused by mineralogical effects inherent in this method. To minimise these effects some fused glass discs were prepared using a mixture of lithium metaborate and lithium tetraborate as a flux. Short range calibrations were then prepared and used to correct the powder briquette analyses. Residual errors are to be expected, particularly for Al and Fe.

A few samples were analysed using a Philips 1212 spectrometer at Bedford College, University of London. Major element analyses were performed on glass discs prepared as above and trace element analyses were performed on pressed powder briquettes.

SAMPLE NO.	GRID REF.	LOCATION	ROCK TYPE	FIELD RELATIONSHIPS
W1	114334	nr Drumbeg	Layered u/m	Northern part of complex
W2	114334	"	"	"
W3	117333	Drumbeg	Retrogressed u/m	From basal unit of complex
W9	117333	"	Layered u/m	From central u/m unit
W11	117333	"	"	5m above W9
J84	113328	"	"	From southern part of complex
W4	117333	"	Gt gabbro	Base of main gabbro, 5m above W2
W6	117333	"	"	60cm garnetite layer, 16m above W4
W7	117333	"	"	10m above W6
W8	117333	"	"	9m above W7
W12	117333	"	Retrogressed gabbro	Upper gabbro unit
W13	117333	"	"	5m above W12
J73	110331	"	Gt gabbro	Top of a 10m thick gabbro band
J74	110331	"	"	5m below J73
J76	110331	"	"	very garnetiferous
J78	110331	"	Retrogressed gabbro	8m above J76
J79	110331	"	"	Below J78
J82	113328	"	Gt gabbro	Part of southern Drumbeg complex
J86	113328	"	"	"
W32	033079	Achiltibuie	Mafic garnet gabbro	2m from base of garnet gabbro
W34a	033079	"	Hb rich u/m	3m above W32
W34b	033079	"	Gt-Hb gabbro	3m above W32
W35	033079	"	Gt gabbro	7m above W34
W36	033079	"	"	7m above W35
W37	033079	"	Garnet rich gabbro	12m above W36

TABLE B.2 List of all samples analysed by X.R.F. giving grid references (all NC) and brief details.

SAMPLE NO.	GRID REF.	LOCATION	ROCK TYPE	FIELD RELATIONSHIPS
073	108307	Loch Poll body	Layered u/m	1m from base of main 100m thick u/m unit
074	108307	"	"	Coarse pyroxene rich layer 10m above 073
076	108309	"	Retrogressed gabbro	Above 077
077a	108309	"	Layered u/m	Olivine rich layer
077b	108309	"	"	"
W29	097210	Culag body	Layered u/m	From main cliffs
058	097210	"	"	"
059	097210	"	"	"
W31	097210	"	Retrogressed gabbro	From N.W. side of Lochan
J21	054263	nr Port Alltan na	Layered u/m	Fairly massive lens in low deformation lens in northern margin of Canisp shear zone
J22	054263	Bradhan		
J65	135301	nr Gorm Loch Mor	Retrogressed layered u/m	Westerly continuation of u/m band that crops out on Gorm Loch
W14	131325	E. of Drumbeg	Gabbro	Layered unit up to 30m thick folded in with the gneisses
W16	131325	"	Gt gabbro	"
J64	132326	"	Retrogressed gabbro	From same band as W14 but now only 2m thick
J95	056288	Loch Poll an Droighinn	Gt gabbro	From gabbro band about 30m thick conformable with the fairly steeply dipping gneisses
J123	056288	"	"	"
J124	056288	"	"	"

TABLE B.2 ( cont. )

SAMPLE NO.	GRID REF.	LOCATION	ROCK TYPE	FIELD RELATIONSHIPS
J101	056245	Achmelvich	Retrogressed ultramafic	From main u/m unit to W of fold
065	057244	"	"	From u/m unit to E of fold
007	056244	"	Gt gabbro retrogressed	Gabbro unit to E of fold axis
063	056244	"	"	"
J103	056244	"	"	Gabbro 10m below 007
J103a	056244	"	"	Adjacent to J103
J1	057302	nr Clash-nessie	Amphibolite	From a conformable lens 6m thick
J16	068307	"	"	From a conformable lens
069	167314	E.of Nedd	Retrogressed gabbro	From a continuous basic band up to 50m thick
J35	067259	Loch an Ordain	Basic rock with Kfsp	Lens in gneiss from N. margin of Glen Canisp shear zone
J49	059261	Alltan na Bradhan	Amphibolite	Conformable band up to 20m thick
J50	059261	"	Scapolite amphibolite	"
J56	075257	Rhicarn	Mafic	Mafic rock from shear zone
J92	048282	Clachtoll	Amphibolite	Lens in steeply dipping gneisses
J108	097312	W.Loch Poll	Retrogressed gabbro	Continuation W.of Loch Poll body
J110	128304	Torr nam Uidhean	Mafic	Sizable area of mafic material in region with retrogressed gneisses. The mafic material is uniform cut by thin felsic veins.
J111	128304	"	"	
J112	128304	"	"	
044	133322	W.of L.Nedd	Amphibolite	Mafic conformable lens
046	135315	"	"	"
D35	088213	Srathan	Amphibolite	Continuation of the Culag Body
S14	080231	Baddidaroch	"	Mafic part of small agmatite
S25	062264	Alltan na Bradhan	Retrogressed gt gabbro	Layered body, northern margin of Canisp shear zone

TABLE B.2 (cont.)

SAMPLE NO.	GRID REF.	LOCATION	ROCK TYPE	FIELD RELATIONSHIPS
D18	063293	Cnoc a Sgiorodaich	Basic(actinolite)	Large area of mafic material, mostly actinolite rich, cut by numerous felsic veins and patches in a structurally very complex area. There are a few garnetiferous horizons.
S5	063293	"	"	"
S20	068293	"	"	"
S21	068293	"	"	"
J4	056315	Rheidh Phort Clashnessie	Hornblendite	Lens of hornblendite cut by thin felsic veins, above low deformation gneisses.
J5	056315	"	"	"
J6	056315	"	Gt amphibolite	"
J7	056315	"	Hornblendite	"
W40	218448	Gorm Loch Laxford Front	Hornblendite u/m,	3m from base of crags
W41	218448	"	"	Lens in W40
W42	218448	"	"	More basic, 14m above W41
W45	218448	"	Gabbro	In parts garnetiferous, 30m above W42
W46	218448	"	Amphibolite	From Loch shore
W47	218448	"	"	More leucocratic
W49	218448	"	Layered u/m	15m thick layer in gabbro
W50	218448	"	Garnet horn blendite	10m thick layer in leucocratic gabbro
J48	070309	E.of Clashnessie	Hornblendite (+ some cpx)	u/m part of agmatite
J70	129308	L.Braighe	"	"
D19	178325	L.Ardhair	Mafic	Conformable lens up to 30m thick, continues along strike for about 1.5km.
D20	178325	"	"	"

TABLE B.2 (cont.)

SAMPLE NO.	GRID REF.	LOCATION	ROCK TYPE	FIELD RELATIONSHIPS
J10	067318	E.end of Clashnessie Bay	Hornblendite	10m thick conformable lens of coarse dark hornblendite
J71	141303	E. of Gorm Loch Mor	Hornblendite	Conformable lens in gneiss
J15	111340	Culkein Drumbeg	Hornblendite	Finer grained conformable lens
J23	058310	Clashnessie	"	"
J61	066316	"	"	"
J69	066316	"	"	"
W59	066316	"	"	"
J47	055295	E.of Stoer	Biotite rich Gneiss	3m thick conformable lens
J94	055289	Loch Poll an Droighinn	Gt-Qz-Bi gneiss	3-4m thick band at base of garnet gabbro unit
J96	058275	nr Maiden Loch	Gt-Hb-Bi-Qz -Pyx-Sulph	1-2m thick bands in vertically dipping gneisses
S10	058275	"	"	"
J113	058275	"	Gt-Qz-Bi-Hb Gneiss	15m thick lens adjacent to shear zone
J114	058275	"	"	"
D17	062293	Cnoc a Sgiorodaich	Gt-Qz-Bi gneiss	Thin(up to 5m) band at base of Cnoc a Sgiorodaich mafic complex
S4	062293	"	"	"
W43	218448	Gorm Loch Laxford Front	Anorthosite	10cm vein cutting W42
W44	218448	"	Granite	35m thick sheet cutting W42
W48	218448	"	Anorthosite	12m thick sheet cutting W47
W51	218448	"	Granite	Homogenous sheet cutting W47
W52	218448	"	Anorthosite	Hb spotted anorthositic sheet
W53	218448	"	"	25m above W52
W54	218448	"	Granite	15m above W53

Table B.2 (cont.)

SAMPLE NO.	GRID REF.	LOCATION	ROCK TYPE	FIELD RELATIONSHIPS
J104	057242	Achmelvich	Trondjhemite	Discordant sheet cutting Achmelvich layered complex
J105	057242	"	"	"
J106	057242	"	"	"
W15	131325	E.of Drumbeg	Anorthosite	Discordant pegmatitic patch cutting mafic complex
W30	097210	Culag	"	"
W38	033079	Achiltibuie	"	"
J28	061311	Clashnessie Bay	Trondjhemite	Conformable lens in fold core
J29	097312	W.side of Loch Poll	Granite	3m thick sheet cutting mafic complex
J107	097312	"	"	"
J115	058273	Maiden Loch	Trondjhemite	5m thick sheet in vertically dipping gneisses
J77	110331	Drumbeg	"	10m thick, discordant sheet cutting J76
J85	113328	Drumbeg	"	Pegmatitic gneiss cutting J86
J120	056288	Loch Poll an Droighinn	Tonalite	5m thick layer conformably above the gt-gabbro horizon
W24	065316	Clashnessie	Tonalite	Low-deformation gneiss adjacent to the amphibolite dykes
J24	058310	"	"	Well banded gneiss in area with many minor folds
078	058310	"	"	"
J27	060311	Irmfada	"	"
J59	065316	Clashnessie	"	Gneiss adjacent to dykes
J60	065316	"	"	"
J116	065316	"	"	"
J117	065316	"	"	Sheared, very near to dyke
J118	065316	"	"	Gneiss near to dykes
J119	065316	"	"	"

TABLE B.2 (cont.)

SAMPLE NO.	GRID REF.	LOCATION	ROCK TYPE	FIELD RELATIONSHIPS
D34	073244	Loch Roe	Tonalite	Ordinary amphibolite facies gneiss in N.Limb of Lochinver antiform
D37	054257	Alltan na Bradhan	"	Fine grained shear zone gneiss
D40	057256	"	Trondjemite	"
D42	058254	"	Tonalite	More mafic gneiss from S. margin of shear zone
D46	100235	Lochinver	"	Vertically dipping gneisses in shear zone, medium grain size (Not recrystallized)
D47	100235	"	"	
081	054242	Achmelvich	Tonalite	From area with numerous hornblendite balls.
080	054244	"	"	Massive, steeply dipping gneiss
079	054246	"	"	Well banded steeply dipping gneiss
J11	067318	Clashnessie	"	Banded gneiss adjacent to J10
J12	111340	Culkein Drumbeg	Trondjemite	Massive 20m thick sheet
J14	111340	"	"	Low-deformation gneiss
J18	067263	Port Alltan na Bradhan	Tonalite	Low deformation lens in shear zone
J20	059258	Alltan na Bradhan	"	From margin of Canisp. shear zone
J39	173318	E. of L. Nedd	Trondjemite	Low-deformation gently dipping gneiss
J42	096247	Manse Loch	"	Gneiss between two dykes
J51	059261	Alltan na Bradhan	Tonalite	Adjacent to J49, J50; Northern margin of shear zone
J52	087193	Inverkirkaig	Mafic	Greasy looking gneiss
J53	085191	"	Trondjemite	"

TABLE B.2 (cont.)

SAMPLE NO.	GRID REF.	LOCATION	ROCK TYPE	FIELD RELATIONSHIPS
J3	056315	Rheidh Phort Clashnessie	Trondjemite	Micaceous gneiss underlying amphibolites.
J8	056315	"	"	"
J9	056315	"	"	"
J55	075257	Rhicarn	Tonalite	Shear zone, vertically dipping gneisses.
J91	104225	nr Lochinver	"	S. limb of Lochinver antiform
J121	056288	Loch Poll an Droighinn	"	Gneiss overlying J120
J62	135332	Duart	Tonalite	Pegmatitic gneiss, conformable
J63	135332	"	"	"
W17	065316	Clashnessie Bay	Amphibolite	Discordant amphibolite dyke
W19	065316	"	"	"
W20	065316	"	"	"
W21	065316	"	"	"
W22	065316	"	"	"
W23	065316	"	"	"
J67	065316	"	"	"
J68	065316	"	"	"
W55	057314	"	"	"
060	097210	Culag	"	From a shear zone cutting the layered complex
061	133326	E. of Drumbeg	"	From a shear zone
062	155326	E. of Nedd	"	From a shear zone marginal to a mafic band
W56	057314	Clashnessie	Hornblendite	15cm thick, possibly discordant band.
J58	065316	"	"	Foliated ultramafic Scourie Dyke
W57	065316	"	"	"

TABLE B.2 (cont)

## DRUMBEG ULTRAMAFICS.

ROCK NO	W1	W2	W3	W9	W11	J84
SiO <sub>2</sub>	44.9	44.7	47.1	45.4	45.2	43.1
TiO <sub>2</sub>	.37	.37	.31	.30	.33	.34
Al <sub>2</sub> O <sub>3</sub>	4.1	5.0	4.4	5.5	4.9	3.0
Fe <sub>2</sub> O <sub>3</sub>	10.44	11.14	12.06	10.43	11.05	12.76
FeO	0.00	0.00	0.00	0.00	0.00	0.00
MnO	0.00	0.00	0.00	0.00	0.00	.21
MgO	30.43	28.44	28.81	29.19	27.96	32.63
CaO	7.19	7.33	9.17	7.11	7.85	7.08
Na <sub>2</sub> O	.27	.53	.12	.17	.49	.32
K <sub>2</sub> O	.07	.08	.04	.06	.14	.05
P <sub>2</sub> O <sub>5</sub>	.02	.04	0.00	.01	.03	.02
TOTAL	97.79	97.63	101.00	98.13	97.69	99.54
TRACE ELEMENTS IN PPM						
NI	1715	1520	0	0	0	1581
CR	2869	3320	1793	2674	2899	2550
ZN	73	68	78	92	69	75
GA	9	7	7	7	7	11
RB	1	1	1	2	3	1
SR	33	38	12	29	39	56
Y	6	4	8	9	5	6
ZR	18	18	35	21	16	12
NB	2	-1	-1	2	-1	-1
BA	15	15	14	16	18	24
LA	-3	2	2	5	1	-1
CE	-3	4	-3	-3	-3	-1
ND	-3	0	-3	-3	-3	-1
PB	-4	-3	-3	-3	-3	-3
TH	-3	-3	-3	-3	-3	-3
ELEMENT RATIOS						
K/RB	581.	564.	332.	249.	387.	415.
BA/PB	16.7	19.0	14.0	8.0	6.0	24.0
K/BA	36.3	44.3	23.7	31.1	64.6	17.3
K/SR	17.6	17.5	27.7	17.2	29.8	7.4
SR/SR	.031	.026	.083	.069	.077	.018
BA/SR	.48	.39	1.17	.55	.46	.43
CE/YN	0.0	2.4	0.0	0.0	1.5	0.0
CE*/MG	.40	.45	.50	.41	.48	.45
ZR/NB	9.00	0.00	0.00	10.50	0.00	0.00
TI/ZR	123.	123.	53.	103.	124.	170.
SR/ZR	1.8	2.1	.3	1.4	2.4	4.7
ZP/Y	3.0	4.5	4.4	2.3	3.2	2.2
CIPW NORMS						
Q	0.0	0.0	0.0	0.0	0.0	0.0
GOR	0.0	0.0	0.0	0.0	0.0	0.0
OR	4.2	.5	.2	.4	.8	.3
AB	2.3	4.0	1.0	1.5	4.2	2.7
AN	8.1	11.4	11.3	14.4	10.9	6.8
NE	0.0	0.0	0.0	0.0	0.0	0.0
DI	21.2	20.2	26.8	17.0	22.5	22.6
HY	14.4	13.8	24.4	24.4	19.7	7.2
OL	43.6	37.1	27.0	37.8	34.3	54.0
MT	5.4	6.5	8.7	3.8	6.6	5.6
ILM	.7	.7	.6	.7	.6	.7
HM	0.0	0.0	0.0	0.0	0.0	0.0
AP	.5	.1	.0	.0	.1	.0

TABLE B.4 Lists of analyses of all samples analysed. Details of localities etc. are given in Table B.2. Negative numbers mean the element concerned is less than the value indicated, 0 for trace elements means that element was not determined. Norms for basic rocks were calculated assuming an  $Fe_2O_3/FeO$  ratio of about 0.3.

Total iron is given as  $Fe_2O_3$ , FeO not determined.

GABRIUS DRUMBEG

ROCK NO.	M4	M6	M7	M8	M12	M13	J73	J74	J76	J78	J79	J82	J86
TOTAL	97.92	98.40	97.19	97.14	97.76	98.01	98.34	96.70	96.85	97.93	96.53	97.32	97.22
TRACE ELEMENTS IN PPM													
NI	0	0	0	0	0	0	150	153	151	312	206	140	122
COBALT	4915	5114	5357	3911	5936	2938	3214	3229	3259	4977	1078	1179	1223
ZN	1119	1124	1188	1033	1222	1115	1115	1116	1115	1033	1100	1144	1159
SR	268	269	118	287	142	1518	130	229	78	220	119	219	169
Y	17	17	14	14	12	19	13	14	20	33	21	17	22
BAR	33	33	14	33	11	157	17	18	55	114	104	35	103
BALEAD	26	26	14	26	9	210	13	7	14	47	17	17	15
LPB	1	1	1	1	1	1	1	1	1	1	1	1	1
PH	1	1	1	1	1	1	1	1	1	1	1	1	1
ELEMENT RATIOS													
LPB	0.000	0.000	0.000	0.000	0.000	0.000	0.000	0.000	0.000	0.000	0.000	0.000	0.000
GA/PA	22.4	22.5	22.5	22.4	22.4	22.4	22.4	22.4	22.4	22.4	22.4	22.4	22.4
SR/SR	19	19	19	19	19	19	19	19	19	19	19	19	19
BA/BA	2.000	2.000	2.000	2.000	2.000	2.000	2.000	2.000	2.000	2.000	2.000	2.000	2.000
FE+MG	21.42	21.42	21.42	21.42	21.42	21.42	21.42	21.42	21.42	21.42	21.42	21.42	21.42
TI/ZR	1.000	1.000	1.000	1.000	1.000	1.000	1.000	1.000	1.000	1.000	1.000	1.000	1.000
SP/ZR	1.000	1.000	1.000	1.000	1.000	1.000	1.000	1.000	1.000	1.000	1.000	1.000	1.000
Z/Y	2.5	2.5	2.5	2.5	2.5	2.5	2.5	2.5	2.5	2.5	2.5	2.5	2.5
GIPW NORMS													
COBALT	10	10	10	10	10	10	10	10	10	10	10	10	10
ZN	18	18	18	18	18	18	18	18	18	18	18	18	18
SR	12	12	12	12	12	12	12	12	12	12	12	12	12
Y	1	1	1	1	1	1	1	1	1	1	1	1	1
BAR	2	2	2	2	2	2	2	2	2	2	2	2	2
BALEAD	1	1	1	1	1	1	1	1	1	1	1	1	1
LPB	1	1	1	1	1	1	1	1	1	1	1	1	1
PH	1	1	1	1	1	1	1	1	1	1	1	1	1

TABLE B.4 ( cont. )

## ACHILTIBUIE GABBROS.

ROCK NO	W32	W34A	W34B	W35	W36	W37
SiO <sub>2</sub>	47.2	48.7	46.7	48.3	49.3	47.8
TiO <sub>2</sub>	.63	.66	.70	.61	.53	.73
Al <sub>2</sub> O <sub>3</sub>	10.1	11.0	11.5	11.2	12.1	13.2
Fe <sub>2</sub> O <sub>3</sub>	13.15	13.68	15.02	12.39	12.45	13.15
FeO	0.00	0.00	0.00	0.00	0.00	0.00
MnO	0.20	0.19	0.30	0.17	0.24	0.22
MgO	13.39	14.27	13.41	12.29	9.96	10.35
CaO	13.37	11.13	13.49	12.75	13.49	14.20
Na <sub>2</sub> O	1.23	1.26	.77	1.61	1.64	1.32
K <sub>2</sub> O	.19	.24	.25	.44	.30	.34
P <sub>2</sub> O <sub>5</sub>	.01	.09	.10	.02	.06	.09
TOTAL	99.47	101.22	102.56	99.78	100.07	101.41
TRACE ELEMENTS IN PPM						
NI	494	352	261	448	153	182
CR	1207	0	0	1199	502	0
ZN	78	0	0	87	77	0
GA	14	0	0	12	11	0
RB	2	3	1	0	0	1
SR	59	65	45	84	71	64
Y	10	4	16	6	21	11
ZR	17	33	31	17	26	30
NB	2	3	1	4	4	1
BA	12	0	0	21	82	0
LA	0	0	0	0	0	0
CE	0	0	0	0	33	0
ND	0	0	0	0	17	0
PB	-3	0	0	-3	-3	0
TH	-3	-3	-3	-3	-3	-3
ELEMENT RATIOS						
K/RB	788.	564.	2075.	0.	0.	2622.
BA/RB	6.0	0.0	0.0	0.0	0.0	0.0
K/BA	131.4	0.0	0.0	173.9	30.4	0.0
K/SR	26.7	30.6	46.1	43.5	35.1	44.1
KB/SR	.034	.046	.022	0.000	0.000	.016
BA/SR	.20	0.00	0.00	.25	1.15	0.00
CE/YN	0.0	0.0	0.0	0.0	0.8	0.0
FE*/MG	1.14	1.11	1.30	1.17	1.45	1.48
ZR/NB	8.50	11.00	31.00	4.25	6.50	30.00
TI/ZR	222.	120.	135.	215.	122.	146.
SR/ZR	3.5	2.2	1.5	4.9	2.7	2.1
ZR/Y	1.7	8.3	1.9	2.8	1.2	2.7
CIPW NORMS						
O	0.0	0.0	0.0	0.0	0.0	0.0
COR	0.0	0.0	0.0	0.0	0.0	0.0
OR	1.1	1.4	1.5	2.6	1.3	2.0
AB	10.6	10.6	6.4	13.8	14.0	11.1
AN	21.8	23.5	26.9	22.3	25.0	29.0
NE	0.0	0.0	0.0	0.0	0.0	0.0
DI	36.4	24.3	30.8	33.3	34.0	32.6
HY	10.9	24.5	14.6	10.4	16.3	10.0
OL	12.2	7.8	11.8	11.0	2.3	7.9
MT	5.8	5.9	6.4	5.5	5.5	5.7
ILM	1.2	1.3	1.3	1.2	1.0	1.4
HM	0.0	0.0	0.0	0.0	0.0	0.0
AP	.0	.2	.2	.0	.1	.2

TABLE B.4 (cont.)

OTHER LOCALITIES. LUCH POLL, GULAG, SLACHTOLL.

WOCK NO	073	074	077A	077B	076	W29	058	059	W31	J21	J22	J65
SI02	45.8	43.3	42.8	47.8	51.2	42.8	44.2	43.1	49.3	42.1	41.3	41.0
TU203	52.8	33.9	35.3	41.3	27.8	33.8	32.6	23.8	33.1	37.8	36.8	33.8
FE00	12.0	13.1	13.3	11.4	7.8	11.3	13.2	2.8	13.9	2.7	2.3	13.7
MM0	0.0	0.0	0.0	0.0	0.0	0.0	0.0	0.0	0.0	0.0	0.0	0.0
MA0	26.7	33.3	39.4	32.1	55.4	32.0	32.5	35.0	8.2	33.5	4.0	33.4
CA20	8.1	3.4	1.2	3.5	3.8	3.0	3.5	5.5	12.8	3.1	4.9	3.4
K20	19.2	14.1	10.4	22.2	1.5	23.5	1.0	14.0	2.2	30.1	30.1	0.0
P205	24.1	10.1	0.1	0.0	1.5	23.5	1.0	14.0	2.2	30.1	30.1	0.0
TOTAL	99.95	99.22	99.89	99.72	98.16	96.75	99.24	101.23	100.74	98.43	99.50	95.59
TRACE ELEMENTS IN PPM												
NI	554	1471	2165	916	356	0	1044	0	257	342	250	255
CR	359	357	4035	3739	227	3096	3473	4249	257	320	250	255
ZN	86	61	80	69	27	143	114	95	97	88	89	88
GA	5	2	1	3	3	1	1	1	1	1	1	1
BR	57	114	111	30	33	2	1	1	1	1	1	1
Y	27	18	21	52	14	2	1	1	1	1	1	1
NR	27	72	100	24	30	3	1	1	1	1	1	1
BA	13	0	1	0	0	0	1	0	1	1	1	1
LU	3	0	0	0	0	0	1	0	1	1	1	1
NO	3	0	0	0	0	0	1	0	1	1	1	1
PB	3	0	0	0	0	0	1	0	1	1	1	1
TH	3	0	0	0	0	0	1	0	1	1	1	1
ELEMENT RATIOS												
K/KRB	198	81.0	32.0	32.0	47.0	0.0	83.0	32.0	100.0	0.0	53.0	10.4
RA/RA	5.4	3.6	3.6	6.5	11.4	0.0	15.0	3.9	3.0	0.0	3.0	3.4
X/CR	73	10.2	30.2	33.0	41.3	13.8	15.0	27.7	26.0	10.0	10.0	10.0
BR/CR	35	10.8	30.9	33.0	41.3	13.8	15.0	27.7	26.0	10.0	10.0	10.0
BA/CR	47	0.16	0.09	1.80	1.01	1.50	1.2	0.75	0.16	0.0	0.0	0.0
CE*/MG	0.58	0.46	0.39	0.40	1.06	0.43	0.5	0.46	1.2	0.0	0.0	0.0
ZR/NB	0.00	0.46	0.40	0.37	1.06	0.43	0.5	0.46	1.2	0.0	0.0	0.0
FR/ZR	0.44	0.97	0.40	0.50	1.18	0.54	0.8	0.46	1.2	0.0	0.0	0.0
TR/ZR	1.1	3.0	2.1	1.5	2.4	1.7	1.4	1.5	3.2	1.5	1.5	1.5
ZR/Y	3.4	3.0	2.1	1.5	2.4	1.7	1.4	1.5	3.2	1.5	1.5	1.5
GIPW NORMS												
CO2	0.0	0.0	0.0	0.0	0.0	0.0	0.0	0.0	0.0	0.0	0.0	0.0
AD	17.0	4.0	7.4	29.0	31.0	27.0	16.0	16.0	30.0	15.0	14.0	14.0
AN	7.0	15.0	10.7	38.0	18.0	18.0	17.0	17.0	30.0	15.0	14.0	14.0
NI	0.5	0.2	0.7	0.2	0.3	0.3	0.3	0.3	0.3	0.3	0.3	0.3
HY	2.5	5.0	3.5	11.0	5.0	5.0	5.0	5.0	5.0	5.0	5.0	5.0
OL	8.0	17.0	12.0	53.0	24.0	24.0	24.0	24.0	24.0	24.0	24.0	24.0
MT	0.0	0.0	0.0	0.0	0.0	0.0	0.0	0.0	0.0	0.0	0.0	0.0
ILM	0.0	0.0	0.0	0.0	0.0	0.0	0.0	0.0	0.0	0.0	0.0	0.0
HP	0.0	0.0	0.0	0.0	0.0	0.0	0.0	0.0	0.0	0.0	0.0	0.0

TABLE B.4 (cont.)

ROCK NO	EAST OF DRUMBEG			LOCH POLL AN DROIGHINN		
	W14	416	J64	J95	J123	J124
SI02	48.0	51.2	49.6	49.3	49.2	47.4
TIO2	1.61	1.71	1.45	1.63	1.69	1.40
AL2O3	16.2	14.5	12.7	16.6	14.9	16.5
FE2O3	10.4	11.4	9.3	10.3	10.0	9.4
FeO	0.0	0.0	0.0	0.0	0.0	0.0
MNO	0.0	0.0	0.0	.15	.19	.17
MgO	7.6	4.9	10.7	5.5	3.7	9.4
CaO	14.1	11.8	12.1	11.4	13.2	14.1
Na2O	1.9	3.3	2.2	3.1	1.9	1.7
K2O	.38	.47	.68	.12	.16	.18
P2O5	.04	.16	.02	.05	.04	.03
TOTAL	99.26	99.44	98.28	97.78	100.31	99.51
TRACE ELEMENTS IN PPM						
NI			101	12	43	35
CR	510	231	671	5	33	167
ZN	76	143	100	62	92	63
GA	18	23	17	15	19	19
RB	18	22	6	2	4	4
SP	9	16	19	15	11	11
Y	18	49	20	14	10	11
ZR	27	100	27	33	16	29
NB	1	5	1	1	1	1
BA	8	17	12	28	33	27
LA	11	7	7	3	4	3
CE	11	20	13	10	9	11
NO	4	15	7	5	3	6
PB	4	7	7	3	3	3
TH	3	3	4	3	3	3
ELEMENT RATIOS						
X/RB	1.0	1.9	1.0	4.9	3.3	3.7
BA/RB	0.4	0.5	0.2	14.0	9.8	6.3
X/BA	0.7	0.8	0.7	35.6	34.1	55.3
X/SR	0.5	0.4	0.6	6.3	11.3	12.8
Y/SR	0.5	0.4	0.3	0.1	0.3	0.3
BA/SR	0.9	1.0	0.5	1.6	0.3	2.3
CE/YN	0.9	1.1	1.6	0.8	2.2	1.7
FE/MG	0.7	0.7	1.0	2.2	1.2	1.1
ZR/NB	27.0	20.0	27.0	33.0	16.0	29.0
TI/ZR	19.0	103.0	102.0	114.0	259.0	83.0
SR/ZR	3.3	1.6	7.1	4.8	7.4	4.0
ZR/Y	1.5	2.2	1.4	2.4	1.6	2.6
GIPW NORMS						
Q	0.0	2.5	0.0	0.0	0.0	0.0
COR	0.0	0.0	0.0	0.0	0.0	0.0
OR	0.0	0.8	4.1	0.7	0.9	1.1
AB	10.0	28.8	19.7	27.3	16.5	14.7
AN	34.0	33.0	23.0	31.8	31.6	37.2
NE	0.0	0.0	0.0	0.0	0.0	0.0
DI	29.0	28.1	31.0	0.0	0.0	0.0
HY	4.0	4.1	7.3	21.7	27.6	27.1
OL	7.0	0.0	9.7	10.0	12.2	3.9
MT	3.0	7.0	4.2	1.7	5.4	11.0
ILM	1.0	3.3	0.9	4.9	4.4	4.2
HM	0.0	0.0	0.0	1.2	1.3	0.8
AP	0.1	0.4	0.0	0.0	0.0	0.0

TABLE B.4 (cont.)

## ACHMELVICH.

ROCK NO	J101	065	007	063	J103	J103A
SiO <sub>2</sub>	48.6	48.6	47.7	48.2	47.6	48.6
TiO <sub>2</sub>	.31	.27	1.33	1.28	1.78	1.49
Al <sub>2</sub> O <sub>3</sub>	4.7	4.2	12.4	12.0	11.8	12.3
Fe <sub>2</sub> O <sub>3</sub>	10.59	11.82	13.68	13.39	15.54	13.45
FeO	0.00	0.00	0.00	0.00	0.00	0.00
MnO	.19	.21	.36	.38	.28	.29
MgO	26.51	26.21	6.78	6.44	7.10	6.86
CaO	7.39	7.67	12.39	13.24	10.74	10.83
Na <sub>2</sub> O	.12	.08	2.12	2.02	1.93	2.65
K <sub>2</sub> O	.01	0.00	.90	.37	.42	.61
P <sub>2</sub> O <sub>5</sub>	0.00	.01	.12	.10	.17	.11
TOTAL	98.50	98.86	97.70	97.92	97.36	97.19
TRACE ELEMENTS IN PPM						
NI	1450	1508	114	130	86	102
CR	2603	2519	236	192	119	211
ZN	64	76	189	141	133	111
GA	8	6	32	20	20	17
RB	1	2	19	7	4	6
SR	15	25	317	159	186	212
Y	6	7	29	31	52	34
ZR	14	12	60	54	82	58
NB	-1	-1	3	-1	6	5
BA	16	6	236	172	247	191
LA	-3	-3	5	6	18	4
CE	-3	-3	10	11	46	19
ND	-3	-3	9	7	27	12
PB	-3	-3	12	22	7	5
TH	-3	-3	3	4	4	-3
ELEMENT RATIOS						
K/RB	83.	0.	393.	436.	871.	843.
BA/RB	16.0	3.0	12.4	24.6	61.8	31.8
K/BA	5.2	0.0	31.7	17.9	14.1	26.5
K/SR	5.5	0.0	23.6	19.3	18.7	23.9
RB/SR	.057	.089	.060	.044	.022	.028
BA/SR	1.07	.24	.74	1.08	1.33	.90
CE/YN	4.0	0.0	.78	.80	2.0	1.3
FE*/MG	4.0	5.3	2.37	2.50	2.54	2.28
ZR/NB	0.00	0.00	20.00	0.00	13.67	11.60
TI/ZR	133.	135.	133.	142.	130.	154.
SR/ZR	1.1	2.1	5.3	2.9	2.3	3.7
ZR/Y	2.3	.6	2.1	1.7	1.6	1.7
CIPW NORMS						
Q	0.0	0.0	0.0	1.4	2.9	.2
CO <sub>3</sub>	0.0	0.0	0.0	0.0	0.0	0.0
OR	.1	0.0	5.5	2.3	2.6	3.7
AB	1.0	.7	18.5	17.6	17.0	23.3
AN	12.9	11.3	22.4	23.3	23.2	20.6
NE	0.0	0.0	0.0	0.0	0.0	0.0
DI	19.7	21.7	33.0	35.4	29.4	23.1
HY	45.0	45.2	9.2	10.6	18.1	14.7
OL	16.3	15.3	2.3	0.0	0.0	0.0
MT	4.7	5.5	5.1	0.0	7.0	6.1
ILM	.6	.5	2.6	2.5	3.5	2.9
HM	0.0	0.0	0.0	0.0	0.0	0.0
AP	0.0	.0	.3	.2	.4	.3

TABLE B.4 (cont.)

OTHER BASIC ROCKS.

ROCK NO	J1	J16	J69	J35	J49	J50	J56	J92
SiO2	49.6	52.6	47.7	57.6	50.6	49.1	49.8	47.7
TiO2	.51	.73	.88	.44	.28	.38	.31	.88
Al2O3	11.8	11.8	12.1	14.4	14.0	13.5	11.6	13.2
Fe2O3	10.27	11.17	13.13	7.55	8.67	9.73	10.42	11.46
FeO	0.00	0.00	0.00	0.00	0.00	0.00	0.00	0.00
MnO	.15	.27	.22	.13	.15	.17	.13	.17
MgO	9.81	6.63	8.62	5.53	11.16	11.31	12.04	9.60
CaO	12.64	13.26	11.68	7.31	11.13	12.52	12.66	12.20
Na2O	2.45	2.50	2.50	4.85	2.66	2.11	1.74	1.86
K2O	.51	.77	.89	2.44	.70	.32	.36	.36
P2O5	.54	.10	.07	.51	.01	.03	.02	.07
TOTAL	97.78	96.83	97.19	100.74	99.36	99.17	99.13	97.50
TRACE ELEMENTS IN PPM								
NI	50	102	134	17	76	78	40	188
CR	15	269	144	63	340	122	40	320
ZN	49	111	120	100	85	94	100	127
GA	19	19	13	20	14	12	17	16
RB	8	11	8	24	8	2	2	4
SR	285	249	145	1024	225	165	294	128
Y	13	20	22	0	10	8	9	22
ZR	28	60	42	104	29	19	19	56
NB	-1	-1	-1	3	1	-1	-1	-1
BA	81	278	195	628	272	64	68	102
LA	21	13	9	37	16	3	7	2
CE	53	28	20	91	42	13	19	11
ND	26	14	11	48	19	7	9	8
PB	4	6	8	7	5	5	-3	5
TH	6	-3	-3	-3	3	-3	-3	3
ELEMENT RATIOS								
K/RB	529.	581.	923.	843.	726.	1328.	1494.	747.
BA/RB	10.1	25.3	24.4	26.2	34.0	32.0	34.0	25.5
K/BA	52.3	33.0	37.9	32.3	21.4	41.5	43.5	23.5
K/SR	14.9	35.7	31.0	19.8	25.5	16.1	11.1	23.3
RB/SR	.028	.044	.055	.023	.036	.012	.007	.031
BA/SR	.28	1.12	1.34	.61	1.21	.59	.23	.30
CE/YN	1.0	3.4	2.2	0.0	10.3	4.0	5.2	1.13
FE*/MG	1.22	1.96	1.77	1.59	1.90	1.00	1.0	1.39
ZR/NB	0.00	0.00	0.00	34.67	29.00	0.00	0.00	0.00
TI/ZR	109.	73.	126.	25.	58.	120.	98.	34.
SR/ZR	10.2	4.2	3.5	9.8	7.8	8.7	15.5	2.5
ZR/Y	2.2	3.0	1.9	0.0	2.9	2.4	2.1	2.5
CIPW NORMS								
Q	0.0	5.6	0.0	0.0	0.0	0.0	0.0	0.0
CR	0.0	0.0	0.0	0.0	0.0	0.0	0.0	0.0
OR	3.1	4.7	5.5	14.4	4.2	4.2	3.2	5.2
AB	21.4	21.9	22.0	19.9	22.8	19.5	19.5	19.0
AN	20.3	13.3	19.9	10.3	24.5	19.2	23.2	27.1
NE	0.0	0.0	0.0	0.0	0.0	0.0	0.0	0.0
DI	35.4	26.7	29.8	18.6	29.1	30.9	32.6	27.6
HY	0.3	15.1	4.1	9.2	6.7	15.9	15.9	11.9
OL	7.9	3.0	1.3	1.4	12.3	5.0	6.1	3.3
MT	4.6	5.0	5.9	3.3	3.8	4.6	4.6	5.1
ILM	1.0	1.4	1.7	.8	.5	.6	.6	1.7
HM	0.0	0.0	0.0	0.0	0.0	0.0	0.0	0.0
AP	.1	.2	.2	1.2	.0	.0	.0	.2

TABLE B.4 (cont.)

OTHER BASIC ROCKS.

ROCK NO	J108	J110	J111	J112	044	046	035	S14	S25
SiO2	55.2	46.6	50.6	49.5	46.3	50.2	48.2	48.0	52.5
TiO2	1.34	1.71	.63	1.10	1.11	.36	1.00	1.70	.92
Al2O3	13.5	12.0	17.4	12.6	11.4	13.5	14.9	12.7	18.9
FeO	11.73	15.26	9.50	13.06	14.59	8.20	13.08	12.38	9.49
MnO	0.00	0.00	0.00	0.00	0.00	0.00	0.00	0.00	0.00
MgO	4.33	5.43	5.55	6.42	9.69	10.99	6.91	9.22	5.15
CaO	8.61	9.38	9.50	10.34	10.63	12.49	13.31	12.88	8.33
Na2O	3.09	1.84	3.77	2.69	1.49	2.26	1.82	1.51	3.85
K2O	.79	1.59	1.36	1.54	1.18	.50	.24	.53	.43
P2O5	.13	.16	.14	.10	.18	.05	.11	.13	.31
TOTAL	98.91	95.25	98.64	97.60	96.66	98.70	99.79	98.78	100.00
TRACE ELEMENTS IN PPM									
NI	59	53	25	73	82	71	127	175	149
CR	72	110	30	163	171	121	0	0	0
ZN	106	162	89	111	306	123	0	0	0
GA	19	17	18	19	28	19	0	0	0
RB	11	49	20	17	30	11	1	4	-1
SR	199	151	526	216	458	376	155	155	724
Y	31	41	16	27	28	9	22	11	25
ZR	37	86	62	58	51	53	55	37	112
NB	1	4	-1	-1	1	-1	1	1	8
BA	268	971	456	465	360	110	0	0	0
LA	10	15	14	12	18	5	0	0	0
CE	26	31	35	26	24	18	0	0	0
ND	15	17	16	15	15	9	0	0	0
PB	4	0	6	7	7	16	0	0	0
TH	3	0	6	-3	6	5	-3	-3	0
ELEMENT RATIOS									
K/RB	596.	269.	564.	751.	326.	377.	1532.	1723.	
BA/RB	24.4	19.8	22.8	27.4	12.0	10.0	0.0	0.0	24.4
K/BA	24.5	13.6	24.8	27.5	27.2	37.7	0.0	0.0	
K/SR	33.0	87.4	21.5	59.2	21.4	11.0	12.9	44.5	4.9
RB/SR	0.55	0.32	0.38	0.79	0.66	0.29	0.06	0.06	0.00
BA/SR	1.35	6.43	.37	2.15	.79	.29	0.00	0.00	0.00
CE/YN	1.9	1.7	5.0	2.2	1.9	4.5	5.2	1.7	1.0
FE*/MG	3.15	2.70	1.99	2.30	1.75	.87	2.2	1.58	2.14
ZR/NB	37.00	21.5	0.00	34.67	51.00	0.00	55.00	37.00	14.00
TI/ZR	217.	119.	61.	114.	130.	41.	109.	113.	49.
SR/ZR	5.4	1.8	3.5	3.7	9.0	7.1	2.8	4.2	8.5
ZR/Y	1.2	2.1	3.9	2.2	1.8	5.9	2.5	3.4	4.5
CIPW NORMS									
Q	10.4	0.9	0.0	0.0	0.0	0.0	0.7	0.0	5.0
CO3	0.0	0.0	0.0	0.0	0.0	0.0	0.0	0.0	0.0
OP	4.8	11.1	0.0	0.0	0.0	0.0	0.0	0.0	0.0
AB	26.7	15.7	31.5	23.4	13.3	31.5	11.4	13.1	31.7
AN	21.0	21.3	27.1	18.6	21.0	23.7	21.1	25.9	21.0
NE	0.0	0.0	0.0	0.0	0.0	0.0	0.0	0.0	0.0
UI	17.9	22.8	16.8	27.7	20.8	20.8	27.9	31.1	11.1
HY	11.2	13.4	10.0	19.9	19.1	19.9	14.8	13.0	11.4
OL	0.0	0.0	1.0	0.0	0.0	0.0	0.0	0.0	0.0
MT	4.2	7.1	1.1	3.3	7.0	3.0	9.7	4.0	0.0
ILM	2.6	3.5	1.2	2.2	2.2	0.7	1.9	1.4	4.5
FM	0.0	0.0	0.0	0.0	0.0	0.0	0.0	0.0	0.0
AP	.3	.4	.3	.2	.2	.2	.5	.3	.7

TABLE B.4 (cont.)

ROCK NO	GNOC A SGIORODAICH.				RHEIDH PHORT AMPHIBOLITES.			
	D18	S5	S20	S21	J4	J5	J6	J7
SiO2	47.4	48.8	48.1	48.3	48.1	47.1	52.4	47.4
TiO2	.32	.31	.41	.46	.56	.40	1.39	.36
Al2O3	15.5	14.0	16.5	15.7	9.7	3.8	11.8	10.0
FeO	10.16	9.36	9.92	9.29	12.34	13.76	15.03	13.65
Fe2O3	0.00	0.00	0.00	0.00	0.00	0.00	0.00	0.00
MnO	.16	.16	.17	.17	.33	.23	.21	.24
MgO	11.58	12.30	9.69	10.01	12.55	11.58	5.04	11.41
CaO	12.29	12.73	10.07	12.65	2.65	11.73	7.96	12.60
Na2O	1.69	1.50	2.21	1.60	1.27	1.30	2.04	1.52
K2O	.44	.40	1.16	.64	.53	.65	.74	.79
P2O5	.08	.08	.08	.09	.04	.04	.23	.02
TOTAL	99.72	93.64	98.32	98.82	98.08	96.69	96.81	97.42
TRACE ELEMENTS IN PPM								
NI	168	173	71	83	109	68	2	77
CR	0	0	0	0	284	821	14	851
ZN	0	0	0	0	126	147	103	170
GA	0	0	0	0	105	25	21	18
RB	4	2	24	8	6	5	9	8
SR	124	122	190	202	72	57	121	85
Y	2	4	11	4	17	10	38	14
ZR	20	20	27	17	27	21	87	34
NR	1	1	1	1	0	1	5	1
BA	0	0	0	0	46	50	115	76
LA	0	0	0	0	5	6	8	5
CE	0	0	0	0	21	16	21	14
NO	0	0	0	0	13	11	11	10
PB	0	0	0	0	10	6	3	3
TH	-3	-3	-3	-3	4	5	-3	-3
ELEMENT RATIOS								
K/RB	913.	1560.	471.	664.	733.	1079.	582.	819.
BA/RB	0.0	0.0	0.0	0.0	6.7	10.0	12.8	9.5
K/BA	0.0	0.0	0.0	0.0	110.0	107.9	53.4	86.3
K/SR	29.5	27.2	50.7	26.3	61.1	94.7	50.8	77.2
RB/SR	.032	.015	.126	.040	.033	.088	.074	.094
BA/SR	0.0	0.0	0.0	0.0	.56	.88	.35	.89
CE/YN	0.0	0.0	0.0	0.0	3.0	3.9	1.4	2.4
FE*/MG	1.41	.88	1.19	1.07	1.13	1.37	3.46	1.39
ZR/NB	20.00	20.00	0.00	0.00	13.50	0.00	17.40	0.00
TI/ZR	96.	93.	91.	162.	124.	114.	96.	63.
SR/ZR	6.2	5.1	7.0	11.9	2.7	2.7	1.4	2.5
ZR/Y	10.0	5.0	2.5	4.3	1.6	2.1	2.3	2.4
CIPW NORMS								
Q	0.0	0.0	0.0	0.0	0.0	0.0	12.6	0.0
CO3	0.0	0.0	0.0	0.0	0.0	0.0	0.0	0.0
OP	2.0	2.3	7.0	3.9	0.0	4.0	4.6	4.8
AB	14.4	12.2	19.2	13.8	14.4	11.5	13.1	13.1
AN	34.7	31.0	32.5	34.4	14.4	19.3	13.8	18.5
NE	0.0	0.0	0.0	0.0	0.0	0.0	0.0	0.0
DI	22.3	25.8	14.7	23.0	3.5	32.3	15.0	3.6
HY	6.3	15.7	7.9	12.8	18.5	17.9	18.0	6.3
OL	15.4	4.1	13.4	7.0	7.0	6.3	6.3	13.9
MT	4.5	4.1	4.4	4.1	5.5	6.3	6.3	6.1
ILM	.6	.6	.8	.9	.0	.6	.8	.7
HM	.6	.6	.0	.0	.0	.0	.0	.0
AP	.2	.2	.2	.2	.1	.1	.5	.0

TABLE B.4 (cont.)

## GORM LOCH LAXFORD FRONT

ROCK NO	W40	W41	W42	W45	W46	W47	W49	W50
SiO <sub>2</sub>	48.3	48.1	47.6	48.2	47.3	51.5	42.6	43.9
TiO <sub>2</sub>	.22	.23	.23	.26	.27	.48	.35	3.15
Al <sub>2</sub> O <sub>3</sub>	13.9	13.3	14.0	17.9	14.9	14.2	8.4	8.3
Fe <sub>2</sub> O <sub>3</sub>	7.81	8.10	7.82	8.55	8.60	9.27	15.32	20.93
FeO	0.00	0.00	0.00	0.00	0.00	0.00	0.00	0.00
MnO	.16	.16	.15	.15	.16	.19	.22	.31
MgO	13.81	13.69	12.30	7.73	11.58	9.44	24.35	7.07
CaO	13.62	13.98	13.31	12.03	13.48	10.01	6.84	12.09
Na <sub>2</sub> O	1.16	1.05	.72	1.28	.83	2.78	.96	.61
K <sub>2</sub> O	.24	.45	1.35	1.90	1.09	1.02	.15	.26
P <sub>2</sub> O <sub>5</sub>	.01	0.00	0.00	0.00	0.00	.04	.01	.18
TOTAL	99.02	99.08	97.48	98.00	98.11	93.93	99.00	96.79
TRACE ELEMENTS IN PPM								
NI	0	0	0	0	0	0	0	0
CR	0	0	0	0	0	0	0	0
ZN	42	45	43	48	43	119	103	128
GA	15	12	14	17	16	19	12	16
RB	5	9	35	44	29	13	4	4
SR	164	175	231	167	248	327	52	42
Y	5	4	3	6	7	19	6	43
ZR	9	9	14	10	8	43	33	76
NB	2	5	3	4	-1	4	-1	20
3A	24	37	73	349	121	195	24	64
LA	0	0	0	0	0	9	-1	-1
CE	0	0	0	0	1	23	3	19
ND	0	0	0	0	-1	10	-1	17
PB	-3	8	-3	-3	-3	8	-3	-3
TH	-3	-3	-3	-3	-3	-3	-3	-3
ELEMENT RATIOS								
K/RB	398.	415.	320.	358.	312.	651.	311.	539.
GA/RB	4.8	4.1	2.1	7.9	4.2	15.0	6.0	16.0
K/BA	83.0	101.0	153.5	45.2	74.8	43.4	51.3	33.7
K/SR	12.1	21.3	48.5	94.4	36.5	25.9	23.9	51.4
RB/SR	.030	.051	.152	.263	.117	.040	.077	.195
3A/SR	.15	.21	.32	2.09	.49	.60	.46	1.52
CE/YN	0.0	0.0	0.0	0.0	.3	3.0	1.2	1.1
FE*/MG	.67	.69	.74	1.28	.86	1.14	.75	3.44
ZR/NB	4.50	1.80	4.67	2.50	0.00	10.75	0.00	3.80
TI/ZR	146.	153.	98.	156.	202.	67.	64.	248.
SR/ZR	18.2	19.4	16.5	16.7	31.0	7.6	1.6	.6
ZR/Y	1.8	2.3	4.7	1.7	1.1	2.3	5.5	1.8
CIPW NORMS								
Q	0.0	0.0	0.0	0.0	0.0	0.0	0.0	0.0
COR	0.0	0.0	0.0	0.0	0.0	0.0	0.0	0.0
OR	1.4	2.7	8.2	11.5	6.6	6.1	.9	1.6
AB	9.9	9.0	6.2	11.1	7.2	23.8	8.2	5.3
AN	32.3	30.5	31.8	38.2	34.1	23.5	18.0	19.8
NE	0.0	0.0	0.0	0.0	0.0	0.0	0.0	0.0
DI	28.6	31.2	28.5	18.4	27.4	21.3	11.8	34.4
HY	12.1	10.8	10.9	7.7	8.4	14.7	9.8	27.8
OL	11.5	10.1	9.1	9.4	12.2	4.8	41.9	.6
MT	3.7	5.2	4.9	3.2	3.6	4.9	3.4	4.0
IL4	.4	.4	.4	.5	.5	.9	.7	6.2
JM	0.0	0.0	0.0	0.0	0.0	0.0	0.0	0.0
AP	0.0	0.0	0.0	0.0	0.0	.1	.1	.4

TABLE B.4 (cont.)

AGMATITES.			LOCH ARDBHAIR.		
ROCK NO	J48	J70	ROCK NO	013	020
SiO2	52.5	50.6	SiO2	51.2	51.4
TiO2	.36	.61	TiO2	.58	.57
Al2O3	3.7	4.3	Al2O3	17.7	17.6
Fe2O3	10.47	10.48	Fe2O3	10.12	3.24
FeO	0.00	0.00	FeO	0.00	0.00
MnO	.19	.19	MnO	.17	.15
MgO	17.14	15.72	MgO	5.83	6.72
CaO	15.11	16.37	CaO	11.29	11.41
Na2O	.71	.63	Na2O	2.75	3.07
K2O	.28	.31	K2O	.39	.52
P2O5	.04	.07	P2O5	.09	.10
TOTAL	100.52	99.28	TOTAL	100.17	100.78
TRACE ELEMENTS IN PPM			TRACE ELEMENTS IN PPM		
NI	257	168	NI	26	44
CR	917	25	CR	0	0
ZN	144	125	ZN	0	0
GA	11	12	GA	0	0
RB	3	1	RB	2	2
SR	127	247	SR	182	147
Y	12	13	Y	10	11
ZR	36	49	ZR	45	45
NB	-1	-1	NB	2	2
BA	20	49	BA	0	0
LA	13	12	LA	0	0
CE	31	36	CE	0	0
ND	15	19	ND	0	0
PB	-3	-3	PB	0	0
TH	-3	-3	TH	-3	-3
ELEMENT RATIOS			ELEMENT RATIOS		
K/RB	774.	2573.	K/RB	1618.	2158.
BA/RB	6.7	49.0	BA/RB	0.00	0.00
K/BA	116.2	52.5	K/BA	0.00	0.00
K/SR	18.3	10.4	K/SR	17.8	29.4
PB/SR	.024	.014	PB/SR	.011	.014
BA/SR	.16	.20	BA/SR	0.00	0.00
CE/YN	6.3	6.8	CE/YN	0.00	0.00
FE*/MG	.71	.77	FE*/MG	2.02	1.60
ZR/NB	0.00	0.00	ZR/NB	22.50	22.50
TI/ZR	60.	75.	TI/ZR	77.	76.
SR/ZR	3.5	5.0	SR/ZR	4.0	3.3
ZR/Y	3.0	3.8	ZR/Y	4.5	4.1
CIPW NORMS			CIPW NORMS		
Q	.2	0.0	Q	1.6	0.0
CR	0.0	0.0	CR	0.0	0.0
OR	1.7	1.9	OR	0.3	3.1
AB	6.0	5.4	AB	23.4	26.2
AN	6.1	3.2	AN	33.2	30.2
NE	0.0	0.0	NE	0.0	0.0
DI	54.6	53.7	DI	16.7	21.2
HY	26.1	17.5	HY	15.1	12.5
OL	0.0	2.4	OL	0.0	1.4
MT	4.6	4.6	MT	4.4	4.1
ILM	.7	1.2	ILM	1.1	1.1
HM	0.0	0.0	HM	0.0	0.0
AP	.1	.2	AP	.2	.2

TABLE B.4 (cont.)

## ULTRAMAFIC LENSES IN BANDED GNEISS

ROCK NO	J19	J71	J15	J23	J61	J69	W59
SiO <sub>2</sub>	42.4	40.2	47.7	53.1	51.4	49.6	48.2
TiO <sub>2</sub>	2.21	1.22	1.36	.24	.23	1.21	2.62
Al <sub>2</sub> O <sub>3</sub>	11.27	19.11	5.5	3.9	4.55	7.33	10.0
FeO	13.87	14.11	14.84	11.14	11.55	12.81	15.88
MnO	.14	.22	.28	.24	.28	.21	.22
MgO	13.66	11.22	15.19	18.59	18.30	14.35	11.66
CaO	11.03	10.07	11.46	10.79	11.73	11.60	12.55
Na <sub>2</sub> O	1.98	1.60	.81	.79	.89	1.22	1.44
K <sub>2</sub> O	1.43	2.00	.28	.13	.07	.20	.48
P <sub>2</sub> O <sub>5</sub>	.03	.67	.13	.03	.65	.11	.90
TOTAL	97.50	96.41	98.33	99.05	99.00	98.66	97.95
TRACE ELEMENTS IN PPM							
NI	99	21	738	1061	801	441	151
CR	166	171	1104	2188	3194	453	181
ZN	92	91	200	160	200	176	145
GA	17	22	15	11	11	15	23
RB	14	40	6	0	2	2	1
SR	209	531	136	17	21	38	177
Y	19	19	16	8	7	21	26
ZP	42	55	83	17	13	56	59
NB	11	1	9	-1	-1	-1	2
BA	528	1400	94	47	25	63	172
LA	19	19	17	-1	6	39	35
CE	46	45	48	1	-1	12	94
ND	26	28	23	-1	-1	31	63
PB	-3	11	3	-3	-3	-3	-3
TH	-3	-3	-3	-3	-3	-3	-3
ELEMENT RATIOS							
K/RB	847.	415.	387.	0.	290.	857.	3984.
BA/RB	37.7	35.0	15.7	0.	12.5	31.5	172.0
K/BA	228.5	11.3	24.7	0.	23.2	26.4	23.2
K/SR	56.6	31.3	17.1	0.	27.7	43.7	23.5
RB/SR	1.57	0.75	0.44	0.	0.95	0.53	0.06
BA/SR	2.56	2.64	0.69	0.	1.19	1.66	0.97
CE/YN	5.9	5.8	7.3	3.	0.0	1.4	8.8
FE*/MG	1.16	1.46	1.12	.70	.73	1.04	1.67
ZP/NB	0.00	0.00	9.22	0.00	0.00	0.00	29.50
TI/ZR	815.	133.	98.	85.	1.6.	110.	268.
SR/ZR	31.0	9.7	1.6	1.0	1.6	.6	3.6
ZR/Y	2.2	2.9	5.2	2.1	1.9	3.1	2.3
CIPW NORMS							
Q	0.0	0.0	0.0	2.8	0.0	.6	0.0
CO <sub>2</sub>	0.0	0.0	0.0	0.0	0.0	0.0	0.0
OP	0.0	12.3	1.7	0.8	0.4	1.2	0.9
AB	0.0	0.0	7.0	6.8	7.7	10.6	12.6
AN	1.4	29.2	13.6	6.8	3.2	14.2	20.0
NE	0.0	7.3	0.0	0.0	0.0	0.0	0.0
DI	2.0	15.0	35.2	37.7	40.4	35.1	30.8
HY	0.0	0.0	30.4	39.6	38.9	30.1	33.8
OL	21.0	25.3	2.5	0.0	.7	0.0	13.5
MT	0.0	0.4	0.5	0.9	5.1	5.7	7.1
ILM	4.0	2.4	2.7	.5	.4	2.3	5.1
HM	0.0	0.0	0.0	0.0	0.0	0.0	0.0
AP	.1	1.6	.3	.1	.1	.3	2.2

TABLE B.4 (cont.)

METASEDIMENTS ?

ROCK NO	J96	J47	J94	J113	J114	D17	S4	S10
SiO2	58.8	63.6	57.2	51.6	63.2	64.0	63.2	51.6
TiO2	.78	1.14	.92	1.04	.51	1.08	1.26	1.43
Al2O3	13.0	14.8	19.4	17.5	16.8	13.0	12.8	18.7
Fe2O3	11.74	6.99	8.36	9.30	5.04	14.59	15.53	13.28
FeO	0.00	0.00	0.00	0.00	0.00	0.00	0.00	0.00
MnO	.19	.55	.15	.16	.16	.21	.22	.24
MgO	8.60	2.71	3.91	4.47	1.43	1.09	1.07	6.46
CaO	4.62	3.18	3.26	8.48	3.96	3.23	3.68	5.55
Na2O	2.24	4.08	5.90	4.18	4.91	2.02	1.79	3.04
K2O	.85	2.34	1.75	.95	1.79	1.54	1.43	1.09
P2O5	.12	.39	.04	.65	.38	.05	.25	.20
TOTAL	100.37	93.28	100.89	98.33	98.08	101.01	101.24	101.38
TRACE ELEMENTS IN PPM								
NI	201	-1	107	13	29	-1	-1	231
CR	689	11	243	8	136	0	0	0
ZN	210	62	75	107	66	0	0	0
GA	19	19	27	25	24	0	0	0
RB	21	20	34	11	27	31	33	26
SR	181	604	431	809	855	1622	1460	2955
Y	23	39	30	26	15	98	60	23
ZR	86	958	317	434	174	127	139	96
NB	2	13	11	6	-1	6	15	4
BA	194	4298	1059	605	1525	0	0	0
LA	19	83	42	46	104	0	0	0
CE	38	175	76	107	189	0	0	0
ND	19	92	26	57	75	0	0	0
PB	7	16	23	19	16	0	0	0
TH	4	3	-3	-3	24	3	0	0
ELEMENT RATIOS								
K/RB	335.	371.	427.	716.	550.	412.	359.	348.
BA/RB	9.2	214.9	31.1	55.0	56.5	0.0	0.0	0.0
K/BA	36.4	4.5	13.7	13.0	9.7	0.0	0.0	0.0
K/SR	39.0	32.2	33.7	9.7	17.4	73.9	83.0	34.7
RB/SR	.116	.033	.079	.014	.032	.191	.232	.088
BA/SR	1.07	7.12	2.46	.75	1.78	0.0	0.0	0.0
CE/YN	3.7	11.0	6.2	10.1	3.8	0.0	0.0	0.0
FE*/MG	1.70	2.99	2.48	2.42	4.09	15.54	16.85	2.39
ZR/NB	43.00	73.69	28.82	72.33	0.00	21.17	9.87	24.40
TI/ZR	54.	7.	17.	14.	16.	51.	54.	8.9
SR/ZR	2.1	.5	1.4	1.9	4.9	1.3	1.0	3.1
ZR/Y	3.7	24.6	10.6	16.7	11.6	2.2	2.2	4.2
CIPW NORMS								
Q	16.7	18.8	.4	0.0	16.6	33.1	32.8	5.0
COR	.2	.3	1.8	0.0	.3	2.7	2.1	.7
OR	5.0	14.0	10.3	5.7	10.8	3.1	3.0	1.4
AB	19.0	34.9	49.8	36.2	42.5	17.1	13.6	20.0
AN	22.3	14.5	15.2	26.8	18.2	14.4	15.7	23.5
NE	0.0	0.0	0.0	0.0	0.0	0.0	0.0	0.0
OI	0.0	0.0	0.0	0.0	0.0	0.0	0.0	0.0
HY	29.7	11.4	16.0	13.2	7.6	14.6	13.0	20.0
OL	0.0	0.0	0.0	.3	0.0	0.0	0.0	0.0
NT	5.1	3.1	3.6	4.1	2.2	6.4	6.7	5.7
ILM	1.5	2.2	1.7	2.0	1.0	2.1	2.4	1.4
HM	0.0	0.0	0.0	0.0	0.0	0.0	0.0	0.0
AP	.3	.9	.1	1.6	.9	.6	.6	.5

TABLE B.4 (cont.)

## FUNNY AMPHIBOLITES

ROCK NO	060	061	062
SiO2	54.3	54.0	54.1
TiO2	12.78	12.88	12.34
Al2O3	12.7	12.7	12.1
FeO	10.76	11.22	10.47
Fe2O3	0.00	0.00	0.00
MnO	0.17	0.17	0.17
MgO	7.74	7.09	6.97
CaO	8.32	7.52	8.01
Na2O	2.50	2.51	2.42
K2O	.83	1.17	1.11
P2O5	.14	.15	.15
TOTAL	98.26	97.41	97.04

TRACE ELEMENTS IN PPM			
NI	40	37	34
CR	213	97	88
ZN	83	83	89
GA	18	16	13
RB	11	13	18
SR	306	415	350
Y	10	19	19
ZR	105	104	101
NB	4	3	2
BA	392	335	307
LA	16	19	14
CE	38	36	36
NO	18	17	17
PB	5	10	12
TH	5	9	8

ELEMENT RATIOS			
K/RB	6.00	7.47	4.60
BA/RB	35.00	30.90	31.70
K/BA	17.00	22.70	14.50
K/SR	2.20	2.90	3.40
RB/SR	1.20	1.30	1.10
BA/SR	1.20	1.81	1.10
CE/YN	4.5	4.3	4.3
FE*/MG	1.51	1.82	1.54
ZR/NB	2.50	34.67	50.00
TI/ZR	4.90	51.00	30.00
SR/ZR	2.9	4.00	3.50
ZR/Y	5.8	5.5	5.3

CIPW NORMS			
Q	8.0	7.3	9.2
CO*	0.0	0.0	0.0
OR	0.0	0.0	0.0
AB	21.7	20.9	21.3
AN	21.0	20.0	19.0
NE	0.0	0.0	0.0
DI	1.0	1.4	1.8
HY	21.0	20.0	17.0
OL	0.0	0.0	0.0
MT	4.0	4.0	4.0
ILM	0.0	0.0	0.0
HM	0.0	0.0	0.0
AP	0.0	0.0	0.0

## ULTRAMAFIC SCOURIE DYKE GLASHNESSIE

ROCK NO	W56	J58	W57
SiO2	44.8	47.5	48.2
TiO2	.87	.49	.56
Al2O3	9.4	7.0	7.1
FeO	14.83	13.42	13.20
Fe2O3	0.00	0.00	0.00
MnO	.29	.21	.22
MgO	12.89	21.27	20.60
CaO	11.34	3.30	9.35
Na2O	1.19	.80	.77
K2O	.95	.18	.08
P2O5	.04	.05	.05
TOTAL	96.42	99.21	99.73

TRACE ELEMENTS IN PPM			
NI	302	724	750
CR	1028	2339	2430
ZN	226	127	130
GA	24	10	9
RB	5	4	1
SR	99	46	44
Y	5	11	16
ZR	33	40	50
NB	1	1	2
BA	175	31	19
LA	8	4	3
CE	11	3	3
NO	1	2	1
PB	1	1	1
TH	1	1	1

ELEMENT RATIOS			
K/RB	1314.	373.	0.
BA/RB	29.2	7.8	0.0
K/BA	45.1	43.2	30.0
K/SR	79.7	32.5	15.1
RB/SR	0.01	0.07	0.01
BA/SR	1.77	0.07	0.43
CE/YN	0.4	0.7	0.0
FE*/MG	1.34	0.73	0.74
ZR/NB	33.0	1.0	25.0
TI/ZR	122.0	73.0	67.0
SR/ZR	3.0	1.2	1.9
ZR/Y	6.6	3.9	3.1

CIPW NORMS			
Q	0.0	0.0	0.0
CO*	0.0	0.0	0.0
OR	0.0	0.0	0.0
AB	10.4	10.0	10.0
AN	10.0	10.0	10.0
NE	0.0	0.0	0.0
DI	3.0	2.0	3.0
HY	10.0	10.0	10.0
OL	17.9	17.5	18.0
MT	0.0	0.0	0.0
ILM	0.0	0.0	0.0
HM	0.0	0.0	0.0
AP	0.1	0.1	0.1

TABLE B.4 (cont.)

## CLASHNESSIE DYKES.

ROCK NO	W17	W19	W20	W21	W22	W23	J57	J68	W55
SiO2	57.4	56.5	57.7	56.2	55.9	55.7	54.2	54.2	55.7
TiO2	1.13	1.05	1.14	1.61	1.59	1.16	1.18	1.18	2.29
Al2O3	12.1	11.8	12.1	12.1	12.1	12.6	12.0	12.0	11.4
Fe2O3	13.69	13.72	13.54	13.15	13.64	13.38	13.3	13.67	14.52
FeO	0.00	0.00	0.00	0.00	0.00	0.00	0.00	0.00	0.00
MnO	.20	.21	.20	.22	.21	.19	.21	.20	.19
MgO	4.49	5.15	4.27	5.04	5.07	4.44	5.85	5.91	4.84
CaO	8.00	3.57	8.29	8.72	8.28	7.32	8.41	8.24	8.20
Na2O	2.38	2.42	2.40	2.65	2.74	2.87	2.50	2.51	2.16
K2O	.70	.57	.70	.60	.70	.53	.70	.71	.85
P2O5	.25	.32	.26	.31	.29	.29	.32	.32	.24
TOTAL	100.34	99.99	100.57	100.58	100.52	99.48	98.71	98.60	100.39
TRACE ELEMENTS IN PPM									
NI	79	0	77	62	71	72	63	66	34
CR	125	0	109	100	114	114	121	127	47
ZN	122	110	116	106	114	114	129	130	105
GA	24	20	19	24	22	22	17	16	23
RB	8	3	7	4	4	4	8	11	3
SR	364	330	385	402	364	363	371	342	574
Y	28	27	28	28	30	30	29	30	40
ZR	137	137	138	141	130	130	130	132	208
NB	8	10	9	9	8	8	4	5	17
BA	283	154	371	197	207	453	319	295	453
LA	20	14	19	17	19	19	14	21	23
CE	48	39	46	49	47	47	39	50	55
ND	25	20	23	23	24	24	25	25	28
PB	6	8	7	9	14	8	5	8	19
TH	4	-3	-3	4	4	6	-3	-3	7
ELEMENT RATIOS									
K/RB	726.	1577.	830.	1245.	1452.	1099.	757.	581.	981.
BA/RB	35.4	51.3	53.0	49.3	51.8	113.3	39.9	26.8	56.6
K/BA	20.5	30.7	15.7	25.3	28.1	9.7	19.1	21.7	15.6
K/SR	16.0	12.1	15.1	12.4	16.0	12.1	16.3	18.7	12.3
RB/SR	0.22	0.08	0.18	0.10	0.11	0.11	0.22	0.32	0.14
BA/SR	.78	.39	.36	.49	.57	1.25	.86	.86	.79
CE/YN	4.2	3.5	4.0	4.3	3.8	3.8	3.3	4.1	3.4
FE*/MG	3.54	3.39	3.68	3.63	3.12	3.50	2.64	2.69	3.48
ZR/NB	17.13	13.70	15.33	15.67	16.25	16.25	32.50	26.4	12.24
TI/ZR	49.	46.	50.	68.	73.	53.	54.	54.	68.
SP/ZP	2.7	2.8	2.8	2.9	2.8	2.8	2.9	2.6	2.8
ZR/Y	4.9	5.1	4.9	5.0	4.3	4.3	4.5	4.4	5.2
SIPW NORMS									
Q	16.7	14.6	17.6	13.6	12.6	18.7	10.8	10.8	15.7
CO2	0.0	0.0	0.0	0.0	0.0	0.0	0.0	0.0	0.0
OR	4.2	3.4	4.1	3.6	4.2	3.1	4.4	4.7	5.1
AB	20.3	20.6	19.8	22.3	23.3	24.4	21.6	21.7	18.4
AN	20.4	19.8	20.4	19.5	18.7	20.0	19.8	19.7	19.0
NE	0.0	0.0	0.0	0.0	0.0	0.0	0.0	0.0	0.0
JI	14.9	17.3	16.0	18.1	17.1	8.9	17.1	16.9	16.9
HY	14.9	15.5	13.4	13.4	14.5	7.0	17.3	17.7	13.6
OL	0.0	0.0	0.0	0.0	0.0	0.0	0.0	0.0	0.0
MT	0.0	0.0	5.9	5.7	6.6	0.0	5.9	5.9	6.4
ILM	2.2	2.0	2.2	3.1	3.0	.4	2.3	2.3	4.4
HM	0.0	0.0	0.0	0.0	0.0	13.4	0.0	0.0	0.0
AP	.6	.8	.6	.7	.7	.7	.9	.8	.6

TABLE B.4 (cont.)



STO2	56.91	61.37	59.34	67.53	69.23	65.41	49.88	60.38	71.23	69.00
TIO2	43.04	45.35	47.99	43.62	46.91	45.73	43.20	45.78	45.33	42.43
FE2O3	0.00	0.00	0.00	0.00	0.00	0.00	0.00	0.00	0.00	0.00
MNO	57.53	4.94	3.74	1.89	0.00	1.00	9.08	2.04	0.00	0.00
CAO	3.93	5.45	5.95	11.51	7.19	5.74	2.07	4.02	5.03	5.13
AL2O3	0.00	0.00	0.00	0.00	0.00	0.00	0.00	0.00	0.00	0.00
ZRO2	0.00	0.00	0.00	0.00	0.00	0.00	0.00	0.00	0.00	0.00
TOTAL	98.13	99.54	100.67	98.40	98.51	98.19	97.50	100.46	99.49	98.35
TRACE ELEMENTS IN PPM										
NI	43	28	2	22	11	8	184	7	95	297
NO	38	17	57	34	10	249	132	94	25	277
NA	68	19	21	17	20	20	122	29	102	117
SR	17	81	67	49	69	53	36	41	38	15
SY	71	17	16	16	1	17	14	8	15	14
ZR	11	6	4	4	0	0	2	0	0	0
BA	15	1	1	1	7	6	9	8	7	8
AL	15	5	23	20	15	26	27	15	10	10
CO	12	1	9	11	2	8	7	5	5	5
MO	17	1	15	11	1	1	3	1	1	1
PH	1	1	1	1	1	1	1	1	1	1
ELEMENT RATIOS										
KA/AB	0.25	0.25	0.25	0.25	0.25	0.25	0.25	0.25	0.25	0.25
KA/BA	0.25	0.25	0.25	0.25	0.25	0.25	0.25	0.25	0.25	0.25
KA/SR	0.25	0.25	0.25	0.25	0.25	0.25	0.25	0.25	0.25	0.25
KA/SY	0.25	0.25	0.25	0.25	0.25	0.25	0.25	0.25	0.25	0.25
KA/AL	0.25	0.25	0.25	0.25	0.25	0.25	0.25	0.25	0.25	0.25
KA/CO	0.25	0.25	0.25	0.25	0.25	0.25	0.25	0.25	0.25	0.25
KA/MO	0.25	0.25	0.25	0.25	0.25	0.25	0.25	0.25	0.25	0.25
KA/PH	0.25	0.25	0.25	0.25	0.25	0.25	0.25	0.25	0.25	0.25
DIPW NORMS										
CO	1.5	1.5	1.5	1.5	1.5	1.5	1.5	1.5	1.5	1.5
OR	1.5	1.5	1.5	1.5	1.5	1.5	1.5	1.5	1.5	1.5
AB	1.5	1.5	1.5	1.5	1.5	1.5	1.5	1.5	1.5	1.5
BA	1.5	1.5	1.5	1.5	1.5	1.5	1.5	1.5	1.5	1.5
SR	1.5	1.5	1.5	1.5	1.5	1.5	1.5	1.5	1.5	1.5
SY	1.5	1.5	1.5	1.5	1.5	1.5	1.5	1.5	1.5	1.5
AL	1.5	1.5	1.5	1.5	1.5	1.5	1.5	1.5	1.5	1.5
CO	1.5	1.5	1.5	1.5	1.5	1.5	1.5	1.5	1.5	1.5
MO	1.5	1.5	1.5	1.5	1.5	1.5	1.5	1.5	1.5	1.5
PH	1.5	1.5	1.5	1.5	1.5	1.5	1.5	1.5	1.5	1.5

TABLE B.4 (cont.)

## ACID AND INTERMEDIATE GNEISSES SHEAR ZONE AND MARGIN

ROCK NO	034	037	040	042	046	047
SiO <sub>2</sub>	65.74	67.5	72.2	69.5	62.9	69.6
TiO <sub>2</sub>	.42	.59	.42	.48	.85	.44
Al <sub>2</sub> O <sub>3</sub>	14.1	14.33	13.3	16.8	16.1	16.5
Fe <sub>2</sub> O <sub>3</sub>	19.89	33.33	20.9	33.36	6.31	3.04
FeO	0.00	0.00	0.00	0.00	0.00	0.00
MnO	0.00	0.00	0.00	0.00	0.00	0.00
MgO	0.00	0.00	0.00	1.00	0.73	1.24
CaO	0.00	0.00	2.33	3.38	0.28	3.89
Na <sub>2</sub> O	3.76	4.19	4.97	4.82	4.30	5.33
K <sub>2</sub> O	.99	.85	1.24	.99	.54	.66
P <sub>2</sub> O <sub>5</sub>	.11	.12	.09	.11	.18	.08
TOTAL	100.47	99.25	99.95	100.43	100.57	100.85
TRACE ELEMENTS IN PPM						
NI	67	20	5	19	62	16
OR	0	0	0	0	0	0
ZN	0	0	0	0	0	0
GA	0	0	0	0	0	0
RB	-1	6	12	1	-1	-1
SR	400	495	409	378	450	442
Y	15	8	11	11	33	2
ZP	114	175	121	113	357	83
NB	1	2	4	3	3	2
BA	0	0	0	0	0	0
LA	0	0	0	0	0	0
CE	0	0	0	0	0	0
ND	0	0	0	0	0	0
PB	0	0	0	0	0	0
TR	0	0	0	0	0	0
ELEMENT RATIOS						
K/23	0.0	1139.	857.	8217.	0.	0.
BA/RB	0.0	0.0	0.0	0.0	0.0	0.0
K/3A	0.0	0.0	0.0	0.0	0.0	0.0
K/SR	7.3	14.4	25.4	21.7	10.0	12.4
3D/SR	0.0	0.12	0.36	0.03	0.0	0.0
BA/SR	0.00	0.00	0.00	0.00	0.00	0.00
CE/YN	0.0	0.0	0.0	0.0	0.0	0.0
FE*/MG	1.74	3.5	8.2	2.31	2.63	2.85
ZP/NB	114.0	87.5	30.25	37.67	119.00	44.00
TI/ZP	22.0	20.8	21.0	25.0	14.0	30.0
SR/ZP	3.5	2.8	3.3	3.3	1.3	5.0
ZR/Y	7.5	21.9	8.0	0.0	119.0	44.0
CIPW NORMS						
Q	25.1	29.1	32.4	29.2	19.1	25.9
CO <sub>3</sub>	0.0	0.0	1.7	1.7	0.0	.1
OR	2.1	5.1	7.3	5.8	3.2	3.9
A <sub>3</sub>	31.7	39.7	42.1	38.9	37.9	44.7
AN	20.5	16.5	11.2	16.1	22.0	13.8
NE	0.0	0.0	0.0	0.0	0.0	0.0
DI	7.2	0.0	0.0	0.0	4.2	0.0
HY	6.4	6.7	2.2	4.2	5.6	3.1
OL	0.0	0.0	0.0	0.0	0.0	0.0
MT	0.0	0.0	0.0	0.0	0.0	0.0
ILM	.2	.2	.1	.1	.2	.1
FM	5.9	5.4	2.5	5.3	6.3	3.6
AP	.3	.3	.2	.3	.4	.2

TABLE B.4 (cont.)

## ACID AND INTERMEDIATE GNEISSES CLASHNESSIE BAY

ROCK NO	W24	J24	J27	J59	J60	J116	J117	J118
SiO <sub>2</sub>	66.1	59.0	70.5	60.6	68.4	61.6	63.7	70.6
TiO <sub>2</sub>	.37	.74	.45	.75	.31	.53	.50	.19
Al <sub>2</sub> O <sub>3</sub>	16.3	15.3	15.7	14.4	16.4	16.8	17.2	16.1
Fe <sub>2</sub> O <sub>3</sub>	3.22	3.13	2.33	7.55	2.57	5.74	5.13	1.81
FeO	0.00	0.00	0.00	0.00	0.00	0.00	0.00	0.00
MnO	.04	.10	.10	.11	.03	.06	.05	.02
MgO	2.41	4.83	.30	4.25	1.03	3.04	3.02	.67
CaO	4.11	5.71	3.10	5.83	3.92	5.67	4.49	3.78
Na <sub>2</sub> O	5.81	4.71	5.97	4.29	5.05	5.02	5.71	6.07
K <sub>2</sub> O	.68	.85	1.12	.93	.60	.90	.80	.47
P <sub>2</sub> O <sub>5</sub>	.18	.20	.10	.22	.10	.40	.19	.07
TOTAL	99.20	101.58	99.93	98.93	93.39	93.86	100.79	99.78
TRACE ELEMENTS IN PPM								
NI	8	54	2	59	10	18	16	2
CR	24	127	3	134	3	54	31	3
ZN	35	74	16	62	28	50	35	16
GA	18	13	20	19	21	19	19	20
RB	7	7	6	10	9	6	11	6
SR	910	632	635	560	743	837	967	635
Y	2	15	-1	8	-1	6	3	-1
ZF	98	161	21	88	41	82	104	21
NB	-1	3	-1	-1	-1	-1	-1	-1
BA	550	453	384	587	605	555	490	384
LA	21	23	11	20	15	23	20	11
CE	32	43	17	36	22	40	31	17
ND	11	22	5	18	7	17	11	5
PB	5	7	9	5	8	4	10	8
TH	-3	-3	-3	-3	-3	-3	-3	-3
ELEMENT RATIOS								
K/RB	806.	1119.	1411.	771.	553.	1245.	603.	650.
BA/RB	78.6	64.7	64.0	58.7	67.2	92.5	44.5	64.0
K/BA	10.3	15.8	22.0	13.2	8.2	13.5	13.6	10.2
K/SR	6.2	11.3	13.3	13.8	6.7	8.9	6.9	6.1
Y/SR	.0006	.011	.009	.018	.012	.007	.011	.009
BA/SR	.60	.72	.60	1.05	.81	.66	.51	.60
CE/YN	39.1	7.0	0.0	11.0	0.0	16.3	25.3	0.0
FE*/MG	1.55	1.95	3.38	2.05	2.90	2.19	1.97	3.14
ZR/NB	0.00	53.67	0.00	0.00	0.00	0.00	0.00	0.00
TI/ZR	23.	28.	128.	51.	45.	39.	29.	54.
SR/ZR	9.3	3.9	30.2	6.4	18.1	10.2	9.3	30.2
ZR/Y	43.0	10.7	0.0	11.0	0.0	13.7	34.7	0.0
CIPW NORMS								
Q	18.5	13.2	24.6	16.2	22.0	14.4	14.1	25.2
CR	0.0	0.0	0.0	0.0	0.0	0.0	0.0	0.0
OR	4.1	5.1	6.0	5.6	3.6	5.3	4.7	2.8
AB	43.0	39.6	50.5	36.7	51.5	42.5	47.9	51.5
AN	16.5	18.3	13.0	17.5	15.9	20.7	18.8	15.3
NE	0.0	0.0	0.0	0.0	0.0	0.0	0.0	0.0
DI	1.6	9.3	.6	6.5	1.9	2.8	.7	2.1
HY	5.3	7.7	1.7	7.7	1.7	6.3	7.1	.7
OL	0.0	0.0	0.0	0.0	0.0	0.0	0.0	0.0
MT	0.0	0.0	0.0	0.0	0.0	0.0	0.0	0.0
ILM	.1	.2	.2	.2	.1	.1	.1	.0
HM	3.2	8.1	2.3	7.6	2.6	5.7	5.1	1.8
AP	.4	.5	.2	.5	.2	.9	.4	.2

TABLE B.4 (cont.)

## OTHER LATE SHEETS

ROCK NO	J28	J29	J107	J115	J77	J85	J120
SiO <sub>2</sub>	75.8	73.8	74.4	69.7	61.9	62.2	59.1
TiO <sub>2</sub>	.23	1.00	0.00	.09	1.00	.06	2.68
Al <sub>2</sub> O <sub>3</sub>	14.4	15.2	15.1	17.6	21.7	22.4	15.1
FeO	.24	.26	.29	.82	1.67	1.47	3.88
MnO	0.00	0.00	0.00	0.00	0.00	0.00	0.00
MgO	.11	.14	.13	.31	.91	1.00	2.17
CaO	2.19	.97	.98	4.22	2.44	1.63	7.14
Na <sub>2</sub> O	6.01	4.16	3.99	6.65	7.02	7.35	4.16
K <sub>2</sub> O	.71	3.83	5.76	.45	4.15	4.71	4.82
P <sub>2</sub> O <sub>5</sub>	.51	.01	.01	.01	.01	.01	1.45
TOTAL	99.30	99.92	100.14	99.65	99.84	100.84	98.57
TRACE ELEMENTS IN PPM							
NI	-1	-1	-1	19	13	-1	14
CR	-1	3	-1	-1	-1	-1	25
ZN	30	22	22	95	55	33	97
GA	19	19	17	16	28	27	20
RB	7	103	104	5	39	50	10
SR	361	124	146	118	874	1017	354
Y	-1	6	9	-1	-1	-1	22
ZR	39	19	37	29	44	20	37
NB	-1	-1	-1	-1	-1	-1	32
BA	482	731	733	28	3328	3352	481
LA	11	6	6	20	45	44	32
CE	19	9	11	28	32	53	60
NO	4	2	3	7	13	12	153
PB	6	23	31	6	28	30	10
TR	-3	-3	5	8	3	-3	-3
ELEMENT RATIOS							
K/RB	341.	469.	464.	747.	883.	781.	680.
BA/RB	63.9	7.1	7.0	5.6	85.3	67.0	48.1
K/BA	12.2	56.2	55.2	133.4	15.4	11.7	14.2
K/SP	16.5	390.3	327.5	31.7	39.4	38.4	19.2
MG/SR	.19	.331	.712	.042	.245	.049	.028
BA/SR	1.34	5.90	5.02	.24	3.81	3.30	1.36
CE/YN	0.0	3.7	3.0	0.0	0.0	0.0	7.0
FE*/MG	2.93	7.55	11.22	2.32	2.15	1.71	3.15
ZR/NB	0.00	1.00	0.00	0.00	0.00	0.00	1.16
TI/ZR	5.0	0.0	0.0	19.0	11.0	18.0	434.0
SR/ZR	9.3	5.5	3.9	4.1	19.9	50.9	9.6
ZR/Y	0.0	3.2	4.1	0.0	0.0	0.0	1.7
CIPW NORMS							
Q	33.6	26.0	28.0	20.8	0.0	0.0	18.9
CO <sub>3</sub>	0.0	1.0	1.2	0.0	.9	1.9	0.0
OP	4.2	34.5	34.0	2.7	24.6	27.6	4.9
AB	11.0	35.2	33.4	55.5	57.0	54.3	5.7
AN	10.2	3.0	3.0	16.9	13.0	8.9	20.3
NE	0.0	0.0	0.0	0.0	1.3	3.7	0.0
DI	0.6	0.0	0.0	1.7	0.0	0.0	0.0
HY	0.0	.1	.1	0.0	0.0	0.0	5.5
OL	0.0	0.0	0.0	0.0	1.6	1.7	0.0
MT	0.0	.1	.1	0.0	0.0	0.0	0.0
ILM	.0	0.0	0.0	.0	0.0	.0	.2
H <sub>2</sub>	.2	.2	.2	.6	1.7	1.5	6.0
AP	.0	.0	.0	.0	.0	.0	3.5

TABLE B.4 (cont.)

ROCK NO	SHEETS CUTTING ACHMELVICH COMPLEX			SHEETS CUTTING OTHER LAYER		
	J104	J105	J106	W15	W30	W38
SI02	74.7	70.8	70.0	57.4	53.6	55.2
TI02	0.00	0.04	0.04	0.06	0.07	.15
AL2O3	14.6	13.5	13.7	22.2	21.0	24.3
FeO	0.00	0.00	0.00	0.00	0.13	2.43
MNO	0.00	0.00	0.00	0.00	0.00	0.30
MGO	0.00	0.00	0.00	0.00	0.03	.02
CAO	3.76	0.64	0.39	11.33	1.46	2.05
Na2O	5.04	0.01	0.04	5.37	4.04	3.17
K2O	0.00	0.00	0.00	8.11	7.64	6.29
P2O5	0.01	0.02	0.01	0.00	2.13	0.55
TOTAL	98.77	99.70	99.16	97.74	101.23	99.68
TRACE ELEMENTS IN PPM						
NI	-1	1	3	0	36	54
CR	-1	23	5	0	4	18
ZN	7	10	11	9	16	16
GA	13	14	15	30	25	30
RB	4	6	8	1	23	1
SR	287	430	419	975	591	535
Y	-1	-1	-1	2	3	-1
ZR	30	173	153	49	18	73
NB	-1	-1	-1	1	-1	1
BA	184	222	206	255	314	344
LA	2	5	4	33	-1	-1
CE	2	4	6	54	13	28
ND	-1	-1	-1	14	5	7
PB	-9	12	16	12	16	8
TH	-3	-3	-3	-3	-3	-3
ELEMENT RATIOS						
K/RB	664.	325.	487.	1826.	509.	4565.
BA/RB	40.0	37.0	29.8	255.0	23.1	344.0
K/BA	14.4	14.2	13.9	7.2	91.7	13.3
K/SP	3.3	7.2	9.3	1.9	23.9	8.5
CB/SR	0.14	0.14	0.19	0.01	0.14	0.02
BA/SR	0.64	0.51	0.49	0.26	1.38	0.64
CE/YN	0.00	0.00	0.00	6.00	14.7	0.00
Fe*/Mg	0.07	1.00	1.70	2.67	1.73	1.38
ZR/NB	0.00	0.00	0.00	43.00	0.00	73.00
TI/ZP	0.00	1.0	2.0	7.0	2.0	12.0
SP/ZR	3.6	2.5	2.7	19.9	32.9	7.3
ZR/Y	0.0	0.0	0.0	24.0	6.0	0.0
CIPW NORMS						
Q	38.9	25.5	24.4	0.0	0.0	0.0
CR	0.0	0.0	0.0	0.0	1.8	0.0
OR	1.0	2.3	2.8	1.0	0.0	3.3
AR	4.3	31.0	51.5	64.1	50.5	48.8
AN	16.0	13.8	14.5	24.1	19.6	37.9
NE	0.0	0.0	0.0	3.3	4.3	2.5
DI	0.0	3.4	2.0	2.4	0.0	1.9
HY	0.0	1.9	2.6	0.0	0.0	0.0
OL	0.0	0.0	0.0	1.6	2.5	3.0
MT	0.0	0.0	0.0	0.0	0.0	0.0
ILM	0.0	0.0	0.1	0.0	0.0	0.0
HM	0.0	2.0	2.1	3.1	2.1	2.1
AP	0.0	0.0	0.0	0.1	0.2	0.0

TABLE B.4 (cont.)

## GORMLOCH SHEETS

ROCK NO	W43	W44	W48	W51	W52	W53	W54
SiO2	53.6	74.7	54.8	74.4	51.8	53.9	74.1
TiO2	.64	.63	.77	.10	.13	.40	.08
Al2O3	24.4	15.4	25.3	14.5	21.9	25.5	14.3
Fe2O3	3.25	.89	2.87	.87	5.59	2.69	1.28
FeO	6.00	0.00	0.00	0.00	0.00	0.00	0.00
MnO	.53	.69	.07	.04	.11	.04	.08
MgO	2.53	.32	1.14	.15	4.01	1.44	.24
CaO	8.64	3.90	8.13	.87	9.11	3.46	.73
Na2O	6.14	.12	8.91	5.20	4.25	6.15	4.29
K2O	1.64	.72	1.57	3.65	1.31	.32	4.35
P2O5	.01	.02	.15	.01	.01	.08	.01
TOTAL	99.17	100.81	99.66	99.79	98.22	99.93	100.01
TRACE ELEMENTS IN PPM							
NI	0	0	0	0	0	0	0
CR	0	0	0	0	0	0	0
ZN	10	9	5	5	58	6	8
GA	30	20	23	26	30	31	30
RB	39	8	36	113	26	4	194
SR	578	447	775	205	433	492	83
Y	1	-1	10	1	3	-1	30
ZR	109	28	46	71	16	42	79
NB	4	8	38	8	5	22	10
BA	172	286	530	606	162	165	408
LA	2	0	30	10	-1	12	26
CE	7	0	80	21	15	26	35
ND	-1	0	43	6	6	7	0
PB	-3	5	17	28	4	10	27
IH	8	-1	-3	14	-3	-3	6
ELEMENT RATIOS							
K/RB	349.	747.	362.	268.	418.	664.	207.
BA/RB	4.4	35.8	16.1	5.4	6.2	41.3	2.1
K/BA	79.1	20.9	22.5	50.0	57.1	16.1	93.7
K/SR	23.6	13.4	16.8	147.8	22.5	3.4	485.1
RB/SR	.067	.018	.046	.551	.054	.068	2.337
BA/SR	.30	.64	.75	2.96	.34	.34	4.92
CE/YN	17.1	0.0	19.5	51.3	12.2	0.0	2.9
Fe*/MG	1.46	3.23	2.92	6.73	1.62	2.17	6.19
Zr/Nb	27.25	3.50	1.21	8.86	3.20	1.91	7.90
Ti/Zr	2.	6.	10.	8.	49.	57.	6.
Sr/Zr	5.3	16.0	16.8	2.9	30.2	11.7	1.1
Zr/Y	109.0	0.0	4.6	71.0	5.3	0.0	2.6
CIPW NORMS							
Q	0.0	33.9	0.0	28.1	0.0	0.0	28.5
CO3	0.0	0.0	1.5	.4	0.0	0.0	.6
OR	9.8	4.2	9.3	21.7	7.9	1.9	28.7
AB	35.7	43.0	43.0	44.1	36.6	44.9	36.3
AN	34.5	16.3	29.4	4.4	37.5	41.1	3.9
NE	9.0	0.0	5.7	0.0	0.0	3.9	0.0
DI	4.6	.6	0.0	0.0	6.7	3.4	0.0
HY	0.0	.5	0.0	.4	1.5	0.0	.6
OL	3.0	0.0	2.0	0.0	3.9	1.4	0.0
MT	.1	.1	0.0	0.0	0.0	0.0	.0
ILM	.1	.1	.2	.1	.2	.1	.2
HM	3.2	.8	2.9	.9	5.7	2.7	1.3
AP	.0	.0	.4	.0	.0	.2	.0

TABLE B.4 (cont.)

Element	Ol	Opx	Cpx	Plag	Hb	Gt	Magt	Phlog
K	0.007	0.014	0.011	0.17	0.96	0.015		2.65
Rb	0.010	0.022	0.015	0.071	0.29	0.042		3.06
Sr	0.004	0.017	0.12	1.83	0.46	0.012		0.081
Ba	0.010	0.013	0.013	0.23	0.42	0.023		1.09
Ce	0.007	0.024	0.070	0.12	0.20	0.028		0.034
Nd	0.007	0.033	0.12	0.081	0.33	0.068		0.032
Sm	0.007	0.054	0.18	0.067	0.52	0.29		0.031
Eu	0.007	0.054	0.18	0.34	0.59	0.49		0.030
Gd	0.008	0.091	0.19	0.063	0.63	0.97		0.030
Yb	0.014	0.34	0.16	0.063	0.49	11.5		0.042
Ti	0.02	0.1	0.3	0.04	1.5	0.3	7.5	0.9
Zr	0.01	0.03	0.1	0.01	0.5	0.3		0.6
Y	0.01	0.2	0.5	0.03	1.0	2.0		0.03

Appendix C Partition coefficient data used in calculations described in the text. REE, K, Rb, Sr and Ba data are from Arth (1976), Ti, Zr and Y data is from Pearce and Norry(1979).

J.D. SILLS    Geochemical studies of the Lewisian complex of the  
Western Assynt region, N.W. Scotland.

#### ABSTRACT

This work examines the petrogenesis of layered ultramafic-gabbro bodies from the Scourian and the metamorphic evolution of the Assynt district of Sutherland. About 150 new rock analyses and 200 new mineral analyses are presented.

The layered bodies comprise ultramafic rocks (amphibole-spinel-lherzolites) and garnetiferous gabbros derived from the same tholeiitic magma which had about 15-20% MgO. The ultramafic rocks are partial cumulates formed by olivine and orthopyroxene settling; with the gabbros being derived liquids. The flat to LREE enriched patterns and trace element levels suggest the magma formed by 30-40% partial melting of undepleted mantle. The bodies may be fragments of Archaean oceanic crust invaded by tonalitic magma generated at a convergent plate boundary followed by ductile deformation and metamorphism to granulite facies. The gabbros show evidence of two periods of granulite facies mineral growth, the first producing a clinopyroxene-garnet-plagioclase assemblage at about 12-15 kb and 1000° C. Uplift caused partial breakdown of the garnet to orthopyroxene-plagioclase-spinel-amphibole symplectites at about 800-900° C and 9-14 kb. Garnet stability depends on both P-T conditions and whole rock Fe/Mg ratio.

The Lewisian complex in Assynt suffered widespread retrogression during the Inverian caused by the influx of large volumes of mantle-derived hydrous fluids associated with the development of NW-trending monoclinical folds. During retrogression the development of a uniform hornblende-plagioclase-quartz assemblage in mafic and intermediate gneisses caused a redistribution of elements. Hornblende and biotite compositions depend on whole-rock composition and paragenesis. The assemblages developed suggest retrogression occurred with falling temperatures in the range 700-500° C remaining above 500° C for the duration of the Inverian and Laxfordian events. The style of deformation became more brittle with time as the complex was uplifted. Amphibolite dykes from Clashnessie Bay are tholeiitic andesites formed from a tholeiitic magma by hornblende fractionation. They were deformed and metamorphosed before the intrusion of the main Scourie dyke swarm. The Canisp shear zone was the site of deformation over a protracted period and there may have been 5-10 km of right-lateral displacement.